Declassified in Part - Sanitized Copy Approved for Release 2012/03/12 : CIA-RDP82-00039R000100190014-6

RESTRICTED

SECURITY INFORMATION

STAT

18 Reports Appearing in the Works of the Main Geophysical Observatory imeni A. I. Voyeykov, No 19(81)

Trudy Glavnoy Geofizicheskoy Observatorii imeni A. I. Voyeykova, Vypusk 19 (81); 18 authors. Leningrad: 1950. (315 pp)

STAT

RESTRICTED

Declassified in Part - Sanitized Copy Approved for Release 2012/03/12 : CIA-RDP82-00039R000100190014-6

Declassified in Part - Sanitized Copy Approved for Release 2012/03/12 : CIA-RDP82-00039R000100190014-6

TABLE OF CONTENTS


| | | page /In the original/ |
|---|---|---|
| 1. | Preface | 3 |
| 2. | Investigation of Effectiveness of the Basic Methods of Combatting Frosts<br>M. E. Berlyand and P. N. Krasikov | 5 |
| 3. | Visibility Range of Real Objects<br>N. G. Boldyrev | 11 |
| 4. | Climatic Factors of the Surface Physico-Geographic Process<br>M. I. Budyko | 25 |
| 5. | Theory of Ground Freezing<br>I. Sh. Volokhonskiy | 41 |
| 6. | The New DM-7 Instrument for Determining the Visibility of Objects and Beacons<br>V. A. Gavrilov | 66 |
| 7. | The Macrometeorological Process of Drought Formation<br>B. S. Gurevich | 79 |
| 8. | Some Properties of Fields of Meteorological Elements<br>O. A. Drozdov | 102 |
| 9. | Water Content and the Distribution of Drops in Cumulus Clouds<br>V. A. Zaytsev | 122 |
| 10. | Total Radiation at Pavlovsk<br>N. N. Kalitin /deceased/ | 133 |
| 11. | Certain Nonstationary Problems in the Theory of Heat Conductivity in Dynamic Meteorology<br>D. L. Laykhtman | 161 |
| 12. | On the Hyperbolic Equation of a Vertical Turbulence Exchange in the Atmosphere<br>E. S. Lyapin | 175 |
| 13. | A Spectrographic Study of the Transparency of the Atmosphere for Ultra-Violet Radiation of the Sun<br>Ye. A. Polyakova | 185 |
| 14. | Dynamics of Climate in Connection with Changes in Solar Activity<br>P. P. Predtechenskiy | 193 |
| 15. | Vertical Movement of the Air and Cosmic Dust<br>L. R. Rakipova | 209 |
| 16. | Certain Conclusions from the Koltusha Observation Station on the Physics of the Surface Layer of Air<br>S. A. Saprozhnikova | 225 |
| 17. | On an Approximate Method of Solving Certain Problems of Geophysics and Aerohydromechanics<br>M. Ye. Shvets | 236 |
| 18. | On the Theory of Light Scatter in the Atmosphere<br>K. S. Shifrin | 255 |
| 19. | Some Problems of the Theory of Meteorological Fields<br>M. I. Yudin | 288 |


END

Declassified in Part - Sanitized Copy Approved for Release 2012/03/12 : CIA-RDP82-00039R000100190014-6

Declassified in Part - Sanitized Copy Approved for Release 2012/03/12 : CIA-RDP82-00039R000100190014-6

Works of the Main Geophysical Observatory imeni A. I. Voyeykov
No 19 (81). Leningrad: 1950 (published by Gidrometeoizdat)

/Trudy Glavnoy Geofizicheskoy Observatorii imeni A. I. Voyeykova
Vypusk 19 (81). Leningrad: 1950 /

Declassified in Part - Sanitized Copy Approved for Release 2012/03/12 : CIA-RDP82-00039R000100190014-6

Declassified in Part - Sanitized Copy Approved for Release 2012/03/12 : CIA-RDP82-00039R000100190014-6

# PREFACE

April 1949 marked the one hundredth anniversary of the inception of the Main Geophysical Observatory.

Prior to the great October Socialist Revolution the observatory was a purely academic establishment remotely concerned with the solution of practical problems. Predominant importance in the work of the observatory at that time was occupied by problems of organization of standard meteorological observations at a network of stations, as well as the processing and publication of these data. This stage in the development of the observatory was of appreciable value, since meteorological observations extended our knowledge of the climate of Russia. Other tasks (synoptic, terrestrial magnetism, instrument making) also occupied a definite place in the activity of the observatory.

During the Soviet period the observatory has been transformed into one of the largest scientific research establishments of the Soviet Union.

The realization of the planned socialist reconstruction of USSR state economy and an increasing number of problems presented by the various branches of state economy have constantly posed new problems before the observatory. Resolution of these problems was connected with the solution of a substantial number of short and long term problems of weather forecasting, special work on the USSR climate, research into atmospheric physics, and other work.



Declassified in Part - Sanitized Copy Approved for Release 2012/03/12 : CIA-RDP82-00039R000100190014-6

Declassified in Part - Sanitized Copy Approved for Release 2012/03/12 : CIA-RDP82-00039R000100190014-6

It can be stated without exaggeration that the Main Geophysical Observatory had in its own way become a meteorological academy, where extensive research was conducted dealing with the physics of the earth's crust, applied meteorology, climatology, aerology, atmospheric optics, atmospheric electricity, terrestrial magnetism, actinometry, atmospheric acoustics, and methodology of meteorological observations.

Restoration and development of our country's national economy during the fourth postwar Five-Year Plan presented new problems, solution of which brought the observatory even closer to practical problems. Some of these tasks were the publication of the 27 volume USSR climatic manual, preparation of a two volume climatic atlas of USSR based on the above manual, compilation of a section "Climatic Influence", estimated manual, climatic descriptions of state forest field-conserving zones, development of the problem of active reaction upon clouds, effective methods of combating frosts in agriculture, quantitative methods of frost forecasting and a number of problems important to the national economy.

The subject symposium of "Works" devoted to the centennial jubilee of the observatory, contains various meteorological papers which reflect only partially the contemporary activity of scientific departments and laboratories of the observatory. Some of the papers are of great practical value, such as papers of Berlyand and Krasikov "Investigation of effectiveness of the basic methods of combating frosts"; Volkenskiy's "Theory of surface soil freezing"; Gavrilov's "New instrument DM-7 for the determination of distant visibility of objects and lights."



Declassified in Part - Sanitized Copy Approved for Release 2012/03/12 : CIA-RDP82-00039R000100190014-6

Declassified in Part - Sanitized Copy Approved for Release 2012/03/12 : CIA-RDP82-00039R000100190014-6

Moreover, the symposium contains a number of papers of principal importance to the further development of meteorology as a science. These papers are exemplified by Laykhtman's article "Certain non-stationary problems of heat conductivity theory in dynamic meteorology", Yudin's "Certain problems of the theory of meteorological fields"; Shifrin's "On the theory of light dispersion in the atmosphere" and other works.

Papers dealing with new climatological ideas are exemplified by the articles of Budyko "Climatic factors of the external physico-geographical process"; Drozdov's "On certain field features of meteorological elements".

The works of Kalitin, Sapozhnikovoy, and Rakipovoy contain interesting data on radiation, earth surface layer of atmosphere, and upper atmospheric layers.

Other papers published in this symposium deal with special questions of meteorological investigations and are of considerable interest. Content of papers in the jubilee symposium indicates the advanced level of theoretical, methodological, and experimental work performed by the Main Geophysical Observatory.

In approaching its centennial anniversary the Main Geophysical Observatory has compiled an impressive record of solid accomplishment by a collective of scientific and scientific-technical workers, and has made its contribution to the task of building communism in our country.



Declassified in Part - Sanitized Copy Approved for Release 2012/03/12 : CIA-RDP82-00039R000100190014-6

Declassified in Part - Sanitized Copy Approved for Release 2012/03/12 : CIA-RDP82-00039R000100190014-6

# INVESTIGATION OF EFFECTIVENESS OF THE BASIC METHODS OF COMBATING FROSTS

M. E. Berlyand and P. N. Krasikov

1. In the USSR great attention has always been devoted to the wide development of valuable warm climate agricultural crops. During the period of soviet power the area of gardens and berry orchards has increased many times.

Successes of soviet agricultural engineering permit the northward movement of such warm climate crops as citrus, grape, etc. It is known that in 1949 in Ukraine, Moldavia, Krasnodav Kray, Crimea, and Dagestan 400,000 citrus trees were planted, and in 1950 it is planned to plant no less than one million.

In the near future every kolkhoz will have its own garden.

According to the historical director of TsK VKP (b) and the Council of Ministers USSR on the creation of field-conserving zones, only in the RSFSR is it necessary to plant fruit and berry crops over an area in excess of half a million hectares. Of decisive importance is the preservation of southern climate plant life in the colder conditions of the northern regions.

In connection with this problem a great role is played by the development of frost-resistant Michurin types of crops. But even to these crops occasional frosts of great intensity can present a real danger.



Declassified in Part - Sanitized Copy Approved for Release 2012/03/12 : CIA-RDP82-00039R000100190014-6

Declassified in Part - Sanitized Copy Approved for Release 2012/03/12 : CIA-RDP82-00039R000100190014-6

What is more, frosts can and do cause great damage to other less frost-resistant crops. Many instances are known when, due to one or several spring or autumn frost nights, the yields of many plantations are sharply decreased or altogether lost. Therefore, the old problem of developing effective plant frost counter measures becomes even more acute.

For each growing plant, at some phase of its growth, there exists a certain critical temperature below which the plant is damaged by frost or altogether destroyed [1]. Climatological analysis of repeated observations of spring and autumn frosts made by I. A. Gol'tsberg [2] indicates that the probability of their onset, as a rule, is greater as the intensity of frosts decreases. Therefore it turns out that the probability of the temperature falling below the critical value by 1 degree is considerably greater than that of a 2 or 3 degree drop, and is much greater than the probability of a 4 or 5 degree drop.

Hence the important conclusion to be drawn is that quite frequently during dangerous frosts it is sufficient to find a method of raising the temperature by only 1 or 2 degrees, in order to save the plant from damage or destruction. From literature on the subject it is known that with methods employed to combat frosts in some instances such temperature increases or even greater ones are possible. At the same time published works on the subject until recently indicate that the effectiveness of the various methods of plant frost protection has been investigated inadequately, nothing being known as to the conditions required for achieving the necessary thermal effect, and nothing being known as to which of the respective methods could be appropriately utilized.



Declassified in Part - Sanitized Copy Approved for Release 2012/03/12 : CIA-RDP82-00039R000100190014-6

Declassified in Part - Sanitized Copy Approved for Release 2012/03/12 : CIA-RDP82-00039R000100190014-6

As a result no answers were given to a number of important practical questions. In particular, there were established no norms of use of protective measures at different meteorological conditions.

Of special practical interest are the mass methods of combating frost designed for plant protection over large areas.

Such basic mass methods are the creation of smoke screens by utilizing various chemical mixtures, burning of smoke-producing trash and direct heating by burners.

Beginning in 1946 the Main Geophysical Observatory has conducted investigations of effectiveness of the basic methods of combating frost.

Initially ~~these~~ physico-meteorological and climatological foundations, underlying the application of the above-stated methods of combating frost, were developed in order to establish the effectiveness of such methods and create grounds for their rationalization.

This work was conducted in accordance with the following plan: studies were made of a method of plant frost protection by means of smudge pots, which have been used in recent years by sovkhozes and kolkhozes; determination was made of the thermal effect of the smoking method (burning of smoke heaps); determination was made of effectiveness of direct heating of plants with burners. Along with this there was performed theoretical analysis of the heating effect, and laboratory investigation was made of the protective properties of the various smokes. Besides, a method was developed to improve frost forecasting, and in this connection, a theoretical investigation was made of the problem of time-temperature variation of the surface air layer. Great



Declassified in Part - Sanitized Copy Approved for Release 2012/03/12 : CIA-RDP82-00039R000100190014-6

Declassified in Part - Sanitized Copy Approved for Release 2012/03/12 : CIA-RDP82-00039R000100190014-6

attention was devoted to the climatological assessments of the danger of frosts in various climatic zones of USSR, and basic frost-combating methods were classified geographically by regions. Abbreviated contents of papers treating these problems are given below. (No results of climatological investigation are given herein; they are given in works of I. A. Gol'tsberg.)

2. During the last several decades chemically created smoke screens have been employed in combating frost. To investigate the effectiveness of this method, a large number of field experiments were conducted in the USSR as well as abroad. However, results of these experiments turned out to be highly contradictory. Comparison and analysis of these experiments becomes quite complicated, and, in the majority of cases, is impossible, since the literature dealing with these investigations does not furnish in detail the most important characteristics of the experiments. Thus, there is frequently a lack of data on meteorological conditions during the experiment, or of data on the discharge of smoke mixtures, and at times neither record is given. As a result of this, thermal effectiveness of smoke screens has been given entirely inadequate study.

Occasional norms of smoke mixture discharge recommended in practice were identical in different meteorological conditions. Therefore, our problem was, before all else, to determine the thermal effect of smoke screens in relation to meteorological conditions and the discharge of smoke-producing substances. For this purpose field and laboratory tests were conducted of the special smudge pots used in our sovkhozes and kolkhozes; these produce dense white smoke [3]. (Hereafter they shall be known as white smudge pots.)



Declassified in Part - Sanitized Copy Approved for Release 2012/03/12 : CIA-RDP82-00039R000100190014-6

Declassified in Part - Sanitized Copy Approved for Release 2012/03/12 : CIA-RDP82-00039R000100190014-6

During field experiments the temperature and effective radiation over the smoke-filled and smoke-free regions were recorded. Also observations were made on smoke concentration, wind velocity, humidity of the air, and other meteorological factors. The resultant thermal effect was compared with the fixed discharge of white smudge pots.

Laboratory experiments permitted the accumulation of supplementary data on the composition of the dispersing phase of the smoke, weight concentration of smoke, combustion heat of the smoke mixture and the ratio of the weight of produced smoke to the weight of the smoke mixture. (This last relationship hereinafter will be known as the smoke production efficiency coefficient - DKPI.)

Obtained data was subjected to theoretical analysis. It was established that the thermal effect during the burning of white smudge pots is determined by the following 3 factors:

1. Decrease of effective soil surface radiation within the smoke screen;

2. Diffusion of heat liberated during the burning of smoke mixture;

3. Condensation of water vapor on hygroscopic smoke particles.

To clarify the role of the first factor, that is, to determine the component of thermal effect connected with the variation of long-wave smoke radiation, there was studied a system of differential equations of thermal air and soil conductivity, considering radiant heat transfer in smoke-charged air [4].



Declassified in Part - Sanitized Copy Approved for Release 2012/03/12 : CIA-RDP82-00039R000100190014-6

Declassified in Part - Sanitized Copy Approved for Release 2012/03/12 : CIA-RDP82-00039R000100190014-6

In solving this problem the method of comparison of temperature and effective radiation of the smoke-charged and smoke-free regions was employed. Solution of this problem was obtained by two methods: first there was employed the approximate method of Fourier series, using 24 hours for the time interval, and then there was found the exact solution by means of the Fourier integral and operational methods. These methods yielded results that agreed closely.

Obtained formulas permit the determination of the decrease in effective radiation and its attendant component of the thermal effect depending on wind velocity, discharge of smoke-producing substances, duration of smoking, etc.

The second factor connected with the liberated heat during the combustion of the smoke mixture, was studied on the basis of similarity between atmospheric diffusion of heat and smoke. It was shown [4] that the accompanying rise in temperature is equal, to the accuracy of factor $\frac{1}{c_p \rho}$, to the product of weight concentration of smoke and the ratio of the heat of combustion of the smoke mixture to DKPI. This permits, on the basis of laboratory experiments and measured concentration, the determination of the second component of the thermal effect of the smoke screen.

The third component of thermal effect, determined by the liberated heat of water vapor condensation, takes place only when the smoke contains a hygroscopic substance and smoking takes place at high relative air humidity. Condensation can take place on condition that the water vapor tension in air exceeds the vapor tension of the saturated solution of the substance constituting the dispersion phase of the smoke. Then, knowing the composition of the latter and the humidity of the air



Declassified in Part - Sanitized Copy Approved for Release 2012/03/12 : CIA-RDP82-00039R000100190014-6

Declassified in Part - Sanitized Copy Approved for Release 2012/03/12 : CIA-RDP82-00039R000100190014-6

and assuming phase equilibrium of the smoke, it is possible to determine the quantity of condensed water per unit volume of smoke by using the method described in [5].

Since by weight the dispersion phase of smoke constitutes a negligible fraction of the dispersion medium, which is air, the heat of condensation is used only for the heating of air, whence it is easy to determine the rise of air temperature [6].

On the basis of the above field experimental data of white smudge pots, and application of the above-mentioned computational scheme of the respective components of the thermal effect, it became possible to establish data on normal discharges of smudge pots. Thus, for wind velocity of 1 meter per second at a height of 2 meters and relative humidity in the neighborhood of 90 percent, to effect a 1 degree rise in temperature it is necessary to burn simultaneously 50 smudge pots for one hectare.

With this, components of the thermal effect arising from the above factors turned out to be approximately equal to each other. For humidities less than 80 percent the third component, relating to the condensation of water vapor, can be regarded as equal to zero, since the experiment indicated that no condensation on smoke particles takes place at such humidities. It should be noted that for low air humidities, due to the lack of condensed water on smoke particles, there also takes place a decrease in the absorption capacity of the smoke screen relative to the long wave radiation.

Essentially, thermal effect depends on the wind velocity. Thus, for calm winds (about 0.3 meters per second) and the above-indicated discharge of 50 smudge pots burned simultaneously over an



Declassified in Part - Sanitized Copy Approved for Release 2012/03/12 : CIA-RDP82-00039R000100190014-6

Declassified in Part - Sanitized Copy Approved for Release 2012/03/12 : CIA-RDP82-00039R000100190014-6

area of one hectare, the thermal effect would amount to about 2.5 degrees. When the wind velocity exceeds 2 meters per second, the thermal effect is reduced considerably and for above conditions amounts to less than 0.5 degree.

3. The suggested analysis of components of the thermal effect of smoke screen can be used to study the method of smoking by means of smudge fires. The method of smudge fires combustion is one of the most widespread mass methods used to combat frosts and has been used extensively during several centuries. However, the question of effectiveness of smudge fires has been scarcely investigated.

In order to study this method we have conducted field and laboratory experiments with smudge fires [3]. These experiments indicated that the value of DKPI for smudge fires is one tenth that of the white smudge pots, but that the quantity of heat liberated per unit of combustible smoke-producing mixture is about 2 or 3 times the quantity of heat obtained from the white smudge pots.

As a result of the above-suggested analysis and comparison with experimental data, it is possible to come to the conclusion that the thermal effect of smudge fires is practically determined solely by the heat of combustion. The latter in turn is noticeably dependent on the moisture content of the combustion materials and relative air humidity. For low relative air humidities it is not expedient to moisten the material burned, as is often done, since in this case part of the heat is expended wastefully on evaporation.

When burning 50 100-kilogram smudge heaps over an area of one hectare, (each heap designed to burn for 8 hours) with wind velocity



Declassified in Part - Sanitized Copy Approved for Release 2012/03/12 : CIA-RDP82-00039R000100190014-6

Declassified in Part - Sanitized Copy Approved for Release 2012/03/12 : CIA-RDP82-00039R000100190014-6

of 1 meter per second, the thermal effect amounts to approximately 0.5 degrees. If the number of smudge heaps is increased to 100 per hectare, the thermal effect, under identical conditions, will be in the neighborhood of one degree.

4. Along with the employment of smoke screens and smudge fires, one of the basic methods of combating frost is that of heating plants directly. In practice direct heating of plants is effected by the combustion of various solid fuels, as well as of solid and liquid fuel in special burners.

In USSR direct heating of plants by oil burners was begun in 1930 to protect Caucasian citrus crops. At the same time experimental studies began to determine the effectiveness of this method. The first supervisor of these studies at the Sochi experimental station was J. T. Selyaninov [7]. Afterwards the most important studies were conducted at the All Union Scientific Research Institute of Humid Subtropical Regions (VNIIVS) with the collaboration of J. B. Nadaraya, V. S. Lavriychuk, V. P. Nikiforov, and others [8]. Works of the VNIIVS and the Sochi Experimental Station represent a great forward step in the investigation of effectiveness of oil burners. V. P. Nikiforov had constructed new burners which excelled U.S.-made burners.

On 25 April 1940 a directive was issued by the TsK VKP (b) and SNK USSR, in which was mentioned the necessity of employing direct heating of citrus plantations located in highly frost-susceptible locations, and there was also established an area of direct heating utilization within the Georgian SSR for the winter of 1944 - 45 amounting to 3000 hectares. The war and absence of frosts in recent



Declassified in Part - Sanitized Copy Approved for Release 2012/03/12 : CIA-RDP82-00039R000100190014-6

Declassified in Part - Sanitized Copy Approved for Release 2012/03/12 : CIA-RDP82-00039R000100190014-6

years in our subtropical regions have postponed the universal usage of burners in actual practice. During recent years attention devoted to the problem of direct heating as a means of protecting plants from frosts was unfortunately decreased.

Without stopping to review the work of VNIIVS and the Sochi experimental station, we can observe that, to a considerable degree, it is incomplete. This is primarily connected with the meteorological aspect of the problem. No investigation was made of the problem of heat distribution from the burners over the surface layer of the atmosphere. The lack of a developed theory of this phenomenon made it difficult to generalize the obtained empirical data. The first stage of our work in connection with this problem was to fill in these gaps of knowledge.

Since Nikiforov's burners proved superior to all other existing ones, they were the basic ones used in our investigation.

There are two types of Nikiforov's burners: the so-called wide and narrow pipe burners.

Both types consist of a conical tank to hold the oil, and a cylindrical pipe. The tank is 0.5 meters high and the pipe is 1.5 meters high. For average combustion tempo the wide pipe burner uses 1.75 kilograms of oil per hour, with the narrow pipe using 1.2 kilograms per hour [9].

Initially the approximate thermal balance of Nikiforov's burner was studied, that is, there was determined the relationship between the heat given up by burner walls by convection, radiation and the heat of heated gas emitted by the burner. Then the theo-



Declassified in Part - Sanitized Copy Approved for Release 2012/03/12 : CIA-RDP82-00039R000100190014-6

Declassified in Part - Sanitized Copy Approved for Release 2012/03/12 : CIA-RDP82-00039R000100190014-6

retical temperature field in the vicinity of the burner was determined. To determine this temperature field the equation of turbulent thermo-conductivity was solved, assuming that the heat source can be represented as a thin vertical cylinder.

Since during frosts burners operate over considerable periods of time, the problem is of stationary nature.

The equation of turbulent thermo-conductivity in stable conditions, accounting for heat lost in the ground, can be represented as:

$$u\frac{\partial \tau}{\partial x} = \frac{\partial}{\partial y}k_y\frac{\partial \tau}{\partial y} + \frac{\partial}{\partial z}k_z\frac{\partial \tau}{\partial z},$$

$$\Delta\theta = 0.$$

Here the X - axis is oriented in the direction of average wind; Y - axis across the wind direction; Z - axis is vertically upward; $\tau$ - temperature difference of air over heated and non-heated regions; $\theta$ - corresponding temperature difference for the ground; $\Delta$ - laplacian; U - wind velocity; $K_y$, $K_3$ - horizontal and vertical components of the turbulent transfer coefficient.

In the first equation there is omitted a term corresponding to the diffusion of heat along the X - axis, since, in the presence of wind, it can be neglected.



Declassified in Part - Sanitized Copy Approved for Release 2012/03/12 : CIA-RDP82-00039R000100190014-6

Declassified in Part - Sanitized Copy Approved for Release 2012/03/12 : CIA-RDP82-00039R000100190014-6

The boundary conditions are as follows: at the ground surface $Z = 0$:

$$\tau = \theta; \quad C_p \rho k_z \frac{\partial \tau}{\partial z} = \lambda \frac{\partial \theta}{\partial z} .$$

When $X = 0$:

$$C_p \rho \tau = \frac{Q}{d(H - h_1)u}, \text{ for } h_1 \leqslant z \leqslant H \text{ and } |y| = d;$$

$$\tau = 0, \ \theta = 0, \text{ for other } z \text{ and } y.$$

At an infinitely great distance from the burner:

$$\tau, \theta = 0.$$

Here the following nomenclature is introduced: $C_p$ and $\rho$ -- specific heat and density of the air; $\lambda$ -- thermal coefficient of the soil; Q -- quantity of heat produced by burning fuel per unit of time; H -- effective height of the above-mentioned cylindrical heat source, which is usually greater than the height of the burner; d -- diameter of the burner; $h_1$ -- height of the oil tank, which usually remains cold.

Complete solution of these equations is very complicated, therefore the investigation proceeded in an indirect manner. Two extreme cases were considered. In the first case it was assumed that the ground heat loss is small, that is, that the thermal conductivity of the ground is zero; in the second case, it was assumed, to the contrary, that the



Declassified in Part - Sanitized Copy Approved for Release 2012/03/12 : CIA-RDP82-00039R000100190014-6

Declassified in Part - Sanitized Copy Approved for Release 2012/03/12 : CIA-RDP82-00039R000100190014-6

thermal conductivity of the earth is infinite. It was taken, in general, that

$$u = u_1 z^n \text{ and } k_z = k_1 z^m.$$

In regard to the horizontal component of the turbulent transfer coefficient $K_y$, it was assumed to be proportional to the velocity of the wind, that is,

$$k_y = k_0 u = k_0 u_1 z^n.$$

It was also considered that the diameter of the burner is considerably smaller than the distances x, for which thermal effect was to be determined.

Using the method of separation of variables it is possible to obtain the final solution for the above-mentioned two extreme cases. A study of these solutions indicates that for the x and z values which are of interest to us, these two solutions approach each other.

This means, that to a first approximation, we do not have to consider the ground heat loss. Limiting ourselves to one of the obtained solutions, we get a formula of practical applicability for the description of the temperature field about one burner.

The temperature field for a system of burners is obtained through superposition of the temperature fields of the respective burners. Thus, if there obtains the so-called square arrangement of burners (distance between rows is the same as the distance between the adjacent burners in one row, this distance being equal to a) then



Declassified in Part - Sanitized Copy Approved for Release 2012/03/12 : CIA-RDP82-00039R000100190014-6

Declassified in Part - Sanitized Copy Approved for Release 2012/03/12 : CIA-RDP82-00039R000100190014-6

it turns out that the thermal effect of a system of burners can be expressed by the following formula, which takes into account the effect of meteorological factors:

$$\Delta T = \frac{QI\left(\frac{a}{2}\right)}{0.6 C_p \rho (H-h_1) k_1 a^2}\left[\Phi\left(\sqrt{\frac{a}{2k_0}}\right) + \frac{I\left(\frac{3a}{2}\right)}{3I\left(\frac{a}{2}\right)}\Phi\left(\sqrt{\frac{a}{6k_0}}\right) + \right.$$

$$\left. + \frac{I\left(\frac{5a}{2}\right)}{5I\left(\frac{a}{2}\right)}\Phi\left(\sqrt{\frac{a}{10k_0}}\right) + \frac{I\left(\frac{7a}{2}\right)}{7I\left(\frac{a}{2}\right)}\Phi\left(\sqrt{\frac{a}{14k_0}}\right)\right].$$

Here

$$I(x) = \int_{h_1}^{H} e^{\frac{z^{1.2}+z^{1.2}}{1.44\frac{k_1}{u_1}x}} I_0\left[\frac{(z\xi)^{0.6}}{0.72\frac{k_1}{u_1}x}\right] d\xi$$

Where $\Phi$ - is the Crump's function; $I_0$ - is the Bessel's function.

In deriving this formula, for the vertical component $k_z$ it was assumed that $m = 1$, that is, linear increase with height, and wind velocity $n = 1/5$.

Approximate value of H was obtained on the basis of analysis of the thermal balance of a burner.

By the obtained formula it is possible to compute the thermal effect of direct heating depending on the density of burners in the plantation, fuel expenditure, height above the ground, and wind velocity. A rectangular burner arrangement was also studied, where the distance between rows in the direction of the wind is twice that the distance between rows perpendicular to the wind. Computations showed that in this case the thermal effect was equal to that of the square arrangement.



Declassified in Part - Sanitized Copy Approved for Release 2012/03/12 : CIA-RDP82-00039R000100190014-6

Declassified in Part - Sanitized Copy Approved for Release 2012/03/12 : CIA-RDP82-00039R000100190014-6

As a result of these derived formulas a number of tables were compiled for determining the thermal effect; these will be published in a separate article.

To give an example: for the wide pipe type of Nikiforov's burner system, for the average combustion tempo, density of 500 burners per one hectare, and wind velocity of 1 meter per second, the thermal effect amounted to 4 - 4.5 degrees. These values agree with the experimental data [9]. Under identical conditions, with oil expenditure at 1 kilogram per burner per hour, or 500 kilograms per hectare per hour, the thermal effect is equal to 2.5 degrees.

5. Up to this point we have studied problems pertaining to the effectiveness of mass methods that are being used to combat frosts. Results of this study permit us also to point out ways and means of rationalizing measures used to protect plant life from frost. In the first place this relates to means of increasing the effectiveness of the smoke methods.

So far as we know, during the introduction of the white smudge pots no studies were made that would establish this smoke as the most effective type for combating frosts. The choice of this smoke was to a certain degree accidental. Therefore, we have investigated a number of neutral smokes harmless to plants, in order to pick out those smokes having the greatest capacity to absorb long wave radiation, as well as the capacity to liberate the maximum amount of heat.

Correspondingly, laboratory experiments were conducted in a chamber (fog chamber of GGO) having a volume of 110 cubic meters.

The bottom of the chamber (about 12 square meters in area) was ice-cooled to zero degrees, while the rest of the chamber remained at



Declassified in Part - Sanitized Copy Approved for Release 2012/03/12 : CIA-RDP82-00039R000100190014-6

Declassified in Part - Sanitized Copy Approved for Release 2012/03/12 : CIA-RDP82-00039R000100190014-6

a temperature of 15 - 20 degrees. Thus, artifical conditions were established under which radiant heat transfer would be similar to that taking place during frosts.

At a height of 4 meters in the middle of the chamber a Moll-Yanishevskiy actinometer and a Savinov pyrgeometer were set up and directed toward the bottom of the chamber.

In these chambers, the white pot smoke, smoke of ammonium chloride, black smoke, smoke of organic mixtures (smoke heaps) and orange smoke were studied.

Methodology of the experiments consisted in determining the radiant heat transfer between the actinometer and pyrgeometer receivers and the bottom of the chamber both prior to and during the generation of smoke.

Simultaneously, smoke concentration was measured by sucking the smoke through glass filters; temperature distribution and air humidity were recorded.

These laboratory experiments established that of the five smokes tested, the greatest absorption capacity is possessed by the black smoke. From supplementary experiments it was also found that during the generation of this smoke the amount of heat liberated per unit mass is 5 times that of the white smudge pots.

For the white smoke and the smoke of organic material, the absorption capacities were approximately equal to those assumed during our previous field experiments.

Moreover, on the basis of the obtained values of smoke concentrations in the chamber and the weight of the combustible mass,



Declassified in Part - Sanitized Copy Approved for Release 2012/03/12 : CIA-RDP82-00039R000100190014-6

Declassified in Part - Sanitized Copy Approved for Release 2012/03/12 : CIA-RDP82-00039R000100190014-6

the DKPI were determined for the tested smokes.

For the black and white smokes the DKPI turned out to be equal, while for the organic material smoke, as in previous experiments with smoke heaps, it was found that DKPI is one tenth that of the DKPI of white smoke.

6. Since the laboratory experiments indicated the great effectiveness of the black smoke, in August 1948 field experiments were conducted using this smoke.

Methodology of these experiments was the same as that employed in our previous experiments with the white smudge pots and smoke heaps. Smoke sources were placed over an open level area, on a line perpendicular to wind direction.

Meteorological observations were conducted at two locations: one within the smoke area; the other control point was without the smoke area. Within the smoke area air temperatures at different heights were recorded and the effective radiation of the ground was measured. At the control point, in addition to the temperature and effective radiation, observations were made of the wind, air humidity, and other factors. The thermal effect of the smoke screen was determined according to the average difference between the air temperatures at both observation points during the time of smoke generation, taking into account the microclimatic peculiarities based on observations prior to the beginning of smoking.

In an analogous manner the decrease of effective radiation was established.



Declassified in Part - Sanitized Copy Approved for Release 2012/03/12 : CIA-RDP82-00039R000100190014-6

Declassified in Part - Sanitized Copy Approved for Release 2012/03/12 : CIA-RDP82-00039R000100190014-6

the DKPI were determined for the tested smokes.

For the black and white smokes the DKPI turned out to be equal, while for the organic material smoke, as in previous experiments with smoke heaps, it was found that DKPI is one tenth that of the DKPI of white smoke.

6. Since the laboratory experiments indicated the great effectiveness of the black smoke, in August 1948 field experiments were conducted using this smoke.

Methodology of these experiments was the same as that employed in our previous experiments with the white smudge pots and smoke heaps. Smoke sources were placed over an open level area, on a line perpendicular to wind direction.

Meteorological observations were conducted at two locations: one within the smoke area; the other control point was without the smoke area. Within the smoke area air temperatures at different heights were recorded and the effective radiation of the ground was measured. At the control point, in addition to the temperature and effective radiation, observations were made of the wind, air humidity, and other factors. The thermal effect of the smoke screen was determined according to the average difference between the air temperatures at both observation points during the time of smoke generation, taking into account the microclimatic peculiarities based on observations prior to the beginning of smoking.

In an analogous manner the decrease of effective radiation was established.



Declassified in Part - Sanitized Copy Approved for Release 2012/03/12 : CIA-RDP82-00039R000100190014-6

Declassified in Part - Sanitized Copy Approved for Release 2012/03/12 : CIA-RDP82-00039R000100190014-6

Observations were analyzed to determine respective components of the thermal effect that are connected with the basic factors, as was done in previous experiments.

Laboratory analysis indicated that the dispersion phase of smoke is barely hygroscopic, therefore we can neglect the component determined by the liberated heat of water vapor condensation.

Using the results of laboratory and field experiments with black smoke and based upon the above described theoretical scheme, it is possible to make an approximate computation which allows a comparison between thermal effects of white and black smokes. Thus, with the discharge of black smoke mixture corresponding to simultaneous combustion of 50 white smudge pots over one hectare, with wind velocity one meter per second, thermal effect will amount to about 2 degrees, while under the same conditions the white smoke thermal effect is only 1 degree. This indicates the high effectiveness of black smoke, which hitherto was not used in combating frost.

There is sufficient evidence to state that black smoke is harmless to plant life. Its usage may result in some dirt contamination of fruits, and, therefore, it is preferable to use black smoke in combating spring frosts.

The practical acceptance of black smoke requires the study of supplementary technical problems connected with refining the composition of the smoke mixture, perfecting the method of combustion, and others.

It is of interest to compare the above cited thermal effect values of black and white smoke with the thermal effect of burners. Simultaneous combustion of 50 smudge pots corresponds to the discharge



Declassified in Part - Sanitized Copy Approved for Release 2012/03/12 : CIA-RDP82-00039R000100190014-6

Declassified in Part - Sanitized Copy Approved for Release 2012/03/12 : CIA-RDP82-00039R000100190014-6

of 500 kilograms of smoke mixture per one hectare per hour. With this, for wind velocity of one meter per second, the thermal effect for white smoke is one degree, and that for black smoke is two degrees. With direct heating, for a wind velocity of one meter per second, density of 500 burners per hectare and hourly oil consumption of one kilogram per burner (500 kilograms of oil per hectare per hour), the thermal effect obtained was 2.5 degrees.

7. As a result of generalization of the theoretical scheme devised for the computation of thermal effect due to smoking, a solution was obtained of a more general problem relating to temperature variation in the air layer at the earth's surface [10]. A particular form of this solution answers a number of significant questions concerning transformation of air masses, temperature forecasting in the air layer at the earth's surface and frost prognosis, as well as determination of thermal effect of smoke screens, connected with the decrease of effective radiation. All of these questions have this in common, namely, that their mathematical formulation reduces to a process of solving a system of differential equations of thermal conductivity in air and ground at different initial and boundary conditions. Solution of these equations was carried out by the operational method, and basic computations, using the obtained formulas, were made for the problem of temperature variation at night, which is necessary in frost prognosis. Questions of frost prognosis are also raised by us, because it seems to us that the existing methods have a number of serious drawbacks, which we attempted to remedy to a certain extent.

8. Summarizing the results of the investigative work conducted by the GGO into the basic methods of combating frost, we can note the following principal results:



Declassified in Part - Sanitized Copy Approved for Release 2012/03/12 : CIA-RDP82-00039R000100190014-6

Declassified in Part - Sanitized Copy Approved for Release 2012/03/12 : CIA-RDP82-00039R000100190014-6

1. The physical bases of plant-life frost protection by means of smoke screens, smoke heaps, and oil burners were investigated.

2. The effectiveness of these methods under various meteorological conditions were established.

3. On the basis of the theoretical and experimental data expenditure norms of the protective substances were suggested.

4. The possibility was determined of employing a newer, more effective method of smoke production by use of black smoke.

Obtained results allow the inference of a number of significant points in connection with perfecting and increasing the effectiveness of the basic methods of combating frosts. Elaboration of these points and their experimental verification constitute the object of further work.



Declassified in Part - Sanitized Copy Approved for Release 2012/03/12 : CIA-RDP82-00039R000100190014-6

Declassified in Part - Sanitized Copy Approved for Release 2012/03/12 : CIA-RDP82-00039R000100190014-6

# VISIBILITY RANGE OF REAL OBJECTS

N. G. Boldyrev

1. The basic factor affecting the visibility of real objects is regarded to be the transparency of the atmosphere. The admittance coefficient of an atmospheric layer having a thickness l is equal to:

$$T = e^{-\alpha l} \qquad (1)$$

where the coefficient $\alpha$ characterizes the properties of the air mass and is known as the decay coefficient. We shall study the case of object observation along directions approaching horizontal and will base ourselves on the light-atmospheric equation of haze brightness Vd, determined by the dispersion of light in an atmospheric layer of thickness l:

$$Vd = B\,(1 - e^{-\alpha l}). \qquad (2)$$

Coefficient of the light-atmospheric formula B is approximately equal to sky brightness in the azimuth of the observed object. When the atmosphere is turbid to such an extent that the coefficient of atmospheric admittance becomes equal to T = 0.05, haze brightness approaches 95 percent of the sky brightness B. Such haze is so intense, that many observed objects will become hardly visible, and others almost indistinguishable. The layer thickness l corresponding to T = 0.05 can be computed by means of formula (1) and assumed equal to the meteorological range of visibility S. Thus, for l = S we have T = 0.05. Therefore,

$$S = -\frac{\ln 0.05}{\alpha} = \frac{3}{\alpha}. \qquad (3)$$



Declassified in Part - Sanitized Copy Approved for Release 2012/03/12 : CIA-RDP82-00039R000100190014-6

Declassified in Part - Sanitized Copy Approved for Release 2012/03/12 : CIA-RDP82-00039R000100190014-6

Instead of the number 3 in the numerator of the right side of formula (3) previously there were used coefficients 3.91 [1] and even 4.2 [2]. However, as was shown by the experiments of O. D. Bartenevoy, the number used in formula (3) is more probable. The choice of this number will be rationalized further along in this work.

From formula (2) it follows that haze brightness increases with the increase of the air layer thickness, at first very rapidly and then more and more slowly. For an infinitely thick air layer ($l = \infty$) haze brightness becomes equal to the coefficient of the light-atmospheric formula B, which is the greatest possible value of haze brightness. Haze brightness reaches 50 percent of its greatest value (Table I) for $\alpha l = 0.69$, which takes place at $l = 0.23S$, as follows from formula (3). Thus, already for the air layer thickness equal to 1/4 of the meteorological visibility range, air haze brightness becomes greater than half of its greatest possible value. We won't be making a serious error (it could not exceed 30 percent), if we assume that brightness of cloudless sky constitutes 70 percent of the coefficient of the light-atmospheric formula. This haze brightness will be achieved for the layer thickness $l = 0.4S$. Sky brightness is therefore determined by light dispersion in the air volume surrounding the observer, and bounded along the horizon by a circle the radius of which constitutes about 40 percent of the meteorological visibility range. This "sky radius" is generally not too large, especially with considerable atmospheric turbidity. For the convenience of computation of the coefficient of atmospheric ~~permeability~~ transparency and the air haze brightness, we give Table I of natural logarithms of numbers from 0.01 to 0.99. If the values of this table are divided by 3, we get a



Declassified in Part - Sanitized Copy Approved for Release 2012/03/12 : CIA-RDP82-00039R000100190014-6

Declassified in Part - Sanitized Copy Approved for Release 2012/03/12 : CIA-RDP82-00039R000100190014-6

relationship between the thickness of air layer l and the meteorological visibility range S, corresponding to transparency or permeation T and haze brightness B (1-T).

TABLE I

Natural logs, $-\ln T = \alpha l$

| T | 00 | 01 | 02 | 03 | 04 | 05 | 06 | 07 | 08 | 09 |
|---|---|---|---|---|---|---|---|---|---|---|
| 0.0 | -- | 4.61 | 3.91 | 3.51 | 3.22 | 3.00 | 2.81 | 2.66 | 2.53 | 2.41 |
| 0.1 | 2.30 | 2.20 | 2.12 | 2.04 | 1.97 | 1.90 | 1.83 | 1.77 | 1.72 | 1.66 |
| 0.2 | 1.61 | 1.56 | 1.51 | 1.47 | 1.43 | 1.39 | 1.35 | 1.31 | 1.27 | 1.24 |
| 0.3 | 1.20 | 1.17 | 1.14 | 1.11 | 1.08 | 1.05 | 1.02 | 0.99 | 0.97 | 0.94 |
| 0.4 | 0.92 | 0.89 | 0.87 | 0.84 | 0.82 | 0.80 | 0.78 | 0.76 | 0.73 | 0.71 |
| 0.5 | 0.69 | 0.67 | 0.65 | 0.63 | 0.62 | 0.60 | 0.58 | 0.56 | 0.54 | 0.53 |
| 0.6 | 0.51 | 0.49 | 0.48 | 0.46 | 0.45 | 0.43 | 0.42 | 0.40 | 0.39 | 0.37 |
| 0.7 | 0.356 | 0.342 | 0.328 | 0.315 | 0.301 | 0.288 | 0.274 | 0.262 | 0.249 | 0.236 |
| 0.8 | 0.223 | 0.211 | 0.198 | 0.186 | 0.174 | 0.162 | 0.151 | 0.139 | 0.128 | 0.117 |
| 0.9 | 0.105 | 0.094 | 0.083 | 0.073 | 0.062 | 0.051 | 0.041 | 0.030 | 0.020 | 0.010 |

2. The possibility of distinguishing a given object depends materially on the contrast between the brightness of the object and background against which the object is viewed. By brightness contrast we mean the ratio of the difference between object and background brightnesses to the greatest of these two brightnesses. This difference is taken as positive; smaller brightness is subtracted from the larger one.

In view of absorption and dispersion of light by the atmosphere, brightness contrast decreases rapidly with the increase in distance between the object and the observer. At some critical distance the eye will



Declassified in Part - Sanitized Copy Approved for Release 2012/03/12 : CIA-RDP82-00039R000100190014-6

Declassified in Part - Sanitized Copy Approved for Release 2012/03/12 : CIA-RDP82-00039R000100190014-6

not perceive the small brightness contrast, and the observed object will become indistinguishable. This distance is called the visibility range of a real object, which, obviously, depends on the properties of the object and does not coincide with the meteorological visibility range. Meteorological visibility range determines only the transparency of the atmosphere and is connected with the properties of the air mass.

We denote by $K_0$ the contrast between the object and the background measured when it is such a small distance away from the object that we can neglect the brightness of air haze between the observer and the object. Distances less than 1/20 or even 1/10 of the meteorological visibility range, can in practice be used for measurement of contrast $K_0$. Theoretically, of course, it is considered that contrast $K_0$ is measured at the distance $l = 0$ from the object. From formulas (1) and (2) it is easy to derive a basic equation of the law of variation of contrast K with distance $l$:

$$K = \frac{K_0}{1 + \frac{1}{b}(e^{-\alpha l} - 1)} \qquad (4)$$

where the coefficient of lightness b is equal to the ratio of the larger brightness (background or the object) and the coefficient of the light-atmospheric formula B. If in equation (4) we let $l = 0$, we get $K = K_0$, as it should be. For perfectly transparent atmosphere $\alpha = 0$, $K = K_0$ regardless of the distance l at which the object is viewed. In the general case $\alpha \neq 0$ and $l \neq 0$, and we have equation (4).

The coefficient B of the light-atmospheric formula will, in the future, be regarded as equal to sky brightness in the azimuth of the



Declassified in Part - Sanitized Copy Approved for Release 2012/03/12 : CIA-RDP82-00039R000100190014-6

Declassified in Part - Sanitized Copy Approved for Release 2012/03/12 : CIA-RDP82-00039R000100190014-6

object. For cloudless sky, and also in overcast weather, with the sky uniformly cloudy, the error will be small. However, in sunshine, if there is a dark cloud in the vicinity of the object, the brightness of which is taken as B, then the coefficient of lightness is exaggerated. Correspondingly, if the cloud is light, the coefficient of lightness will be underestimated. In the first case the visibility range of an object determined on the basis of formula (4) will be greater than the actual one; in the second instance it will be less than the actual one, which should be kept in mind.

If the object is observed against the sky background, the coefficient of lightness becomes unity and formula (4) simplifies to:

$$K = K_0 e^{-\alpha l} \qquad (5)$$

Formula (5) is usually employed for visual determination of meteorological visibility range according to observations of objects silhouetted against the sky background. As much as possible, the objects selected should be dark, whose sky contrast $K_0$ is close to unity.

3. If the contrast K is measured by one or the other method, then $\alpha$ can be determined from equation (5):

$$\alpha = \frac{\ln K_0 - \ln K}{l}$$

and the meteorological visibility range:

$$S = \frac{3l}{\ln K_0 - \ln K}$$

Since real objects are not perfectly black, $K_0 < 1$. Correction $\ln K_0$, in the majority of cases, is of material importance, and should be made.



Declassified in Part - Sanitized Copy Approved for Release 2012/03/12 : CIA-RDP82-00039R000100190014-6

Declassified in Part - Sanitized Copy Approved for Release 2012/03/12 : CIA-RDP82-00039R000100190014-6

Assume for example, that an object is observed at a distance $\ell = 4$ kilometers and K = 0.8. Computations are made using Table I.

To contrast K = 0.45 there corresponds the number 0.8

Contrast K = 0.8 yields the correction — 0.22

We get $\alpha \ell = 0.58$

$\frac{\ell}{S} \quad \frac{1}{3} \alpha \ell = 0.19$

Meteorological visibility range $S = \frac{4}{0.19} \approx 20$ kilometers.

If the correction is not made of the object brightness (considering $K_0 = 1$) we would get $\frac{\ell}{S} = 0.27$ and S = 15 kilometers.

Contrast can be measured by means of a telephotometer, Sharonov's diaphanoscope - - all photometric methods, or, less precisely by means of type DM-7 smokemeter - - extinguishing method. Construction of the smokemeter permits weakening the contrast of the object, viewed through its optical system, M times. The value of M is determined by means of the calibration curve of the instrument according to a regular computation. During measurements two series of observations are taken. One series is taken during the washout (loss of visibility) of the object of contrast K, with the determination of $\bar{M}_\ni$ as the average of n observations, which yields various values of M. The other series yields the average value $M_\ni$ at the washout of standard contrast $K_\ni$, which is known to the observer. We assume that n observations are also made in the second series, which results in the individual values $M_\ni$.

The smokemeter theory yields the following basic equation:

$$KM = K_\ni M_\ni$$



Declassified in Part - Sanitized Copy Approved for Release 2012/03/12 : CIA-RDP82-00039R000100190014-6

Declassified in Part - Sanitized Copy Approved for Release 2012/03/12 : CIA-RDP82-00039R000100190014-6

which is free of systematic error. The random error is given by the formula:

$$S = \sqrt{\frac{K_3^2 \sum (M_3 - \bar{M}_3)^2 + K^2 \sum (M - \bar{M})^2}{n(n-1)}}$$

To an accuracy of 0.99 we can say that:

$$-tS < MK - M_3 K_3 < +tS$$

where the number t should be taken, depending on the number of observations n in each series, from the following table:

| n = | 3 | 4 | 5 | 6 | 7 | 8 | 9 | 10 |
|---|---|---|---|---|---|---|---|---|
| t = | 4.6 | 3.7 | 3.4 | 3.2 | 3.1 | 3.0 | 2.9 | 2.9 |

Photometric observations are processed by the methods usually used in ordinary light measurements.

Measurements by means of Sharonov's diaphanoscope, in view of the step-like scale, can yield only one result. The measuring error can be considered as not exceeding 20 percent of the measured contrast.

4. If the observer does not have measuring instruments, he still can make a visual estimate of the meteorological visibility range. For this purpose it is necessary to use objects of large angular dimensions silhouetted against the sky background, the objects being preferably dark. Therefore, such observations should be avoided when the sun is behind the observer, since in such circumstances objects are strongly illuminated, and their sky contrast $K_0$ cannot be reliably determined. Relatively light objects can also be used, if they are far enough away



Declassified in Part - Sanitized Copy Approved for Release 2012/03/12 : CIA-RDP82-00039R000100190014-6

Declassified in Part - Sanitized Copy Approved for Release 2012/03/12 : CIA-RDP82-00039R000100190014-6

from the observer. A necessary requirement is the perception of haze on the object. If the haze is hardly noticeable, then the meteorological visibility range is at least 10 times the distance of the object. Therefore, if all the objects accessible to observation, even when positioned against the light, are visible clearly and distinctly, and the haze is not perceptible or hardly noticeable, then the meteorological visibility range is 10 times the distance to the remotest object. For visual estimate of the range of visibility it is necessary to view carefully all the objects which are accessible to observation and estimate for each of those objects the effect of the atmospheric haze by one of the points of the scale given below.

OBJECT VISIBILITY SCALE

1. Object is hardly distinguishable, discerned with difficulty, and easily lost from view.

2. Object is seen as a silhouette differing little in brightness and color from the sky. Visibility of the object is considerably impaired and regarded as poor by the observer.

3. While the object is covered by an intense haze, according to its brightness it is obviously darker than the sky.

4. Object can be seen well, but is covered by considerable haze, which is clearly perceived by the observer. A dark object has become considerably lighter, while a light object has noticeably changed its usual color.

5. Atmospheric haze is altogether absent or hardly noticeable.



Declassified in Part - Sanitized Copy Approved for Release 2012/03/12 : CIA-RDP82-00039R000100190014-6

Declassified in Part - Sanitized Copy Approved for Release 2012/03/12 : CIA-RDP82-00039R000100190014-6

TABLE III

| OBJECT | K | —ln K | Correction |
|---|---|---|---|
| | OVERCAST WEATHER | | |
| Coniferous forest | 0.85 | 0.16 | —0.05 |
| Leafy forest in summer | 0.75 | 0.29 | —0.10 |
| Dark buildings | 0.65 | 0.43 | —0.15 |
| Light hills | 0.55 | 0.60 | —0.20 |
| Openwork towers (triangulation towers, etc.) | 0.50 | 0.69 | —0.25 |
| | SUN IN FRONT OF THE OBSERVER (OBSERVATION AGAINST LIGHT) | | |
| Openwork towers | 0.50 | 0.69 | —0.25 |
| White towers | 0.80 | 0.22 | —0.05 |
| All other objects | 1.00 | 0.00 | —0.00 |
| | SIDEWISE SOLAR ILLUMINATION | | |
| Coniferous forest | 0.75 | 0.29 | —0.10 |
| Leafy forest in summer | 0.55 | 0.60 | —0.20 |
| Hills | 0.45 | 0.80 | —0.25 |
| Openwork towers | 0.50 | 0.69 | —0.25 |
| | DIRECT SOLAR ILLUMINATION (SUN BEHIND THE OBSERVER) | | |
| Coniferous forest | 0.70 | 0.36 | —0.15 |
| Openwork towers | 0.50 | 0.69 | —0.25 |



Declassified in Part - Sanitized Copy Approved for Release 2012/03/12 : CIA-RDP82-00039R000100190014-6

Declassified in Part - Sanitized Copy Approved for Release 2012/03/12 : CIA-RDP82-00039R000100190014-6

We shall study an example using the above-described methodology. Assume that the observer estimated the visibility of a hill located at a distance S = 15 kilometers by the number 3 of degree of haze intensity (Table II) for overcast weather.

From Table II we get $\frac{l}{S} = 0.4$, and from Table III we get the correction - 0.2. With this correction we have $\frac{l}{S} = 0.4 - 0.2 = 0.20$. The meterological visibility range is equal to $S = \frac{15}{0.2} = 75$ kilometers.

6. Small objects are less visible than large ones, and the coefficient in formula (3) has the numerical value of $-\ln 0.05 = 3$ only for objects seen over a wide angle of vision. The least contrast still perceptible by the eye depends on the angular dimensions of the object.

For objects viewed over a wide angle, it can be considered that the object will be distinguishable if the contrast exceeds 0.05 (5 percent). As the angle of vision decreases there is an increase in the least perceptible contrast.

Angular dimensions should be determined as follows. If there is known to the observer the visible silhouette area of the object Q, defined as a plane area bounded by ~~conforms~~ contours of the object with all perspective contractions, by denoting l as the distance to the object, we obtain the angle of vision $\gamma$ according to the formula:

$$\gamma = 3.438 \sqrt{\frac{Q}{l}}, \qquad (5')$$

where the angle $\gamma$ is in minutes, Q - - in square meters and l - - in kilometers.

Table IV gives the relationship between the least perceptible



Declassified in Part - Sanitized Copy Approved for Release 2012/03/12 : CIA-RDP82-00039R000100190014-6

Declassified in Part - Sanitized Copy Approved for Release 2012/03/12 : CIA-RDP82-00039R000100190014-6

contrast K and angle $\gamma$ for two cases: greater distinguishing probability (appearance of the object) and small distinguishing probability (loss of object visibility).



Declassified in Part - Sanitized Copy Approved for Release 2012/03/12 : CIA-RDP82-00039R000100190014-6

Declassified in Part - Sanitized Copy Approved for Release 2012/03/12 : CIA-RDP82-00039R000100190014-6

TABLE IV

| Angle $\gamma$ | Discernment object | | Loss of visibility | | Angle $\gamma$ | Discernment object | | Loss of visibility | |
|---|---|---|---|---|---|---|---|---|---|
| | K | -lnK | K | -lnK | | K | -ln K | K | -lnK |
| 1 | 1.00 | 0.00 | 0.67 | 0.40 | 18 | 0.074 | 2.60 | 0.038 | 3.26 |
| 2 | 0.55 | 0.61 | 0.35 | 1.05 | 20 | 0.073 | 2.61 | 0.036 | 3.31 |
| 3 | 0.35 | 1.06 | 0.21 | 1.55 | 25 | 0.072 | 2.63 | 0.034 | 3.37 |
| 4 | 0.24 | 1.44 | 0.14 | 1.95 | 30 | 0.071 | 2.64 | 0.033 | 3.42 |
| 5 | 0.16 | 1.71 | 0.11 | 2.24 | 40 | 0.070 | 2.66 | 0.031 | 3.47 |
| 6 | 0.15 | 1.91 | 0.090 | 2.41 | 60° | 0.068 | 2.69 | 0.030 | 3.50 |
| 7 | 0.13 | 2.06 | 0.077 | 2.56 | 2° | 0.062 | 2.78 | 0.027 | 3.61 |
| 8 | 0.11 | 2.18 | 0.067 | 2.70 | 3 | 0.057 | 2.86 | 0.024 | 3.73 |
| 9 | 0.10 | 2.28 | 0.058 | 2.84 | 4 | 0.054 | 2.91 | 0.022 | 3.81 |
| 10 | 0.093 | 2.37 | 0.050 | 2.98 | 5 | 0.051 | 2.97 | 0.021 | 3.86 |
| 12 | 0.086 | 2.45 | 0.047 | 3.06 | 6 | 0.050 | 2.99 | 0.020 | 3.89 |
| 14 | 0.080 | 2.52 | 0.044 | 3.13 | 7 | 0.050 | 3.00 | 0.020 | 3.91 |
| 16 | 0.076 | 2.57 | 0.041 | 3.20 | | | | | |

Declassified in Part - Sanitized Copy Approved for Release 2012/03/12 : CIA-RDP82-00039R000100190014-6

Declassified in Part - Sanitized Copy Approved for Release 2012/03/12 : CIA-RDP82-00039R000100190014-6

Let us take an example. For overcast weather at a distance $l = 5$ kilometers a dark structure with dimensions $Q = 2.5 \cdot 7 =$ 17.5 square meters is observed silhouetted against the sky background. This outline is visible over an angle of:

$$\gamma = \frac{3.438\sqrt{17.5}}{5} \approx 3'.$$

From Table IV we get the corresponding value of contrast: for discernment $-\ln K = 1.06$; for loss of visibility $-\ln K = 1.55$.

By introducing the contrast correction from Table III we get, for the first instance $\alpha l = 1.06 - 0.43 = 0.63$; and for the second instance $\alpha l = 1.55 - 0.43 = 1.12$. Since $l = 5$ for the discernment of the object (the outline is visible), it can be expected that the coefficient of extinction $\alpha < 0.13$. If the structure is invisible, then it is probable that $\alpha > \frac{1.12}{5} = 0.22$. Correspondingly, discernment of the structure for a meteorological visibility range of $S > 24$ kilometers is highly probable. For the meteorological visibility range of $S < 13$ kilometers, discernment of the object should be considered as improbable.

This example can be looked upon from another viewpoint. The observer, having noticed that the structure is hardly visible will estimate the range of visibility as 24 kilometers. However, if the observer possesses exceedingly keen eyesight, then, on comparison of the visibility of distant objects with the visibility of the structure, he might obtain for the meteorological visibility range the value of 17 kilometers. In this case the observer's eyesight would be characterized by the numbers of Table IV in the loss of visibility column. For the meteorological range visibility the observer will use the formula:

$$S = \frac{3.91}{q}$$



Declassified in Part - Sanitized Copy Approved for Release 2012/03/12 : CIA-RDP82-00039R000100190014-6

Declassified in Part - Sanitized Copy Approved for Release 2012/03/12 : CIA-RDP82-00039R000100190014-6

As was previously assumed, the structure is located at the threshold of visibility:

$$l = \frac{1.55}{2}$$

The distance to the object $l$ is 5 kilometers, whence it follows that $S = 17$ kilometers.

Summarizing all of the above, it can be stated that the threshold of visibility in the above instance is reached for the meteorological visibility range equal to approximately 20 kilometers.

The above example indicates the way of utilizing small objects capable of observation, for the visual estimate of the visibility range. Table IV gives the coefficient $A = -\ln K$ in the visibility range formula:

$$S = \frac{A}{\alpha} \qquad (6)$$

for objects of different angular dimensions. If the object is not perfectly black, its contrast should be considered, which can be made on the basis of Table III. Table IV, therefore, yields the correction for the angular size of the object. If there are no large size objects at the observer's disposal, he can determine the meteorological visibility range of objects, by introducing the necessary corrections for their size.

7. Now we can study the visibility range of an arbitrary object against any background. The range of visibility depends on geophoto-



Declassified in Part - Sanitized Copy Approved for Release 2012/03/12 : CIA-RDP82-00039R000100190014-6

Declassified in Part - Sanitized Copy Approved for Release 2012/03/12 : CIA-RDP82-00039R000100190014-6

tometric as well as upon physiological factors. The observer's vision can be adequately characterized by two numbers: threshold of contrast sensitivity $\varepsilon$, determined for the case of a very large object, and the least angle of resolution $\delta$, which is equal to the angle over which there is yet visible a very small perfectly black object on a white background. Instead of the relationship given in Table IV, we can take the analytical dependence:

$$(K-\varepsilon)\,\gamma^2 = \delta^2,$$

where K is the least perceptible contrast for an observed object of angular size $\gamma$. This formula does not fully correspond to the data of Table IV; however, it is sufficiently accurate for practical purposes. Introducing into this formula the area of the object Q and distance to the object L, we get:

$$(K-\varepsilon)\,\frac{Q}{L^2} = a \qquad (7)$$

where $a = 0.085\,\delta^2$.

Contrast K is related to distance through formula (4):

$$K = \frac{K_0}{1+\frac{1}{b}\left(e^{-\alpha L}-1\right)}, \qquad (4')$$

where $\alpha$ is determined through the formula (6) of the meteorological visibility range:

$$S = \frac{A}{\alpha}. \qquad (6')$$

If there are known the meteorological visibility range S, coefficients of lightness b, contrast between the object and background $K_0$, and the area Q of the object, then the system of equations (7), (4), and (6) can be solved for L, which is the visibility range of a real object.



Declassified in Part - Sanitized Copy Approved for Release 2012/03/12 : CIA-RDP82-00039R000100190014-6

Declassified in Part - Sanitized Copy Approved for Release 2012/03/12 : CIA-RDP82-00039R000100190014-6

We introduce the following quantities:

Relative contrast - $\frac{K}{\varepsilon}$ ;

Relative visibility range - $\frac{L}{S}$;

Relative object size - $\frac{1.18 \varepsilon Q}{\delta^2 S^2}$

Relative contrast $K/\varepsilon$

b - background lightness

$\frac{\varepsilon Q}{AS^2}$ relative object size

Figure 1. Nomograph of the daytime visibility range with a sliding indicator.

Relative visibility range:



Declassified in Part - Sanitized Copy Approved for Release 2012/03/12 : CIA-RDP82-00039R000100190014-6

Declassified in Part - Sanitized Copy Approved for Release 2012/03/12 : CIA-RDP82-00039R000100190014-6

$$а)\ \frac{K}{\varepsilon} = \left[1 + \frac{aL^2}{\varepsilon Q}\right]\left[1 + \frac{1}{b}\left(20^{\frac{L}{S}} - 1\right)\right]$$

$$б)\ \frac{K}{\varepsilon} = \left[1 + \frac{aL^2}{\varepsilon Q}\right]\left[1 + \frac{1}{b}\left(50^{\frac{L}{S}} - 1\right)\right].$$

The system of equations (7), (4), and (6) can be transformed into one equation

$$\frac{K_0}{\varepsilon} = \left[1 + \frac{\delta^2 S^2}{11.8\varepsilon Q}\left(\frac{L}{S}\right)^2\right]\left\{1 + \frac{1}{b}\left[\left(e^A\right)^{\frac{L}{S}} - 1\right]\right\}$$

which can be nomographed. To construct the nomograph we set

$$X = 2\lg\frac{L}{S};\quad a = \lg\frac{11.8Q}{\delta^2 S^2};$$

$$Y = \lg\left(e^{A\frac{L}{S}} - 1\right);\quad \beta = \lg b;$$

$$\frac{K_0}{\varepsilon} = (1 + 10^{X'})(1 + 10^{Y'}), \qquad (8)$$



Declassified in Part - Sanitized Copy Approved for Release 2012/03/12 : CIA-RDP82-00039R000100190014-6

Declassified in Part - Sanitized Copy Approved for Release 2012/03/12 : CIA-RDP82-00039R000100190014-6

$$X' = X - \alpha;$$
$$Y' = Y - \beta. \qquad (9)$$

We construct a family of curves defined by equation (8) for various values of the parameter $K/\varepsilon$ - the relative contrast. On a separate drawing we draw the curve:

$$X = 2 \lg \frac{L}{S},$$
$$Y = \lg \left( A_e \frac{L}{S} - 1 \right) \qquad (10)$$

and upon this curve we designate points corresponding to the different values of the parameter $\frac{L}{S}$. This second drawing must be overlaid upon the first drawing in such a way that the origin of coordinates (X, Y) coincides with the point $(-\alpha, -\beta)$ of the first drawing, wherein by means of coordinates (X', Y') the family of curves is constructed (8). From equations (9) it follows that in order to find $\frac{L}{S}$ we must find the point of intersection of the moveable curve (10) with one of the curves of the (8) family, to which there corresponds the required value of $\frac{K}{\varepsilon}$.

The nomograph is shown in Figure 1. A sliding triangular shaped indicator with a curvilinear hypotenuse must be cut out and overlaid



Declassified in Part - Sanitized Copy Approved for Release 2012/03/12 : CIA-RDP82-00039R000100190014-6

Declassified in Part - Sanitized Copy Approved for Release 2012/03/12 : CIA-RDP82-00039R000100190014-6

upon the remainder of the drawing, having a grid and a family of curves drawn upon it. The arrow index of the sliding indicator must be placed at the point of the grid determined by the coordinates "relative size of the object" and "background lightness". In overlaying, care must be taken to see that the straight edges of the indicator are parallel to the coordinate lines of the stationary drawing. Inscriptions "relative visibility range" and "relative object size" must be placed below. Let us choose a curve on the stationary drawing which corresponds to the required value of the relative contrast and note its point of intersection with the curve of the sliding indicator. This value is read off on the curvilinear scale of the sliding indicator, wherein there is given the relative visibility range $\frac{L}{S}$.

Let us examine now the solution of the reverse problem -- determination of the meteorological visibility range from known distances of discernment or disappearance of the object. For this purpose we utilize the straight-edge scale of the sliding indicator. In this case the indicator arrow must be displaced over a distance corresponding to the tenfold increase of the relative size of the object. Therefore, having determined the relative object size, we multiply it by 10 and, upon overlaying the sliding indicator, we read the answer on the straight-edge scale of the indicator. Multiplication by 10 is necessitated only by the graphical displacement of the straight-edge scale, in order to prevent it intersecting the curvilinear scale.

8. It remains only now to select some numerical value in order to use the nomograph. In constructing the nomograph the threshold of contrast eye sensitivity was taken to be equal to 0.02, to which there



Declassified in Part - Sanitized Copy Approved for Release 2012/03/12 : CIA-RDP82-00039R000100190014-6

Declassified in Part - Sanitized Copy Approved for Release 2012/03/12 : CIA-RDP82-00039R000100190014-6

corresponds the number A = 3.91. Actually the threshold of eye sensitivity is greater, approaching 0.05 in the conditions of the meteorological practice of visibility range determination, to which there corresponds the number A = 3.00. Therefore, the meteorological visibility range should be multiplied by a coefficient 1.3 in order to get S for the use with the nomograph. Sharonov takes A = 4.2; therefore, the meteorological visibility range, as determined by Sharonov, should be multiplied by 0.93 in order to get S for the nomograph. The relative contrast is defined as the ratio $K_o/\varepsilon$. Contrast $K_o$ should be either measured, or taken from a table. In Table V are given contrast values measured by Bartenev. In using Sharonov's method in the determination of the discernibility Ch and the weather coefficient W is employed the identity:

$$\frac{K_o}{\varepsilon} = \frac{Ch}{W} + 1.$$

The least angle of resolution $\delta$ depends on the individual characteristics of the observer's vision and conditions of observation. Acuity of vision $1/\delta$ on the average can be taken as equal to 1.5 ($\delta$ = 0.67 minutes) going up to 2 ($\delta$ = 0.5 minutes) for specially selected observers. For unfavorable conditions of observation $\delta$ = one minute.



Declassified in Part - Sanitized Copy Approved for Release 2012/03/12 : CIA-RDP82-00039R000100190014-6

Declassified in Part - Sanitized Copy Approved for Release 2012/03/12 : CIA-RDP82-00039R000100190014-6

TABLE V

CONTRASTS OF SOME OBJECTS

| Background | Object | Contrast |
|---|---|---|
| Meadow | Tree | 0.15 |
| | Shadow of a tree | 0.8 |
| | Persons in dark attire | 0.15 |
| | Grayish colored settlement | 0.1 |
| | Dirt road | 0.3 |
| | Pole | 0.2 |
| | Shadow of a pole | 0.8 |
| Forest | White building | 0.9 |
| | Brick building | 0.35 |
| | Gray pole | 0.20 |

VISUAL ESTIMATE

| | |
|---|---|
| Strong contrast | 0.7-1.0 |
| Average contrast | 0.6-0.4 |
| Weak contrast | 0.3-0.2 |
| Very weak contrast | 0.2-0.1 |

Taking $\varepsilon = 0.05$, $\delta = 0.67$ minutes, we get the following formula for determinating the relative size of the object.

The relative size of the object is equal to $1.33 \frac{Q}{S^2} = 0.087\ Q\alpha^2$, since in this formula, as stated above,



Declassified in Part - Sanitized Copy Approved for Release 2012/03/12 : CIA-RDP82-00039R000100190014-6

Declassified in Part - Sanitized Copy Approved for Release 2012/03/12 : CIA-RDP82-00039R000100190014-6

$$S = \frac{3.91}{\alpha}$$

Visibility range L is obtained as a fraction of S, the relative visibility range being equal to:

$$\frac{L}{S} = 0.256\alpha L.$$

Coefficients of lightness for typical cases are given in Table VI.

TABLE VI

Coefficients of lightness - b

| Background | Overcast weather | Sun behind the observer | Sun to one side of the observer | Sun in front of the observer |
|---|---|---|---|---|
| Sky | 1.0 | 1.0 | 1.0 | 1.0 |
| Sand | 0.4 | 1.0 | 0.8 | 0.2 |
| Meadow | 0.25 | 0.5 | 0.4 | 0.1 |
| Foliate forest | 0.15 | 0.25 | 0.1 | 0.015 |
| Coniferous forest | 0.1 | 0.2 | 0.05 | 0.010 |
| Extremely light object against dark background | 0.35 | 3.0 | 1.0 | 0.15 |
| Calm water | 0.8 | 0.8 | 0.8 | 0.8 |
| Water - - 1-2 point ripple | 0.5 | 0.5 | 0.5 | 0.5 |
| Water - - 3-4 point ripple | 0.35 | 0.35 | 0.35 | 0.35 |



Declassified in Part - Sanitized Copy Approved for Release 2012/03/12 : CIA-RDP82-00039R000100190014-6

Declassified in Part - Sanitized Copy Approved for Release 2012/03/12 : CIA-RDP82-00039R000100190014-6

We shall analyze an example of nomographic computation. Let it be necessary to determine the visibility range of an openwork tower having a $Q = 300$ square meters viewed against a sky background for atmospheric transparency, characterized by the coefficient of extinction $\alpha = 0.0265$. We take the threshold of contrast sensitivity $\varepsilon = 0.06$. By Table III contrast is equal $K_0 = 0.5$. The relative contrast $K/\varepsilon = 8$. The relative size $0.087\, Q\alpha^{-2} = 1.8 \cdot 10^{-2}$; against the sky background $b = 1$; from the nomograph we read $\frac{L}{S} = 0.24$. Consequently, $L = 0.24\, \frac{3.91}{\alpha} = 35$ kilometers. Actually the visibility range was determined to be 37 kilometers.

9. The nomograph has two sliding indicators. The right hand indicator is designed for the universally accepted value for the threshold of contrast sensitivity $\varepsilon = 0.02$. This indicator should be used in those cases when the meteorological visibility range is computed by the formula

$$S = \frac{3.91}{\alpha}$$

The left hand indicator is designed for the threshold of contrast sensitivity $\varepsilon = 0.05$. In this case the meteorological visibility range is equal to

$$S = \frac{3.00}{\alpha}$$

It is 30 percent less than the former one, corresponding to $\varepsilon = 0.02$.

The nomograph was constructed in 1946. In 1948 O. D. Bartenova, at the request of this author, conducted an experiment to verify the nomograph and to obtain introductory data for illustrating the methods



Declassified in Part - Sanitized Copy Approved for Release 2012/03/12 : CIA-RDP82-00039R000100190014-6

Declassified in Part - Sanitized Copy Approved for Release 2012/03/12 : CIA-RDP82-00039R000100190014-6

of nomograph application. Data on the visibility of real objects obtained by O. D. Barteneva agree with the data in the table, published by V. V. Sharonov [2].

The methodology of computation of the visibility range of real objects must be regarded as commonly known at this time. Sharonov [2] described a method of computation not using the nomograph. Subsequently Dantley [3] published nomographs for the computation of visibility ranges. Dantley does not refer to Sharonov's work. The nomograph published herein is more compact than Dantley's nomographs.



Declassified in Part - Sanitized Copy Approved for Release 2012/03/12 : CIA-RDP82-00039R000100190014-6

Declassified in Part - Sanitized Copy Approved for Release 2012/03/12 : CIA-RDP82-00039R000100190014-6

# CLIMATIC FACTORS OF THE SURFACE PHYSICO-GEOGRAPHIC PROCESS

M. I. Budyko

The external (surface) physico-geographic process represents, according to A. A. Grigor'yev (/8/ and others) a complexity of climatic, hydrological, soil, exogenous, geomorphological, and biological processes which develop in the atmosphere, hydrosphere, and upper layers of lithosphere.

Development of the surface physico-geographic process takes place under the extremely close interaction of all of the component processes ("links") whose immediate connection with each other is determined, to a considerable extent, by the constant exchange of a number of most important substances (water, nitrogen, carbon dioxide and others) taking place between the atmosphere, hydrosphere, soil, and animal matter.

The common reserve of all categories of organic and mineral substances in the developmental sphere of the surface physico-geographic process (in the entire surface physico-geographical shell), as well as the energy reserve, vary comparatively slightly within the time limits, characteristic in the development of the surface physico-geographic process.

The relatively small variability of the amount of substance in the surface physico-geographic shell is connected with the negligible (compared to the available reserves) rate of exchange of substance between the surface physico-geographic shell on one hand, and the deep



Declassified in Part - Sanitized Copy Approved for Release 2012/03/12 : CIA-RDP82-00039R000100190014-6

Declassified in Part - Sanitized Copy Approved for Release 2012/03/12 : CIA-RDP82-00039R000100190014-6

layers of lithosphere and the outer atmospheric space on the other hand. In contrast to this the reserve of energy within the surface physico-geographic shell is maintained approximately at the same level in the presence of extremely intensive exchange of energy with the outer atmospheric space, wherein the input of absorbed solar radiation is equal to the expenditure of heat energy for the earth's radiation.

The approximate constancy of the very slowly varying reserves of different categories of substances and energy within the entire physico-geographic shell as a whole is connected with the appreciable and relatively rapid variation of these reserves over local regions of the surface physico-geographic shell. Such variation, of somewhat periodic (diurnal and annual periodicity) and somewhat non-periodic nature.

The work of A. A. Grigor'yev established that the dynamics of the exchange of substance and energy within the surface physico-geographic shell is determined, first of all, by climatic factors, that is, that the climatic link is the determining one of the entire surface physico-geographic process. (Here, as elsewhere in this work is discussed the surface physico-geographic process for comparatively extensive territories, and not for separate geographic regions or landscapes.)

From this point of view, it is possible to pose the problem of finding of those climatic characteristics which determine the nature of the separate natural processes and the level of development ("intensity") of the entire surface physico-geographic process as a whole.



Declassified in Part - Sanitized Copy Approved for Release 2012/03/12 : CIA-RDP82-00039R000100190014-6

Declassified in Part - Sanitized Copy Approved for Release 2012/03/12 : CIA-RDP82-00039R000100190014-6

To solve this problem it is necessary before everything else to study the basic laws of thermal and moisture exchanges in the surface physico-geographic shell.

1. The energy of solar radiation entering the surface physico-geographic shell of the earth undergoes therein a number of complex changes and transformations, differing materially in the various geographic zones.

The most significant effect upon the development of physico-geographic processes is due to the differences of thermal balances in low and high latitudes determined by the non-uniform heating of the earth's spherical surface. Since the atmosphere and hydrosphere possess considerable horizontal thermal conductivity (circulationary and macroturbulent), the difference in the amount of absorbed radiation at different latitudes leads to the formation of considerable heat transfer in the meridional direction, which decreases the contrasts between the thermal behavior of high and low latitude locations. Besides the purely advective heat transfer, certain redistribution of heat also takes place in view of the inequality of quantities of evaporated and condensed water in the various latitudinal zones.

A general representation of the comparative roles of the respective components of thermal balance of latitudinal zones of the surface physico-geographic shell (the earth-atmosphere system) is given by our scheme [6] based on the materials of contemporary studies and partly on original data. We represent the equation of the average annual long-term thermal balance of the earth-atmosphere system in the form:



Declassified in Part - Sanitized Copy Approved for Release 2012/03/12 : CIA-RDP82-00039R000100190014-6

Declassified in Part - Sanitized Copy Approved for Release 2012/03/12 : CIA-RDP82-00039R000100190014-6

$$R_s = A + F + L(\varepsilon - r), \qquad (1)$$

where $R_s$ is the radiation balance of the earth-atmosphere system; A is the heat consumption for atmospheric advection; F is the heat consumed by the oceanic advection (redistribution of heat by ocean currents); L is the latent heat of vaporization; $\varepsilon$ is the evaporation total; r is the precipitation total. We note, that in the computation of the thermal balance of latitudinal zones we need the data on aqueous balance ($\varepsilon$ and r).

Distribution of the components of aqueous balance of latitudinal zones of the Northern hemisphere encompassing both land and oceans is given in the graph of Figure 1.

Distribution of evaporation ($\varepsilon$) for this graph was determined according to the data of M. I. L'vovich [9] (for the continents) and that of Jacobs [12] (for oceans); distribution of precipitation (r) was computed for continents according to M. I. L'vovich's data, and for oceans on the basis of Maynardus' data [14], which were appreciably corrected in order to bring them in correspondence with the existing estimates of oceanic evaporation.

The difference between precipitation and evaporation (curve f) represents the total flow-quantity of water which flows in fluid form from one latitudinal zone into another and is compensated by an equal transformation of water vapor.

The quantity of the total flow is directly proportional to the input or expenditure of heat due to the moisture cycle in a given



Declassified in Part - Sanitized Copy Approved for Release 2012/03/12 : CIA-RDP82-00039R000100190014-6

Declassified in Part - Sanitized Copy Approved for Release 2012/03/12 : CIA-RDP82-00039R000100190014-6

latitudinal zone (difference between expenditure due to evaporation and input due to condensation). Since in the near-equatorial and north of the 39th northern latitude the total flow is positive, these regions receive a definite quantity of heat due to moisture cycle (in other words, the output L ($\mathcal{E}$ - r) within them is negative). In tropical zones evaporation is noticeably greater than the precipitation total, in view of which there takes place the expenditure of heat in the moisture cycle.

In view of the equality of precipitation and evaporation totals for the entire earth, it is obvious that the moisture cycle leads only to some non-redistribution of heat, without changing the total thermal balance of the entire earth. The average latitudinal distribution of output (or input) of heat due to the moisture cycle, computed on the basis of the obtained total flow data, is shown by the curve L ($\mathcal{E}$ - r) of Figure 2.

Distribution of the radiation balance in the northern hemisphere is shown on Figure 2 by the curve $R_s$ (Simpson's data [15]); distribution of the average zonal output (or input) of heat due to ocean currents is shown by the curve F (based on Sverdrup's data [16]). Subtracting from the values of $R_s$ the sum of L ($\mathcal{E}$ - r) and F, we get the output or input of heat due to atmospheric advection, which is shown in Figure 2 by the curve A. On the basis of the above data relative to the general interrelationship of the components of thermal balance of the surface physico-geographic shell, we can divide the northern hemisphere into 4 basic latitudinal zones.

1. The near-equatorial zone, from the equator up to 10 - 15 degrees of latitude northern, where to the heat input, due to the large



Declassified in Part - Sanitized Copy Approved for Release 2012/03/12 : CIA-RDP82-00039R000100190014-6

Declassified in Part - Sanitized Copy Approved for Release 2012/03/12 : CIA-RDP82-00039R000100190014-6

positive radiation balance, is added a considerable input of heat due to moisture cycle. These sources of heat insure large output of heat for atmospheric and oceanic advections, for which the comparatively narrow near-equatorial zone represents the basic source of heat energy.

2. The tropical zone, (this zone also includes a part of the subtropical zone), which is north of the near-equatorial zone, where for a positive radiation balance, gradually decreasing toward the north, output of heat is observed for the moisture cycle, which reaches appreciable values. Over the greater portion of this zone, the output of heat for the moisture cycle approaches the value of the radiation balance, in view of which the output of heat for atmospheric advection is negligible, and there is also an inappreciable redistribution of heat by the ocean currents.

centimeters/year

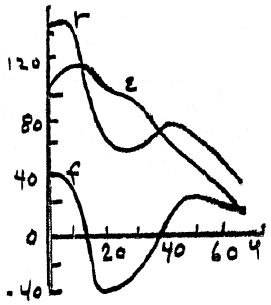


Figure 1. Aqueous balance in the northern hemisphere

large calories/cm$^2$ per year

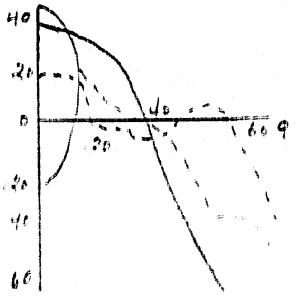


Figure 2. Thermal balance of the earth-atmosphere system (northern hemisphere)
1-$R_s$; 2-$L(\varepsilon-r)$; 3-F; 4-A.



Declassified in Part - Sanitized Copy Approved for Release 2012/03/12 : CIA-RDP82-00039R000100190014-6

Declassified in Part - Sanitized Copy Approved for Release 2012/03/12 : CIA-RDP82-00039R000100190014-6

3. Transition zone, extending several degrees north and south of the 38th north latitude, where the input and output of heat for all the components of the thermal balance are approximately balanced, that is, all the components are close to zero as averaged over a year's period.

4. The northern zone, which is north of the transition zone, where the negative radiation balance is compensated by the heat input due to atmospheric advection, moisture cycle, and, in higher latitudes, from oceanic currents.

In order to get a complete picture of the horizontal heat exchange in the entire surface physico-geographic shell, data of Figure 2 should be supplemented by the estimate of the intralatitudinal heat exchange; data thus obtained will, however, be inadequate for the analysis of the effect of climatic factors on the surface physico-geographic process.

As it was noted in our preceding work, interaction between natural processes which takes place in some form within the entire surface physico-geographic shell, is of materially different intensity at the various levels.

This circumstance is connected with certain localization of the sphere of the most intensive development of the basic natural processes. Thus, the biological link of the surface physico-geographic process is developed entirely, except for a relatively negligible portion of the biological mass, in the thin layer adjacent to the underlying surface (from several meters below to several tens of meters above the level of the underlying surface).



Declassified in Part - Sanitized Copy Approved for Release 2012/03/12 : CIA-RDP82-00039R000100190014-6

Declassified in Part - Sanitized Copy Approved for Release 2012/03/12 : CIA-RDP82-00039R000100190014-6

Analogous to this, river flow forms in the underlying surface; soil formation and the exogenous geomorphological process are actively developed in the thin upper lithospheric layer, and most actively in the immediate vicinity of the underlying surface.

centimeter/year

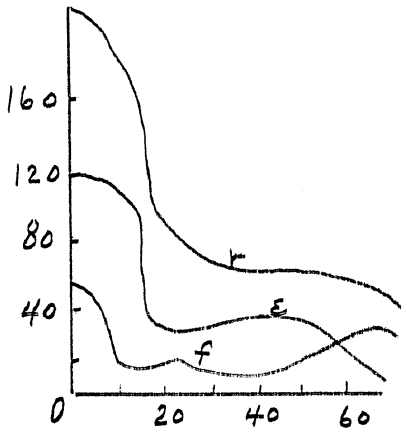


Figure 3. Aqueous balance of land (northern hemisphere)

large calories/cm$^2$ year

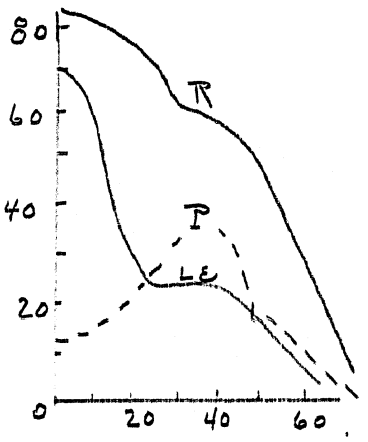


Figure 4. Thermal balance of land (northern hemisphere)

It is obvious that the intensity of interaction of all of these processes among themselves, as well as with the climatic link should be greatest in the vicinity of the level of the underlying surface.

In view of this, in order to analyze the effects of the thermal transfer and moisture cycle on the physico-geographic process, it is necessary to compile data on the thermal and aqueous balances of the underlying surface.



Declassified in Part - Sanitized Copy Approved for Release 2012/03/12 : CIA-RDP82-00039R000100190014-6

Declassified in Part - Sanitized Copy Approved for Release 2012/03/12 : CIA-RDP82-00039R000100190014-6

As is known, the thermal balance of the land surface for average annual conditions represents the equality between the radiation balance of the underlying surface and the amount of heat used up on evaporation and turbulent heat transfer. In order to determine the average latitudinal distribution of thermal balance of the land portion of the northern hemisphere, it is necessary to determine the distribution of heat used up on evaporation, which, having the aqueous balance data, can be done.

The average latitudinal aqueous balance of the land portion of the northern hemisphere is shown in Figure 3 (according to M. I. L'vovich [9]). By utilizing the data on zonal distribution of evaporation, it is possible to compute heat expenditure on evaporation (curve $L\varepsilon$ in Figure 4). Subtracting these values from the totals of the radiation balance of the underlying surface (curve R, drawn on the basis of data by T. G. Berlyand [2] and this author [6]) we get the average heat transfer distribution between the atmosphere and the underlying surface (curve P).

Comparing Figures 4 and 2, it is not difficult to establish that variations of the components of the thermal balance of land along the geographical latitude are entirely different from the variations of the components of the earth-atmosphere thermal balance. It is important, in particular, to note that the radiation balance of the underlying surface, as compared with the radiation balance of the earth-atmosphere system, does not change its sign (being positive everywhere); the other two components of the thermal balance of the underlying surface also do not change their signs.



Declassified in Part - Sanitized Copy Approved for Release 2012/03/12 : CIA-RDP82-00039R000100190014-6

Declassified in Part - Sanitized Copy Approved for Release 2012/03/12 : CIA-RDP82-00039R000100190014-6

In the distribution of the total turbulent heat output of the underlying atmospheric surface attention is drawn to the characteristic maximum in "any latitudes" between 15 and 30 degrees of north latitude, which was first found by this author and M. I. Yudin [7]. To this maximum there corresponds a weakly-pronounced minimum of heat expended for evaporation.

Figure 4 clearly shows the considerable variability of the absolute values and the mutual inter-relationships of the thermal balance components of land surface in different latitudinal zones. From the available data it can be concluded that these components also vary considerably within the limits of the same latitudinal zones (especially the quantities $L\varepsilon$ and P in connection with changes in the aqueous balance).

It is obvious that in order to study the effect of the thermal transfer and moisture cycle upon the surface physico-geographic process, it is necessary to have adequate methodology for the determination of at least two out of three basic components of thermal balance of the underlying surface. Having the aqueous balance data (precipitation and flow), we can easily determine the amount of heat expended for evaporation ($L\varepsilon$) while the determination of the other components of the thermal balance (R and P) is connected with certain difficulties.

In a number of preceding works the value of the radiation balance was computed for separate points utilizing observational data, as well as indirect methods of computation, the turbulent heat transfer being computed as the remaining term of the thermal balance equation. The value of these computations was diminished by the impossibility of direct verification of the computed quantities, which made it difficult



Declassified in Part - Sanitized Copy Approved for Release 2012/03/12 : CIA-RDP82-00039R000100190014-6

Declassified in Part - Sanitized Copy Approved for Release 2012/03/12 : CIA-RDP82-00039R000100190014-6

to assess the correctness of computational methods.

In one work [3] all the components of the thermal balance of a given land surface point were determined independently, in view of which the completion of the balance equation was achieved, thus proving the appreciable accuracy of the employed methods of computation. In the next work [4] such computation was performed not for a single point, but for considerable territory, and there, for the first time maps of the thermal balance components of the underlying land surface were constructed.

Possibility of comparatively detailed and accurate computations of the distribution of the thermal balance components of land surface clarified in works [3] and [4] created grounds for the use of the thermal balance data of underlying surface in the investigation of the effect of climatic factors upon the surface physico-geographic process. In this connection it can be stated that at present computations of thermal balance of underlying surface have been made with certain degrees of accuracy for a considerable part of the entire land surface (works of T. G. Berlyand [1], [2] and others).

Having the data on the thermal and aqueous balances of land surface, it is natural to pose this question: are the components of the thermal and aqueous balances independent qualities, or are they connected by relationships supplementary to the balance equations? In the work [5], chapter 7 it was established that the terms of the thermal and aqueous balances are connected by one supplementary relationship, which is called the connecting equation. The basis of the deviation of the connecting equation is predicated upon the following physical considerations.



Declassified in Part - Sanitized Copy Approved for Release 2012/03/12 : CIA-RDP82-00039R000100190014-6

Declassified in Part - Sanitized Copy Approved for Release 2012/03/12 : CIA-RDP82-00039R000100190014-6

Let us study the relationships between terms of the thermal and aqueous balances for two extreme cases: in very dry and hot climate, and in very moist and cold climate. In the first instance which is characterized by small precipitation totals and relatively large values of radiation balance, the soil is dry, in view of which all the moisture of precipitation is retained by molecular forces on the soil particles and is expended through evaporation without river flow formation. In view of this it can be concluded that for sufficiently large values of the $\frac{R}{Lr}$ ratio, coefficient of flow approaches zero or, what is equivalent, the value $\frac{\varepsilon}{r}$ approaches unity.

In the second case, when the radiation balance is small and precipitation is relatively large, soil is in a state of surplus moistness, the possible maximum available amount of thermal energy being used for evaporation. The value of this maximum outlay can be estimated considering the valve-like nature of the turbulent thermal exchange between the underlying surface and the atmosphere.

In a study by this author, M. I. Yudin [7] and in some other works it was determined that the turbulent thermoconductivity of the lower air layer depends considerably on the direction of the vertical turbulent heat flow. In those instances when the turbulent flow is directed from the earth toward the atmosphere, the considerably greater intensity of turbulent intermixing permits it to attain large values comparable with the basic components of the radiation and thermal balances. For a reverse turbulent flow the inverse temperature distribution considerably reduces the intensity of the transfer, in view of which the turbulent flow of heat turns out to be comparatively small.



Declassified in Part - Sanitized Copy Approved for Release 2012/03/12 : CIA-RDP82-00039R000100190014-6

Declassified in Part - Sanitized Copy Approved for Release 2012/03/12 : CIA-RDP82-00039R000100190014-6

is compensated by the radiation balance only, in view of which the upper limit of increase of the component $L\mathcal{E}$ is the quantity R.

On this basis it can be considered that for small values of the ratio $\frac{R}{Lr}$ the quantity $\frac{\mathcal{E}}{r}$ approaches $\frac{R}{Lr}$ (or that the coefficient of flow $\frac{f}{r}$ approaches unity or $\frac{R}{Lr}$).

For verification of the stated consideration on the nature of relationship between $\frac{\mathcal{E}}{r}$ and $\frac{R}{Lr}$ for small and large values of the latter parameter it is necessary to utilize various factual data.

In figure 6 the assumed dependence of $\frac{\mathcal{E}}{r}$ on $\frac{R}{Lr}$ (for small $\frac{R}{Lr}$) values is shown by the straight line OA, and for large values of $\frac{R}{Lr}$ by the straight line AB. There are also shown points which represent the average values of deviation of $\frac{\mathcal{E}}{r}$ obtained from the factual data compiled by Wundt [17] for rivers of different continents (except mountain reservoirs), with the averaging of the $\frac{\mathcal{E}}{r}$ values over certain intervals of the parameter $\frac{R}{Lr}$ (the value of R was determined from its mean latitudinal values). The experimental points indicate that actually there is observed a smooth transition in the $\frac{\mathcal{E}}{r}$, $\frac{R}{Lr}$ relationship, going from line OA to line AB, which lines, as it was assumed above, are of limiting nature.

Using the conclusion that the $\frac{R}{Lr}$ value represents the upper limit of possible evaporation from the surface of river basins, which can be considered as physical evaporability in given climatic conditions, in one work: [5], chapter 7 there were determined the functional forms of the $\frac{\mathcal{E}}{r}$, $\frac{R}{Lr}$ dependence, which generalize the known hydrological equations of Shreiber and Ol'dekop.



Declassified in Part - Sanitized Copy Approved for Release 2012/03/12 : CIA-RDP82-00039R000100190014-6

Declassified in Part - Sanitized Copy Approved for Release 2012/03/12 : CIA-RDP82-00039R000100190014-6

As a result of comparing the obtained relationships with the more accurate experimental data on precipitation, flow, evaporation, and radiation balances, it was established that the $\frac{\mathcal{E}}{r}$, $\frac{R}{Lr}$ relationship satisfies the equation:

$$\frac{\varepsilon}{r} = \sqrt{\frac{R}{Lr} th \frac{Lr}{R}\left(1 - ch\frac{R}{Lr} + sh\frac{R}{Lr}\right)} \qquad (2)$$

where th, ch, sh represent the hyperbolic tangent, cosine, and sine respectively.

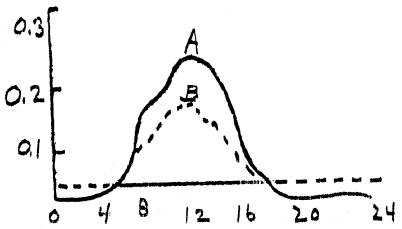


Figure 5. Diurnal variation of turbulent heat transfer during warm period of the year

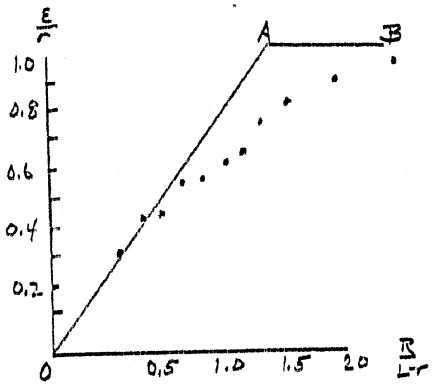


Figure 6. Relationship between the thermal and aqueous balances according to Wundt's data

Writing the equations of the thermal and aqueous balances of the underlying surface in the form:

$$\frac{R}{Lr} = \frac{\varepsilon}{r} + \frac{P}{Lr}, \qquad (3)$$



Declassified in Part - Sanitized Copy Approved for Release 2012/03/12 : CIA-RDP82-00039R000100190014-6

Declassified in Part - Sanitized Copy Approved for Release 2012/03/12 : CIA-RDP82-00039R000100190014-6

$$I = \frac{\varepsilon}{Lr} + \frac{f}{r} \qquad (4)$$

(thermal balance components are divided by Lr, and aqueous balance components are divided by r). We can state that the 4 relative values of the components of the thermal and aqueous balances are connected by 3 equations, and that, consequently, only one of these quantities is an independent variable. This conclusion has a certain value in the study of the effect of climatic factors on the surface physico-geographic process.

2. The study of the effect of climatic conditions on the surface physico-geographic process can have for its purpose the solution of 3 important problems.

The first one resolves to the establishment of quantitative connections between the climatic factors and zonality (zone boundaries) of the basic natural processes, which in future should permit the finding of a general theoretical explanation of the zonality phenomenon.

Solution of this problem is facilitated by the comparatively thorough empirical study of zonality of vegetation, topsoil, hydrological phenomena, and others.

The second problem consists in the establishment of definite connections between the climatic factors and the quantitative characteristics of the basic natural processes. Studies in this direction are surrounded with great difficulties in those fields of physical geography having inadequately developed quantitative characteristics of process intensity (biogeography). Comparatively greater possibilities for the



Declassified in Part - Sanitized Copy Approved for Release 2012/03/12 : CIA-RDP82-00039R000100190014-6

Declassified in Part - Sanitized Copy Approved for Release 2012/03/12 : CIA-RDP82-00039R000100190014-6

development of the second problem are furnished by the land hydrology having voluminous quantitative material on the river flow totals, which was repeatedly employed for the establishment of empirical connections with climatic factors.

The third problem in the study of climate effect upon the surface physico-geographic process, solution of which is connected with the solution of the second problem, consists in the analysis of the role of climatic conditions in the complex characterization of the entire physico-geographic process -- intensity of the process.

Of the available studies the basic place in the elaboration of the cited problems, especially the third one, is occupied by the known works of A. A. Grigor'yev.

In our works in this connection [4], [5] there a number of A. A. Grigor'yev's ideas were utilized; specifically, the concept of the determining effect of the thermal and moisture balances upon the development of the surface physico-geographic process was accepted.

Considering the previously cited thesis of the special role in the development of the surface physico-geographic process of climatic characteristics, relating to the underlying surface level, we assumed that the physico-geographic zonality is immediately connected with the distribution of parameters which determine the components of the thermal and aqueous balances of the underlying surface.

It was established that for the parameter determining the relative values of components of the thermal and aqueous balances we can take the ratio $\frac{R}{Lr}$ or $\frac{P}{Lr}$. (Ratios $\frac{E}{r}$ and $\frac{f}{r}$ do not determine



Declassified in Part - Sanitized Copy Approved for Release 2012/03/12 : CIA-RDP82-00039R000100190014-6

Declassified in Part - Sanitized Copy Approved for Release 2012/03/12 : CIA-RDP82-00039R000100190014-6

the first two quantities for large values of $\frac{R}{Lr}$ due to the special nature of the semi-empirical relationship [27.] The absolute values of the terms of the equation systems (2), (3), (4) are determined by the combinations of two parameters, such as R and $\frac{R}{Lr}$.

For comparison of geographic distribution of these parameters with the boundaries of the physico-geographic zones it is necessary to have sufficiently accurate data on the radiation balance of the underlying surface. In moderate latitudes (except for mountain regions) is basically of latitudinal distribution and can be approximately expressed by a single average latitudinal dependence.

As a result of appropriate computations it was established that the radiation balance of land surface

Utilizing data by means of precipitation maps on the mean latitudinal distribution of radiation balance for the European territory of USSR, Western Siberia and Central Asia, we found the $\frac{R}{Lr}$ values for these regions. In Figure 7, 4 isolines corresponding to the following values of $\frac{R}{Lr}$ are shown: 1) 0.35; 2) 1.1; 3)2.3; 4) 3.4. These isolines can be compared with the boundaries of the tundra, forest, steppe, semidesert, and desert shown in Figure 8.

By comparing the maps of Figures 7 and 8, one can become easily convinced that the discrepancy between the isolines of parameter $\frac{R}{Lr}$ and the boundaries of the geobotanical zones is comparatively small and depends basically on the degree of accuracy in determining the beginning parameters -- precipitation and the radiation balance. It can be noted that the valley structure of the basic portion of the studied territory is important to the derived agreement, since an accurate account of the vertical zonality, employing the mean latitudinal values of radiation balance, is obviously impossible.



Declassified in Part - Sanitized Copy Approved for Release 2012/03/12 : CIA-RDP82-00039R000100190014-6

Declassified in Part - Sanitized Copy Approved for Release 2012/03/12 : CIA-RDP82-00039R000100190014-6

A somewhat less accurate, but still satisfactory agreement between the isolines of $\frac{R}{Lr}$ and the geobotanical zones was found for the North American territory, although the available radiation balance and precipitation data for this continent were of comparatively low accuracy. It is interesting to note the correct reflection in this computation of the extreme southward displacement of tundra on Newfoundland (up to the 48th northern latitude).

Figure 7. Isolines of the parameter $\frac{R}{Lr}$ (cross-hatched areas depict high mountain regions.)

At the same time attention is directed to some displacement of the tundra-forest boundary toward the north as compared with actuality; this discrepancy can be explained to a considerable degree by the obviously underestimated precipitation totals for these regions taken from the available maps (/11/ and others) due to the lowered estimate of the totals of solid precipitation. As a result of appropriate correction of the precipitation data, agreement between estimated and actual location of the geobotanical zones can be considerably improved.

Performed computations indicate that the distribution of the basic geobotanical zones generally corresponds to the distribution of the parameter $\frac{R}{Lr}$, which determines the relative values of the components of the thermal and aqueous balances. It is obvious that within the boundaries of the same zones there are observed materially different values of the radiation balance of the underlying surface ("energy basis" of the surface physico-geographic process), which leads to differences in the intensity levels of the surface physico-geographic



Declassified in Part - Sanitized Copy Approved for Release 2012/03/12 : CIA-RDP82-00039R000100190014-6

Declassified in Part - Sanitized Copy Approved for Release 2012/03/12 : CIA-RDP82-00039R000100190014-6

process. In order to characterize zonal regions with different "energy bases" it is necessary to employ two parameters, which determine the absolute values of the components of the thermal and aqueous balances. For this purpose, it is convenient for a number of reasons to select the quantities R and $\frac{R}{Lr}$.

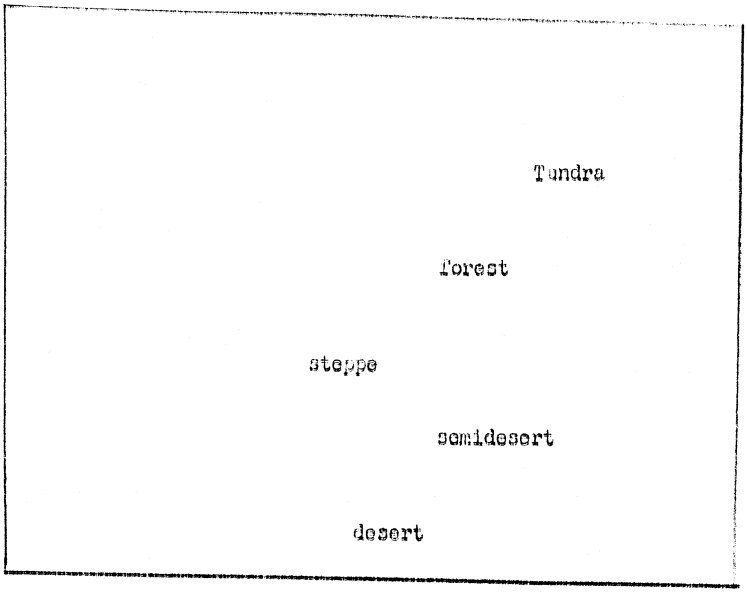


Figure 8. Boundaries of the basic geobotanical zones. (crosshatched areas depict high mountain regions.)

Connection of the geobotanical zonality with the parameters R and $\frac{R}{Lr}$ can be portrayed in general as a graph, with R and $\frac{R}{Lr}$ along the corresponding axes, the basic geobotanical boundaries being shown by vertical and horizontal lines. A schematic form of such a graph is shown in Figure 9. In view of the inaccuracy of the available data on radiation balance in the tropical and equatorial regions, location of the corresponding geobotanical zones is approximate and is subject to further elucidation.



Declassified in Part - Sanitized Copy Approved for Release 2012/03/12 : CIA-RDP82-00039R000100190014-6

Declassified in Part - Sanitized Copy Approved for Release 2012/03/12 : CIA-RDP82-00039R000100190014-6

The solid line in Figure 9 bounds the region of actual values of R and $\frac{R}{Lr}$ (except for mountain regions), within the limits of which definite values of the $\frac{R}{Lr}$ parameter (vertical lines) define the basic geobotanical zones: tundra, forest, steppe, semidesert, and desert. Large variations in the values of the forest zone radiation balance and somewhat smaller changes in the steppe zone are due to noticeable geobotanical variations within the boundaries of these zones, with the unchanged nature of the plant life. (From the special features of the graph in Figure 9, we can note the inclusion, according to the characteristic values of R and $\frac{R}{Lr}$, of moist savannas in the forest region instead of the steppe region; this is generally in agreement with the presence of forest plant life in such savannas.)

Since the zonality of soils is closely connected with the zonality of plant life conclusions reached relative to the connection of plant life zones with definite values of parameters R and $\frac{R}{Lr}$ apply as well to the soil zones. Corresponding to this it is possible to establish that as the parameter $\frac{R}{Lr}$ increases the soil types also change in the following order: (a) tundra soils; (b) podzols, brown forest soils, yellow ochers, red soils, and laterite soils (the variety of soil types in this group is connected with wide variations of the R parameter); (c) black earths and black soils of savannas; (d) chestnut soils; and (e) gray soils. Dependence of soil zonality on the climatic parameters $\frac{R}{Lr}$ and R can be expressed in the general form of a graph similar to that of the plant life zone graph of Figure 9.



Declassified in Part - Sanitized Copy Approved for Release 2012/03/12 : CIA-RDP82-00039R000100190014-6

Declassified in Part - Sanitized Copy Approved for Release 2012/03/12 : CIA-RDP82-00039R000100190014-6

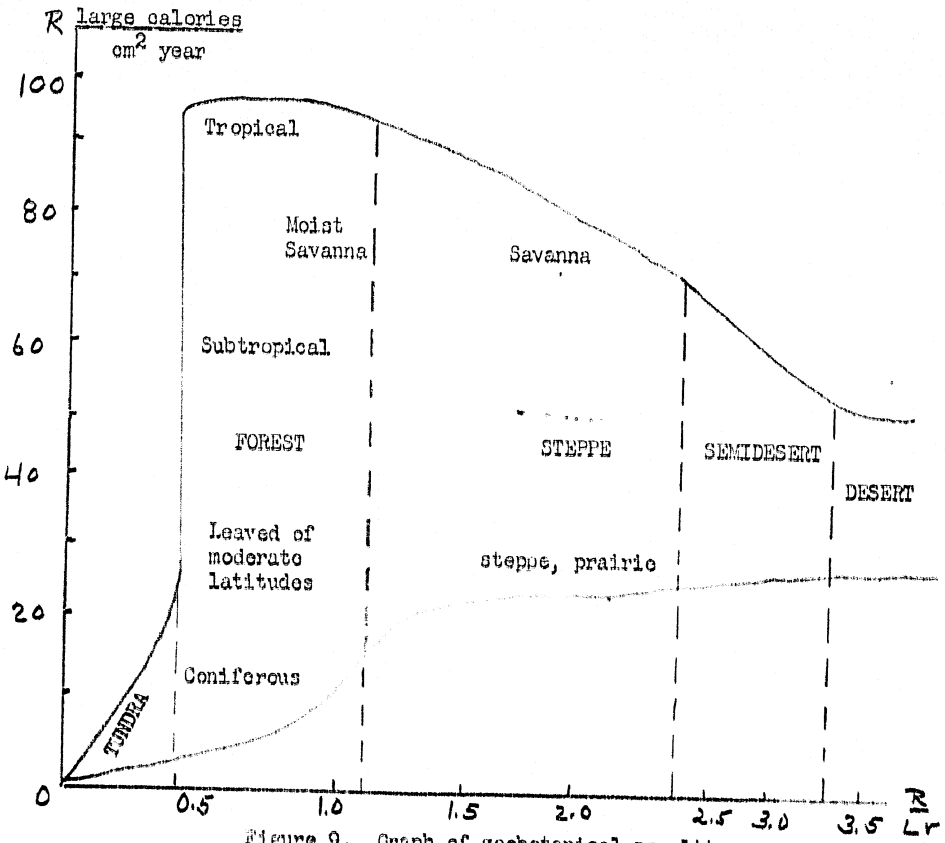


Figure 9. Graph of geobotanical zonality.

Connection between the zonality of hydrological regimes and the parameters R and $\frac{R}{Lr}$ is the immediate consequence of the system (2), (3), (4), from which it follows that the coefficient of flow is simply defined by the parameter $\frac{R}{Lr}$, and the mean annual flow total by the quantities $\frac{R}{Lr}$ and R.

Using the relationships (2), (3), (4) and the above-cited values of the $\frac{R}{Lr}$ parameter for the boundaries of the geobotanical zones, it is not difficult to establish that in the tundra zone the coefficient of flow should be in excess of 0.7; in the forest zone between 0.7 to 0.27;



Declassified in Part - Sanitized Copy Approved for Release 2012/03/12 : CIA-RDP82-00039R000100190014-6

Declassified in Part - Sanitized Copy Approved for Release 2012/03/12 : CIA-RDP82-00039R000100190014-6

in steppe from 0.27 - 0.08, etc. It was pointed out that these values agree satisfactorily with the results of empirical determination of flow coefficients of physico-geographic zones.

The absolute values of flow totals, computed by means of equations (2), (3), (4) are shown as a function of R and $\frac{R}{Lr}$ in the form of isolines in the graph of Figure 10, which is analogous to the graph of Figure 9 (the flow totals are given in centimeters per year). The graph of Figure 10 gives a general idea of the average flow totals in the basic physico-geographic zones.

From the given data it follows that to physico-geographic zones having certain types of plant life and soil there correspond definite gradations of the flow coefficient values and values of the climatic parameters R and $\frac{R}{Lr}$. With this, the climatic characteristics are the predominant ones and determine the nature of plant life and soils, and the order of magnitude of flow coefficients for the valley-like and non-mountainous character of the underlying surface.

It can be supposed that in mountainous regions the importance of climatic factors and particularly of the indicated parameters on the surface physico-geographic process remains very great; however, it is quite probable that, besides the climatic factors, in a number of cases the vertical physico-geographic zonality is affected directly by the topography of the underlying surface, which changes the conditions of surface flow.



Declassified in Part - Sanitized Copy Approved for Release 2012/03/12 : CIA-RDP82-00039R000100190014-6

Declassified in Part - Sanitized Copy Approved for Release 2012/03/12 : CIA-RDP82-00039R000100190014-6

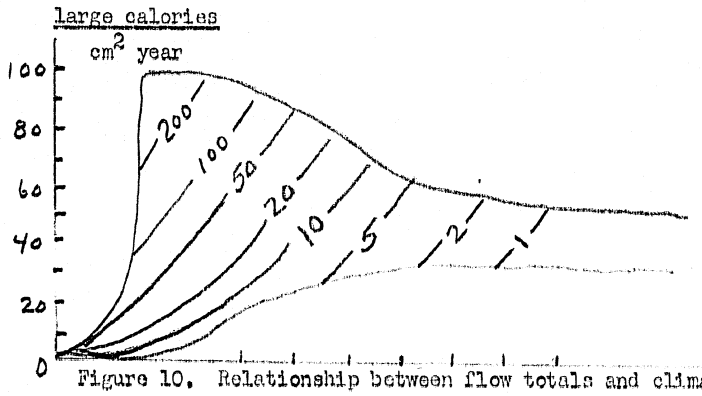


Figure 10. Relationship between flow totals and climatic factors.

The "connecting equation" depicted graphically in Figure 10 can be used not only for computation of the characteristic values of coefficients and flow totals in physico-geographic zones, but also for direct determinations of flow in any geographic region according to climatic data. Effecting such computations would obviously correspond to the solution of one of the problems, entering into the second problem of study of the effects of climatic factors upon the surface physico-geographic process.

In order to verify the results of flow computation by equation (2) a comparison was made between the computed flow values of 29 comparatively large European river reservoirs with the data of hydrometric flow determination by Wundt [17]. Results of this comparison are shown by Figure 11, where the measured values of flow coefficients $(\frac{f}{r})_o$ are shown along the abscissa, and the computed values of $(\frac{f}{r})$ are shown along the ordinate.

By means of the equation (2) and the radiation balance data of the underlying surface, it is possible to give an exact theoretical



Declassified in Part - Sanitized Copy Approved for Release 2012/03/12 : CIA-RDP82-00039R000100190014-6

Declassified in Part - Sanitized Copy Approved for Release 2012/03/12 : CIA-RDP82-00039R000100190014-6

explanation of certain empirical dependencies of flow totals upon the climatic factors, and, particularly of the dependences of flow on precipitation found by Keller [13] and D. L. Sokolovskiy [10]. Figure 12 shows these relationships graphically (curve C represents D. L. Sokolovskiy's relationship for rivers of Eastern Europe; curve B represents Keller's equation for the Western European rivers). There is also shown the dependence of total flow on precipitation in accordance with the equation (2) for the average value of radiation balance characteristic of the European plains region (curve A).

The good agreement of the results of flow determination based on climatic data and equation (2) with the actual flow materials (Figure 11) and with the empirical dependencies of flow upon the climatic characteristics (Figure 12) proves that climatic factors are the determining ones in the formation of flow in medium-size reservoirs and that the connection of the total flow with the climatic conditions is well shown by the equation (2).

Solution of the analogous problem involving the soil and biological links of the surface physico-geographic process, that is, the establishment of quantitative connections between the balances of organic and mineral soil content and the formation of the biological mass and the climatic factors is complicated by the considerable complexity and the insufficient knowledge of the quantitative characteristics of corresponding processes. The possibility of establishing such connection in the more or less near future appears slight.



Declassified in Part - Sanitized Copy Approved for Release 2012/03/12 : CIA-RDP82-00039R000100190014-6

Declassified in Part - Sanitized Copy Approved for Release 2012/03/12 : CIA-RDP82-00039R000100190014-6

centimeter/year

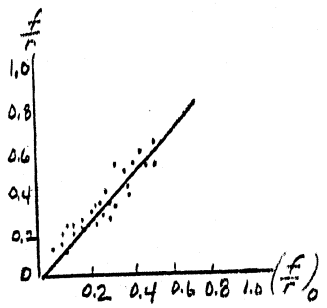


Figure 11. Determination of flow by climatic data.

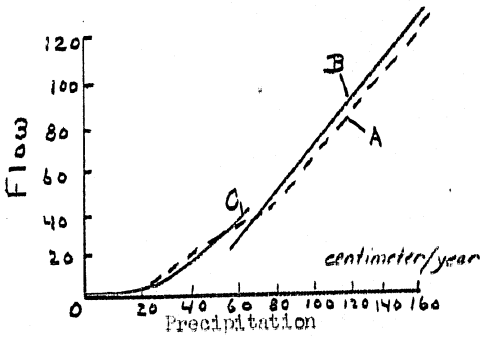


Figure 12. Relationship between flow and precipitation.

The third problem in studying the effect of climatic conditions on the surface physico-geographic process consists in the establishment of connections between the intensity of the surface physico-geographic process and the climatic factors.

An extremely important conception of the intensity of the physico-geographic process introduced and developed by A. A. Grigor'yev is characterized by a complex of symptoms relating to the development of all of the components of physico-geographic process.

In this connection the general quantitative study of links between the intensity of the surface physico-geographic process and the climatic factors is possible only upon the establishment of quantitative relationships between all of the characteristics of the basic components of the physico-geographic process and the climatic conditions.



Declassified in Part - Sanitized Copy Approved for Release 2012/03/12 : CIA-RDP82-00039R000100190014-6

Declassified in Part - Sanitized Copy Approved for Release 2012/03/12 : CIA-RDP82-00039R000100190014-6

In the absence of adequate data which would permit the study of the entire complex of the intensity characteristics of the surface physico-geographic process as a whole, it is possible to set up a narrower problem limiting the study to that of certain particular characteristics particularly significant to the general intensity of the physico-geographic process in the light of A. A. Grigor'yev's conception.

From these particular characteristics especially significant is the amount of annual intake of energy within the organic substance throughout the entire thickness of the surface physico-geographic shell per unit area of the underlying surface.

As is known, the energy contained in the organic substance represents the sole source of existence of heterotrophic organisms, which play a very important role in the development of the surface physico-geographic process. At the same time, changes in the reserves of this energy, and its different annual levels in different physico-geographic zones reflect directly and fully the interaction of all the basic components of the surface physico-geographic process.

Accumulating of energy within the biological mass takes place predominantly through the process of photosynthesis, and its final expenditure is realized by the mineralization of the soil humus, which is accompanied by the liberation of heat. The total input and, on the average, the approximately equal expenditure of energy of the biological mass vary widely in different physico-geographic zones -- from several large calories per square centimeter per year in a tropical forest, down to negligibly small values in sand deserts and in regions of perpetual snow.



Declassified in Part - Sanitized Copy Approved for Release 2012/03/12 : CIA-RDP82-00039R000100190014-6

Declassified in Part - Sanitized Copy Approved for Release 2012/03/12 : CIA-RDP82-00039R000100190014-6

A relatively greater level of energy within the biological mass for a given radiation balance of the underlying surface (for a given "energetic basis" of the surface physico-geographic process) is reached at optimum conditions of soil moisturization and for optimum balance of the mineral substances of the soil. It is obvious that in cases of excessive or insufficient moisturization (flooding or drying up of soil) as well as in cases of excessive or insufficient soil irrigation, the energy level of the biological mass will decrease as compared with the maximum possible at given thermal conditions.

In our work [4] it was assumed that the optimum conditions of moisturization and the mineral balance of the soil are independent and characterized by two different parameters. It further turned out that these conditions to a considerable extent are interconnected.

From equations (2), (3), (4) it follows that for a given radiation balance a definite flow total and flow coefficient correspond to each value of evaporation. Since the total evaporation is directly connected with the average soil moisture characteristics, while the flow and coefficient of flow, according to A. A. Grigor'yev, regulate the mineral balance of soil, it can be concluded that to definite conditions of soil moisturization, for a given radiation balance, there must correspond definite characteristics of soil mineral balance.

From this it also follows that the parameter $\frac{R}{Lr}$, which for a given radiation balance determines the values of evaporation, flow, and the coefficient of flow, can be looked upon as the characteristic of the relative productivity of energy within the biological mass. The absolute productivity of energy within the biological mass will depend,



Declassified in Part - Sanitized Copy Approved for Release 2012/03/12 : CIA-RDP82-00039R000100190014-6

Declassified in Part - Sanitized Copy Approved for Release 2012/03/12 : CIA-RDP82-00039R000100190014-6

obviously, on two parameters (R and $\frac{R}{Lr}$ ) increasing as the radiation balance for constant $\frac{R}{Lr}$ increases.

The insufficiency of data on the formation and energy reserves of the biological mass in different physico-geographic regions hinders the determination of the quantitative aspect of this relationship. The general nature of the assumed variations in energy production within the biological mass as dependent on R and $\frac{R}{Lr}$ is shown by Figure 13, where the values of the biological energy formation, shown by means of isolines, increase in the directions of the arrows. It should be emphasized that the graph in Figure 13 furnishes only the qualitative aspect of this relationship, and is not quantitative.

Considering conditionally that the fluctuating values of biological mass energy formation characterize the fluctuating intensity of the physico-geographic process, we can note that the relative maxima in biological energy formation (corresponding to definite values of the $\frac{R}{Lr}$ parameter) which are close to each other in value for different radiation balances, determine the relatively great intensity of the physico-geographic process. (As was noted before, according to A. A. Grigor'yev, the intensity of the physico-geographic process is the complex characteristic which determines the level of development of all of the respective components of the surface physico-geographic process. Since the variations of the respective characteristic components of the process are substantially different for varying climatic factors, in order to make a quantitative comparison of intensity of the various process components it is more convenient to utilize the data of a single characteristic, which takes into account most fully the interaction of all of the basic components of the surface physico-geographic



Declassified in Part - Sanitized Copy Approved for Release 2012/03/12 : CIA-RDP82-00039R000100190014-6

Declassified in Part - Sanitized Copy Approved for Release 2012/03/12 : CIA-RDP82-00039R000100190014-6

process.) From Figure 13 it follows that the absolute intensity maximum will correspond to such a relative maximum when R attains its greatest possible values.

Figure 13. Effect of climatic factors on the intensity of the surface physico-geographic process.

In one of our preceding works it was assumed that the conditions of relative maximum intensity of the surface physico-geographic process correspond to the values of parameter $\frac{R}{Lr}$ in the order of 1-2. Subsequently, it was pointed out by A. A. Grigor'yev that the more correct estimate of this value is 1. This opinion was confirmed by the scheme of relationship of zachotanical zonality and the parameters R and $\frac{R}{Lr}$ shown by Figure 9.

For further development in the study of intensity of the surface physico-geographic process, of great importance, in our opinion, is the elaboration of detailed quantitative characteristics of production in various categories of the biological mass and the dynamics of biological energy reserves in all the physico-geographic zones; this is an important problem of biological geography.

The author expresses his sincere gratitude to Academician A. A. Grigor'yev, who reviewed the manuscript of this paper and made a number of significant criticisms.



Declassified in Part - Sanitized Copy Approved for Release 2012/03/12 : CIA-RDP82-00039R000100190014-6

Declassified in Part - Sanitized Copy Approved for Release 2012/03/12 : CIA-RDP82-00039R000100190014-6

# THEORY OF GROUND FREEZING

L. Sh. Volokhonskiy

## INTRODUCTION

On the basis of studies during recent years, ground freezing has come to be considered a highly complex physical phenomenon. Before everything else we should note the important fact that ground moisture has a wide continuum of freezing temperatures extending, for example, to — 70 degrees Centigrade [17]. The second important circumstance is the intensive absorption of moisture below the freezing front. All of this further complicates the already highly difficult problem, solution of which is of interest for many reasons. It is desirable for meteorological science to be able to relate thermal processes within the ground and atmosphere throughout the year. Prolonged existence of frozen ground at a certain depth facilitates the accumulation of moisture in the upper layer, which leads to crop destruction.

In regions of perpetual frozen state, thawing of the top layer has a vital effect upon the construction industry and agricultural techniques. This thawing represents a problem very close to that of freezing. The presence of the temperature continuum of ground moisture freezing results in partial freezing of the ground, and therefore it does not lose its water permeability entirely.

In this article we shall investigate only the one-dimensional problem, considering the ground as a vertical shaft. We shall take any horizontal plane in the frozen portion of the ground and compute



Declassified in Part - Sanitized Copy Approved for Release 2012/03/12 : CIA-RDP82-00039R000100190014-6

Declassified in Part - Sanitized Copy Approved for Release 2012/03/12 : CIA-RDP82-00039R000100190014-6

for it the percentage of frozen moisture. This value, which is a function of depth and time, can be considered as a measure of the degree of freezing. We shall denote it as W. All of the existing types of freeze meters, that is, the instruments which register the depth of the freezing front, are based on the assumption that at some depth the value W undergoes a discontinuity changing its initial value from 1 to zero. Actually this does not happen, and therefore freeze meters indicate only a certain effective position of the freezing front. Thus, indications of freeze meters depend materially on the physical principle underlying the basis of measurement.

## FORMULATION OF THE PROBLEM

Definitions of Terms:

$A^2$ - coefficient of temperature conductivity;

K - coefficient of thermal conductivity;

cD - volume heat capacity;

$\rho$ - weight of moisture per unit volume;

X - depth; t-time;

$\xi(t)$ - coordinates of the freezing front;

$\theta(x,t)$ - temperature.

Index 1 shows that the subject quantity refers to the frozen portion of the ground, index 2 refers to the unfrozen portion of the ground. Difficulty of the problem necessitates its schematization.



Declassified in Part - Sanitized Copy Approved for Release 2012/03/12 : CIA-RDP82-00039R000100190014-6

Declassified in Part - Sanitized Copy Approved for Release 2012/03/12 : CIA-RDP82-00039R000100190014-6

We assume that ground moisture changes its aggregate state at zero degrees Centigrade (Figure 1).

We also consider that each medium has its own constant with time and in space -- thermophysical constants. All of this permits the writing of heat propagation equations for each medium:

$$\frac{\partial}{\partial t}\theta_1(x,t) = a_1^2 \frac{\partial^2}{\partial x^2}\theta_1(x,t); \qquad (1)$$

$$\theta_1(x,t) \leqslant 0;\ 0 \leqslant x \leqslant \xi(t);$$

$$\theta_1(x,t)\Big|_{x=\xi(t)} = 0;\ t \geqslant 0; \qquad (1a)$$

$$\frac{\partial}{\partial t}\theta_2(x,t) = a_2^2 \frac{\partial^2}{\partial x^2}\theta_2(x,t); \qquad (2)$$

$$\theta_2(x,t) \geqslant 0;\ \xi(t) \leqslant x \leqslant h;$$

$$\theta_2(x,t)\Big|_{x=\xi(t)} = 0. \qquad (2a)$$

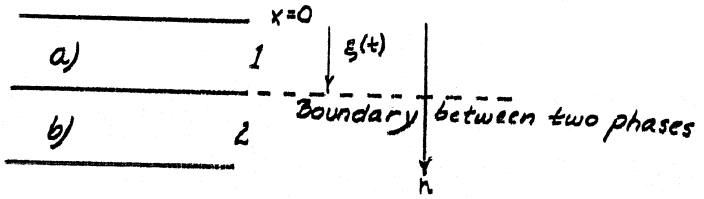


Figure 1.

To a certain extent we can take into account the presence of the freezing temperature continuum and migration of ground moisture. We shall apply to medium 1 the analytical method of determination of $\Lambda^2$, suggested by D. L. Laykhtman, Doctor of Physico-mathematical



Declassified in Part - Sanitized Copy Approved for Release 2012/03/12 : CIA-RDP82-00039R000100190014-6

Declassified in Part - Sanitized Copy Approved for Release 2012/03/12 : CIA-RDP82-00039R000100190014-6

sciences [2]. Liberation of the latent heat of fusion of ice and migration of moisture result in that, instead of the actual coefficient, we obtain its effective value for a heterogeneous medium, which consists of the ground and two water phases, wherein there is liberated heat of convection. Migration of ground moisture takes place also by means of vapor thermodiffusion. The latent heat of condensation is taken into account automatically in computing the effective value of $A^2$.

We can continue the formulation of the abstract problem. The upward flow of heat from the boundary between the two phases is equal to the downward flow of heat plus the latent heat of fusion of ice. This is the so-called Stefan's condition. This formula is written in its integral form (3)

$$\gamma \rho \xi(t) = K_1 \int_0^t \left.\frac{\partial \theta_1(x,\tau)}{\partial x}\right|_{x=\xi(\tau)} \cdot d\tau - K_2 \int_0^t \left.\frac{\partial \theta_2(x,\tau)}{\partial x}\right|_{x=\xi(\tau)} \cdot d\tau.$$

L - is the latent heat of fusion of ice.

It seems that up to now, there has been no clear idea as to which index should be used with $\rho$. Some authors (for example [16]) omit this index altogether. Actually the fronts of the various media have unequal velocities of movement, and depending on our point of reference we take either $\rho_1$, or $\rho_2$.

Different velocities result in the emergence of great stresses. If ice floats in water, there are no stresses, since the depth of immersion follows the principle of Archimedes' law. Here we take $\rho_1$, since we are interested in the thickness of ice.



Declassified in Part - Sanitized Copy Approved for Release 2012/03/12 : CIA-RDP82-00039R000100190014-6

Declassified in Part - Sanitized Copy Approved for Release 2012/03/12 : CIA-RDP82-00039R000100190014-6

There are two types of ground freezing:

1. (The case studies herein). Freezing moisture expands into the free portion of the capillaries $\rho_1 = \rho_2$, since $\rho$ refers to the macrovolume of the heterogeneous medium.

2. The ground is highly moist, there is little free space in the capillaries, and the ground swells.

Boundary conditions (h is a certain fixed depth which is not reached by the freezing front.):

$$\theta_1(x,t)\Big|_{x=0} = \phi(t) \leqslant 0 \qquad (4a)$$

or

$$\frac{\partial}{\partial x}\theta_1(x,t)_{x=0} = \psi(t); \qquad (4b)$$

$$\theta_2(x,t)_{x=h} = \Phi(t) \geqslant 0. \qquad (5)$$

$\phi(t)$ [or $\psi(t)$] and $\Phi(t)$ should be given for $t \geqslant 0$; $\phi(0) = 0$.

The initial condition:

$$\theta_2(x,t) = f(x) \geqslant 0, \qquad (6)$$

and f(x) is taken in the interval [0, h]; $f(0) = 0$;

$$f(h) = \Phi(0).$$



Declassified in Part - Sanitized Copy Approved for Release 2012/03/12 : CIA-RDP82-00039R000100190014-6

Declassified in Part - Sanitized Copy Approved for Release 2012/03/12 : CIA-RDP82-00039R000100190014-6

We look for $\xi$ (t) for the condition $\xi(0) = 0$.

In such a setting the problem has been considerably generalized as compared with its solution by Stefan.

Later more or less successful attempts were made to solve this problem in formulations intermediate to Stefan's system and that of equations (1) - (6).

We note only certain of these attempts. A. G. Kolesnikov in his work "On the theory of ice formation on the sea's surface" [3] had made a serious error in his solution of this problem, thus rendering his results completely valueless. This error, detected by M. Kh. Shurets, candidate of physico-mathematical sciences, consists in using the Fourier series with medium /1, while in the derived characteristic equation Kolesnikov had tacitly assumed $\xi$ (t) to be a constant. L. I. Rubinstein in a number of papers [4], [13], [14] showed that the system (1) - (6) is a correct one and supplied its exact solution. The significant disadvantage of this solution is the impossibility of practical application in view of the extreme complexity of the algorithm. L. I. Rubinstein attempted to take into account the continuum of freezing temperatures [15] of ground moisture, but carried out his computations only for the simplest instance.

Presence of the condition (5) limits materially the possible errors in the solution and reduces the importance of the initial condition. In formulating a prognostic theory the necessity of knowing $\Phi$ (t) is not a detriment, since this function is very close to being periodic.



Declassified in Part - Sanitized Copy Approved for Release 2012/03/12 : CIA-RDP82-00039R000100190014-6

Declassified in Part - Sanitized Copy Approved for Release 2012/03/12 : CIA-RDP82-00039R000100190014-6

Since the exact solution of the system (1) - (6) leads to a useless, from a practical standpoint, algorithm, we have devised an approximate (quasilinear) solution, based on the assumption that function $\xi$ (t) approaches linearity.

Determining the function $\xi$ (t) for the time $t = \bar{t}$, we consider that in the interval $[0, \bar{t}]$ freezing proceeds with a constant velocity $V = \frac{\xi(\bar{t})}{\bar{t}}$, and with this it is possible to find $\frac{\partial}{\partial x}\theta_{1,2}\Big|_{x=\xi(t)}$. [illegible]. Condition (3) yields a numerical value for v, as a result of which we get the function v(t); $\bar{\xi}(t) = v(t) \cdot t$ is an approximation of the required function $\xi$ (t). In the future we shall omit the bar superscripts.

Region 1, Case a

The problem can be formulated as follows:

To find

$$\int_0^t \frac{\partial}{\partial x}\theta(x,\tau)\Big|_{x=v\tau} d\tau ,$$

given

$$\frac{\partial}{\partial t}\theta(x,t) = a^2 \frac{\partial^2\theta}{\partial x^2};\ 0 \leqslant x \leqslant vt, \text{ when } t \geqslant 0;$$

$$\theta\Big|_{x=0} = \varphi(t) \leqslant 0;\ \theta\Big|_{x=vt} = 0;\ \varphi(0) = 0.$$



Declassified in Part - Sanitized Copy Approved for Release 2012/03/12 : CIA-RDP82-00039R000100190014-6

Declassified in Part - Sanitized Copy Approved for Release 2012/03/12 : CIA-RDP82-00039R000100190014-6

This problem was in general solved by B. Ya. Lyubov [5].

Employing the source method he sought the solution in the form:

$$\theta(x,t)=\frac{1}{a}\int_0^t\left[\mu(\eta)e^{-\frac{(x-v\eta)^2}{4a^2(t-\eta)}}+\lambda(\eta)e^{-\frac{k^2}{a^2(t-\eta)}}\right]\frac{d\eta}{\sqrt{\pi(t-\eta)}}\quad(*)$$

Functions $\mu$ and $\lambda$ are determined on the basis of boundary conditions from the two joint integral equations, using operational methods. The author had made a significant error in this determination, which resulted in a divergent integral entering into the final expression.

Let

$$\bar{\psi}(p)=p\int_0^\infty e^{-pt}\psi(t)\,dt$$

denote the function $\psi(t)$. Solution of this equation will be denoted by subscript dash, or

$$\underline{\varphi}(t)=\frac{1}{2\pi i}\int_{\gamma-i\infty}^{\gamma+i\infty}e^{pt}\frac{\varphi(p)}{p}\,dp$$

is the original of the function $\varphi(p)$.

In the course of the solution, B. Ya. Lyubov had to determine (find the original) operational equation:

$$\bar{\rho}(p)=\sqrt{p}\,\bar{\sigma}(p).$$

The sequence of operations, omitted in the article, was as follows:



Declassified in Part - Sanitized Copy Approved for Release 2012/03/12 : CIA-RDP82-00039R000100190014-6

Declassified in Part - Sanitized Copy Approved for Release 2012/03/12 : CIA-RDP82-00039R000100190014-6

$$\bar{\rho}(p) = \frac{1}{p} \times p^{3/2} \times \sigma(p) .$$

Considering that $p^{3/2} = \frac{1}{\Gamma(-\frac{3}{2}+1)3/2}$ (this already is absurd, since the formula $p^{-n} = \frac{t^n}{\Gamma(n+1)}$ is only valid for $n > -1$) and using Borel's theorum, B. Ya. Lyubov obtained:

$$\rho(t) = \frac{1}{\Gamma(-\frac{1}{2})} \int_0^t \frac{\sigma(\tau)}{(t-\tau)^{3/2}} d\tau ,$$

that is, a divergent integral.

Actually we should do the following:

$$\bar{\rho}(p) = \frac{1}{p} \times p^{1/2} \times p\sigma(p)$$

and since:

$$\underline{\sqrt{p}} = \frac{1}{\sqrt{\pi t}} \quad \text{and} \quad \underline{p\bar{\sigma}(p)} = \sigma'(t)$$

(since in B. Ya. Lyubov's work $\sigma(0) = 0$), then

$$\rho(t) = \int_0^t \frac{\sigma'(\tau)}{\sqrt{\pi(t-\tau)}} d\tau .$$

Differentiating (*) with respect to X and taking $X = vt$, we get ($\beta = \frac{v}{2a}$):



Declassified in Part - Sanitized Copy Approved for Release 2012/03/12 : CIA-RDP82-00039R000100190014-6

Declassified in Part - Sanitized Copy Approved for Release 2012/03/12 : CIA-RDP82-00039R000100190014-6

$$\left.\frac{\partial\theta}{\partial x}\right|_{x=vt} = -\frac{\beta}{a^2}\int_0^t \left[\mu(\eta)e^{-\beta^2(t-\eta)} + \lambda(\eta)e^{-\beta^2\frac{t^2}{t-\eta}}\cdot\frac{t}{t-\eta}\right]\frac{d\eta}{\sqrt{\pi(t-\eta)}} \quad \text{(A)}$$

However (*) for $X = vt$ it yields

$$0 = \int_0^t \left[\mu(\eta)e^{-\beta^2(t-\eta)} + \lambda(\eta)e^{-\beta^2\frac{t^2}{t-\eta}}\right]\frac{d\eta}{\sqrt{\pi(t-\eta)}} . \quad \text{(B)}$$

Forming the combination (A) $+ \frac{\beta}{a^2}$ (B):

$$\left.\frac{\partial\theta}{\partial x}\right|_{x=vt} = X(t) = -\frac{\beta}{a^2}\int_0^t \lambda(\eta)\cdot e^{-\beta^2\frac{t^2}{t-\eta}}\frac{\eta}{\sqrt{\pi}(t-\eta)^{3/2}}d\eta ;$$

$$\overline{X}(p) = -\frac{\beta}{a^2}p\int_0^\infty e^{-pt}dt\int_0^t \lambda(\eta)e^{-\beta^2\frac{t^2}{t-\eta}}\frac{\eta}{\sqrt{\pi}(t-\eta)^{3/2}}d\eta .$$

Changing the order of Integration:

$$\overline{X}(p) = -\frac{\beta}{a^2}p\int_0^\infty \lambda(\eta)\eta\,d\eta\int_\eta^\infty e^{-pt-\beta^2\frac{t^2}{t-\eta}}\frac{dt}{\sqrt{\pi}(t-\eta)^{3/2}} .$$



Declassified in Part - Sanitized Copy Approved for Release 2012/03/12 : CIA-RDP82-00039R000100190014-6

Declassified in Part - Sanitized Copy Approved for Release 2012/03/12 : CIA-RDP82-00039R000100190014-6

We denote the interior integral by I and making a substitution

$t = \eta + \chi$ we get

$$I = \int_0^\infty e^{-p(\chi+\eta)-\beta^2\frac{(\chi+\eta)^2}{\chi}} \frac{d\chi}{\chi\sqrt{\pi\chi}} = e^{-\eta(p+2\beta^2)} \int_0^\infty e^{-\chi(p+\beta^2)-\frac{\beta^2\eta^2}{\chi}} \frac{d\chi}{\chi\sqrt{\pi\chi}} =$$

$$= \frac{e^{-\eta(p+2\beta^2)}}{p+\beta^2} \cdot \left[\frac{e^{-\beta^2\frac{\eta^2}{\chi}}}{\chi\sqrt{\pi\chi}}\right]\Bigg|_{\text{instead of } p \text{ take } p+\beta^2} \frac{1}{\beta\eta} e^{-\eta(\sqrt{p+\beta^2}+\beta)^2}.$$

And so

$$\overline{X}(p) = -\frac{p}{a^2}\int_0 \lambda(\eta) e^{-\eta(\sqrt{p+\beta^2}+\beta)^2} d\eta = -\frac{p}{a^2}\frac{\overline{\lambda}[(\sqrt{p+\beta^2}+\beta)^2]}{(\sqrt{p+\beta^2}+\beta)^2}.$$

Let

$$Z(t) = \kappa\int_0^t \frac{\partial\theta(x,\tau)}{dx}\Big|_{x=v\tau} d\tau \text{ and } \Lambda(p) = \frac{\overline{\lambda}(p)}{p},$$

then

$$\overline{Z}_1(p) = -\frac{\kappa_1}{a_1^2}\Lambda\left[(\sqrt{p+\beta^2}+\beta)^2\right].$$



Declassified in Part - Sanitized Copy Approved for Release 2012/03/12 : CIA-RDP82-00039R000100190014-6

Declassified in Part - Sanitized Copy Approved for Release 2012/03/12 : CIA-RDP82-00039R000100190014-6

But according to (5)

$$\Lambda(p) = a\sum_{s=0}^{\infty} \frac{\bar{\varphi}\left[(\sqrt{p}+2s\beta)^2\right]}{\sqrt{p}+2s\beta}$$

and since $\frac{k}{a} = acD$

then

$$\bar{Z}_1(p) = -(acD)_1 \sum_{s=0}^{\infty} \frac{\bar{\varphi}\left\{\left[\sqrt{p+\beta^2}+(2s+1)\beta\right]^2\right\}}{\sqrt{p+\beta^2}+(2s+1)\beta}$$

To use this equation we use Efros' theorem [5]:

$$v(p)\bar{\varphi}[q(p)] = \int_0^{\infty} w(\xi,t)\varphi(\xi)\,d\xi,$$

where

$$w(\xi,t) = e^{-\xi q(p)} \cdot q(p)v(p) .$$

Thus

$$\frac{\bar{\varphi}\left\{\left[\sqrt{p+\beta^2}+(2s+1)\beta\right]^2\right\}}{\sqrt{p+\beta^2}+(2s+1)\beta} = \int_0^{\infty} \varphi(\xi) w_s(\xi,t)\,d\xi ,$$



Declassified in Part - Sanitized Copy Approved for Release 2012/03/12 : CIA-RDP82-00039R000100190014-6

Declassified in Part - Sanitized Copy Approved for Release 2012/03/12 : CIA-RDP82-00039R000100190014-6

where

$$w_s(\xi, t) = \underline{e^{-\xi[\sqrt{p+\beta^2}+(2s+1)\beta]^2}\,[\sqrt{p+\beta^2}+(2s+1)\beta]} =$$

$$= e^{-[(2s+1)^2+1]\beta^2\xi}\,\underline{e^{-p\xi-2(2s+1)\beta\sqrt{p+\beta^2}}\cdot[\sqrt{p+\beta^2}+(2s+1)\beta]}\,.$$

But [6]

$$\underline{e^{-2(2s+1)\xi\beta\sqrt{p+\beta^2}}} = \frac{1}{2}\left\{e^{-2(2s+1)\xi\beta^2}\,\mathrm{erfc}\left[\frac{(2s+1)\beta\xi}{\sqrt{t}}-\beta\sqrt{t}\right]+\right.$$

$$\left.+\,e^{-2(2s+1)\xi\beta^2}\,\mathrm{erfc}\left[\frac{(2s+1)\xi\beta}{\sqrt{t}}+\beta\sqrt{t}\right]\right\}.$$

using the formula for $\underline{e^{-\lambda p}\,f(p)}$ [7], we get:



Declassified in Part - Sanitized Copy Approved for Release 2012/03/12 : CIA-RDP82-00039R000100190014-6

Declassified in Part - Sanitized Copy Approved for Release 2012/03/12 : CIA-RDP82-00039R000100190014-6

$$\underline{e^{-\left[\sqrt{p+\beta^2}+(2s+1)\beta\right]^2\xi}} = \begin{cases} 0 \text{ for } t<\xi \\ \frac{1}{2}e^{-\left[(2s+1)^2+1\right]\beta'\xi} \times \end{cases}$$

$$\times \left[ e^{-2(2s+1)\beta^2\xi} \operatorname{erfc} \beta\left(\frac{2s+1}{\sqrt{t-\xi}}\xi - \sqrt{t-\xi}\right) + \right.$$

$$\left. + e^{2(2s+1)\beta^2\xi} \operatorname{erfc}\left(\frac{2s+1}{\sqrt{t-\xi}}\xi + \sqrt{t-\xi}\right) \right] \text{ for } t>\xi .$$



Declassified in Part - Sanitized Copy Approved for Release 2012/03/12 : CIA-RDP82-00039R000100190014-6

Declassified in Part - Sanitized Copy Approved for Release 2012/03/12 : CIA-RDP82-00039R000100190014-6

Similarly we get

$$\underline{e^{-\left[\sqrt{p+\beta^2}+(2s+1)\beta\right]^2\xi}\sqrt{p+\beta^2}} =$$

$$= \begin{cases} 0 \text{ for } t<\xi \\ e^{-\left[(2s+1)^2+1\right]\beta^2\xi} \times \end{cases}$$

$$\times \left\{ \frac{1}{\sqrt{\pi(t-\xi)}} e^{-(2s+1)^2\frac{\beta^2\xi^2}{t-\xi}-\beta^2(t-\xi)} + \frac{\beta}{2}\left[ e^{-2(2s+1)\beta^2\xi} \times \right.\right.$$

$$\times \operatorname{erfc}\beta\left(\frac{2s+1}{\sqrt{t-\xi}}\xi+\sqrt{t-\xi}\right) - e^{2(2s+1)\beta^2\xi}$$

$$\left.\left. \operatorname{erfc}\beta\left(\frac{2s+1}{\sqrt{t-\xi}}\xi+\sqrt{t-\xi}\right)\right]\right\} \text{ for } t>\xi \text{ ;}$$



Declassified in Part - Sanitized Copy Approved for Release 2012/03/12 : CIA-RDP82-00039R000100190014-6

Declassified in Part - Sanitized Copy Approved for Release 2012/03/12 : CIA-RDP82-00039R000100190014-6

$$Z_1(t) = -(acD)_1 \int_0^t \varphi(\xi) \sum_{s=0}^{\infty} e^{-[(2s+1)^2+1]\beta^2\xi} \times$$

$$\left\{ \frac{1}{\sqrt{\pi(t-\xi)}} e^{-(2s+1)^2 \frac{\beta^2\xi^2}{t-\xi} - \beta^2(t-\xi)} + \right.$$

$$+ (s+1)\beta e^{-2(2s+1)\beta^2\xi} \cdot \operatorname{erfc} \beta\left(\frac{2s+1}{\sqrt{t-\xi}}\xi - \sqrt{t-\xi}\right) +$$

$$\left. + s\beta e^{2(2s+1)\beta^2\xi} \cdot \operatorname{erfc} \beta\left(\frac{2s+1}{\sqrt{t-\xi}}\xi + \sqrt{t-\xi}\right) \right\} d\xi .$$



Declassified in Part - Sanitized Copy Approved for Release 2012/03/12 : CIA-RDP82-00039R000100190014-6

Declassified in Part - Sanitized Copy Approved for Release 2012/03/12 : CIA-RDP82-00039R000100190014-6

But

$$\sum_{s=0}^{\infty} e^{-(2s+1)^2\beta^2\xi - (2s+1)^2\frac{\beta^2\xi^2}{t-\xi}} =$$

$$= \sum_{s=0}^{\infty} e^{-(2s+1)^2\beta^2\frac{t\xi}{t-\xi}} =$$

$$= \frac{1}{2}\theta_2\left(v=0, q=e^{-4\beta^2\frac{t\xi}{t-\xi}}\right)$$



Declassified in Part - Sanitized Copy Approved for Release 2012/03/12 : CIA-RDP82-00039R000100190014-6

Declassified in Part - Sanitized Copy Approved for Release 2012/03/12 : CIA-RDP82-00039R000100190014-6

(nomenclature according to [7]) and after other elementary transformations we get:

$$Z(t) = -acD\int_0^t \varphi(\xi)\left\{\frac{e^{-\beta^2 t}}{\sqrt{\pi(t-\xi)}}\,\theta_2\left(0, e^{-4\beta^2\frac{t\xi}{t-\xi}}\right) + \right.$$

$$\left. + \beta\sum_{s=0}^{\infty} s e^{-4s^2\beta^2\xi}\left[\operatorname{erfc}\beta\frac{2s\xi - t}{\sqrt{t-\xi}} + \operatorname{erfc}\beta\frac{2s\xi + t}{\sqrt{t-\xi}}\right]\right\} d\xi .$$

Let us look especially at the evaluation of the function under the integral sign for $\xi = 0$ and for $\xi = t$.

a) $\xi = 0$. If k is a modulus and K - a complete elliptical integral of the first kind, then [8]

$$\frac{1}{2}\theta_2(0, q) = \sqrt{\frac{\pi K}{2\pi}} .$$

Further

$$\frac{\pi K}{\pi} sn u = \sum_{s=1}^{\infty} \frac{\sin(2s+1)\kappa}{\operatorname{sh}(2s+1)\rho} ; \kappa = \frac{\pi}{2}\frac{u}{K}, \rho = \frac{1}{2}\ln\frac{1}{q} .$$



Declassified in Part - Sanitized Copy Approved for Release 2012/03/12 : CIA-RDP82-00039R000100190014-6

Declassified in Part - Sanitized Copy Approved for Release 2012/03/12 : CIA-RDP82-00039R000100190014-6

there we have

$$\rho = 2\beta^2 \frac{t\xi}{t-\xi} \longrightarrow 2\beta^2 . \xi \longrightarrow 0 .$$

Let $u = K$, which yields $x = \frac{\pi}{2}$ and $snu = 1$, therefore

$$\frac{\varkappa K}{\pi} = \sum_{s=1}^{\infty} \frac{\sin(2s+1)\frac{\pi}{2}}{\operatorname{sh}[(2s+1)2\beta_1^2\xi} \longrightarrow \frac{1}{2\beta_1^2\xi} \sum_{s=1}^{\infty} \frac{(-1)^s}{2s+1} ;$$

$$\xi \frac{\varkappa K}{\pi}\Big|_{\xi\to 0} \longrightarrow \frac{1}{2\beta_1^2} \sum_{s=1}^{\infty} \frac{(-1)^s}{2s+1} = \frac{\frac{\pi}{4} - 1}{2\beta_1^2} .$$

Whence it follows that

$$\xi \sqrt{\varkappa K}\Big|_{\xi\to 0} \longrightarrow 0 ,$$

therefore, and

$$\varphi(\xi) \sqrt{\varkappa K}\Big|_{\xi\to 0} \longrightarrow 0.$$



Declassified in Part - Sanitized Copy Approved for Release 2012/03/12 : CIA-RDP82-00039R000100190014-6

Declassified in Part - Sanitized Copy Approved for Release 2012/03/12 : CIA-RDP82-00039R000100190014-6

In the second component of the function under the integral sign:

$$\operatorname{erfc}(-\beta_1\sqrt{t})+\operatorname{erfc}(\beta_1\sqrt{t})=2.$$

Thus we have to find

$$\lim 2\varphi(\xi)\sum_{s=1}^{\infty} s e^{-4s^2\beta_1^2\xi}$$

The following method was proposed by N. R. Malkin, candidate of physico-mathematical sciences. (It is also applicable to the preceding problem.) Let us study the function

$$y=\kappa e^{-4\kappa^2\beta^2\xi}.$$

It is not difficult to see that:

$$\xi\sum_{s=1}^{\infty} s e^{-4s^2\beta^2\xi}$$

is Darboux's sum for

$$\int_0^{\infty}\xi\kappa e^{-4\kappa^2\beta^2\xi}\,d\kappa.$$

Thus, for $\xi \to 0$:



Declassified in Part - Sanitized Copy Approved for Release 2012/03/12 : CIA-RDP82-00039R000100190014-6

Declassified in Part - Sanitized Copy Approved for Release 2012/03/12 : CIA-RDP82-00039R000100190014-6

$$2\varphi(\xi)\beta\sum_{s=1}^{\infty} s e^{-4s^2\beta^2\xi} \longrightarrow 2\varphi'(0)\beta\int_0^{\infty}\xi\kappa e^{-4\kappa^2\beta^2\xi}\,d\kappa = \frac{\varphi'(0)}{4\beta}$$

(b) $\xi = t$, function under the integral sign is equal to 0.

Medium 1, Case b

To determine

$$\int_0^t \left.\frac{\partial\theta(x,\tau)}{\partial x}\right|_{x=v\tau} d\tau$$

given

$$\frac{\partial\theta}{\partial t} = a^2\frac{\partial^2\theta}{\partial x^2};\ 0\leq x\leq vt;\ t\geq 0;$$

$$\left.\frac{\partial\theta}{\partial x}\right|_{x=0} = \psi(t) \text{ and } \left.\theta\right|_{x=vt} = 0.$$

from (*) we can obtain:

$$\psi(t) = \frac{\beta}{a^2}\int_0^t \eta\mu(\eta)e^{-\beta^2\frac{\eta^2}{t-\eta}}\frac{d\eta}{\sqrt{\pi}(t-\eta)^{3/2}};$$

$$\bar{\psi}(p) = \frac{\beta p}{a^2}\int_0^{\infty} e^{-pt}dt\int_0^t \eta\mu(\eta)e^{-\beta^2\frac{t^2}{t-\eta}}\frac{d\eta}{\sqrt{\pi}(t-\eta)^{3/2}} =$$



Declassified in Part - Sanitized Copy Approved for Release 2012/03/12 : CIA-RDP82-00039R000100190014-6

Declassified in Part - Sanitized Copy Approved for Release 2012/03/12 : CIA-RDP82-00039R000100190014-6

$$= \frac{\beta p}{a^2} \int_0^\infty \eta \mu(\eta) e^{-p\eta} \, d\eta \int_0^\infty e^{-p\chi - \beta^2 \frac{\eta^2}{\chi}} \frac{d\chi}{\chi \sqrt{\pi \chi}} .$$

We evaluate the interior integral:

$$I = \int_0^\infty e^{-p\chi - \beta^2 \frac{\eta^2}{\chi}} \frac{d\chi}{\chi \sqrt{\pi \chi}} = \frac{1}{\beta \eta} e^{-2\beta\eta\sqrt{p}} ,$$

thus

$$\bar{\psi}(p) = \frac{p}{a_1^2} \int_0^\infty \mu(\eta) e^{-\eta(p+2\beta\sqrt{p})} d\eta = \frac{p}{a^2} \frac{\bar{\mu}(p+2\beta\sqrt{p})}{p+2\beta\sqrt{p}} .$$

If we introduce

$$M(p) = \frac{\bar{\mu}(p)}{p} ,$$

then

$$\bar{\psi}(p) = \frac{p}{a^2} M(p+2\beta\sqrt{p}) ,$$

However, before we had

$$\bar{Z}_1(p) = -(cD)_1 \Lambda \left[ (\sqrt{p+\beta^2} + \beta)^2 \right] ;$$

besides (5)



Declassified in Part - Sanitized Copy Approved for Release 2012/03/12 : CIA-RDP82-00039R000100190014-6

Declassified in Part - Sanitized Copy Approved for Release 2012/03/12 : CIA-RDP82-00039R000100190014-6

$$M(p)+\Lambda\left[\left(\sqrt{p+\beta^2}+\beta\right)^2\right]=0.$$

Eliminating A, we obtain the system:

$$\overline{Z}_1(p)=(cD)_1 M(p);$$

$$\overline{\psi}(p)=\frac{p}{a_1^2}M(p+2\beta_1\sqrt{p}),$$

i.e.

$$\overline{Z}_1(p)=\kappa_1\frac{\overline{\psi}\left[\left(\sqrt{p+\beta^2}-\beta\right)^2\right]}{\left(\sqrt{p+\beta^2}-\beta\right)^2}.$$

Consequently

$$Z_1(t)=\kappa_1\int_0^\infty \psi(\xi)w(t,\xi)\,d\xi,$$

where

$$w(p,\xi)=e^{-\xi\left(\sqrt{p+\beta^2}-\beta\right)^2}$$



Declassified in Part - Sanitized Copy Approved for Release 2012/03/12 : CIA-RDP82-00039R000100190014-6

Declassified in Part - Sanitized Copy Approved for Release 2012/03/12 : CIA-RDP82-00039R000100190014-6

We study

$$e^{\frac{-\frac{1}{\xi}\left(\frac{1}{p}-\beta\right)^2}{}} = \sum_{s=0}^{\infty} \frac{(-\xi\beta^2)^s}{s!}\left(\frac{1}{\beta p}-1\right)^{2s},$$

$$\text{but } \left(\frac{1}{p}-1\right)^{2s} = \frac{1}{(2s)!}\angle_{2s}(t)$$

($L_{2s}$ - Laguerre's polynominals).

Therefore $\left(\frac{1}{\beta p}-1\right)^{2s} = \frac{1}{(2s)!} L_{2s}\left(\frac{t}{\beta}\right)$.

We introduce the function $l(x, y) = \sum_{s=0}^{\infty} \frac{(-x)^s}{s!\,(2s)!} L_{2s}(y)$.

(For positive values of arguments, the series is rapidly convergent.)

$$e^{\frac{-\xi\left(\frac{1}{p}-\beta\right)^2}{}} = l\left(\xi\beta^2; \frac{t}{\beta}\right).$$

As the second argument tends to $\infty$, the function rapidly approaches 0. This is seen from its description at $p \longrightarrow 0$.

We employ the transformation $f\left(\frac{1}{\sqrt{p+\beta^2}}\right)$. The formula indicated for this case in [6] refers actually to $\frac{1}{p+\beta^2} f\left(\sqrt{p+\beta^2}\right)$.



Declassified in Part - Sanitized Copy Approved for Release 2012/03/12 : CIA-RDP82-00039R000100190014-6

Declassified in Part - Sanitized Copy Approved for Release 2012/03/12 : CIA-RDP82-00039R000100190014-6

Actually

$$f\left(\frac{1}{\sqrt{p+\beta^2}}\right) = \int_0^\infty \nu(t,\xi) f(\xi)\, d\xi$$

where

$$\nu(t,\xi) = \frac{1}{\sqrt{p+\beta^2}}\, e^{-\frac{\xi}{\sqrt{p+\beta^2}}}$$

Considering that

$$\frac{1}{\sqrt{p}} e^{-\frac{\xi}{\sqrt{p}}} = \frac{1}{\xi^2\sqrt{\pi t}} \int_0^\infty e^{-\frac{\tau^2}{4\xi^2 t}} \sqrt{\tau}\, I_1(2\sqrt{\tau})\, d\tau,$$

we get

$$f\left(\frac{1}{\sqrt{p+\beta^2}}\right) = \int_0^\infty \frac{f(\xi)}{\xi^2}\, d\xi \int_0^\infty \left\{ \frac{e^{-p^2 t - \frac{\tau^2}{4\xi^2 t}}}{\sqrt{\pi t}} + \frac{\beta}{2}\left[ e^{-\frac{\beta\tau}{\xi}} \operatorname{erfc}\left(\frac{\tau}{2\xi\sqrt{t}} - \beta\sqrt{t}\right) - e^{p\frac{\tau}{\xi}} \operatorname{erfc}\left(\frac{\tau}{2\xi\sqrt{t}} + \beta\sqrt{t}\right)\right]\right\} \sqrt{\tau}\, I_1(2\sqrt{\tau})\, d\tau.$$



Declassified in Part - Sanitized Copy Approved for Release 2012/03/12 : CIA-RDP82-00039R000100190014-6

Declassified in Part - Sanitized Copy Approved for Release 2012/03/12 : CIA-RDP82-00039R000100190014-6

Consequently

$$\frac{e^{-\xi(\sqrt{p+\beta^2}-\beta)^2}}{} = \int_0^\infty \frac{J\left(\xi\beta^2\frac{\chi}{\beta}\right)}{\chi^2}\,d\chi \int_0^\infty \left\{ \frac{e^{-\beta^2 t-\frac{\tau^2}{4\chi^2 t}}}{\sqrt{\pi t}} + \right.$$

$$\left. + \frac{\beta}{2}\left[ e^{-\beta\frac{\tau}{\chi}} \operatorname{erfc}\left(\frac{\tau}{2\chi\sqrt{t}} - \beta\sqrt{t}\right) - e^{\beta\frac{\tau}{\chi}} \operatorname{erfc}\left(\frac{\tau}{2\chi\sqrt{t}} + \beta\sqrt{t}\right)\right]\right\} .$$

$$\sqrt{\tau}\, I_1(2\sqrt{\tau})\,d\tau = w(t,\xi).$$

Now is it convenient to determine the soil heat loss through its surface:

$$A(t) = \kappa \int_0^t \psi(\tau)\,d\tau ;$$

$$\bar{A}(p) = (cD)\,M(p+2\beta_1\sqrt{p}) = -(cD)_1\,\Lambda\left[(\sqrt{p}+2\beta)^2\right] =$$

$$= -(acD)_1 \sum_{s=0}^{\infty} \frac{\bar{\Phi}\left\{\left[\sqrt{p}+2(s+1)\beta\right]^2\right\}}{\sqrt{p}+2(s+1)\beta} =$$

$$= -(acD)_1 \sum_{s=1}^{\infty} \frac{\bar{\Phi}\left\{\left[\sqrt{p}+2s\beta\right]^2\right\}}{\sqrt{p}+2s\beta} .$$



Declassified in Part - Sanitized Copy Approved for Release 2012/03/12 : CIA-RDP82-00039R000100190014-6

Declassified in Part - Sanitized Copy Approved for Release 2012/03/12 : CIA-RDP82-00039R000100190014-6

But

$$\frac{\varphi[(\sqrt{p}+2s\beta)^2]}{\sqrt{p}+2s\beta} = \int_0^\infty \varphi(\xi) w(t,\xi)\, d\xi ;$$

$$w(p,\xi) = [\sqrt{p}+2s\beta]\, e^{-\xi(\sqrt{p}+2s\beta)^2}$$

Since

$$\frac{\sqrt{p}\, e^{-4s\beta\xi\sqrt{p}}}{} = \frac{1}{\sqrt{\pi t}}\, e^{-4s^2\beta^2\frac{\xi^2}{t}}$$

and

$$\frac{e^{-s\beta\xi\sqrt{p}}}{} = \operatorname{erfc}\left(\frac{2s^2\beta^2\xi^2}{t}\right),$$

then

$$A(t) = -(acD)\sum_{s=1}^{\infty} \int_0^t e^{-4\xi^2\beta^2 s^2} \varphi(\xi) \left\{ \frac{1}{\sqrt{\pi(t-\xi)}} e^{-4s^2\beta^2\frac{\xi^2}{t-\xi}} + \right.$$



Declassified in Part - Sanitized Copy Approved for Release 2012/03/12 : CIA-RDP82-00039R000100190014-6

Declassified in Part - Sanitized Copy Approved for Release 2012/03/12 : CIA-RDP82-00039R000100190014-6

$$+2s\beta\,\mathrm{erfc}\left(\frac{2s^2\beta^2\xi^2}{t-\xi}\right)\Big\}d\xi=-(acD)_1\int_0^t\varphi(\xi)\left\{\frac{\theta_1\left(0,e^{-4\beta^2\frac{t\xi}{t-\xi}}\right)-1}{2\sqrt{\pi(t-\xi)}}+\right.$$

$$\left.+2\beta_1\sum_{s=1}^{\infty}Se^{-4\xi^2\beta^2s^2}\,\mathrm{erfc}\left(\frac{2s^2\beta^2\xi^2}{t-\xi}\right)\right\}d\xi\,.$$

This interesting formula permits the computation of heat transfer through the earth's surface according to its temperature variation (during winter season). This result should be referred to point (a)

Medium 2

To find

$$X_2(t)=\kappa_2\int_0^t\frac{\partial}{\partial x}\theta_2(x,\tau)\Big|_{x=v\tau}d\tau\,,$$

given

$$\frac{\partial}{\partial t}\theta_2=a_2^2\frac{\partial^2}{\partial x^2}\theta_2\,;\ vt\leqslant x\leqslant h;\ 0\leqslant t\leqslant\frac{h}{v};$$

$$\theta\Big|_{x=vt}=0;\ \theta\Big|_{x=h}=\Phi(t)\geqslant 0;$$

$$\theta\Big|_{t=0}=f(x)\geqslant 0;\ 0\leqslant x\leqslant h;\ f(0)=0;\ \Phi(0)=f(h).$$



Declassified in Part - Sanitized Copy Approved for Release 2012/03/12 : CIA-RDP82-00039R000100190014-6

Declassified in Part - Sanitized Copy Approved for Release 2012/03/12 : CIA-RDP82-00039R000100190014-6

We look for a temperature function in the form:

$$\theta_2(x,t)=\frac{1}{a^2}\int_0^t\left[\lambda(\eta)e^{-\frac{(x-v\eta)^2}{4a^2(t-\eta)}}+\mu(\eta)e^{-\frac{(x-h)^2}{4a^2(t-\eta)}}\right]\frac{d\eta}{\sqrt{\pi(t-\eta)}}+$$

$$+\frac{2}{h}\sum_{n=1}^{\infty}e^{-\left(\frac{an\pi}{h}\right)^2 t}\sin\frac{n\pi}{h}x\int_0^h f(y)\sin\frac{n\pi y}{h}dy.$$

This integral satisfies the equation of thermal conductivity (for any $\lambda$ and $\mu$ ) and reduces to 0 for $t=0$. As far as the sum is concerned, it enters as a component in the solution of the limited shaft problem [10], and therefore it also satisfies the equation of thermal conductivity as well as the initial condition.

Thus, for determining the unknown functions $\lambda$ and $\mu$ there remain two boundary conditions ($x=vt$ and $x=h$). They yield two integral equations:

$$\frac{1}{a}\int_0^t\left[\lambda(\eta)e^{-\beta^2(t-\eta)}+\mu(\eta)e^{-\frac{(h-vt)^2}{4a^2(t-\eta)}}\right]\frac{d\eta}{\sqrt{\pi(t-\eta)}}+$$

$$+\frac{2}{h}\sum_{n=1}^{\infty}e^{-\left(\frac{a^2n\pi}{h}\right)^2 t}\sin\frac{n\pi vt}{h}\int_0^h f(y)\sin\frac{n\pi y}{h}dy=0. \quad (a)$$



Declassified in Part - Sanitized Copy Approved for Release 2012/03/12 : CIA-RDP82-00039R000100190014-6

Declassified in Part - Sanitized Copy Approved for Release 2012/03/12 : CIA-RDP82-00039R000100190014-6

$$\frac{1}{a_2}\int_0^t \left[\lambda(\eta)e^{-\frac{(h-v\eta)^2}{4a^2(t-\eta)}}+\mu(\eta)\right]\frac{d\eta}{\sqrt{\pi(t-\eta)}}=\Phi(t). \qquad (\beta)$$

Having found their operational versions, we have:

$$\overline{\frac{e^{-t}}{\sqrt{\pi t}}}=\frac{p}{\sqrt{p+1}}\ ,\ i.e.\ \overline{\frac{e^{-\beta^2 t}}{\sqrt{\pi t}}}=\frac{p}{\sqrt{p+\beta^2}}\ . \qquad (9)$$

According to the fold theorem:

$$\overline{\int_0^t \lambda(\eta)e^{-\beta^2(t-\eta)}\frac{d\eta}{\sqrt{\pi(t-\eta)}}}=\frac{\bar{\lambda}(p)}{\sqrt{p+\beta^2}}\ .$$

Furthermore,

$$A=\overline{\int_0^t \mu(\eta)e^{-\frac{(h-vt)^2}{4a^2(t-\eta)}}\frac{d\eta}{\sqrt{\pi(t-\eta)}}}=$$



Declassified in Part - Sanitized Copy Approved for Release 2012/03/12 : CIA-RDP82-00039R000100190014-6

Declassified in Part - Sanitized Copy Approved for Release 2012/03/12 : CIA-RDP82-00039R000100190014-6

$$= p\int_0^\infty \mu(\eta)\,d\eta \int_\eta^\infty e^{-pt-\frac{(h-vt)^2}{4a^2(t-\eta)}} \frac{dt}{\sqrt{\pi(t-\eta)}} =$$

$$= p\int_0^\infty \mu(\eta)\, e^{-p\eta+\frac{\beta}{a}(h-v\eta)}\,d\eta \int_0^\infty e^{-p\chi-\beta^2\chi-\frac{(h-v\eta)^2}{4a^2\chi}} \frac{d\chi}{\sqrt{\pi\chi}} =$$

$$= pe^{\frac{vh}{2a^2}} \int_0^\infty \mu(\eta)\, e^{-\eta(p+2\beta^2)}\,d\eta \int_0^\infty e^{-\chi(p+\beta^2)-\frac{(h-v\eta)^2}{4a^2\chi}} \frac{d\chi}{\sqrt{\pi\chi}} .$$

But

$$\overline{\frac{e^{-\frac{\lambda}{t}}}{\sqrt{\pi t}}} = \sqrt{p}\; e^{-2\sqrt{\lambda p}}$$

( $\lambda > 0$ condition is mandatory), therefore

$$A = pe^{\frac{\beta h}{a}} \int_0^\infty \mu(\eta)\, e^{-\eta(p+2\beta^2)\left|\frac{h}{a}-v\eta\right|\sqrt{p+\beta^2}} \frac{d\eta}{\sqrt{p+\beta^2}} .$$



Declassified in Part - Sanitized Copy Approved for Release 2012/03/12 : CIA-RDP82-00039R000100190014-6

Declassified in Part - Sanitized Copy Approved for Release 2012/03/12 : CIA-RDP82-00039R000100190014-6

Let us consider that, according to the conditions of the problem for $t=\frac{h}{v}$ the shaft reduces to a point with zero temperature. Let us take $\Phi\left(\frac{h}{v}\right)=0$, which is not a limitation, since $h$ is the depth to which freezing does not extend. Therefore, we can consider that $\theta|_{t\geq h:v}=0$ and, consequently, then $\lambda\equiv\mu\equiv 0$. Therefore in the integral for A we can, for $\eta\geq\frac{h}{v}$, arbitrarily change the factor of $\mu$.

Let

$$A=\frac{p}{\sqrt{p+\beta^2}}e^{-\frac{h}{a}(\sqrt{p+\beta^2}-\beta)}\int_0^\infty \mu(\eta)e^{-\eta(\sqrt{p+\beta^2}-\beta)^2}d\eta=$$

$$=\frac{p}{\sqrt{p+\beta^2}}e^{-\frac{h}{a}(\sqrt{p+\beta^2}-\beta)}\frac{\bar{\mu}\left[(\sqrt{p+\beta^2}-\beta)^2\right]}{(\sqrt{p+\beta^2}-\beta)^2}.$$

We introduce an expression $M(p)=\frac{\mu(p)}{p}$:

$$A=\frac{p}{\sqrt{p+\beta^2}}e^{-\frac{h}{a}(\sqrt{p+\beta^2}-\beta)}M\left[(\sqrt{p}+\beta^2-\beta)^2\right].$$

Now we find:

$$\underset{\rightarrow}{C}=\sum_{n=1}^{\infty}e^{-\left(\frac{an\pi}{h}\right)^2 t}\sin\frac{n\pi vt}{h}\int_0^t f(y)\sin\frac{n\pi}{h}y\,dy,$$



Declassified in Part - Sanitized Copy Approved for Release 2012/03/12 : CIA-RDP82-00039R000100190014-6

Declassified in Part - Sanitized Copy Approved for Release 2012/03/12 : CIA-RDP82-00039R000100190014-6

since

$$\overline{e^{-at}\sin\omega t} = \frac{\omega p}{(p+a)^2+\omega^2} ,$$

therefore

$$C = \frac{\pi v p}{h} \sum_{n=1}^{\infty} \frac{n \int_0^h f(y) \sin \frac{n\pi}{h} y \, dy}{\left[p+\left(\frac{an\pi}{n}\right)\right]^2 + \left(\frac{n\pi v}{h}\right)^2} .$$

We factor the common ter. into simplest, relative to $x = n^2$, fractions:

$$C = \frac{hp}{2a\pi\sqrt{p+\beta^2}} \int_0^h f(y)\,dy \left[ \sum_{n=1}^{\infty} \frac{n \sin \frac{n\pi}{n}}{n^2+\left[\frac{h}{a\pi}\left(\sqrt{p+\beta^2} \mp \beta\right)\right]^2} - \right.$$

$$\left. - \sum_{n=1}^{\infty} \frac{n \sin \frac{n\pi}{h}}{n^2+\left[\frac{h}{a\pi}\left(\sqrt{p+\beta^2}+\beta\right)\right]^2} \right] .$$



Declassified in Part - Sanitized Copy Approved for Release 2012/03/12 : CIA-RDP82-00039R000100190014-6

Declassified in Part - Sanitized Copy Approved for Release 2012/03/12 : CIA-RDP82-00039R000100190014-6

There is a formula (8):

$$\sum_{n=1}^{\infty} \frac{n \sin nx}{n^2+\alpha^2} = \frac{\pi}{2} \frac{\operatorname{sh}\alpha(\pi-x)}{\operatorname{sh}\alpha\pi}\,; \quad 0<x<2\pi. \qquad (8)$$

Therefore,

$$C = \frac{hp}{4a\sqrt{p+\beta^2}} \int_0^h f(y) \left[ \frac{\operatorname{sh}\frac{h-y}{a}(\sqrt{p+\beta^2}-\beta)}{\operatorname{sh}\frac{h}{a}(\sqrt{p+\beta^2}-\beta)} - \frac{\operatorname{sh}\frac{h-y}{a}(\sqrt{p+\beta^2}+\beta)}{\operatorname{sh}\frac{h}{a}(\sqrt{p+\beta^2}+\beta)} \right] dy.$$

We refer to the second integral equation:

$$D = \int_0^t \lambda(\eta) e^{-\frac{|h-v\eta|^2}{4a^2(t-\eta)}} \frac{d\eta}{\sqrt{\pi(t-\eta)}} =$$

$$= p \int_0^{\infty} \lambda(\eta)\, d\eta \int_{\eta}^{\infty} e^{-pt - \frac{|h-v\eta|^2}{4a^2(t-\eta)}} \frac{dt}{\sqrt{\pi(t-\eta)}} =$$

$$= \frac{\sqrt{p}}{p-2\beta\sqrt{p}} e^{-\frac{h}{a}\sqrt{p}}\, \bar{\lambda}\left[p-2\beta\sqrt{p}\right].$$



Declassified in Part - Sanitized Copy Approved for Release 2012/03/12 : CIA-RDP82-00039R000100190014-6

Declassified in Part - Sanitized Copy Approved for Release 2012/03/12 : CIA-RDP82-00039R000100190014-6

Let $\Lambda(p) = \frac{\lambda(p)}{p}$, then

$$D = \sqrt{p}\, e^{-\frac{h}{a}\sqrt{p}}\, \Lambda(p - 2\beta\sqrt{p});$$

$$\int_0^t \mu(\eta) \frac{d\eta}{\sqrt{\pi(t-\eta)}} = \sqrt{p}\, M(p).$$

Consequently

$$(\gamma)\begin{cases} \Lambda(p) + e^{-\frac{h}{a}(\sqrt{p+\beta^2}-\beta)} M\left[(\sqrt{p+\beta^2}-\beta)^2\right] + \frac{1}{2}\int_0^h f(y) \times \\ \times\left[\dfrac{\operatorname{sh}\frac{h-y}{a}(\sqrt{p+\beta^2}-\beta)}{\operatorname{sh}\frac{h}{a}(\sqrt{p+\beta^2}-\beta)} - \dfrac{\operatorname{sh}\frac{h-y}{a}(\sqrt{p+\beta^2}+\beta)}{\operatorname{sh}\frac{h}{a}(\sqrt{p+\beta^2}+\beta)}\right] dy = 0; \\ e^{-\frac{h}{a}\sqrt{p}}\, \Lambda(p - 2\beta\sqrt{p}) + M(p) = \dfrac{a}{\sqrt{p}}\, \overline{\Phi}(p). \end{cases}$$



Declassified in Part - Sanitized Copy Approved for Release 2012/03/12 : CIA-RDP82-00039R000100190014-6

Declassified in Part - Sanitized Copy Approved for Release 2012/03/12 : CIA-RDP82-00039R000100190014-6

Referring to the expression for $\theta_2$, we can obtain:

$$\left.\frac{\partial\theta}{\partial x}\right|_{x=vt} = \frac{1}{2a^3}\int_0^t \left[-v\lambda(\eta)e^{-\beta^2(t-\eta)} + \frac{h-vt}{t-\eta}\mu(\eta)e^{-\frac{(h-vt)^2}{4a^2(t-\eta)}}\right] \times$$

$$\times \frac{d\eta}{\sqrt{\pi(t-\eta)}} + \frac{2\pi}{h^2}\sum_{n=1}^{\infty} n e^{-\left(\frac{an\pi}{h}\right)^2 t} \cos\frac{n\pi v}{h} t \int_0^h f(y)\sin\frac{n\pi y}{h}\,dy .$$

Adding to this equation ($\alpha$) multiplied by $\frac{\beta}{a}$, we get:

$$x\left.\frac{\partial\theta}{\partial x}\right|_{x=vt} = \frac{x}{2a^3}\int_0^t \frac{h-v\eta}{\sqrt{\pi}(t-\eta)^{3/2}}\mu(\eta)e^{-\frac{(h-vt)^2}{4a^2(t-\eta)}}d\eta +$$

$$+ \frac{2x}{h}\sum_1^{\infty}\left(\frac{n\pi}{h}\cos\frac{n\pi vt}{h} + \frac{\beta}{a}\sin\frac{n\pi vt}{h}\right)e^{-\left(\frac{an\pi}{h}\right)^2 t}\int_0^h f(y)\sin\frac{n\pi y}{h}\,dy .$$

Denoting the first term as $E(t)$:

$$\bar{E}(p) = \frac{px}{2a^3}\int_0^{\infty}(h-v\eta)\mu(\eta)\,d\eta\int_0^{\infty} e^{-p(x+\eta)-\frac{(h-v\eta-vx)^2}{4a^2x}}\frac{dx}{x\sqrt{\pi x}} =$$



Declassified in Part - Sanitized Copy Approved for Release 2012/03/12 : CIA-RDP82-00039R000100190014-6

Declassified in Part - Sanitized Copy Approved for Release 2012/03/12 : CIA-RDP82-00039R000100190014-6

$$= \frac{pK}{a^2} e^{-\frac{h}{a}(\sqrt{p+\beta^2}-\beta)} \int_0^\infty \mu(\eta) e^{-\eta(\sqrt{p+\beta^2}-\beta)^2} d\eta =$$

$$= \frac{pK}{a^2} e^{-\frac{h}{a}(\sqrt{p+\beta^2}-\beta)} M\left[(\sqrt{p+\beta^2}-\beta)^2\right].$$

Denoting the second term as F(t):

$$\int_0^t F(\tau)\, d\tau =$$

$$= \frac{2K}{h} \sum_{n=1}^{\infty} \frac{e^{-\left(\frac{a_2 n\pi}{h}\right)^2 t}\left\{\frac{\beta^2}{a^2}\sin n\pi\frac{vt}{h} - \frac{h}{n\pi}\left[\frac{2}{a_2^2}\beta_2^2 + \left(\frac{n\pi}{h}\right)^2\right]\cos\frac{n\pi vt}{h}\right\} + \frac{h}{n\pi}\left[\frac{2}{a_2^2}\beta_2^2 + \left(\frac{n\pi}{h}\right)^2\right] t}{4\beta_2^2 + \left(\frac{a_2 n\pi}{h}\right)^2} \times$$

$$\times e^{-\left(\frac{a n\pi}{h}\right)^2 t} \int_0^h f(y) \sin\frac{n\pi y}{h}\, dy.$$

Eliminating $\Lambda$ from the $\gamma$ system; for this we get $\Lambda(p)$ from the first equation; forming $\Lambda(p-2\beta\sqrt{p})$ and substituting into the second equation we get:

$$M(p) - e^{-2\frac{h}{a}(\sqrt{p}-\beta)} M\left[(\sqrt{p}-2\beta)^2\right] =$$

$$= a\frac{\Phi(p)}{\sqrt{p}} + \frac{1}{2} e^{-\frac{h}{a}\sqrt{p}} \times$$



Declassified in Part - Sanitized Copy Approved for Release 2012/03/12 : CIA-RDP82-00039R000100190014-6

Declassified in Part - Sanitized Copy Approved for Release 2012/03/12 : CIA-RDP82-00039R000100190014-6

$$\times \int_0^h f(y)\left[\frac{\operatorname{sh}\frac{h-y}{a}(\sqrt{p}-2\beta)}{\operatorname{sh}\frac{h}{a}(\sqrt{p}-2\beta)} - \frac{\operatorname{sh}\frac{h-y}{a}\sqrt{p}}{\operatorname{sh}\frac{h}{a}\sqrt{p}}\right] dy = \sigma(p).$$

By the method of mathematical induction we can obtain a solution, correctness of which can be easily verified by the substitution:

$$M(p) = \sum_{n=0}^{\infty} e^{-2\frac{h}{a}(n\sqrt{p}-n^2\beta)}\, \sigma\left[(\sqrt{p}-2n\beta)^2\right].$$

Since we're looking for $X(t)$, we have to find:

$$\overline{E}(p) = cDe^{-\frac{h}{a}(\sqrt{p+\beta^2}-\beta)} M\left[(\sqrt{p+\beta^2}+\beta)^2\right] =$$

$$= cDe^{\frac{h\beta}{2a}} \sum_{n=0}^{\infty} e^{2\frac{\beta h}{a}\left(n+\frac{1}{2}\right)^2-(2n+1)\frac{h}{a}\sqrt{p+\beta^2}}\, \sigma\left\{\left[\sqrt{p+\beta^2}-(2n+1)\beta\right]^2\right\}.$$



Declassified in Part - Sanitized Copy Approved for Release 2012/03/12 : CIA-RDP82-00039R000100190014-6

Declassified in Part - Sanitized Copy Approved for Release 2012/03/12 : CIA-RDP82-00039R000100190014-6

We have introduced designations:

$$\sigma(p)=a\frac{\bar{\Phi}(p)}{\sqrt{p}}+\frac{1}{2}e^{-\frac{h}{a}\sqrt{p}}\int_0^h f(y)\left[\frac{\operatorname{sh}\frac{h-y}{a}(\sqrt{p}-2\beta)}{\operatorname{sh}\frac{h}{a}(\sqrt{p}-2\beta)}-\frac{\operatorname{sh}\frac{h-y}{a}\sqrt{p}}{\operatorname{sh}\frac{h}{a}\sqrt{p}}\right]dy=$$

$$=\frac{a}{\sqrt{p}}\left\{\bar{\Phi}(p)+\frac{\sqrt{p}}{2a}e^{-\frac{h}{a}\sqrt{p}}\int_0^h f(y)\left[\frac{\operatorname{sh}\frac{h-y}{a}(\sqrt{p}-2\beta)}{\operatorname{sh}\frac{h}{a}(\sqrt{p}-2\beta)}-\frac{\operatorname{sh}\frac{h-y}{a}\sqrt{p}}{\operatorname{sh}\frac{h}{a}\sqrt{p}}\right]dy\right\}$$

Expression inside the outside parentheses can be represented as a description of the fictitious temperature:



Declassified in Part - Sanitized Copy Approved for Release 2012/03/12 : CIA-RDP82-00039R000100190014-6

Declassified in Part - Sanitized Copy Approved for Release 2012/03/12 : CIA-RDP82-00039R000100190014-6

$$u(t) = \Phi(t) + \frac{\sqrt{p}}{2a} e^{-\frac{h}{a}\sqrt{p}} \int_0^h f(y) \left[ \quad \right] dy .$$

Working out the last expression:

$$\overline{A}(p) = \sqrt{p}\, e^{-\frac{h}{a}\sqrt{p}} \left[ \frac{\operatorname{sh} \frac{h-y}{a}(\sqrt{p} - 2\beta)}{\operatorname{sh} \frac{h}{a}(\sqrt{p} - 2\beta)} - \frac{\operatorname{sh} \frac{h-y}{a}\sqrt{p}}{\operatorname{sh} \frac{h}{a}\sqrt{p}} \right].$$

Expressing it as a series yields:

$$\frac{\operatorname{sh} \frac{h-y}{a}(\sqrt{p} - 2\beta)}{\operatorname{sh} \frac{h}{a}(\sqrt{p} - 2\beta)} = \sum_{s=0}^{\infty} e^{-\frac{2sh+y}{a}\sqrt{p} + 2\frac{\beta}{a}(2sh+y)} - \sum_{s=1}^{\infty} e^{-\frac{2sh-y}{a}\sqrt{p} + 2\frac{\beta}{a}(2sh-y)}.$$

Consequently:

$$\overline{A}(p) = \sqrt{p} \left\{ \sum_{s=0}^{\infty} e^{-\frac{(2s+1)h+y}{a}\sqrt{p}} \left[ e^{2\frac{\beta}{a}(2sh+y)} - 1 \right] - \right.$$



Declassified in Part - Sanitized Copy Approved for Release 2012/03/12 : CIA-RDP82-00039R000100190014-6

Declassified in Part - Sanitized Copy Approved for Release 2012/03/12 : CIA-RDP82-00039R000100190014-6

$$-\sum_{s=1}^{\infty} e^{-\frac{(2s+1)h-y}{a}\sqrt{p}}\left[e^{2\frac{\beta}{a}(2sh-y)}-1\right]\Bigg\};$$

$$A(t)=\frac{1}{\sqrt{\pi t}}\Bigg\{\sum_{s=0}^{\infty} e^{-\left[\frac{(2s+1)h+y}{2a}\right]^2\frac{1}{t}}\left[e^{2\frac{\beta}{a}(2sh+y)}-1\right]-$$

$$-\sum_{s=1}^{\infty} e^{-\left[\frac{(2s+1)h-y}{2a}\right]^2\frac{1}{t}}\left[e^{2\frac{\beta}{a}(2sh-y)}-1\right]\Bigg\}=$$

$$=\frac{2}{\sqrt{\pi t}}\Bigg\{e^{-\left(\frac{h+y}{2a}\right)^2\frac{1}{t}+\frac{\beta}{a}y}\operatorname{sh}\frac{\beta}{a}y+\sum_{s=1}^{\infty}\Bigg[e^{-\left[\frac{(2s+1)h+y}{2a}\right]^2\frac{1}{t}+\frac{\beta}{a}(2sh+y)}\times$$

$$\times\operatorname{sh}\frac{\beta}{a}(2hs+y)-e^{-\left[\frac{(2s+1)h-y}{2a}\right]^2\frac{1}{t}+\frac{\beta}{a}(2sh-y)}\operatorname{sh}\frac{\beta}{a}(2hs-y)\Bigg]\Bigg\}.$$



Declassified in Part - Sanitized Copy Approved for Release 2012/03/12 : CIA-RDP82-00039R000100190014-6

Declassified in Part - Sanitized Copy Approved for Release 2012/03/12 : CIA-RDP82-00039R000100190014-6

In view of the rapid convergence A(t) can be conveniently determined, consequently

$$u(\xi) = \Phi(\xi) + \frac{1}{2a}\int_0^h f(y)A(\xi)\,dy\ ;$$

$$\frac{\bar{E}(p)}{p} = acDe^{\frac{h\beta}{2a}} \sum_{n=0}^{\infty} e^{\frac{2h}{a}\beta\left(n+\frac{1}{2}\right)^2 - (2n+1)\frac{h}{a}\sqrt{p+\beta^2}} \times$$

$$\times \frac{\bar{u}\left[\left(\sqrt{p+\beta^2} - (2n+1)\beta\right)^2\right]}{\sqrt{p+\beta^2} - (2n+1)\beta}\ ;$$

but

$$e^{-(2n+1)\frac{h}{a}\sqrt{p+\beta^2}} \frac{\bar{u}\left[\left(\sqrt{p+\beta^2} - (2n+1)\beta\right)^2\right]}{\sqrt{p+\beta^2} - (2n+1)\beta} = \int_0^{\infty} u(\xi)w(t,\xi)\,d\xi\ ,$$



Declassified in Part - Sanitized Copy Approved for Release 2012/03/12 : CIA-RDP82-00039R000100190014-6

Declassified in Part - Sanitized Copy Approved for Release 2012/03/12 : CIA-RDP82-00039R000100190014-6

where

$$\overline{w}(p,\xi)=\left[\sqrt{p+\beta^2}-(2n+1)\beta\right]e^{-\xi\left[p+(4n^2+4n+2)\beta^2\right]-(2n+1)\frac{h-v\xi}{a}\sqrt{p+\beta^2}},$$

therefore

$$\int_0^\infty u(\xi)w(t,\xi)\,d\xi=\int_0^t e^{-\xi\left[(2n+1)^2+1\right]\beta^2}u(\xi)w_1(t-\xi,\xi)\,d\xi,$$

where

$$\overline{w}_1(p,\xi)=\left[\sqrt{p+\beta^2}-(2n+1)\beta\right]e^{-(2n+1)\frac{h-v\xi}{a}\sqrt{p+\beta^2}},$$



Declassified in Part - Sanitized Copy Approved for Release 2012/03/12 : CIA-RDP82-00039R000100190014-6

Declassified in Part - Sanitized Copy Approved for Release 2012/03/12 : CIA-RDP82-00039R000100190014-6

that is,

$$w_1(t,\xi)=\frac{1}{\sqrt{\pi t}}\,e^{-\frac{(2n+1)^2}{t}\left(\frac{h-v\xi}{2a}\right)^2-\beta^2 t}\,-\beta\quad\times$$

$$\times\left\{ne^{-\beta\frac{h-v\xi}{a}(2n+1)}\operatorname{erfc}\left[(2n+1)\frac{h-v\xi}{2a\sqrt{t}}-\beta\sqrt{t}\right]+\right.$$

$$\left.+(n+1)e^{\beta\frac{h-v\xi}{a}(2n+1)}\operatorname{erfc}\left[(2n+1)\frac{h-v\xi}{2a\sqrt{t}}+\beta\sqrt{t}\right]\right\}.$$

$$\int_0^\infty u(\xi)w(t,\xi)\,d\xi=\int_0^t e^{-\xi\beta^2[(2n+1)^2+1]}u(\xi)\cdot\left(\frac{1}{\sqrt{\pi(t-\xi)}}\cdot e^{-\frac{(2n+1)^2}{t-\xi}\left(\frac{h-v\xi}{2a}\right)^2-\beta^2(t-\xi)}\right.$$

$$-\beta\left\{ne^{-\beta\frac{h-v\xi}{a}(2n+1)}\operatorname{erfc}\left[(2a+1)\frac{h-v\xi}{2a\sqrt{t-\xi}}-\beta\sqrt{t-\xi}\right]+\right.$$

$$\left.\left.+(n+1)e^{\beta\frac{h-v\xi}{a}(2n+1)}\operatorname{erfc}\left[(2a+1)\frac{h-v\xi}{2a\sqrt{t-\xi}}+\beta\sqrt{t-\xi}\right]\right\}\right)d\xi.$$



Declassified in Part - Sanitized Copy Approved for Release 2012/03/12 : CIA-RDP82-00039R000100190014-6

Declassified in Part - Sanitized Copy Approved for Release 2012/03/12 : CIA-RDP82-00039R000100190014-6

The factor with $\dfrac{(acD)_2\, u(\xi)}{\sqrt{\pi(t-\xi)}}$ is

$$\sum_{n=0}^{\infty} e^{\frac{h\beta_2}{2a_2} + 2\frac{h}{a_2}\left(n+\frac{1}{2}\right)^2\beta - \xi\beta_2^2\left[(2n+1)^2+1\right] - \frac{(2n+1)^2}{t-\xi}\left(\frac{h-v\xi}{2a}\right)^2 - \beta^2(t-\xi)} =$$

$$= \frac{1}{2} e^{\frac{\beta_2}{2a_2}(h-vt)}\, \theta_2\left(0, e^{-\frac{(h-vt)(h-v\xi)}{a^2(t-\xi)}}\right).$$

After elementary transformations we have:

$$\frac{\bar{E}(p)}{p} = (acD)_2 \int_0^t u(\xi)\left\{\theta_2\left(0, e^{-\frac{(h-v\xi)(h-vt)}{a_2^2(t-\xi)}}\right) \times\right.$$



Declassified in Part - Sanitized Copy Approved for Release 2012/03/12 : CIA-RDP82-00039R000100190014-6

Declassified in Part - Sanitized Copy Approved for Release 2012/03/12 : CIA-RDP82-00039R000100190014-6

$$\times \frac{e^{\frac{\beta}{2a}(h-vt)}}{2\sqrt{\pi(t-\xi)}} - \beta \sum_{n=1}^{\infty} n e^{2n^2 \frac{\beta}{a}(h-v\xi)} \left[ \operatorname{erfc} \frac{2n(h-v\xi)+h-vt}{2a\sqrt{t-\xi}} + \right.$$

$$\left. + \operatorname{erfc} \frac{2n(h-v\xi)(h-vt)}{2a\sqrt{t-\xi}} \right] \Bigg\} d\xi \cdots$$

Considering the aryptotic expression (7)

$$\operatorname{erfc} \Phi(u) \sim \frac{e^{-u^2}}{\sqrt{\pi}\, u} \sum_{n=0}^{\infty} (-1)^n \frac{1 \cdot 3 \cdot 5 (2n-1)}{(2u^2)^n},$$

it is easy to show the convergence of the series contained in the function under the integral sign. Stefan's condition finally yields:

$$\lambda \rho v t = -(acD)_1 \int_0^t \varphi(\xi) \left\{ \frac{e^{-\beta_1^2 t}}{2\sqrt{\pi(t-\xi)}} \theta_2 \left(0, e^{-4\beta_1^2 \frac{t\xi}{t-\xi}}\right) + \right.$$



Declassified in Part - Sanitized Copy Approved for Release 2012/03/12 : CIA-RDP82-00039R000100190014-6

Declassified in Part - Sanitized Copy Approved for Release 2012/03/12 : CIA-RDP82-00039R000100190014-6

$$+\beta_1\sum_{n=1}^{\infty} n e^{-4n^2\beta_1^2\xi}\left[\operatorname{erfc}\beta_1\frac{2n\xi-t}{\sqrt{t-\xi}}+\operatorname{erfc}\beta_1\frac{2n\xi+t}{\sqrt{t-\xi}}\right]\Bigg\}-$$

$$-(acD)_2\int_0^t u(\xi)\left\{\frac{e^{\frac{\beta_2}{2a_2}(h-vt)}}{2\sqrt{\pi(t-\xi)}}\,\theta_2\left(0,e^{-\frac{(h-v\xi)(h-vt)}{a_2^2(t-\xi)}}\right)-\right.$$

$$-\beta_2\sum_{n=1}^{\infty} n e^{2n^2\beta_2^2\frac{h-\xi v}{a_2}}\left[\operatorname{erfc}\frac{2n(h-v\xi)+h-vt}{2a_2\sqrt{t-\xi}}+\operatorname{erfc}\frac{2n(h-v\xi)-(h-vt)}{2a_2\sqrt{t-\xi}}\right]\Bigg\}d\xi-$$

$$-\int_0^t F(\tau)\,d\tau\,.$$

The values $u(\xi)$ and $\int_0^t F(\tau)\,d\tau$ were given above.

Here v, and consequently $\beta$ are functions of t, but the equation itself is finally relative to v. The complex form of the equation forces us to use a solution by the method of successive approximations.



Declassified in Part - Sanitized Copy Approved for Release 2012/03/12 : CIA-RDP82-00039R000100190014-6

Declassified in Part - Sanitized Copy Approved for Release 2012/03/12 : CIA-RDP82-00039R000100190014-6

$(acD)_1 \int_0^t$ expresses the upward flow of heat from the freezing front; $(acD)_2 \int_0^t$ is the heat flow toward the bottom freezing front.

To simplify the computational work we should select such initial conditions as would have the least effect on the result. Therefore h should be taken as small as possible.

Example: Finding suitable data for a numerical example presents considerable difficulties. Before everything else it should be noted that the literature has no data on ground freezing connected with the variation of ground temperature. Therefore we had to limit ourselves to observations of ground temperatures made in Pavlovsk during the winter of 1901 - 1902 [17], taking the 0 degree isotherm as the boundary between two phases. The second circumstance which considerably complicates carrying out the computation is the unavailability in the Annals of thermophysical constants of the ground. These had to be determined from data of analogous soil (in the Forestry Institute). Therefore, the given computation must be looked upon mainly as an illustration.

The computation was performed for exposed ground, since under this condition, freezing penetrates more deeply, and, therefore, the laws that obtain can be observed more clearly.

Analytical determination of the coefficient of temperature conductivity yields the values

$A_1^2 = 1900$ square centimeters/month $A_2^2 = 5200$ square centimeters/month



Declassified in Part - Sanitized Copy Approved for Release 2012/03/12 : CIA-RDP82-00039R000100190014-6

Declassified in Part - Sanitized Copy Approved for Release 2012/03/12 : CIA-RDP82-00039R000100190014-6

According to [12] we take $(cD)_1 = (cD)_2 = 0.5$.

Since observations in Slutsk were made on a sandy hill, where conditions were favorable for water flow, we took $\rho = 0.1$.

The function $\varphi(t)$ was smoothed out, its values being taken as the average monthly data from [11]. The initial time was determined graphically to be 1 November 1901. Unit of time was taken to be one month.

| t | 0 | 0.5 | 1.5 | 2.5 | 3.5 | 4.5 | 5.2 |
|---|---|---|---|---|---|---|---|
| $\varphi(t)$ | 0° | −3.9 | −9.7 | −10.3 | −8.0 | −3.7 | 0 |

$h = 160$ centimeters

| t | 0 | 1 | 2 | 3 | 4 | 5 | 5.2 |
|---|---|---|---|---|---|---|---|
| $\Phi(t)$ | 6.9° | 4.4 | 2.5 | 1.1 | 0.7 | 0.6 | 0.7 |

Computation was performed for $t = 5.2$, with the selection of the maximum period during which it is possible to dispense with the theory of thawing. Thus, we can get an idea on the maximum accumulation of errors.

Under the conditions at Pavlovsk the maximum depth of freezing is reached before the advent of spring $\varphi = 0$. As was pointed out by N. K. Malkin, candidate of physico-mathematical sciences, application of quasilinear theory to a region where the function is a maximum should result in a supplementary error. Therefore, in this example we selected the least favorable case.



Declassified in Part - Sanitized Copy Approved for Release 2012/03/12 : CIA-RDP82-00039R000100190014-6

Declassified in Part - Sanitized Copy Approved for Release 2012/03/12 : CIA-RDP82-00039R000100190014-6

After 2 trials we took $v = 15$ centimeters per month; therefore around 6 April 1902 freezing had to penetrate the depth $\xi(5.2) = 15 \cdot 5.2 = 78$ centimeters. With this, it turned out that there were 122 calories of heat supplied from below, 625 calories of heat $= L\rho\xi$ were liberated through freezing, 684 calories flowed upward from the freezing front (all for a column one square centimeter in cross-section). 1. For $v = 20$ cm/month $\frac{L\rho\xi}{\int_0^\tau \frac{\partial\theta}{\partial x}\Big|_{x=v\tau} d\tau} \cong -1.25$; for $v = 25$ cm/month $\frac{L\rho\xi}{\int_0^\tau \frac{\kappa}{t}} \cong -2.8$.

Since $625 + 122 > 684$, this indicates that v should be slightly decreased. Effect of the initial conditions turned out to be completely negligible. The greatest portion of the computation is given in the supplement.

No further elaboration of the results was made, since the nearest depth, for which control is possible, according to [17], is $h = 40$ centimeters.

## THAWING OF GROUND

When the earth's temperature becomes positive, we get 3 media with 4 boundaries, 2 of which are movable.

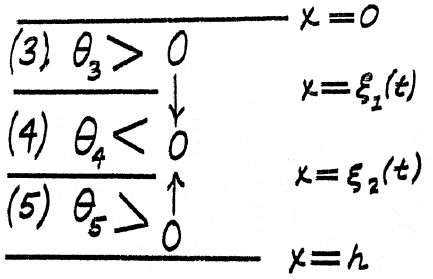




Declassified in Part - Sanitized Copy Approved for Release 2012/03/12 : CIA-RDP82-00039R000100190014-6

Declassified in Part - Sanitized Copy Approved for Release 2012/03/12 : CIA-RDP82-00039R000100190014-6

In the media (3) and (5) the thermophysical constants are of index 2, and in medium (4) they are of index 1.

Again we base ourselves on the quasilinear theory. Taking the line of transition of the earth's surface to positive temperatures, as initial moment, that is, $\varphi(0) = 0$.

$$\xi_1(0) = 0 \quad \text{and} \quad \xi_2 = \xi_0 .$$

From the preceding we can immediately obtain

$$\varkappa_1 \int_0^t \left.\frac{\partial \theta_3}{\partial x}\right|_{x=v\tau} d\tau .$$

For the medium (4) the solution is to be sought in the form:

$$\theta_4 = \frac{1}{a_1}\int_0^t \left[\lambda(\eta) e^{-\frac{(x-v_1\eta)^2}{4a_1^2(t-\eta)}} + \mu(\eta) e^{-\frac{(x-\xi_0+v_2\eta)^2}{4a_1^2(t-\eta)}}\right]\frac{d\eta}{\sqrt{\pi(t-\eta)}} +$$

$$+ \frac{2}{\xi_0}\sum_{n=1}^{\infty} e^{-\left(\frac{an\pi}{\xi_0}\right)^2 t} \sin n\pi\frac{x}{\xi_0}\int_0^h f(y)\sin n\pi\frac{y}{\xi_0}\,dy .$$



Declassified in Part - Sanitized Copy Approved for Release 2012/03/12 : CIA-RDP82-00039R000100190014-6

Declassified in Part - Sanitized Copy Approved for Release 2012/03/12 : CIA-RDP82-00039R000100190014-6

f(y) should be given in $[0, \xi_0]$

Boundary conditions yield:

$$\frac{1}{a_1}\int_0^t \left[\lambda(\eta)e^{-\beta_1^2(t-\eta)} + \mu(\eta)e^{-\frac{(v_2 t + v_2\eta - \xi_0)^2}{4a_1^2(t-\eta)}}\right]\frac{d\eta}{\sqrt{\pi(t-\eta)}} +$$

$$+ \frac{2}{\xi_0}\sum_{n=1}^{\infty} e^{-\left(\frac{a_1 n\pi}{\xi_0}\right)^2 t} \sin\frac{n\pi}{\xi_0} v_1 t \int_0^h f(y)\sin\frac{n\pi}{\xi_0} y\, dy = 0;$$

$$\frac{1}{a_1}\int_0^t \left[\lambda(\eta)e^{-\frac{(\xi_0 - v_1\eta - v_2 t)^2}{4a_1^2(t-\eta)}} + \mu(\eta)e^{-\beta_{2.1}^2(t-\eta)}\right]\frac{d\eta}{\sqrt{\pi(t-\eta)}} +$$

$$+ \frac{2}{\xi_0}\sum_{n=1}^{\infty} e^{-\left(\frac{a_1 n\pi}{\xi_0}\right)^2 t} \sin\frac{n\pi}{\xi_0}(\xi_0 - v_1 t)\int_0^h f(y)\sin\frac{n\pi}{\xi_0} y\, dy = 0;$$

$$\beta_{2.1} = \frac{v_2}{2a_1}.$$



Declassified in Part - Sanitized Copy Approved for Release 2012/03/12 : CIA-RDP82-00039R000100190014-6

Declassified in Part - Sanitized Copy Approved for Release 2012/03/12 : CIA-RDP82-00039R000100190014-6

We can also conduct computations for the medium (5). Thus we obtain 2 systems with 2 integral equations each for the determination of 4 functions.

Applying Stefan's conditions to the two movable boundaries yields a system of two equations for the determination of $v_1$ and $v_2$.

However, it is characteristic of seasonal freezing that thawing takes place considerably faster at the top than below. Basing on this we get a more practical and sufficiently accurate method of solution: we consider

$$\xi_2(t) = \xi_0 = \text{constant and } f_0(x) = 0.$$

The latter is based on the fact that while the earth's surface temperature is changing from negative to positive, the frozen layer is still at a negative temperature close to zero degrees.

Therefore

$$\left.\frac{\partial \theta_4}{\partial x}\right|_{x=\xi_1(t)} = 0$$

and Stefan's condition yields:

$$L\rho v_1 = -(acD)_2 \int_0^{\infty} \varphi(\xi)\left\{\frac{e^{-\beta^2 t}}{2\sqrt{\pi(t-\xi)}}\,\theta_2\left(0, e^{-4\beta^2 \frac{t\xi}{t-\xi}}\right) + \right.$$

$$\left. + \beta \sum_{n=1}^{\infty} n e^{-4n^2\beta^2\xi}\left[\operatorname{erfc}\beta\frac{2n\xi - t}{\sqrt{t-\xi}} + \operatorname{erfc}\beta\frac{2n\xi + t}{\sqrt{t-\xi}}\right]\right\} d\xi;$$

$$\beta = \frac{v_1}{2a_2}.$$



Declassified in Part - Sanitized Copy Approved for Release 2012/03/12 : CIA-RDP82-00039R000100190014-6

Declassified in Part - Sanitized Copy Approved for Release 2012/03/12 : CIA-RDP82-00039R000100190014-6

The same formula applies to the computation of summertime thawing of perpetual frozen states. With the advent of winter 3 media are formed with 4 boundaries two of which are movable.



Declassified in Part - Sanitized Copy Approved for Release 2012/03/12 : CIA-RDP82-00039R000100190014-6

Declassified in Part - Sanitized Copy Approved for Release 2012/03/12 : CIA-RDP82-00039R000100190014-6

SUPPLEMENT

COMPUTATION FOR FREEZING for v = 15 cm/month, t = 5.2 months

A. Computation $K_1 \int_0^t \frac{\partial \theta_1}{\partial x}\Big|_{x=v\tau} d\tau$

| $\xi$ | $-4\beta_1^2 M\xi$ | $t-\xi$ | $\lg q$ | $\alpha$ | $\theta_2(q,0)$ | $\frac{e^{-\beta_1^2 t}}{2\sqrt{\pi(t-\xi)}}\theta_2(q,0)$ |
|---|---|---|---|---|---|---|
| 0.5 | 9.9742 | 4.7 | 9.9715 | | 6.924 | 0.772 |
| 1.5 | 9.9229 | 3.7 | 9.8916 | | 3.544 | 0.446 |
| 2.5 | 9.8713 | 2.7 | 9.7520 | | 2.340 | 0.3444 |
| 3.5 | 9.8199 | 1.7 | 9.4499 | | 1.570 | 0.2912 |
| 4.5 | 9.7682 | 0.7 | 8.28 | $30^0 50'.8$ | 0.7035 | 0.2034 |

Where the column $\alpha$ has empty squares $\theta_2$ was computed by formula (7).

$$\theta_2(q,0) = \sqrt{-\frac{\pi M}{\lg q}}\,\theta_0\left(\frac{(\pi M)^2}{\lg q}, 0\right)$$

| $\xi$ | $\frac{(\pi M)^2}{\lg q} = \lg q'$ | $\alpha$ | $\theta_0(q',0)$ | $\sqrt{-\frac{\pi M}{\lg q}}$ |
|---|---|---|---|---|
| 0.5 | — 65.6 | 0 | 1 | 6.924 |
| 1.5 | — 18.61 | 0 | 1 | 3.544 |
| 2.5 | — 7.51 | 0 | 1 | 2.34 |
| 3.5 | — 3.375 | 0 | 1 | 1.57 |



Declassified in Part - Sanitized Copy Approved for Release 2012/03/12 : CIA-RDP82-00039R000100190014-6

Declassified in Part - Sanitized Copy Approved for Release 2012/03/12 : CIA-RDP82-00039R000100190014-6

$2n\xi - t$

| $\xi$ \ $n$ | 1 | 2 | 3 | 4 | 5 | 6 | 7 | 8 | 9 | 10 | 11 |
|---|---|---|---|---|---|---|---|---|---|---|---|
| 0.5 | -4.2 | -3.2 | -2.2 | -1.2 | -0.2 | 0.8 | 1.8 | 2.8 | 3.8 | 4.8 | 5.8 |
| 1.5 | -2.2 | 0.8 | 3.8 | 6.8 | 9.8 | | | | | | |
| 2.5 | -0.2 | 4.8 | | | | | | | | | |
| 3.5 | 1.8 | 8.8 | | | | | | | | | |
| 4.5 | 3.8 | | | | | | | | | | |

$2n\xi + t$

| $\xi$ \ $n$ | 1 | 2 | 3 | 4 | 5 | 6 | 7 | 8 | 9 | 10 | 11 |
|---|---|---|---|---|---|---|---|---|---|---|---|
| 0.5 | 6.2 | 7.2 | 8.2 | 9.2 | 10.2 | 11.2 | 12.2 | 13.2 | 14.2 | 15.2 | 16.2 |
| 1.5 | 8.2 | 11.2 | 14.2 | 17.2 | 20.2 | | | | | | |
| 2.5 | 10.2 | 15.2 | | | | | | | | | |
| 3.5 | 12.2 | 19.2 | | | | | | | | | |
| 4.5 | 14.2 | | | | | | | | | | |

$\beta_1 \frac{2n\xi - t}{\sqrt{t - \xi}}$

| $\xi$ \ $n$ | 1 | 2 | 3 | 4 | 5 | 6 | 7 | 8 | 9 | 10 | 11 |
|---|---|---|---|---|---|---|---|---|---|---|---|
| 0.5 | -0.333 | -0.254 | -0.174 | -0.095 | -0.016 | 0.063 | 0.143 | 0.222 | 0.316 | 0.380 | 0.460 |
| 1.5 | -0.197 | 0.072 | 0.339 | 0.608 | 0.876 | | | | | | |
| 2.5 | -0.021 | 0.502 | | | | | | | | | |
| 3.5 | 0.238 | 1.161 | | | | | | | | | |
| 4.5 | 0.782 | | | | | | | | | | |



Declassified in Part - Sanitized Copy Approved for Release 2012/03/12 : CIA-RDP82-00039R000100190014-6

Declassified in Part - Sanitized Copy Approved for Release 2012/03/12 : CIA-RDP82-00039R000100190014-6

$$\beta_1 \frac{2n\xi + t}{\sqrt{t-\xi}}$$

| $\xi$ \ $n$ | 1 | 2 | 3 | 4 | 5 | 6 | 7 | 8 | 9 | 10 | 11 |
|---|---|---|---|---|---|---|---|---|---|---|---|
| 0.5 | 0.492 | 0.571 | 0.650 | 0.730 | 0.810 | 0.890 | 0.969 | 1.049 | 1.128 | 1.204 | 1.276 |
| 1.5 | 0.733 | 1.000 | 1.269 | 1.538 | | | | | | | |
| 2.5 | 1.068 | 1.590 | | | | | | | | | |
| 3.5 | 1.61 | 2.528 | | | | | | | | | |
| 4.5 | 2.92 | | | | | | | | | | |

$$erfc\beta_1 \frac{2n\xi - t}{\sqrt{t-\xi}}$$

| $\xi$ \ $n$ | 1 | 2 | 3 | 4 | 5 | 6 | 7 | 8 | 9 | 10 | 11 |
|---|---|---|---|---|---|---|---|---|---|---|---|
| 0.5 | 1.3623 | 1.2804 | 1.1948 | 1.1069 | 1.0179 | 0.9285 | 0.8403 | 0.7536 | 0.6550 | 0.5909 | 0.5152 |
| 1.5 | 1.2194 | 0.9194 | 0.6316 | 0.3899 | 0.2154 | | | | | | |
| 2.5 | 1.0236 | 0.4777 | | | | | | | | | |
| 3.5 | 0.7364 | 0.1006 | | | | | | | | | |
| 4.5 | 0.2688 | | | | | | | | | | |



Declassified in Part - Sanitized Copy Approved for Release 2012/03/12 : CIA-RDP82-00039R000100190014-6

Declassified in Part - Sanitized Copy Approved for Release 2012/03/12 : CIA-RDP82-00039R000100190014-6

$$erfc\,\beta_1 \frac{2n\xi + t}{\sqrt{t-\xi}}$$

| $\xi$ \ $n$ | 1 | 2 | 3 | 4 | 5 | 6 | 7 | 8 | 9 | 10 |
|---|---|---|---|---|---|---|---|---|---|---|
| 0.5 | 0.4866 | 0.4194 | 0.3580 | 0.3019 | 0.2520 | 0.2082 | 0.1706 | 0.1379 | 0.1107 | 0.[redacted] .0886 |
| 1.5 | 0.2999 | 0.1573 | 0.0727 | 0.0296 | 0.0100 | | | | | |
| 2.5 | 0.1309 | 0.0245 | | | | | | | | |
| 3.5 | 0.0228 | | | | | | | | | |

$$erfc\,\beta_1 \frac{2n\xi - t}{\sqrt{t-\xi}} + erfc\,\beta_1 \frac{2n\xi + t}{\sqrt{t-\xi}}$$

| $\xi$ \ $n$ | 1 | 2 | 3 | 4 | 5 | 6 | 7 | 8 | 9 | 10 | 11 |
|---|---|---|---|---|---|---|---|---|---|---|---|
| 0.5 | 1.8497 | 1.6998 | 1.5528 | 1.4088 | 1.2699 | 1.1367 | 1.0109 | 0.8915 | 0.7657 | 0.6791 | 0.5863 |
| 1.5 | 1.5193 | 1.0767 | 0.7043 | 0.4195 | 0.2254 | | | | | | |
| 2.5 | 1.1545 | 0.5022 | | | | | | | | | |
| 3.5 | 0.7592 | 0.1009 | | | | | | | | | |
| 4.5 | 0.2688 | | | | | | | | | | |



Declassified in Part - Sanitized Copy Approved for Release 2012/03/12 : CIA-RDP82-00039R000100190014-6

Declassified in Part - Sanitized Copy Approved for Release 2012/03/12 : CIA-RDP82-00039R000100190014-6

$-4n^2\beta_1^2\xi M$

| ξ \ n | 1 | 2 | 3 | 4 | 5 | 6 | 7 | 8 | 9 | 10 | 11 |
|---|---|---|---|---|---|---|---|---|---|---|---|
| 0.5 | 9.9743 | 9.8971 | 9.7685 | 9.5899 | 9.358 | 9.075 | 8.740 | 8.352 | 7.92 | 7.43 | 6.9 |
| 1.5 | 9.9230 | 9.692 | 9.3075 | 8.770 | 8.079 | 7.23 | 6.270 | | | | |
| 2.5 | 9.8720 | 9.488 | | | | | | | | | |
| 3.5 | 9.8211 | 9.285 | | | | | | | | | |
| 4.5 | 9.7701 | | | | | | | | | | |

$$ne^{-4n^2\beta_1^2\xi}\left[\operatorname{erfc}\frac{2n\xi-t}{\sqrt{t-\xi}}+\operatorname{erfc}\beta_1\frac{2n\xi+t}{\sqrt{t-\xi}}\right]$$

| ξ \ n | 1 | 2 | 3. | 4 | 5 | 6 | 7 | 8 | 9 | 10 | 11 |
|---|---|---|---|---|---|---|---|---|---|---|---|
| 0.5 | 1.742 | 2.65 | 2.73 | 2.19 | 1.45 | 0.81 | 0.43 | 0.25 | 0.06 | 0.002 | 0.001 |
| 1.5 | 1.279 | 1.06 | 0.43 | 0.10 | 0.01 | | | | | | |
| 2.5 | 0.859 | 0.31 | | | | | | | | | |
| 3.5 | 0.759 | 0.04 | | | | | | | | | |
| 4.5 | 0.158 | | | | | | | | | | |



Declassified in Part - Sanitized Copy Approved for Release 2012/03/12 : CIA-RDP82-00039R000100190014-6

Declassified in Part - Sanitized Copy Approved for Release 2012/03/12 : CIA-RDP82-00039R000100190014-6

| $\xi$ | 0.5 | 1.5 | 2.5 | 3.5 | 4.5 | 5.2 |
|---|---|---|---|---|---|---|
| $\sum_{n=1}^{\infty}$ | 12.34 | 2.88 | 1.17 | 0.80 | 0.16 | |
| $\beta_1 \sum_{n=1}^{\infty}$ | 2.12 | 0.50 | 0.21 | 0.14 | 0.03 | |
| $\{\ \}$ | 2.89 | 0.95 | 0.55 | 0.43 | 0.23 | |
| $y$ | -11.3 | -9.2 | -5.7 | -3.4 | -0.8 | |

$\{\ \}$ denotes a factor of $\varphi(\xi)$ under the sign $\int_0^t$;

y - function under the integral sign.

$$v\big|_{\xi=0} = \frac{\varphi'(0)}{4\beta_1} = -11.8.$$

$$y\big|_{\xi=t} = 0.$$

Graphical integration yielded 31.4 and upon multiplying by (acD), 684 calories. This is the quantity of heat transmitted upward from the freezing front.

B. Computation $k_2 \int_0^t \frac{\partial \theta_2}{\partial x}\Big|_{x=v\tau} d\tau$

| $\xi$ | $v\xi$ | $h-v\xi$ | $t-\xi$ | $\lg q$ | $\alpha$ | $\theta_2(0,q)$ |
|---|---|---|---|---|---|---|
| 1 | 15 | 145 | 4.2 | 9.764 | | 2.100 |
| 2 | 30 | 130 | 3.2 | 9.722 | | 2.215 |
| 3 | 45 | 115 | 2.2 | 9.642 | | 1.949 |
| 4 | 60 | 100 | 1.2 | 9.43 | | 1.545 |
| 5 | 75 | 85 | 0.2 | 7.09 | 8°02' | 0.354 |



Declassified in Part - Sanitized Copy Approved for Release 2012/03/12 : CIA-RDP82-00039R000100190014-6

Declassified in Part - Sanitized Copy Approved for Release 2012/03/12 : CIA-RDP82-00039R000100190014-6



Denoting $Arg_{\pm} = \dfrac{2n(h-v\xi) \pm (h-vt)}{2a_2\sqrt{t-\xi}}$

n = 1

| ξ | 2n(h−vξ) | 2n(h−vξ)+h−vt | 2n(h−vξ)−(h−vt) | $Arg_+$ | $Arg_-$ | $erfc_+$ | $erfc_-$ | $erfc_+ + erfc_-$ | $\frac{Mv}{a^2}(h-v\xi)$ | $ne^{2n^2\beta_z^2}\frac{h-\xi v}{a}[erfc_+ + erfc_-]$ |
|---|---|---|---|---|---|---|---|---|---|---|
| 0 | 320 | 402 | 238 | 1.220 | 0.724 | 0.0845 | 0.3059 | 0.3904 | 0.2000 | 0.6200 |
| 1 | 290 | 372 | 208 | 1.260 | 0.685 | 0.0748 | 0.3327 | 0.4075 | 0.1818 | 0.6190 |
| 2 | 260 | 342 | 178 | 1.328 | 0.690 | 0.0604 | 0.3292 | 0.3896 | 0.1629 | 0.5665 |
| 3 | 230 | 312 | 148 | 1.460 | 0.693 | 0.0389 | 0.3271 | 0.3660 | 0.1440 | 0.4955 |
| 4 | 200 | 282 | 118 | 1.785 | 0.747 | 0.0116 | 0.2908 | 0.3024 | 0.1252 | 0.4040 |
| 5 | 170 | 252 | 88 | 3.906 | 1.366 | 0 | 0.0534 | 0.0534 | 0.1064 | 0.0684 |

n = 2

| ξ | 4(h−vξ) | 4(h−vξ)+h−vt | 4(h−vξ)−(h−vt) | $Arg_+$ | $Arg_-$ | $erfc_+$ | $erfc_-$ | $erfc_+ + erfc_-$ | $4\frac{Mv}{a^2}(h-v\xi)$ | $ne^{2n^2\beta_z^2}\frac{h-\xi v}{a}[erfc_+ + erfc_-]$ |
|---|---|---|---|---|---|---|---|---|---|---|
| 0 | 640 | 722 | 558 | 2.20 | 1.695 | 0.0019 | 0.0165 | 0.0184 | 0.800 | 0.232 |
| 1 | 580 | 662 | 498 | 2.24 | 1.685 | 0.0015 | 0.0172 | 0.0187 | 0.725 | 0.197 |
| 2 | 520 | 602 | 438 | 2.33 | 1.699 | 0.0010 | 0.0163 | 0.0173 | 0.650 | 0.1545 |
| 3 | 460 | 542 | 378 | 2.57 | 1.770 | 0.0003 | 0.0123 | 0.0126 | 0.575 | 0.09515 |
| 4 | 400 | 482 | 318 | | 2.140 | | 0.0025 | 0.0025 | 0.502 | 0.01585 |
| 5 | 340 | 422 | 258 | | | | | | | |

Declassified in Part - Sanitized Copy Approved for Release 2012/03/12 : CIA-RDP82-00039R000100190014-6

Declassified in Part - Sanitized Copy Approved for Release 2012/03/12 : CIA-RDP82-00039R000100190014-6

$n = 3$

| $\xi$ | $6(h-v\xi)$ | $6(h-v\xi)+h-vt$ | $6(h-v\xi)-(h-vt)$ | Arg _ | erfc _ | $9\frac{Mv}{a^2}(h-v\xi)$ | $ne\{\}/7^1$ |
|---|---|---|---|---|---|---|---|
| 0 | 960 | 1042 | 878 | 2.67 | 0.0002 | 1.800 | 0.038 |
| 1 | 870 | 952 | 788 | 2.67 | 0.0002 | 1.638 | 0.026 |
| 2 | 780 | 862 | 698 | 2.71 | 0.0001 | 1.467 | 0.009 |
| 3 | 690 | 772 | 608 | 2.84 | 0.0001 | 1.450 | 0.008 |

(As usual, parentheses do not contain the standard expressions found many times in the text.)

Determination of the function under the integral sign

| $\xi$ \ $n$ | 1 | 2 | 3 | $\sum_1$ | $-\beta_2\sum_1$ | $\frac{e^{\beta_2\frac{h-vt}{2a^2}}}{2\sqrt{\pi(t-\xi)}}\theta_2(q,0)$ |
|---|---|---|---|---|---|---|
| 0 | 0.620 | 0.232 | 0.038 | 0.890 | -0.0926 | 0.334 |
| 1 | 0.619 | 0.197 | 0.026 | 0.842 | -0.0876 | 0.350 |
| 2 | 0.566 | 0.154 | 0.009 | 0.729 | -0.0758 | 0.360 |
| 3 | 0.496 | 0.095 | 0.008 | 0.599 | -0.0623 | 0.393 |
| 4 | 0.404 | 0.016 | | 0.420 | -0.0437 | 0.421 |
| 5 | 0.068 | | | 0.068 | -0.0071 | 0.237 |

| $\xi$ | 0 | 1 | 2 | 3 | 4 | 5 | 5.2 |
|---|---|---|---|---|---|---|---|
| $\frac{1}{2\sqrt{\pi(t-\xi)}}e^{[\,]}\theta_2(0,q)-\beta_2\sum$ | 0.241 | 0.262 | 0.284 | 0.331 | 0.377 | 0.230 | |
| y (function under the integral sign) | 1.66 | 1.20 | 0.71 | 0.36 | 0.26 | 0.14 | 0 |



Declassified in Part - Sanitized Copy Approved for Release 2012/03/12 : CIA-RDP82-00039R000100190014-6

Declassified in Part - Sanitized Copy Approved for Release 2012/03/12 : CIA-RDP82-00039R000100190014-6

$$\int_0^t \left.\frac{\partial A_2}{\partial x}\right|_{x=v\tau} d\tau = 3.38;$$

$$(acD)_2 \int_0^{\infty} = 122 \text{ calories}$$

Effect of the initial conditions decreases to the vanishing point. Relative to the term $\int_0^{\tau} F(\tau)\,d\tau$ this can be seen immediately by estimating the factor $e^{-(\frac{n\pi}{l})^2 t}$. As regards the upheaval $u(t) - \Phi(t)$, for $t = 5.2$ it constitutes about 0.1 degrees, and reduces to zero as the temperature decreases.



Declassified in Part - Sanitized Copy Approved for Release 2012/03/12 : CIA-RDP82-00039R000100190014-6

Declassified in Part - Sanitized Copy Approved for Release 2012/03/12 : CIA-RDP82-00039R000100190014-6

# THE NEW DM-7 INSTRUMENT FOR DETERMINING THE VISIBILITY OF OBJECTS AND BEACONS

(Patent application Number 381331-IV dated 8 July 1948; class 42, sub-class gr 17/05)

V. A. Gavrilov

## I. INTRODUCTORY REMARKS

The necessity for determining and knowing the visibility range became particularly acute as World War I drew to a close, for the problem was posed by the practical requirements of the naval and air fleets, artillery, transport, etc. of the warring powers.

It would be possible to solve the problem of determining visibility by simple visual observation with an accuracy sufficient for practical purposes, if every meteorological station had within its field of vision a sufficient number of natural or artificial objects suitable for observation.

If this situation had obtained, it could be said that the problem of determining visibility would never have arisen.

As a practical matter however, in most if not all instances, meteorological stations have a very limited field of vision and only an insignificant number of objects available for observations, thus excluding the possibility of determining visibility so easily. The prevalent methods of visually estimating visibility on one or two objects, "by eye", "according to the amount of haze", "by intuition", etc. are subject to extremely gross errors, making such visual estimates unsuitable for operational uses. It was this circumstance that made it imperative to search immediately for a



Declassified in Part - Sanitized Copy Approved for Release 2012/03/12 : CIA-RDP82-00039R000100190014-6

Declassified in Part - Sanitized Copy Approved for Release 2012/03/12 : CIA-RDP82-00039R000100190014-6

solution to the problem in the shape of instrumental methods suitable for mass use. But although about thirty years have already passed since that search for instrumental systems adaptable to mass distribution and giving reliable results first began, we are today confronted by the fact that the majority of meteorological systems both at home and abroad are still to this day not equipped with satisfactorily functioning visibility meters.

One of the first instruments of this type was the Wigand visibility meter, which was widely publicized and distributed; Bennett's "clarnet", based on a similar principle, was another. The physical basis of these instruments, however, was vitiated in principle by the assumption of a complete analogy between the diffusion of light in the atmosphere and that diffusion within ground glass, and could not assure satisfactory results.

After Koschmieder published his theory of horizontal visibility in 1926, the methodology of determining visibility by instrument became essentially clarified. As is generally known, the main conclusion of this theory concerns the visibility of a distant object projected against the background of the sky, the albedo of which may be taken as equal to zero (conditions which, within a certain degree of approximation, correspond to those of densely wooded hills). It is shown that

$$S = \frac{1}{\alpha} \ln \frac{1}{\epsilon}$$

where $\alpha$ is the absorption coefficient or extinction coefficient of the atmosphere and $\epsilon$ is the threshold of contrast.



Declassified in Part - Sanitized Copy Approved for Release 2012/03/12 : CIA-RDP82-00039R000100190014-6

Declassified in Part - Sanitized Copy Approved for Release 2012/03/12 : CIA-RDP82-00039R000100190014-6

This first well-defined relationship to be established between the visibility of a black object and the absorption coefficient imparted a new direction to the search for instrumental methods of solving the problem. This new direction resulted in visibility meters, instead of being constructed as empirical instruments in the true sense of the word (such as, for instance, the Wigand meter), now beginning to be designed primarily for the purpose of measuring the absorption $\alpha$ or the transparency $\tau$ of the atmosphere. From the value found for $\alpha$, the visibility could be calculated by equation (1). Only the persistence of tradition can account for the fact that even after the theory of Koschmieder the new instruments continued to be designated visibility meters, though by rights they should have been called extinction or transparency meters.

In the USSR, instruments based on the principle of photometric extinction of the contrast between the image of an object and its background have come into widespread use.

The first of such instruments was the Tikhanovskiy visibility meter, constructed in 1927. The process of eliminating the observed contrast between object and background was effected by introducing neutral color filters of known density into the instrument's field. The total coefficients of transmission of all the filters introduced supposedly corresponded to the value of the transparency of the atmosphere at which an object would lose perceptibility. However, an apparatus based on so primitive an arrangement did not give and could not have given satisfactory results. With the sharp reduction in brightness which takes place



Declassified in Part - Sanitized Copy Approved for Release 2012/03/12 : CIA-RDP82-00039R000100190014-6

Declassified in Part - Sanitized Copy Approved for Release 2012/03/12 : CIA-RDP82-00039R000100190014-6

in the field of vision when color filters are introduced and, consequently, with the sharply reduced amount of light impinging on the retina, the eye's adaptation to light creates an intermittent disturbance which leads to a highly significant rise in the threshold of contrast; this in turn results in a lack of correspondence between the visual and instrumental discrimination.

In 1934 Sharonov devised a system for visibility meters, new in principle, but also based on photometric extinction. In order to eliminate the effect of adaptive changes in the eye's sensitivity which disturb the extinction of the observed contrast, Sharonov produced, in his well-known "haze-meter", an additional brightness in the background, or an artificial haze. The inventor felt that this additional brightness would probably act to weaken the observed contrast until the moment the photometric apparatus began to function, and then during the subsequent process of contrast extinction would maintain the minimum level or retinal illumination necessary to assure the continued unchanging adaptation of the eye to light, thereby avoiding all the inconveniences involved in the sharp reduction of brightness within the field of vision which was characteristic of the Tikhanovskiy device. In practice, however, the "haze-meter" proved to have a fundamental defect because of the insufficient brightness imparted by the artificial haze. The subsequent reduction of contrast to the threshold value again led to a significant reduction in the over-all brightness of the field of vision, with all the consequences involved, including unsatisfactory results.

During the years 1938 to 1941, V. A. Faas, in the former



Declassified in Part - Sanitized Copy Approved for Release 2012/03/12 : CIA-RDP82-00039R000100190014-6

Declassified in Part - Sanitized Copy Approved for Release 2012/03/12 : CIA-RDP82-00039R000100190014-6

Institute of Experimental Meteorology, constructed a series of his instruments for the purpose of measuring visibility (transparency) in fogs and artificial mists (whence the name of the instrument -- "dymkomer" or haze-meter -- abbreviated to DM). The optical system of the DM represented a considerable improvement over that of Sharonov's "haze-meter". This will be clear from the following discussion. The value of the contrast between a background and an object of which the albedo may be disregarded, is, as is commonly known, given by the expression:

$$K = \frac{B_H - \beta}{B_H} \qquad (2)$$

where $B_H$ is the background (sky) brightness, and $\beta$ is the brightness of a dark object equivalent to the brightness of the atmospheric layer intervening between object and observer.

Inasmuch as the threshold of visual perception of the eye for contrast is generally taken as equal to 0.02 or 2 percent, it follows that in cases where $\beta \ll B_H$ (as is usually the case for objects not very remote) the contrast between object and background becomes imperceptible when the brightness $\beta$ of the object is increased by a few tens of times. The purpose of the superimposed haze in instruments of this type is to increase artificially the value of $\beta$ for the observed object and thereby to reduce the observed contrast until the photometric apparatus functions. In the "haze-meter" of Sharonov, and also in the similar Piskun VP-3 visibility meter (constructed in 1939), $\beta$ remains $\ll B_H$ as a result of the insufficiency of the superimposed brightness. In order to render $\beta$ commensurable with $B_H$, V. A. Faas, in his



Declassified in Part - Sanitized Copy Approved for Release 2012/03/12 : CIA-RDP82-00039R000100190014-6

Declassified in Part - Sanitized Copy Approved for Release 2012/03/12 : CIA-RDP82-00039R000100190014-6

DM-3, DM-4 and DM-5 instruments, considerably increased the effect of the superimposed haze by providing for a difference between the sections of the pencil of light furnishing the superimposed brightness and that forming the observed contrasting image. It should be noted that in the DM-4 the section of the former is several times greater than that of the latter. The superimposed haze will therefore increase the apparent brightness of the image of the object to such an extent as to make the observed value of $\beta$ in the instrument $\approx \frac{1}{2} B_н$ and greater.

Experimental tests of DM-3 and DM-4, as well as [redacted] of DM-5, showed, however, that the superimposed haze was still not sufficiently great to free the observer completely from the adaptation effect. Further extinction of contrast down to the disappearance level led once more to a change in the value of $\epsilon$, the threshold of contrast, though this change was not as great as in the Sharonov and Piskun instruments.

It must be noted that the adaptation effect, which appears in the course of immediate observation with the instrument, consists in the reappearance of the extinguished image after 5-15 seconds, thus forcing the observer to readjust again to extinction and thus again disturbing his adjustments. The image then reappears, and so on.

This cycle of extinction and reappearance is shown by observation to occur 3-4 times in the Sharonov instrument, 2-3 times in the Piskun VP-3, and 1-2 times in the DM-4 (and sometimes in the DM-5). The readings were very significantly affected in



Declassified in Part - Sanitized Copy Approved for Release 2012/03/12 : CIA-RDP82-00039R000100190014-6

Declassified in Part - Sanitized Copy Approved for Release 2012/03/12 : CIA-RDP82-00039R000100190014-6

consequence. If the very narrow graduations on the scales of these instruments is also taken into account -- and the very wide range of natural atmospheric turbidity encountered in the readings as well -- the unsatisfactory performance of these instruments becomes entirely clear, in the light of this discussion.

The failure of visibility meters based on the principle of photometric extinction has caused a number of specialists to conclude that this principle was entirely unsuitable for solving the problems of visibility measurement.

This accounts for the fact that instruments appeared during and after the war based on the principle of comparison of the observed brightness contrast (for instance of a forest against sky background) with that shown by a variable neutral-gray scale. The diaphanoscope of Professor Sharonov is one such instrument. But this new photometric method has even more disadvantages, as we see it, than the extinction principle. In the first place, perfectly gray objects are never observed in nature. Even an evergreen forest, if not very remote from the observer, has appreciable, though slight, greenish hue. This makes it extremely difficult to select the part of the scale that has an equivalent darkening; we find ourselves confronted here with all the complex problems of heterochromatic photometry. It is primarily to this that the unsatisfactory results obtained with the diaphanoscope must be ascribed. In the second place, the use of instruments of this type necessarily requires the presence of evergreen forests or of black artificial objects and is thus excluded from extensive use in steppe regions, while instruments based on the extinction prin-



Declassified in Part - Sanitized Copy Approved for Release 2012/03/12 : CIA-RDP82-00039R000100190014-6

Declassified in Part - Sanitized Copy Approved for Release 2012/03/12 : CIA-RDP82-00039R000100190014-6

ciple are free from this restriction, as we shall show below.

After the war we had the opportunity of trying out another instrument based on an entirely new principle -- the nephelometer constructed by Engineer N. E. Kityn'. But this apparatus too gave unsatisfactory results in practice.

In the light of the above considerations it is obvious that the process of measuring the atmospheric transparency and the related visibility of objects is not so simple as might appear at first glance. It appears to be somewhat difficult in using these instruments to escape the distorting influence of instrumental and psycho-physiological factors. Naturally, then, when we undertake the task of constructing an instrument that will not only function satisfactorily but also will be adapted to mass distribution, we should proceed with exceptional care to the analysis of the rationale of preceding instruments as well as the methods used in them before attempting to design anything new ourselves.

Instruments based on the principle of comparison of observed contrast with a variable neutral-gray scale should, in our opinion, be rejected because of the existence of a difference in hue between scale and object (which color filters cannot completely overcome), and also because such instruments require completely uniform objects in order to function properly.

In the light of the failures by Faas, as well as by Gerlich and Pollak, it is most doubtful whether any success at all can be expected from efforts to construct objective photoelectric instruments for mass production.



Declassified in Part - Sanitized Copy Approved for Release 2012/03/12 : CIA-RDP82-00039R000100190014-6

Declassified in Part - Sanitized Copy Approved for Release 2012/03/12 : CIA-RDP82-00039R000100190014-6

Any methodology involving the application of simplified and approximate methods of photometry, of the nature of those proposed at one time by V. F. Piskun, is destined in our opinion to complete and unmitigated failure.

The same negative appraisal is warranted for a number of other instruments and methods, including foreign ones as well, on which we cannot dwell here.

A relatively extensive experience in testing various instruments (at different times the writer has tested in practice the haze-meter and diaphanoscope of Sharonov, the DM-3, DM-4, and DM-5 instruments of Faas, the VP-3 instrument of Piskun and a number of its photometric attachments, the KOL-8 and KOL-10 nephelometers of Kityn' and Gurevich, the Gold apparatus, the Wiegand wedge, the photometric EKS-1 and EKS-2 of Faas, etc.) has shown that the best results may be expected from an instrument based on the principle of photometric extinction, but free of the faults inherent in the instruments of Sharonov, Faas and Piskun. It is this principle that best serves the purpose of solving the various problems involved in visibility, since, as we shall show below, the transparency of the atmosphere may be determined by using any object at all, even if it is colored; and the method of using this principle allows us to take the influence of psycho-physiological factors into account and enables us thereby to eliminate them. It is only necessary that such a new instrument be free of the adaptation effect and have a sufficiently extensive range in its measurement scales.

The first model of an adaptation-free instrument was built in the summer of 1947. Its basic principle was as follows: A



Declassified in Part - Sanitized Copy Approved for Release 2012/03/12 : CIA-RDP82-00039R000100190014-6

Declassified in Part - Sanitized Copy Approved for Release 2012/03/12 : CIA-RDP82-00039R000100190014-6

wedge-shaped semidisc of ordinary crown glass is placed in front of the objective of a telescopic system, so as to cover half of the aperture of the objective and allow an image of the observed object to lie in the same focal plane. This image is caused to disappear by rotating a shutter about the optical axis of the apparatus and gradually covering the wedge-shaped semidisc as it opens the free half of the aperture not occupied by the wedge. In this way the brightness of the field of vision is constant. This apparatus, however, which was constructed by developing an idea of V. A. Faas (In Autumn of 1947 it was learned that V. F. Piskun had suggested in 1940 a very similar method of constructing an instrument with constant brightness of field.), showed in practice that although the adaptation effect was completely absent, it still afforded no significant extension of the range of measurement. This circumstance continued to be a serious disadvantage of the instrument.

In the search for a way of eliminating this defect, all possible methods of causing the rays forming the secondary image to pass through a diaphragm were tried in order to further strengthen the action of the superimposed haze. Although all these numerous attempts proved unsuccessful, they did nevertheless succeed in revealing a relationship by which the problem of extending the measurement-range of the instrument could be accurately solved; the faster that the brightness of the superimposed haze increased during the process of extinction of the observed object, the wider became the range of the measurement scale.

The realization of this rule led to the construction of an



Declassified in Part - Sanitized Copy Approved for Release 2012/03/12 : CIA-RDP82-00039R000100190014-6

Declassified in Part - Sanitized Copy Approved for Release 2012/03/12 : CIA-RDP82-00039R000100190014-6

instrument in which the over-all brightness of the field of vision increased during the process of extinction. It was precisely this method that finally permitted the construction of an instrument free from the adaptation effect and with a considerably wider range of measurement scale than the earlier instruments offered.

Inasmuch as the basic design of the instrument described below represents a further development of the DM design, it has been given the name of DM-7, as the successor of that instrument and in memory of V.A. Faas.

## II. BASIC DESIGN AND THEORY OF THE DM-7 VISIBILITY METER

The instrument consists of a tube 1, at one end of which is placed the wedge-shaped glass semidisc $K_T$, which has a fixed coefficient of transmission, and the photometric device $Sh_T$ in the form of a semicircular shutter. The tube is set into the mounting of the objective of the telescopic system 6. The wedge-shaped semidisc covers half of the aperture of the objective, leaving the other half $O_T$ open. (Figures 1 and 2).

The pencil of rays from the object viewed impinges on the objective and is divided into two pencils, of which one passes through the open half of the objective and forms an image of the object in the central part of the focal plane, while the other pencil falls at first on the wedge, undergoes a certain amount of diffraction and absorption, and only then falls on the objective,



Declassified in Part - Sanitized Copy Approved for Release 2012/03/12 : CIA-RDP82-00039R000100190014-6

Declassified in Part - Sanitized Copy Approved for Release 2012/03/12 : CIA-RDP82-00039R000100190014-6

forming a displaced secondary acentric image of the same object in the focal plane.

By rotating the shutter $Sh_1$ relative to the optical axis of the tube, by means of the worm 2 and the toothed sector 3, the wedge-shaped semidisc may be closed and the active area of the open half of the objective simultaneously increased. The shutter is rotated to cover more and more of the wedge until the secondary image in the field of vision disappears against the background created by the superimposed brightness. The entire process of observation thus reduces to causing the disappearance of the secondary image. We note that either the free aperture or the wedge-shaped semi-disc may be completely covered by the shutter.

Because of this optical system, the increase in the apparent brightness of the object and, consequently, the reduction of the observed contrast are accomplished not only by closing the wedge-shaped semidisc with the shutter but also (because of the increasing area of the free aperture of the objective) by the uninterrupted strengthening of the additional brightness or "haze" effect superimposed on the observed contrast. The latter circumstance is due to the increasing brightness of the field of vision involved in the process of extinction. Inasmuch as the value of the coefficient of transmission T is taken as equal to 1% percent, by rotating the shutter on the side of the wedge-shaped semidisc through the angle $\varphi$, we obtain an increase in the superimposed brightness (and therefore of the apparent brightness of the object) proportional to $T\varphi$.

This dual process of weakening the observed contrast leads



Declassified in Part - Sanitized Copy Approved for Release 2012/03/12 : CIA-RDP82-00039R000100190014-6

Declassified in Part - Sanitized Copy Approved for Release 2012/03/12 : CIA-RDP82-00039R000100190014-6

to rapid and reliable extinction, without any distortion by the visual functions of the observer.

As is generally known, the brightness of the atmospheric haze increases with the distance of any object. The motion of the shutter on the wedge-shaped semidisc, leading to the uninterrupted increase in the brightness of the superimposed haze and of the overall brightness of the field of vision, is optically equivalent to increasing the brightness of the intervening air layer by increasing the distance between observer and object. Expressed figuratively, the photometric system of the DM-7 acts with respect to object and observer as though the observer were on an airplane flying away from or toward the object, with the difference that the angular dimensions of the object remain unchanged. We note that the photometric system[5] of all instruments previously proposed, if based on the extinction principle, act in a manner directly contrary to the natural course of events, in that the over-all brightness of the field of vision of such instruments is either reduced during extinction or, at best, remains constant.

We pass now to the theory of the DM-7.

Figure 1. The photometric mechanism of the DM-7.

Figure 2. General view of the DM-7: (1) tube; (2) worm; (3) toothed sector; (4) scale; (5) attachment to sight tube; (6) sight tube; (7), (8), (9), attachment to tripod.



Declassified in Part - Sanitized Copy Approved for Release 2012/03/12 : CIA-RDP82-00039R000100190014-6

Declassified in Part - Sanitized Copy Approved for Release 2012/03/12 : CIA-RDP82-00039R000100190014-6

As is already known, the contrast K between the brightness of the background (sky) $B'_H$ and the brightness of the object $B'_O$, projected against this background, is expressed by the relation:

$$K = \frac{B'_H - B'_O}{B'_H} \qquad (3)$$

When the object projected against the background of the sky has an albedo which may be disregarded, its contrast $K_L$ at distance L will be:

$$K_L = \frac{B_H - \beta'}{B_H}$$

where $\beta'$ is the brightness of the air layer between object and observer, or the apparent brightness of the object.

As is well known, the distance at which the contrast between object and background falls to the value $\epsilon$ of the eye's threshold of contrast is called the visibility S. The value of the contrast at a distance equal to the visibility S is thus:

$$K_S = \epsilon = \frac{B'_H - \beta'}{B'_H} \qquad (4)$$

In order to measure the visibility by the DM-7 instrument, the observed contrast must be caused to disappear. This, as we have seen, is accomplished by a dual process: by reducing the brightness of the observed image and at the same time rapidly increasing the brightness of the haze superimposed on this image.

Let $\Sigma$ be the area of the free aperture of the objective at the moment when the observed contrast vanishes, $\sigma$ be the area of the wedge-shaped semidisc not covered by the shutter at that moment, and T be the transmission of that semidisc.



Declassified in Part - Sanitized Copy Approved for Release 2012/03/12 : CIA-RDP82-00039R000100190014-6

Declassified in Part - Sanitized Copy Approved for Release 2012/03/12 : CIA-RDP82-00039R000100190014-6

We now assume the free aperture of the objective to be completely closed by the shutter. We then see in the field of vision of the instrument only the secondary image of the dark object and the background formed by rays all of which have passed through the wedge-shaped semidisc. The apparent brightness $\beta$ of that image will be equal to $\beta\sigma T$, and the apparent brightness of the background will be $B_H \sigma T$.

If now the shutter is turned to uncover the free aperture of the objective on these two brightness values, then a supplementary brightness (" a haze") will be superimposed, representing the brightness of the background (the sky) at the azimuth of the object, and proportional to the uncovered area of the free aperture of the objective, that is, proportional to $B_H \Sigma$.

Then the final total apparent brightness $\beta'$ of the image of the object in the field of vision will be equal to:

$$\beta' = \beta\sigma T + B_H \Sigma \qquad (5)$$

and the total brightness of the background will be

$$B_H = B_H \sigma T + B_H \Sigma \ . \qquad (6)$$

The physical meaning of the superimposed brightness is graphically portrayed by the relation (5); it reduces to the increase in the apparent brightness of the image and to the reduction of contrast between image and background.

Substituting in equation (4) the values given in equations (5) and (6), we obtain for the moment when the contrast between



Declassified in Part - Sanitized Copy Approved for Release 2012/03/12 : CIA-RDP82-00039R000100190014-6

Declassified in Part - Sanitized Copy Approved for Release 2012/03/12 : CIA-RDP82-00039R000100190014-6

secondary image and background vanishes:

$$\epsilon = \frac{(B_H \sigma T + B_H \Sigma) - (\beta \sigma T + B_H \Sigma)}{B_H \sigma T + B_H \Sigma} = \frac{B_H \sigma T - \beta \sigma T}{B_H \sigma T + B_H \Sigma} \quad (7)$$

We now write instead of $\beta$ the expression given by Löhle for the brightness of an infinitely thick layer of air:

$$\beta = \beta_\infty (1 - e^{-\alpha L}) = B_H (1 - e^{-\alpha L}) . \quad (8)$$

where $\alpha$ is the absorption coefficient or extinction coefficient of the atmosphere, L is the distance of the observed object, and e is the base of natural logarithms.

Combination of equations (7) and (8) gives

$$\epsilon = \frac{B_H \sigma T \cdot e^{-\alpha L}}{B_H \sigma T + B_H \Sigma} \quad (9)$$

If in equation (9) denominator and numerator are both divided by $B_H \Sigma$ and M is written for $\frac{\sigma T}{\Sigma}$, we obtain:

$$\epsilon = \frac{M \cdot e^{-\alpha L}}{1 + M}$$

whence

$$e^{-\alpha L} = \frac{\epsilon (1 + M)}{M} . \quad (10)$$

In equation (10), besides $\alpha$, $\epsilon$, the value of the threshold of contrast, is also an unknown quantity. Its value may be simply taken from the laboratory determinations and substituted. However, experience with observations has shown that this quantity is not at all constant, not only for different persons but also for the same person at different times. Therefore operation with unchanged values of $\epsilon$ at all times only serves as a source of very significant additional errors. The value of $\epsilon$, however,



Declassified in Part - Sanitized Copy Approved for Release 2012/03/12 : CIA-RDP82-00039R000100190014-6

Declassified in Part - Sanitized Copy Approved for Release 2012/03/12 : CIA-RDP82-00039R000100190014-6

can be very simply determined from a supplementary observation of a model having the shape, angular dimensions, and albedo approximating those of the observed object, but located so close (10-15 meters) as to make it possible to neglect the value of extinction and make

$$e^{-\alpha L} = 1.$$

Then from (10)

$$\epsilon = \frac{M_M}{M_M+1} = \frac{\frac{\sigma_M T}{\Sigma_M}}{\frac{\sigma_M T}{\Sigma_M}+1} = \frac{1}{1+\frac{\Sigma_M}{\sigma_M T}}, \qquad (11)$$

where $\sigma_M$ and $\Sigma_M$ are the areas of the wedge-shaped semidisc and the free aperture of the objective, respectively, at the moment of extinction of the model.

This method for the immediately determining the value of $\varepsilon$ at the time of observation under field conditions, carried on with great convenience and simplicity by the extinction of contrast between a model and the background, is of great fundamental importance. For this method permits us to free ourselves completely, as we shall see below, from the distorting influence of psychophysiological factors. Thereby it considerably increases the precision with which atmospheric transparency and the related visibility of objects are determined.

Substituting in (11) the value of $\epsilon$ from (10), we have:

$$e^{-\alpha L} = \frac{M_M}{M_M+1} \cdot \frac{M+1}{M}. \qquad (11a)$$

Whence

$$\alpha = \frac{2.3}{L} \lg \frac{M(M_M+1)}{M_M(M+1)}, \qquad (12)$$



Declassified in Part - Sanitized Copy Approved for Release 2012/03/12 : CIA-RDP82-00039R000100190014-6

Declassified in Part - Sanitized Copy Approved for Release 2012/03/12 : CIA-RDP82-00039R000100190014-6

where $M = \frac{\sigma T}{\Sigma}$, the ratio between the acting surface of the wedge and that of the free aperture of the objective at the moment of extinction of the object.

For further treatment it is more convenient to rewrite the expression (12) in another form. For this purpose we divide the fraction after the logarithm sign by $M\Sigma_M$. We obtain

$$\alpha = \frac{2.3}{L} \lg \frac{1 + \frac{\Sigma_M}{\sigma_M T}}{1 + \frac{\Sigma}{\sigma T}} \qquad (13)$$

As is commonly known, the visibility S of a dark object projected against the background of the sky is given by Koschmieder's equation:

$$S = \frac{1}{\alpha} \ln \frac{1}{\epsilon} . \qquad (14)$$

From this formula the so-called meteorological visibility is calculated. This represents the distance at which the contrast between a dark object (wooded hills, soot-covered top of a factory smokestack, tar-paper on a roof, etc.) and the sky falls to the value of the threshold of contrast.

In calculating S from equation (14), $\epsilon$ is assumed to be a constant, and is put at 0.02, the value obtained by laboratory determinations. It must be understood that this value, however, is very much subject to variation under different conditions. If, in keeping with established practice, we still put $\epsilon = 0.02$, then (14) becomes:

$$S = \frac{3.91}{\alpha} . \qquad (15)$$



Declassified in Part - Sanitized Copy Approved for Release 2012/03/12 : CIA-RDP82-00039R000100190014-6

Declassified in Part - Sanitized Copy Approved for Release 2012/03/12 : CIA-RDP82-00039R000100190014-6

From this relationship the existence of a single-valued dependence between the meteorological visibility S and the absorption coefficient $\alpha$ is clearly apparent.

Substituting for $\alpha$ in (15) its value from (13), found by observation, we finally obtain

$$S = \frac{1.7 \times L}{\lg\left(1 + \frac{\Sigma_M}{\sigma_M T}\right) - \lg\left(1 + \frac{\Sigma}{\sigma T}\right)} = \frac{1.7 \times L}{u_M - u_0}, \quad (16)$$

where

$$u_M = \lg\left(1 + \frac{\Sigma_M}{\sigma_M T}\right)$$

corresponds to the observation of the model, and

$$u_0 = \lg\left(1 + \frac{\Sigma}{\sigma T}\right)$$

corresponds to the observation of the object.

A table will be supplied for each instrument, giving the computed values of $u_M$ and $u_0$ as the functions of the readings of that instrument.

## III. METHOD OF OBSERVATION

As we have shown, equation (14) obtained by Koschmieder led to the fact that the instrumental methods of determining S reduced in fact to the instrumental determination of $\alpha$; and therefore the so-called visibility meters would be more correctly designated as extinctometers or transparency meters.

The usual method of determining $\alpha$ is by observing only a



Declassified in Part - Sanitized Copy Approved for Release 2012/03/12 : CIA-RDP82-00039R000100190014-6

Declassified in Part - Sanitized Copy Approved for Release 2012/03/12 : CIA-RDP82-00039R000100190014-6

single object with one azimuth or the other. This method, however, as we shall show, is a source of very significant error.

When with the aid of a photometric device we reduce the observed contrast to the threshold value, we must assume that the value of $\epsilon$ remains constant for all observers and in all cases, and that the readings obtained and the consequent value of $\alpha$ depend only on the brightness of the air layer between object and observer. If this were actually so, we could, instead of (12), write

$$\alpha = \frac{2.3N}{L} \log \frac{M}{M+1}, \qquad (17)$$

where $N = \log \frac{1}{\epsilon}$, and $\epsilon$ is a given constant threshold value.

Unfortunately practical experience does not confirm the hypothesis of an unchanging and constant value of $\epsilon$. According to the data of our field observations, the value of $\epsilon$ varies within a range of $\pm$ 30 percent from its mean value obtained from several hundred observations. Thus when we observe only a single object and assume that $\alpha$ depends solely on the brightness A of the haze, that is that $\alpha = f(A)$, what we are actually getting is data for which $\alpha = f(A,\epsilon)$. Considering that a variation in the value of $\epsilon$ by 0.01 results in a variation of S by 5-10 percent, it is obvious that a difference between the actual value of $\epsilon$ at the moment of observation and its assumed value as a constant may lead to errors in the determination of S ranging up to 30 and 40 percent of the value of S.

How can we eliminate this error and make $\alpha = f(A)$?



Declassified in Part - Sanitized Copy Approved for Release 2012/03/12 : CIA-RDP82-00039R000100190014-6

Declassified in Part - Sanitized Copy Approved for Release 2012/03/12 : CIA-RDP82-00039R000100190014-6

In instruments of type DM-7, this elimination may be accomplished by the very simple method indicated above. This consists in setting up a model with the same angular dimensions, shape and albedo as the object, at the same azimuth as the object, but at a distance of 10 to 15 meters. Observations are then made on this model in exactly the same way as on the object itself, that is, its image in the field of view of the instrument is caused to disappear.

Then equation (11) will define the actual value of the threshold $\epsilon$ at which the object vanishes, which threshold is characterized by the ratio $\frac{M}{M+1}$.

Thus, on observing both object and model, and then calculating $\epsilon$ by equation (12), we are automatically freed from the influence of variations in the value of $\epsilon$ on the result. It is apparent therefore that equation (12) now actually gives $\alpha = f(\Lambda)$, while by using equation (17), $\alpha = f(\Lambda, \epsilon)$.

It is, of course, true that the additional observation of the model represents a certain added complexity in the method. But this complexity is entirely compensated by the sharply-increased precision in the determination of $\alpha$ and S which it makes possible. Logic demands that in calculating S the value of $\epsilon$ found by observation as per equation (11) should be substituted for the constant 0.02. It is precisely in this case that the quantity S will actually represent the meteorological visibility.

The method of determining and eliminating $\epsilon$ from the observations may be most simply and accurately effected only with



Declassified in Part - Sanitized Copy Approved for Release 2012/03/12 : CIA-RDP82-00039R000100190014-6

Declassified in Part - Sanitized Copy Approved for Release 2012/03/12 : CIA-RDP82-00039R000100190014-6

instruments based on the principle of extinction, and in this may lie the great advantage of this system over all others. But this is not all. The system of contrast extinction by increasing the brightness of the superimposed haze leads to yet another clearly discernible phenomenon. When we look through the instrument at any colored object against the background of the sky, that is, when we observe a color contrast, we note that when the haze is superimposed, the color saturation of the contrasted object is very abruptly reduced, so that the eye subsequently perceives that object as gray, not as colored. In other words, the superimposition of haze on the observed image of a colored object leads to the perception of color contrast being changed to one of brightness contrast. We observe the same thing in nature, when we note how some red object like a factory smokestack or a building painted any color appears dark gray to us in a fog. This circumstance, which constantly attracted the attention of V. A. Fass as early as 1937, permits us to draw the very important conclusion that in dealing with visibility we are concerned exclusively with contrasts of brightness and not with contrasts of color.

Thus, instruments based on the principle of contrast extinction, if used with the method described above of supplementary observation of a model, succeed in determining the values of $\alpha$ and S independently of the varying values of $\epsilon$.

Moreover, even if there are no dark objects available in the field of view, the determination of $\alpha$ and the subsequent calculation of S may be carried out with the same precision by observing any other object, including colored objects as well.



Declassified in Part - Sanitized Copy Approved for Release 2012/03/12 : CIA-RDP82-00039R000100190014-6

Declassified in Part - Sanitized Copy Approved for Release 2012/03/12 : CIA-RDP82-00039R000100190014-6

The only necessary condition is the preparation of a model with approximately the same angular dimensions (as viewed through the instrument), the same shape and same albedo as the object itself, which can be done without any trouble at all.

## IV. RESULTS OF OBSERVATIONS WITH THE DM-7

Visual estimates of visibility carried out on the roofs of watertowers at the field base of GGO in the village of Voyeykovo were used to check the accuracy of the results given by the DM-7. The use of these criteria were justified by the fact that the panorama from the place of observation offered a large number of objects and formed a natural polygon for the study of visibilities. The character of the natural dark objects and their number at the various azimuths allowed the determination of actual visibilities with errors not exceeding 20 to 25 percent of their values, and, with reduced visibility, determination could be made within 10 percent. The distance of the objects was determined by using a 1:50,000 map. Analysis of the results of 1948 observations with the DM-7 show that the error between the instrumental visibility so obtained and its actual value by the most careful visual estimate lies within the range of 10 to 20 percent. In 80 percent of all observations the error did not exceed 15 percent, while in 12 percent of all observations it ranged from 15 to 20 percent. In the remaining 8 percent of the observations, the error was over 20 percent. If we assume a 20 percent error in determining visibility to be entirely admissible for operational purposes, then it follows that 92 percent of all observations meet this



Declassified in Part - Sanitized Copy Approved for Release 2012/03/12 : CIA-RDP82-00039R000100190014-6

Declassified in Part - Sanitized Copy Approved for Release 2012/03/12 : CIA-RDP82-00039R000100190014-6

standard of precision. As an illustration we present a table giving the results of observations with visibilities of 5 to 10 kilometers.

| No. | Date | Visual Estimate of Visibility in kilometers | Visibility according to DM-7 in kilometers | Remarks |
|---|---|---|---|---|
| 1 | July 28 | 6 - 8 | 9.3 | Variable cloudiness and |
| | | | 8.7 | haze changing in density |
| 2 | August 2 | 5 - 6 | 6.3 | Overcast |
| 3 | August 3 | 5 - 8 | 7.9 | Overcast |
| 4 | August 7 | 6 - 8 | 8.4 | Overcast |
| 5 | August 11 | 4 - 6 | 4.2 | Overcast |
| 6 | August 11 | 5 - 7 | 7.9 | |
| 7 | August 11 | 5 - 7 | 8.9 | |
| 8 | August 24 | 5 - 7 | 8.1 | Data of two observers |
| | | | 7.3 | |
| 9 | August 25 | 5 - 7 | 6.5 | Data of two observers |
| | | | 5.8 | with three different |
| | | | 6.3 | instruments |
| | | | 6.2 | |
| | | | 6.1 | |
| | | | 6.3 | |
| 10 | August 25 | 8 - 10 | 7.5 | Data of three observers |
| | | | 10.4 | with two different |
| | | | 8.2 | instruments |
| | | | 10.3 | |
| | | | 9.0 | |
| | | | 8.4 | |
| 11 | October 17 | 7 - 9 | 7.2 | |

Note: The distances of the observed objects were from 15 to 25 percent of the actual visibilities.



Declassified in Part - Sanitized Copy Approved for Release 2012/03/12 : CIA-RDP82-00039R000100190014-6

Declassified in Part - Sanitized Copy Approved for Release 2012/03/12 : CIA-RDP82-00039R000100190014-6

## V. USE OF THE DM-7 DURING THE DARK PART OF THE DAY

The possibility of using the DM-7 for determining the absorption coefficient $\alpha$ in the dark hours as well is of great practical value. In the first place such a determination of $\alpha$ will allow the meteorological stations in the Far North which must work for a few months each year under the conditions of polar night, to characterize the air masses by the values for $\alpha$ or S, as the other stations in the network do. In the second place, the determination of $\alpha$ by night will allow the visibility of various signal beacons to be calculated throughout the entire network.

Figure 3.

We now discuss the conditions for the determination of $\alpha$ by night, using the DM-7.

Let O be the point where the observer is situated (Figure 3), with one light-source of intensity $I_1$ candlepower at point A, at distance $L_1$ from O, and another light-source of intensity $I_2$ candlepower at point B, at distance $L_2$ from O.

The observer will see four images of these light sources as points of light in the field of view of the DM-7: two images in the central part of the field and two acentric images. The central, undisplaced images are formed by rays passing through the free aperture of the objective. The acentric images are formed by rays passing through the wedge-shaped glass semidisc. The acentric images may be readily distinguished from the central images by a slight rotation of the DM-7 around the mounting of the objective of the sight tube.



Declassified in Part - Sanitized Copy Approved for Release 2012/03/12 : CIA-RDP82-00039R000100190014-6

Declassified in Part - Sanitized Copy Approved for Release 2012/03/12 : CIA-RDP82-00039R000100190014-6

Two of these four images are selected for photometry -- the acentric image of the nearer beacon (the bright beacon) and the undisplaced image of the far (faint) beacon. We pay no attention to the other pair. By moving the instrument in one way or another relative to the line of sight between the two beacons, and also by fixing the instrument in one angular position or another on the mounting of the objective, the photometric pair may be caused to move nearer to the field of view, or farther away from it, as convenient for observation (Figure 4).

Figure 4: 1. Displaced near beacon; 2. Non-displaced near beacon; 3. Photometric gauge of beacons; 4. Non-displaced distant beacon; 5. Displaced distant beacon.

By moving the shutter upon the wedge-shaped semidisc and thus reducing the section of the pencil or rays forming the acentric image of the nearer beacon, we may reduce its observed luminosity to zero. At the same time, in consequence of the increase in the section of the other pencil of the pair, the luminosity of the undisplaced image of the farther beacon is increased.

The observation itself consists in making the luminosity or "brightness" of these two points equal. The luminous flux forming the acentric image of the farther beacon is obviously proportional to

$$F_1 = \sigma T E_1$$

and the flux forming the undisplaced image of the farther beacon to

$$F_2 = \Sigma E_2$$

where $E_1$ and $E_2$ are the retinal illuminations due respectively to



Declassified in Part - Sanitized Copy Approved for Release 2012/03/12 : CIA-RDP82-00039R000100190014-6

Declassified in Part - Sanitized Copy Approved for Release 2012/03/12 : CIA-RDP82-00039R000100190014-6

the nearer and farther beacons, and $\sigma$ and $\Sigma$ are the respective functioning areas of the wedge-shaped semidisc and the free aperture of the objective.

At the moment of photometric match $F_1 = F_2$, and therefore

$$\sigma T E_1 = \Sigma E_2 \tag{18}$$

Inasmuch as the illumination E on the retina from a point source of light of intensity I candle power at a distance L from the observer is expressed by Allar's equation:

$$E = \frac{I}{L^2} e^{-\alpha L}$$

thus, substituting this value in equation 18, we have

$$\sigma T \frac{I_1 e^{-\alpha L}}{L_1^2} = \Sigma \frac{I_2 e^{-\alpha L_2}}{L_2^2} \tag{19}$$

where $\alpha$ is the absorption coefficient of the atmosphere, $L_1$ and $L_2$ are the respective distances of the near and the far beacons, and $I_1$ and $I_2$ are the respective intensities of the near and far beacons.

By simple rearrangement, we finally obtain

$$\alpha = \frac{2.3}{L_2 - L_1} \left[ \log \frac{I_2}{I_1} \cdot \frac{L_1^2}{L_2^2} + \log \frac{\Sigma}{\sigma T} \right]. \tag{20}$$

It should be noted that for this method it is enough to know the ratio between the intensities of the two beacons, and that it is not necessary to know the intensities themselves. Under any circumstances knowledge of this ratio simplifies the organization of the observations.

It is clear that for the given pair of beacons,



Declassified in Part - Sanitized Copy Approved for Release 2012/03/12 : CIA-RDP82-00039R000100190014-6

Declassified in Part - Sanitized Copy Approved for Release 2012/03/12 : CIA-RDP82-00039R000100190014-6

$$\frac{2.3}{L_2 - L_1} \quad \text{and} \quad \frac{I_2 L_1^2}{I_1 L_2^2}$$

are constants. Designating them respectively as A and B, equation (20) may be rewritten in a form more convenient for use:

$$\alpha = A \log \left[ B \frac{\Sigma}{\sigma T} \right] \qquad (21)$$

It is easy to draw a graph, using equation 21, determining the values of $\alpha$ and S as functions of the instrument readings.

It is generally known that trained observers can establish the equality of illumination for two luminous points within an error of the order of 15 to 20 percent. Such low accuracy in the photometry of point beacons may be explained by the fact that the retinal image of a luminous point occupies only a few of the retinal receptors. The great accuracy of ordinary photometry, based on the matching of the illumination of two mixed fields, is explained by the very fact that the image of the field of comparison occupies millions of retinal receptors. From this point of view there could be no hope at all of increasing the precision of photometry of point sources, for it is hard to imagine any possible way of raising the level of irritability of two or three elements of the retina to the level of thousands and millions of such elements. Yet such a possibility does exist. It is only necessary, for this, to find some way of obtaining the degeneration of luminous points into Lissajous figures of any form. Such an attempt has been made by simply imparting a vibratory motion by hand to the tripod on which the DM-7 was mounted. The effect proved to be



Declassified in Part - Sanitized Copy Approved for Release 2012/03/12 : CIA-RDP82-00039R000100190014-6

Declassified in Part - Sanitized Copy Approved for Release 2012/03/12 : CIA-RDP82-00039R000100190014-6

remarkable. Equality of brilliance of the two sources under examination was achieved not only with great precision, but more consistently and with less eye strain.

## CONCLUSIONS

1. The results of field tests of DM-7 show that using the principle of increasing the over-all brightness of the field of view during the process of extinction of the observed contrast resulted in the construction of an instrument free from the adaptation effect and possessing a wide range of the measurement scale, assuring entirely satisfactory accuracy in its functioning.

2. The methods of using the DM-7 allow us to circumvent any limitations imposed by climatic or physical and geographic factors, and permits us to obtain data independent of the psycho-physiological characteristics of the observer's eye.

3. The possibility of solving the following problems with the aid of the DM-7 has been verified in practice:

   a. measurement of any contrasts of brightness against sky background;

   b. determination of the meteorological visibility (transparency or absorption of the atmosphere) during both light and dark portions of the day;

   c. determination of the thresholds of contrast and point sensitivity (thresholds of disappearance and appearance).

The satisfactory accuracy in determining $\alpha$ or S, together



Declassified in Part - Sanitized Copy Approved for Release 2012/03/12 : CIA-RDP82-00039R000100190014-6

Declassified in Part - Sanitized Copy Approved for Release 2012/03/12 : CIA-RDP82-00039R000100190014-6

with its simplicity and inexpensiveness make possible the mass distribution of the DM-7 among the network of meteorological stations.

The following persons participated in the work of constructing and developing the DM-7 and in its field trials: Senior Scientist of the GGO, V. A. Berezkin (since deceased), and Senior Technician, N. M. Suderevskaya.

E N D



Declassified in Part - Sanitized Copy Approved for Release 2012/03/12 : CIA-RDP82-00039R000100190014-6

Declassified in Part - Sanitized Copy Approved for Release 2012/03/12 : CIA-RDP82-00039R000100190014-6

# THE MACROMETEOROLOGICAL PROCESS OF DROUGHT FORMATION

B. S. Gurevich

1. The immense damage done to agriculture by drought has long since forced a number of sciences -- meteorology above all -- to undertake numerous and detailed, painstaking investigations (3, 4, 6, 10, 24, 30, 32, 34 etc.). These investigations have resulted in many disagreements, unresolved to this day.

The concept of drought in agriculture was a varied one and was the object of a number of contradictory definitions. The reason for this lay in the absence of any uniform method of evaluating droughts no less than in the complexity of agricultural production, which added supplementary interpretations to the original concept. Meteorology laid down its own definitions without troubling itself about the actual circumstances involved in agricultural droughts. Agrometeorology as a rule either underestimated or exaggerated the role of meteorological factors. We confine ourselves to two examples, so as not to overload this paper with innumerable citations. For the first group we present the definition given by A. A. Kaminskiy (21).

"By droughts we understand those rainless periods during the period from the disappearance of the snow cover in spring to the onset of frequent frosts in autumn, in the course of which the maximum diurnal temperature of the air (or the temperature at 1300 hours) increases uniformly after a sharp initial rise, the relative humidity is low (not over 40 percent) after a consider-



Declassified in Part - Sanitized Copy Approved for Release 2012/03/12 : CIA-RDP82-00039R000100190014-6

Declassified in Part - Sanitized Copy Approved for Release 2012/03/12 : CIA-RDP82-00039R000100190014-6

able drop, and continues to fall, the absolute humidity fluctuates within narrow limits, and cloudiness is slight."

This definition is the most finished expression of the viewpoint of the meteorologists during the first third of the present century. It insists on the most exhaustive description of complex phenomena. However, its numerical data does not refer to agricultural drought at all but to a certain abstract meteorological condition which is observed annually over a widespread territory of the Caspian steppes, in years both of drought and of plenty. This formulation represents drought as a purely meteorological phenomenon, not depending on either social and economic causes or on the technology of agricultural production, and in any case is a formulation valid only for the South and Southeast of the European part of the USSR.

The definition of N. V. Bov (2) may serve as an example of the second group -- the agrometeorological characterizations of drought:

"We consider drought as a combination of various phenomena taking place in the soil and in the air and resulting in a lack of correspondence between the necessary consumption of water by plants and its actual supply from the soil to those plants."

This definition is essentially a statistical one, and suffers from extreme vagueness in its meteorological aspect, since it focuses its entire attention of agrobiological factors.

It seems indubitable to us that drought is the agricultural



Declassified in Part - Sanitized Copy Approved for Release 2012/03/12 : CIA-RDP82-00039R000100190014-6

Declassified in Part - Sanitized Copy Approved for Release 2012/03/12 : CIA-RDP82-00039R000100190014-6

appearance of a temporary water famine for cultivated plants, arising from the insufficiency of soil water or from excessive evaporation. This famine is due on the one hand to weather conditions, and on the other to social and economic practices and in particular to agricultural practices. Categorical definition of the damage due to drought is rendered considerably more difficult by the complexity of agriculture, the large number of species and varieties of the cultivated plants, and the physical and geographical conditions in a given region (the geographic coordinates, exposure, elevation above sea level, soil, etc.). As the social and economic level rises with the introduction of progressive agricultural practices and with improvement in the work of breeding and selection, the damage caused by unfavorable meteorological conditions is considerably reduced.

Taking into account the incompleteness in the formulations of both these types of thought, a definition integrating the two along the following lines is to be preferred:

Drought is the temporary failure of the water supply to agricultural plants, It arises, in dependence on social and economic, agrotechnical, physical and geographic conditions, as a result of a macrometeorological process and leads to a substantial reduction or loss of crops.

The task of the present paper is to analyze the meteorological factors of drought. In this aspect the phenomenon of drought is conditioned by a complex* meteorological process on a massive scale.

First to turn their attention to the dynamic character of



Declassified in Part - Sanitized Copy Approved for Release 2012/03/12 : CIA-RDP82-00039R000100190014-6

Declassified in Part - Sanitized Copy Approved for Release 2012/03/12 : CIA-RDP82-00039R000100190014-6

the origin of drought were S. D. Griboyedov (13) and B. P. Mul'tanovskiy (25). The latter wrote:

"In its very essence the phenomenon of drought must be understood as a process uninterruptedly supported by definite atmospheric influences. In a word, drought is not a static phenomenon, and in this it closely recalls many phenomena which occur in connection with definite processes in the atmosphere, for instance the high levels reached by the waters in Petrograd."

In the formulation just presented, the phenomenon of drought is identified with the meteorological process evoking it. It seems to us more expedient to distinguish these two concepts, since the influence of drought is not dependent on meteorological processes alone. The process evoking drought is a great link in the macrometeorological process determined by the weather conditions of the whole hemisphere and connected simultaneously with the appearance of drought in different territories.

The macrometeorological drought-forming process may be defined as the origin, development and decline of successive circulatory currents in the atmosphere which, during an extended portion of the growing season of agricultural plants, sustain a condition of rainlessness, accompanied by low relative humidities and relatively high temperatures, in a given territory or in a number of territories.

By this definition we emphasize the dependence of the occurrence of droughts on the development and condition of the general circulation of the earth's atmosphere. As far as we know,



Declassified in Part - Sanitized Copy Approved for Release 2012/03/12 : CIA-RDP82-00039R000100190014-6

Declassified in Part - Sanitized Copy Approved for Release 2012/03/12 : CIA-RDP82-00039R000100190014-6

this aspect of the question has not yet been investigated.

Thus drought, in its meteorological context, is the ultimate expression of a long and complex process which develops over a given territory in the course of a fairly extended period. This process is a normal link in the circulation of the moderate latitudes, but it must reach a certain intensity before it does any economic damage.

There is not a single year when a synoptic chart of the Northern Hemisphere would appear entirely free from drought-forming processes, though they are highly variable in both localization and intensity.

2. By the general circulation we understand the tropo-stratospheric exchange of air masses between the equatorial-tropical zone and the high latitudes, which embraces directly or indirectly all circulatory zones without exception. This exchange is generated by, and on the whole is due to, the transfer of energy between the heated portions of the system and its cooler portions; and in detail it is determined by local energy transfers. The air masses are the principal carriers of energy. The deflecting influence of the earth's rotation is responsible for the division of the tropospheric circulation into great zonal belts. The circulation of the basic one of these zones -- the equatorial-tropical -- in the troposphere is closed within itself.

In the region of the tropopause and above it -- in the stratosphere -- this closure of the circulation does not occur, owing to the very low density of the air and to its increased velocities. For this reason the boundaries of the zonal circu-



Declassified in Part - Sanitized Copy Approved for Release 2012/03/12 : CIA-RDP82-00039R000100190014-6

Declassified in Part - Sanitized Copy Approved for Release 2012/03/12 : CIA-RDP82-00039R000100190014-6

lations are completely different in the stratosphere from those in the troposphere.

The system of ascending, horizontal, and descending currents makes up a complex vertical-horizontal system of circulation divided into regions of which only the lowest two may be considered as well known: the troposphere and the lower stratosphere to a height of 20 to 25 kilometers. The currents of air which commence their motion from the equator in a meridional direction are deflected from their original direction to the right in the Northern Hemisphere and to the left in the Southern Hemisphere. At some distance from the Equator -- say approximately 25 to 30 degrees latitude -- these currents then turn and flow along the parallels, and, forming a cell of convergence for the subtropical high pressure zone, powerfully block the tropospheric circulation of the equatorial-tropical zone.

The subtropical high pressure belt is primarily a belt of convergence between the internal currents of the equatorial-tropical zone on the one hand and the east-west transfer of the zone of temperate latitudes on the other. The subtropical high pressure belt is very active in the narrow strips bordering the equatorial-tropical zone. There accumulate the masses of warm dry tropical air, which are formed because of the regional transformation of the converging air masses. The excess portions of these air masses so formed overflow into the zone of temperate latitudes. The polar boundaries of the subtropical high pressure zones are unstably formed and can be distinguished only with difficulty on the chart by virtue of their activity.



Declassified in Part - Sanitized Copy Approved for Release 2012/03/12 : CIA-RDP82-00039R000100190014-6

Declassified in Part - Sanitized Copy Approved for Release 2012/03/12 : CIA-RDP82-00039R000100190014-6

The air currents that flow in the upper troposphere and stratosphere from the equatorial-tropical zone toward the poles possess a high potential temperature, and are responsible for the basic part of the heat balance of the polar zones. Thanks to their existence, great excess air masses accumulate in the polar zones which result from radiational cooling and are discharged from time to time into the zones of temperate latitudes (16), (17). The latter temperate zones play the role of passive zones and are the arena of conflict between two aggressors.

In the interaction between two circulations -- zonal or regional -- the regimen of one is subject to stronger variation than that of the other. One circulation, as it were, reorganizes the neighboring circulation. For instance, the Siberian winter monsoon anticyclone, gathering strength and forcing its air masses to the west, proceeds to reorganize the passive circulation of Europe. The Siberian anticyclone in this case is in expansion, while the European circulation is in depression.

The circulation of the zone of temperate latitudes consists, on the whole, of two components: a west-east transfer and a meridional circulation. They are mutually antagonistic: one of them strengthens while the other weakens.

The circulation of the northern zone of temperate latitudes undergoes disturbance from the regional circulations, and, in the first place, from the Atlantic and Pacific circulations (4). The influence of the monsoon circulations also increases in strength as the general circulation grows weaker. With increasing



Declassified in Part - Sanitized Copy Approved for Release 2012/03/12 : CIA-RDP82-00039R000100190014-6

Declassified in Part - Sanitized Copy Approved for Release 2012/03/12 : CIA-RDP82-00039R000100190014-6

activity of the sun and of the general circulation, the role of the monsoon circulations diminishes, while that of the oceanic circulations increases.

The regional circulations enter as elements in the general circulation and in the zonal circulation. These elements are usually unstable and sometimes of seasonal character as, for example, the monsoon circulations of Asia. A few of these local circulations, however, are very stable by virtue of the physical and geographic properties of their circulation regions such as, for instance, the circulations of the Atlantic and Pacific Oceans. Stable regional circulations maintain a certain autonomy in their energy households, and their influence is exerted on processes of very considerable power and extent, and during reorganizations of the general circulation they sometimes determine the direction of the latter.

The discharge of the excess air masses built up in the subtropical high pressure zone and in the Arctic zone proceeds uninterruptedly. The rate of such discharges, however, does not remain constant. In the first place, the frequency of such discharges increases as the general circulation strengthens and decreases as the general circulation weakens. Then their rate also varies in such a way that greater frequency occurs now in one zone and now in another.

Thus the development of the zones of expansion adjacent to the zones of temperate latitudes is accomplished by means of a fluctuating process. It is important to note that their intensity increases with solar activity, and weakens as the latter decreases.



Declassified in Part - Sanitized Copy Approved for Release 2012/03/12 : CIA-RDP82-00039R000100190014-6

Declassified in Part - Sanitized Copy Approved for Release 2012/03/12 : CIA-RDP82-00039R000100190014-6

The complete cycle of such fluctuation from the inception of expansion in one zone to the repetition of such expansion varies in accordance with the phases of the 11-year cycle of solar activity (monar) and with the fluctuations of solar activity from roughly 3 months during its stormy peak to the 11 months during its deep trough.

Besides this there are even wider fluctuations of the temperature and pressure background of a whole hemisphere; these fluctuation patterns are fairly stable over a year's time or even for whole 11-year periods. The first form appears over an entire hemisphere in the predominance of stable anomalies of a single sign. Tentatively, we have formulated the following explanation of this form. The dynamic barrier of the Equator divides the circulation within the troposphere. In the upper regions of the atmosphere, however, the flow of air from one hemisphere to the other is increased, and, without doubt, is accomplished in an alternating manner. First one hemisphere and then the other possesses excess air masses, in consequence of which the dynamic Equator is deflected now to the south and now to the north of the geographic Equator, into the region of the hemisphere that is relatively impoverished in air. By virtue of this, the heating area of the equatorial-tropical zone, which warms the air of the relatively enriched hemisphere, is considerably increased over its mean value, while the flow of heat is reduced into the hemisphere impoverished in air.

The second form of such fluctuations -- which already belong to the following class -- are the temperature anomalies, in terms



Declassified in Part - Sanitized Copy Approved for Release 2012/03/12 : CIA-RDP82-00039R000100190014-6

Declassified in Part - Sanitized Copy Approved for Release 2012/03/12 : CIA-RDP82-00039R000100190014-6

of the standard intervals of elapsed time, which depend on climatic fluctuations similar, from our point of view, to the first form and leading to the warming of the Arctic regions (9, 31).

Finally, the west-east transfer of processes is an important element in the circulation relationships. It appears only when the general circulation is sufficiently active. However, when a certain stage of pressure is reached in the general circulation, this transfer ceases to be distinguishable, being masked by the successive strong expansions of the arctic and subtropical high pressure belts. It is similarly indiscernable when the pressure of the general circulation is low, being then masked by the development of stationary processes. This transfer of processes is entirely distinct from the west-east transfer of air masses forming pressure systems. It may be traced on the charts by the large-scale displacement of weather phenomena, for instance of droughts, areas of excess precipitation, temperature anomalies, hurricane areas, etc. The transfer of temperature anomalies of ocean and sea currents serves as its cause (14).

The connection between the development of the general circulation and the progress of solar activity is now no longer in doubt. The dynamics of the basic components of the general circulation are still, however, in need of clarification. We accept the scheme of P. P. Predtechenskiy: both components increase with increasing solar activity, but the meridional circulation increases more, while the west-east transfer increases relatively less. Conversely, with the weakening of solar activity both these components weaken, but the meridional circulation weakens more, while



Declassified in Part - Sanitized Copy Approved for Release 2012/03/12 : CIA-RDP82-00039R000100190014-6

Declassified in Part - Sanitized Copy Approved for Release 2012/03/12 : CIA-RDP82-00039R000100190014-6

the west-east transfer weakens relatively less.

Solar activity acts in the first place on the processes of condensation, through them on the development of regional circulations, and then on the macrometeorological process. Because of this, solar activity becomes the principal organizing and stimulating agent, determining the development of the general circulation, which itself bears the indelible impress of a decisive influence (27).

The consistent application of this concept to the investigation of atmospheric processes will allow us to identify the links which are essentially determined by world-wide reasons, such as the distribution of land and sea areas, the structure of continental surfaces, the transfer of heat in ocean waters, etc.

3. The general circulation of the earth's atmosphere does not remain invariable. Besides the annual rhythm of change, there is uninterrupted change in its general stress, which may be characterized by the frequency of substitutions of air masses, calculated over a large enough territory and a sufficiently extensive network of meteorological stations.

Changes in stress of the general circulation are expressed in variations in its intensity, territorial distribution and type. These variations are accomplished primarily in the fundamental component mechanisms, the west-east and meridional transfers.

It is also important to consider the regularity of the general circulation. By regularity we understand the accuracy or



Declassified in Part - Sanitized Copy Approved for Release 2012/03/12 : CIA-RDP82-00039R000100190014-6

Declassified in Part - Sanitized Copy Approved for Release 2012/03/12 : CIA-RDP82-00039R000100190014-6

rhythmic quality of the recurrence, territorial distribution and duration of any major analogous synoptic processes (29). Regularity of the general circulation is determined by regularity of the active impulses emitted by the sun.

In irregular circulation the kinetic energy of motion of the air masses is unproductively expended in complex displacements of the pressure formations. In regular circulation it is, on the whole, expended in the displacement of air masses. In irregular circulation the velocity of displacement of the pressure formations may be very great, while at the same time the velocity of displacement of the air masses is low. Conversely, in regular circulation, even in cases where the pressure systems are slowly displaced, the transfer of the air masses themselves takes place rapidly.

If it is desired to characterize the condition of the general circulation at a given moment, we should take the following factors into account: (1) the relation between west-east and meridional transfers; (2) the relation between the expansion of active neighbors, that is, of the Arctic and subtropical high pressure belts; (3) the regularity of the general circulation; (4) the condition of the regional circulations and, first of all, that of the oceanic and monsoon circulations; (5) the development of the west-east transfer of processes.

The different circulation zones react differently to intensification or weakening of the general circulation. To some extent they depend on their complex interaction at the moment of observation, and to some extent on the [redacted] previous history of



Declassified in Part - Sanitized Copy Approved for Release 2012/03/12 : CIA-RDP82-00039R000100190014-6

Declassified in Part - Sanitized Copy Approved for Release 2012/03/12 : CIA-RDP82-00039R000100190014-6

duction of measurable radiation. This phenomenon may be called "hothouse effect."

The dry winds play an important role in the development of drought. By a dry wind as an element of drought we mean the occurrence of damage to agricultural crops under the influence of a considerable drop in the relative humidity. The soil moisture conditions are here of only secondary importance.

5. Turning now to the synoptic processes, the process of drought formation is generated either by the stable transfer of dry air masses, primarily -- though not exclusively -- in anticyclonic systems, which is the advective type; or else by the transformation of air masses with consequent relative dryness into widespread quasi-stationary anticyclones, which is the stationary type. Advection and transformation constitute the basis of the process of drought formation, and lead to a sharp fall in relative humidity and to the rapid evaporation of the moisture in plants and on the surface of the ground. Relative humidity falls rapidly. Stunting of growth commences much earlier than when only stagnant reserves of moisture still remain in the soil (that is, moisture unassimilated by plants and adsorbed as molecular film on particles of silicates in the soil). This is explained by the increased transpiration (due to evaporation) relative to the absorption of moisture through the roots. In the southern regions of the USSR, for instance in Turkmenistan, Uzbekistan, where during July and August, even in the absence of drought, and even under irrigation, wilting of plants and reduction of moisture-assimilation is observed in the hot afternoon hours.



Declassified in Part - Sanitized Copy Approved for Release 2012/03/12 : CIA-RDP82-00039R000100190014-6

Declassified in Part - Sanitized Copy Approved for Release 2012/03/12 : CIA-RDP82-00039R000100190014-6

If the gradual fall in the relative humidity lasts long enough, and especially if it coincides with the flowering phase and the development of the ovaries, it unavoidably leads to agricultural damage, and in extreme cases to catastrophic drought and consequent crop failure. The separate details whose occurrence is linked to other meteorological factors, are superimposed upon this simple pattern. Thus the presence of large amounts of dust in the air, which is always the case with tropical and continental Turanian air masses, leads to rapidly increasing overheating of the air. By virtue of the absorption of solar radiation by the dust particles and the subsequent release of this supply of energy in the long-wave spectrum already absorbed by the air, the heating of dust-laden air proceeds far more intensively than is the case with pure air. Besides this, as a result of the reduction in the transparency of the atmosphere because of its dust content and the formation of a dry haze (and sometimes also because of the existence of a turbidity detectable only by actinometric means in the upper strata of the atmosphere), outward radiation from the ground is sharply reduced both by day and by night. There is in consequence a considerable rise in daytime temperatures, while the nocturnal temperature minima remain extremely high and there is no dew whatever.

The nightly condensation of moisture in the surface stratum of the atmosphere provides a supplementary source of water for plants. We know of immense physico-geographic regions, such as Peru or Southwest Africa, where plants supplement their intake of water to a considerable extent by absorbing water condensed in the



Declassified in Part - Sanitized Copy Approved for Release 2012/03/12 : CIA-RDP82-00039R000100190014-6

Declassified in Part - Sanitized Copy Approved for Release 2012/03/12 : CIA-RDP82-00039R000100190014-6

surface layer of the atmosphere in the form of dew and fog. The absence of nightly condensation therefore represents still another handicap for plants in regions of drought. Besides this, wind velocity and intensification of turbulent agitation play a significant role in the acceleration of soil dessication.

Drought also takes a different course in places protected by forests or shelter-belts from the course it takes on the open steppe. Exposure of the site also plays a role: if it is on the northern or southern slope of a hill, ravine, or open field, or finally, if it is on a passage in a sequence of terraced hills gently sloping toward the south or southeast. The darker the soil, the more devastating will be insolation during a spring drought. It is for this reason that droughts assume so severe a character on black mould and chestnut brown soils.

6. The dry wind, that is, the sharp reduction in relative humidity, is always an element of the process of drought formation, but is observed during its initial stages only in a certain, though still rather high, intensity. There are undoubtedly different types of dry winds. Sometimes they occur with only modest temperature rises, though much oftener they are accompanied by substantial increases in temperature. Wind velocities in dry winds are sometimes imperceptible, while sometimes they reach 3 to 4 meters a second and higher.

On analyzing the development of the process of drought formation, it may be said that there are two basic types of dry wind, the stationary and advective. To these basic types a third should



Declassified in Part - Sanitized Copy Approved for Release 2012/03/12 : CIA-RDP82-00039R000100190014-6

Declassified in Part - Sanitized Copy Approved for Release 2012/03/12 : CIA-RDP82-00039R000100190014-6

be added -- the radiational type, which has been only slightly studied and is observed mostly in the south of the USSR, especially in Central Asia.

Stationary dry winds arise as a result of the foehn-type fallwinds in stationary anticyclones. They cause considerable heating of the air, and sharply reduce its humidity. It is just these dry winds that observers unacquainted with meteorology attribute to "the scorching winds of the glowing Central Asian steppes." This type has negligibly small horizontal velocities.

Advective dry winds are caused by currents of dry air masses, which may be either hot or cold. If they are hot, the air masses of the lower strata of the troposphere, transformed into a form of stationary anticyclone system, have a very low relative humidity and a high dust content, and are transferred toward the North at perceptible velocities. Under way they become still more heated as a result of their dust content. This type of dry wind as well is incorrectly called a Central Asian wind. In fact it only happens very rarely that Central Asian air masses impinge on the European territory of the USSR. The dust-free dry air masses of the Arctic intrusion are immediately heated as they move southward, and although they are supplied with moisture from the underlying surface of the earth, still retain their dangerously low relative humidity. The advection type of dry wind has the highest velocities.

The third type of dry wind -- the radiational -- has been studied very little. The Central Asian agrometeorologists furnished



Declassified in Part - Sanitized Copy Approved for Release 2012/03/12 : CIA-RDP82-00039R000100190014-6

Declassified in Part - Sanitized Copy Approved for Release 2012/03/12 : CIA-RDP82-00039R000100190014-6

the first information about it, but did not work out the meteorological circumstances of its occurrence. It originates either in the thermal depression of Summer or in a stationary anticyclone with imperceptible wind velocities. At such a time a turbidity is observed in the atmosphere -- not cloudiness, but only turbidity -- while the measurable solar radiation drops; this is confirmed by actinometric observation. This turbidity is opaque to infra-red rays and produces a hothouse effect in the lower strata of the atmosphere: temperature and absolute humidity rise rapidly, while relative humidity rapidly falls. "Heat flashes" without thunder occur in the air.

The dry wind as an element of the drought formation process is thus manifold in nature and demands a considerable amount of investigation to discover its characteristics. It is also necessary to strengthen and stimulate the observation of actual dry winds.

The stationary type of dry wind develops during a stationary drought. The advective type develops principally during drought of advective type, but may also originate on the periphery of a stationary anticyclone. The radiation type occurs during all types of drought.

7. The development of weather throughout the grain regions everywhere includes periods with high temperatures during the hot half of the year. Such periods, however, are not alone sufficient to originate drought. The factor of intensity as well as the time factor play a role in the development of the meteorological con-



Declassified in Part - Sanitized Copy Approved for Release 2012/03/12 : CIA-RDP82-00039R000100190014-6

Declassified in Part - Sanitized Copy Approved for Release 2012/03/12 : CIA-RDP82-00039R000100190014-6

ditions for drought. Long rainless periods may by themselves damage the development of certain agricultural crops. Injury to specific crops commences with the increasing intensity of unfavorable conditions and with the lengthening of the period of their action, depending on the species and variety of the plant in question. Buckwheat crops may fail completely at the same time that oats, wheat and rye give average or even above-average yields. Thus a rainless period, accompanied by a rise in temperature, may turn into a sporadic drought.

A drought may be light or severe, short or prolonged. When only those crops in certain stages of development are affected, or when the affected crops can subsequently recover with favorable weather, we have a sporadic drought. In cases of intense or prolonged drought, many or all crops are affected, the damage to agriculture becomes very substantial, and we have a catastrophic drought.

A sporadic drought is distinguished from a simple rainless period by the greater intensity of the unfavorable factors (fall in relative humidity, rise in temperature and wind velocity, etc) and the rapidity with which the reserves of soil moisture are consumed.

If no crop damage can be noted during the rainless period itself, the inception of a sporadic drought provides the further conditions for such damage. Some crops will suffer more and others less, according to the selective physiological qualities of the plants and according to the respective stages of development at



Declassified in Part - Sanitized Copy Approved for Release 2012/03/12 : CIA-RDP82-00039R000100190014-6

Declassified in Part - Sanitized Copy Approved for Release 2012/03/12 : CIA-RDP82-00039R000100190014-6

the time when sporadic drought strikes.

With progressive increase in intensity and duration, a sporadic drought, with its partial crop damage, turns into a catastrophic drought, with damage to all crops or a very considerable part of them. Sporadic droughts, ended by rainfall, after which drought recurs over an extensive territory, are frequently forerunners of catastrophic droughts. Catastrophic droughts result either from the powerful development of a stationary anticyclone or from the formation of a stable transfer of dry air masses in non-stationary processes.

In essence sporadic and catastrophic droughts are distinguished only in their duration, that is, the degree of stability of the circulations responsible for them; they are further distinguished in the degree of damage caused, whence the names.

Statistical analysis shows the existence of a wide belt in the European part of the USSR which is visited mostly by sporadic droughts, and of territories that are affected by catastrophic droughts (33). The territorial extent of sporadic droughts, especially in years marked by the development of thunderstorm processes, that is, in years of increased general circulation, remains small. The economic damage done by them is also small and does not reach the catastrophic level for whole physical and geographic provinces.

The occurrence of sporadic droughts allows us to analyze the formation of droughts in general. The basic factors are: (1) a difference between the total precipitation and the total evaporation



Declassified in Part - Sanitized Copy Approved for Release 2012/03/12 : CIA-RDP82-00039R000100190014-6

Declassified in Part - Sanitized Copy Approved for Release 2012/03/12 : CIA-RDP82-00039R000100190014-6

during the preceding Autumn, up to the beginning of the period and during it, whereby the amount of soil-moisture reserves in the layer inhabited by the roots is determined, and (2) the march of the positive departures of air and soil temperatures from the fixed optimum values. The processes responsible for reduction of the moisture balance and for overheating are normal links in the circulatory sequence. Every sporadic drought, and every catastrophic drought as well, has its own peculiar character to which the influence of soil moisture reserves, of the relative humidity, of the wind velocities, of the development of cloudiness, of atmospheric transparency, site exposure, soil qualities, etc., all contribute.

We may arrange these phenomena in the following order of increasing harmfulness for agriculture: rainless period; sporadic drought; catastrophic drought. The differences in intensity between the members of this series are determined by the stability and stress of the regional atmospheric circulation over a given territory. This circulation is in turn determined by the development of the general circulation, which is dependent on solar activity.

8. We pass now to the consideration of the process of drought formation in its manifestations: in the sporadic and catastrophic droughts of the European part of the USSR. The quality of the observational material recorded earlier than 1890 makes it impossible to use it in this work, for it contains neither general meteorological description nor sufficiently detailed description of the agricultural situation. Only the disastrous drought of 1891 compelled pre-revolutionary Russia to turn its attention to the



Declassified in Part - Sanitized Copy Approved for Release 2012/03/12 : CIA-RDP82-00039R000100190014-6

Declassified in Part - Sanitized Copy Approved for Release 2012/03/12 : CIA-RDP82-00039R000100190014-6

~~to the~~ study of droughts and ~~in the first place~~ primarily to the collection and preservation of data.

Even to the most recent times, however, the study of droughts was still conducted in a purely formal manner, confined at best to the determination of the synoptic situation. The connection of droughts with the development of the general circulation remained outside the field of vision of these investigators, as did the dependence of droughts on solar activity.

The predecessors of our work held the conviction that a solution of the question could be sought only by investigating the dependence of the general circulation on the development of solar activity and by defining catastrophic droughts as normal links in the development of the general circulation.

From this point of view all available papers on drought (1, 11, 18, 19, 20, 23, 26, 36, etc.) were examined and the concrete data on agricultural conditions extracted. In addition, all available basic sources were consulted, such as The Agricultural Year (12), Meteorologicheskiy Vestnik, Meteorologicheskoye Obozreniye, the monthly and ten-day agricultural surveys and weather surveys, literary material (V. I. Lenin [22], L. N. Tolstoy, V. G. Korolenko, etc.), and articles in newspapers and periodicals.

All this data was organized into a system based on examination and analysis of the synoptic charts of Eurasia from 1890 to 1948, and of the circumpolar regions from 1900 to 1939. The mechanism of the general circulation in its dependence on solar activity (7, 8, 9, 27) was the guiding principle. This relationship is responsible



Declassified in Part - Sanitized Copy Approved for Release 2012/03/12 : CIA-RDP82-00039R000100190014-6

Declassified in Part - Sanitized Copy Approved for Release 2012/03/12 : CIA-RDP82-00039R000100190014-6

on the one hand for the clear dependence on solar activity of the acceleration and retardation of the general circulation, suppression and development of monsoon influences, acceleration and retardation of the expansion of the active neighbors of the zone of temperate latitudes, and on the other hand for the manifestation of that activity in the regimen of precipitation and thunderstorm activity.

We formulated a hypothesis on the formation, development and localization of the drought-forming process in connection with the development of solar activity and with its regularity.

The vast extent and diversity in quality of our original material did not permit of complete uniformity in the analysis and description of individual droughts. For some of them data was lacking on the meteorological conditions of individual territories (the years of civil war, intervention, patriotic war); for others the existing descriptions were incomplete and also, to some extent, not scientific; much of the data in them was contradictory; this necessitated side by side comparison in the analysis and also required verification by the use of synoptic charts and charts of precipitation and temperature anomalies.

9. The types of catastrophic droughts also vary in accordance with the types of drought-forming processes. From the synoptic point of view such processes may be classified into two modifications: the stationary (radiational) and the advective.

Drought in the former case is determined by the transformation of stationary air masses, mostly of arctic origin or resulting



Declassified in Part - Sanitized Copy Approved for Release 2012/03/12 : CIA-RDP82-00039R000100190014-6

Declassified in Part - Sanitized Copy Approved for Release 2012/03/12 : CIA-RDP82-00039R000100190014-6

from foehn-type warming of descending air masses (foehns in open atmosphere). (35)

Drought of stationary or radiational type may afflict vast territories at the same time. All crops suffer more or less throughout the entire area afflicted. This type of drought is characteristic of epochs of slackening in the general circulation and fall of solar activity to very low levels. The influence of regional monsoon circulations is manifested most clearly in this type. With the slackening of the general circulation and the intensification of stationary processes, the winter monsoon circulation is intensified, while the oceanic circulations (taking hydrologic inertia into account) are slackened.

Stationary droughts are originated in anticyclone systems with slow west-east transfer as well as with meridional transfer, but under any circumstances there must be development of quasi-stationary processes to facilitate and accelerate the transformation of the air masses. Expansion of the subtropical high pressure belt is the usual cause of such droughts, but in rare cases it may also be connected with the expansion of the arctic belt.

The agricultural results of a catastrophic drought depend to a considerable degree on conditions in the preceding fall and winter (21). If these were favorable and the soil succeeded in accumulating sufficient reserves of moisture by spring, and the weather conditions were sufficiently favorable for the development of the winter crops, then the damage done by drought will be sharply reduced. The stationary or radiational droughts of 1890, 1891, 1900, 1901, 1911, 1921, 1931 and 1943 all occurred during epochs



Declassified in Part - Sanitized Copy Approved for Release 2012/03/12 : CIA-RDP82-00039R000100190014-6

Declassified in Part - Sanitized Copy Approved for Release 2012/03/12 : CIA-RDP82-00039R000100190014-6

of strongly reduced solar activity and slackened general circulation.

Advective type droughts arise with intensified general circulation and solar activity. They are accompanied and characterized by strong development of thunderstorm processes and consequently result in new network or cell distribution of the affected localities over the map. Very often limited islands of drought-free areas are observed in the midst of relatively large afflicted territories.

The process of drought formation in this type of drought is determined by the transfer of dry air masses under conditions of stable meridional circulation. These transfers may come from the south in the form of superheated southern air masses, or from the north when the former arctic air masses, now transformed, are transferred. In the former case the drought is limited in territorial extent, since as time passes the superheated air masses undergo cooling and their relative humidity rises; but in the latter case the drought extends over a vast area, inasmuch as the air masses are warmed and dried more and more during their southward movement.

Advective droughts occur in epochs of increased solar activity and high intensity of atmospheric circulation. 1893, 1905, 1906, 1907, 1917, 1927, 1928, 1936, 1938 and 1939 were years of advective drought. Characteristic of these years was the almost complete absence of quasi-stationary processes, with slackening of the west-east transfer; and the transfer of dry air masses proceeded along stable, localized tracks.



Declassified in Part - Sanitized Copy Approved for Release 2012/03/12 : CIA-RDP82-00039R000100190014-6

Declassified in Part - Sanitized Copy Approved for Release 2012/03/12 : CIA-RDP82-00039R000100190014-6

We shall not consider in the present paper droughts of the intermediate types: stationary-advective and advective-stationary. The droughts of 1897, 1898 and 1920 belonged to the former type, while that of 1924 belonged to the latter.

The actual existence of these types is confirmed by computations, in the literature, of the number of days with anticyclonic and cyclonic weather, during the months of the growing season in drought years. We present these computations in Table I, giving the mean number of days of anticyclonic weather in years of catastrophic drought for the drought region in the southeast of the European part of the USSR.

When the general circulation slackens, we encounter quasi-stationary processes and drought of stationary type, no matter which transfer has been dominant up to the time of drought formation. On strengthening of the general circulation, the number of quasi-stationary processes falls slowly at first, while the number of advective processes rises more and more rapidly with increased strengthening of the general circulation. By this is determined the evolution of stationary droughts within the general type, following the rising secular trend of solar activity observed with particular distinctness during the 20th century.

Evolution of the advective type of drought is similarly observed during the 20th century. In them the part played by stationary processes has steadily declined. In this case, however, the evolution does not reduce to fundamental modification, while with the stationary type it does: in the development of such droughts,



Declassified in Part - Sanitized Copy Approved for Release 2012/03/12 : CIA-RDP82-00039R000100190014-6

Declassified in Part - Sanitized Copy Approved for Release 2012/03/12 : CIA-RDP82-00039R000100190014-6

the participation of meridional processes has been increasing.

TABLE I

| Type of Drought | Number of Days with Anticyclonic weather | | | |
|---|---|---|---|---|
| | May | June | July | May-July Total |
| Stationary | 10.8 | 10.2 | 7.5 | 28.5 |
| Stationary-advective | 9.0 | 14.0 | 4.0 | 27.0 |
| Advective-Stationary | 4.7 | 5.7 | 10.6 | 21.0 |
| Advective | 1.6 | 4.4 | 9.8 | 15.8 |

During the 1930's, as a result of the secular increase in solar activity, we note that the two types of drought were clearly approaching each other. The last drought that can be classified as purely stationary in character occurred in 1921. The droughts during the 30's already testify to the inception of a new phase in the general circulation -- a phase which had never before been observed during the entire history of synoptic meteorology.

During a state of insufficient stress of the general circulation, no period of stable dominance of the basic expansions can be recognized in pure form. In such a case, besides the manifestation of activity of the zone undergoing actual expansion, the influence of a second zone is also present in some measure. At times these influences become so marked that the question arises: is the dominant expansion still being maintained? In months with stressed general circulation this mutual approach of the stresses of zonal expansion is not observed.



Declassified in Part - Sanitized Copy Approved for Release 2012/03/12 : CIA-RDP82-00039R000100190014-6

Declassified in Part - Sanitized Copy Approved for Release 2012/03/12 : CIA-RDP82-00039R000100190014-6

Research into the process of drought formation will make it possible to discover the mechanism of the general circulation, inasmuch as this process is always a component of the circulation in the temperate latitudes. Research into drought cannot pretend to aspire to attain a complete understanding of the circulatory relations, but will allow us to penetrate more profoundly into them and thereby to cast light on the least understood area of the general circulation, to wit: the distribution of the processes of condensation. Down to the present time there has been no single dominating idea in the investigation of the complex -- at first glance chaotic -- interrelations between the separate elements of the macrometeorological process; in our own work we have accepted the variation of solar activity as the decisive factor.

The regulatory influence of the sun is manifested in two ways: in the ultimate resolution of unstable conditions of moisture equilibrium, resulting in regional effects, and in the general reorganizations of the macrometeorological process, which are determined by the sum total, (that is, by the distribution) of the intensity and rhythm of all regional disturbances.

When the general circulation slackens and the west-east transfer dominates, quasi-stationary processes develop, and the process of drought formation assumes a static form. This process, when of stationary type, occurs in epochs of minimum solar activity and results in droughts which are continuous and unbroken over immense areas.

In epochs of the most lively general circulation, that is,



Declassified in Part - Sanitized Copy Approved for Release 2012/03/12 : CIA-RDP82-00039R000100190014-6

Declassified in Part - Sanitized Copy Approved for Release 2012/03/12 : CIA-RDP82-00039R000100190014-6

in epochs of peak solar activity, processes for the most part advective develop, and advective transfer assumes a dominant significance. Only when it is characterized by a high degree of regularity can such transfer provide the conditions for a dangerous development of the process of drought formation. The advective type of drought-forming process results in drought scattered in dot formation on the map: over a region of catastrophic or sporadic drought, thunderstorm processes develop from place to place, resulting in cloudbursts. Thereby, upon a map of the drought, islets or even islands appear, which are more or less favored from the agricultural point of view.

There is constant fluctuation in the development of solar activity, causing substantial variations around the mean level of any given phase of solar activity. Due to this, the process of drought formation often acquires a transitional character: stationary-advective or advective-stationary. In the former type, which occurs against the background of a weak stress of the general circulation and of the rapid rise of solar activity, it takes on the features of stationary development; while in the latter case, occurring against a background of a high stress of the general circulation, and a rapid drop in solar activity, it takes on the features of advective development.

We thus assume four genetic types of the drought-forming process and of droughts: the basic types, stationary or radiational and advective; and the transitional types, stationary-advective and advective-stationary. All the droughts in the European part of the USSR studied by us -- those that occurred between 1890 and 1939 -- fit into these four groups. Columns 2, 3, 4 and 5 of Table II



Declassified in Part - Sanitized Copy Approved for Release 2012/03/12 : CIA-RDP82-00039R000100190014-6

Declassified in Part - Sanitized Copy Approved for Release 2012/03/12 : CIA-RDP82-00039R000100190014-6

show respectively the years of catastrophic droughts, the region affected, the intensity and the genetic type of the drought. This list is very far from including all the droughts observed during the nineteenth and twentieth centuries; but it does include all the substantial agricultural disasters. The droughts of the past decade, to and including 1948, do not depart from the indicated types; the drought of 1943 belongs to the stationary type (with some reservation as to its mildness) while those of 1946 and 1948 belong to the advective type.



Declassified in Part - Sanitized Copy Approved for Release 2012/03/12 : CIA-RDP82-00039R000100190014-6

Declassified in Part - Sanitized Copy Approved for Release 2012/03/12 : CIA-RDP82-00039R000100190014-6

T A B L E

CATASTROPHIC DROUGHTS IN THE USSR, THEIR TYPES AND

| LINE NO. (1) | YEAR (2) | BASIC REGION AFFECTED (3) | INTENSITY OF DROUGHT (4) |
|---|---|---|---|
| 1 | 1890 | Southeast ETS | Average |
| 2 | 1891 | Southeast ETS, Ukraine, Central Chernozem Province, Kazakhstan | Maximum |
| 3 | 1893 | Ukraine, Central Chernozem Province | Average |
| 4 | 1897 | Southeast ETS | Average |
| 5 | 1898 | Southeast ETS | Average |
| 6 | 1900 | Western Siberia, Northern Kazakhstan, Irkutsk and Zabaykal Oblasts, Parts of Southwestern and Southeastern ETS | Average |
| 7 | 1901 | Southeastern ETS, Part of Eastern Ukraine | Average |
| 8 | 1905 | Southeastern ETS | Average |
| 9 | 1906 | Southeastern ETS, Central Chernozem Province, Ukraine | Maximum |
| 10 | 1907 | Southeastern ETS | Average |
| 11 | 1911 | Southeastern ETS, Kazakhstan, Western Siberia | Maximum |
| 12 | 1917 | Southeastern ETS, Central Asia Kazakhstan | Average |



Declassified in Part - Sanitized Copy Approved for Release 2012/03/12 : CIA-RDP82-00039R000100190014-6

Declassified in Part - Sanitized Copy Approved for Release 2012/03/12 : CIA-RDP82-00039R000100190014-6

II

DISTRIBUTION BY MICROSTAGES OF THE MONARS

| GENETIC TYPE OF DROUGHT (5) | MICROSTRUCTURAL STAGE OF MONAR (6) | LEVEL OF SOLAR ACTIVITY IN RELATIVE NUMBERS OF SUNSPOTS FROM OCT TO JULY (7) |
|---|---|---|
| Stationary | Normal Microbinar | 3.9 |
| Stationary | Normal Microbinar | 24.3 |
| Advective | Microsingular | 77.8 |
| Advective-Stationary | Second Asymmetric Microsingular Series | 29.8 |
| Advective-Stationary | Second Asymmetric Microsingular Series | 23.2 |
| Stationary | Depressive Microbinar | 11.4 |
| Stationary | Depressive Microbinar | 4.2 |
| Advective | Microsingular | 55.3 |
| Advective | Microsingular | 66.2 |
| Advective | First Asymmetric Microsingular Series | 55.2 |
| Stationary | Depressive Microbinar | 10.0 |
| Advective | Microsingular | 83.4 |



Declassified in Part - Sanitized Copy Approved for Release 2012/03/12 : CIA-RDP82-00039R000100190014-6

Declassified in Part - Sanitized Copy Approved for Release 2012/03/12 : CIA-RDP82-00039R000100190014-6

| (1) | (2) | (3) | (4) |
|---|---|---|---|
| 13 | 1920 | Southeastern ETS | Average |
| 14 | 1921 | Southeastern ETS | Maximum |
| 15 | 1924 | Southeastern ETS, Ukraine | Average |
| 16 | 1927 | Southeastern ETS | Average |
| 17 | 1928 | Ukraine | Average |
| 18 | 1931 | Southeastern ETS, Western Siberia | Average |
| 19 | 1936 | Southeastern ETS, Western Siberia | Average |
| 20 | 1938 | Southeastern ETS, | Average |
| 21 | 1939 | Southeastern ETS, | Average |
| 22 | 1943 | Southeastern ETS | Average |



Declassified in Part - Sanitized Copy Approved for Release 2012/03/12 : CIA-RDP82-00039R000100190014-6

Declassified in Part - Sanitized Copy Approved for Release 2012/03/12 : CIA-RDP82-00039R000100190014-6

| (5) | (6) | (7) |
|---|---|---|
| Advective-Stationary | Second Asymmetric Microsingular Series | 41.9 |
| Stationary | Depressive Microbinar | 32.3 |
| Stationary-Advective | Normal Microbinar | 11.6 |
| Advective | Microsingular | 74.2 |
| Advective | First Asymmetric Microsingular Series | 76.5 |
| Stationary | Depressive Microbinar | 27.2 |
| Advective | Microsingular | 64.5 |
| Advective | Microsingular | 108.3 |
| Advective | First Asymmetric Microsingular Series | 96.2 |
| Stationary | Depressive Microbinar | 20.2 |



Declassified in Part - Sanitized Copy Approved for Release 2012/03/12 : CIA-RDP82-00039R000100190014-6

Declassified in Part - Sanitized Copy Approved for Release 2012/03/12 : CIA-RDP82-00039R000100190014-6

Conditions determining the occurrence of these modifications do not violate the unity of development of the drought-forming process: as under all conditions the general circulation remains unitary, just as the macrometeorological process, of which the drought-forming process is always a link, also remains unitary.

10. At one time the writer proposed a scheme for the microstructure of the 11-year cycles of solar activity -- the monars (15). According to this scheme, each monar is composed of groups of fluctuations of solar activity, united by an internal physical linkage and representing the final microstages of solar activity. The distribution of microstages is subject to well-known regularities: monars of symmetric type are comparable to a long subperiod of the 190-year cycle -- the indiktion (28). The structure of asymmetric monars is similar to that of the short subperiod of the 190-year cycle. The indiktion is composed of monars. In turn, monars are composed of fluctuation microstages. This similarity represents not merely an external resemblance, but the manifestation of a unity of physical causation which is responsible for the development of solar activity in its various orders of significance. As the long arm of the indiktion is composed of tens of monars, so the symmetric monar is composed of tens of fluctuation-groups, divided into four microseries. The asymmetric monar, like the short arm of the indiktion, is composed of seven fluctuation-groups.

The resemblance is not confined to external similarity of structure, but manifests itself also in the internal relationship between the characteristics of analogous phases. The maximum development of activity in the subperiods of the indiktion is ob-



Declassified in Part - Sanitized Copy Approved for Release 2012/03/12 : CIA-RDP82-00039R000100190014-6

Declassified in Part - Sanitized Copy Approved for Release 2012/03/12 : CIA-RDP82-00039R000100190014-6

served in the singular series. In the individual monars the maximum manifestation of energy is during the microsingular series. The duration of the peak periods during the symmetric cycles is therefore greater than during the asymmetric cycles; during the former the microsingular series are composed of four members, the microsingular and three microasymmetrics, while during the latter they are composed of only three members, the microsingular and two microasymmetrics. The activity in the symmetric cycles is lower than that of the asymmetric cycles inasmuch as the short arm of the indiktion undergoes a more stormy development than the long arm. The minimums of activity coincide in the indiktion with the depressive binars, and in the separate monars with the depressive microbinars. As in the indiktion, there is a fundamental difference between the initial phase of a cycle and its final phase of a cycle and its final phase, that is, the physical asymmetry of the subperiods of the indiktion find adequate expression in the asymmetry of the monars. This close analogy between the phenomena at different levels of subdivision is confirmed by the course of the gradual accumulation of characteristics during the period of development of all monars which have been observed.

Table III. gives the distribution of the separate stages and groups of stages of 5 monars from 1889 to 1944 (15). Columns 6 and 7 of Table II give the microstructural stages of the monars and the indices of the mean stress of solar activity expressed by the relative number of sun spots during the ten months from October of the preceding year to July of the drought year. On examining Table II and Figure 7, we note that the depressive microbinars



Declassified in Part - Sanitized Copy Approved for Release 2012/03/12 : CIA-RDP82-00039R000100190014-6

Declassified in Part - Sanitized Copy Approved for Release 2012/03/12 : CIA-RDP82-00039R000100190014-6

coincide in time with the principal development of drought-forming processes of stationary type. The development of circulatory processes of stationary type is also noted during the course of other microcycles, but to a lesser degree -- the nearer the given microstage is to the microsingular of the cycle, the lower the mean activity of the given monar (Figures 1-6).

It must be noted that the development of advective processes in the general circulation is encountered with particular frequency during the course of the microsingular cycles. Although advective processes are also found in other microcycles, their frequency decreases as the distance between the given microcycle and the microsingular increases, and the higher the mean activity of the given monar. For this reason advective type processes of drought formation occur as a rule during the singular and during the first asymmetric microsingular series.

It follows from the tables and from Figures 2-6 that the catastrophic droughts of stationary type in 1900, 1901, 1921, 1911, 1931 and 1943 coincide in time with depressive microbinars and low levels of solar activity: a mean relative number of sunspots during the period from October to July ranging from 3.9 to 32.3.

The catastrophic droughts of 1890 and 1891, which belonged to the stationary type, coincided in time not with depressive microbinars but with normal ones. This is explained as follows: (1) during the course of the binar from 1878 to 1901 (Figures 1 and 2), the level of solar activity remained low, and consequently stationary traits predominated in the general circulation; (2) the



Declassified in Part - Sanitized Copy Approved for Release 2012/03/12 : CIA-RDP82-00039R000100190014-6

Declassified in Part - Sanitized Copy Approved for Release 2012/03/12 : CIA-RDP82-00039R000100190014-6

particularly low levels of activity observed from 1887 to 1890 (Figure 1) resulted in the general circulation remaining at a low level and thus being responsible for the protracted predominance of stationary factors in the development of the macrometeorological process.

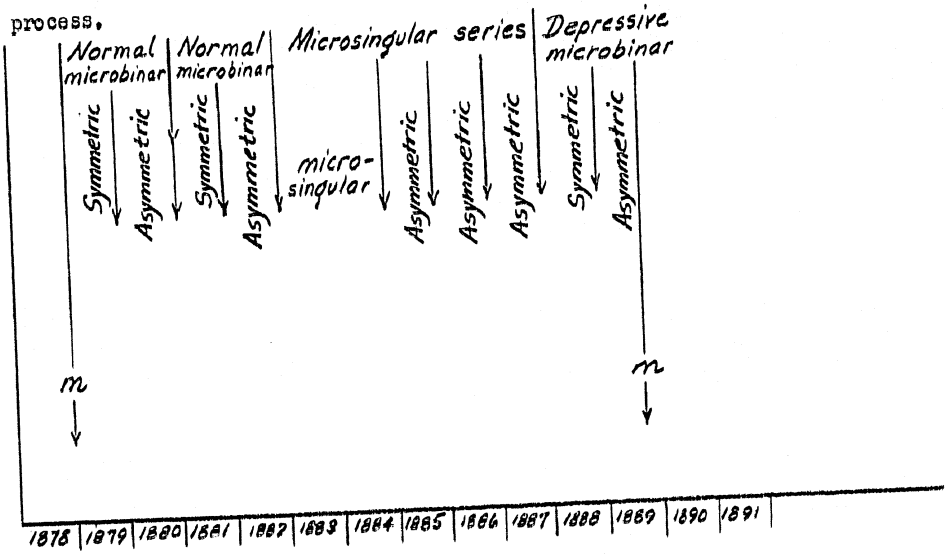


Figure 1. Relative number of sunspots and microstructure of the monar, 1878 - 1889.

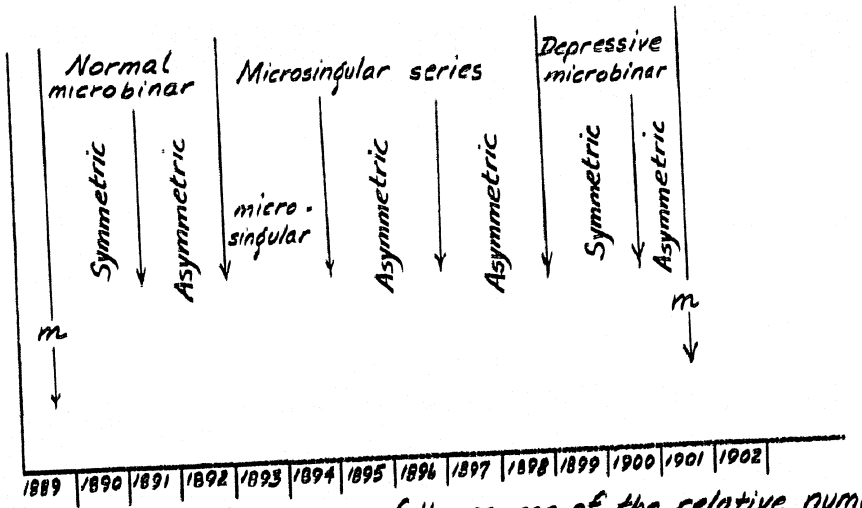


Figure 2. Comparison of the course of the relative numbers of sunspots and the microstructure of the monar from 1889 to 1901 with the types of catastrophic droughts.



Declassified in Part - Sanitized Copy Approved for Release 2012/03/12 : CIA-RDP82-00039R000100190014-6

Declassified in Part - Sanitized Copy Approved for Release 2012/03/12 : CIA-RDP82-00039R000100190014-6

[Legend, figure 2] Types of catastrophic drought: 1-advective, 2-stationary, 3-advective-stationary, 4-stationary-advective.

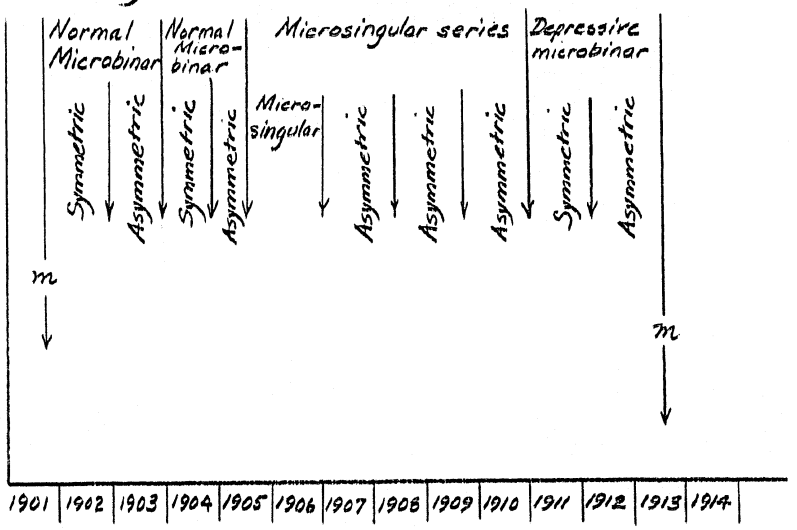


Figure 3. Comparison of the course of the relative numbers of sunspots and the microstructure of the monar from 1901-1913 with the types of catastrophic droughts. (See fig. 2 for Legend.)

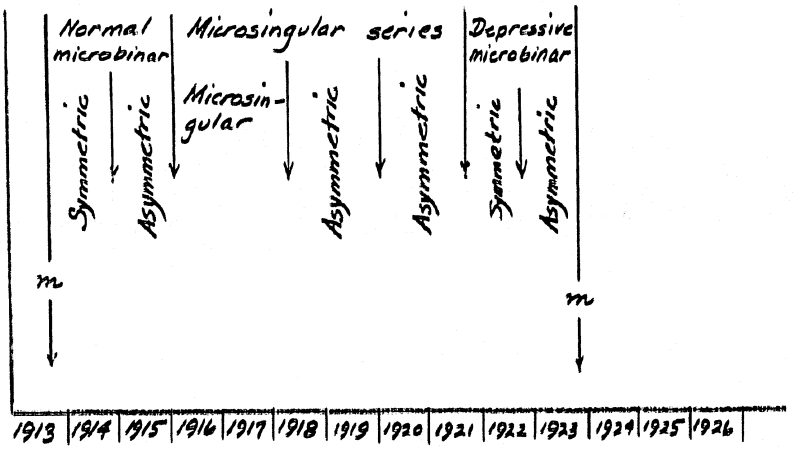


Figure 4. Comparison of the course of the relative numbers of sunspots and the microstructure of the monar from 1913-1923 with the types of catastrophic droughts. (See fig. 2 for Legend.)



Declassified in Part - Sanitized Copy Approved for Release 2012/03/12 : CIA-RDP82-00039R000100190014-6

Declassified in Part - Sanitized Copy Approved for Release 2012/03/12 : CIA-RDP82-00039R000100190014-6

We conclude further, from the tables presented and Figures 2-6, that all the catastrophic droughts of advective type in 1893, 1905, 1906, 1907, 1917, 1927, 1928, 1936, 1938, and 1939 coincide in time with microsingular series and high levels of solar activity; the mean relative number of sunspots during the period from October to July varies from 55.2 to 108.3, and in 1948, according to preliminary data, it reached about 140.

The droughts of 1893, 1905, 1906, 1917, 1927, 1936 and 1938 occurred during microsingular cycles proper, while those of 1907, 1928 and 1939 occurred during the first asymmetrics of the microsingular cycles. The droughts of advective-stationary transitional type in 1897, 1898 and 1920 occurred during the last asymmetrics of the microsingular series, while the drought of stationary-advective type in 1924 occurred during a normal microbinar.

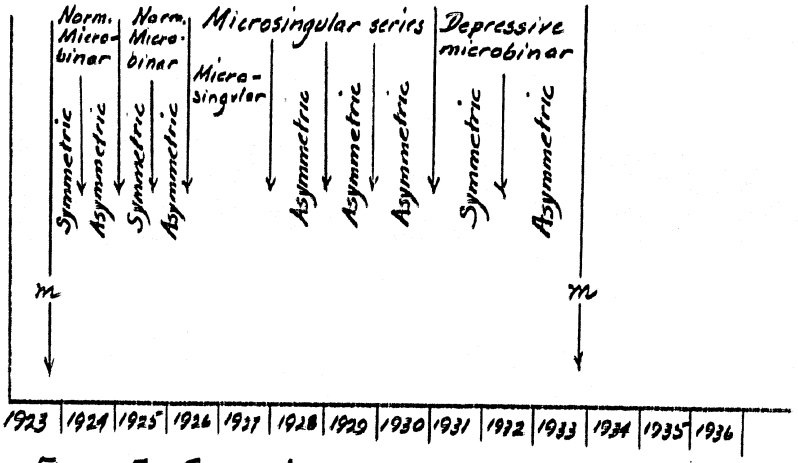


Figure 5. Comparison of the course of the relative numbers of sunspots and the microstructure of the monar from 1923-1933 with the types of catastrophic droughts. (See fig. 2 for Legend.)



Declassified in Part - Sanitized Copy Approved for Release 2012/03/12 : CIA-RDP82-00039R000100190014-6

Declassified in Part - Sanitized Copy Approved for Release 2012/03/12 : CIA-RDP82-00039R000100190014-6

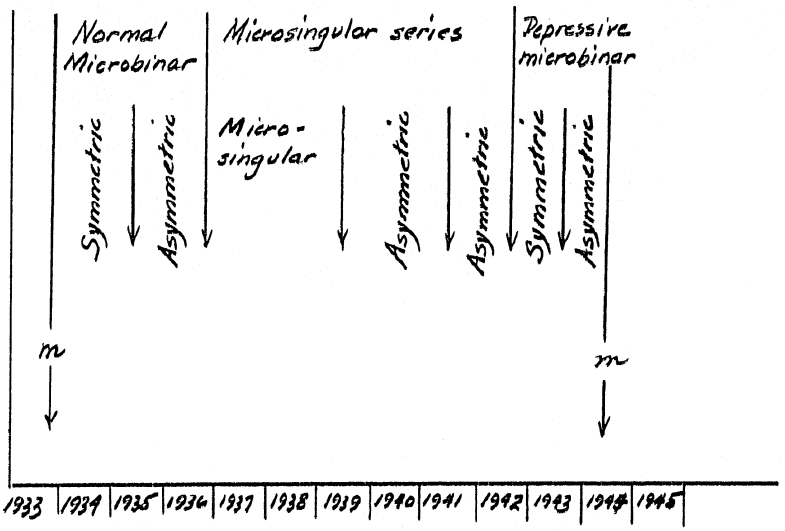


Figure 6. Comparison of the course of the relative numbers of sunspots and the microstructure of the menar from 1933-1944 with the types of catastrophic droughts. (See fig. 2 for Legend.)

11. The accurate prediction of drought is possible only if a reliable forecast of the general circulation of the planetary atmosphere can be made. Besides a knowledge of current processes and of the preceding development of the general circulation, a forecast of solar activity is also necessary for this. Such a forecast need not necessarily predict in detail each individual impending fluctuation of solar activity. For the purpose of long-term climatic forecasting it is necessary to know only the type of cycle, its activity, intensity at the peak epoch, and the dates of its extremes.

Statistical methods at the present time are applicable neither to forecasting solar activity not to forecasting the development of the planetary general circulation, in view of the brief period



Declassified in Part - Sanitized Copy Approved for Release 2012/03/12 : CIA-RDP82-00039R000100190014-6

Declassified in Part - Sanitized Copy Approved for Release 2012/03/12 : CIA-RDP82-00039R000100190014-6

covered by the series of observations on which the forecaster is compelled to rely. A forecast of the development of the general circulation is made up on the whole of separate forecasts of its intensity, type of prevailing processes, development of the regional circulations, prevailing expansions and development of the processes of west-east transfer. A climatic forecast cannot establish the aim of predicting the weather by days. The margin of error in the prediction of the time of onset and of close of the individual stages of a circulation increases with the length of the forecast period. Thus an error of a single month in the forecast of solar activity or of the general circulation has no practical effect on the reliability of a climatic forecast. The forecaster needs only to know the mean values for the microstages of solar activity (15); the reliability of these is entirely sufficient for making a breakdown of the planetary general circulation. The mean level of the separate microstages can be predicted well enough from a table showing microstructure as a function of the expected stress during the epoch of the peak activity. It is frequently possible for the forecaster, who takes the preceding history into account, to work out the territorial distribution of the most important circulation members on this basis. But this is possible -- it must be understood -- only with processes that are stable and of sufficient scope.

12. The strengthening and slackening of the general circulation of the planetary atmosphere is broadly parallel to the smoothed curve of solar activity, excluding the abrupt reversals during the epoch of maximum activity. The inertia of the general



Declassified in Part - Sanitized Copy Approved for Release 2012/03/12 : CIA-RDP82-00039R000100190014-6

Declassified in Part - Sanitized Copy Approved for Release 2012/03/12 : CIA-RDP82-00039R000100190014-6

circulation is determined by its entire development during the preceding two or three years, with which the forecaster should be familiar. Solar activity exerts only an indirect effect toward modifying this inertia, by way of its action on the hydrological condition of the oceans. The higher the level of solar activity for a given monar (11-year cycle of solar activity) the higher will be the stress of the general circulation. The role of advective processes grows more important with the strengthening of the general circulation, while that of stationary processes grows with its slackening. This relationship depends primarily on the mean stress of the general circulation in a given epoch (of the order of a single monar), and the forecaster should be very familiar with this magnitude; and in the second place on the expected mean cause of solar activity according to the stages. When the mean level of the relative number of sunspots exceeds 40, it may be confidently expected that the stress of the general circulation will attain a high level and that the stationary processes will assume a clearly subordinate position in that circulation, becoming stronger only during epochs of considerable depression of solar activity. The following cycles in recent times constituted such monars:

| YEAR | Mean Relative Number of Sunspots for the Monar |
|---|---|
| 1917 | 44.4 |
| 1928 | 40.3 |
| 1937 | 57.2 |
| 1948 | 60.0 (only estimated for purposes of orientation) |



Declassified in Part - Sanitized Copy Approved for Release 2012/03/12 : CIA-RDP82-00039R000100190014-6

Declassified in Part - Sanitized Copy Approved for Release 2012/03/12 : CIA-RDP82-00039R000100190014-6

while, on the contrary, during the cycles:

| YEAR | Mean Relative Number of Sunspots for the Monar |
|---|---|
| 1889 | 35.5 |
| 1894 | 37.8 |
| 1907 | 31.6 |

stationary process predominated over advective processes. The effect of this circumstance was reinforced by the fact that a profound depression of the indiktion (190-year cycle) occurred during these latter cycles (28).

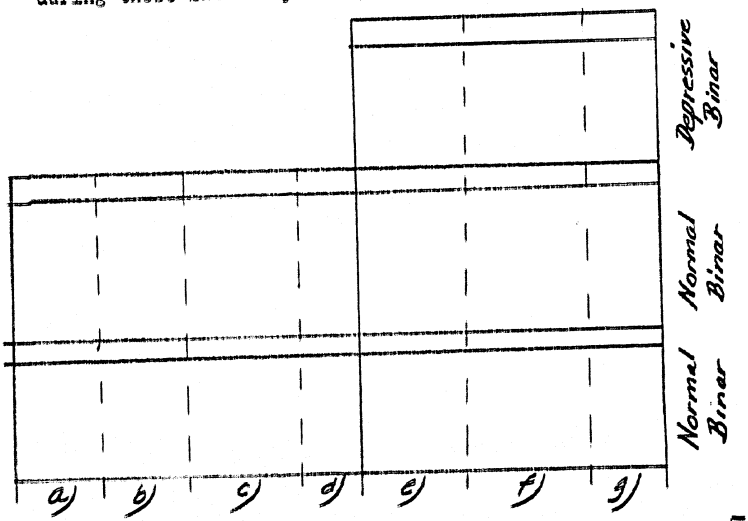


Figure 7. Distribution of catastrophic droughts in European USSR by microstages of the last five monars.

(a) first normal microbinar; (b) second normal microbinar; (c) long microsingular; (d) depressive microbinar; (e) normal microbinar; (f) short microsingular; (g) depressive microbinar. (1) symmetric micromonars; (2) asymmetric micromonars; (3) singular micromonars; (4) depressive microbinars. Catastrophic Droughts by Types: (5) stationary type; (6) advective type; (7) stationary-advective type; (8) advective-stationary type.

Note: The horizontal line of Roman numerals shows the month in which a new microstage commenced; the next horizontal line shows the dates of beginning of the microstages in years and tenths of a year; the horizontal line below the triangles shows the years of drought.



Declassified in Part - Sanitized Copy Approved for Release 2012/03/12 : CIA-RDP82-00039R000100190014-6

Declassified in Part - Sanitized Copy Approved for Release 2012/03/12 : CIA-RDP82-00039R000100190014-6

13. It is far more difficult to forecast the type of circulation, that is, to indicate whether the west-east or meridional transfer will be predominant. Such forecasts must be based on the empirical fact that the duration of the period during which one transfer or the other is predominant increases with decreasing solar activity and decreases with increasing solar activity. Neither transfer is observed in its pure form at the present time. A second transfer is always associated to some degree with the dominant transfer. With a calendar showing the dates of these transfer phenomena during the past two or three years, the changes in type of circulation can be rather reliably forecast with the aid of the forecast for the intensity of the solar cycle. In forecasting such changes of type, over periods up to one year, an accuracy of the order of one month is attainable.

14. Stability in the rhythm of these changes also depends on the regularity of the general circulation. By the latter is understood the correspondence in extent and in time of recurrence between corresponding processes in the cycle (29). Regularity of the general circulation depends on the regularity of solar activity, and its curve can be smoothed with relative ease into an accurate alternation with the fluctuations of solar activity. The 1907, 1928, 1937 and 1948 cycles were regular, while those in 1883 and 1894 were irregular, and the 1917 cycle was regular for only some of its stages.

It must be noted that the regularity of solar activity is subject to a secular upward trend. The single-type cycles of the nineteenth century show far less regularity than those enumerated



Declassified in Part - Sanitized Copy Approved for Release 2012/03/12 : CIA-RDP82-00039R000100190014-6

Declassified in Part - Sanitized Copy Approved for Release 2012/03/12 : CIA-RDP82-00039R000100190014-6

above. This regularity must be distinguished from the inertia of the general circulation. Regularity is introduced into the general circulation by the rhythm-imparting influence of solar activity, while the inertia of the general circulation is due fundamentally to the transfers of heat in ocean waters and to the character of the surfaces underlying that circulation.

15. Expansion of the active zones of the subtropical high pressure belt and the arctic high pressure belt into the zone of temperate latitudes is a determining factor in the development of the general circulation. For this reason the next stage in formulating a forecast is the determination of the dominant expansion. Analysis of the cause of semiannual temperature fluctuations during the respective monars confirms the fact that at certain levels of solar activity the zone of temperate latitudes is divided into two subzones: a northern and a southern. This division manifests itself more strikingly with increasing solar activity; on the other hand, it becomes less apparent as solar activity slackens. With intensification of advection the character of the weather process in the northern subzone is primarily determined by the influence of the arctic, while in the southern subzone it is correspondingly determined by the influence of the subtropical high pressure belt. The processes of expansion are strengthened or weakened with the strengthening or weakening of solar activity, with first one and then the other expansion predominating in turn. At any given stage of development of the general circulation, the circulations of the separate physical and geographical provinces take on the general color of precisely that expansion which happens



Declassified in Part - Sanitized Copy Approved for Release 2012/03/12 : CIA-RDP82-00039R000100190014-6

Declassified in Part - Sanitized Copy Approved for Release 2012/03/12 : CIA-RDP82-00039R000100190014-6

to be dominant at that particular time. This is due to the fact that the expansions of the active zones determine the dominating areas of formation of the air masses transported to a given territory by the west-east transfer and the meridional circulation.

When the expansion of the subtropical high pressure belt is intensified, the frequency of the inflow of warm air masses rises (tropical, formerly tropical and warm polar air), with unstable weather and very rapidly changing synoptic processes. Total precipitation as well as the number of days with precipitation falls. At the same time the inflow of air from the arctic are frequent and weak. The transport of the masses of cold dry air proceeds in fractions, without changing the general picture, which is composed of extensive and stable warm anticyclones. This also results in negative anomalies of precipitation.

When the arctic expansion is intensified against the background of a strongly stressed general circulation, predominance of the cold air masses results (arctic, formerly arctic and cold polar air), with instability of weather and increased total precipitation and a greater number of days with precipitation. With arctic expansion the Atlantic cells are frequent and weak; but the moisture transported by them from the ocean duly condenses, and a positive anomaly of precipitation is thus assured.

The following signs of a slackening arctic expansion may be pointed out: (a) the more northerly position of the transcontinental high pressure belt, as compared with the time of full development of that expansion; (b) the northward shift of the line of demarcation



Declassified in Part - Sanitized Copy Approved for Release 2012/03/12 : CIA-RDP82-00039R000100190014-6

Declassified in Part - Sanitized Copy Approved for Release 2012/03/12 : CIA-RDP82-00039R000100190014-6

between the northern and southern subzones of the zone of temperate latitudes.

16. The relation between the expansions of both these active zones constitutes the decisive condition for the meteorological circumstances of both subzones. The modification of this relation is a fluctuating process which demands a definite interval of time for its development.

With insufficient stress of the general circulation, it is impossible to make any clear-cut division of the period of stable predominance of the basic expansions. Usually, in addition to the manifestation of activity of the zone undergoing expansion, there also exists the influence of a second zone. These interferences occasionally become so marked that they raise the question as to whether or not the dominant expansion is still being maintained. This phenomenon is not observed in monars with highly stressed general circulation. The displacement of the dominant expansion is entirely distinct, and the development of the new expansion proceeds in analogous fashion. The change-over between the expansions of the active zones is due to the march of the accumulation of air masses in the Arctic and in the subtropical high pressure belt. The strengthening of the general circulation results in the first place in the strengthening of the circulation of the equatorial-tropical zone and the expulsion of air masses toward the poles and into the subtropical high pressure belts.

17. The forecast, moreover, should follow the conditions in the regional circulations. The most difficult of these is the



Declassified in Part - Sanitized Copy Approved for Release 2012/03/12 : CIA-RDP82-00039R000100190014-6

Declassified in Part - Sanitized Copy Approved for Release 2012/03/12 : CIA-RDP82-00039R000100190014-6

forecast of the monsoon circulation. With the strengthening of the general circulation the monsoon phenomena subside as a rule. However, at very high levels of stress of the circulation, the usual monsoon phenomena are complicated to a considerable extent by dynamic factors. Incipient monsoon phenomena are connected with readjustments in the energy balance between land and sea. In years of slack circulation this aspect of the phenomenon becomes intensified and then represents the entire monsoon circulation. In years of strengthened circulation, dynamic factors are added to the basic stimulus. The winter monsoon anticyclones then develop powerfully and at first glance can be reckoned among the normal monsoon formations.

This phenomenon develops on an especially broad scale in the cold half-year, owing to the temperature contrast between land and sea. The monsoon-dynamic winter anticyclones, however, disintegrate in the spring and leave behind them summer quasi-stationary continental anticyclones, the occurrence of which stands in glaring contradiction to the customary physical concept of a monsoon. At the same time the pure monsoon phenomena of the warm half of the year, such as the thermal Asiatic depression, remain incompletely developed.

Forecasting is facilitated by the following additional considerations: in order for the monsoon circulation to be completely free from dynamic factors, it is necessary to have a low level of the general circulation, accompanied by weak and unstable transfers. In years of considerable stress in the general circulation only monsoon-dynamic processes can develop; on the other hand, with a



Declassified in Part - Sanitized Copy Approved for Release 2012/03/12 : CIA-RDP82-00039R000100190014-6

Declassified in Part - Sanitized Copy Approved for Release 2012/03/12 : CIA-RDP82-00039R000100190014-6

stormy growth of the stress of the general circulation or with its very rapid abatement, its dynamic transfers are so strong that the existence of a monsoon-dynamic complex becomes impossible. The time of the appearance and the duration of the monsoon circulation follow from the forecast of the stress and type of the general circulation and of the relation between the expansions.

The territorial distribution of monsoons and monsoon-dynamic processes is rigidly determined by physical and geographic conditions, which change only at geological velocities. Therefore, if once the places of origin of monsoons and monsoon-dynamic phenomena are known in advance, the forecaster then has only to solve the problem of fixing the territorial boundaries of the monsoon phenomena.

The next stage -- forecasting the state of the oceanic circulations -- is relatively easy because of the stability and inertial qualities of their energy balance, and is based on the preceding record of the circulation.

The oceanic circulations determine to a large extent the character of the basic transfers over the continental areas of Eurasia and America. G. Ya. Vangengeym's eastern type of circulation apparently depends on the relation between, and on the stresses of, the oceanic circulations (4). In our opinion it is a subspecies of the meridional circulation.

18. From year to year the regions of sharp weather anomalies undergo a shift from west to east. The magnitude of the annual displacement and the change in the intensity of the processes at the time of each shift depends primarily on the level of solar acti-



Declassified in Part - Sanitized Copy Approved for Release 2012/03/12 : CIA-RDP82-00039R000100190014-6

Declassified in Part - Sanitized Copy Approved for Release 2012/03/12 : CIA-RDP82-00039R000100190014-6

vity. This dependence, however, is complicated not by the stress of the general circulation, but by the violation of its regularity of that circulation in the corresponding regional -- and especially oceanic -- circulations. The course of the anomalies of the elements indicates the spatial and temporal displacements of major links in the weather process, while the scope of the phenomenon allows us to go so far as to speak even of shifts in the spatial and temporal location of a number of factors of climate formation.

The distribution of the drought forming processes in time and space is subordinated, at mean levels of development of solar activity and of the general circulation, to the west-east displacement of anomalies and processes. At high stresses in the general circulation, the expansion of the active zones screens the west-east transfer of processes.

The basic factors which determine the conditions during the growing season are:

1. type and stress of the basic transfer;
2. dates of beginning and end of the alternating expansion of the subtropical high pressure belt or the expansion of the arctic, which alternately dominate;
3. the regularity of the general circulation;
4. the state of the monsoon circulation -- whether stimulated or depressed;
5. the oceanic circulations;
6. the west-east transfer of processes.

19. We shall now consider the territorial and temporal



Declassified in Part - Sanitized Copy Approved for Release 2012/03/12 : CIA-RDP82-00039R000100190014-6

Declassified in Part - Sanitized Copy Approved for Release 2012/03/12 : CIA-RDP82-00039R000100190014-6

distribution of the process of drought formation. Under the domination of the meridional transfer the processes of drought formation never simultaneously embrace both the South Russian plain and Central Asia. Across these territories in general the transfer of humid marine air masses from the eastern Mediterranean and from the Black Sea is accomplished. If one of these areas is occupied by superheated continental air masses, then the other is taken over at the same time by marine and former marine air masses, and conversely.

When the relatively dry and the relatively moist air masses move irregularly, their paths intersect each other frequently. When they move regularly, they remain apart. In the former case both physical and geographic provinces have climatic and agricultural conditions close to the mean values for a term of years. In the latter case, one of the territories will have a plainly unfavorable agricultural environment as the process of drought formation develops, while the other will have a clearly favorable agricultural environment as expressed by the increase of humidity. This statement is accurate both for the stationary type of circulation (1921, the drought in European USSR) and for its advective type (1917, the drought in the southeast part of European USSR, in Central Asia and in Kazakhstan).

Paths of transport for humid air masses are as follows:

a. Tyrrhenian Sea -- Rhone basin -- northward;
b. Adriatic Sea -- upper Danube -- Elbe and Oder;
c. Black Sea -- Dnepr basin;
d. Black Sea -- basin of Middle and Lower Volga -- Kama basin;



Declassified in Part - Sanitized Copy Approved for Release 2012/03/12 : CIA-RDP82-00039R000100190014-6

Declassified in Part - Sanitized Copy Approved for Release 2012/03/12 : CIA-RDP82-00039R000100190014-6

e. Southern Caspian -- to the east from the Aral Sea;

f. Murgab basin -- Syr-Dar'ya basin -- Balkhash.

Paths e and f merge and flow together in the direction of Lake Baikal. Paths a and b also merge to the north of latitude 55 degrees + ; Paths c and d merge at the Upper Volga -- from Selizhar to Gor'kiy.

The northern dry air masses, as well, frequently follow the course of the river basins. Only the western type of Kara Sea intrusions are determined by the Ural chain.

The regularity of the general circulation, too, is of decisive influence in cases where advective processes predominate. When this regularity is great, then -- if monsoon influences are absent or weakened -- the outward paths of the humid air masses will bring drought either in the Dnepr basin (in the broad sense of the word) or in the Kama-Volga basin. When the dynamic-monsoon circulation is strongly developed, it determines the location of the process of drought formation.

If circulation is not regular, then, due to the physical and geographic conditions, catastrophic drought cannot develop on the European part of the USSR, except for its eastern and southeastern portions. In the former case, a forecast of the distribution of the affected areas must rely on the inertial qualities of the general circulation and on the stability of distribution of the air masses paths. In the latter case forecasting is easier. The role of the regularity of the general circulation reduces to the following: when the processes are regular, sporadic droughts recur in a fixed



Declassified in Part - Sanitized Copy Approved for Release 2012/03/12 : CIA-RDP82-00039R000100190014-6

Declassified in Part - Sanitized Copy Approved for Release 2012/03/12 : CIA-RDP82-00039R000100190014-6

rhythm and strengthen their activity, very often forming catastrophic droughts (1906, 1917). When the circulation is irregular, sporadic droughts do not recur rhythmically. The periods of rain that divide them grow longer, and a catastrophic drought can develop only in localities where the physical and geographical circumstances favor such development, (1897 and 1898). Each time, the existing relationships between the expansions of the basic active zones must be taken into account.

20. When the west-east transfer is dominant, the location of the boundary between the northern and southern subzones is the first problem which must be solved. This is determined by the forecast for the expansions. When the arctic expansion dominates, this boundary is shifted southward, and the development of the drought-formation process is then concentrated on the steppes of Southern Russia, in the Krimea, Pre-Caucasus, Lower Volga, and the Transvolga steppes. When the expansion of the subtropical high pressure belt dominates, the boundary is shifted northward, and the process of drought formation embraces the northern regions of the Ukraine, the Central Chernozem Province, Central Povol'zhe and all of Western Siberia.

In the same way the process here can be regular or irregular. If it is regular, then the region of development of the drought formation process is located to the south of the division between the subzones, resulting in the development of sporadic drought over great areas. The distribution of catastrophic drought is determined by monsoon influences. When the general circulation is weakly developed, that is, when independent monsoon processes are developed,



Declassified in Part - Sanitized Copy Approved for Release 2012/03/12 : CIA-RDP82-00039R000100190014-6

Declassified in Part - Sanitized Copy Approved for Release 2012/03/12 : CIA-RDP82-00039R000100190014-6

droughts of the 1931 type are formed. When the general circulation is strongly developed and the monsoon-dynamic processes are also developed, 1945 type droughts (Danube basin) are built up. When the circulation is irregular, the distribution of catastrophic drought is determined by the distribution of quasi-stationary processes (together with the monsoon-dynamic circulation) and by the physical and geographic conditions (1901 and 1911).

When the process of drought formation evolves under the aegis of the west-east transfer, the paths of discharge of arctic air on to the continent of Europe acquire essential significance. If the circulation is regular they take up a permanent territory and are responsible for the formation of zones of merger and of regions of precipitation. When the circulation is irregular, these transfers take place along different paths. Thanks to this fact, the regions of rainfall embrace various territories where sporadic drought has developed and thus lessen the agricultural effect.

The present paper gives only a first rough outline of the methodology of climatic forecasting of the development of the drought-formation process on the European territory of the USSR. The development of the methodology of climatic forecasting will serve as a subject of further research.

E N D



Declassified in Part - Sanitized Copy Approved for Release 2012/03/12 : CIA-RDP82-00039R000100190014-6

Declassified in Part - Sanitized Copy Approved for Release 2012/03/12 : CIA-RDP82-00039R000100190014-6

# SOME PROPERTIES OF FIELDS OF METEOROLOGICAL ELEMENTS

(Temperature, pressure, wind, and precipitation)

O. A. Drozdov

Down to recent times climatology was concerned, with rare exceptions (breezes, mountain-valley circulation), only with the study of the climate of discrete points, independently of whether climate could be analyzed into separate elements or complexes of elements. There was relatively little research into the structure of the course of the weather in any given place from time to time.

Under such conditions, when one referred to the climate of a territory, what was really meant was merely the more or less successful interpolation of the data for separate areas within the territory. It is true that the connections between the course of the weather at neighboring points were investigated, but they were used only for working out numerical data, without any characterization of the climate in essence. The spatial distribution of weather is nevertheless a very important climatic factor; it is of concern to the most diverse branches of the national economy and is not devoid of interest to the armed forces.

The various meteorological phenomena simultaneously affect territories of varying dimensions. Heavy rains on the European territory of the USSR are observed at individual points or over an area covering at most a few rayons. Such points of torrential rain may be observed simultaneously, or almost so, at a number of places spread over the territories of a number of oblasts.



Declassified in Part - Sanitized Copy Approved for Release 2012/03/12 : CIA-RDP82-00039R000100190014-6

Declassified in Part - Sanitized Copy Approved for Release 2012/03/12 : CIA-RDP82-00039R000100190014-6

Droughts, depending on their origin, may possess very different territorial structures, ranging from the continuous inclusion of a vast and unbroken territory down to the manifold distribution of precipitation and crop yields according to the paths of thunderstorms across a territory in times of drought. The dimensions of the regions covered by widespread and continuous rains, snowstorms, thunderstorms, or sleet are of interest, for these dimensions determine the degree of the difficulties caused by these phenomena to railroad and air transportation and to communication lines. For instance, in predicting the path of a thunderstorm for the aviation service it is by no means irrelevant to know whether we are dealing with areas of heat lightning, small in extent and easily by-passed, or with large-scale thunderstorm fronts which are hard to by-pass.

The very concept of the frequency of harmful weather phenomena occurring along a given route completely differs to the observer at a fixed point on the route and the observer on a moving point (an airplane in flight, etc). Even during the summer months, a thunderstorm confined to a single point is comparatively rare in any given area in European USSR. In flight it is met much oftener, since when the airplane flies under conditions in which thunderstorms are possible, the probability of encountering one or more thunderstorm centers is greater. The number of days with thunderstorms at a given point is, moreover, no general indication of the number of days with thunderstorms or other harmful weather phenomena along the route.

Let us elucidate this by the following example. Let there be 10 equidistant stations along a certain route. The number of thunderstorm days per month is three at each of them. How many thunderstorm



Declassified in Part - Sanitized Copy Approved for Release 2012/03/12 : CIA-RDP82-00039R000100190014-6

Declassified in Part - Sanitized Copy Approved for Release 2012/03/12 : CIA-RDP82-00039R000100190014-6

days per month will there be for an airplane flying along that route? If we are ignorant of the structure of the phenomena the answer will be very indeterminate; from 3 to 30.

If the thunderstorms simultaneously extend over the entire length of the route, there will be three thunderstorm days a month; in that case, on three days of the month thunderstorms will be observed simultaneously over the entire route; and those days will presumably be non-flying days. Thunderstorms will occur daily (on 30 days) in the event that the occurrence of a thunderstorm at any ~~two~~ point on the route (precludes the appearance of a thunderstorm at another) ~~are mutually exclusive~~. In fact the probability of an airplane flying along the route encountering harmful phenomena lies somewhere between these two extreme limits, but it will differ for different regions and different phenomena, depending not only on their frequency along the route but also on the length of the route and on the spatial structure of the phenomenon itself. The study of the climate of a moving point must rely therefore on the study of the structure of a field of meteorological elements. This has been graphically shown by A. N. Lebedev, N. F. Nakorenko, F. G. Tokar and others.

What problems confront the climatologist in his study of the structure of the fields of meteorological elements?

The first problem of great importance theoretically and practically is that of the climatology of gradients of meteorological elements, their character, and the discontinuity and intermittence in space and time of the fields of meteorological elements. The mathematical apparatus for the convenient investigation of this



Declassified in Part - Sanitized Copy Approved for Release 2012/03/12 : CIA-RDP82-00039R000100190014-6

Declassified in Part - Sanitized Copy Approved for Release 2012/03/12 : CIA-RDP82-00039R000100190014-6

problem has been developed to some extent with the aid of probability theory and of statistical physics; and the most important work in this field has been done by Soviet scholars (1), (2), (3), (4), etc. A certain amount of work has been done by meteorologists themselves in the study of field structure from this point of view (5), (6) (7). Knowledge is needed of the mean values of the gradients of the meteorological elements under various conditions (on mountain slopes and near bodies of water). In connection with this problem there are associated questions of the application of meteorology and climatology which are concerned with interpolation in the fields of meteorological elements, the intervals separating stations and posts for meteorological observation and the structure of their network, the distribution of station locations required for plotting climatic charts or charts of departure from normal with the necessary degree of detail.

Next comes the study of the forms of the temporal connections observed between the values of meteorological elements in a given territory. Down to the present time this question has interested climatologists from the point of view of developing long-term mean values, but it has its own independent theoretical and practical importance and is connected to a considerable extent with the preceding problem.

Third is the problem of the probability of encountering a given meteorological phenomenon along a section of a route of given length, and of the dimensions of the path followed by such a phenomenon. This is the above-mentioned problem of the climate of a moving point.



Declassified in Part - Sanitized Copy Approved for Release 2012/03/12 : CIA-RDP82-00039R000100190014-6

Declassified in Part - Sanitized Copy Approved for Release 2012/03/12 : CIA-RDP82-00039R000100190014-6

Finally, in the fourth place (a problem closely related to the general sense of the preceding problems), is the question of the dimensions, distribution, and structural properties of the meteorological elements (horizontal and vertical); for instance, the number and distribution of the cloud layers over a given point, the dimensions and structure of regions covered by unbroken low cloud or fog, the regions of development of snowstorms, sleet, icing in the air, and anomalies of pressure, temperature, precipitation, etc.

In the course of the present article it will only be possible to mention work done by the GGO during the past 10 or 15 years.

Many meteorological elements are characterized by a considerable regularity of territorial variation in time. Atmospheric temperature and pressure on flatlands belong to this category, as does also, to a considerable extent, the probability of overcast skies, atmospheric humidity, etc. Of course, in different climates variability with time is also different, but for distances expressed in hundreds of kilometers, the quantity

$$\sigma_t^2 = \frac{\sum_1^N (t_i - t_0)^2}{N} \qquad (1)$$

where $t_1,\ldots,t_N$ -- the successive values of the elements in time at a given time of the year (a given month) -- show very little change over a period of years.

The essence of this phenomenon reduces to the fact that the fluctuation of the element proceeds at various observation points on different levels, but the amplitude of these fluctuations does not depend on the level of the element. Over small distances the



Declassified in Part - Sanitized Copy Approved for Release 2012/03/12 : CIA-RDP82-00039R000100190014-6

Declassified in Part - Sanitized Copy Approved for Release 2012/03/12 : CIA-RDP82-00039R000100190014-6

course of the weather remains similar or even uniform.

This phenomenon is connected with the fact that the limits of the physically possible values of similar quantities lie far from the limits within which they fluctuate. Given a connection between the readings at neighboring points, this leads to low variability of the difference between the values of these quantities at stations close to each other. In cases where the variation in the value of an element substantially influences the course of a geophysical process, the constancy of the difference is also disturbed. This may be noted for temperature if we operate not on the mean monthly values, but with values for periods or mean daily temperatures for individual days. When the temperature at one station crosses 0 degrees, the thermal balance of the locality is upset, especially where there is snow cover -- progress of the temperature slows, and the constancy of the differences is disturbed. This phenomenon may be readily followed on the curves of temperature distribution. The sharp negative asymmetry of the distribution curves in winter for the western part of the European USSR is also due to this. In the south, where snow cover is substantially or entirely lacking, and at the center of the mainland, where winter thaws are seldom or never observed, this asymmetry in the distribution of winter temperatures disappears. Asymmetry appears again, but this time a positive asymmetry, at the border of Yakutiya, where it is also connected with disruption of the uniformity of the meteorological cycle (and possibly with the method of differences as well, but for different reasons in this case). With a uniform anticyclonic area in Yakutiya, there is very slight variability of temperature and no reason at all to expect any considerable fall in temperature. The



Declassified in Part - Sanitized Copy Approved for Release 2012/03/12 : CIA-RDP82-00039R000100190014-6

Declassified in Part - Sanitized Copy Approved for Release 2012/03/12 : CIA-RDP82-00039R000100190014-6

infrequent rises in temperature are connected with strengthening of the wind and advection from almost any direction, which is also responsible for the positive asymmetry of distribution, illustrating the possibility of considerable rises in temperature from disturbance of the anticyclonic area.

In April the great expenditure of heat with the thawing of the snow leads to a high occurrence of temperatures close to 0 degrees, which results in a characteristic type of sharp-peaked distribution curve for the central zone of the USSR [67], which is not found in the extreme south. A direct study of the temperature frequency-curves undertaken by M. D. Pavlova confirms the disappearance of similarity, at temperatures near 0 degrees, of temperature-distribution curves for stations with non-uniform temperatures.

The above-mentioned peculiarities determine to a certain extent the form of the correlation in time between the temperatures at neighboring points, predetermining its linearity, which, however, suffers a certain distortion when the temperature passes through 0 degrees.

The coefficient of correlation thus appears in the present case to be an almost complete indication of the closeness of the relation.

We pass now to the question of the mean gradients of temperature and pressure. The relationship of the mean variability F of the temperature or pressure differences at neighboring stations (expressed by the variance or by the standard deviation) to the distance $\rho$ between the stations is practically linear. This has been verified for temperatures up to a distance of 500 kilometers, and for barometric pressures up to a distance of 600 kilometers. This testifies to the very wide range of



Declassified in Part - Sanitized Copy Approved for Release 2012/03/12 : CIA-RDP82-00039R000100190014-6

Declassified in Part - Sanitized Copy Approved for Release 2012/03/12 : CIA-RDP82-00039R000100190014-6

regional anomalies of a single-sign for these elements and to the relatively simple laws of temperature variation within them. This allows the wide and effective application of linear interpolation (on a plane surface) of deviations from the mean temperatures and pressures on the flatlands of the USSR, for individual days as well as for monthly values, which is very important to the synoptic method of weather analysis. The mean values themselves, for temperature and pressure, may be interpolated with a certain degree of accuracy only after converting them to sea-level equivalents, in view of the great influence exerted on them by elevations above sea-level. Adjustments must be made in advance to allow for the influence of local factors based on physico-geographic descriptions, for without such adjustments interpolation may lead to rather large errors. P. I. Kolovskiy (9) has well indicated the order of importance of the various local factors within the confines of a single region.

In referring to the charts of the mean deviations which include to a considerable extent the influence of local factors, one marked peculiarity should be mentioned: The discontinuities in the temperature field expressed on a micro-scale (from the order of meters to that of kilometers) affect the form of the relationship that the differences between station readings bear to the distances between stations, and produce, along with accidental measurement errors, an over-all error reflecting those discontinuities -- even for near zero distances in the order of a few kilometers; nevertheless the temperature discontinuities affecting atmospheric fronts, an influence generally increasing the error when interpolating across the front, do not substantially effect the form of the function $F(\rho)$. In practice the variance is not ordinarily used to characterize $F(\rho)$, but the standard deviation



Declassified in Part - Sanitized Copy Approved for Release 2012/03/12 : CIA-RDP82-00039R000100190014-6

Declassified in Part - Sanitized Copy Approved for Release 2012/03/12 : CIA-RDP82-00039R000100190014-6

instead (and in some cases the probable error which is calculated from the standard deviation). We present a few characteristics of the temperature cycle -- for the mean monthly temperatures and also for the temperatures for individual periods.

It has been empirically established (10), (11), that the increase in the variability of temperature differences is approximately linear for distances from 0 to 600 kilometers. The form of the function for greater distances has not yet been investigated, but it may be assumed that beyond this point this increase gradually dies away; that is, for very great distances the correlation between the readings of different stations approaches zero. No research has ever been done on the structure of this damping. In general, two possibilities present themselves: (1) the value of the coefficient of correlation between the readings of two stations approaches zero as a limit, remaining positive all the time (a similar phenomenon may be observed, for instance, for precipitation); or (2), and this is more probable for temperatures, in view of the wide territorial extent of single-sign temperature anomalies, the coefficient of correlation, as it approaches zero, passes, when the distance reaches a certain value, through negative values as well (damped oscillation). Inasmuch as for some values of the distance it may prove most probable that the stations under comparison will fall within a field of anomalies of different sign. In connection with the form of the dependence of $F(\rho)$ on $(\rho)$, a number of essential questions on the structure of the quantities under investigation may be formulated.

In the neighborhood of $\rho = 0$, F approaches not zero but some finite quantity, reflecting the errors of instrumental measurement



Declassified in Part - Sanitized Copy Approved for Release 2012/03/12 : CIA-RDP82-00039R000100190014-6

Declassified in Part - Sanitized Copy Approved for Release 2012/03/12 : CIA-RDP82-00039R000100190014-6

and the inaccuracy of station readings under the influence of microclimatic and micrometeorological conditions; $\alpha = \frac{F(0)}{\sqrt{2}}$ will characterize the mean error of station readings under the conditions of the meteorological network.

$$\Phi(\rho) = F^2(\rho) - 2\alpha^2 \qquad (2)$$

Formula (2) gives the true form of the correlation between the variability of the differences and the distance between the stations in question. The derivative $\Phi'(0)$ shows (if it is finite) the continuity of the field of the element, or, if it is infinite, shows the presence of discontinuities in the field of the element under study. However, this criterion, with respect to the field of temperature, does not yield a determinate solution of the problem. The linearity of $F(\rho)$ is inevitably connected with the discontinuity of the field of temperatures, but the departures of $F(\rho)$ from linearity required to establish the continuity of the deviations of the temperatures from the norms, are so small that empirical data cannot give a clear answer to the question.

The value of $\alpha$ varies widely with the variations in the weather, reaching its maximum in clear calm winter weather.

This naturally leads to territorial differences in the value of $\alpha$.

For temperatures at fixed times, $\alpha$ is greater in summer than in winter in Western USSR, but the opposite is true in Eastern USSR. The reason is that the microclimatic peculiarities of the windy and overcast winters of Western USSR, with a uniform snow cover throughout,



Declassified in Part - Sanitized Copy Approved for Release 2012/03/12 : CIA-RDP82-00039R000100190014-6

Declassified in Part - Sanitized Copy Approved for Release 2012/03/12 : CIA-RDP82-00039R000100190014-6

are smoothed out in summer. On the other hand, in Krasnoyarsk Kray the quiet clear weather under conditions of broken relief can result in very great temperature differences even over extremely short distances. For example $\alpha$ = 0.2 for the Belorussian SSR in January, and 0.3 in July (its value being about the same at 0700 and 1300), while in the western part of Siberia it is 0.6 (at 0700 hours) in January and 0.4 (at 1300 hours), and in July it is 0.5 ( at 0700 hours) and 0.6 (at 1300 hours).

At 0700 hours the still calm weather and the rapid rise of temperature at the time contribute toward increasing the value of $\alpha$, while at 1300 hours there is local cloudiness and thunderstorms (with increased turbulence also probable).

If the temperature conditions for different periods and days were independent of each other, the values of $\alpha$ for the month would be 9.5 times less than for the observations periods, but in reality the diminution in $\alpha$ proceeds within narrower limits, amounting in the Belorussian SSR to 4.2 times in January and 5.8 times in July.

In the central belt of the European USSR, $\alpha$, is 0.11 degrees in winter and 0.13 degrees in summer. Bearing in mind that there is relatively small probability of deviations greater than twice the mean deviation, and that deviations of at least four times the mean error in the departure from the norms, of the order of 0.2 degrees are possible and should be taken into consideration, a difference in the departure amounting to 0.5 degree should be taken as very substantial. It is obvious that the isolines must not be drawn closer than 0.5 degree. However, the advisable density for isolines depends



Declassified in Part - Sanitized Copy Approved for Release 2012/03/12 : CIA-RDP82-00039R000100190014-6

Declassified in Part - Sanitized Copy Approved for Release 2012/03/12 : CIA-RDP82-00039R000100190014-6

not only upon the precision of the original data but also upon the density of distribution and the nature of the location of stations in the network. The precision of linear interpolation for plane surfaces has been considered by A. Kh. Khrgian, O. A. Drozdoviy, A. A. Chepelevskiy and M. V. Zavarina (5), (12), (13), (14).

For the simplest case of interpolation for three equidistant points, situated at the vertices of an equilateral triangle, O. A. Drozdovly obtained the following formula connecting the standard error of interpolation f ( $\rho$ ) (the differences between observed and interpolated quantities) and F ( $\rho$ ):

$$f(\rho)=\sqrt{F^2\left(\frac{\rho}{\sqrt{3}}\right)-\frac{1}{3}F^2(\rho)} \qquad (3)$$

In most cases interpolation to the center gives the greatest error. In drawing isolines through a climatically uniform locality three-point interpolation is sufficiently typical. In connection with this we consider it useful to present calculations of the accuracy with which isolines were plotted for the mean monthly temperatures in January and July for the central part of the European territory of the USSR (all figures subject to the standard error) (8).

| Month | Degrees | $\rho$ KM | | | | |
|---|---|---|---|---|---|---|
| | | 0 | 50 | 100 | 200 | 400 |
| January | $F^\circ(\rho)$ | 0.15 | 0.25 | 0.30 | 0.60 | 1.08 |
| | $f^\circ(\rho)$ | 0.12 | 0.14 | 0.17 | 0.25 | 0.30 |
| July | $F^\circ(\rho)$ | 0.20 | 0.26 | 0.33 | 0.47 | 0.68 |
| | $f^\circ(\rho)$ | 0.16 | 0.19 | 0.22 | 0.28 | 0.35 |



Declassified in Part - Sanitized Copy Approved for Release 2012/03/12 : CIA-RDP82-00039R000100190014-6

Declassified in Part - Sanitized Copy Approved for Release 2012/03/12 : CIA-RDP82-00039R000100190014-6

It must be taken into account that because of the lack of uniformity of the surrounding circumstances as a whole, departures in the weather elements may reach four times the mean departure. Therefore only a network of stations with distances of about 50 kilometers between them can assure in all cases the accuracy of isolinear departure from the norm of up to 0.5 degree; inter-station distances of 200 kilometers will still assure accuracy within 1 degree; while errors exceeding 0.5 degree in plotting will be observed in approximately only 45 percent of the area. Finally, with inter-station distances on the order of 400 kilometers, although errors will only rarely exceed 1 degree, errors over 0.5 degree will already be observed in 10 to 15 percent of all the localities. With greater distances between stations, the accuracy of isolines up to 1 degree is not entirely assured. At climatic boundaries (sea, dry land, mountain regions) accuracy falls correspondingly, and additional stations should be used.

A similar type of calculation, but applied to the values of meteorological elements, was used as the basis of numerous studies by the GGO on the theory of rational location within a network.

A few observations may be made, however, with respect to the calculations presented above. In the first place, the divergence between the observed and interpolated quantity still does not represent the error of interpolation, since the observed quantity is also not entirely accurate and the mean errors of interpolation are less than $f(\rho)$. The true error of interpolation

$$\rho(\rho) = \sqrt{f^2(\rho) - \frac{E^2(0)}{2}}, \qquad (4)$$



Declassified in Part - Sanitized Copy Approved for Release 2012/03/12 : CIA-RDP82-00039R000100190014-6

Declassified in Part - Sanitized Copy Approved for Release 2012/03/12 : CIA-RDP82-00039R000100190014-6

Comparing the mean square values $F^2(\rho)$ with $\sqrt{2}\sigma(y)$ the value of the coefficient of correlation may be determined to be

$$r = 1 - \frac{F^2(\rho)}{2\sigma_y^2}, \qquad (6)$$

an approximate value of which may also be obtained from the relation of the standard deviations.

Based on the foregoing, the value of r for January and July is expressed as a function of the distance by the formula:

| $\rho$ km | 0 | 50 | 100 | 200 | 400 |
|---|---|---|---|---|---|
| $r_I$ | 0.9987 | 0.9965 | 0.9918 | 0.9796 | 0.9330 |
| $r_{VII}$ | 0.9879 | 0.9796 | 0.9672 | 0.9324 | 0.8609 |

In this case, the values of the coefficients of correlation between the mean monthly temperatures of neighboring stations are impressively high. It is only natural that the method of differences should prove to be more accurate here than the application of series to a single period by the regression method. In the given case, r diminishes as the square of the distance. By carrying this law to hold up to r = 0, the effective distance at which r would be equal to zero may be computed; while this distance would be less than the mean dimensions of an anomaly, it would still be surprising enough. In this way we may obtain about 1300 kilometers as the mean radius of the January anomaly and about 1300 kilometers as the mean radius of the July anomaly.



Declassified in Part - Sanitized Copy Approved for Release 2012/03/12 : CIA-RDP82-00039R000100190014-6

Declassified in Part - Sanitized Copy Approved for Release 2012/03/12 : CIA-RDP82-00039R000100190014-6

It must be observed that in fact the increase of F ($\rho$) is not uniform (not isotropic) for different distances, and that, in particular, this increase is less along the line of the most frequent transports of air masses than in a direction perpendicular to it, as was shown at one time by Ye. S. Selezneva, and later, independently of her and with more data, by D. [illegible] Kuznetsov. Unfortunately, however, neither of these studies were published.

It is interesting to investigate the decline of the correlation of [redacted] readings at separate stations with time as well as distance. Unfortunately there has been almost no research on this subject, since A. I. Voyeykov and V. Kaminskiy. It is true that Ye. S. Rubinshteyn has calculated the statistical distribution of the day to day variability of mean daily temperature, but except for a single article on one aspect of this question [15], all of this material is still unpublished. The decline in the correlation of temperatures during a number of consecutive days has similarly not been investigated. The only data given in the literature is on the mean duration of the period of departures from the mean in one direction at one single given point. It has been shown that the anomalies of mean monthly temperatures also reveal a connection over a period of several months (14), (17), (20). Only a very slight connection, however, is revealed between the mean daily temperatures of corresponding months in successive years, which connection is entirely negligible for winter but somewhat larger in summer and was revealed for a number of successive summers. This characterizes the relatively feeble role of the rhythmic processes with periods longer than a single year in the temperature cycle observed at any given point. T. N. Kozlova attempted, on the basis of data in the literature, to establish a connection between temperatures by times and types of spatial



Declassified in Part - Sanitized Copy Approved for Release 2012/03/12 : CIA-RDP82-00039R000100190014-6

Declassified in Part - Sanitized Copy Approved for Release 2012/03/12 : CIA-RDP82-00039R000100190014-6

distribution over the European territory of the USSR with existing 3 and 5 month rhythms of Trans-Polar activity; but the result was also negative. Further details are given below.

During the past 15 years, in the USSR, A. A. Kaminskiy (19), (20), M. A. Omshanskiy (7), O. A. Drozdoviy and A. A. Shepelevskiy (5) have investigated the pressure field, which in general has a structure analogous to that of the temperature field. Interesting studies were made abroad by Z. Yev'yen on the secular course of the variability of pressure differences between successive days or periods. The pressure field is closely connected with the question of weather prediction, and therefore most synoptic work, especially in the realm of long-term forecasting, is concerned in one way or another with the structure of the pressure field. In the present article we shall only consider the essence of the investigated fields together with unpublished researches on climatology.

The value of F ($\rho$) for mean monthly pressures has been studied by A. A. Kaminskiy (20). Unfortunately the scattering of the points on graphs of the relationship between F and $\rho$ is so great as to make rigorous calculation of the form of the function F ($\rho$) difficult, although it is clearly almost linear up to distances of 600-800 kilometers. This scattering is explained by the fact that data for highly dissimilar regions of the USSR has been entered on the same chart, and that this data is distinguished by low quality of the observations (in particular no barometric corrections have been noted). In spite of this, the dependence of the mean annual barometric values is still very definite, A. A. Kaminskiy defines the form of the relation between the mean departure F in



Declassified in Part - Sanitized Copy Approved for Release 2012/03/12 : CIA-RDP82-00039R000100190014-6

Declassified in Part - Sanitized Copy Approved for Release 2012/03/12 : CIA-RDP82-00039R000100190014-6

millimeters of mercury and $\rho$ in kilometers by the formula:

$$F(\rho) = 0.065 + 0.0004\rho. \qquad (7)$$

The fact that $F(0) \neq 0$, with so large a number of observations (the annual mean is of 1,195 observations), is connected with the mean error of observation of the barometric pressure; the total error in this about 0.7 meters, that is, the mean error of observation of the barometric height is about 0.5 meters [Sic].

The data for atmospheric pressure at stations in the southwest of the European territory of the USSR, worked out by A. A. Chepelevskiy, also yielded a linear relation between them; and for the data of the reliable stations over short distances, the dependence $F(\rho)$ in millimeters of mercury on $\rho$ in kilometers has the form:

$$F(\rho) = 0.04 + 0.0061(\rho). \qquad (8)$$

If the data of stations with lower quality of observation be taken into account,

$$F(\rho) = 0.19 + 0.0059\rho. \qquad (9)$$

For the shores of the Kara Sea, using corrections to this formula given by M. A. Gashunskiy and A. A. Chepelevskiy, we obtain:

$$F(\rho) = 0.18 + 0.0057\rho. \qquad (10)$$

Comparison of formula 3 with (8), (9) and (10) shows that the value of $F(0)$ depends mainly on the accuracy of the separate readings, that is, mainly on the quality of the observations and the accuracy of the calculations of the differences between the heights of the baro-



Declassified in Part - Sanitized Copy Approved for Release 2012/03/12 : CIA-RDP82-00039R000100190014-6

Declassified in Part - Sanitized Copy Approved for Release 2012/03/12 : CIA-RDP82-00039R000100190014-6

metric columns.

As for the theoretical determination of the form of the dependence of the pressure difference on the difference between the stations, A. M. Obukhov, starting with his representation of wind structure, has given it exponential form with index of $\frac{7}{8}$, which is little less than unity. However, since the relation obtained by him for the wind as well does not exist on the scale we are considering, it is all the more impossible to follow up the data on pressure. Our calculations from I. I. Yudin's formula for wind structure give a dependence $F(\rho)$, for the case of pressure, which is not, generally speaking, linear, but over a considerable interval of $\rho$ it approaches linearity, which is confirmed in practice. The inaccuracies involved in this concept will be discussed below.

Somewhat more work has been done on the elucidation of the temporal structure of the barometric field.

In 1939, M. I. Yudin (21) made an analysis of the fluctuations of pressure waves with separate aperiodic members, based on material of the II International Polar Year. According to his classification, the following structural components may be distinguished in the variations of the barometric pressure (and also of other meteorological elements).

1. Random fluctuations, independent in time.

2. Perturbation-fluctuations of random character but manifesting a connection within a certain time-interval.



Declassified in Part - Sanitized Copy Approved for Release 2012/03/12 : CIA-RDP82-00039R000100190014-6

Declassified in Part - Sanitized Copy Approved for Release 2012/03/12 : CIA-RDP82-00039R000100190014-6

3. Rhythmic fluctuations: the alternating of perturbations of different sign, having a certain mean period, but with each successive perturbation depending only on the end of the preceding one; and any assigned phase difference from the fluctuations with their mean period can be built up after the succession of a certain number of cycles (Bradovitskiy gives a similar definition of the rhythms).

4. Periodic fluctuations: rhythmic fluctuations with the strict alternation of the same cycles.

There is a latent periodicity within the rhythmic fluctuations which should not be overlooked. The differences in the length and intensity of the separate cycles are the actual result of the superimposition of other fluctuations (random perturbations or rhythms) on the periodic members. The 11-year solar cycle is an example; the mean duration of the period is distinguished by a remarkable stability, but its pure periodicity is disturbed by processes that take place in the sun itself.

5. Changes of field, in which its mean value, around which the levels fluctuate, undergoes a change (for instance in consequence of change in the height of the barometer).

The use of periodograms, which is usually recommended for studying the periodic processes, rhythmic processes and perturbations, is unsuitable because it damps the rhythms, although slowly; moreover, the periodogram method results in large errors when applied to connected series. Analysis of the general form of a series may be done with the aid of one of the following methods: construction



Declassified in Part - Sanitized Copy Approved for Release 2012/03/12 : CIA-RDP82-00039R000100190014-6

Declassified in Part - Sanitized Copy Approved for Release 2012/03/12 : CIA-RDP82-00039R000100190014-6

of correlograms, construction of spectrograms or simplified methods similar to it (for instance rhythmograms, structural functions, etc).

The correlation functions (correlograms) are of the greatest interest, since they allow the structural properties of the series to be analyzed at the same time.

The random errors are almost eliminated from the correlograms (creating, as they do, only a dispersion of the order of $\frac{1}{n}$). Over a definite interval t there is a gradual decline in the connection of the perturbation with the correlated members of the series, allowing the spectrum of perturbations to be duly evaluated. The rhythms form waves on the correlogram with maximum ordinates at t = 0 and gradually damped amplitude. The periodic members in pure form yield periodic fluctuations on the correlogram as well with identical phases at t = 0.

Figure 1 is an example of correlogram construction from the data showing annual maximum depths (during ten-day periods) of snow cover at Kazan (Figure 2). The periodic members at 2 and 5.5 years appear with great distinctness.

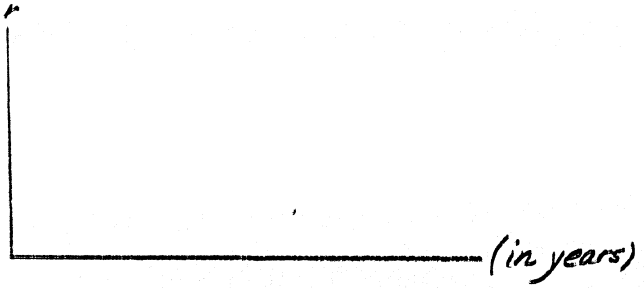


Figure 1. Maximum depth of snow cover at Kazan. 1 -- (heavy line), raw data curve; 2 -- (light line), curve with both members smoothed.



Declassified in Part - Sanitized Copy Approved for Release 2012/03/12 : CIA-RDP82-00039R000100190014-6

Declassified in Part - Sanitized Copy Approved for Release 2012/03/12 : CIA-RDP82-00039R000100190014-6

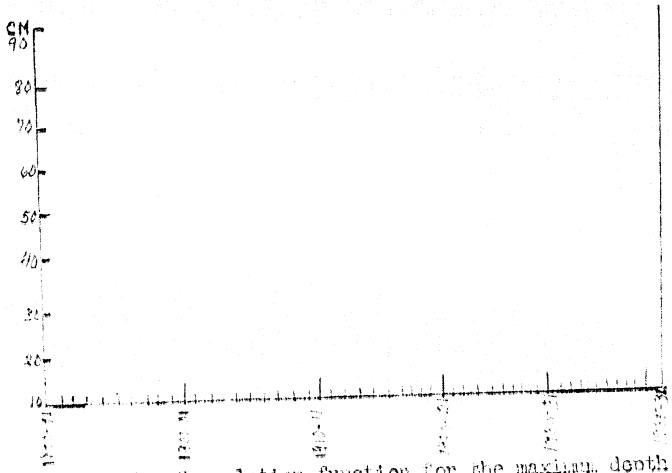


Figure 2. Correlation function for the maximum depth of snow cover at Kazan' (1891-1936).

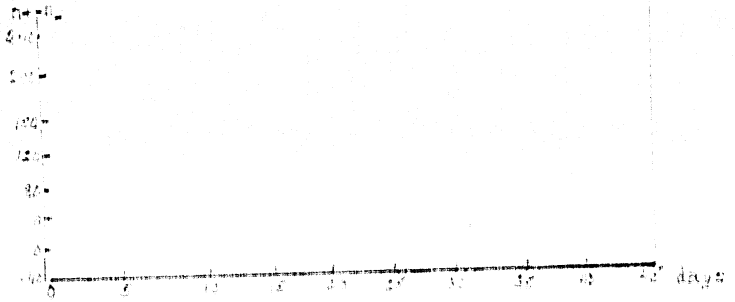


Figure 3. Correlogram of pressure at Poltava station with the shifts ranging from 1 to 45 days, from 1928 to 1940. $n_+ - n_-$ : number of coincidences per year between signs of the departures from normal.

During a number of years analysis of the pressure field for a few points of European USSR (Poltava, Bryansk Forest Station, Leningrad) was made on the basis of calculations carried out by student-trainees of the GIDROMETEOROLOGICHNYY. The connections were almost invariably of a simple sign up to t = 5-6 days. Beyond that point it either remained within limits close to zero or fluctuated rhythmically with a mean period of about 15 days, but very faintly (within the limits of error) (figure 3). Thus the fluctuations of pressure, connected with the change in natural synoptic periods, bear the character of perturbations



Declassified in Part - Sanitized Copy Approved for Release 2012/03/12 : CIA-RDP82-00039R000100190014-6

Declassified in Part - Sanitized Copy Approved for Release 2012/03/12 : CIA-RDP82-00039R000100190014-6

of faintly rhythmic tinge. The mean duration of these perturbations is 5-6 days. In Leningrad, however, this period was longer (about 7-8 days) while the rhythmic character was somewhat more distinct.

The results of the work of T. N. Kozlova on the influence of the 3- and 5-month rhythms on the barometric and temperature fields is very interesting. For this purpose she selected examples of rhythmic processes from the book Fundamental Principles of the Synoptic Methods of Long-Range Weather Forecasting, editor S. T. Pagav. Thereupon the correlation was computed between the barometer readings at 0700 hours for 16 stations located in various parts of European USSR and also of the mean temperatures for the selected day, with the rhythmic repetitions in all cases presented in the book in question (taking the annual cycle of the normal values into due consideration). The mean value of the coefficient of correlation for pressure at all the points mentioned was r = 0.23, while for temperature r = 0.095. On the other hand, the spatial distribution of pressure was correlated in the same way for the same 16 points from the occurrence of the value on the base date to its rhythmic repetition, with the result that, for pressure, r = 0.21 was obtained, and for temperature, r = 0.13.

It may be pointed out for comparison that the correlation between the pressure data for 20 years and that for 3 or 5 months, presented in S. T. Pagav's book as an example of purely random distribution of pressure produced a higher correlation than the presence of rhythms emphasized by the author of the book.

The reason for the absence of any real relationship under the influence of existing rhythms is found in the considerable territorial



Declassified in Part - Sanitized Copy Approved for Release 2012/03/12 : CIA-RDP82-00039R000100190014-6

Declassified in Part - Sanitized Copy Approved for Release 2012/03/12 : CIA-RDP82-00039R000100190014-6

extent of the rhythmic repetition in comparison with the base phenomena, and, in particular, with the varying intensity of repetition in one case or another. The data presented render comprehensible the reasons why long-range weather forecasting based on the method of calculating the rhythms has only achieved inconsequential success. Correlations of territorial pressure distributions furnished by T. A. Dulatova for the base periods (1) 2-5 February 1942; (2) 3-5 March 1942; (3) 15-16 March 1943; (4) 19-22 March 1942 were presented for comparison. The rhythmic processes were visible very distinctly almost at first glance on the synoptic charts, and the territorial correlation of the pressure field gave a mean value for r of 0.29 in the first case, 0.34 in the second, 0.75 in the third, and 0.02 in the fourth. The reason for the low correlation was again the territorial extent of the process.

We pass now to the characteristics of the wind field. The wind field was of special interest for research, since its character had already been theoretically calculated by a number of authors and conclusions could be drawn about the structure of atmospheric macro turbulence on the basis of the empirical data. Besides this, the principal part of the work was devoted to the distribution of wind in the free atmosphere. Near the earth's surface the direction and especially the velocity of the wind is so strongly subject to the influence of local conditions that investigation of the separate cases of wind distribution becomes extremely difficult. M. Ye. Poltyagin, and E. A. Sapozhnikova have worked on the structure of the field of mean wind velocity in its dependence on local conditions,



Declassified in Part - Sanitized Copy Approved for Release 2012/03/12 : CIA-RDP82-00039R000100190014-6

Declassified in Part - Sanitized Copy Approved for Release 2012/03/12 : CIA-RDP82-00039R000100190014-6

while V. Yu. Milevskiy has worked on the frequency distribution of wind velocities. The present paper will not discuss this work, as it is all of purely climatological character. In addition, there are a few papers of M. A. Omshanskiy which stand rather in disagreement with these (25).

Based on considerations of dimensions, Academician A. N. Kolmogorov has pointed out that for the isotropic field of velocities which condition macroturbulence, the variance of the velocities (in vector form, although this can be obtained for scalar wind velocities as well) is equal to:

$$F^2(\rho) = \alpha D^{2/3} \rho^{2/3} \quad , \qquad (11)$$

where $\alpha$ is an arbitrary constant depending on the location of the stations with reference to the direction of flow; D is the dissipation, which is constant for a given altitude in an isotropic atmosphere; and $\rho$, w in the previous formulae, is the distance between the stations.

A. M. Obukhov (4) arrived at the same formula by a more circumstantial but rather complicated route. Thence he also deduced the theoretical value of $F(\rho)$ for atmospheric pressure and temperature.

Comparison of these results with the empirical data, however, resulted in poor reconciliation with theory. M. V. Kazarina (14) obtained especially important results in which $F(\rho)$, on the basis of a large amount of data for distances ranging from a few kilometers up to 600 kilometers, was expressed by the exponential function $\rho^n$ where n proved to have on value equal to 1/3 and another one somewhat greater than 1/2. These discrepancies were reconciled in a paper of



Declassified in Part - Sanitized Copy Approved for Release 2012/03/12 : CIA-RDP82-00039R000100190014-6

Declassified in Part - Sanitized Copy Approved for Release 2012/03/12 : CIA-RDP82-00039R000100190014-6

M. I. Yudin (6), who verified the conclusion of A. M. Obukhov, but giving effect to the vertical anisotropy of the atmosphere, that is to say: (1) the energy of vertical motion in the atmosphere is immeasurably less than the energy of the horizontal field of velocities; (2) the vertical velocity gradients are immeasurably greater than the horizontal velocity gradients.

He found that in the absence of error $F(\rho)$ increases proportionately to $\rho^{\frac{1}{2}}$. He also showed that the form of the relationship between $F(\rho)$ and $(\rho)$ established by A. N. Kolmogorov and A. M. Obukhov is actually true for small-scale phenomena; the limits of its applicability vary, depending on the season, from hundreds of meters in the winter to tens of kilometers in the summer. Confirmation of his conclusions by data of L. V. Zavarina shows that the conditions postulated by him actually exist in the atmosphere, though only as first approximations. The investigation by E. S. Solomonova into the change with time in the form of the given relations of the wind at different altitudes over the same point (32) have once again confirmed the fact that the dependence of $F(t)$ on $t$ is also proportional at first to $t^{\frac{1}{2}}$, and is then keeped for greater time-intervals (which may also be the case for the function $F(\rho)$ for large values of $\rho$). M. I. Yudin explains the above form of the function $F(\rho)$ by the horizontal displacement of perturbations, which leads to the variability in time of the wind at a given point, and regards this fact as one of the confirmations of his theory.

The deduction made by M. I. Yudin is rather complicated. A. M. Obukhov and A. N. Kolmogorov attempted to controvert its accuracy. However, analogous results based on his fairly obvious postulates may



Declassified in Part - Sanitized Copy Approved for Release 2012/03/12 : CIA-RDP82-00039R000100190014-6

Declassified in Part - Sanitized Copy Approved for Release 2012/03/12 : CIA-RDP82-00039R000100190014-6

also be obtained in other and considerably simpler ways. For instance, one might consider the basic sources of energy at the expenditure of which the kinetic energy of turbulent flow is created at each point at a definite elevation above a given territory. The kinetic energy perpendicularly transferred in unit time to a stream and producing a turbulence-inducing effect at a given point, is proportional to:

$$K_z\left(\frac{\partial w}{\partial z}\right)^2 + K_n\left(\frac{\partial w}{\partial n}\right)^2 , \qquad (12)$$

where $K_z = v_z l_z$ and $K_n = v_n l_n$, $v_z$ and $v_n$ are the pulsations of the vertical and horizontal velocities in a direction perpendicular to the main stream; $l_z$ and $l_n$ are the corresponding paths of transfer (displacement) respectively in a vertical direction and in a direction perpendicular to the stream; $k_z$ and $k_n$ are the coefficients of turbulent diffusion in the corresponding directions; and $n$ is the direction of flow (in the center between the points compared).

The kinetic energy transferred along the stream and distinguished by an effect producing turbulence at any given point, will be proportional to $(k_s + wl_s)\left(\frac{\partial w}{\partial n}\right)^2$, where $s$ is the direction along the flow.

Then the total quantity of energy entering in unit time into the creation of turbulence of various orders at a given point will be equal to



Declassified in Part - Sanitized Copy Approved for Release 2012/03/12 : CIA-RDP82-00039R000100190014-6

Declassified in Part - Sanitized Copy Approved for Release 2012/03/12 : CIA-RDP82-00039R000100190014-6

$$E = \partial \kappa_z \left(\frac{\partial w}{\partial z}\right)^2 + \delta \kappa_n \left(\frac{\partial w}{\partial n}\right)^2 + \delta(\kappa_s + w l_s)\left(\frac{\partial w}{\partial s}\right)^2, \qquad (13)$$

where $\delta$ is the density of air.

By virtue of horizontal isotropy, the mean value of E is constant in time for a given altitude, just as the mean values of $\left|\frac{\partial w}{\partial z}\right|, \left|\frac{\partial w}{\partial n}\right|, \left|\frac{\partial w}{\partial s}\right|, |w|, v_z, F(\rho), v_s$ and $v_n$ are also constant.

It may consequently be assumed that $l_s$, $l_n$, and $l_z$ are proportional in first approximation among themselves and that the coefficient of proportionality is $\rho$, which characterizes the order of turbulence. Finally, according to M. I. Yudin, all terms except the first on the right hand side of equation 13 should be disregarded. Then

$$E \cong \delta \kappa_z \left(\frac{\partial w}{\partial z}\right)^2 = \delta \frac{v_z}{l_z} \Delta w^2$$

or

$$\Delta w^2 = \frac{E}{v_z \delta} l_z = \beta \rho, \qquad (14)$$

which was to be proved.



Declassified in Part - Sanitized Copy Approved for Release 2012/03/12 : CIA-RDP82-00039R000100190014-6

Declassified in Part - Sanitized Copy Approved for Release 2012/03/12 : CIA-RDP82-00039R000100190014-6

More rigorously considered, we should still retain in equation 12 the term $wl_z\left(\frac{\delta w}{\delta z}\right)^2$, which is the basic term in the work of E. S. Selemenev, but this would not involve any change in the substance, since in this case

$$\frac{\delta v_z}{l_z}\Delta_z(w^2)+\frac{\delta w}{l_s}\Delta_s(w^2)\approx E,$$

whence similarly follows

$$\Delta^2 w^2 \cong \beta\rho. \qquad (14c)$$

It may nevertheless be doubted that the vertical scale of perturbation $l_z$ is proportional to the horizontal $l_x$ and $l_y$. This is a weak point in Yudin's calculation. However, if it be assumed that $l_x$ and $l_y$ increase, $l_z$ approaches a certain limit $l_\infty$, then, if it be postulated that the transfer of energy takes place at a certain effective altitude for which terms containing $l_x$ and $l_y$ are intermediate (the altitude of the flow occurring), once again we get proportionality between the square of the difference of the velocities at two points and the distance between them.

The good agreement of formula (14) and the practical results gives the advantage of Yudin's formula.

The following two circumstances, however, must be borne in mind. The structure of the pressure field, and consequently of the wind field as well, consists not only of perturbations on various scales, but also of waves. Consequently the correlation function should contain not only the odd powers but also the even powers of



Declassified in Part - Sanitized Copy Approved for Release 2012/03/12 : CIA-RDP82-00039R000100190014-6

Declassified in Part - Sanitized Copy Approved for Release 2012/03/12 : CIA-RDP82-00039R000100190014-6

the distance between the points; this is ignored by A. N. Kolmogorov and A. M. Obukhov, and by M. I. Yudin as well. It is very probable that the influence of the even powers should manifest itself at greater distances than that of the odd powers, but this has not yet been confirmed, except by M. V. Zavarina and E. S. Selezneva getting exponents of $\rho$ in $F(\rho)$ somewhat higher than $\frac{1}{2} F(\rho) = a\rho^{0.56}$ with Zavarina and $F(t) = b\rho\, t^{0.53}$ with Selezneva. These results lie within the limits of possible error, but were obtained by the investigators mentioned in a number of variants.

The second circumstance is more substantive. The law $F(\rho) = a\sqrt{\rho}$ cannot be extended without limit, since at a certain value of $\rho$ all connection between the two points will have been lost. This transition occurs gradually, but the law defining it has not yet been studied analytically.

It is a familiar fact that for stationary processes with fundamental field and derivative field (of quasi-wave character) of continuous character, the correlation function $r$ contains only even powers of $\rho$ in its expansion, and is expressed by the formula

$$r = \int_{-\infty}^{+\infty} \cos m\rho\, f(m)\, dm. \qquad (2')$$

where $m$ represents frequency (inverse scale of perturbation) and $f(m)$ is a function of the distribution of the perturbation effect on the given scale.

If we have a field in which the increase of $F(\rho)$ proceeds by way of the accumulation of discontinuous jumps in the values of the given element (again of different scales) then by analogy we should write:



Declassified in Part - Sanitized Copy Approved for Release 2012/03/12 : CIA-RDP82-00039R000100190014-6

Declassified in Part - Sanitized Copy Approved for Release 2012/03/12 : CIA-RDP82-00039R000100190014-6

$$r = \int_0^\infty e^{-m\rho} f(m)\,dm. \qquad (16)$$

Here r is an exponential function of $\rho$. Apparently a structural wind function for all great distances may be obtained in the first approximation from formula 16.

The very important question of the structure of the pressure field is connected with the form of the correlation function for wind. O. A. Drozdov and A. A. Shepelevskiy have accepted the linearity, in first approximation, of the dependence F ($\rho$) for periodic pressure observations up to a distance of 800 kilometers. This was in agreement with the results of observation, which did, it is true, give a certain amount of scatter. M. I. Yudin recently discovered that the errors of interpolation determined for a given F ($\rho$) by formula (3) were sharply reduced (by about three times) as compared with those calculated immediately. He considered it necessary to proceed to the calculation of $F^2$ ($\rho$), accepting for it, in agreement with M. A. Omshanskiy, a polynomial formula of the third degree. Linear dependence presupposes that the scale of the phenomenon shall be substantially greater than the distances involved, which is doubtful in this case. From this point of view the influence of the terms of higher degree, overshadowed by the dispersion of the points on the graph of F ($\rho$), is entirely probable, although without further research it cannot be proved.



Declassified in Part - Sanitized Copy Approved for Release 2012/03/12 : CIA-RDP82-00039R000100190014-6

Declassified in Part - Sanitized Copy Approved for Release 2012/03/12 : CIA-RDP82-00039R000100190014-6

It can be shown on the basis of the general formulae of the theory of O. A. Drozdov and A. A. Shepelevskiy that the formula adopted by M. I. Yudin corresponds precisely to his structural wind function in the postulated continuity of the pressure field. In this case the basic assumptions are as follows:

1. The pressure field p is assumed to be continuous; consequently $\left(\frac{\partial F}{\partial \rho}\right)_{\rho=0} = 0$ and the correlation function does not contain in its exponential expansion any term in the first power of $\rho$.

2. The wind field is considered to be proportional to the derivative $v = k\frac{\partial p}{\partial \rho}$.

3. The structural wind function is adopted in the form $\Phi(\rho) = a\sqrt{\rho}$, and therefore the correlation function $R = r_v = 1 - b\rho$.

4. For the sake of simplifying the deductions, we shall consider the random errors in the determination of pressure and wind to have been eliminated, that is, R(0) = 1 and r(0) = 1.

(Figure 4, page 115 -- no legend.)

In the above mentioned paper of O. A. Drozdov and A. A. Shepelevskiy, the coefficient of correlation between the gradients $R(\overline{\delta_{14}}/\overline{\delta_{23}})$, where $\overline{\delta_{14}}$ is the increment in pressure between the adjacent points 4 and 1, in terms of the distance $\rho_{14}$ between them, and $\delta_{23}$ is the analogously calculated increment in pressure at point 2 (Figure 4), is expressed in the form:



Declassified in Part - Sanitized Copy Approved for Release 2012/03/12 : CIA-RDP82-00039R000100190014-6

Declassified in Part - Sanitized Copy Approved for Release 2012/03/12 : CIA-RDP82-00039R000100190014-6

$$R(\bar{\xi}_{14}\bar{\xi}_{23}) = \frac{r_{12}-r_{42}-r_{13}+r_{34}}{2\sqrt{(1-r_{14})(1-r_{23})}}, \tag{17}$$

as

$$\rho_{14} \longrightarrow 0 \text{ and } \rho_{23} \longrightarrow 0$$

$$1-r_{14} = \frac{\rho_{14}^2}{2}\left(\frac{d^2 r_1}{d\rho^2}\right)_{\rho=0}; \quad 1-r_{23} = \rho_{23}^2\left(\frac{dz^2}{d\rho}\right)_{\rho=0};$$

$$\rho_{12} = \rho; \ \rho_{14} = \rho_{23} = \Delta\rho \longrightarrow 0,$$

$$r_{12} = r(\rho).$$

Thus

$$r_{12}-r_{13}-r_{42}+r_{34} = \left(\frac{dr(\rho)}{d(\rho)} - \frac{dr(\rho-\Delta\rho)}{d(\rho)}\right)\Delta\rho = -r''(\rho)\Delta\rho^2 + \cdots$$

from which

$$R(\xi_1\xi_2) = \lim_{\Delta\rho\to 0} R\bar{\xi}_1\bar{\xi}_2 = -\frac{r''(\rho)}{\sqrt{\left(\frac{d^2 r_2}{d\rho^2}\frac{d^2 r_2}{d\rho^2}\right)_{\rho\to 0}}} = -\frac{r''(\rho)}{r''(0)}. \tag{18}$$



Declassified in Part - Sanitized Copy Approved for Release 2012/03/12 : CIA-RDP82-00039R000100190014-6

Declassified in Part - Sanitized Copy Approved for Release 2012/03/12 : CIA-RDP82-00039R000100190014-6

If the correlation function for wind $R = 1 - b\rho$, then, assuming the formula for a geostrophic wind still holds true as $\rho \longrightarrow 0$, we have

$$-\frac{r''(\rho)}{r''(0)} = 1 - b\rho$$

or

$$r(\rho) = 1 - \alpha\rho^2 + \beta\rho^3, \qquad (19)$$

whence the desired structural function for pressure assumes the form:

$$F(\rho) = 2\sigma_p^2(\alpha\rho^2 - \beta\rho^3). \qquad (20)$$

An analogous formula was previously obtained, based in part on suggestions of N. A. Obukhovskiy.

It is interesting to note that this function has a somewhat different structure from that which follows from formula (15), as here it contains both an even and an odd power of $\rho$.

Investigation of the precipitation field has been mostly done on the monthly precipitation figures. The field of precipitation has a very peculiar structure with obvious discontinuity. Accordingly the correlation between even the monthly values falls rapidly with increasing distance; and even for very short distances it is still rather low, especially for the summer months in the steppe zone of the USSR. Winter precipitation often suffers from the influence of the wind, but in these cases, when the rain gages at the compared stations are satisfactorily set up, comparability for considerable distances is



Declassified in Part - Sanitized Copy Approved for Release 2012/03/12 : CIA-RDP82-00039R000100190014-6

Declassified in Part - Sanitized Copy Approved for Release 2012/03/12 : CIA-RDP82-00039R000100190014-6

greater in winter than in summer.

The following table may serve to illustrate this point. It shows data from the work of V. P. Kurskoy for the central zone of European USSR (Moscow Oblast, Gorkiy Oblast, etc):

| $\rho$ KM | 0 | 25 | 50 | 100 | 200 |
|---|---|---|---|---|---|
| I, II | 0.94 | 0.82 | 0.65 | 0.64 | 0.60 |
| VII, VIII | 0.97 | 0.74 | 0.66 | 0.46 | 0.29 |

For distances over 50 kilometers in the summer, the relationship weakens rapidly, leading in practice to complete independence for distances of about 250 kilometers, while in the winter, when precipitation is linked to larger-scale processes, the coefficient of correlation for the same distance remains over 0.5

The anisotropy in distance of the precipitation field is rather marked, but its regularities remain almost unexplored in practice, and therefore the type of distance table presented above is still the only criterion for determining the accuracy of the anomaly charts.

In the same Moscow Oblast the probable errors of interpolation of monthly norms of summer precipitation (for three stations), in relation to distance, are expressed by the following table:

| $\rho$ KM | 0 | 25 | 50 | 100 | 200 |
|---|---|---|---|---|---|
| $f(\rho)$ % | 8 | 17 | 18 | 26 | 27 |



Declassified in Part - Sanitized Copy Approved for Release 2012/03/12 : CIA-RDP82-00039R000100190014-6

Declassified in Part - Sanitized Copy Approved for Release 2012/03/12 : CIA-RDP82-00039R000100190014-6

If we consider that in separate instances the errors may deviate from the mean values by more than 4 times, since the distribution of errors does not follow a normal distribution, it follows that to plot the precipitation isolines in summer, even for 50 percent departures, a network of stations no farther apart than 20-25 kilometers is required, while to draw such charts from data of stations 100 kilometers apart involves the possibility of gross errors, which can reach 100 percent of the norms in isolated cases, thus rendering entirely futile the compilation of such charts. It should be considered that there are regions where these errors are even considerably greater. In the steppe part of Crimea, even after eliminating observational errors which create an exaggerated impression of the errors of interpolation, the chart errors for the winter short distances are about 15 percent, reaching 21 percent for 25 kilometers and attaining 42 percent at 100 kilometers. Values close to these are observed in the downstream Volga areas. Without a sufficiently dense network of pluviographic stations the construction of rainfall distribution charts for the separate months of any given year becomes almost senseless. There is even less connection between the separate rains. By comparing the daily maxima of rainfall during the month, it will be seen that except in mountainous regions and in the Far East, the relationship between them decreases very rapidly with increasing distance; and therefore these values are practically independent for distances of 50-100 kilometers. In the steppes and semi-desert areas, for instance even in Saratov Kray, the relationship between such linear precipitations is almost completely lost even in the environs of a city. On the contrary, in the foothills and windy parts of the mountains, a significant connection is revealed between



Declassified in Part - Sanitized Copy Approved for Release 2012/03/12 : CIA-RDP82-00039R000100190014-6

Declassified in Part - Sanitized Copy Approved for Release 2012/03/12 : CIA-RDP82-00039R000100190014-6

the precipitation at points separated by distances sometimes exceeding 200 kilometers, even in the warm period. In flatland regions where the connection between the amounts of rainfall is lost even for the shortest distances (Crimea and the mountains of Central Asia), there is still a significant connection between precipitations at different points in the western foothills. However, on plateaus (for instance in Armenia) and on slopes below the level of wind exposure (Dagestan, Transural, Chitin Oblast) only very feeble connections are obtained.

Precipitation and the number of days with various phenomena -- rainfall, thunder, strong wind -- change their variability as the absolute value of the element increases, which is also apparent on the correlation graphs of the connections between neighboring stations. This property is common to a whole class of values which may be represented as the sum of a number of positive components (even though dependent). The variability k of the sum of independent values should increase proportionally to the square root of their number, or approximately proportionally (exactly so for the single components) to the square root of the observed value.

If these values are correlated among themselves during the course of the period for which they are summated, then, in addition to a term depending on $\sqrt{p}$, a term depending on the first power of p must enter into the expression for the variability. According to the investigations of V. Kerpen, recently confirmed by E. S. Rubinshteyn, it is well known that a considerable balance is observed in the quantity of rainfall from month to month, which proves the reality of the correlations of long duration in rainfall series,



Declassified in Part - Sanitized Copy Approved for Release 2012/03/12 : CIA-RDP82-00039R000100190014-6

Declassified in Part - Sanitized Copy Approved for Release 2012/03/12 : CIA-RDP82-00039R000100190014-6

extending over a number of successive months. On the other hand, O. A. Drozdov has shown, on the ground of extensive empirical data for the most varied regions of the USSR, that there exists between $\sigma_p$ and p an approximate relationship of the form:

$$\sigma_p^2 = \alpha p^2 + \beta p, \tag{21}$$

where $\alpha$ and $\beta$ are constant within the limits of a definite geographical region; this is the direct consequence of the above mentioned correlation. From this there follows the relationship for the variational coefficients v:

$$v_p = \sqrt{\alpha + \frac{\beta}{p}}. \tag{22}$$

The low degree of variability of v for rainfall together with a certain tendency of its distribution to reflect that of p has already been remarked in the literature and corresponds completely to the formula obtained.

A consequence of (22) is the correspondence between the daily maxima of rainfall and the quantity of rainfall during a season: the relation $i = \frac{n}{p}$ is approximately proportional to v. The dependence of i on p is shown in Figure 5, which very clearly reveals the regularity we have indicated.

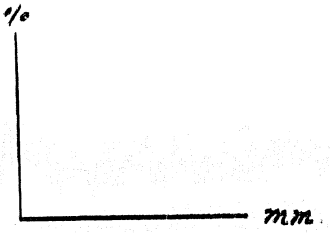


Figure 5. Central Asia.
i % as a function of P mm.



Declassified in Part - Sanitized Copy Approved for Release 2012/03/12 : CIA-RDP82-00039R000100190014-6

Declassified in Part - Sanitized Copy Approved for Release 2012/03/12 : CIA-RDP82-00039R000100190014-6

The determination of the two-dimensional spatial structure of the precipitation field is more complicated. M. A. Omshanskiy (25) has elucidated the form of the dependence of $\sigma_p$ on p, in the course of his investigation of the departures from the means at 10 stations approximately covering the territory of the present Leningrad Oblast for 10 successive Julys. He obtained a relationship of the form

$$\sigma_p = 1.57 p^{2/3}, \qquad (8)$$

which showed a good correspondence with the factual observational data, except for cases of minor rains (or single rains at one of the stations), giving an average of not more than 0.5 millimeters throughout the region, in which instances the connection was practically linear. O. A. Drozdov subsequently studied the connection for various regions of the USSR between the standard deviations of pairs of readings at stations close together as a function of the mean value of the sum of the quantity of rainfall at these stations. It developed that initially (sometimes up to 10-15 millimeters) the increment of $\overline{|x - y|}$ in the function $\frac{x + y}{2}$ was linear (and naturally $\overline{|x - y|}$ proved to be somewhat smaller than in the instance of M. A. Omshanskiy, inasmuch as $\overline{|x - y|} \ll x + y$; while with M. A. Omshanskiy, $\sigma_p$ could in one case be 9 times as high as the mean for the region); then however, for large amounts of rainfall in a number of regions, this increase slowed down, and in a few instances $\overline{|x - y|}$, that is, a quantity proportional to $\sigma_p$, even decreases as p increases (Figure 6). This points to the increase in the coefficient of correlation between rains falling on a given territory as the quantity



Declassified in Part - Sanitized Copy Approved for Release 2012/03/12 : CIA-RDP82-00039R000100190014-6

Declassified in Part - Sanitized Copy Approved for Release 2012/03/12 : CIA-RDP82-00039R000100190014-6

of that rainfall increases. If the increase in that quantity were attained by way of an increase of its intensity, then this phenomenon would be in general incomprehensible, but if it is connected with a modification of the very type of rainfall or if it were even with greater duration of its fall, that is, with an increase of the area covered by the rain in large rainfalls, then it could be explained as a result of the diminished influence, as rainfall became more prolonged, of the factors making for dispersion in the process of natural summation.

Figure 6. Dependence of the spread in the readings at stations very close to ether on the daily precipitations in millimeters.

We shall now present a very elementary and simplified theory of this phenomenon, disregarding differences in the intensity of the rain and connecting the differences in the daily precipitation only with the increase in their duration.

Let us assume that there is a region of rain, which for simplicity will be considered circular, with radius R. Let two stations be located at the distance $h_p - h_q$, perpendicular to the line of motion of the area of rain, which line of motion is assumed to be rectilinear, uniform, and without change in time of the intensity of the rain.

The duration of the rainfall, and consequently also its quantity, will be the function R of the distance h between the



Declassified in Part - Sanitized Copy Approved for Release 2012/03/12 : CIA-RDP82-00039R000100190014-6

Declassified in Part - Sanitized Copy Approved for Release 2012/03/12 : CIA-RDP82-00039R000100190014-6

station and the center of the circle. This quantity will be equal to

$$p_1 = a\sqrt{R^2 - h_1^2}\ , \qquad (24)$$

where a is the coefficient of proportionality.

For the second station, if it lies within the area of rainfall, the quantity of rainfall will be

$$p_2 = a\sqrt{R^2 - h_2^2}\ ,$$

whence

$$\left|\overline{p_2 - p_1}\right|^2 \cong \frac{a}{2}\,\overline{\frac{h_1 + h_2}{R}\left|h_1 - h_2\right|} = b\left|h_1 - h_2\right|\ . \qquad (25)$$

In this case the difference in rainfall undergoes a linear increase with increasing distance, up to the point where $h_1 - h_2 = R$; for $h_1 - h_2 > R$, rainfall becomes constant (where $h_1$ and $h_2$ are on opposite sides of the center, $h_1 + h_2$ replaces $h_1 - h_2$ and $2R$ replaces $R$). The probability q of one of the stations not falling within the area of rainfall is inversely proportional to the radius R of the rainfall and proportional to the distance between the stations, that is, for $\left|\overline{h_1 - h_2}\right| < R$, $q = \frac{h_1 - h_2}{2R}$, while for $\left|\overline{h_1 - h_2}\right| > 2R$, $q = 1$.

Then the mathematical expectation of the variance between the precipitation at nearby stations is equal to



Declassified in Part - Sanitized Copy Approved for Release 2012/03/12 : CIA-RDP82-00039R000100190014-6

Declassified in Part - Sanitized Copy Approved for Release 2012/03/12 : CIA-RDP82-00039R000100190014-6

$$b|h_1-h_2|(1-q)+qbh_1 \approx \frac{a}{2R}(1+h_1)|h_1-h_2|-\frac{a(h_1-h_2)^2}{2R}, \quad (36)$$

reaching the maximum values indicated above. If all rainfall were on the same scale, then the curve expressing the dependence of $(\rho_2-\rho_1)^2$ on $|h_1-h_2|$ would begin as a linear function, the growth of which would subsequently be damped, a result independently obtained by O. A. Drozdov and V. P. Kurdinya. When a whole spectrum of values of $h$ exists, the problem becomes more complicated, but still for short distances

$$F^2(\rho)=(\overline{p_1-p_2})^2 \cong \alpha\rho-\beta\rho^2, \quad (37)$$

where $\alpha$ and $\beta$ are constants, and $\rho$ is the distance between the stations. (The sign of the correlation moment changes if $h_1$ and $h_2$ are located on opposite sides of the center.)

On the other hand, we may write

$$\rho = 2R\sin\phi,$$

whence

$$p_1-p_2 = 2R(\cos\varphi_1-\cos\varphi_2),$$

$$F(\rho)=|\overline{p_1-p_2}|=\bar{R}|\cos\varphi_1-\cos\varphi_2|,$$

$$p=\frac{\overline{p_1+p_2}}{2}=\bar{R}|\overline{\cos\varphi_1}+\overline{\cos\varphi_2}|$$



Declassified in Part - Sanitized Copy Approved for Release 2012/03/12 : CIA-RDP82-00039R000100190014-6

Declassified in Part - Sanitized Copy Approved for Release 2012/03/12 : CIA-RDP82-00039R000100190014-6

or

$$p = F(\rho)\frac{\overline{\cos\varphi_1 + \cos\varphi_2}}{\cos\varphi_1 - \cos\varphi_2}, \qquad (28)$$

that is, the diffusion is proportional to $F(\rho)$, subject to the condition that the change in the scale of R is of decisive importance for the quantity of rainfall, which also finds confirmation in Figure 3. A different correspondence is obtained where R is constant or almost constant and $\rho$ is determined by the value of h. Then

$$\frac{\overline{p_1 + p_2}}{2} \approx \frac{a}{2}\left(2R - \frac{\overline{h_1^2 + h_2^2}}{2R}\right) \approx aR\left[1 - c\left(\overline{h_1 + h_2}\right)^2\right], \qquad (29)$$

which leads to an inverse dependence between $F(\rho)$ and $(\rho)$ where $h_1 < h$ and $h_2 < h$, which dependence is linear only for the instance in which rain is observed at only one of the stations.

In this case, the variability increases initially with the increase in rainfall, but begins to decrease again when rainfall appears at both stations. In actuality, the natural process of reduction in variability with increasing rainfall commences very late and does not always occur in all cases investigated by us. Sometimes (Figure 3) there is a linear increase in variability as far as the largest sums investigated. This results from the combination of both the cases considered above, and the immeasurably



Declassified in Part - Sanitized Copy Approved for Release 2012/03/12 : CIA-RDP82-00039R000100190014-6

Declassified in Part - Sanitized Copy Approved for Release 2012/03/12 : CIA-RDP82-00039R000100190014-6

more complex structure of the precipitation field than that which we have been discussing, particularly as regards the increasing intensity of precipitation from the periphery inward to the center.

We pass now to the question of the form of the connection between the quantities of precipitation at stations a short distance apart, but having different mean quantities of precipitation.

We consider first the limiting case in which all factors making for dispersion are eliminated and the connection between the quantities of rainfall is precise, functional, and linear. In this case the connection can only have the form

$$y = kx \tag{20}$$

since these factors can attain the physical limit 0 of precipitation only simultaneously and are never observed below that level. It is well known that the approximate constancy from year to year of the relations in series of rainfall quantities was discovered as early as the middle of the Nineteenth Century. If this correspondence is precisely followed in the form of the simple solution of the correlation equation

$$y - y_0 = \frac{\sigma_y}{\sigma_x}(x - x_0) \tag{21}$$

it leads to $y = \frac{\sigma_y}{\sigma_x}\bar{x}$ or to the equivariance of the precipitation series.

It has been shown previously by A. A. Chepelevskiy and the present author that a similar correspondence can occur only where the growth in the influence of the factors making for dispersion is



Declassified in Part - Sanitized Copy Approved for Release 2012/03/12 : CIA-RDP82-00039R000100190014-6

Declassified in Part - Sanitized Copy Approved for Release 2012/03/12 : CIA-RDP82-00039R000100190014-6

proportional to the increase in the rainfall, that is, the part of the rainfall that results from processes which differ for each station is on the average proportional to the quantities of rainfall at these stations. This indicates that the coefficient of correlation between such quantities is not a function of their mean level. At the same time, according to equation 21, the relative variability of rainfall is less at a station with heavy precipitation than that at a station where precipitation is lighter. From this it follows that the correlation between the rainfall at points having unequal mean precipitation must be non-linear, and that this non-linearity is manifested not only in the lines of regression but also in the so-called unique solution of correlation used by climatologists in the form of a method of relations.

These peculiarities may be readily observed in practice as well. We are now in a position better to appreciate the physical significance of formula 21. The fundamental reason for the departure of the precipitation at neighboring stations from equivariance is that the difference of these values according to location depends not only on variations in the intensity of rainfall but also on variations in its duration. And thus the variability of precipitation naturally diminishes.

These are the results achieved by the GGO in this problem during the past ten years.

For a number of reasons we must dispense with a detailed analysis of the work of Ye. I. Abramova, G. L. Gaken, A. N. Lebedev and R. F. Sokhrina, which has yielded exceedingly interesting results



Declassified in Part - Sanitized Copy Approved for Release 2012/03/12 : CIA-RDP82-00039R000100190014-6

Declassified in Part - Sanitized Copy Approved for Release 2012/03/12 : CIA-RDP82-00039R000100190014-6

on the regularities of spatial fields of snow cover, thunder, cloudiness, and soil temperature. It should be noted, however, that the work in this respect permits the elucidation of a number of new properties of the climate, which are of enormous importance in the various fields of their application.



Declassified in Part - Sanitized Copy Approved for Release 2012/03/12 : CIA-RDP82-00039R000100190014-6

Declassified in Part - Sanitized Copy Approved for Release 2012/03/12 : CIA-RDP82-00039R000100190014-6

# WATER CONTENT AND THE DISTRIBUTION OF DROPS IN CUMULUS CLOUDS

V. A. Zaytsev

In recent years the Department of Physics of the Free Atmosphere of the GGO has been making a study of cumulus clouds. Elucidation of the microstructure of these clouds in its dependence on their stage of development has occupied a significant place in these studies. The first investigations in this direction concerned only the distribution of drops (1, 4). In the summer of 1948 the measurement of water content was successfully initiated. In the present article the results of simultaneous measurements of water contents and cloud drops will be reviewed.

The development and testing of the instruments for these microphysical measurements was done by us; the observations were mostly carried out by Senior Technician L. P. Nikandrov; and the flights were made by aviators V. N. Denisov and F. I. Medvedev.

A PO-2 airplane was used in 1948, making it possible to investigate cumuli 2000-2500 meters in thickness. A total of 60 flights were made during the summer, ten of which were practice flights to test the instruments in the air. The other 50 were fully operational and yielded about 600 determinations of water content; 360 cloud drop samples were taken and some 600 microphotographs of these drops were made.



Declassified in Part - Sanitized Copy Approved for Release 2012/03/12 : CIA-RDP82-00039R000100190014-6

Declassified in Part - Sanitized Copy Approved for Release 2012/03/12 : CIA-RDP82-00039R000100190014-6

## METHOD OF MEASUREMENT

The dimensions of the cloud drops were determined by the microphotographic method adopted by the Central Geophysical Observatory (1, 2). This method allows the measurement of cloud drops from 2 to 500 microns in diameter. For two reasons it was impossible to determine the dimensions of drops smaller than 2 microns in diameter with the airborne microphotographic equipment: in the first place most of these drops flowed around the glass and failed to adhere; in the second place, short-focus objectives could not be used on account of the vibration, and therefore 20X objectives and 15X oculars were employed. There is reason to assume that drops larger than 500 microns in diameter cannot be measured by airborne microphotographic equipment because of the fact that large drops break up into smaller drops on striking the oil-covered surface of the glass. In spite of these inadequacies, the method is still the most accurate and convenient one at present, and makes it possible to determine the indicated dimensions within the indicated limits, of the cloud drops present in a state of "suspension" within a cloud.

The microphotographs were processed by projecting the images of the drops on a ground-glass counting-screen ruled in millimeters, with a 1 micron power of resolution. The frequency of drops was then calculated for various drop diameters on the basis of these measurements, and a distribution curve with 2 micron intervals was then constructed.

## DETERMINATION OF WATER CONTENT

The water content of clouds was determined by a new method making use of the inertia of the drops falling in a jet, and of the



Declassified in Part - Sanitized Copy Approved for Release 2012/03/12 : CIA-RDP82-00039R000100190014-6

Declassified in Part - Sanitized Copy Approved for Release 2012/03/12 : CIA-RDP82-00039R000100190014-6

capacity of filter paper for rapidly absorbing water. An instrument was devised (3) and constructed for the measurement from airplane of the quantity of moisture in liquid-drop form in clouds (Figure 1).

Figure 1. Airborne water content meter.

As the airplane enters the cloud, the observer opens the shutter of the instrument by means of a cable for 3 to 15 seconds. The number of seconds of exposure and the speed of the airplane are entered in the log for each measurement of water content. The samples are then processed in the following manner. The velocity of flow through the head of the instrument is computed from the airspeed by using a graduated curve; and the volume of air flowing through the head each time is determined from the velocity of flow and the number of seconds. The weight of the water and hence the water content for each measurement is found from the diameter of the colored spot on the graduated tables. The liquid is measured in terms of grams per cubic meter.

We note that the measurement of cloud-drop size is subject to a certain error [7], the mean value of which is ± microns for drops 2 to 10 microns in diameter, and ± 1.2 microns for drops over 10 microns in diameter. The total error in water content determination is made up of the error in measuring the colored spot, of the error of graduation of the paper, and of the error in determining the volume of air passed through. The mean value of this total error is ± 10 percent, and its maximum value does not exceed 16 percent.



Declassified in Part - Sanitized Copy Approved for Release 2012/03/12 : CIA-RDP82-00039R000100190014-6

Declassified in Part - Sanitized Copy Approved for Release 2012/03/12 : CIA-RDP82-00039R000100190014-6

## THE RESULTS OF THE MEASUREMENTS

Analysis of the data on the structure of cumulus clouds shows that the individual measurements of the clouds as well as the mean values of the measurements confirm the conclusions (4) of the 1947 investigations on drop distribution: in the very heart of the cumuli the drops are smaller, and the mean maximum percentage frequency falls to the interval between 4.1 and 6 microns, while the maximum drop size does not exceed 26 microns in diameter.

The size of the drops increases with the altitude: at a height of 200 meters above the cloud base, the modal diameter of the drops is 9 microns, and no drops are found of diameter over 50 microns; at a height of 600 meters the modal diameter is 11 microns; and at a height of 800 meters it is 17 microns, while drops of diameter of the order of 100 microns appear as a rule at an height of 350 meters above cloud-base level. Thus, in a cumulus convectus (25 July 1948 between 0650 and 0935 hours) the modal drop-size was 9-10 microns on the periphery at height 620 meters above the cloud-base, while the largest drops were not over 20 microns in diameter. Consequently the four zones discovered during the 1947 measurements are clearly expressed in cumuli.

## THE DISTRIBUTION OF WATER-CONTENT

The results of the measurements of the quantity of liquid-drop moisture show the water content of cumuli to increase with height above cloud-base. From Table I and also from the graph in Figure 2 it will be seen that the water-content in the layer from 0 to 50 meters, that is, at the very base of the cloud, is 0.09 grams per



Declassified in Part - Sanitized Copy Approved for Release 2012/03/12 : CIA-RDP82-00039R000100190014-6

Declassified in Part - Sanitized Copy Approved for Release 2012/03/12 : CIA-RDP82-00039R000100190014-6

cubic meter; while at a height 300-350 meters, W increases to 0.31 grams per cubic meter. The mean water content at the periphery of cumuli fluctuates between 0.12 to 0.31 grams per cubic meter. The maximum values of water content, both for the means and individual cases, are encountered at heights 900-1000 meters above cloud base: its mean value there is about 0.9 grams per cubic meter, while at the same height above cloud base the mean value of W = 1.7 grams per cubic meter in dense cumulus congestus.

Thus the water content in cumuli only infrequently exceeds 1 gram per cubic meter, while more often this value is small. According to E. S. Selezneva's estimates based on indirect evaluation, clouds of other types (stratus, stratocumulus, etc.) also have water content of the same order of magnitude.

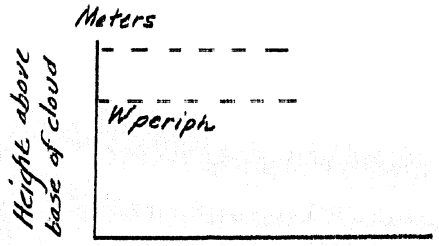


Figure 2. Mean distribution of water content by elevation above base of cloud in cumuli 500-2000 meters deep.

$W_o$ is water content in Cumulus Humilis; $W_{periph}$ -- water content at periphery of cumulus; $W_c$ -- mean water content for cumulus clouds of various densities; W -- the water content in dense cumulus congestus; n -- the number of measurements.



Declassified in Part - Sanitized Copy Approved for Release 2012/03/12 : CIA-RDP82-00039R000100190014-6

Declassified in Part - Sanitized Copy Approved for Release 2012/03/12 : CIA-RDP82-00039R000100190014-6

TABLE

MEAN DISTRIBUTION OF WATER CONTENT

| Elevation of center of layer above base of cloud (M) | Thickness of layer (M) From | To | Mean water-content ($G/M^3$) in Cu simpl and Cu cong of different densities | | | |
|---|---|---|---|---|---|---|
| | | | Center | | Periphery | |
| | | | W | n' | W | n' |
| 25 | 0 - | 50 | 0.09 | 42 | - | - |
| 150 | 51 - | 250 | 0.23 | 116 | 0.12 | 6 |
| 350 | 251 - | 450 | 0.31 | 127 | 0.16 | 10 |
| 550 | 451 - | 650 | 0.54 | 104 | 0.27 | 6 |
| 750 | 651 - | 850 | 0.56 | 81 | 0.13 | 9 |
| 950 | 851 - | 1050 | 0.86 | 43 | 0.31 | 2 |
| 1150 | 1051 - | 1250 | 0.76 | 33 | - | - |
| 1350 | 1251 - | 1450 | 0.69 | 25 | 0.15 | ? |
| 1550 | 1451 - | 1650 | 0.53 | 19 | - | - |
| 1750 | 1651 - | 1850 | 0.52 | 7 | - | - |



Declassified in Part - Sanitized Copy Approved for Release 2012/03/12 : CIA-RDP82-00039R000100190014-6

Declassified in Part - Sanitized Copy Approved for Release 2012/03/12 : CIA-RDP82-00039R000100190014-6

I

ACCORDING TO ELEVATION IN CUNULI

| Mean water content ($G/M^3$) in dense Cu cong | | Mean water content ($G/M^3$) in Cu hum | | Remarks |
|---|---|---|---|---|
| W | n' | W | n' | |
| 0.1 | 9 | 0.08 | 8 | W -- water content in $G/M^3$ |
| 0.33 | 16 | 0.17 | 35 | n'-- number of measurements |
| 0.36 | 23 | 0.33 | 37 | |
| 0.65 | 29 | 0.36 | 2 | |
| 1.06 | 27 | - | - | |
| 1.70 | 17 | - | - | |
| 0.19 | 20 | - | - | |
| 0.99 | 16 | - | - | |
| 0.77 | 3 | - | - | |
| 0.81 | 2 | - | - | |



Declassified in Part - Sanitized Copy Approved for Release 2012/03/12 : CIA-RDP82-00039R000100190014-6

Declassified in Part - Sanitized Copy Approved for Release 2012/03/12 : CIA-RDP82-00039R000100190014-6

The maximum values for water content were observed in cumulus congestus, which in most instances quickly changed into cumulo-nimbus and developed precipitation. For instance, on 30 June 1948, between 1504 and 1601 hours, at elevation 1550-1600 meters above sea level, at 1000 meters above the base of a cumulus congestus, the water content was 4.1 grams per cubic meter. This cumulus congestus then changed into a cumulo-nimbus and formed rain. Further, on 26 July 1948, between 0949 and 1047 hours, at elevation 1450 meters above the base of the cloud, a water content of 3.1 grams per cubic meter was measured in a cumulus congestus. This cloud also changed into a cumulo-nimbus. In both instances a very strong lung was observed in the clouds, and the variometer showed a lift of 5-7 meters per second with the airplane in level flight. It may be assumed that the water content at isolated points of a cumulo-nimbus type cloud can attain values of the order of 10 grams per cubic meter or higher.

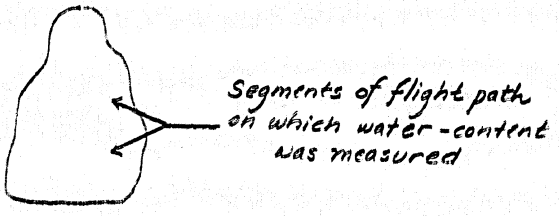


Figure 5. Distribution of water content in cumulus congestus, 24 July 1948, 1028 to 1115 hours.
h -- elevation in meters above sea level; [redacted]
$H_s$ -- height in meters above level of base of cloud.

In investigating each cumulus the airplane as a rule made three to ten flights through it against the wind, depending on the vertical



Declassified in Part - Sanitized Copy Approved for Release 2012/03/12 : CIA-RDP82-00039R000100190014-6

Declassified in Part - Sanitized Copy Approved for Release 2012/03/12 : CIA-RDP82-00039R000100190014-6

dimensions of the cloud; the airplane thus crossed the cloud in virtually a single vertical plane. At each crossing it was possible to make from one to three measurements of water content. Each cloud therefore had from six to eighteen measurements in a vertical plane from its base to its summit; this made it possible to construct isolines of water content for each cumulus. In Figures 3 and 4 such isolines have been constructed for two separate cumuli congesti.

As may be seen from the plottings, in one instance (Figure 3) the maximum water content lies in the zone of positive temperatures at a height 950 meters above the base of the cloud, and is 3.36 grams per cubic meter; in the second instance (Figure 4) the maximum water content is found in a zone of negative temperatures at a height 1160 meters above the base of the cloud.

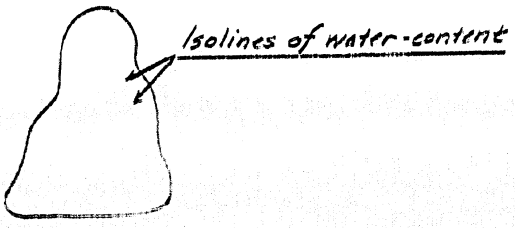


Figure 4. Distribution of water content in cumulus congestus, 26 July 1948, 1416 to 1500 hours. h — elevation in meters above sea level in meters; $H_c$ — height in meters above level of base of cloud.

The measurements also show the water content to be distributed unevenly throughout a cumulus. The accumulation of water drops in some regions evidently depends on the pulsations of anabatic currents of air. The



Declassified in Part - Sanitized Copy Approved for Release 2012/03/12 : CIA-RDP82-00039R000100190014-6

Declassified in Part - Sanitized Copy Approved for Release 2012/03/12 : CIA-RDP82-00039R000100190014-6

accumulation of water at the mean height of 1000 meters above the base of the cloud is characteristic of clouds 1500-2000 meters thick and is due to the fact that the size of drops at this level increases until their rate of fall relative to the air is equal to the upward velocity of the anabatic current (5). In cumulus congestus, in which there are powerful anabatic air currents, the maximum value of the water content is observed at a height of 1350-1400 meters and higher, above the base of the cloud. It may be assumed that for cumuli congesti 2000-2500 meters thick, the zone of maximum water content will be found within the limits of 800 to 1600 meters above the base of the cloud.

It is also interesting to observe that in eight of the ten cases of cumulus congestus that changed into cumulo-nimbus, as well as in cumuli that did not develop completely into cumulo-nimbus, but remained close to the form of thunder clouds, the maximum water content was found above the level of the zero isotherm, that is, in the zone of negative temperatures. In those instances in which a cloud did not develop into a cumulo-nimbus, the zone of maximum water content was located below the zero isotherm, although the summit of the cloud was situated in the zone of negative temperatures.

DETERMINATION OF THE NUMBER OF DROPS PER CUBIC CENTIMETER

Since water content was measured at the same time drop samples were taken for microphotography, water content and drops may be considered to have been taken from the same area. If we know the number of drops found in a sample, together with their size, the total volume of all the drops in a given sample may be found by the formula



Declassified in Part - Sanitized Copy Approved for Release 2012/03/12 : CIA-RDP82-00039R000100190014-6

Declassified in Part - Sanitized Copy Approved for Release 2012/03/12 : CIA-RDP82-00039R000100190014-6

$$V = \frac{\pi}{6} \sum d_i^3 n_i \ (cm^3) \qquad (1)$$

where V is the volume of all the drops found in the given sample, $d_i$ is the diameter of drops of the i-th size and $n_i$ is the number of such drops.

On the other hand, the water content is determinated by instrument and expressed as grams per cubic foot.

Taking the density of water as unity, we may consider the water content W equal to the volume of liquid water in cubic centimeters contained in 1 cubic meter of air.

By dividing the volume of water W, ascertained by the instrument, by the volume V of all measured drops, we obtain:

$$\frac{W}{V} = K \qquad (2)$$

K shows how many times the volume V of all measured drops is contained in the volume of water W determined by the instrument. Then the number of drops in 1 cubic centimeter may be found by the formula:

$$N = n \cdot K \qquad (3)$$

where n is the number of drops counted in the given sample.

The number of drops in unit volume was calculated by formulae (1), (2), and (3) for each cloud; and the mean of the total number of simultaneous readings was similarly calculated.

As appears from Table II and from the graph in Figure 5, the



Declassified in Part - Sanitized Copy Approved for Release 2012/03/12 : CIA-RDP82-00039R000100190014-6

Declassified in Part - Sanitized Copy Approved for Release 2012/03/12 : CIA-RDP82-00039R000100190014-6

number of drops per cubic centimeter declines with increasing height, although the water content increases. The mean maximum number of drops per cubic centimeter -- N = 460 -- was observed at a height 100 meters above the base of the cloud, that is, in zone II. In most of the clouds N may be similarly observed to increase in the second zone. Thus, for instance, in the cumulus congestus of 20 July 1948, between 1105 and 1205 hours, (figure 6), N = 380 at a height 80 meters above the base of the cloud, N = 700 at a height of 300 meters, and N = 25 at a height of 1200 meters.

Table II. Mean distribution according to height in cumulus clouds of the number of drops per cubic centimeter and of the water content, from simultaneous observations.

| Height of center of layer ($\bar{h}$) above base of cloud | Thickness (h') of layer from | To | N Drops per cm3 | W Water content g/m3 | n' Number of measurements |
|---|---|---|---|---|---|
| 25 | 0 -- | 50 | 300 | 0.09 | 23 |
| 100 | 51 -- | 150 | 460 | 0.18 | 25 |
| 225 | 151 -- | 300 | 290 | 0.27 | 43 |
| 400 | 301 -- | 500 | 140 | 0.41 | 57 |
| 600 | 501 -- | 700 | 90 | 0.45 | 32 |
| 800 | 701 -- | 900 | 70 | 0.72 | 16 |
| 1000 | 901 -- | 1100 | 50 | 0.97 | 18 |
| 1450 | 1101 -- | 1800 | 40 | 0.77 | 18 |

The lower number of drops per cubic centimeter in Zone I as compared with Zone II may be explained first by the fact that drops up to 2.5 microns were discarded in the process of microphotography, and second by the low density of the bottom layer of a cumulus. With the



Declassified in Part - Sanitized Copy Approved for Release 2012/03/12 : CIA-RDP82-00039R000100190014-6

Declassified in Part - Sanitized Copy Approved for Release 2012/03/12 : CIA-RDP82-00039R000100190014-6

transition to Zone II, the density of the cloud apparently increases because of the formation of new drops on the condensation nuclei.

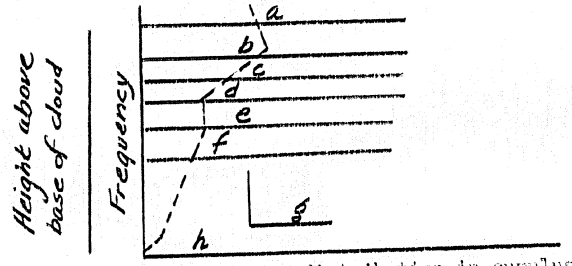


Figure 5. Mean distribution in cumulus congestus, according to height, of drop size, water content and number of drops per cubic centimeter.

1. W -- water content in grams per cubic meter; 2. N -- number of drops per cubic centimeter; n -- number of measurements of drops; $H_o$ -- height in meters of center of layer above base of cumulus.

| | Values n | Values $H_o$ |
|---|---|---|
| a | 4,321 | 1,450 |
| b | 4,062 | 1,000 |
| c | 6,010 | 800 |
| d | 11,883 | 600 |
| e | 21,277 | 400 |
| f | 17,267 | 225 |
| g | 8,326 | 100 |
| h | 4,439 | 25 |



Declassified in Part - Sanitized Copy Approved for Release 2012/03/12 : CIA-RDP82-00039R000100190014-6

Declassified in Part - Sanitized Copy Approved for Release 2012/03/12 : CIA-RDP82-00039R000100190014-6

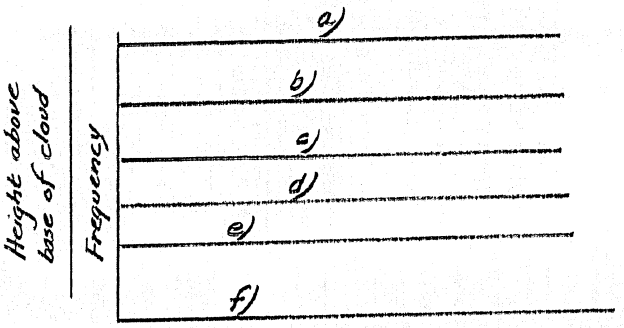


Figure 6. Mean distribution in cumulus congestus, according to height, of drop size, water content and number of drops per cubic centimeter. 20 July 1948 (1105 -- 1205 hours).

1. W -- water content in grams per cubic meter; 2. N -- number of drops per cubic centimeter; n -- number of measurements of drops; $H_0$ -- height in meters of center of layer above base of cumulus.

| | Values n | Values $H_0$ | |
|---|---|---|---|
| a | 121 | 1,200 | |
| b | 313 | 250 | |
| c | 418 | 700 | |
| d | 446 | 500 | |
| e | 609 | 300 | center dense, airplane drenched |
| f | 333 | 80 | |

Figure 7 shows the distribution according to height of water content, size and number of drops, in a cumulus congestus that turned to cumulo-nimbus. The maximum number of drops per cubic centimeter here is equal to 700 and occurs at a height of 550 meters above the base of the cloud. The second increase in this value with increasing



Declassified in Part - Sanitized Copy Approved for Release 2012/03/12 : CIA-RDP82-00039R000100190014-6

Declassified in Part - Sanitized Copy Approved for Release 2012/03/12 : CIA-RDP82-00039R000100190014-6

height is found at the height of 1350 meters above the base, where N = 350 and W = 3.2 grams per cubic meter. At this height 19 microns is the size of highest frequency, while individual drops attain diameters of 100 microns and over. Consequently in the zone of high water content the drops grow considerably in size, with their diameters distributed over a range from 10 to 100 microns. The regions of high water content in the cloud (of the order of 2 grams per cubic meter and over) are apparently the foci where stormy formation of "incipient" raindrops 1-2 millimeters in diameter occurs. These regions are also in all probability places of active formation of snow, soft hail, and hail because of the crystallization or freezing of large drops 40 microns and more in diameter, if such drops are found in the zone of negative temperatures (on the order of -4 to -12 degrees Centigrade).

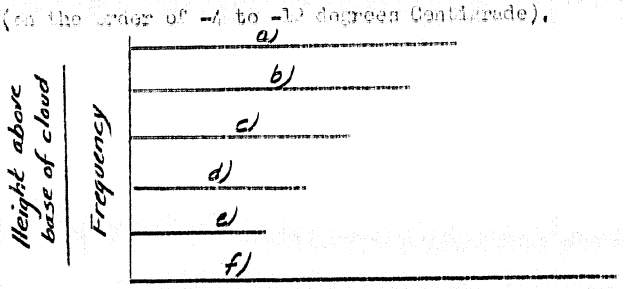


Figure 7. Zone distribution in cumulus congestus, according to height, of drop size, water content and number of drops per cubic Centimeter. 24 July 1948 (0249 to 1047 hours).

1. W -- water content in grams per cubic meter; 2. N -- number of drops per cubic Centimeter; n -- number of measurements of drops; $H_b$ -- height in meters of center of layer above base of cumulus.



Declassified in Part - Sanitized Copy Approved for Release 2012/03/12 : CIA-RDP82-00039R000100190014-6

Declassified in Part - Sanitized Copy Approved for Release 2012/03/12 : CIA-RDP82-00039R000100190014-6

| | Values $n$ | Values $H_o$ | |
|---|---|---|---|
| a | 501 | 1,400, | dome-shaped summit of cumulus congestus with bumpiness; airplane drenched |
| b | 279 | 1,100, | airplane drenched at center |
| c | 304 | 800 | " " " " |
| d | 316 | 550 | " " " " |
| e | 903 | 400 | center dense and uniform |
| f | 389 | 200 | base of cloud; density uniform. |

There is reason to assume that the crystallisation or freezing of cloud drops of sizes from 30 to 40 microns and over proceeds as a result of the appearance of ice in the form of crystals or amorphous formations around the hard particles enclosed within the drops. As is generally known, besides the condensation nuclei which, on the whole, are hygroscopic and soluble, there are considerable numbers of particles in the air which are hard and insoluble in water: dust, products of weathering, combustion, organic dusts etc, of sizes ranging from $10^{-5}$ to $10^{-4}$ centimeters. We consider it probable that the mean number of hard particles insoluble in water beneath the base of a cumulus cloud amounts to one-half percent of the total number of condensation nuclei (6), or 20-25 particles per cubic centimeter. As a result of the Brownian movement and electrical forces, these hard particles adsorb the water droplets in the first and second zones of a cumulus.

It may therefore be postulated that some of the drops even in the lower layers of the cloud contain hard particles. The cloud droplets from 30 to 40 microns in diameter can freeze earlier than the others when they fall into a zone of negative temperatures from -4 to



Declassified in Part - Sanitized Copy Approved for Release 2012/03/12 : CIA-RDP82-00039R000100190014-6

Declassified in Part - Sanitized Copy Approved for Release 2012/03/12 : CIA-RDP82-00039R000100190014-6

-12 degrees Centigrade, and thus create favorable conditions for their development as water vapor is successively transferred to them from the unfrozen drops and from the air.

## CONCLUSIONS

On the basis of these investigations, the following conclusions as to the microstructure of cumulus clouds may be drawn.

1. At consecutively higher levels from base to summit of a cumulus, increase in drop size, increase in water content, and decrease in number of drops per cubic centimeter is observed. Increase in drop size and in water content depends on the vertical dimension of the cloud and on the strength of the anabatic currents within it. Drops of over 50 microns in diameter are almost never encountered in clouds of the cumulus humilis type, and the water content in such clouds does not exceed 0.4 grams per cubic meter, while single drops up to 400 microns and over are not in dense cumuli congesti, and in places the water content in these instances reaches as much as 1.7 grams per cubic meter.

2. The distribution of drops and of water content is irregular both vertically and horizontally in cumuli 1800-2000 meters thick. In the lower 60-meter layer, which we call Zone I, the drops are small, 90 percent of them being between 3 and 16 microns in diameter, while drops larger than 24 microns are not met at all. The water content in this zone is 0.08 grams per cubic meter, and N = 300 drops per cubic centimeter. Zone I is located on the condensation level, and the new drops which are continuously being formed in it are carried upward by the anabatic current.



Declassified in Part - Sanitized Copy Approved for Release 2012/03/12 : CIA-RDP82-00039R000100190014-6

Declassified in Part - Sanitized Copy Approved for Release 2012/03/12 : CIA-RDP82-00039R000100190014-6

Zone II is located above Zone I and occupies a layer of the mean thickness of 300 meters. In this zone the drops grow larger because of condensation, and new drops are also formed by condensation about condensation nuclei. 96 percent of all the drops here are between 3 and 30 microns in diameter, while no drops larger in diameter than 50 microns are encountered. The water content ranges from 0.18 grams per cubic meter in the lower part of the zone to 0.27 grams per cubic meter in the upper part, with N at 460 to 200 drops per cubic centimeter respectively. Zone II may be as much as 500-600 meters thick in clouds with powerful anabatic currents.

Zone III occupies the entire central part of a cumulus. Its lower limit begins at 350-400 meters above the base of the cloud, and it extends upward almost to the very summit. 96 percent of the drops in this zone are between 3 and 30 microns in diameter, while the largest drops reach 300-400 microns. In the lower part of the zone, W = 0.41 grams per cubic meter and N = 140; in the upper part, W = 0.77 grams per meter and N = 40. We call this zone the zone of drizzling drops, and airplanes became badly drenched.

Zone IV embraces the entire periphery of a cumulus. It is a layer 50-100 meters thick. In this zone, the modal diameter of the drops is 8 to 14 microns, while drops larger than 50 microns are almost never met. Water content fluctuates between 0.05 and 0.3 grams per cubic meter. In consequence of the contact between the cloud masses and the surrounding air, which has a relative humidity under 100 percent, the processes of evaporation probably predominate in Zone IV.



Declassified in Part - Sanitized Copy Approved for Release 2012/03/12 : CIA-RDP82-00039R000100190014-6

Declassified in Part - Sanitized Copy Approved for Release 2012/03/12 : CIA-RDP82-00039R000100190014-6

3. The region of maximum water content is located in the central part of zone III. In this region, in dense clouds, the water content attains a mean value of 1.7 grams per cubic meter, while in individual clouds it goes as high as 4.1 grams per cubic meter; 94 percent of all drops are between 3 and 40 microns in diameter, and the largest drops may reach 100-400 microns. The mean value of N is 70. This region may undergo both vertical and horizontal displacement within the cloud, depending on the pulsations and power of ascending air currents. The region of maximum water content is currently the place where incipient rain drops 1 to 2 millimeters in diameter are formed, and is also the most dangerous icing region when the drops are supercooled.

4. The method and instrument employed by us for determining the water content of clouds, with the use of an airplane, have fully justified themselves in accuracy and simplicity of measurement, and may be applied successfully by aerologic stations for the regular measurement by airplane of the amount of liquid-drop moisture in clouds.



Declassified in Part - Sanitized Copy Approved for Release 2012/03/12 : CIA-RDP82-00039R000100190014-6

Declassified in Part - Sanitized Copy Approved for Release 2012/03/12 : CIA-RDP82-00039R000100190014-6

# TOTAL RADIATION AT PAVLOVSK

N. N. Kalitin [deceased]

The year 1890 must be considered the beginning of actinometric work at Pavlovsk. In that year Professor O.D. Khvol'son of the University of St. Petersburg designed and constructed an actinometer at the observatory there for the purpose of measuring the intensity of direct solar radiation. The actinometer was put into operation as soon as constructed, making it possible for Professor Khvol'son to publish a paper in 1893 entitled "Actinometric Investigations carried out in 1891 and 1892 at the Konstantinovsk Observatory in Pavlovsk."

From that time to August 1941 the actinometric work at Pavlovsk was uninterrupted, and continued to develop throughout the entire period.

The Khvol'son actinometer was not only inconvenient to use but also of unsatisfactory accuracy, and the observations with it consumed much time; consequently its use received no particular or widespread development.

Actinometric measurements became considerably more widespread in 1905, when the observatory acquired an Angstrom compensating pyrheliometer, which had recently been recommended at the International Meteorological Congress at Innsbruck, Austria, as the standard instrument for measuring the intensity of solar radiation. Down to the present day, over a period of more than 40 years, the excellent quality of this instrument has kept it, almost without modification, among the standard equipment for



Declassified in Part - Sanitized Copy Approved for Release 2012/03/12 : CIA-RDP82-00039R000100190014-6

Declassified in Part - Sanitized Copy Approved for Release 2012/03/12 : CIA-RDP82-00039R000100190014-6

geophysical observatories. But even with this instrument observations were not made very often as its operation required a highly qualified technician.

In 1907 the number of observations was significantly expanded when a remarkable instrument was put into operation: the bimetallic strip actinometer designed in 1906 by our noted physicist V. A. Mikhel'son, which is simple, convenient and accurate. In 1910-1911, S. I. Savinov worked in the Pavlovsk Observatory with the improved French actinograph of Krov. An improved radiation receiver, the so-called Savinov thermoelectric control wheel, was the result of this work. The Krov actinograph -- a capricious instrument -- frequently gives distorted readings of the radiation.

With the utilization of a new receiver the recordings became faultless; this permitted use of the actinograph for the first time anywhere in the world, for systematic, continuous research; this commenced 1 April 1912 and proceeded without interruption until the end of August, 1941, when all instruments were evacuated to Leningrad as the war front neared Pavlovsk.

Since 1912 there has been an uninterrupted registration of the heat inflow from solar radiation. It was clear even at that time that the record of incoming solar radiation alone was insufficient, and that it was necessary also to take account of the diffuse sky radiation which plays no small role in the total radiation. But the lack of reliable methods at the time prevented study of the diffuse sky radiation. It is true that at that time S.I. Savinov worked out a method for measuring diffuse sky radiation by constructing a "checkerboard" actinometer, or pyranometer, which was subsequently remodeled into a "strip type," but the



Declassified in Part - Sanitized Copy Approved for Release 2012/03/12 : CIA-RDP82-00039R000100190014-6

Declassified in Part - Sanitized Copy Approved for Release 2012/03/12 : CIA-RDP82-00039R000100190014-6

instruments were still unreliable, and their readings were frequently so unsatisfactory (1) that they could not be used in systematic work. Therefore, although measurement and registration of the diffuse sky radiation was carried out from 1923 to 1927, the material was worked up only selectively and served methodological purposes principally.

In 1927 a model of a vacuum pyranometer (2) was developed at the observatory. It was constructed according to the principle laid down by Ångstrom (magnesium oxide and lampblack) and gave more or less satisfactory results. The systematic study of diffuse radiation was also hampered by the unsuitable location of the actinometric pavilion in a clearing surrounded on all sides by forests and buildings, which made it impossible to take account of the diffuse radiation from the full arch of the sky, which for some azimuths was shut off from an altitude of 40-60 degrees down to the horizon.

The situation took a change for the better in 1930 when the building for the Institute of Actinometry and Atmospheric Optics was erected on an open field not far from the Meteorological Observatory at Pavlovsk and all actinometric and optical observations were transferred there. From the autumn of 1930 the diffuse sky radiation, among other radiation elements, was uninterruptedly registered in the new building up to the end of August 1941. Until 1932 a Kalitin pyranometer No 4 was used; a Kalitin No 27 was used from 1932 to 1935; and a Yanishevskiy pyranometer (3) was used from 1935 to the end. Moreover, it should be taken into account that since 1931 the observations were made under entirely



Declassified in Part - Sanitized Copy Approved for Release 2012/03/12 : CIA-RDP82-00039R000100190014-6

Declassified in Part - Sanitized Copy Approved for Release 2012/03/12 : CIA-RDP82-00039R000100190014-6

favorable conditions for diffuse sky radiation (open field), and furthermore, the same type of apparatus was used throughout. Because of these two factors it proved possible to make an accurate record during the ten years from 1931 to 1940 of the solar radiation falling on a horizontal surface S', of the diffuse sky radiation D, and therefore of the total radiation q equals S' plus D.

The conclusions from the observations for Pavlovsk of solar radiation (4) -- (9) and for diffuse sky radiation (10) -- (12) have been separately published, but the total radiation for this long period is studied here for the first time in this paper, except for a few short papers (13) and (14) published in 1943 and 1946.

The object of the present investigation is the study of the total radiation for the climatic conditions of Leningrad Oblast on the basis of a long series of uniform observations consisting of readings of direct and diffuse radiation, with the thought that Pavlovsk is rather typical of the entire Oblast so far as radiation conditions are concerned. The total radiation will be considered not merely as such, but will also be studied in its components as well: solar and diffuse radiation.

Yu. D. Yanishevskiy completed his investigation "Questions of Accuracy of the Pyranometric Observations at Pavlovsk" when the present paper had already gone to press; his study contains the corrections for the Savinov and Kalitin pyranographs that were operated up to 1939, and these corrections make the entire series



Declassified in Part - Sanitized Copy Approved for Release 2012/03/12 : CIA-RDP82-00039R000100190014-6

Declassified in Part - Sanitized Copy Approved for Release 2012/03/12 : CIA-RDP82-00039R000100190014-6

of observations completely uniform by converting them to the scale of readings of the Yanishevskiy pyranometer.

Inasmuch as there was no time for this recomputation, my article uses the data as originally observed, in the form in which it was worked up at that time.

If there should be future occasion for it, this data can be recomputed on the basis of the data in the Yanishevskiy article.

## TOTAL RADIATION OF A CLOUDLESS SKY

First of all it is of interest and importance to study the value of the total radiation and its components for a cloudless sky. The values obtained for a cloudless sky may serve as basic values for the further study of radiation under natural conditions.

This question has been investigated previously, in part, but on the basis of limited data (15), (16), while in the present paper the study is based on the results of ten years' of observations.

The daily and annual cycle of the value of total radiation in a cloudless sky depends on the altitude of the sun, the transparency of the atmosphere, and the albedo of the ground. Since the material for the study of total radiation consists of actinograph and pyranograph records, days were first selected that could all be determined from these records to have been cloudless. To be absolutely sure of this, the days in question were then checked



Declassified in Part - Sanitized Copy Approved for Release 2012/03/12 : CIA-RDP82-00039R000100190014-6

Declassified in Part - Sanitized Copy Approved for Release 2012/03/12 : CIA-RDP82-00039R000100190014-6

for cloudlessness against the hourly cloudiness record, covering amount and type of clouds, maintained by the Meteorological Observatory.

There were in all 79 completely cloudless days in the ten years, which is only 2.2 percent of the total number of days (3,653) in ten years; besides being very few in number, these days were also distributed very irregularly among the various months, so that the material was rendered completely inadequate for the study of the relationships sought.

In order to increase the amount of data subject to this study, it was decided to add those days that were completely cloudless from sunrise to noon or from noon to sunset; there were 131 of these half-days during the ten-year period. Their distribution by months is shown in Table I. This table shows that the highest mean monthly number of cloudless days during the period under study was 13, in March, and the lowest was 2, in September. The annual cycle of cloudless days from the maximum in March to the minimum in September and November is well defined. Cloudless half-days were most frequent in May, with 1[illegible], and least frequent in November, with three. Thus the total radiation in a cloudless sky must be studied on the basis of rather scanty material, but nothing can be done about this climate in the Leningrad Oblast.

TABLE I

TEN YEARS NUMBERS OF COMPLETELY CLOUDLESS DAYS AND HALF DAYS BY MONTHS, AND MEAN ANNUAL NUMBERS OF SUCH DAYS

1931 - 1940



Declassified in Part - Sanitized Copy Approved for Release 2012/03/12 : CIA-RDP82-00039R000100190014-6

Declassified in Part - Sanitized Copy Approved for Release 2012/03/12 : CIA-RDP82-00039R000100190014-6

| | JAN. | FEB. | MAR. | APR. | MAY | JUNE |
|---|---|---|---|---|---|---|
| Whole days | 10 | 11 | 13 | 8 | 6 | 5 |
| Half days | 15 | 15 | 14 | 11 | 18 | 13 |

| | JULY | AUG. | SEPT. | OCT. | NOV. | DEC. | YEAR |
|---|---|---|---|---|---|---|---|
| Whole days | 3 | 3 | 2 | 5 | 4 | 3 | 79 |
| Half days | 12 | 7 | 8 | 8 | 3 | 7 | 131 |

The total radiation was worked up according to the following method.

From the prepared tabulations of the recorded instrument readings, the hourly totals for diffuse sky radiation between sunrise and sunset were taken off for all years, and the monthly means computed. Graphs of the daily cycle of total diffuse sky radiation were then plotted on the basis of these data.

Since the material for some months was inadequate, there was a considerable degree of scatter among the points on the graphs in consequence of variations in atmospheric transparency, and it was necessary in some cases to smooth the curves extensively.

The data for solar radiation falling on a horizontal surface were assembled in analogous fashion for these years, and the daily cycle of the hourly total heat of solar radiation by months was likewise obtained.

From these curves (for diffuse and solar radiation) the values of the hourly totals were then taken and compiled in Table



Declassified in Part - Sanitized Copy Approved for Release 2012/03/12 : CIA-RDP82-00039R000100190014-6

Declassified in Part - Sanitized Copy Approved for Release 2012/03/12 : CIA-RDP82-00039R000100190014-6

II, which shows for each month and for each hourly interval the mean values of the incoming solar radiation falling on a horizontal surface ($\Sigma S_0'$), of the incoming diffuse sky radiation ($\Sigma D$), and of the total incoming radiation ($\Sigma Q_0$) as their sum.

The mean diurnal hourly totals $\Sigma Q_0$ were thus secured for each month. The total incoming heat of radiation during the daylight intervals of each month were obtained by multiplying these totals by the number of days in the month. The values so obtained are shown as $\Sigma Q_0$ in the last line for each month in Table II.

[See next page for table.]

Curves of mean monthly diurnal cycles of the total radiation through a cloudless sky with the mean atmospheric transparency at Pavlovsk may be drawn on the basis of the figures in Table II; these graphs in turn allow the plotting of isopleths of the hourly total heats of the total radiation for a cloudless sky (Figure 1).

The figures on the isopleths are in hundreds of calories. The distribution of isopleths in Figure 1 shows symmetrical distribution under the mean conditions of atmospheric transparency at Pavlovsk. There is only a slight reduction in the incoming total radiation for June in the hours around noon and during the latter half of the day; this reduction is apparently produced by the lowered intensity of solar radiation resulting from the diminished atmospheric transparency in its annual and diurnal cycle.



Declassified in Part - Sanitized Copy Approved for Release 2012/03/12 : CIA-RDP82-00039R000100190014-6

Declassified in Part - Sanitized Copy Approved for Release 2012/03/12 : CIA-RDP82-00039R000100190014-6



MEAN ANNUAL DIURNAL AND HOURLY AMOUNTS OF SOLAR, DIFFUSE, AND TOTAL RADIATION,

TOGETHER WITH MONTHLY TOTAL RADIATION, FOR CLOUDLESS SKY, IN CALORIES.

Table 2.

| MONTHS | | HOURS | | | | | | | | | | | | | | | | | | | |
|---|---|---|---|---|---|---|---|---|---|---|---|---|---|---|---|---|---|---|---|---|---|
| | | (1) 2-3 | (2) 3-4 | (3) 4-5 | (4) 5-6 | (5) 6-7 | (6) 7-8 | (7) 8-9 | (8) 9-10 | (9) 10-11 | (10) 11-12 | (11) 12-13 | (12) 13-14 | (13) 11-15 | (14) 15-16 | (15) 16-17 | (16) 17-18 | (17) 18-19 | (18) 19-20 | (19) 20-21 | (20) 21-22 |
| January | Σ So' | | | | | | | 0.3 | 2.5 | 6.2 | 8.3 | 8.0 | 5.6 | 2.0 | 0.1 | | | | | | |
| | Σ Do | | | | | | | 0.8 | 2.2 | 3.4 | 1.0 | 3.9 | 3.3 | 2.1 | 0.5 | | | | | | |
| | Σ Qo | | | | | | | 1.1 | 4.7 | 9.6 | 12.3 | 11.9 | 8.9 | 4.1 | 0.6 | | | | | | |
| | Σ Qm | | | | | | | 31 | 146 | 298 | 381 | 369 | 276 | 127 | 19 | | | | | | |
| February | Σ So' | | | | | | 0.3 | 4.0 | 11.1 | 16.6 | 19.4 | 19.0 | 18.3 | 11.2 | 4.6 | 0.4 | | | | | |
| | Σ Do | | | | | | 1.2 | 3.2 | 4.7 | 5.5 | 6.0 | 5.6 | 4.9 | 3.8 | 2.4 | 0.8 | | | | | |
| | Σ Qo | | | | | | 1.5 | 7.2 | 15.8 | 22.1 | 25.4 | 24.6 | 23.2 | 15.0 | 7.0 | 1.2 | | | | | |
| | Σ Qm | | | | | | 42 | 202 | 442 | 619 | 711 | 689 | 650 | 420 | 196 | 34 | | | | | |
| March | Σ So' | | | | | 0.5 | 6.2 | 11.6 | 23.0 | 29.0 | 32.0 | 31.1 | 27.7 | 22.0 | 13.2 | 4.2 | 0.3 | | | | |
| | Σ Do | | | | | 0.8 | 3.1 | 4.5 | 5.4 | 6.0 | 6.3 | 6.2 | 5.7 | 5.1 | 4.2 | 2.6 | 0.8 | | | | |
| | Σ Qo | | | | | 1.3 | 9.3 | 19.1 | 28.4 | 35.0 | 38.3 | 37.3 | 33.4 | 27.1 | 17.4 | 6.8 | 1.1 | | | | |
| | Σ Qm | | | | | 40 | 288 | 592 | 880 | 1085 | 1187 | 1156 | 1035 | 840 | 539 | 211 | 34 | | | | |

Declassified in Part - Sanitized Copy Approved for Release 2012/03/12 : CIA-RDP82-00039R000100190014-6

Declassified in Part - Sanitized Copy Approved for Release 2012/03/12 : CIA-RDP82-00039R000100190014-6



| | | (1) | (2) | (3) | (4) | (5) | (6) | (7) | (8) | (9) | (10) | (11) | (12) | (13) | (14) | (15) | (16) | (17) | (18) | (19) | (20) |
|---|---|---|---|---|---|---|---|---|---|---|---|---|---|---|---|---|---|---|---|---|---|
| April | $\Sigma So'$ | | | 0.2 | 2.2 | 10.1 | 20.8 | 31.4 | 40.5 | 46.3 | 49.0 | 47.2 | 44.0 | 37.0 | 28.0 | 18.5 | 9.0 | 2.0 | 0.1 | | |
| | $\Sigma Do$ | | | 0.3 | 2.5 | 3.7 | 4.6 | 5.1 | 5.3 | 5.4 | 5.6 | 5.8 | 5.7 | 5.4 | 4.9 | 4.2 | 3.1 | 1.6 | 0.3 | | |
| | $\Sigma Qo$ | | | 0.5 | 4.7 | 13.8 | 25.4 | 36.5 | 45.8 | 51.7 | 54.6 | 53.0 | 49.7 | 42.4 | 32.9 | 22.7 | 12.1 | 3.6 | 0.4 | | |
| | $\Sigma Qm$ | | | 15 | 141 | 414 | 762 | 1095 | 1374 | 1551 | 1638 | 1590 | 1491 | 1272 | 987 | 681 | 363 | 108 | 12 | | |
| May | $\Sigma So'$ | | 0.3 | 3.5 | 12.5 | 22.5 | 33.0 | 42.7 | 50.5 | 56.5 | 59.0 | 58.0 | 54.5 | 49.0 | 42.0 | 32.0 | 21.8 | 12.6 | 3.8 | 0.1 | |
| | $\Sigma Do$ | | 1.1 | 2.8 | 4.0 | 4.9 | 5.5 | 6.1 | 6.5 | 6.8 | 6.9 | 6.9 | 6.7 | 6.3 | 5.9 | 5.3 | 4.5 | 3.5 | 2.4 | 0.6 | |
| | $\Sigma Qo$ | | 1.4 | 6.3 | 16.5 | 27.4 | 38.5 | 48.8 | 57.0 | 63.3 | 65.9 | 64.9 | 61.2 | 55.3 | 47.9 | 37.3 | 26.3 | 16.1 | 6.2 | 0.7 | |
| | $\Sigma Qm$ | | 43 | 195 | 512 | 819 | 1194 | 1513 | 1767 | 1962 | 2043 | 2012 | 1897 | 1714 | 1485 | 1156 | 815 | 499 | 192 | 22 | |
| June | $\Sigma So'$ | | 0.6 | 6.0 | 14.2 | 24.0 | 34.2 | 44.0 | 51.8 | 55.5 | 59.0 | 60.0 | 57.7 | 52.0 | 43.5 | 34.5 | 24.5 | 14.4 | 5.8 | 0.9 | |
| | $\Sigma Do$ | 0.1 | 1.4 | 3.1 | 4.1 | 5.0 | 5.6 | 6.1 | 6.4 | 6.6 | 6.6 | 6.6 | 6.4 | 6.2 | 5.8 | 5.3 | 4.8 | 4.1 | 2.9 | 1.4 | 0.2 |
| | $\Sigma Qo$ | 0.1 | 2.0 | 9.1 | 18.3 | 29.0 | 39.8 | 50.1 | 58.2 | 62.1 | 65.6 | 66.0 | 64.1 | 58.2 | 49.3 | 39.8 | 29.3 | 18.5 | 8.7 | 2.3 | 0.2 |
| | $\Sigma Qm$ | 3 | 60 | 273 | 549 | 870 | 1194 | 1503 | 1746 | 1863 | 1968 | 1998 | 1923 | 1746 | 1479 | 1194 | 879 | 555 | 261 | 69 | 6 |

Declassified in Part - Sanitized Copy Approved for Release 2012/03/12 : CIA-RDP82-00039R000100190014-6

Declassified in Part - Sanitized Copy Approved for Release 2012/03/12 : CIA-RDP82-00039R000100190014-6



| | | (1) | (2) | (3) | (4) | (5) | (6) | (7) | (8) | (9) | (10) | (11) | (12) | (13) | (14) | (15) | (16) | (17) | (18) | (19) | (20) |
|---|---|---|---|---|---|---|---|---|---|---|---|---|---|---|---|---|---|---|---|---|---|
| July | $\Sigma So'$ | | 0.3 | 3.6 | 10.5 | 20.6 | 31.2 | 40.4 | 46.4 | 54.0 | 58.3 | 60.0 | 58.2 | 52.8 | 44.4 | 34.0 | 23.3 | 13.2 | 5.0 | 0.6 | |
| | $\Sigma Do$ | 0.1 | 1.1 | 2.9 | 4.7 | 5.9 | 6.5 | 6.8 | 7.0 | 7.2 | 7.2 | 7.1 | 6.9 | 6.5 | 6.0 | 5.5 | 4.7 | 3.8 | 2.6 | 0.9 | |
| | $\Sigma Qo$ | 0.1 | 1.4 | 6.5 | 15.2 | 26.5 | 37.7 | 47.2 | 55.4 | 61.2 | 65.5 | 67.1 | 65.1 | 59.3 | 50.4 | 39.5 | 28.0 | 17.0 | 7.6 | 1.5 | |
| | $\Sigma Qm$ | 3 | 43 | 202 | 468 | 822 | 1169 | 1463 | 1717 | 1897 | 2030 | 2080 | 2018 | 1838 | 1562 | 1225 | 868 | 527 | 236 | 46 | |
| August | $\Sigma So'$ | | | 0.4 | 4.0 | 11.6 | 19.8 | 29.4 | 35.4 | 41.4 | 45.5 | 47.5 | 46.8 | 42.0 | 34.0 | 24.2 | 14.3 | 5.1 | 0.5 | | |
| | $\Sigma Do$ | | 0.1 | 1.4 | 3.4 | 5.8 | 7.6 | 8.9 | 9.4 | 9.6 | 9.6 | 9.4 | 8.9 | 8.3 | 7.7 | 6.6 | 5.4 | 3.4 | 1.4 | 0.2 | |
| | $\Sigma Qo$ | | 0.1 | 1.8 | 7.4 | 17.4 | 27.4 | 36.3 | 44.8 | 51.0 | 55.1 | 56.9 | 55.7 | 50.3 | 41.7 | 30.8 | 19.7 | 8.5 | 1.9 | 0.2 | |
| | $\Sigma Qm$ | | 3 | 56 | 229 | 539 | 849 | 1167 | 1369 | 1581 | 1708 | 1764 | 1727 | 1559 | 1293 | 945 | 611 | 264 | 59 | 6 | |
| September | $\Sigma So'$ | | | | 0.2 | 3.1 | 12.0 | 22.0 | 29.8 | 38.6 | 39.0 | 37.5 | 34.4 | 29.4 | 20.5 | 10.7 | 2.6 | 0.1 | | | |
| | $\Sigma Do$ | | | | 0.6 | 2.3 | 3.5 | 4.2 | 4.6 | 4.8 | 4.9 | 4.7 | 4.5 | 4.1 | 3.5 | 2.6 | 1.3 | 0.2 | | | |
| | $\Sigma Qo$ | | | | 0.8 | 5.4 | 15.5 | 26.2 | 34.4 | 43.4 | 43.9 | 42.2 | 38.9 | 33.5 | 24.0 | 13.3 | 3.9 | 0.3 | | | |
| | $\Sigma Qm$ | | | | 24 | 162 | 465 | 786 | 1032 | 1302 | 1317 | 1266 | 1167 | 1005 | 720 | 399 | 117 | 9 | | | |

Declassified in Part - Sanitized Copy Approved for Release 2012/03/12 : CIA-RDP82-00039R000100190014-6

Declassified in Part - Sanitized Copy Approved for Release 2012/03/12 : CIA-RDP82-00039R000100190014-6



| | | (1) | (2) | (3) | (4) | (5) | (6) | (7) | (8) | (9) | (10) | (11) | (12) | (13) | (14) | (15) | (16) | (17) | (18) | (19) | (20) |
|---|---|---|---|---|---|---|---|---|---|---|---|---|---|---|---|---|---|---|---|---|---|
| October | $\Sigma$ So' | | | | | 0.1 | 2.7 | 10.0 | 17.6 | 23.6 | 26.8 | 26.7 | 23.3 | 17.2 | 9.1 | 5.2 | 0.1 | | | | |
| | $\Sigma$ Do | | | | | 0.2 | 1.7 | 3.1 | 3.9 | 4.4 | 4.7 | 4.5 | 4.2 | 3.6 | 2.6 | 1.3 | 0.1 | | | | |
| | $\Sigma$ Qc | | | | | 0.3 | 4.4 | 13.1 | 21.5 | 28.0 | 31.5 | 30.2 | 27.5 | 20.8 | 11.7 | 6.5 | 0.2 | | | | |
| | $\Sigma$ Qm | | | | | 9 | 136 | 406 | 666 | 868 | 977 | 936 | 852 | 645 | 363 | 202 | 6 | | | | |
| November | $\Sigma$ So' | | | | | | | 0.8 | 4.8 | 9.5 | 12.5 | 10.6 | 8.1 | 4.1 | 1.0 | | | | | | |
| | $\Sigma$ Do | | | | | | 0.1 | 1.2 | 2.0 | 2.7 | 3.0 | 2.9 | 2.4 | 1.6 | 0.5 | | | | | | |
| | $\Sigma$ Qc | | | | | | 0.1 | 2.0 | 6.8 | 12.2 | 15.5 | 13.5 | 10.5 | 5.7 | 1.5 | | | | | | |
| | $\Sigma$ Qm | | | | | | 3 | 60 | 204 | 366 | 465 | 405 | 315 | 171 | 45 | | | | | | |
| December | $\Sigma$ So' | | | | | | | | 0.6 | 3.6 | 5.6 | 5.4 | 3.2 | 0.2 | | | | | | | |
| | $\Sigma$ Do | | | | | | | 0.1 | 1.1 | 2.1 | 2.5 | 2.5 | 2.1 | 1.1 | 0.1 | | | | | | |
| | $\Sigma$ Qc | | | | | | | 0.1 | 1.7 | 5.7 | 8.1 | 7.9 | 5.3 | 1.3 | 0.1 | | | | | | |
| | $\Sigma$ Qm | | | | | | | 3 | 53 | 177 | 254 | 245 | 164 | 40 | 3 | | | | | | |

Declassified in Part - Sanitized Copy Approved for Release 2012/03/12 : CIA-RDP82-00039R000100190014-6

Declassified in Part - Sanitized Copy Approved for Release 2012/03/12 : CIA-RDP82-00039R000100190014-6

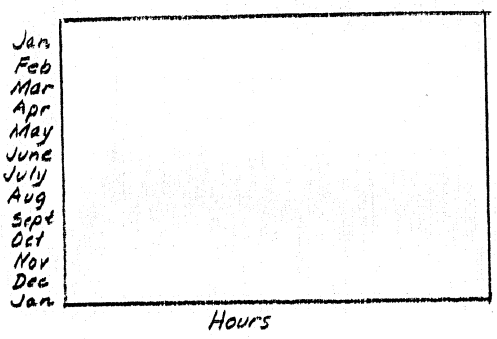


FIGURE 1. ISOPLETHS OF THE HOURLY TOTALS OF TOTAL RADIATION WITH A CLOUDLESS SKY

Total Radiation Under Natural Conditions

As has been already stated, the ten-year period of actinograph and pyranograph operation, 1931-1940 inclusive, was selected for study of total radiation. Since the instrument readings had been immediately tabulated in the course of the routine work, and the records for each month have been processed by the middle of the following month, tables of the hourly totals of solar and diffuse radiation were available. The simple computation of the ten-year mean values of the hourly totals of solar and diffuse radiation, and thus also of total radiation under natural conditions, was rendered possible by this, using the existing annual tables for this purpose. Table III contains these values. Each month has three lines; the first one, designated by $\Sigma S'$, shows the incoming heat of solar radiation falling on a horizontal surface, during each hourly interval; the second line -- $\Sigma D$ -- shows the diffuse



Declassified in Part - Sanitized Copy Approved for Release 2012/03/12 : CIA-RDP82-00039R000100190014-6

Declassified in Part - Sanitized Copy Approved for Release 2012/03/12 : CIA-RDP82-00039R000100190014-6

sky radiation; and the third -- $\Sigma Q$ -- shows total incoming radiation as the sum of the first two. Table III is thus of analogous structure to Table II.

In order to construct isopleths of the hourly total heats of total radiation under natural conditions, auxiliary graphs (Figures 2a and 2b) were first plotted, on which were entered the diurnal cycle of the hourly totals for each month. As will be seen, ten years of observations have made it possible to draw curves which are perfectly smooth, except for a single month -- June -- in which there is a slight unevenness in the progress of the curve for the interval between 1000 and 1500 hours.

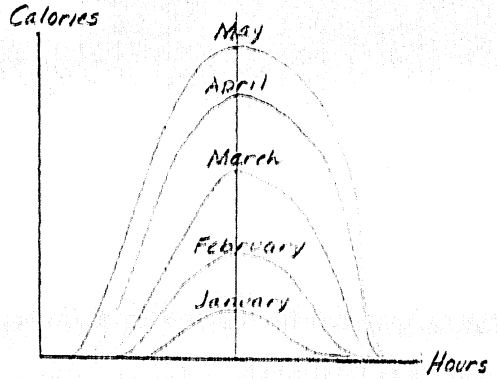


FIGURE 2A. DIURNAL CYCLE OF HOURLY TOTALS OF TOTAL RADIATION UNDER NATURAL CONDITIONS, JANUARY TO MAY.

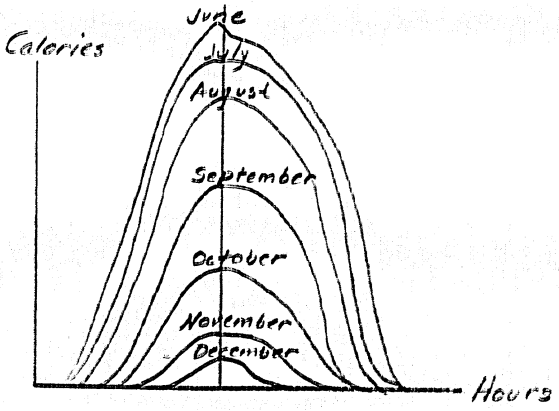




Declassified in Part - Sanitized Copy Approved for Release 2012/03/12 : CIA-RDP82-00039R000100190014-6

Declassified in Part - Sanitized Copy Approved for Release 2012/03/12 : CIA-RDP82-00039R000100190014-6

FIGURE 2B. DIURNAL CYCLE OF HOURLY TOTALS OF TOTAL RADIATION UNDER NATURAL CONDITIONS, JUNE TO DECEMBER.

The isopleths presented in Figure 3 are constructed according to the curves of Figures 2a and 2b. The figures on each isopleth show the incoming heat of total radiation in hundreds of calories at hourly intervals.

[See next page for table.]

It will be noted that the positions of the isopleths with respect to the midday line are entirely symmetric, except for May, June, and July, during which a slight increase in incoming radiation is observed in the morning hours close to noon, which is apparently explained by the influence of cloudiness; this will be elucidated in the near future.

As for symmetry with respect to the line of the summer solstice AB, here a slight increase in the amount of incoming radiation is observed in the first half of the year as compared with the second half, which increase is particularly marked during the hours around noon.

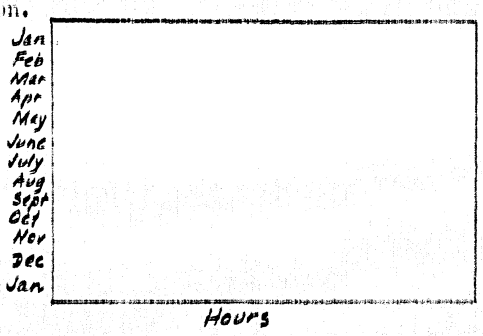


FIGURE 3. ISOPLETHS OF THE HOURLY TOTALS OF TOTAL RADIATION UNDER NATURAL CONDITIONS.



Declassified in Part - Sanitized Copy Approved for Release 2012/03/12 : CIA-RDP82-00039R000100190014-6

Declassified in Part - Sanitized Copy Approved for Release 2012/03/12 : CIA-RDP82-00039R000100190014-6



MEAN MONTHLY HOURLY AMOUNTS OF SOLAR, DIFFUSE, AND TOTAL RADIATION UNDER NATURAL CONDITIONS, IN CALORIES

Table 3.

| MONTHS | | HOURS | | | | | | | | | | | | | | | | | | |
|---|---|---|---|---|---|---|---|---|---|---|---|---|---|---|---|---|---|---|---|---|
| | | (1) | (2) | (3) | (4) | (5) | (6) | (7) | (8) | (9) | (10) | (11) | (12) | (13) | (14) | (15) | (16) | (17) | (18) | (19) | (20) |
| | | 2-3 | 3-4 | 4-5 | 5-6 | 6-7 | 7-8 | 8-9 | 9-10 | 10-11 | 11-12 | 12-13 | 13-14 | 14-15 | 15-16 | 16-17 | 17-18 | 18-19 | 19-20 | 20-21 | 21-22 |
| January | $\Sigma S'$ | | | | | | | 0.5 | 9 | 25 | 43 | 42 | 28 | 10 | 0.4 | | | | | | |
| | $\Sigma D$ | | | | | | 0.1 | 13 | 56 | 107 | 134 | 134 | 98 | 52 | 10 | 0.1 | | | | | |
| | $\Sigma Q$ | | | | | | | 14 | 65 | 133 | 177 | 175 | 126 | 62 | 10 | | | | | | |
| February | $\Sigma S'$ | | | | | | 7 | 23 | 62 | 114 | 130 | 128 | 118 | 74 | 29 | 2 | | | | | |
| | $\Sigma D$ | | | | | 1 | 20 | 84 | 164 | 226 | 256 | 249 | 223 | 154 | 77 | 16 | | | | | |
| | $\Sigma Q$ | | | | | 1 | 22 | 107 | 226 | 310 | 386 | 377 | 341 | 228 | 106 | 18 | | | | | |
| March | $\Sigma S'$ | | | | 0.3 | 10 | 59 | 147 | 244 | 325 | 358 | 364 | 335 | 270 | 168 | 72 | 11 | 0.3 | | | |
| | $\Sigma D$ | | | | 3 | 44 | 137 | 236 | 319 | 379 | 409 | 396 | 358 | 297 | 216 | 126 | 38 | 3 | | | |
| | $\Sigma Q$ | | | | 3 | 54 | 196 | 383 | 563 | 704 | 767 | 760 | 693 | 567 | 384 | 198 | 49 | 3 | | | |
| April | $\Sigma S'$ | | | 1 | 24 | 111 | 228 | 334 | 477 | 549 | 567 | 567 | 512 | 438 | 316 | 227 | 108 | 34 | 1 | | |
| | $\Sigma D$ | | | 10 | 65 | 148 | 231 | 307 | 356 | 410 | 426 | 433 | 406 | 356 | 306 | 221 | 110 | 58 | 8 | | |
| | $\Sigma Q$ | | | 11 | 89 | 259 | 459 | 641 | 833 | 959 | 993 | 1000 | 918 | 794 | 652 | 448 | 248 | 92 | 9 | | |

Declassified in Part - Sanitized Copy Approved for Release 2012/03/12 : CIA-RDP82-00039R000100190014-6

Declassified in Part - Sanitized Copy Approved for Release 2012/03/12 : CIA-RDP82-00039R000100190014-6



| | | (1) | (2) | (3) | (4) | (5) | (6) | (7) | (8) | (9) | (10) | (11) | (12) | (13) | (14) | (15) | (16) | (17) | (18) | (19) | (20) |
|---|---|---|---|---|---|---|---|---|---|---|---|---|---|---|---|---|---|---|---|---|---|
| May | $\Sigma S'$ | | 2 | 37 | 118 | 296 | 476 | 616 | 761 | 828 | 892 | 873 | 814 | 711 | 590 | 435 | 282 | 134 | 35 | 1 | |
| | $\Sigma D$ | | 14 | 70 | 144 | 224 | 293 | 364 | 413 | 444 | 460 | 464 | 443 | 429 | 355 | 293 | 219 | 144 | 67 | 11 | |
| | $\Sigma Q$ | | 16 | 107 | 292 | 520 | 769 | 980 | 1194 | 1272 | 1352 | 1337 | 1257 | 1140 | 945 | 728 | 501 | 278 | 102 | 12 | |
| June | $\Sigma S'$ | | 14 | 98 | 231 | 397 | 584 | 742 | 863 | 890 | 895 | 818 | 793 | 752 | 628 | 512 | 373 | 215 | 94 | 9 | |
| | $\Sigma D$ | 4 | 44 | 109 | 170 | 230 | 294 | 347 | 389 | 454 | 472 | 473 | 449 | 425 | 367 | 316 | 249 | 179 | 109 | 44 | 3 |
| | $\Sigma Q$ | 4 | 58 | 207 | 401 | 627 | 878 | 1089 | 1252 | 1344 | 1367 | 1321 | 1282 | 1177 | 995 | 828 | 622 | 394 | 203 | 53 | 3 |
| July | $\Sigma S'$ | | 6 | 53 | 140 | 315 | 462 | 610 | 739 | 822 | 843 | 792 | 719 | 636 | 523 | 424 | 298 | 160 | 57 | 3 | |
| | $\Sigma D$ | 1 | 28 | 94 | 172 | 250 | 315 | 372 | 434 | 477 | 473 | 479 | 457 | 420 | 358 | 296 | 236 | 170 | 89 | 24 | 1 |
| | $\Sigma Q$ | 1 | 34 | 147 | 332 | 565 | 797 | 1012 | 1173 | 1299 | 1316 | 1271 | 1206 | 1056 | 881 | 720 | 534 | 330 | 146 | 27 | 1 |
| August | $\Sigma S'$ | | | 7 | 62 | 252 | 359 | 520 | 629 | 722 | 728 | 698 | 639 | 538 | 435 | 317 | 190 | 64 | 6 | | |
| | $\Sigma D$ | | 2 | 38 | 118 | 201 | 280 | 343 | 381 | 424 | 445 | 441 | 420 | 389 | 331 | 261 | 188 | 106 | 33 | 2 | |
| | $\Sigma Q$ | | 2 | 45 | 180 | 453 | 639 | 863 | 1013 | 1146 | 1173 | 1139 | 1059 | 927 | 766 | 578 | 378 | 170 | 39 | 2 | |

Declassified in Part - Sanitized Copy Approved for Release 2012/03/12 : CIA-RDP82-00039R000100190014-6

Declassified in Part - Sanitized Copy Approved for Release 2012/03/12 : CIA-RDP82-00039R000100190014-6

| | | (1) | (2) | (3) | (4) | (5) | (6) | (7) | (8) | (9) | (10) | (11) | (12) | (13) | (14) | (15) | (16) | (17) | (18) | (19) | (20) |
|---|---|---|---|---|---|---|---|---|---|---|---|---|---|---|---|---|---|---|---|---|---|
| September | $\Sigma$ S' | | | | 2 | 30 | 109 | 222 | 324 | 397 | 442 | 439 | 389 | 312 | 218 | 110 | 33 | 2 | | | |
| | $\Sigma$ D | | | | 18 | 84 | 168 | 245 | 309 | 355 | 364 | 353 | 339 | 284 | 221 | 146 | 70 | 13 | | | |
| | $\Sigma$ Q | | | | 20 | 114 | 277 | 467 | 629 | 752 | 806 | 792 | 728 | 596 | 439 | 256 | 103 | 15 | | | |
| October | $\Sigma$ S' | | | | | 0.4 | 12 | 52 | 94 | 141 | 172 | 173 | 154 | 112 | 60 | 5 | 0.1 | | | | |
| | $\Sigma$ D | | | | | 5 | 43 | 106 | 168 | 214 | 231 | 222 | 192 | 152 | 96 | 36 | 4 | | | | |
| | $\Sigma$ Q | | | | | 5 | 55 | 158 | 262 | 355 | 403 | 395 | 346 | 264 | 156 | 51 | 4 | | | | |
| November | $\Sigma$ S' | | | | | | | 1 | 12 | 31 | 42 | 44 | 33 | 14 | 2 | | | | | | |
| | $\Sigma$ D | | | | | | 2 | 20 | 58 | 97 | 118 | 115 | 91 | 56 | 16 | | | | | | |
| | $\Sigma$ Q | | | | | | 2 | 21 | 70 | 128 | 160 | 159 | 124 | 70 | 18 | | | | | | |
| December | $\Sigma$ S' | | | | | | | | 2 | 12 | 21 | 23 | 14 | 2 | | | | | | | |
| | $\Sigma$ D | | | | | | | 2 | 26 | 61 | 88 | 89 | 64 | 25 | 2 | | | | | | |
| | $\Sigma$ Q | | | | | | | 2 | 28 | 73 | 109 | 112 | 78 | 27 | 2 | | | | | | |



Declassified in Part - Sanitized Copy Approved for Release 2012/03/12 : CIA-RDP82-00039R000100190014-6

Declassified in Part - Sanitized Copy Approved for Release 2012/03/12 : CIA-RDP82-00039R000100190014-6

If the values for total radiation given in the last line for every month in Table III, are divided by the number of days in a month and the quotient then divided by 60 (the number of minutes in an hour), we obtain the mean intensity of total radiation at the midpoint of each hourly interval. The values so obtained are shown in Table IV.

[See next page for table.]

The maximum value, 0.76 calory, occurs during the interval 1100-1200 hours in June. The minimum noon value in the annual cycle falls in December.

Curves of the diurnal cycle of the intensity of total radiation for each month were plotted from the values of Table IV. The curves so obtained are presented in Figures 4a and 4b.

Table IV and Figures 4a and 4b were then used to construct the isopleths of intensity of total radiation shown in Figure 5.

It is entirely natural that the form of these isopleths should be analogous to those in Figure 3. The figures on the isopleths of Figure 5 indicate hundredths of a calory.

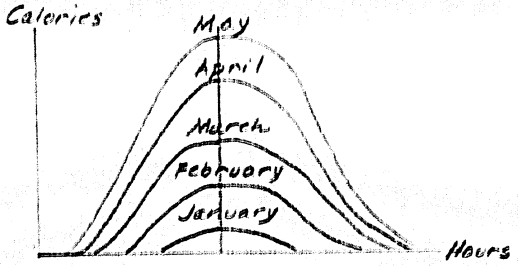


FIGURE 4A. DIURNAL CYCLE OF THE INTENSITY OF TOTAL RADIATION UNDER NATURAL CONDITIONS, JANUARY TO MAY.



Declassified in Part - Sanitized Copy Approved for Release 2012/03/12 : CIA-RDP82-00039R000100190014-6

Declassified in Part - Sanitized Copy Approved for Release 2012/03/12 : CIA-RDP82-00039R000100190014-6

MEAN INTENSITY OF TOTAL RADIATION Q AT THE MIDPOINTS OF HOURLY INTERVALS, 1931-1940, IN CALORIES

Table 4.

| MONTHS | Hours (1) 2-3 | (2) 3-4 | (3) 4-5 | (4) 5-6 | (5) 6-7 | (6) 7-8 | (7) 8-9 | (8) 9-10 | (9) 10-11 | (10) 11-12 | (11) 12-13 | (12) 13-14 | (13) 14-15 | (14) 15-16 | (15) 16-17 | (16) 17-18 | (17) 18-19 | (18) 19-20 | (19) 20-21 | (20) 21-22 |
|---|---|---|---|---|---|---|---|---|---|---|---|---|---|---|---|---|---|---|---|---|
| January | | | | | | | 0.00 | 0.03 | 0.07 | 0.09 | 0.09 | 0.07 | 0.03 | 0.00 | | | | | | |
| February | | | | | 0.00 | 0.01 | 0.04 | 0.13 | 0.20 | 0.23 | 0.22 | 0.20 | 0.14 | 0.06 | 0.01 | 0.00 | | | | |
| March | | | | 0.00 | 0.03 | 0.10 | 0.21 | 0.30 | 0.38 | 0.41 | 0.41 | 0.37 | 0.31 | 0.21 | 0.11 | 0.03 | 0.00 | | | |
| April | | | 0.00 | 0.05 | 0.14 | 0.26 | 0.36 | 0.46 | 0.53 | 0.55 | 0.56 | 0.51 | 0.44 | 0.36 | 0.25 | 0.14 | 0.05 | 0.00 | | |
| May | | 0.00 | 0.06 | 0.16 | 0.28 | 0.41 | 0.52 | 0.61 | 0.68 | 0.73 | 0.72 | 0.68 | 0.61 | 0.51 | 0.39 | 0.27 | 0.15 | 0.05 | 0.00 | |
| June | 0.00 | 0.03 | 0.11 | 0.22 | 0.35 | 0.49 | 0.61 | 0.70 | 0.75 | 0.76 | 0.73 | 0.69 | 0.63 | 0.55 | 0.46 | 0.35 | 0.22 | 0.11 | 0.03 | 0.00 |
| July | 0.00 | 0.02 | 0.08 | 0.18 | 0.30 | 0.43 | 0.54 | 0.63 | 0.70 | 0.71 | 0.68 | 0.64 | 0.57 | 0.47 | 0.39 | 0.29 | 0.18 | 0.08 | 0.01 | 0.00 |
| August | | 0.00 | 0.02 | 0.10 | 0.24 | 0.34 | 0.46 | 0.55 | 0.62 | 0.65 | 0.61 | 0.57 | 0.50 | 0.41 | 0.31 | 0.20 | 0.09 | 0.02 | 0.00 | |
| September | | | 0.00 | 0.01 | 0.08 | 0.19 | 0.26 | 0.35 | 0.42 | 0.45 | 0.44 | 0.40 | 0.33 | 0.24 | 0.14 | 0.06 | 0.01 | 0.00 | | |
| October | | | | 0.00 | 0.03 | 0.09 | 0.14 | 0.19 | 0.22 | 0.21 | 0.19 | 0.14 | 0.08 | 0.03 | 0.00 | | | | | |
| November | | | | | 0.00 | 0.01 | 0.04 | 0.07 | 0.09 | 0.09 | 0.07 | 0.04 | 0.01 | 0.00 | | | | | | |
| December | | | | | | 0.00 | 0.02 | 0.04 | 0.06 | 0.06 | 0.04 | 0.02 | 0.00 | | | | | | | |

Declassified in Part - Sanitized Copy Approved for Release 2012/03/12 : CIA-RDP82-00039R000100190014-6

Declassified in Part - Sanitized Copy Approved for Release 2012/03/12 : CIA-RDP82-00039R000100190014-6

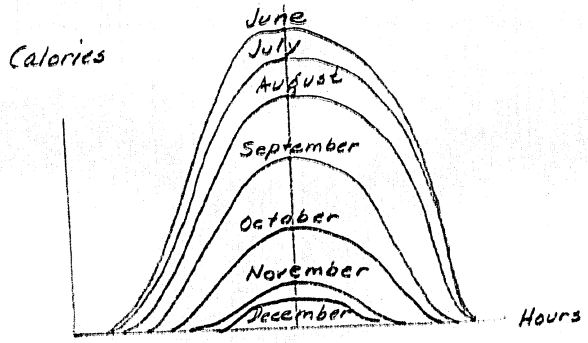


FIGURE 1b. DIURNAL CYCLE OF THE INTENSITY OF TOTAL RADIATION UNDER NATURAL CONDITIONS, JUNE TO DECEMBER.

See [redacted] page 314 for table.

Now that we have the data on the incoming total radiation under natural conditions as well as with a cloudless sky, the extent to which the theoretical influx of radiation is disturbed by conditions of cloudiness may now be elucidated. This may be seen from Table V.

The values for $\sum Q_0$ and $\sum Q$ are rounded out to the nearest 10 calories in Table V. The first hourly interval in the morning and the last one in the evening are excluded from consideration. This is done because accuracy of measurement at these times is low, and when values for hourly incoming radiation of the order of a few tens of calories are rounded out to even multiples of 10, arbitrary values sometimes result and enter the computations; consequently Table V shows that the ratio between these values



Declassified in Part - Sanitized Copy Approved for Release 2012/03/12 : CIA-RDP82-00039R000100190014-6

Declassified in Part - Sanitized Copy Approved for Release 2012/03/12 : CIA-RDP82-00039R000100190014-6

varies from 0.35 to 0.75, if values near the beginning and end of the day are not considered.

During the midday hours in the warm season about 70 percent of the possible influx of radiation with a cloudless sky is actually received, while 50 percent is received in the cold season.

From the last line for each month in Table V it may be noted that, as compared to the amount of total incoming radiation possible with a cloudless sky, the months fall into three groups with respect to total influx of radiation under natural conditions. The first group, in which the amount is more than 60 percent of possible maximum, includes March, April, May, June, July, August, and September, with a mean value of 65 percent for these months. The third group, with amount under 50 percent, includes October, November, December, and January, with a mean value of 42 percent. The second group, intermediate between these two, is made up only of February, with 54 percent. We have already pointed out that the isopleths of total radiation are distributed in highly symmetrical fashion with respect to the annual cycle, but nevertheless a slight predominance of the forenoon totals over the afternoon totals is discernible in all months except December. This may be seen from Table VI, which presents a computation for all months of the values of the forenoon totals (a) and the afternoon totals (p) for hourly intervals symmetrically located around the moment of noon, and also computed on an annual basis. The table also gives the ratio ($\Delta$) of the forenoon values to the afternoon values.



Declassified in Part - Sanitized Copy Approved for Release 2012/03/12 : CIA-RDP82-00039R000100190014-6

Declassified in Part - Sanitized Copy Approved for Release 2012/03/12 : CIA-RDP82-00039R000100190014-6

[See next page for tables.]

The final column of Table VI shows that the maximum difference in favor of the forenoon values occurs in August, where it amounts to 9 percent. In December the forenoon radiation is 3 percent less than that in the afternoon. In the annual mean for Pavlovsk the difference is 5 percent in favor of the forenoon radiation.

## TOTAL RADIATION AND CLOUDINESS

Cloudiness is the fundamental factor which affects the value of total radiation. It may either operate to increase it, or, what is predominantly significant, to decrease it; for this influence is very manifold, depending on amount and type of the clouds, their position in the arch of the sky and on the altitude of the sun above the horizon. For the purpose of studying the role of cloudiness, we worked up the observations of amount and type of clouds made at the grounds of the Meteorological Observatory only a few hundred meters from the site of the actinometric observations.

These cloud observations were first commenced at the Observatory on the initiative of Ye. Ye. Fedorov in 1922, and con-



Declassified in Part - Sanitized Copy Approved for Release 2012/03/12 : CIA-RDP82-00039R000100190014-6

Declassified in Part - Sanitized Copy Approved for Release 2012/03/12 : CIA-RDP82-00039R000100190014-6

MEAN ANNUAL AMOUNTS OF HEAT OF TOTAL RADIATION: [illegible] ($\Sigma Q_0$), AND [illegible] ($\Sigma Q$); IN CALORIES; AND THE RATIO ($\Delta$) OF THE FORMER ($\Sigma Q_0$) TO THE LATTER ($\Sigma Q$)

Table 5.

| MONTHS | HOURS | | | | | | | | | | | | | | | | | | | |
|---|---|---|---|---|---|---|---|---|---|---|---|---|---|---|---|---|---|---|---|---|
| | (1) 2-3 | (2) 3-4 | (3) 4-5 | (4) 5-6 | (5) 6-7 | (6) 7-8 | (7) 8-9 | (8) 9-10 | (9) 10-11 | (10) 11-12 | (11) 12-13 | (12) 13-14 | (13) 14-15 | (14) 15-16 | (15) 16-17 | (16) 17-18 | (17) 18-19 | (18) 19-20 | (19) 20-21 | (20) 21-22 |
| January | $\Sigma Q_0$ | | | | | | | 190 | 300 | 350 | 370 | 280 | 130 | | | | | | | |
| | $\Sigma Q$ | | | | | | | 40 | 130 | 180 | 180 | 130 | 60 | | | | | | | |
| | $\Delta$ | | | | | | | 0.40 | 0.43 | 0.47 | 0.49 | 0.46 | 0.46 | | | | | | | |
| February | $\Sigma Q_0$ | | | | | | 200 | 110 | 420 | 710 | 690 | 650 | 420 | 200 | | | | | | |
| | $\Sigma Q$ | | | | | | 110 | 230 | 340 | 390 | 380 | 340 | 230 | 110 | | | | | | |
| | $\Delta$ | | | | | | 0.55 | 0.42 | 0.35 | 0.55 | 0.55 | 0.52 | 0.55 | 0.55 | | | | | | |
| March | $\Sigma Q_0$ | | | | | 290 | 590 | 680 | 1080 | 1190 | 1160 | 1040 | 810 | 510 | 210 | | | | | |
| | $\Sigma Q$ | | | | | 200 | 380 | 540 | 700 | 770 | 760 | 690 | 570 | 380 | 200 | | | | | |
| | $\Delta$ | | | | | 0.69 | 0.61 | 0.61 | 0.65 | 0.65 | 0.66 | 0.66 | 0.68 | 0.70 | 0.95 | | | | | |
| April | $\Sigma Q_0$ | 110 | 110 | 760 | 1100 | 1570 | 1.50 | 1410 | 1190 | 1190 | 1270 | 990 | 480 | 360 | 110 | | | | | |
| | $\Sigma Q$ | 90 | 260 | 460 | 619 | 830 | 960 | 990 | 1000 | 920 | 790 | 650 | 450 | 250 | 90 | | | | | |
| | $\Delta$ | 0.64 | 0.43 | 0.61 | 0.58 | 0.63 | 0.62 | 0.60 | 0.63 | 0.62 | 0.62 | 0.66 | 0.66 | 0.69 | 0.82 | | | | | |



Declassified in Part - Sanitized Copy Approved for Release 2012/03/12 : CIA-RDP82-00039R000100190014-6

Declassified in Part - Sanitized Copy Approved for Release 2012/03/12 : CIA-RDP82-00039R000100190014-6



| | | (1) | (2) | (3) | (4) | (5) | (6) | (7) | (8) | (9) | (10) | (11) | (12) | (13) | (14) | (15) | (16) | (17) | (18) | (19) | (20) |
|---|---|---|---|---|---|---|---|---|---|---|---|---|---|---|---|---|---|---|---|---|---|
| May | $\Sigma Q_o$ | | | 200 | 510 | 850 | 1190 | 1510 | 1770 | 1960 | 2040 | 2000 | 1900 | 1710 | 1480 | 1160 | 820 | 500 | 190 | |
| | $\Sigma Q$ | | | 110 | 290 | 520 | 770 | 960 | 1190 | 1270 | 1350 | 1340 | 1260 | 1110 | 950 | 730 | 500 | 280 | 100 | |
| | $\Delta$ | | | 0.55 | 0.57 | 0.61 | 0.65 | 0.45 | 0.67 | 0.65 | 0.66 | 0.67 | 0.66 | 0.67 | 0.64 | 0.63 | 0.61 | 0.56 | 0.53 | |
| June | $\Sigma Q_o$ | | | 270 | 550 | 870 | 1190 | 1500 | 1750 | 1660 | 1970 | 2600 | 1920 | 1750 | 1480 | 1190 | 880 | 560 | 260 | |
| | $\Sigma Q$ | | | 210 | 400 | 630 | 880 | 1090 | 1250 | 1210 | 1370 | 1320 | 1240 | 1180 | 1000 | 830 | 620 | 390 | 200 | |
| | $\Delta$ | | | 0.78 | 0.73 | 0.73 | 0.74 | 0.73 | 0.71 | 0.72 | 0.69 | 0.66 | 0.65 | 0.67 | 0.68 | 0.70 | 0.71 | 0.70 | 0.77 | |
| July | $\Sigma Q_o$ | | | 200 | 470 | 820 | 1170 | 1460 | 1720 | 1900 | 2050 | 2080 | 2020 | 1840 | 1560 | 1220 | 870 | 530 | 240 | |
| | $\Sigma Q$ | | | 150 | 330 | 560 | 800 | 1010 | 1170 | 1300 | 1320 | 1270 | 1210 | 1060 | 880 | 720 | 530 | 330 | 150 | |
| | $\Delta$ | | | 0.75 | 0.70 | 0.68 | 0.68 | 0.69 | 0.68 | 0.68 | 0.65 | 0.61 | 0.60 | 0.58 | 0.54 | 0.59 | 0.61 | 0.62 | 0.63 | |
| August | $\Sigma Q_o$ | | | | 230 | 510 | 850 | 1190 | 1390 | 1560 | 1710 | 1760 | 1730 | 1560 | 1290 | 940 | 610 | 260 | | |
| | $\Sigma Q$ | | | | 180 | 450 | 640 | 860 | 1010 | 1150 | 1170 | 1110 | 1060 | 930 | 770 | 580 | 380 | 170 | | |
| | $\Delta$ | | | | 0.78 | 0.83 | 0.75 | 0.72 | 0.73 | 0.73 | 0.68 | 0.65 | 0.61 | 0.60 | 0.60 | 0.62 | 0.62 | 0.65 | | |

Declassified in Part - Sanitized Copy Approved for Release 2012/03/12 : CIA-RDP82-00039R000100190014-6

Declassified in Part - Sanitized Copy Approved for Release 2012/03/12 : CIA-RDP82-00039R000100190014-6



| | | (1) | (2) | (3) | (4) | (5) | (6) | (7) | (8) | (9) | (10) | (11) | (12) | (13) | (14) | (15) | (16) | (17) | (18) | (19) |
|---|---|---|---|---|---|---|---|---|---|---|---|---|---|---|---|---|---|---|---|---|
| September | $\Sigma Q_o$ | | | | | | 140 | 140 | 790 | 1030 | 1300 | 1320 | 1300 | 1170 | 1000 | 720 | 400 | 120 | | |
| | $\Sigma Q$ | | | | | | 110 | 280 | 470 | 630 | 750 | 810 | 790 | 730 | 600 | 440 | 260 | 100 | | |
| | $\Delta$ | | | | | | 0.69 | 0.61 | 0.59 | 0.61 | 0.58 | 0.61 | 0.61 | 0.62 | 0.60 | 0.61 | 0.65 | 0.83 | | |
| October | $\Sigma Q_o$ | | | | | | | 110 | 110 | 670 | 870 | 980 | 940 | 850 | 610 | 360 | 200 | | | |
| | $\Sigma Q$ | | | | | | | 60 | 160 | 260 | 360 | 400 | 400 | 350 | 260 | 160 | 50 | | | |
| | $\Delta$ | | | | | | | 0.43 | 0.39 | 0.39 | 0.41 | 0.41 | 0.43 | 0.41 | 0.41 | 0.44 | 0.25 | | | |
| November | $\Sigma Q_o$ | | | | | | | | | 200 | 370 | 460 | 400 | 320 | 170 | | | | | |
| | $\Sigma Q$ | | | | | | | | | 70 | 130 | 160 | 160 | 120 | 70 | | | | | |
| | $\Delta$ | | | | | | | | | 0.35 | 0.35 | 0.35 | 0.40 | 0.38 | 0.41 | | | | | |
| December | $\Sigma Q_o$ | | | | | | | | | | 180 | 250 | 210 | 160 | | | | | | |
| | $\Sigma Q$ | | | | | | | | | | 70 | 110 | 110 | 80 | | | | | | |
| | $\Delta$ | | | | | | | | | | 0.39 | 0.44 | 0.46 | 0.50 | | | | | | |

Declassified in Part - Sanitized Copy Approved for Release 2012/03/12 : CIA-RDP82-00039R000100190014-6

Declassified in Part - Sanitized Copy Approved for Release 2012/03/12 : CIA-RDP82-00039R000100190014-6



RELATION BETWEEN VALUES OF TOTAL RADIATION DURING FORENOON AND AFTERNOON HOURS

Table 6.

| MONTHS | | HOURS (1) 11-12 12-13 | (2) 10-11 13-14 | (3) 9-10 14-15 | (4) 8-9 15-16 | (5) 7-8 16-17 | (6) 6-7 17-18 | (7) 5-6 18-19 | (8) 4-5 19-20 | (9) TOTAL |
|---|---|---|---|---|---|---|---|---|---|---|
| January | a | 180 | 130 | 60 | | | | | | 370 |
| | p | 180 | 130 | 60 | | | | | | 370 |
| | Δ | 1.00 | 1.00 | 1.00 | | | | | | 1.00 |
| February | a | 390 | 340 | 230 | 110 | | | | | 1070 |
| | p | 380 | 340 | 230 | 110 | | | | | 1060 |
| | Δ | 1.03 | 1.00 | 1.00 | 1.00 | | | | | 1.03 |
| March | a | 770 | 700 | 540 | 380 | 200 | | | | 2610 |
| | p | 760 | 690 | 570 | 380 | 200 | | | | 2600 |
| | Δ | 1.01 | 1.01 | 0.98 | 1.00 | 1.00 | | | | 1.00 |
| April | a | 990 | 960 | 830 | 610 | 460 | 260 | 90 | | 4230 |
| | p | 1000 | 920 | 790 | 640 | 450 | 250 | 90 | | 4150 |
| | Δ | 0.99 | 1.04 | 1.05 | 0.98 | 1.02 | 1.04 | 1.00 | | 1.02 |

Declassified in Part - Sanitized Copy Approved for Release 2012/03/12 : CIA-RDP82-00039R000100190014-6

Declassified in Part - Sanitized Copy Approved for Release 2012/03/12 : CIA-RDP82-00039R000100190014-6

| | | (1) | (2) | (3) | (4) | (5) | (6) | (7) | (8) | (9) |
|---|---|---|---|---|---|---|---|---|---|---|
| May | a | 1250 | 1270 | 1190 | 980 | 770 | 520 | 290 | 110 | 6480 |
| | p | 1240 | 1260 | 1110 | 950 | 730 | 500 | 280 | 100 | 6300 |
| | Δ | 1.01 | 1.01 | 1.04 | 1.03 | 1.06 | 1.04 | 1.04 | 1.10 | 1.03 |
| June | a | 1370 | 1340 | 1250 | 1090 | 880 | 630 | 400 | 210 | 7170 |
| | p | 1320 | 1210 | 1150 | 1000 | 830 | 620 | 390 | 200 | 6780 |
| | Δ | 1.04 | 1.06 | 1.06 | 1.09 | 1.06 | 1.02 | 1.03 | 1.05 | 1.06 |
| July | a | 1320 | 1300 | 1170 | 1010 | 800 | 560 | 330 | 150 | 6640 |
| | p | 1270 | 1210 | 1060 | 880 | 720 | 530 | 330 | 150 | 6150 |
| | Δ | 1.04 | 1.07 | 1.10 | 1.15 | 1.11 | 1.06 | 1.00 | 1.00 | 1.08 |
| August | a | 1170 | 1150 | 1010 | 860 | 610 | 450 | 180 | | 5460 |
| | p | 1110 | 1060 | 930 | 770 | 580 | 380 | 170 | | 5030 |
| | Δ | 1.03 | 1.08 | 1.07 | 1.12 | 1.10 | 1.18 | 1.06 | | 1.09 |

-5/6-

Declassified in Part - Sanitized Copy Approved for Release 2012/03/12 : CIA-RDP82-00039R000100190014-6

Declassified in Part - Sanitized Copy Approved for Release 2012/03/12 : CIA-RDP82-00039R000100190014-6

| | | (1) | (2) | (3) | (4) | (5) | (6) | (7) | (8) | (9) |
|---|---|---|---|---|---|---|---|---|---|---|
| September | a | 810 | 750 | 630 | 170 | 280 | 110 | | | 3050 |
| | p | 790 | 730 | 600 | 110 | 260 | 100 | | | 2920 |
| | Δ | 1.03 | 1.03 | 1.05 | 1.07 | 1.08 | 1.10 | | | 1.04 |
| October | a | 100 | 360 | 280 | 160 | 60 | | | | 1240 |
| | p | 100 | 350 | 260 | 150 | 50 | | | | 1220 |
| | Δ | 1.00 | 1.03 | 1.08 | 1.00 | 1.20 | | | | 1.02 |
| November | a | 160 | 130 | 70 | | | | | | 360 |
| | p | 160 | 120 | 70 | | | | | | 350 |
| | Δ | 1.00 | 1.08 | 1.00 | | | | | | 1.03 |
| December | a | 110 | 70 | | | | | | | 180 |
| | p | 110 | 80 | | | | | | | 190 |
| | Δ | 1.00 | 0.85 | | | | | | | 0.95 |
| Year | | | | | | | | | | 38860 |
| | | | | | | | | | | 37120 |
| | | | | | | | | | | 1.05 |

-313-

Declassified in Part - Sanitized Copy Approved for Release 2012/03/12 : CIA-RDP82-00039R000100190014-6

Declassified in Part - Sanitized Copy Approved for Release 2012/03/12 : CIA-RDP82-00039R000100190014-6

sisted in hourly readings, which were uninterrupted until the end of August, 1941. The material from 1931 to 1940 was used for analysis, that is, for the same years covered by the actinometric data studied. During this period, the hourly cloudiness readings were made in various ways; in some years round the clock, while in other years they commenced only at 0500 or at 0700 hours.

Thus since cloudiness data were available from 0700 to 2200 hours for all the years, they were tabulated in juxtaposition to the radiation data for the study of the effect of cloudiness on the incoming total radiation.

The tabulation shows that there were 46,200 cloudiness readings made during the ten years, and since there were as many total radiation measurements during that period, the material was thus very comprehensive. Table VII was obtained by this processing of the cloud data.

In this table the mean monthly values of total and low-lying cloudiness are shown for each full hour from 0700 until the end of the day.

[See next page for table.]



Declassified in Part - Sanitized Copy Approved for Release 2012/03/12 : CIA-RDP82-00039R000100190014-6

Declassified in Part - Sanitized Copy Approved for Release 2012/03/12 : CIA-RDP82-00039R000100190014-6

TOTAL CLOUDINESS (T) AND LOW-LYING CLOUDINESS (L)

MONTHLY VALUES BY MONTHS

Table 7.

| MONTHS | | HOURS | | | | | | | | | | | | | | | |
|---|---|---|---|---|---|---|---|---|---|---|---|---|---|---|---|---|---|
| | | 7 | 8 | 9 | 10 | 11 | 12 | 13 | 14 | 15 | 16 | 17 | 18 | 19 | 20 | 21 | 22 |
| January | (T | - | 8.4 | 8.8 | 8.8 | 8.7 | 8.6 | 8.6 | 8.6 | 8.5 | 8.2 | | | | | | |
| | (L | - | 7.3 | 7.4 | 7.2 | 7.1 | 6.8 | 6.7 | 6.5 | 6.4 | 6.8 | | | | | | |
| February | (T | 8.0 | 8.3 | 8.2 | 8.3 | 8.1 | 8.0 | 8.0 | 7.8 | 8.0 | 7.9 | 7.7 | | | | | |
| | (L | 6.9 | 6.7 | 6.5 | 6.2 | 5.8 | 5.7 | 5.9 | 5.7 | 6.1 | 6.0 | 6.0 | | | | | |
| March | (T | 7.8 | 7.8 | 7.5 | 7.3 | 7.3 | 7.5 | 7.5 | 7.3 | 7.2 | 7.4 | 7.4 | 6.9 | | | | |
| | (L | 5.8 | 5.5 | 5.4 | 5.2 | 5.1 | 5.3 | 5.3 | 5.0 | 5.1 | 5.1 | 4.9 | 4.7 | | | | |
| April | (T | 7.2 | 7.0 | 6.9 | 7.0 | 7.1 | 7.1 | 7.2 | 7.3 | 7.1 | 6.9 | 6.9 | 7.0 | 6.7 | | | |
| | (L | 4.7 | 4.7 | 4.7 | 4.6 | 4.7 | 4.8 | 4.9 | 5.0 | 4.6 | 4.3 | 4.5 | 4.4 | 4.0 | | | |



Declassified in Part - Sanitized Copy Approved for Release 2012/03/12 : CIA-RDP82-00039R000100190014-6

Declassified in Part - Sanitized Copy Approved for Release 2012/03/12 : CIA-RDP82-00039R000100190014-6

HOURS

| MONTHS | | 7 | 8 | 9 | 10 | 11 | 12 | 13 | 14 | 15 | 16 | 17 | 18 | 19 | 20 | 21 | 22 |
|---|---|---|---|---|---|---|---|---|---|---|---|---|---|---|---|---|---|
| May | (T | 6.3 | 6.2 | 6.1 | 6.1 | 6.3 | 6.5 | 6.6 | 6.5 | 6.5 | 6.3 | 6.1 | 6.2 | 6.2 | 6.0 | | |
| | (L | 3.7 | 3.8 | 3.4 | 3.6 | 3.8 | 4.1 | 4.3 | 4.3 | 4.0 | 3.7 | 3.4 | 3.2 | 3.3 | 3.0 | | |
| June | (T | 5.4 | 5.5 | 5.6 | 5.8 | 6.4 | 6.7 | 6.9 | 6.4 | 6.3 | 6.2 | 6.3 | 6.0 | 5.9 | 5.8 | 5.4 | 5.2 |
| | (L | 2.9 | 3.1 | 3.2 | 3.5 | 4.1 | 4.6 | 5.0 | 4.4 | 4.2 | 3.9 | 3.4 | 2.7 | 2.6 | 2.6 | 2.3 | 2.7 |
| July | (T | 6.5 | 6.2 | 6.1 | 6.4 | 6.5 | 6.7 | 7.1 | 6.9 | 6.8 | 6.7 | 6.7 | 6.5 | 6.6 | 6.5 | 6.2 | 5.7 |
| | (L | 3.4 | 3.3 | 3.4 | 3.5 | 3.7 | 4.2 | 4.6 | 4.4 | 4.1 | 3.8 | 3.6 | 3.2 | 3.2 | 2.8 | 2.6 | 2.9 |
| August | (T | 6.3 | 6.1 | 6.0 | 6.2 | 6.3 | 6.4 | 6.6 | 6.4 | 6.6 | 6.3 | 6.2 | 6.2 | 6.3 | 5.8 | 5.2 | |
| | (L | 3.2 | 3.0 | 3.0 | 3.1 | 3.6 | 3.9 | 4.1 | 4.0 | 4.0 | 3.6 | 3.4 | 3.0 | 3.1 | 2.9 | 2.8 | |



Declassified in Part - Sanitized Copy Approved for Release 2012/03/12 : CIA-RDP82-00039R000100190014-6

Declassified in Part - Sanitized Copy Approved for Release 2012/03/12 : CIA-RDP82-00039R000100190014-6



HOURS

| MONTHS | | 7 | 8 | 9 | 10 | 11 | 12 | 13 | 14 | 15 | 16 | 17 | 18 | 19 | 20 | 21 | 22 |
|---|---|---|---|---|---|---|---|---|---|---|---|---|---|---|---|---|---|
| September | (T | 7.3 | 7.2 | 7.2 | 7.2 | 7.4 | 7.1 | 7.4 | 7.1 | 7.3 | 7.4 | 7.1 | 7.1 | 6.6 | 5.8 | | |
| | ( | | | | | | | | | | | | | | | | |
| | (L | 5.0 | 5.0 | 4.8 | 5.0 | 5.0 | 5.1 | 5.3 | 5.0 | 5.2 | 4.8 | 4.3 | 4.2 | 4.3 | 4.1 | | |
| October | (T | 8.4 | 8.6 | 8.6 | 8.4 | 8.3 | 8.4 | 8.1 | 8.2 | 8.0 | 8.1 | 8.0 | 7.5 | | | | |
| | ( | | | | | | | | | | | | | | | | |
| | (L | 7.2 | 7.2 | 7.3 | 7.1 | 6.9 | 6.9 | 6.7 | 6.6 | 6.6 | 6.6 | 6.5 | 6.3 | | | | |
| November | (T | 9.0 | 9.1 | 9.1 | 9.1 | 8.9 | 8.8 | 8.9 | 8.9 | 9.0 | 8.8 | 8.4 | | | | | |
| | ( | | | | | | | | | | | | | | | | |
| | (L | 8.4 | 8.1 | 8.3 | 7.9 | 7.9 | 7.6 | 7.8 | 7.8 | 7.7 | 7.6 | 7.7 | | | | | |
| December | (T | - | 8.7 | 8.8 | 8.8 | 8.7 | 8.8 | 8.7 | 8.6 | 8.8 | 8.6 | | | | | | |
| | ( | | | | | | | | | | | | | | | | |
| | (L | - | 8.0 | 8.2 | 8.0 | 7.7 | 7.5 | 7.3 | 7.6 | 7.5 | 7.4 | | | | | | |

Declassified in Part - Sanitized Copy Approved for Release 2012/03/12 : CIA-RDP82-00039R000100190014-6

Declassified in Part - Sanitized Copy Approved for Release 2012/03/12 : CIA-RDP82-00039R000100190014-6

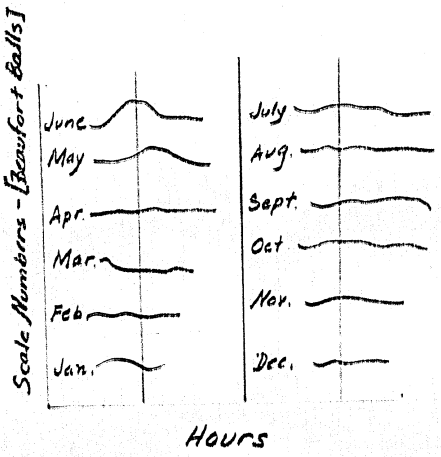


FIGURE 6. DIURNAL CYCLE OF TOTAL CLOUDINESS. TEN-YEAR MEAN VALUES.

From Table VII and also from Figures 6 and 7, it will be seen that under the climatic conditions at Pavlovsk the amplitude of the diurnal cycle of cloudiness is small during the daylight portion of the day which concerns us, especially for the low clouds (Figures 6 and 7). The lowest value of the latter occurs in December, with 0.2 ball, and its highest is in June, with 1.7 ball. Figure 7 shows the diurnal cycle of low-lying cloudiness to be most marked in May, June, July and August, with respective values of 1.5, 2.7, 2.0, and 1.3 balls.

This feebly expressed diurnal cycle of cloudiness explains the symmetrical course of the isopleths of intensity and totals of total radiation, which has already been pointed out. The variation of cloudiness during its annual cycle is shown in Table VIII, which has six lines, of which the two top lines respectively give the total and low-lying cloudiness at 0000 hours, the two middle



Declassified in Part - Sanitized Copy Approved for Release 2012/03/12 : CIA-RDP82-00039R000100190014-6

Declassified in Part - Sanitized Copy Approved for Release 2012/03/12 : CIA-RDP82-00039R000100190014-6

lines give the same data at noon, and the two bottom lines contain the values for 1600 hours; while Figure 8 shows the annual cycle of cloudiness at noon.

FIGURE 7. DIURNAL CYCLE OF LOW-LYING CLOUDINESS. TEN-YEAR MEAN VALUES.

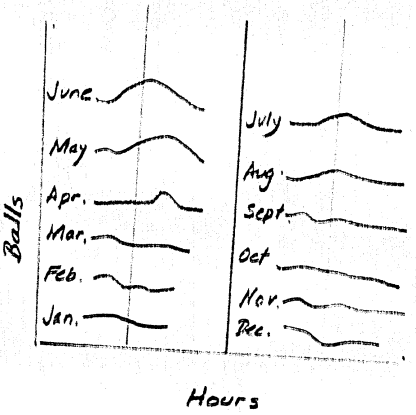


(See next page for Table VIII)

If we consider how cloudiness in its annual cycle varies with respect to June (when the sun is at maximum altitude) we see that the amount of cloudiness varies upwards and downwards in markedly symmetric fashion, which fact is also expressed in the symmetrical distribution of the isopleths of total radiation.

The effect of the altitude of the sun must be eliminated in order to study the influence of cloudiness alone -- amount and type -- on the total radiation; that is, the relationship between cloudiness and radiation must be studied with the sun at the same altitude.



Declassified in Part - Sanitized Copy Approved for Release 2012/03/12 : CIA-RDP82-00039R000100190014-6

Declassified in Part - Sanitized Copy Approved for Release 2012/03/12 : CIA-RDP82-00039R000100190014-6

lines give the same data at noon, and the two bottom lines contain the values for 1600 hours; while Figure 8 shows the annual cycle of cloudiness at noon.

FIGURE 7. DIURNAL CYCLE OF LOW-LYING CLOUDINESS. TEN-YEAR MEAN VALUES.

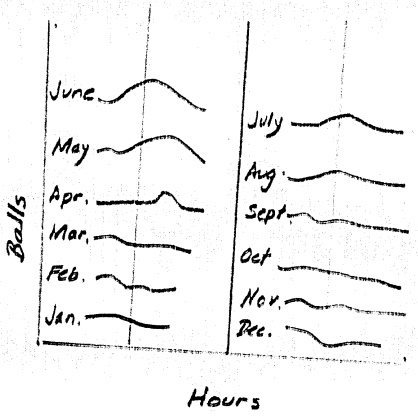


(See next page for Table VIII.)

If we consider how cloudiness in its annual cycle varies with respect to June (when the sun is at maximum altitude) we see that the amount of cloudiness varies upwards and downwards in markedly symmetric fashion, which fact is also expressed in the symmetrical distribution of the isopleths of total radiation.

The effect of the altitude of the sun must be eliminated in order to study the influence of cloudiness alone -- amount and type -- on the total radiation; that is, the relationship between cloudiness and radiation must be studied with the sun at the same altitude.



Declassified in Part - Sanitized Copy Approved for Release 2012/03/12 : CIA-RDP82-00039R000100190014-6

Declassified in Part - Sanitized Copy Approved for Release 2012/03/12 : CIA-RDP82-00039R000100190014-6



ANNUAL COURSE OF TOTAL CLOUDINESS (T) AND LOW-LYING CLOUDINESS (L)

Table 8.

| | | JANUARY | FEBRUARY | MARCH | APRIL | MAY | JUNE | JULY | AUGUST | SEPTEMBER | OCTOBER | NOVEMBER | DECEMBER |
|---|---|---|---|---|---|---|---|---|---|---|---|---|---|
| 8 | T | 8.4 | 8.3 | 7.8 | 7.0 | 6.2 | 5.5 | 6.2 | 6.1 | 7.2 | 8.6 | 9.1 | 8.7 |
| | L | 7.3 | 6.7 | 5.5 | 4.7 | 3.8 | 3.1 | 3.3 | 3.0 | 5.0 | 7.2 | 8.1 | 8.0 |
| 12 | T | 8.6 | 8.0 | 7.5 | 7.1 | 6.5 | 6.7 | 6.7 | 6.4 | 7.1 | 8.4 | 8.8 | 8.8 |
| | L | 6.8 | 5.7 | 5.3 | 4.5 | 4.4 | 4.6 | 4.2 | 3.9 | 5.1 | 6.9 | 7.6 | 7.5 |
| 16 | T | 8.2 | 7.9 | 7.4 | 6.9 | 6.3 | 6.2 | 6.7 | 6.3 | 7.4 | 8.1 | 8.8 | 8.6 |
| | L | 6.8 | 6.0 | 5.1 | 4.3 | 3.7 | 3.9 | 3.8 | 3.6 | 4.8 | 6.6 | 7.6 | 7.4 |

Declassified in Part - Sanitized Copy Approved for Release 2012/03/12 : CIA-RDP82-00039R000100190014-6

Declassified in Part - Sanitized Copy Approved for Release 2012/03/12 : CIA-RDP82-00039R000100190014-6

If observations are selected with the sun at an altitude which is encountered throughout the year, this altitude would have to be lower than 7 degrees, but since for typical observations, the lower the altitude of the sun the less will be the accuracy of radiation measurements, the altitude of 10 degrees was selected instead, which altitude does not occur during December and January at the latitude of Pavlovsk.

TABLE IX

TOTAL RADIATION IN CALORIES AND CLOUDINESS, BOTH DURING HOURLY INTERVALS, WITH SUN AT ALTITUDE OF 10 DEGREES

| | FEB. | MAR. | APR. | MAY | JUNE | JULY | AUG. | SEPT. | OCT. | NOV. |
|---|---|---|---|---|---|---|---|---|---|---|
| $\Sigma Q$ | 212 | 223 | 200 | 214 | 253 | 205 | 230 | 175 | 155 | 130 |
| Total Cloudiness | 8,0 | 6,7 | 7,0 | 6,2 | 5,8 | 6,5 | 6,2 | 7,1 | 8,0 | 9,0 |

Table IX and Figure 9 show an inverse relationship between total incoming radiation and cloudiness.

The maximum cloudiness of 9.0 balls in November corresponds to the minimum hourly total radiation of 130 calories, while the minimum cloudiness of 5.8 balls in June corresponds to the maximum radiation of 253 calories.

Only the afternoon observations were used in constructing Table 9 and Figure 9, since no data was available for cloudiness



Declassified in Part - Sanitized Copy Approved for Release 2012/03/12 : CIA-RDP82-00039R000100190014-6

Declassified in Part - Sanitized Copy Approved for Release 2012/03/12 : CIA-RDP82-00039R000100190014-6

earlier than 0700 hours, and consequently there were no cloud observations during the summer with the sun at altitude 10 degrees. The values for total radiation were taken from Figures 2a and 2b, while those for cloudiness were taken from Figure 6.

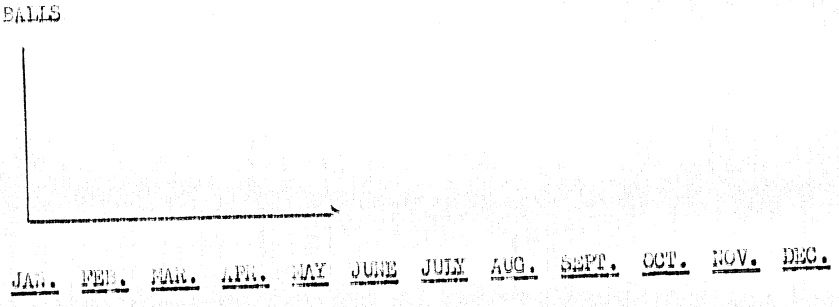


FIGURE 6. ANNUAL CYCLE OF TOTAL CLOUDINESS AT NOON (1) AND LOW-LYING CLOUDINESS AT NOON (2).

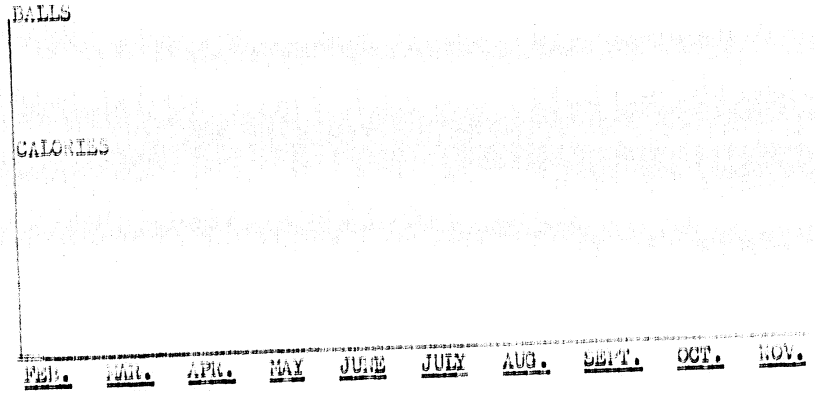


FIGURE 7. RELATIONSHIP BETWEEN TOTAL INCOMING RADIATION AND CLOUDINESS WITH SUN AT ALTITUDE 10 DEGREES



Declassified in Part - Sanitized Copy Approved for Release 2012/03/12 : CIA-RDP82-00039R000100190014-6

Declassified in Part - Sanitized Copy Approved for Release 2012/03/12 : CIA-RDP82-00039R000100190014-6

As a rule cloudiness reduces the total radiation, but there are times when it increases it. We may picture the following case: there is great cloudiness at the middle cloud zones, which as a rule results in larger values for diffuse sky radiation, and there are breaks in the clouds through which the rays of the sun pass. In this case there will be an undiminished influx of direct solar radiation, to which high values of diffuse sky radiation must also be added, making a very considerable amount of total radiation.

Let us take 14 July 1929, as an example. At 1125 hours, with cloudiness 10, type altocumulus, the value of diffuse sky radiation was determined to be 0.61 calories. If there had been a small break in the clouds and the sun had shone through it, the intensity of solar radiation falling on a horizontal surface, with the mean atmospheric transparency what it was at that moment, would have been 0.99 calories, making up a total of 1.60 calories. From the isopleths of Figure 1, it may be determined that with this mean atmospheric transparency the total radiation through a cloudless sky would have been 1.37 calories at 1125 hours on June 14; so that in this case cloudiness increased the intensity of total radiation by 20 percent. This example of the increase of total radiation by cloud influence is exceptional in degree.

In most cases cloudiness diminishes the influx of total radiation; the altitude of the sun plays an important role in this. The relationship between solar, diffuse, and total radiation under varying cloud conditions is shown for the examples given. The observations presented in Table X were made with the sun at altitude 40 degrees, while in Table XI its altitude is 10 degrees (afternoon



Declassified in Part - Sanitized Copy Approved for Release 2012/03/12 : CIA-RDP82-00039R000100190014-6

Declassified in Part - Sanitized Copy Approved for Release 2012/03/12 : CIA-RDP82-00039R000100190014-6

observations). The first column of the tables shows the date of the month; the second, third, and fourth columns show the influx of the corresponding radiations at mean solar altitude of 40 degrees or 10 degrees, respectively; while the fifth column gives amount and types of clouds. July 1938 was chosen as an example of a month with variable and variegated cloud conditions.

The relationship presented between the values of radiation and cloudiness is more graphically portrayed in Figures 10 and 11, which have been plotted from the values of Tables X and XI.

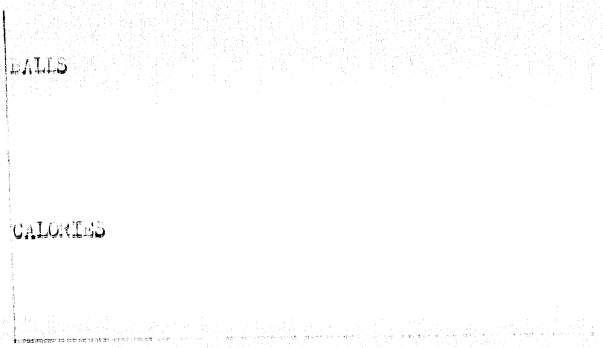


FIGURE 10. RELATIONSHIP BETWEEN RADIATION AND CLOUDINESS IN JUNE 1938, WITH SUN AT ALTITUDE OF 40 DEGREES.



Declassified in Part - Sanitized Copy Approved for Release 2012/03/12 : CIA-RDP82-00039R000100190014-6

Declassified in Part - Sanitized Copy Approved for Release 2012/03/12 : CIA-RDP82-00039R000100190014-6

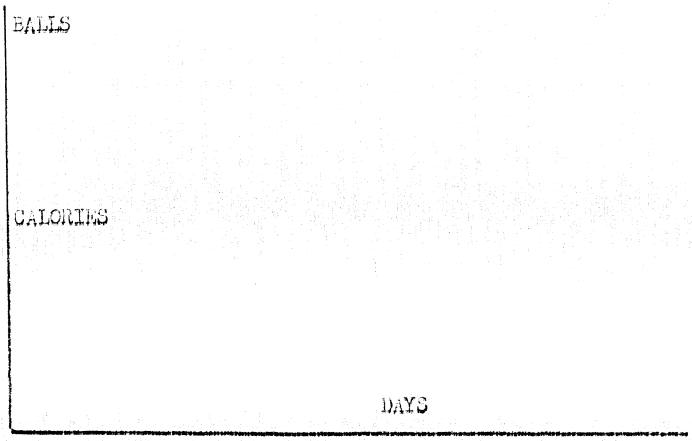


FIGURE 11. RELATIONSHIP BETWEEN RADIATION AND CLOUDINESS IN JUNE 1936, WITH SUN AT ALTITUDE OF 10 DEGREES.

See next page for Tables X and XI.

The dotted curves in these drawings show the hourly values of solar radiation, while the unbroken lines show total radiation. Consequently the value of the diffuse sky radiation is characterized by the distance between these two curves. The mean values of the cloudiness during these hourly intervals is presented in the upper part of each system. The comparison between the values of radiation and cloudiness presented in these drawings graphically indicates the effect of cloudiness on the influx of radiation.

The influence of cloudiness on total radiation was the subject of an earlier study by me, based on data of observations from 1930 to 1935 at Pavlovsk, and the conclusions of this study were published in the Reports of the Academy of Sciences USSR (17). The results are shown in Table XII. The values in Table XII were



Declassified in Part - Sanitized Copy Approved for Release 2012/03/12 : CIA-RDP82-00039R000100190014-6

Declassified in Part - Sanitized Copy Approved for Release 2012/03/12 : CIA-RDP82-00039R000100190014-6

TABLE 10

SOLAR, DIFFUSE AND TOTAL RADIATION IN CALORIES DURING JUNE, 1938,

WITH SUN AT ALTITUDE OF 40 DEGREES, TOGETHER WITH CLOUDINESS

| Date | ΣS' | ΣD | ΣQ | | Cloudiness |
|---|---|---|---|---|---|
| 1 | 0 | 21 | 21 | 10/10 | CN |
| 2 | 27 | 15 | 42 | 4/4 | Cu |
| 3 | 29 | 19 | 48 | 10/1 | Cs, Cu |
| 4 | 38 | 9 | 47 | 0/0 | FrCu |
| 5 | 31 | 10 | 41 | 3/1 | Ci, FrCu |
| 6 | 36 | 10 | 46 | 0/0 | Cu |
| 7 | 4 | 25 | 49 | 10/0 | Ci, Cs |
| 8 | 34 | 11 | 45 | 2/2 | Ci, Cu |
| 9 | 40 | 11 | 51 | 6/0 | Ci, Ac |
| 10 | 26 | 17 | 43 | 10/1 | Ci, FrCu |
| 11 | 10 | 18 | 28 | 10/10 | Fc |
| 12 | 4 | 23 | 27 | 10/8 | Ac, CN |
| 13 | 8 | 21 | 29 | 10/8 | Ci, CN |
| 14 | 37 | 11 | 48 | 2/2 | Cu, Sc |
| 15 | 0 | 23 | 23 | 10/10 | Fc |



Declassified in Part - Sanitized Copy Approved for Release 2012/03/12 : CIA-RDP82-00039R000100190014-6

Declassified in Part - Sanitized Copy Approved for Release 2012/03/12 : CIA-RDP82-00039R000100190014-6

TABLE 10

(Continued)

| Date | $\Sigma S'$ | $\Sigma D$ | $\Sigma Q$ | | Cloudiness |
|---|---|---|---|---|---|
| 16 | 0 | 7 | 7 | 10/10 | Ns |
| 17 | 6 | 15 | 21 | 8/8 | Ac, Cu |
| 18 | 7 | 22 | 29 | 10/9 | Cu |
| 19 | 17 | 18 | 35 | 6/6 | Cu, Sc |
| 20 | 0 | 23 | 23 | 10/10 | Cs, Sc |
| 21 | 13 | 26 | 39 | 10/6 | Ac, Cu |
| 22 | 20 | 16 | 36 | 7/7 | Cu |
| 23 | 20 | 19 | 39 | 10/2 | Cs, Ac, Cu |
| 24 | 19 | 22 | 41 | 10/6 | Ci, Ac, Cu |
| 25 | 39 | 13 | 52 | 8/8 | Ci, Cu |
| 26 | 0 | 10 | 10 | 10/10 | Ns |
| 27 | 4 | 23 | 27 | 10/10 | Ns |
| 28 | 13 | 24 | 37 | 10/8 | Sc |
| 29 | 3 | 16 | 19 | 10/8 | Ac, Sc |
| 30 | 4 | 18 | 22 | 9/6 | Ns |



Declassified in Part - Sanitized Copy Approved for Release 2012/03/12 : CIA-RDP82-00039R000100190014-6

Declassified in Part - Sanitized Copy Approved for Release 2012/03/12 : CIA-RDP82-00039R000100190014-6

TABLE 11

SOLAR, DIFFUSE AND TOTAL RADIATION IN CALORIES DURING JUNE, 1938,

WITH SUN AT ALTITUDE OF 10 DEGREES, TOGETHER WITH CLOUDINESS

| Date | ΣS' | ΣD | ΣQ | Cloudiness | |
|---|---|---|---|---|---|
| 1 | 1 | 7 | 8 | 10/2 | Ci, [redacted], Ac, Cu |
| 2 | 0 | 4 | 4 | 2/2 | Cu |
| 3 | 3 | 5 | 8 | 10/0 | Ci |
| 4 | 0 | 3 | 8 | 0/0 | - |
| 5 | 1 | 9 | 10 | 9/0 | Ci |
| 6 | 1 | 4 | 8 | 2/0 | Ci |
| 7 | 6 | 3 | 9 | 6/0 | Ci, Cs |
| 8 | 5 | 4 | 9 | 2/0 | [redacted] |
| 9 | 0 | 6 | 6 | 10/0 | Ci, Cs |
| 10 | 3 | 5 | 8 | 10/0 | Ci, Cs |
| 11 | 0 | 2 | 2 | 10/9 | Ac, Sc |
| 12 | 1 | 2 | 13 | 7/0 | Ci, Sc |
| 13 | 0 | 1 | 1 | 10/2 | Ac, Frnb |
| 14 | 2 | 1 | 9 | 1/0 | Ac |
| 15 | | | 2 | 10/6 | Sc, Ac |



Declassified in Part - Sanitized Copy Approved for Release 2012/03/12 : CIA-RDP82-00039R000100190014-6

Declassified in Part - Sanitized Copy Approved for Release 2012/03/12 : CIA-RDP82-00039R000100190014-6

TABLE 11

(Continued)

| Date | ΣS' | ΣD | ΣQ | | Cloudiness |
|---|---|---|---|---|---|
| 16 | 2 | 8 | 10 | 1/0 | Ac |
| 17 | 0 | 2 | 2 | 10/10 | Ns |
| 18 | 0 | 5 | 5 | 10/10 | Cu, Ns |
| 19 | 0 | 4 | 4 | 2/2 | FrCu |
| 20 | 0 | 1 | 1 | 10/10 | Ns |
| 21 | 0 | 8 | 8 | 10/10 | Cu |
| 22 | 7 | 4 | 11 | 0/0 | - |
| 23 | 0 | 3 | 3 | 10/2 | Ac, As, FrCu |
| 24 | 1 | 7 | 8 | 10/10 | Ci, Ac, Sc |
| 25 | 0 | 2 | 2 | 0/0 | - |
| 26 | 2 | 5 | 7 | 10/7 | Ac, Ns |
| 27 | 1 | 3 | 1 | 10/10 | Ns |
| 28 | 0 | 1 | 1 | 10/10 | Sc |
| 29 | 0 | 1 | 1 | 10/10 | Sc |
| 30 | 2 | 3 | 5 | 9/9 | Ac, FrCu |



Declassified in Part - Sanitized Copy Approved for Release 2012/03/12 : CIA-RDP82-00039R000100190014-6

Declassified in Part - Sanitized Copy Approved for Release 2012/03/12 : CIA-RDP82-00039R000100190014-6

obtained in the following manner. The actinograph and pyranograph records during the five years were taken as the basic material, together with the hourly observations of cloud conditions during the same period. Only those hourly intervals of the radiation records were chosen for further processing where the cloudiness was one definite form and was 10 tails in amount. Table XII shows that the influence of the following cloud forms types was studied: cirrus, cirrostratus, altocumulus, altostratus, fracto-stratus, stratocumulus, and stratus.

The upper part of Table XII shows the influence of these forms of cloudiness on the intensity of solar radiation, while the first line of the table gives the intensity of solar radiation through a cloudless sky for each altitude of the sun. The table shows that at solar altitudes lower than 15 degrees the solar radiation fails to pass through high cloud forms, such as cirrus. The transmission of radiation increases with the altitude of the sun; and with the sun at altitude 50 degrees, the influx of radiation is only 10 percent less than with the sun not covered by clouds.

Clouds of the cirrus type, of which a typical representative is altocumulus, combine to diminish radiation when the sun reaches an altitude of about 40 degrees. This of course is an average, for in individual instances the transmission of radiation through clouds of this type may depend to a greater extent on the altitude of the sun than it does with cirrus clouds.

See next page for Table XII.



Declassified in Part - Sanitized Copy Approved for Release 2012/03/12 : CIA-RDP82-00039R000100190014-6

Declassified in Part - Sanitized Copy Approved for Release 2012/03/12 : CIA-RDP82-00039R000100190014-6

INTENSITY IN CALORIES OF SOLAR, DIFFUSE, AND TOTAL RADIATION WITH VARYING CLOUD TYPES AND VARYING ALTITUDE OF THE SUN

Table. 12.

| CLOUD TYPE | ALTITUDE OF SUN IN DEGREES | | | | | | | | | | |
|---|---|---|---|---|---|---|---|---|---|---|---|
| | (1) | (2) | (3) | (4) | (5) | (6) | (7) | (8) | (9) | (10) | (11) |
| | 0 | 2.5 | 5 | 7.5 | 10 | 15 | 20 | 25 | 30 | 40 | 50 |
| | Solar Radiation S' | | | | | | | | | | |
| Cloudless | 0.00 | 0.03 | 0.06 | 0.09 | 0.13 | 0.22 | 0.33 | 0.46 | 0.59 | 0.84 | 0.10 |
| Ci | 0.00 | 0.00 | 0.00 | 0.00 | 0.00 | 0.04 | 0.11 | 0.21 | 0.32 | 0.60 | 0.90 |
| Cs | 0.00 | 0.00 | 0.00 | 0.00 | 0.00 | 0.00 | 0.01 | 0.09 | 0.18 | 0.42 | 0.70 |
| Ac | 0.00 | 0.00 | 0.00 | 0.00 | 0.00 | 0.00 | 0.00 | 0.00 | 0.00 | 0.12 | 0.31 |
| As | 0.00 | 0.00 | 0.00 | 0.00 | 0.00 | 0.00 | 0.00 | 0.00 | 0.01 | 0.05 | 0.10 |
| Frst | 0.00 | 0.00 | 0.00 | 0.00 | 0.00 | 0.00 | 0.00 | 0.00 | 0.00 | 0.01 | 0.05 |
| Sc | 0.00 | 0.00 | 0.00 | 0.00 | 0.00 | 0.00 | 0.00 | 0.00 | 0.00 | 0.00 | 0.00 |
| St | 0.00 | 0.00 | 0.00 | 0.00 | 0.00 | 0.00 | 0.00 | 0.00 | 0.00 | 0.00 | 0.00 |

Declassified in Part - Sanitized Copy Approved for Release 2012/03/12 : CIA-RDP82-00039R000100190014-6

Declassified in Part - Sanitized Copy Approved for Release 2012/03/12 : CIA-RDP82-00039R000100190014-6

| | (1) | (2) | (3) | (4) | (5) | (6) | (7) | (8) | (9) | (10) | (11) |
|---|---|---|---|---|---|---|---|---|---|---|---|
| | | | | | Diffuse Sky Radiation D | | | | | | |
| Cloudless | 0.00 | 0.02 | 0.03 | 0.04 | 0.05 | 0.07 | 0.08 | 0.09 | 0.10 | 0.11 | 0.12 |
| Ci | 0.01 | 0.03 | 0.05 | 0.07 | 0.09 | 0.13 | 0.16 | 0.19 | 0.22 | 0.26 | 0.29 |
| Cs | 0.02 | 0.04 | 0.06 | 0.09 | 0.11 | 0.15 | 0.19 | 0.23 | 0.27 | 0.34 | 0.40 |
| Ac | 0.01 | 0.04 | 0.06 | 0.09 | 0.11 | 0.16 | 0.22 | 0.26 | 0.31 | 0.39 | 0.44 |
| As | 0.02 | 0.03 | 0.05 | 0.07 | 0.09 | 0.13 | 0.17 | 0.20 | 0.24 | 0.30 | 0.35 |
| Frst | 0.00 | 0.01 | 0.02 | 0.02 | 0.03 | 0.05 | 0.08 | 0.13 | 0.16 | 0.21 | 0.24 |
| Sc | 0.00 | 0.00 | 0.01 | 0.02 | 0.04 | 0.08 | 0.13 | 0.17 | 0.20 | 0.27 | 0.33 |
| St | 0.00 | 0.01 | 0.02 | 0.02 | 0.04 | 0.06 | 0.08 | 0.10 | 0.13 | 0.16 | 0.19 |
| | | | | | Total Radiation Q = S' + D | | | | | | |
| Cloudless | 0.00 | 0.05 | 0.09 | 0.13 | 0.18 | 0.29 | 0.41 | 0.55 | 0.69 | 0.96 | 1.22 |
| Ci | 0.01 | 0.03 | 0.05 | 0.07 | 0.09 | 0.17 | 0.27 | 0.40 | 0.54 | 0.86 | 1.19 |
| Cs | 0.02 | 0.04 | 0.06 | 0.09 | 0.11 | 0.15 | 0.20 | 0.32 | 0.45 | 0.76 | 1.10 |
| Ac | 0.01 | 0.04 | 0.06 | 0.09 | 0.11 | 0.16 | 0.22 | 0.26 | 0.31 | 0.51 | 0.75 |
| As | 0.02 | 0.03 | 0.05 | 0.07 | 0.09 | 0.13 | 0.17 | 0.20 | 0.25 | 0.35 | 0.45 |
| Frst | 0.00 | 0.01 | 0.02 | 0.02 | 0.03 | 0.05 | 0.08 | 0.13 | 0.16 | 0.22 | 0.29 |
| Sc | 0.00 | 0.00 | 0.01 | 0.02 | 0.04 | 0.08 | 0.13 | 0.17 | 0.20 | 0.27 | 0.35 |
| St | 0.00 | 0.01 | 0.02 | 0.02 | 0.04 | 0.06 | 0.08 | 0.10 | 0.13 | 0.16 | 0.19 |

Declassified in Part - Sanitized Copy Approved for Release 2012/03/12 : CIA-RDP82-00039R000100190014-6

Declassified in Part - Sanitized Copy Approved for Release 2012/03/12 : CIA-RDP82-00039R000100190014-6

With altocumulus clouds, the size and thickness dimensions of the separate cloud elements, as well as the distance between them, is very important. The greater this distance, and the smaller the thickness of the clouds, the lower the sun's attitude at which radiation may be transmitted through them (18). A fractostratus cloud in the lower region commences to transmit radiation, though in very insignificant amount, when the sun reaches an altitude of about 50 degrees; while stratocumulus and stratus clouds do not transmit solar radiation at all.

The middle part of Table XI shows how the increase of diffuse sky radiation by cirrus or cirrostratus clouds of the upper region over that in a cloudless sky ranges from 0 percent for cirrus when the sun is at altitude 5 degrees, to 102 percent for altitude 50 degrees. Clouds of the middle region increase diffuse sky radiation by far more than this, for instance altocumulus increases it by 100 percent at solar altitude 5 degrees, and by as much as 307 percent at altitude 50 degrees.

Since the clouds of the lower region are distinguished by great thickness and density, they act differently on diffuse sky radiation. When the sun's altitude is low, the presence of these clouds does not increase this radiation in comparison to its value in a cloudless sky, but reduces it; and only when the sun has gained very considerably in altitude does the diffuse sky radiation begin to increase. At 5 degrees altitude of the sun, a stratus cloud reduces radiation by 33 percent; at 20 degrees altitude the radiation through such a cloud is equivalent to that in a cloudless sky;



Declassified in Part - Sanitized Copy Approved for Release 2012/03/12 : CIA-RDP82-00039R000100190014-6

Declassified in Part - Sanitized Copy Approved for Release 2012/03/12 : CIA-RDP82-00039R000100190014-6

while when the sun is still higher the radiation is increased, but by an insignificant amount; thus, this increase attains 58 percent at solar altitude 50 degrees. For clouds of fractostratus type the transmission of diffuse sky radiation is lower than that through a cloudless sky so long as the sun is below 20 degrees, but above that solar altitude the transmission increases. For stratocumulus clouds this "critical" altitude of the sun is 12 degrees.

The top and middle parts of Table XII show the influence of cloudiness on both direct and diffuse radiation. By summing these two parts of the table, we find the general influence of cloudiness on total radiation. The result obtained is entered in the lower part of Table XII. It is plain that on the whole all forms of clouds reduce the influx of radiation compared to that of a cloudless sky.

The relationship between solar, diffuse, and total radiations for a few cloud types is presented in figures 12, 13, and 14. These graphs were constructed in the following manner: the radiation was laid off along the axes of abscissas, while the altitude of the sun was plotted along the axes of ordinates. The curve S' shows the mean intensity of solar radiation, while the curve $\gamma$ shows the total radiation. Thus the horizontal distance between these two curves represents the mean diffuse sky radiation.



Declassified in Part - Sanitized Copy Approved for Release 2012/03/12 : CIA-RDP82-00039R000100190014-6

Declassified in Part - Sanitized Copy Approved for Release 2012/03/12 : CIA-RDP82-00039R000100190014-6

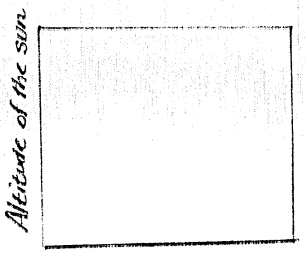


CALORIES

FIGURE 12. SOLAR, DIFFUSE, AND TOTAL RADIATION AT VARYING ALTITUDES OF THE SUN, WITH CLOUDINESS 10, CIRRUS.

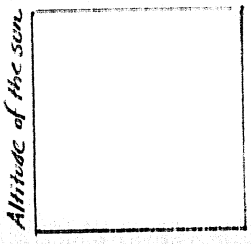


CALORIES

FIGURE 13. SOLAR, DIFFUSE, AND TOTAL RADIATION AT VARYING ALTITUDES OF THE SUN, WITH CLOUDINESS 10, ALTOCUMULUS.

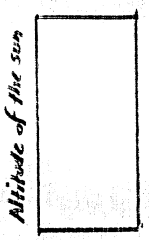


CALORIES

FIGURE 14. SOLAR, DIFFUSE, AND TOTAL RADIATION AT VARYING ALTITUDES OF THE SUN, WITH CLOUDINESS 10, STRATOCUMULUS.



Declassified in Part - Sanitized Copy Approved for Release 2012/03/12 : CIA-RDP82-00039R000100190014-6

Declassified in Part - Sanitized Copy Approved for Release 2012/03/12 : CIA-RDP82-00039R000100190014-6

The extent to which total radiation is reduced by the various cloud types studied, at altitudes of the sun ranging from 5 to 50 degrees, is shown by Table XIII, in which this reduction is expressed as percent of total radiation in a cloudless sky.

Table XIII sums up the results of the study of the influence of cloudiness on total radiation, and shows that:

1. All types of clouds, at all altitudes of the sun, reduce the influx of total radiation compared with that occurring in a cloudless sky;

2. The dependence of the reduction in influx of radiation on the altitude of the sun is well marked for the high clouds, and ranges from 40-50 percent with low sun altitudes to 10-2 percent for high sun altitudes.

3. No dependence on the altitude of the sun was discovered for the low clouds, and, on the average, clouds of these types reduce the influx of radiation by about 80 percent.

Apparently the high clouds do not reduce total radiation, but increase it, when the sun is higher than 30 degrees. This conclusion requires confirmation by observations in more southerly latitudes.



Declassified in Part - Sanitized Copy Approved for Release 2012/03/12 : CIA-RDP82-00039R000100190014-6

Declassified in Part - Sanitized Copy Approved for Release 2012/03/12 : CIA-RDP82-00039R000100190014-6

TABLE XIII

REDUCTION OF INTENSITY OF TOTAL RADIATION FOR CLOUDS OF VARIOUS TYPES, WITH VARIOUS ALTITUDES OF THE SUN.

| TYPE OF CLOUD | ALTITUDE OF SUN IN DEGREES. | | | | | |
|---|---|---|---|---|---|---|
| | 5 | 10 | 20 | 30 | 40 | 50 |
| Ci | -44 | -50 | -34 | -22 | -10 | - 2 |
| Cs | -33 | -39 | -51 | -35 | -20 | -10 |
| Ac | -33 | -39 | -46 | -55 | -46 | -38 |
| As | -44 | -50 | -59 | -64 | -63 | -63 |
| Frst | -78 | -83 | -80 | -77 | -77 | -76 |
| Sc | -89 | -78 | -68 | -71 | -72 | -73 |
| St | -76 | -78 | -80 | -81 | -83 | -84 |

IN CALORIES

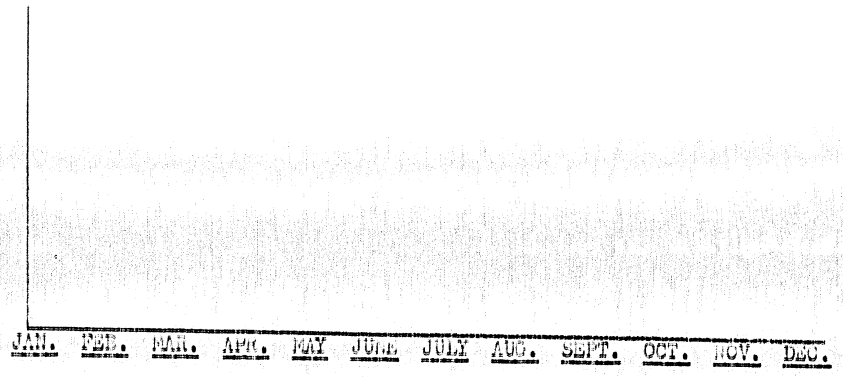


FIGURE 15. ANNUAL RANGE OF THE MONTHLY TOTALS OF SOLAR, DIFFUSE AND TOTAL RADIATION AT PAVLOVSK

1 - SOLAR RADIATION 2 - DIFFUSE RADIATION 3 - TOTAL RADIATION



Declassified in Part - Sanitized Copy Approved for Release 2012/03/12 : CIA-RDP82-00039R000100190014-6

Declassified in Part - Sanitized Copy Approved for Release 2012/03/12 : CIA-RDP82-00039R000100190014-6

## Monthly Values of Total Radiation

Ten years of uninterrupted registration of solar and diffuse radiation, and consequently of total radiation as well, allowed us to compile Table XIV, in which the monthly totals are given for each month of each year. This makes it possible to study the variation and the relationship through time of the values under investigation. The question of the relationship between solar and diffuse radiation at Pavlovsk and a few other points (Yakutsk, Karadag, Tashkent) was already studied, in part, in 1946 (14).

Besides the monthly values, Table XIV also gives the ratio for each month between the maximum and minimum values of total radiation. The highest ratios occur during the cold time of the year (with a maximum ratio in November of 2.49), while lowest ratios are during the latter half of spring and early summer (April, with 1.49). Thus November showed the widest range of variation in total radiation -- from 470 to 1,170 calories -- while June was the month that is most stable in this respect: from 11,160 to 16,520 calories.

Figure 15 shows the annual cycle of the monthly totals of solar, diffuse, and total radiation. This cycle is expressed with the greatest sharpness for direct solar radiation. The minimum of 70 calories occurs in December, while the maximum of 8,940 calories is in June; thus from December to June, under the climatic conditions of Pavlovsk, the influx of heat from solar radiation increased by 128 times. The existence of an influx of diffuse sky radiation tones down this relationship very considerably because of the fact that the contrast between winter and summer values is much less for diffuse radiation than for solar radiation; thus the influx is 360 calories for December and 5,130 calories in June, or an increase of



Declassified in Part - Sanitized Copy Approved for Release 2012/03/12 : CIA-RDP82-00039R000100190014-6

Declassified in Part - Sanitized Copy Approved for Release 2012/03/12 : CIA-RDP82-00039R000100190014-6

14 times between winter and summer. Owing to this the actual influx of total radiation at Pavlovsk increases only 32 times, from 430 calories in December to 14,070 calories in June. Such is the equilibrating influence of the diffuse sky radiation on the total influx of the stream of radiation.

It may also be seen from Figure 15 that twice a year -- at the beginning of April and the middle of September -- the influx of solar radiation equals that of diffuse sky radiation. During the six months October, November, December, January, February, and March, more heat is received from diffuse sky radiation than from solar radiation. During September the influx is the same from both radiations, so that solar radiation preponderates only during five months.

This fact once again emphasizes the significance of diffuse sky radiation for points located in the high latitudes.

The last two lines of Table XIV show the ratio between the influx of solar radiation and that of diffuse sky radiation, expressed in percent.

In June, which is the sunniest month, 64 percent of the total radiation was received from the sun, and only 36 percent from diffuse sky radiation, while in December the sun contributed 17 percent, and diffuse sky radiation 83 percent.

The mean annual value of the total radiation falling on each square centimeter of horizontal surface at Pavlovsk is 76.5 large calories, composed of 42.7 large calories of solar radiation and 33.8 large calories of diffuse sky radiation, or 56 and 44 percent



Declassified in Part - Sanitized Copy Approved for Release 2012/03/12 : CIA-RDP82-00039R000100190014-6

Declassified in Part - Sanitized Copy Approved for Release 2012/03/12 : CIA-RDP82-00039R000100190014-6

respectively.

If we examine the annual values of total radiation obtained from year to year, we see that this total radiation at Pavlovsk is a fairly stable value: during ten years its maximum departure from the mean was 12 percent.

There can be no doubt whatsoever that this type of investigation of total radiation is of great interest, especially if solar and diffuse radiation are separately considered, since this allows us to study the interesting relationships between the influx of the two types of radiation, which may be very diversified under various climatic conditions.

This investigation also shows that in the geophysical observatories it is necessary to carry out research on total radiation by studying its components separately, while the general network of actinometric stations may confine its work to the registration of total radiation alone.



Declassified in Part - Sanitized Copy Approved for Release 2012/03/12 : CIA-RDP82-00039R000100190014-6

Declassified in Part - Sanitized Copy Approved for Release 2012/03/12 : CIA-RDP82-00039R000100190014-6

MONTHLY VALUES OF INFLUX OF SOLAR, DIFFUSE, AND TOTAL RADIATION AT PAVLOVSK, IN CALORIES

Table 11.

| Years | | JANUARY | FEBRUARY | MARCH | APRIL | MAY | JUNE | JULY | AUGUST | SEPTEMBER | OCTOBER | NOVEMBER | DECEMBER | ANNUAL VALUES |
|---|---|---|---|---|---|---|---|---|---|---|---|---|---|---|
| 1931 | (ΣS' | 150 | 700 | 2630 | 3620 | 9750 | 6890 | 7790 | 6170 | 2020 | 1140 | 60 | 140 | 41300 |
| | (ΣD | 730 | 1710 | 3510 | 4760 | 4000 | 4270 | 3390 | 3560 | 2850 | 1170 | 410 | 420 | 30800 |
| | (ΣQ | 880 | 2410 | 6370 | 8380 | 13750 | 11160 | 11180 | 9730 | 4900 | 2310 | 470 | 560 | 72100 |
| 1932 | (ΣS' | 270 | 990 | 3170 | 3660 | 7210 | 7600 | 10600 | 5230 | 3670 | 1030 | 180 | 60 | 43930 |
| | (ΣD | 850 | 1310 | 3060 | 3050 | 4450 | 4620 | 4100 | 4330 | 2510 | 1370 | 580 | 290 | 30800 |
| | (ΣQ | 1120 | 2300 | 6230 | 6710 | 11720 | 12620 | 14700 | 9560 | 6180 | 2400 | 760 | 350 | 74700 |
| 1933 | (ΣS' | 260 | 290 | 2500 | 3550 | 7210 | 9020 | 8690 | 5070 | 2520 | 820 | 420 | 100 | 41300 |
| | (ΣD | 600 | 1640 | 2840 | 3240 | 4320 | 4390 | 4030 | 4270 | 2720 | 1480 | 750 | 440 | 30900 |
| | (ΣQ | 860 | 1930 | 5360 | 6790 | 11510 | 14210 | 12720 | 9340 | 5240 | 2500 | 1170 | 510 | 72200 |
| 1934 | (ΣS' | 90 | 490 | 1540 | 5710 | 4840 | 9070 | 5220 | 7400 | 4190 | 900 | 40 | 60 | 41500 |
| | (ΣD | 490 | 1380 | 1870 | 2880 | 3020 | 3930 | 4440 | 3300 | 2270 | 1320 | 440 | 260 | 26400 |
| | (ΣQ | 550 | 2070 | 3420 | 8590 | 10660 | 13000 | 9620 | 10400 | 6460 | 2220 | 480 | 320 | 67900 |

Declassified in Part - Sanitized Copy Approved for Release 2012/03/12 : CIA-RDP82-00039R000100190014-6

Declassified in Part - Sanitized Copy Approved for Release 2012/03/12 : CIA-RDP82-00039R000100190014-6



| | | (1) | (2) | (3) | (4) | (5) | (6) | (7) | (8) | (9) | (10) | (11) | (12) | (13) |
|---|---|---|---|---|---|---|---|---|---|---|---|---|---|---|
| 1935 | ΣS' | 200 | 330 | 2530 | 5020 | 7150 | 10130 | 5200 | 1630 | 1630 | 910 | 350 | 4 | 38900 |
| | ΣD | 420 | 850 | 2350 | 3350 | 4360 | 4430 | 5030 | 4340 | 2070 | 1120 | 460 | 250 | 28900 |
| | ΣQ | 620 | 1180 | 4780 | 9170 | 11510 | 14560 | 10230 | 8970 | 3700 | 2060 | 810 | 254 | 67800 |
| 1936 | ΣS' | 100 | 620 | 2120 | 4260 | 7990 | 10710 | 7580 | 5100 | 3660 | 960 | 440 | 50 | 43600 |
| | ΣD | 600 | 1990 | 3450 | 4310 | 5210 | 5810 | 6420 | 5340 | 3400 | 1780 | 710 | 290 | 39300 |
| | ΣQ | 700 | 2610 | 5570 | 8570 | 13200 | 16420 | 14000 | 10710 | 7660 | 2740 | 850 | 340 | 82900 |
| 1937 | ΣS' | 230 | 720 | 1620 | 4410 | 9010 | 10530 | 6180 | 7160 | 3400 | 1470 | 60 | 50 | 44900 |
| | ΣD | 500 | 1470 | 2810 | 4450 | 5530 | 6660 | 6660 | 5100 | 3500 | 1680 | 610 | 420 | 38500 |
| | ΣQ | 730 | 2190 | 4430 | 8970 | 14570 | 16190 | 12810 | 12280 | 6900 | 3150 | 670 | 470 | 83400 |
| 1938 | ΣS' | 50 | 710 | 2170 | 3460 | 5680 | 5870 | 10330 | 7030 | 2830 | 780 | 210 | 180 | 39300 |
| | ΣD | 740 | 1550 | 2800 | 4350 | 5580 | 6910 | 5800 | 4410 | 3750 | 1490 | 520 | 310 | 38400 |
| | ΣQ | 790 | 2260 | 4970 | 7810 | 11260 | 12780 | 15130 | 11470 | 6580 | 2270 | 730 | 490 | 77700 |

Declassified in Part - Sanitized Copy Approved for Release 2012/03/12 : CIA-RDP82-00039R000100190014-6

Declassified in Part - Sanitized Copy Approved for Release 2012/03/12 : CIA-RDP82-00039R000100190014-6



| | | (1) | (2) | (3) | (4) | (5) | (6) | (7) | (8) | (9) | (10) | (11) | (12) | (13) |
|---|---|---|---|---|---|---|---|---|---|---|---|---|---|---|
| 1939 | $\Sigma S'$ | 110 | 400 | 1960 | 5160 | 8350 | 10850 | 7110 | 8770 | 3760 | 1010 | 120 | 40 | 48000 |
| | $\Sigma D$ | 620 | 1270 | 3160 | 4120 | 5730 | 4900 | 6110 | 4790 | 3400 | 1380 | 480 | 330 | 36600 |
| | $\Sigma Q$ | 760 | 1870 | 5120 | 9280 | 14110 | 15750 | 13280 | 13560 | 7160 | 2420 | 600 | 370 | 84600 |
| 1940 | $\Sigma S'$ | 90 | 1060 | 3160 | 5400 | 10200 | 7680 | 8300 | 5080 | 2610 | 720 | 220 | 40 | 44800 |
| | $\Sigma D$ | 570 | 1510 | 3460 | 4170 | 5480 | 6140 | 5330 | 4380 | 3150 | 1720 | 780 | 540 | 37200 |
| | $\Sigma Q$ | 660 | 2570 | 6660 | 9770 | 15680 | 13820 | 13630 | 9460 | 5760 | 2140 | 1000 | 580 | 82000 |
| $\frac{\Sigma Q}{\Sigma Q}$ | max / min | 1.93 | 2.21 | 1.95 | 1.85 | 1.47 | 1.48 | 1.68 | 1.51 | 1.90 | 1.53 | 2.49 | 2.28 | |
| Mean | $\Sigma S'$ | 140 | 670 | 2360 | 4520 | 7950 | 8910 | 7700 | 6170 | 3030 | 980 | 380 | 70 | 42700 |
| | $\Sigma D$ | 610 | 1470 | 2960 | 3880 | 4950 | 5130 | 5130 | 4400 | 2960 | 1470 | 570 | 360 | 33800 |
| | $\Sigma Q$ | 770 | 2140 | 5320 | 8400 | 12800 | 11070 | 12830 | 10170 | 5990 | 2150 | 750 | 430 | 76500 |
| Mean | $\Sigma S'(\%)$ | 21 | 31 | 44 | 54 | 62 | 61 | 60 | 58 | 51 | 40 | 24 | 17 | |
| | $\Sigma D(\%)$ | 79 | 69 | 56 | 46 | 38 | 36 | 40 | 42 | 49 | 60 | 76 | 83 | |

Declassified in Part - Sanitized Copy Approved for Release 2012/03/12 : CIA-RDP82-00039R000100190014-6

Declassified in Part - Sanitized Copy Approved for Release 2012/03/12 : CIA-RDP82-00039R000100190014-6

# CERTAIN NON-STATIONARY PROBLEMS IN THE THEORY OF HEAT CONDUCTIVITY IN DYNAMIC METEOROLOGY

D. L. Laykhtman

1. The foremost problem in contemporary theoretical meteorology -- the pre-calculation in the field of meteorological elements such as temperature, humidity, and wind -- at the present time may be formulated as a fully defined theoretical problem (in the sense that the systems of differential equations and boundary conditions may be extracted). The only exception may be instances in which the presence of phase conversion of water is substantially taken into account. However, the processes taking place in natural conditions are so complicated, the number of determining factors so numerous, that a full resolution of the problem concerning the pre-calculation of meteorological elements still presents quite serious mathematical difficulties. In connection with this, the theoretical analysis of specific processes, for which the system of equations of thermohydrodynamics are simplified and may be integrated, presents itself as an actuality. The importance of the results of such an analysis in connection with the problem of forecasts consists not only in our obtaining the means of pre-calculating meteorological elements for certain cases, but also in our use of such results as the first approach to the complete solution of the problem, which may be visualized as being some process of successive approximations.

Investigated in the present work is a group of problems which is reduced to the integration of a differential equation with respect to special derivatives of parabolic type. The difficulties in arriving at a solution lie in the fact that the coefficients of the



Declassified in Part - Sanitized Copy Approved for Release 2012/03/12 : CIA-RDP82-00039R000100190014-6

Declassified in Part - Sanitized Copy Approved for Release 2012/03/12 : CIA-RDP82-00039R000100190014-6

equation are functions of the coordinates.

2. The problem of first priority before us concerns the measurement of temperature, humidity, and daily fluctuations in wind velocity. These questions were investigated earlier, mainly by the Soviet scientists A. A. Dorodnitsyn, A. F. Chudnovskiy and I. G. Lytershteyn, M. E. Shvets, N. R. Malkin and others. The known results have a series of defects: in the majority of cases deviations from the daily average values were sought; some authors first took an erroneous relation between the coefficient of turbulence viscosity and altitude; and, finally, the solution often came out in a form not convenient for computation. We shall in the future endeavor to avoid the above-mentioned defects. It appears rational to seek a solution simultaneously for the three stated meteorological elements. In general, the theoretical investigation of changes in temperature, humidity, or wind vector is reduced to the search of the solution of the following differential equation:

(1)

$$\frac{\partial q}{\partial t} + u\frac{\partial q}{\partial x} + v\frac{\partial q}{\partial y} = \frac{\partial}{\partial z}\kappa\frac{\partial q}{\partial z} + f(t, x, y, z).$$

Here t, x, y, z are time and right-angle coordinates of the point; u, v are components of wind velocity; q is temperature when changes in temperature are sought, relative humidity when changes in humidity are sought, and $u+iv$ when daily changes in wind vector are



Declassified in Part - Sanitized Copy Approved for Release 2012/03/12 : CIA-RDP82-00039R000100190014-6

Declassified in Part - Sanitized Copy Approved for Release 2012/03/12 : CIA-RDP82-00039R000100190014-6

being investigated.

The function:

$$f(t,x,y,z) = -2i\omega_2(u+iv-u_\infty-iv_\infty)$$

in the wind problem is the inflow of heat for each unit of time from known sources to each gram of air; it is divided by specific heat capacity in the temperature problem; and it is the inflow of water vapor for each unit of time in grams for each gram of air, produced in the process of either evaporation or condensation, in the problem of fluctuations of humidity.

The solution of equation (1) in general form produces insurmountable mathematical difficulties. We will limit ourselves to a few instances in which one or more components in the equation may be disregarded. For this we shall classify the changes in the distribution of investigable meteorological elements with respect to the physical processes which determine these changes.

Let us assume that the order of the unknown function $q_0$ is the same as the order of the magnitude of the difference of its values in the area investigated, if the magnitude studied enters only under the symbol of derivatives, inasmuch as for such amounts their absolute values do not appear as substantial physical characteristics. If the unknown function, however, enters not only under the symbol of derivaties, then under the order of magnitudes let us assume the order of the magnitudes of its modulus in the area investigated.



Declassified in Part - Sanitized Copy Approved for Release 2012/03/12 : CIA-RDP82-00039R000100190014-6

Declassified in Part - Sanitized Copy Approved for Release 2012/03/12 : CIA-RDP82-00039R000100190014-6

Let us introduce further characteristic scales: vertical $l$, horizontal h, characteristic scale of time $\tau$, characteristic scale of velocity v. And then let us determine the scales in this fashion, so that

$$\frac{\partial q}{\partial x} = \frac{q_0}{l}\frac{\partial q_*}{\partial x_*} = \frac{q_0}{l}O(1); \qquad (2)$$

$$\frac{\partial q}{\partial y} = \frac{q_0}{l}\frac{\partial q_*}{\partial y_*} = \frac{q_0}{l}O(1);$$

$$\frac{\partial}{\partial z}k\frac{\partial q}{\partial z} = \frac{\partial p}{\partial z} = \frac{kq_0}{h^2}\frac{\partial}{\partial z_*}k_*\frac{\partial p_*}{\partial z} = \frac{kq_0}{h^2}O(1);$$

$$\frac{\partial q}{\partial t} = \frac{q_0}{\tau}\frac{\partial q_*}{\partial \tau_*} = \frac{q_0}{\tau}O(1).$$

Here O (1) denotes that the magnitude has the order of unity. In this manner the selected scales (of time and space) appear as certain intervals on which the changes of variable magnitudes have the order of the magnitudes themselves.

Under such a selection of scales, equation (1) in abstract variables may be stated in the following form:

$$\frac{\partial q_*}{\partial t_*} + \left[u_*(z)\frac{\partial q_*}{\partial x_*} + v_*(z)\frac{\partial q_*}{\partial y}\right]\frac{U_\tau}{l} = \frac{k_0\tau}{h^2}\frac{\partial}{\partial z_*}k_*\frac{\partial q_*}{\partial z_*} + \qquad (3)$$

$$+ \frac{f(t,x,y,z)\tau}{q_0}.$$

In this equation, all items with asterisks by convention have the order of unity, which means that the comparative weight of each of the component items is determined by the values of two



Declassified in Part - Sanitized Copy Approved for Release 2012/03/12 : CIA-RDP82-00039R000100190014-6

Declassified in Part - Sanitized Copy Approved for Release 2012/03/12 : CIA-RDP82-00039R000100190014-6

abstract parameters:

$$\frac{U\tau}{l} \quad \text{and} \quad \frac{k_0 \tau}{h^2} .$$

In accordance with this, the classification of changes of the investigated meteorological elements are presented in Table I.

The four cases presented cover the more important types. The given criteria allow some numerical characteristics which determine the dominant processes under the given variations. For example, when investigating changes in temperature, 1 degree Centigrade may be accepted as the characteristic scale for temperature. If it is assumed that during 24 hours the order of change in temperature is —10 degrees, then the characteristic scale of time is $\sim 10^4$ seconds; in this case the characteristic scale of altitude is 100 meters. Besides that, accordingly, $U \approx 10$ meters per second, $k_0 \approx 1$ square meter per second. Then, $\frac{k_0}{h^2} \sim O(1)$, and for horizontal convection such a horizontal field is accorded in which $\frac{U\tau}{l} \ll 1$, that is, $l \gg 100$ kilometers. This means that at distances of 100 kilometers the temperature changes by substantially less than 1 degree. (Table I).

TABLE I

| $\frac{U\tau}{l}$ \ $\frac{k_0}{h^2}$ | O (1) | $\gg 1$ | $\ll 1$ |
|---|---|---|---|
| O (1) | General case | - | pure advection |
| $\gg 1$ | - | Stationary transformation | - |
| $\ll 1$ | Vertical convection | - | = |



Declassified in Part - Sanitized Copy Approved for Release 2012/03/12 : CIA-RDP82-00039R000100190014-6

Declassified in Part - Sanitized Copy Approved for Release 2012/03/12 : CIA-RDP82-00039R000100190014-6

It is easy to obtain the figures of the characteristic of pure transformation. In this instance, for distances of 100 kilometers, the temperature changes by substantially more than 1 degree. Vertical gradients of temperature must accordingly be great, owing to which $\frac{k_0 \tau}{h^2} \gg 1$.

An analogical estimate may be obtained for characteristic magnitudes in other processes.

In the cases shown we shall study two: the variations determined by vertical convection in which the problem of daily fluctuations of meteorological elements is applied, and the distribution of meteorological elements in transformation.

As follows from the aforesaid, the differential equation which describes each of the stated processes after transition to the original variables may be stated in the following form:

$$\frac{\partial q}{\partial t} = \frac{\partial}{\partial z} \kappa \frac{\partial q}{\partial z} + f(t, z) \tag{4}$$

for vertical convections, and

$$u(z) \frac{\partial q}{\partial x} = \frac{\partial}{\partial z} \kappa \frac{\partial q}{\partial z} + f(x, z) \tag{5}$$

for pure transformation. In the latter case only temperature and humidity may be considered.

Formula (3) may indicate the possibility of disregarding



Declassified in Part - Sanitized Copy Approved for Release 2012/03/12 : CIA-RDP82-00039R000100190014-6

Declassified in Part - Sanitized Copy Approved for Release 2012/03/12 : CIA-RDP82-00039R000100190014-6

sources, actually always taking place in natural conditions. Heat sources arise from the inflow of heat from a radiation exchange and the liberation of latent heat of vaporization. Sources of water vapor appear where the processes of phase transformation of water occur. If we should accept the aforestated characteristic scales for temperature and time, then it appears that we may disregard the source of heat when each kilogram of air receives less than one calorie of heat per minute; inasmuch as there must be:

$$f\frac{\tau}{q_0} = \frac{\frac{\Delta Q}{\Delta t}}{C}\frac{\tau}{q_0} \ll 1$$

or

$$\frac{\Delta Q}{\Delta t} \ll 1.4 \frac{\text{calories}}{\text{kilograms} \cdot \text{minutes}}$$

Analogous reasoning may indicate the advisability of disregarding sources of water vapor or Coriolis force when analyzing daily fluctuations in wind vector.

3. Let us consider the daily fluctuations of meteorological elements under the influence of vertical convections. In order to formulate the problem fully, it is necessary first of all to extract boundary conditions. At the start let us take the level at which the mean velocity converts to zero; the value of the coefficient of turbulent diffusion at this level we may designate by $\nu (\nu \geqslant 0)$. With the increase of vertical stability $\nu$ approaches the coefficient of molecular diffusion.



Declassified in Part - Sanitized Copy Approved for Release 2012/03/12 : CIA-RDP82-00039R000100190014-6

Declassified in Part - Sanitized Copy Approved for Release 2012/03/12 : CIA-RDP82-00039R000100190014-6

It is simpler to state boundary conditions for wind; in this case

$$q(t,z)\Big|_{z=0} = 0; \tag{6}$$

$$q(t,z)\Big|_{z=\infty} = q_\infty = u_\infty + iv_\infty .$$

It is considerably more difficult to formulate boundary conditions for temperature and humidity. In order to state the conditions at the lower limit for temperature, it is possible to utilize the equation of heat balance of the active surface. As is known, if the axis z is directed upward, then the indicated equation has the following form:

$$\left| -k\rho C_p \frac{\partial q}{\partial z} + 4\sigma T_0^3 (q - T_0) = R + B + \epsilon \right|_{z=0} . \tag{7}$$

Here $\rho$ is the air density; $C_p$ is specific thermocapacity; $T_0$ is a constant temperature near the mean daily air temperature; $\sigma$ is Boltzmann's constant; R, B, $\epsilon$ are respectively radiational inflow of heat, inflow of ground heat, and inflow of heat through condensation. All three must be expressed in calories per unit of surface and per unit of time.

For the solution of the problem concerning fluctuations at



Declassified in Part - Sanitized Copy Approved for Release 2012/03/12 : CIA-RDP82-00039R000100190014-6

Declassified in Part - Sanitized Copy Approved for Release 2012/03/12 : CIA-RDP82-00039R000100190014-6

the lower limits either humidity or flow may be sought, that is,

$$q(t,z)\Big|_{z=0} = \varphi(t)$$

or

$$\rho K(z)\frac{\partial q}{\partial t} = p(t). \qquad (8)$$

It should be noted that in equation (7) unknown functions enter on the right a priori. In order that the system of equations determining daily fluctuations of temperatures be closed, it is necessary to add equations of transition of radiation and the equation of thermotransmission of the earth. However, inasmuch as the radiation inflow of heat in the lower troposphere does not greatly affect the daily fluctuations of temperature, and the fluctuations of the radiation balance during 24 hours are comparatively well studied and may be forecast (if the forecast for cloudiness is known) then it is natural to accept in (7) R as the desired value. As to the inflow of heat from condensation, it is usually small, and we shall disregard it. The value of B will be determined, if equation (4) is considered, in the field $-L \leqslant z \leqslant \infty$, where $z = -L$ -- depth, at which daily fluctuations of temperatures are exceptionally small. Such a condition does not appear as the only one. There is reason to assume that solving for $R+B+\varepsilon$ may be no less successful than solving for R. The solution may be obtained for both variations. We shall state the conditions at the upper boundaries for temperatures and humidity by



Declassified in Part - Sanitized Copy Approved for Release 2012/03/12 : CIA-RDP82-00039R000100190014-6

Declassified in Part - Sanitized Copy Approved for Release 2012/03/12 : CIA-RDP82-00039R000100190014-6

taking advantage of the known fact concerning the dampening of daily fluctuations of temperatures with altitude, that is,

$$q(t,z)\Big|_{z=\infty} = q_\infty = const. \tag{9}$$

Besides the conditions (6), (7), and (8), the solution should satisfy the original conditions:

$$q(t,z)\Big|_{t=0} = q^0(z). \tag{10}$$

Solving for the coefficient of turbulent diffusion remains. First of all it is important to consider the coefficient's dependence on altitude. At the present time it is an indisputable fact that up to altitudes between 100 and 300 meters the coefficient of turbulence increases almost linearly and at higher altitudes it changes comparatively little. The important factor in considering diurnal fluctuations of meteorological elements is the change of the coefficient of turbulent diffusion in time. These changes appear as the only reason for diurnal fluctuations in the wind vector. In accordance with the stated facts, let us assume that k(t,z) may be presented by the following function:

$$\bar{k}(t,z) = [1+\varphi(t)] \cdot \begin{cases} \nu + cz & \text{for } z \leqslant H \\ \nu + cH & \text{for } z \geqslant H \end{cases}, \tag{11}$$



Declassified in Part - Sanitized Copy Approved for Release 2012/03/12 : CIA-RDP82-00039R000100190014-6

Declassified in Part - Sanitized Copy Approved for Release 2012/03/12 : CIA-RDP82-00039R000100190014-6

where

$$\int_0^\tau \varphi(t)\,dt = 0. \tag{12}$$

So that the diurnal mean value of the coefficient of turbulent diffusion is:

$$\bar{K}(z) = \begin{cases} \nu + cz & \text{for } z \leqslant H \\ \nu + cH & \text{for } z \geqslant H \end{cases}. \tag{13}$$

4. Before attempting the solution of the formulated problems, let us solve the following integral equation, fundamental to the entire future analysis:

$$u_*(t,\lambda) = \int_a^\infty F(\lambda, r)\,u(t,r)\,dr. \tag{14}$$

Here t, $\lambda$ are non-negative parameters; u(t, r) -- an unknown function; F($\nu$, r) is the nucleus of the equation which represents the following differential equation:

$$\frac{d}{dr}\left[p(r)\frac{dF}{dr}\right] + F(\lambda, r)\left[\lambda^2 + q(r)\right] = 0 \tag{15}$$



Declassified in Part - Sanitized Copy Approved for Release 2012/03/12 : CIA-RDP82-00039R000100190014-6

Declassified in Part - Sanitized Copy Approved for Release 2012/03/12 : CIA-RDP82-00039R000100190014-6

and the boundary conditions:

$$\lim_{r \to a} \left[ \alpha p(r) \frac{dF}{dr} - \beta F \right] = 0; \tag{16}$$

$$\lim_{r \to \infty} \left[ F(\lambda, r) \frac{\partial u(t,r)}{\partial r} - u(t,r) \frac{\partial F(\lambda, r)}{\partial r} \right] p(r) \neq \infty. \tag{17}$$

Let us introduce in equation (15) the following substitution of variables:

$$w = \sqrt[4]{\lambda p(r)}\, (\lambda, r); \tag{18}$$

$$\tau = \lambda \int_{r_0}^{r} \frac{dr}{\sqrt{p(r)}}.$$

Then the differential equation for the nucleus may be stated as follows:

$$\frac{d^2 w}{d\tau^2} + w \left[ \frac{1}{16 \lambda^2 p} \left( \frac{dp}{dr} \right)^2 - \frac{1}{4\lambda^2} \frac{d^2 p}{dr^2} + \frac{q(r)}{\lambda^2} + 1 \right] = 0. \tag{19}$$

Of further interest for us will be such values as p(r) and q(r), for which, at great values for r, the following inequality will take place:



Declassified in Part - Sanitized Copy Approved for Release 2012/03/12 : CIA-RDP82-00039R000100190014-6

Declassified in Part - Sanitized Copy Approved for Release 2012/03/12 : CIA-RDP82-00039R000100190014-6

$$\left|\frac{1}{16p}\left(\frac{dp}{dr}\right)^2 - \frac{1}{4}\frac{d^2p}{dr^2} + q(r)\right| \leqslant \frac{M}{\tau^{1+\alpha}}, \tag{20}$$

and

$$\lim_{r \to \infty} \tau = \infty. \tag{21}$$

Here $M \neq 0, \alpha > 0$. In this case, as is known from the theory of Sturm and Liouville, the asymptotic solution of the equation has the following form:

$$w(\tau, \lambda) \sim a'_\lambda \sin(\tau + b_\lambda),$$

and means that

$$\left.\begin{aligned} F(\lambda, r) &= \frac{a_\lambda \sin(\tau + b_\lambda)}{\sqrt[4]{p(r)}} + n_1; \\ \frac{dF(\lambda, r)}{dr} &= \frac{a_\lambda \cos(\tau + b_\lambda)}{\sqrt[4]{p(r)}} \frac{\lambda}{\sqrt{p(r)}} + n_2 \end{aligned}\right\} \tag{22}$$



Declassified in Part - Sanitized Copy Approved for Release 2012/03/12 : CIA-RDP82-00039R000100190014-6

Declassified in Part - Sanitized Copy Approved for Release 2012/03/12 : CIA-RDP82-00039R000100190014-6

Here

$$a_\lambda = \lim_{r \to \infty} \frac{\sqrt[4]{p(r)}\,F(\lambda, r)}{\sin \tau(r)}. \tag{23}$$

Let us find the solution to equation (14) in the form:

$$u(t, r) = \int_0^\infty F(\lambda, r)\,\Phi(t, \lambda)\,d\lambda. \tag{24}$$

Let us multiply (24) by $F(\mu, r)dr$ and integrate from a to R. Then we shall have

$$\int_a^R u(t, r)F(\mu, r)\,dr = \int_a^R F(\mu, r)\,dr \int_0^\infty F(\lambda, r)\,\Phi(t, \lambda)\,d\lambda.$$

Let us now make the following assumption:

$$\int_a^R F(\mu, r)\,dr \int_0^\infty F(\lambda, r)\,\Phi(t, \lambda)\,d\lambda = \int_0^\infty \Phi(t, \lambda)\,d\lambda \int_a^R F(\lambda, r)F(\mu, r)\,dr. \tag{25}$$

Then it will not be difficult to obtain from (15):

$$F(\mu, r)F(\lambda, r) = \frac{1}{\mu^2 - \lambda^2} \frac{d}{dr}\left\{p(r)\left[\frac{dF(\lambda, r)}{dr}F(\mu, r) - F(\lambda, r)\frac{dF(\mu, r)}{dr}\right]\right\},$$



Declassified in Part - Sanitized Copy Approved for Release 2012/03/12 : CIA-RDP82-00039R000100190014-6

Declassified in Part - Sanitized Copy Approved for Release 2012/03/12 : CIA-RDP82-00039R000100190014-6

then

$$\int_a^R u(t,r)F(\mu,r)\,dr = \tag{26}$$

$$= \int_0^\infty \frac{\Phi(t,\lambda)}{\mu^2-\lambda^2}\left\{p(r)\left[\frac{dF(\lambda,r)}{dr}F(\mu,r) - F(\lambda,r)\frac{dF(\mu,r)}{dr}\right]_{r=R}\right\}d\lambda .$$

In this we have utilized condition (22) and assumed that

(27)

$$p(r)\frac{dF(\lambda,r)}{dr}\bigg|_{r=x-0} = p(r)\frac{dF(\mu,r)}{dr}\bigg|_{r=x+0};$$

$$F(\lambda,r)\Big|_{r=x-0} = F(\lambda,r)\Big|_{r=x+0}$$

for $a \leqslant x \leqslant R$.

Let us now select R so large that in stating integral (26) we may use the asymptotic formulas (22). Then, after elementary conversion, (26) will become:

$$\int_a^\infty u(t,r)F(\mu,r)\,dr = \lim_{R\to\infty}\int_0^\infty \frac{\Phi(t,\lambda)a_\lambda a_\mu}{2}\left[\frac{\sin(\mu\tau_1-\lambda\tau_1+b_\mu-b_\lambda)}{\mu-\lambda} - \right.$$

$$\left. - \frac{\sin(\mu\tau_1+\lambda\tau_1+b_\mu+b_\lambda)}{\mu+\lambda}\right]d\lambda .$$



Declassified in Part - Sanitized Copy Approved for Release 2012/03/12 : CIA-RDP82-00039R000100190014-6

Declassified in Part - Sanitized Copy Approved for Release 2012/03/12 : CIA-RDP82-00039R000100190014-6

Let us suppose that $\Phi(t,\lambda)a_\lambda$ satisfies the conditions of Dirichlet. Then

$$\int_a^\infty u(t,r)F(\mu,r)\,dr = \frac{\Phi(t,\mu)a_\mu^2}{2}. \tag{28}$$

By comparing (14) and (28) we shall obtain:

$$\Phi(t,\mu) = \frac{2}{\pi}\,\frac{u_*(t,\mu)}{a_\mu^2} \tag{29}$$

In this manner we shall obtain, if

$$u_*(t,\lambda) = \int_a^\infty F(\lambda,r)u(t,r)\,dr,$$

the following:

$$u(t,r) = \frac{2}{\pi}\int_0^\infty \frac{F(\lambda,r)u_*(t,\lambda)}{\left[\lim\limits_{r\to\infty}\dfrac{\sqrt[4]{p(r)}F(\lambda,r)}{\sin\tau(r)}\right]^2}\,d\lambda. \tag{30}$$

5. In the foregoing paragraphs we have obtained differential equations, we have formulated boundary conditions, and have obtained



Declassified in Part - Sanitized Copy Approved for Release 2012/03/12 : CIA-RDP82-00039R000100190014-6

Declassified in Part - Sanitized Copy Approved for Release 2012/03/12 : CIA-RDP82-00039R000100190014-6

the solution of an integral equation with which we shall seek the solutions which interest us. Let us first of all begin to consider variations of wind under the influence of vertical convection. Equation (4) in this case becomes:

$$\frac{\partial(u+iv)}{\partial t}=\frac{\partial}{\partial z}\left[\bar{k}(z)(1+\varphi)\frac{\partial(u+iv)}{\partial z}\right]-2il(u+iv-u_\infty-iv_\infty). \tag{31}$$

Let us assume, as is usually done, that ox is directed along the geostrophic wind, then $v_\infty=0$; let us seek the solution in the following form:

$$u+iv-u_\infty=\bar{y}(z)+y(t,z). \tag{32}$$

Whereby $\bar{y}(z)$ is the daily mean profile of the wind ($\bar{y}=\bar{u}+i\bar{v}-u_\infty$, the velocity of the wind, for convenience, is reckoned in relation to the system of coordinates moving with the velocity of the geostrophic wind) that is

$$\frac{d}{dz}\bar{k}\frac{d\bar{y}}{dz}-2il\bar{y}=0; \tag{33}$$

$$\bar{y}\Big|_{z=0}=-u_\infty,\ \bar{y}\Big|_{z=\infty}=0. \tag{34}$$



Declassified in Part - Sanitized Copy Approved for Release 2012/03/12 : CIA-RDP82-00039R000100190014-6

Declassified in Part - Sanitized Copy Approved for Release 2012/03/12 : CIA-RDP82-00039R000100190014-6

Then from (31) we obtain:

$$\frac{\partial y}{\partial t} = (1+\varphi)\frac{\partial}{\partial z}\bar{\kappa}\frac{\partial y}{\partial z} + \varphi\frac{\partial}{\partial z}\bar{\kappa}\frac{\partial \bar{y}}{\partial z} - 2i\lambda y, \tag{35}$$

whereby

$$y(t,z)\Big|_{z=0} = 0; \tag{36}$$

$$y(t,z)\Big|_{z=\infty} = 0. \tag{37}$$

Let us multiply (35) by some arbitrary number, for the present, we shall the function $F_1(z,\lambda)\,dz$ and let us integrate from 0 to $\infty$. Then obtain:

$$\frac{d}{dt}\int_0^\infty F_1(z,\lambda)\,y(t,z)\,dz = (1+\varphi)\int_0^\infty \frac{\partial}{\partial z}\left(\bar{\kappa}\frac{\partial y}{\partial z}\right)F_1(z,\lambda)\,dz + \tag{38}$$

$$+\varphi\int_0^\infty F_1\frac{\partial}{\partial z}\left(\bar{\kappa}\frac{\partial \bar{y}}{\partial z}\right)dz - 2i\lambda\int_0^\infty y(t,z)\,p_1(z,\lambda)\,dz.$$

Let us now separately consider,

$$\left.\begin{aligned}\int_0^\infty \frac{\partial}{\partial z}\left(\bar{\kappa}\frac{\partial y}{\partial z}\right)F_1(z,\lambda)\,dz &= \bar{\kappa}\frac{\partial y}{\partial z}F_1(z,\lambda)\Big|_0^\infty - y\bar{\kappa}\frac{dF_1}{\partial z}\Big|_0^\infty + \int_0^\infty y(t,z)\frac{\partial}{\partial z}\left(\bar{\kappa}\frac{dF_1}{dz}\right)dz;\\ \int_0^\infty \frac{d}{dz}\left(\bar{\kappa}\frac{\partial \bar{y}}{dz}\right)F_1(z,\lambda)\,dz &= \bar{\kappa}\frac{d\bar{y}}{dz}F_1(z,\lambda)\Big|_0^\infty - \bar{\kappa}\bar{y}\frac{dF_1}{dz}\Big|_0^\infty + \int_0^\infty \bar{y}(z)\frac{d}{dz}\left(\bar{\kappa}\frac{dF_1}{dz}\right)dz.\end{aligned}\right\} \tag{39}$$



Declassified in Part - Sanitized Copy Approved for Release 2012/03/12 : CIA-RDP82-00039R000100190014-6

Declassified in Part - Sanitized Copy Approved for Release 2012/03/12 : CIA-RDP82-00039R000100190014-6

Let us select $F_1(z, \lambda)$ in such a manner, that

$$\frac{d}{dz}\left[\bar{\kappa}(z)\frac{dF_1}{dz}\right] + \lambda^2 F_1 = 0; \tag{40}$$

$$F_1(z,\lambda)\Big|_{z=0} = 0;$$

$$\bar{\kappa}\frac{dF_1}{dz}\Big|_{z=\infty} < \infty \tag{41}$$

(the parameter $\lambda$ may vary within the limits of $0 \leqslant \lambda \leqslant \infty$). Then from (39) it follows that:

$$\int_0^\infty \frac{d}{dz}\left(\bar{\kappa}\frac{dy}{dz}\right) F_1(z,\lambda)\,dz = -\lambda^2 \int_0^\infty y(t,z) F_1(z,\lambda)\,dz; \tag{42}$$

$$\int_0^\infty \frac{d}{dz}\left(\bar{\kappa}\frac{d\bar{y}}{dz}\right) F_1(z,\lambda)\,dz = -u_\infty \left(\bar{\kappa}\frac{dF_1}{dz}\right)\Big|_{z=0} - \lambda^2 \int_0^\infty \bar{y}(z) F_1(z,\lambda)\,dz. \tag{43}$$

On the other hand, having utilized the differential equation (33), we have

$$\int_0^\infty \frac{d}{dz}\left(\bar{\kappa}\frac{d\bar{y}}{dz}\right) F_1(z,\lambda)\,dz = 2il \int_0^\infty \bar{y}(z) F_1(z,\lambda)\,dz. \tag{44}$$

Then, on the basis of (43) and (44) we obtain:



Declassified in Part - Sanitized Copy Approved for Release 2012/03/12 : CIA-RDP82-00039R000100190014-6

Declassified in Part - Sanitized Copy Approved for Release 2012/03/12 : CIA-RDP82-00039R000100190014-6

$$2il\int_0^\infty \bar{y}(z)F_1(z,\lambda)\,dz = -u_\infty\left(\bar{\kappa}\frac{dF_1}{dz}\right)\Big|_{z=0} - \lambda^2\int_0^\infty \bar{y}(z)F_1(z,\lambda)\,dz. \tag{45}$$

Finding in the last relation $\int_0^\infty \bar{y}(z)F_1(z,\lambda)\,dz$ and substituting it in (43), we shall obtain:

$$\int_0^\infty \frac{d}{dz}\left(\bar{\kappa}\frac{d\bar{y}}{dz}\right)F_1(z,\lambda)\,dz = -u_\infty\left(\bar{\kappa}\frac{dF_1}{dz}\right)\Big|_{z=0}\left\{1-\frac{\lambda^2}{\lambda^2+2il}\right\} = \tag{46}$$

$$= -u_\infty\left(\bar{\kappa}\frac{dF_1}{dz}\right)\Big|_{z=0}\frac{2il}{\lambda^2+2il}.$$

If now we substitute (45) and (42) in (38), then we shall obtain:

$$\frac{du_*}{dt} = -(1+\varphi)\lambda^2 u_* - u_*\left(\bar{\kappa}\frac{dF_1}{dz}\right)\Big|_{z=0}\frac{2il\varphi}{\lambda^2+2il} - 2il u_*, \tag{47}$$

where

$$u_*(t,\lambda) = \int_0^\infty y(t,z)F_1(z,\lambda)\,dz; \tag{48}$$

$$u_{*0} = u_*(t,\lambda)\Big|_{t=0} = \int_0^\infty \left[(u+iv-u_\infty)\Big|_{t=0} - \bar{u}+i\bar{v}-u_\infty\right]F_1(z,\lambda)\,dz. \tag{49}$$



Declassified in Part - Sanitized Copy Approved for Release 2012/03/12 : CIA-RDP82-00039R000100190014-6

Declassified in Part - Sanitized Copy Approved for Release 2012/03/12 : CIA-RDP82-00039R000100190014-6

Integrating we shall obtain:

$$u_*(t,\lambda)=e^{2il t+\lambda^2\int(1+\varphi)\,dt}\left[u_{*0}-\frac{2ilu_\infty\left(\bar{k}\frac{dF_1}{dz}\right)\Big|_{z=0}}{\lambda^2+2il}\int_0^t e^{-2il\xi-\lambda^2\int(1+\varphi)\,d\xi}\varphi(\xi)\,d\xi\right]. \tag{50}$$

On the basis of the formula of reduction (30), we obtain:

$$y(t,z)=\frac{2}{\pi}\int_0^\infty\frac{F_1(\lambda,z)\,u_*(t,\lambda)}{\left[\lim\limits_{z\to\infty}\frac{\sqrt[4]{p(z)}F_1(\lambda,z)}{\sin\tau(z)}\right]^2}\,d\lambda. \tag{51}$$

Concerning the methods of calculating the obtained integrals we shall speak later. Let us only note that if the initial distribution is near the daily mean, then item $u_{*0}$ in formula (50) may disregarded.

6. Let us now take up the question of diurnal fluctuations of temperature and humidity. Basing on the results of a series of investigations made in the last few years, we shall disregard the radiational inflow of heat in comparison with turbulent inflow. In those exceptional cases when this is not permissible, radiational inflow of heat may be accounted for by a respective change in the coefficient of turbulent diffusion (as this was at one time proposed by Simpson and Brent). In the quality of boundary conditions of the problem let us seek the following:

$$\left|\alpha k(z,t)\frac{\partial q}{\partial z}+\beta q(t,z)=P(t)\right|_{z=0}. \tag{52}$$



Declassified in Part - Sanitized Copy Approved for Release 2012/03/12 : CIA-RDP82-00039R000100190014-6

Declassified in Part - Sanitized Copy Approved for Release 2012/03/12 : CIA-RDP82-00039R000100190014-6

Here $\alpha$ and $\beta$ are some constant coefficients not equalling zero simultaneously. (The solution will be given for either $\alpha = 0$, or $\beta = 0$. The general case may be obtained on the basis of either of these examples.)

To solve in the mentioned manner for the boundary conditions is rational because the obtained solution will be acceptable when: (1) solving for flow with the underlying surface as a function of time ($\beta = 0$); (2) solving only for the limiting value of the sought function ($\alpha = 0$); (3) solving for full thermal radiation into the air (turbulent flow and radiation).

We shall obtain conditions for infinity benefiting from the fact that at high enough altitudes the temperature is constant (according to altitude and according to time). Then

$$q(t,z)\Big|_{z=\infty} = q_\infty = const. \tag{53}$$

Let us note that from equation (4), in such a case, it follows that

$$k(z,t)\frac{\partial q}{\partial z}\Big|_{z=\infty} = 0 \tag{54}$$

(if we disregard radiational inflow of heat).



Declassified in Part - Sanitized Copy Approved for Release 2012/03/12 : CIA-RDP82-00039R000100190014-6

Declassified in Part - Sanitized Copy Approved for Release 2012/03/12 : CIA-RDP82-00039R000100190014-6

In general form, let the initial conditions be solved:

$$\left| q(t,z) = q^0(z) \right|_{t=0} . \tag{55}$$

Let us seek the solution in the following form:

$$q(t,z) q_\infty + \theta(t,z) . \tag{56}$$

Then, for $\theta(t, z)$ we shall obtain the following differential equation:

$$\frac{\partial \theta}{\partial t} = \frac{\partial}{\partial z} K(t,z) \frac{\partial \theta}{\partial z} . \tag{57}$$

Let us note that there are difficulties of principle involved in stating the problem concerning the solution for the deviation of temperature from its diurnal mean value, if we take into account the dependency of the coefficient of turbulent diffusion on time.

The boundary conditions of $\theta$ will take the following form:

$$\left| \alpha K(z,t) \frac{\partial \theta}{\partial z} + \beta \theta(t,z) = P(t) - \beta q_\infty = P_1(t) \right|_{z=0} ; \tag{58}$$

$$\theta(t,z)\Big|_{z=\infty} = 0 ; \tag{59}$$

$$K(z,t) \frac{\partial \theta}{\partial z}\Big|_{z=\infty} = 0. \tag{60}$$



Declassified in Part - Sanitized Copy Approved for Release 2012/03/12 : CIA-RDP82-00039R000100190014-6

Declassified in Part - Sanitized Copy Approved for Release 2012/03/12 : CIA-RDP82-00039R000100190014-6

Let us multiply (57) by $F_2(z,\lambda)$ and let us integrate in respect to z from 0 to $\infty$ :

$$\frac{d}{dt}\int_0^\infty \theta(t,z)F_2(z,\lambda)\,dz = \int_0^\infty F_2(z,\lambda)\frac{\partial}{\partial z}\left[\kappa(t,z)\frac{\partial\theta}{\partial z}\right]dz. \tag{61}$$

But

$$\int_0^\infty F_2(z,\lambda)\frac{\partial}{\partial z}\left[\kappa(t,z)\frac{\partial\theta}{\partial z}\right]dz = F_2(z,\lambda)\kappa(t,z)\frac{\partial\theta}{\partial z}\Big|_0^\infty - \theta(t,z)\kappa(t,z)\frac{dF_2}{dz}\Big|_0^\infty +$$

$$+\int_0^\infty \theta(t,z)\frac{d}{dz}\left[\kappa(t,z)\frac{dF_2(z,\lambda)}{dz}\right]dz.$$

Let us now select $F_2(z,\lambda)$ so that

$$\frac{d}{dz}\bar{\kappa}(z)\frac{dF_2}{dz} = -\lambda^2 F_2\ ; \tag{62}$$

$$\left|\alpha\bar{\kappa}(z)\frac{dF_2}{dz} - \beta F_2 = 0\right|_{z=0}. \tag{63}$$

Then, when $\lambda^2 > 0$, it must be that $F_2\big|_{z=\infty} < \infty$; $\frac{\partial F_2}{\partial z}\Big|_{z=\infty} < \infty$.

In such a case, if we utilize conditions (58), (59) and (60) we shall obtain:

$$\int_0^\infty F_2(z,\lambda)\frac{\partial}{\partial z}\left[\kappa(t,z)\frac{\partial\theta}{\partial z}\right]dz = -\lambda^2(1+\varphi)\int_0^\infty \theta(t,z)F_2(z,\lambda) + \tag{64}$$

$$+\begin{cases}\left(\bar{\kappa}\dfrac{dF_2}{dz}\right)\Big|_{z=0}(1+\varphi)\dfrac{p_2(t)}{\beta} & \text{when } \alpha=0;\\[2ex] F_2(0,\lambda)\dfrac{p_2(t)}{\sigma} & \text{when } \beta=0.\end{cases}$$



Declassified in Part - Sanitized Copy Approved for Release 2012/03/12 : CIA-RDP82-00039R000100190014-6

Declassified in Part - Sanitized Copy Approved for Release 2012/03/12 : CIA-RDP82-00039R000100190014-6

Let us for brevity designate

$$P_2(t) = \begin{cases} \left(\bar{k}\frac{dF_2}{dz}\right)\Big|_{z=0}(1+\varphi)\frac{P_1(t)}{\beta} & \text{when } \alpha = 0; \\ F_2(0,\lambda)\frac{P_1(t)}{\alpha} & \text{when } \beta = 0. \end{cases} \tag{65}$$

Then, substituting (64) in (61) and introducing a new function $P_2(z)$, we shall obtain:

$$\frac{du_*}{dt} = -\lambda^2(1+\varphi)u_* - P_2(t), \tag{66}$$

where

$$u_*(\lambda,t) = \int_0^\infty \theta(t,z)F_2(z,\lambda)\,dz, \tag{67}$$

and whereby

$$u_*(\lambda,0) = \int_0^\infty \left[q^0(z) - q_\infty\right]F_2(z,\lambda)\,dz. \tag{68}$$

Integrating in respect to (64), we shall obtain:

$$u_*(\lambda,t) = e^{-\lambda^2\tau}\left[u_*(0,t) - \int_0^t P_2(\xi)e^{\lambda^2\tau(\xi)}\,d\xi\right], \tag{69}$$



Declassified in Part - Sanitized Copy Approved for Release 2012/03/12 : CIA-RDP82-00039R000100190014-6

Declassified in Part - Sanitized Copy Approved for Release 2012/03/12 : CIA-RDP82-00039R000100190014-6

where

$$\tau(t) = \int (1+\rho)\,dt.$$

Because $F_2(z, \lambda)$ satisfies the conditions (15), (16), and $k(z)$ is such that (20) and (21) are also satisfied, we can utilize the formulas of conversion (30). After that the solution sought will be:

$$\theta(t,z) = \frac{2}{\pi}\int_0^\infty \frac{F_1(\lambda,z)\,u_*(\lambda,t)}{\left[\lim\limits_{r\to\infty} \frac{\sqrt[4]{p(r)}\,F_2(\lambda,r)}{\sin\tau(r)}\right]^2}\,d\lambda. \qquad (70)$$

7. In the considering of the question concerning the transformation of a moving air mass under the influence of an underlying surface, we must state a law according to which the velocity varies. The substitution of velocity in equation (5) by one of its constants of altitude of mean value in the given case should give a considerable error due to the fact that the relative horizontal shift of separate layers (which in this case is disregarded) sharply changes the vertical stratification. In connection with this, taking into account the basic peculiarities of the vertical profile of velocity -- great gradients in the lower layers and sharp decrease in them beginning at an altitude on the order of several hundred meters -- let us accept that u(z) may be approximated in the following manner:



Declassified in Part - Sanitized Copy Approved for Release 2012/03/12 : CIA-RDP82-00039R000100190014-6

Declassified in Part - Sanitized Copy Approved for Release 2012/03/12 : CIA-RDP82-00039R000100190014-6

$$u(z) = U\left[\frac{\bar{k}(z)}{k(H)}\right]^{m-1}, \tag{71}$$

where, $\bar{k}(z)$ is specified by formula (13); m is some proper fraction having a mean in the order of 1/10.

The boundary conditions in the problem concerning transformation are the following:

$$q(x,z)\Big|_{x=0} = q^0(z); \tag{72}$$

$$q(x,z)\Big|_{\substack{z=0\\x>0}} = q_0(x); \tag{73}$$

$$q(x,z)\Big|_{z=\infty} = q^0(z)\Big|_{z=\infty} = q_\infty . \tag{74}$$

In the given case, from the differential equation (5) it follows that

$$\bar{k}\frac{\partial q}{\partial z}\Big|_{z=\infty} = 0. \tag{75}$$

Equation (5) in the given case is stated

$$u(z)\frac{\partial q}{\partial x} = \frac{\partial}{\partial z}\left[\bar{k}(z)\frac{\partial q}{\partial z}\right]. \tag{76}$$



Declassified in Part - Sanitized Copy Approved for Release 2012/03/12 : CIA-RDP82-00039R000100190014-6

Declassified in Part - Sanitized Copy Approved for Release 2012/03/12 : CIA-RDP82-00039R000100190014-6

Let $q(x,z) = q_\infty + \theta(x,z)$, then for $\theta(x,z)$ the differential equation will remain unchanged, but the boundary conditions will take the following form:

$$\theta(x,z)\Big|_{x=0} = q^0(z) - q_\infty ; \tag{77}$$

$$\theta(x,z)\Big|_{\substack{z=0 \\ x>0}} = q_0(x) - q_\infty ; \tag{78}$$

$$\theta(x,z)\Big|_{z=\infty} = 0; \tag{79}$$

$$\bar{\kappa}(z)\frac{\partial\theta(x,z)}{\partial z}\Big|_{z=\infty} = 0. \tag{80}$$

We shall seek the solution in the same manner as in the foregoing cases. We shall multiply equation (74) by $F_3(z,\lambda)dz$ and integrate in respect to z between 0 and $\infty$. Then

$$\frac{d}{dx}\int_0^\infty u(z)\theta(x,z)F_3(z,\lambda)\,dz = \int_0^\infty F_3(z,\lambda)\frac{\partial}{\partial z}\left[\bar{\kappa}(z)\frac{\partial q}{\partial z}\right]dz. \tag{81}$$

Let us now consider the right integral

$$\int_0^\infty F_3(z,\lambda)\frac{\partial}{\partial z}\left[\bar{\kappa}(z)\frac{\partial\theta}{\partial z}\right]dz = F_3(z,\lambda)\kappa\frac{\partial\theta}{\partial z}\Big|_0^\infty - \theta\bar{\kappa}\frac{dF_3}{dz}\Big|_0^\infty + \tag{82}$$

$$+\int_0^\infty \theta\frac{\partial}{\partial z}\left(\bar{\kappa}\frac{dF_3}{\partial z}\right)dz = [q_0(x)-q_\infty]\left(\bar{\kappa}\frac{dF_3}{dz}\right)\Big|_{z=0} - \lambda^2\int_0^\infty \theta(x,z)F_3(z,\lambda)u(z)\,dz.$$



Declassified in Part - Sanitized Copy Approved for Release 2012/03/12 : CIA-RDP82-00039R000100190014-6

Declassified in Part - Sanitized Copy Approved for Release 2012/03/12 : CIA-RDP82-00039R000100190014-6

If only

$$F_3(z,\lambda)=0; \tag{83}$$

$$F_3(z,\lambda)\Big|_{z=\infty} < \infty; \tag{84}$$

$$\bar{\kappa}\frac{\partial F_3}{dz}\Big|_{z=\infty} < \infty; \tag{85}$$

$$\frac{d}{dz}\left(\bar{\kappa}\frac{dF_3}{dz}\right)=-\lambda^2 u(z)F_3 . \tag{86}$$

In such a solution of F3(z, $\lambda$ ), (79) will be stated in the following form:

$$\frac{du_*''}{dx}+\lambda^2 u_*''-[q_0(x)-q_\infty]\left(\bar{\kappa}\frac{dF_3}{dz}\right)\Big|_{z=0}=0, \tag{87}$$

whereby

$$u_*''(x,\lambda)=\int_0^\infty \theta(x,z)u(z)F_3(z,\lambda)\,dz . \tag{88}$$



Declassified in Part - Sanitized Copy Approved for Release 2012/03/12 : CIA-RDP82-00039R000100190014-6

Declassified in Part - Sanitized Copy Approved for Release 2012/03/12 : CIA-RDP82-00039R000100190014-6

Let us designate:

$$u_*''(0,\lambda)=\int_0^\infty [q^0(z)-q_\infty]u(z)F_3(z,\lambda)\,dz\,. \tag{89}$$

Utilizing the formulas of conversion (29) and (30, we shall obtain:

$$\theta(x,z)u(z)=\frac{2}{\pi}\int_0^\infty \frac{F_3(\lambda,z)u_*''(t,\lambda)}{\left[\lim\limits_{z\to\infty}\dfrac{\sqrt[4]{p(z)}\,F_3(\lambda,z)}{\sin\tau(z)}\right]^2}\,d\lambda\,. \tag{90}$$

8. The solutions obtained above as follows from the calculations, represent general solutions of the problems for the functions of the class k(z) and u(z). The limitations placed on k(z) and u(z) follow only from the laws governing the use of the formulas of conversion (29) and (30).

In this manner a series of conclusions concerning the laws of diurnal variations of meteorological elements and their transformations may be made even without problems such as the functions u(z) and k(z). It is sufficient to utilize only some of their properties (behavior at infinity, limit and continuity along the entire area).

Let us now give expressions for the functions $F_1(z,\lambda)$, $F_2(z,\lambda)$, $F_3(z,\lambda)$, specifying k(z) and u(z) in accordance with formulas (13) and (69). First of all, let us note that any of the functions $F_i$ may be determined on the basis of known boundary conditions



Declassified in Part - Sanitized Copy Approved for Release 2012/03/12 : CIA-RDP82-00039R000100190014-6

Declassified in Part - Sanitized Copy Approved for Release 2012/03/12 : CIA-RDP82-00039R000100190014-6

only with an accuracy approaching the constant factor. However, this is sufficient to obtain the solution sought since in the last formulas (50), (68), (88), the functions $F_i(z, \lambda)$ appear so, that the unknown factor will appear in the numerator and the denominator in the same degree and will cancel out. For simplicity when seeking $F_i(z, \lambda)$ we shall consider this multiplier as equal to unity. The solutions for $F_i(z, \lambda)$, if k(z) and u(z) are specified by formulas (13) and (69), appear as cylindrical functions with a zero symbol for $0 \leqslant z \leqslant H$ and a trigonometric function for $z > H$. Integrating with respect to equations (40), (62), and (84), having utilized the conditions on the lower boundary and the continuity of $F_i$, $dF_i/dz$ on the level of $z=H$, and taking one of the arbitrary constants as equal to unity, we obtain:

$$F_i = A_i I_0\left[2\lambda b_i (\nu+cz)^{r_i}\right] + B_i N_0\left[2\lambda b_i (\nu+cz)^{r_i}\right] \qquad (91)$$

for $0 \leqslant z \leqslant H$

and

$$F_i = C_i \sin \lambda N_i (z-H+\delta_i) \quad \text{for } z \geqslant H. \qquad (92)$$

Values obtained for coefficients are contained in Table II. $\delta_i$ is determined from the following equation:



Declassified in Part - Sanitized Copy Approved for Release 2012/03/12 : CIA-RDP82-00039R000100190014-6

Declassified in Part - Sanitized Copy Approved for Release 2012/03/12 : CIA-RDP82-00039R000100190014-6

$$-\tan \lambda N_i \delta_i = \frac{A_i J_0[2\lambda b_i (\nu+cH)^{r_i}] + B_i N_0[2\lambda b_i (\nu+cH)^{r_i}]}{A_i J_1[2\lambda b_i (\nu+cH)^{r_i}] + B_i N_0[2\lambda b_i (\nu+cH)^{r_i}]} \quad (93)$$

In order to compute according to the formulas obtained, it is possible to change the sequence in the integrals representing the solution. Then the internal integrals may be tabulated and computation for concrete examples in each case will be reduced to simple quadratics, which may be solved by computation or graphically.



Declassified in Part - Sanitized Copy Approved for Release 2012/03/12 : CIA-RDP82-00039R000100190014-6

Declassified in Part - Sanitized Copy Approved for Release 2012/03/12 : CIA-RDP82-00039R000100190014-6



Table 2.

| | $r_i$ | $b_i$ | $A_i$ | $B_i$ | $N_i^2$ | $C_i^2 = \frac{1}{\sqrt{\nu+cH}} \lim_{z\to\infty}\left[\frac{\sqrt{p(z)}F_2(\lambda)z}{\sin\tau(z)}\right]^2$ |
|---|---|---|---|---|---|---|
| $i=1$<br>$i=2$<br>$\alpha=0$ | $\frac{1}{2}$ | $\frac{1}{C}$ | $N_0(2\lambda b_1\sqrt{\nu})$ | $-J_0(2\lambda b_1\sqrt{\nu})$ | $\frac{1}{\nu+cH}$ | $[A_1J_1(2\lambda b_1\sqrt{\nu+cH})+B_1N_1(2\lambda b_1\sqrt{\nu+cH})]^2 +$<br>$+[A_1J_0(2\lambda b_1\sqrt{\nu+cH})+B_1N_0(2\lambda b_1\sqrt{\nu+cH})]^2$ |
| $i=2$<br>$\beta=0$ | $\frac{1}{2}$ | $\frac{1}{C}$ | $N_1(2\lambda b_2\sqrt{\nu})$ | $-J_1(2\lambda b_2\sqrt{\nu})$ | $\frac{1}{\nu+cH}$ | $[A_2J_1(2\lambda b_2\sqrt{\nu+cH})+B_2N_1(2\lambda b_2\sqrt{\nu+cH})]^2 +$<br>$+[A_2J_0(2\lambda b_2\sqrt{\nu+cH})+B_2N_0(2\lambda b_2\sqrt{\nu+cH})]^2$ |
| $i=3$ | $\frac{m}{2}$ | $\sqrt{\frac{N}{m^2c^2(\nu+cH)^{m-1}}}$ | $N_0(2\lambda b_3\nu^{m/2})$ | $-J_1(2\lambda b_3\nu^{m/2})$ | $\frac{U}{\nu+cH}$ | $[A_3J_1(2\lambda b_3(\nu+cH)^{m/2})+B_3N_1(2\lambda b_3(\nu+cH)^{m/2})]^2 +$<br>$+[A_3J_0(2\lambda b_3(\nu+cH)^{m/2})+B_2N_0(2\lambda b_3(\nu+cH)^{m/2})]^2$ |

Declassified in Part - Sanitized Copy Approved for Release 2012/03/12 : CIA-RDP82-00039R000100190014-6

Declassified in Part - Sanitized Copy Approved for Release 2012/03/12 : CIA-RDP82-00039R000100190014-6

# ON THE HYPERBOLIC EQUATION OF A VERTICAL TURBULENCE EXCHANGE IN THE ATMOSPHERE

E. S. Lyapin

1. Displacements of large air masses along the surface of the earth are important phenomena that affect the climate of separate areas of the world sphere and cause changes in weather in either one or another point on the earth's surface. Movement of air of the character mentioned appears in the form of wind whose intensity and direction of average velocity (measured at a considerable distance from the surface of the earth) show with what speed and in what direction movements of air masses are taking place at the moment. Along with the given phenomena of movement of air, there is one more important characteristic: neither the velocity of the wind nor its direction remain unchanged for even the smallest period of time. These constant changes in each moment of time and at each point are not ordered and cannot be studied in each of their individual developments, and together consist in what we call the turbulent condition of the atmosphere. Because the movement of air in the atmosphere is always of a turbulent nature, it determines many important processes occurring in the atmosphere itself, as well as on the surface of the earth subject to the action of atmospheric air.

The exchange of heat from one air mass to another or between the air and the surface of the earth, as well as between separate areas of the surface of the earth, is determined by no means solely (and even not so much) by the molecular exchange of heat in the air or in a mass of earth, but is principally attributed to the exchange



Declassified in Part - Sanitized Copy Approved for Release 2012/03/12 : CIA-RDP82-00039R000100190014-6

Declassified in Part - Sanitized Copy Approved for Release 2012/03/12 : CIA-RDP82-00039R000100190014-6

of heat between separate turbulent bodies, that is, separate air masses completing one or another individual movements apart from the overall movement of greater air masses. The same pertains to the distribution and exchange of moisture in the atmosphere. By this we determine the important processes of evaporation. The study of the mechanics of movement of the air is based wholly on the study of the characteristics of turbulence.

Turbulence exchange is of particular interest, that is, the mixing of air due to the turbulent features of its movement in a vertical direction in relation to the earth's surface. Nearly all of the many faceted and extremely difficult processes of interaction of the earth's surface with the atmosphere are determined precisely by vertical turbulence exchange. The considerable heterogeneity of the various characteristics of the air with regard to changes in altitude (considerably greater than horizontal differences) is in the same way determined by vertical turbulence exchange. The aim of the present article is the consideration of some questions regarding the study of vertical turbulence exchange of the atmosphere.

The process of turbulence exchange is most conveniently described by assuming the presence in the air of some mixture-substance which is passively transferred by the moving air and which does not in the least affect the movement of the air. Changes in the concentration of such a substance and its flow along such or other surfaces will be best of all characterized by the complex process of turbulence exchange. Therefore, we will in the future consistently consider turbulence exchange from



Declassified in Part - Sanitized Copy Approved for Release 2012/03/12 : CIA-RDP82-00039R000100190014-6

Declassified in Part - Sanitized Copy Approved for Release 2012/03/12 : CIA-RDP82-00039R000100190014-6

this point of view. We shall suppose that there is such a substance, whose concentration for each unit of volume we shall designate with the letter $\varphi$, and the flow along a certain unit of surface we shall designate with the letter p. In connection with the problem of studying the vertical exchange only, we shall consider these values in relation to two independent variables: time t and space coordinate z directed vertically upward from the surface of the earth and whose equation, let us assume, is $z = \epsilon$ (where $\epsilon \neq 0$, which for purely technical reasons will be more convenient than the commoner $\epsilon = 0$).

In this manner our $\varphi$ and p in reality will be values averaged along given horizontal surfaces. The latter may be regarded as extensive enough (in connection with the above-mentioned property of relatively small change in the character of the air in the horizontal as compared to the vertical direction). This, in particular, allows us to regard $\varphi$ and p, as well as other values, as changing sufficiently regularly in time and direction z that is, particularly as regards the capacity of being differentiated a sufficient number of times in respect to z and t), which in the future we shall not specifically limit.

The process of turbulence exchange, both in a general way and specifically in various meteorological problems, is fully studied and described in scientific literature. Usually, the basis for the study of the process has been the so-called Fick's equation of turbulence diffusion. It has the following form:



Declassified in Part - Sanitized Copy Approved for Release 2012/03/12 : CIA-RDP82-00039R000100190014-6

Declassified in Part - Sanitized Copy Approved for Release 2012/03/12 : CIA-RDP82-00039R000100190014-6

$$\frac{\partial \varphi}{\partial t} = \frac{\partial}{\partial z}\left[k_z \frac{\partial \varphi}{\partial z}\right] . \qquad (1)$$

The process of vertical turbulence intermixing appears as the most important characteristic of the process of turbulence exchange (other characteristics appear by the addition of boundary conditions to this equation). It was discovered long ago that $k_z$ is the value that is essentially dependent on z. In order to study comparatively lengthy processes it is necessary as well to consider the dependence of $k_z$ on t.

With the aid of Fick's equation in meteorology, a certain number of valuable results were obtained. Of the latter, in the order of their appearance, let us mention first of all the work of M. I. Yudin [1] and M. I. Budyko [2]. The usual fully satisfactory correspondence of theoretical calculations with experiments and observation of natural processes proves that the above-mentioned equation basically provides the correct mechanism of actual phenomena. However, at the same time, there appear some divergencies with actuality. For example, Fick's equation gives an instantaneous velocity to the diffusion of admixtures in the atmosphere, which, of course, is fiction. The area in which it is permissible to apply Fick's equation is also not clear. And here, observations leave no doubt that this area does not coincide with the area of all conditions actually encountered which are of interest (for example, Fick's equation does not serve to describe phenomena



Declassified in Part - Sanitized Copy Approved for Release 2012/03/12 : CIA-RDP82-00039R000100190014-6

Declassified in Part - Sanitized Copy Approved for Release 2012/03/12 : CIA-RDP82-00039R000100190014-6

$$\frac{\partial \varphi}{\partial t} = \frac{\partial}{\partial z}\left[k_z \frac{\partial \varphi}{\partial z}\right] . \qquad (1)$$

The process of vertical turbulence intermixing appears as the most important characteristic of the process of turbulence exchange (other characteristics appear by the addition of boundary conditions to this equation). It was discovered long ago that $k_z$ is the value that is essentially dependent on z. In order to study comparatively lengthy processes it is necessary as well to consider the dependence of $k_z$ on t.

With the aid of Fick's equation in meteorology, a certain number of valuable results were obtained. Of the latter, in the order of their appearance, let us mention first of all the work of M. I. Yudin [1] and M. I. Budyko [2]. The usual fully satisfactory correspondence of theoretical calculations with experiments and observation of natural processes proves that the above-mentioned equation basically provides the correct mechanism of actual phenomena. However, at the same time, there appear some divergencies with actuality. For example, Fick's equation gives an instantaneous velocity to the diffusion of admixtures in the atmosphere, which, of course, is fiction. The area in which it is permissible to apply Fick's equation is also not clear. And here, observations leave no doubt that this area does not coincide with the area of all conditions actually encountered which are of interest (for example, Fick's equation does not serve to describe phenomena



Declassified in Part - Sanitized Copy Approved for Release 2012/03/12 : CIA-RDP82-00039R000100190014-6

Declassified in Part - Sanitized Copy Approved for Release 2012/03/12 : CIA-RDP82-00039R000100190014-6

on the limit of distribution of substance; it cannot be applied to the study of processes under conditions of fully developed thermal convections, etc).

The given situation should not cause any special perplexity, because actually we do not have sufficient proof for the derivation of Fick's equation; it is not derived so much as guessed or selected (according to natural but unproved and little competent analogy with the processes of molecular diffusion and heat conductivity). A more detailed consideration of the problem will result in more-or-less unexpected conclusions that a sufficiently strict basis for Fick's equation, applicable to the conditions of the actual atmosphere, in reality cannot be demonstrated. This equation appears to be merely a simplification applicable only under certain conditions and always resulting in certain essential distortions compared with another differential equation which describes much more accurately the process of vertical turbulence. This latter equation was started and developed elsewhere by me [3]. Its description and certain hints as to the method of solution we must take up below.

Here we must note that due to the lack of sufficient proof of Fick's equation, the question whether or not it is possible to use it for the consideration of turbulence of atmosphere has been raised more than once in scientific literature. At one time it even seemed that the investigations of L. F. Richardson [7], [8] and A. M. Obukhov [4] gave a negative answer. In this respect the arguments were in some cases made not only against



Declassified in Part - Sanitized Copy Approved for Release 2012/03/12 : CIA-RDP82-00039R000100190014-6

Declassified in Part - Sanitized Copy Approved for Release 2012/03/12 : CIA-RDP82-00039R000100190014-6

Fick's equation itself, but also against any differential equations of the same character which sought to describe the process herein studied. However, the attempts to utilize the above-mentioned results for refuting Fick's equation appeared incompetent and were based, in the main, on a misunderstanding of the idea of Fick's equation (or any other equation for this same process). This situation was clarified by M. I. Yudin [7]. Our opposition, or comment rather, against the area of admissibility of application of Fick's equation is based on completely different considerations and does not hinder the utilization of this equation under certain conditions.

2. The development of the equation, or rather, the systems of the equation obtained in the above-mentioned work [3] is based on the following considerations.

The particles of our assumed substance are divided into two classes. To the first (+) belong the particles moving at a given moment in a positive direction of axis oz, and to the second (-), those traveling in a negative direction. Further in space a thin horizontal layer P, of substantial horizontal extent, is taken out. A balance of inflow and diminution of particles of both classes is formed for this layer.

Let us designate $\varphi^{\mp}$ and $\bar{\varphi}$ as the concentration of particles of both classes; $s^{\mp}$ and $\bar{s}$ as the mean values of absolute magnitudes composing their velocities along axis oz; and, finally, $\rho^{\mp}$ as the ratio to the general "number" of class (+) particles, (that is $\varphi^{\mp}$) the amount of particles transferring



Declassified in Part - Sanitized Copy Approved for Release 2012/03/12 : CIA-RDP82-00039R000100190014-6

Declassified in Part - Sanitized Copy Approved for Release 2012/03/12 : CIA-RDP82-00039R000100190014-6

inside P in a unit of volume per unit of time from class (+) into class (-) (analogously for $\bar{\rho}$ ). Then the above-mentioned balance may be expressed by the equations:

$$\left.\begin{aligned} \frac{\partial \varphi}{\partial t} &= -\frac{\partial(\overset{+}{s}\overset{+}{\varphi})}{\partial t} + \bar{\rho}\bar{\varphi} - \overset{+}{\rho}\overset{+}{\varphi}; \\ \frac{\partial \varphi}{\partial t} &= \frac{\partial(\bar{s}\bar{\varphi})}{\partial z} - \bar{\rho}\bar{\varphi} + \overset{+}{\rho}\overset{+}{\varphi}. \end{aligned}\right\} \qquad (2)$$

And now let us introduce new values:

$$u = \frac{\overset{+}{s} + \bar{s}}{2}, \quad v = \frac{\overset{+}{s} - \bar{s}}{2}, \qquad (3)$$

$$\varphi = \overset{+}{\varphi} + \bar{\varphi}, \quad \tau = \overset{+}{\varphi} - \bar{\varphi}.$$

The physical meaning of u and v is evident; $\varphi$ is of course the amount of concentration introduced earlier. As regards $\tau$, it is a convenient auxiliary value related to flow $p$, because it (and in the important case, when $\bar{s} - \bar{s} = 0$ (or is sufficiently small), $\tau$ is directly) is evident that:

$$p = \overset{+}{\varphi}\overset{+}{s} - \bar{\varphi}\bar{s}$$

and in this case

$$\overset{+}{s} = \bar{s} = u, \quad p = \tau u.$$



Declassified in Part - Sanitized Copy Approved for Release 2012/03/12 : CIA-RDP82-00039R000100190014-6

Declassified in Part - Sanitized Copy Approved for Release 2012/03/12 : CIA-RDP82-00039R000100190014-6

The further consideration of the present study will refer not to the general case described by system (4), but to a certain narrower area of conditions characterized by certain additional supplementary relationships which simplify the investigation of system (4). These conditions are more favorable for utilizing Fick's equation and therefore are more applicable to the aims of comparing results obtained with the aid of equations (1) and (4).

Let us now evolve the conditions of the aforementioned area. First of all, let us make the supposition on the so-called local symmetry, that is, let us consider that the following takes place:

$$1)\ \overset{+}{s} = s\ (\text{that is, } v = 0);\quad 2)\ \overset{+}{\rho} = \overset{-}{\rho}. \tag{5}$$

Essentially, these equalities imply the supposition concerning the fact that with any z the character of the movement in a positive direction of the axis oz does not differ as such from that of the negative direction of oz, because their respective characteristics are equal in number. Without doubt, a like supposition for a surface layer of air will not be actually true. Under some conditions it will be absolutely inadmissible. For example, under a strongly expressed convection, when the temperature of the air diminishes considerably with altitude, an orderly movement in a vertical direction, acting on the mixing of the air, is formed. The character of this movement is such that the rise is accomplished with a velocity different from that of the fall. It follows then,



Declassified in Part - Sanitized Copy Approved for Release 2012/03/12 : CIA-RDP82-00039R000100190014-6

Declassified in Part - Sanitized Copy Approved for Release 2012/03/12 : CIA-RDP82-00039R000100190014-6

that local symmetry does not hold. However, under moderate temperature gradients, the difference in the character of the movement of air upward or downward is not so essential, and suppositions (5) may evoke only a small error. Let us note that usually similar suppositions were made quite arbitrarily without supplementary explanations, which, generally speaking, appears as carelessness that may react upon the noticeable errors. For an illustration of the property considered herein let us take up the results of experiments in the work of A. R. Konstantinov [5].

Here the value $\left(\frac{\bar{s}'}{\bar{s}}\right)$, measured at altitudes of 2 meters and 11 meters, is considered in relation to the change in the value $\frac{\Delta\Theta}{u_1^2}$, where $\Delta\Theta$ is the difference of the air temperatures at heights of 55 centimeters and 200 centimeters and is the mean value of the air velocity at 100 centimeters.

Of late, the employment of this value for the characteristics of the degree of stability of the atmosphere is becoming more and more frequent. Besides [7], see, for example, the works of M. I. Budyko [2] and D. L. Laykhtman [6].

From Figure 1 we see that within the limits of the considered meaning of the value $\frac{\Delta\Theta}{u_1^2}$, the value $\left(\frac{\bar{s}'}{\bar{s}}\right)$ on an average deviates not more than 10 percent (of which we have previously spoken).

The second assumption, limiting the area of the considered conditions, is that $u$ does not change with altitude. Even though $u$ actually depends on altitude (it increases with altitude), such



Declassified in Part - Sanitized Copy Approved for Release 2012/03/12 : CIA-RDP82-00039R000100190014-6

Declassified in Part - Sanitized Copy Approved for Release 2012/03/12 : CIA-RDP82-00039R000100190014-6

an assumption was always stated or implied in all analogical investigations. Not risking to state a definite judgment on this account, we still believe that under certain conditions this is admissible. Were it absolutely inadmissible, it would be difficult to explain the relatively acceptable verifications in experience by the results of countless investigations based on this assumption (in a direct form or in a form of equivalent hypotheses).

Finally, the third assumption is the hypothesis concerning the linear increase of $k_z = \frac{u^2}{2\rho}$ ($\rho$ is $\rho^+$, equal, in accordance with (5) to $\bar{\rho}$) with altitude.

In the above assumptions, $k_z$, as is not difficult to see, in our equations becomes the coefficient of vertical exchange, the same coefficient which participates in Fick's equation, obtained in our equations by means of disregarding several members, concerning which see (3). The increase of $k_z$ with altitude has been investigated fully, and there are very convincing data [2], [5] regarding the fact that in a sufficiently wide area of conditions k increases with altitude in near accordance with a linear rule. Let us in this connection note that the values $k_z$ are just as strongly dependent on stability. For example, in the above-mentioned work of A. R. Konstantinov [5] there is the following graph of the relationships of $k_z$ and the value $\frac{\Delta\Theta}{u_1^2}$. Here the points relate to the values of $k_z$, computed on the basis of observations with the aid of formulas stated in (3), and the curve corresponds to the values of $k_z$ according to the theory of M. I. Budyko.



Declassified in Part - Sanitized Copy Approved for Release 2012/03/12 : CIA-RDP82-00039R000100190014-6

Declassified in Part - Sanitized Copy Approved for Release 2012/03/12 : CIA-RDP82-00039R000100190014-6

In connection with the assumption concerning the linear increase of z, it is natural to introduce further the value $k = \frac{k_z}{z} = \frac{u^2}{2\rho z}$, [redacted] which may be considered as independent of z. (In a linear expression of $k_z$ to z we need not express a free member because the surface of the earth is given by us by the equation $z = \epsilon$, where $\epsilon$ may be considered as selected so that $k_z$ would equal $k_z$). Further, those parameters entering into the coefficients of the equation will be expressed through k and through $u^2$ (in particular $\rho = \frac{u^2}{2kz}$). Because the changes in time of the mean characteristics are comparatively slow, we will consider that k and $u^2$ do not depend solely on z, but also on t.

As a result of the assumptions made, system (4) will have the following form:

$$\varphi_t' = -p_z' \; ; \tag{6}$$

$$p_t' = -u^2 \varphi_z' - \frac{u^2}{k_z} p .$$

For the integration of this sytem it is best to first exclude the value $\varphi$. For this it is necessary to multiply the first equation by $(-u^2)$ and to differentiate in respect to z; the second equation is differentiated in respect to t, after which both equations are added. As a result we obtain a new equation:

$$p_{tt}'' - u^2 p_{zz}'' + \frac{u^2}{k_z} p_t' = 0. \tag{7}$$



Declassified in Part - Sanitized Copy Approved for Release 2012/03/12 : CIA-RDP82-00039R000100190014-6

Declassified in Part - Sanitized Copy Approved for Release 2012/03/12 : CIA-RDP82-00039R000100190014-6

In this manner the problem has resulted in the integration of equation (7), to which, for the singleness of solution, these or other boundary conditions must be added. Having found p, we can from (6) obtain with facility an expression for $\varphi$ .

3. Having as an aim the solution of the problem formulated at the end of paragraph 2, we shall begin to search for the general solution of the equation which on the one hand will be a certain generalization of equation (7), inasmuch as the new equation is heterogeneous, and on the other hand will give (7) only a particular incident where the parameters are bounded by the relation $u = 2k$:

$$S''_{tt} - 4k^2 S''_{zz} + \frac{4k}{z} S'_t = H(z,t). \qquad (8)$$

Let us introduce a new unknown:

$$r = \frac{\alpha}{z} S + \beta S_z + \gamma S'_t ;$$

$$r_t = \frac{\alpha}{z} S_t + \beta S''_{zt} + \gamma S''_{tt} ;$$

$$r_z = -\frac{\alpha}{z^2} S + \frac{\alpha}{z} S_z + \beta S''_{zz} + \gamma S''_{tz} .$$

Here $\alpha, \beta, \gamma$ are constants, for the present arbitrary. Let us add all three equations, having previously multiplied the first by $\frac{\lambda}{z}$ , the second by $\gamma$ , and the third by $-\beta$ .

$$\frac{\lambda}{z} r + \gamma r'_t - \beta r'_z = \gamma^2 S''_{tt} - \beta^2 S'_{zz} + \left(\frac{\lambda\gamma}{z} + \frac{\alpha\gamma}{z}\right) S'_t + \left(\frac{\lambda\beta}{z} - \frac{\alpha\beta}{z}\right) S'_z + \left(\frac{\alpha\lambda}{z^2} + \frac{\alpha\beta}{z^2}\right) S .$$



Declassified in Part - Sanitized Copy Approved for Release 2012/03/12 : CIA-RDP82-00039R000100190014-6

Declassified in Part - Sanitized Copy Approved for Release 2012/03/12 : CIA-RDP82-00039R000100190014-6

Let us assume

$$\alpha = \lambda = -\beta = 2\kappa, \quad \gamma = 1.$$

Then

$$r_t' + 2\kappa r_z + \frac{2\kappa}{z} r = s_{tt}'' - 4\kappa^2 s_{zz}'' + \frac{4\kappa}{r} s_t.$$

In agreement with (3) we obtain:

$$r_t' + 2\kappa r_z' + \frac{2\kappa}{z} r = H(z,t).$$

Let us solve the equation with respect to the unknown r. For this we shall introduce new independent variables:

$$\kappa_1 = z, \quad \kappa_2 = z - 2\kappa t.$$

The equation becomes:

$$-2\kappa r_2' + 2\kappa r_1' + 2\kappa r_2 + \frac{2\kappa}{\kappa_1} r = H\left(\kappa_1, \frac{\kappa_1 - \kappa_2}{2\kappa}\right);$$

$$r_1' + \frac{1}{\kappa_1} r = \frac{1}{2\kappa} H(z,t);$$

$$r = -\frac{A}{\kappa_1};$$

$$-\frac{A'}{\kappa_1} + \frac{A}{\kappa_1^2} - \frac{A}{\kappa_1^2} = \frac{1}{2\kappa} H(z,t);$$

$$A' = -\frac{\kappa_1}{2\kappa} H(z,t)$$

$$A = f(\kappa_2) - \frac{1}{2\kappa} \int_{\epsilon}^{\kappa_1} \kappa_1 H\left(\kappa_1, \frac{\kappa_1 - \kappa_2}{2\kappa}\right) d\kappa_1;$$

$$r = -\frac{1}{z} f(z - 2\kappa t) + \frac{1}{2\kappa z} \int_{\epsilon}^{z} \beta H\left(\beta, \frac{\beta - z + 2\kappa t}{2\kappa}\right) d\beta.$$



Declassified in Part - Sanitized Copy Approved for Release 2012/03/12 : CIA-RDP82-00039R000100190014-6

Declassified in Part - Sanitized Copy Approved for Release 2012/03/12 : CIA-RDP82-00039R000100190014-6

Here f is a completely arbitrary function. Let us mentally place the found value for r in a relation between r and s:

$$S_t - 2\kappa S_z r + \frac{2\kappa}{z} s = r.$$

Let us introduce new independent variables:

$$k_1 = z, \quad k_2 = z + 2\kappa t$$

We obtain:

$$r = -\frac{1}{\kappa} f(2k_1 - k_2) + \frac{1}{2\kappa k_1} \int_{\epsilon}^{k_1} \beta H\left(\beta, \frac{\beta - 2k_1 + k_2}{2\kappa}\right) d\beta;$$

$$2\kappa s_2' - 2\kappa s_1' - 2\kappa s_2' + \frac{2\kappa}{k_1} s = r; \quad s_1' - \frac{1}{k_1} s = -\frac{1}{2\kappa} r; \quad s = A k_1;$$

$$A_{k_1}' + A - A = -\frac{1}{2\kappa} r; \quad A' = -\frac{1}{2\kappa k_1} r;$$

$$A = -\frac{1}{2\kappa} \int_{\epsilon}^{k_1} \frac{r}{k_1} dk_1 + \varphi(k_2);$$

$$s = -\frac{z}{2\kappa} \int_{\epsilon}^{\bar{z}} \frac{r}{k_1} dk_1 + z\varphi(z + 2\kappa t);$$

$$S = -\frac{z}{4\kappa^2} \int_{\epsilon}^{z} \frac{d\alpha}{\alpha^2} \int_{\epsilon}^{k} \beta H\left(\beta, \frac{\beta - 2\alpha + z + 2\kappa t}{2\kappa}\right) d\beta +$$

$$+ \frac{z}{2\kappa} \int_{\epsilon}^{z} f \frac{(2\alpha - z - 2\kappa t) d\alpha}{\alpha^2} + z\varphi(z + 2\kappa t). \qquad (9)$$

This is the general solution of equation (8). The functions f and g are arbitrary. Let us return to our equation (7) for the flow of p.

$$p_{tt}'' - u_*^2 p_{zz}'' + \frac{u_*^2}{\kappa z} p_t = 0.$$



Declassified in Part - Sanitized Copy Approved for Release 2012/03/12 : CIA-RDP82-00039R000100190014-6

Declassified in Part - Sanitized Copy Approved for Release 2012/03/12 : CIA-RDP82-00039R000100190014-6

The general solution of this equation we shall seek in the form of a power series from (u - 2k):

(10)

$$p = \sum_{n=0}^{\infty} \frac{(u-2k)^n}{n!} \left[\frac{\partial^n p}{\partial u^n}\right]_{u=2k}.$$

Utilizing the general solution (9) of equation (8), it is possible to define further the method of finding derivatives

$$\left[\frac{\partial^n p}{\partial u^n}\right]_{u=2k},$$

appearing as coefficients in series (10).

Actually,

$$[p]_{u=2k}$$

as we have already noted, is equal to z when H=0. Let all of

$$\left[\frac{\partial^m p}{\partial u^m}\right]_{u=2k}$$

be already determined for $m < n$. In order to find

$$\left[\frac{\partial^n p}{\partial u^n}\right]_{u=2k}$$



Declassified in Part - Sanitized Copy Approved for Release 2012/03/12 : CIA-RDP82-00039R000100190014-6

Declassified in Part - Sanitized Copy Approved for Release 2012/03/12 : CIA-RDP82-00039R000100190014-6

we differentiate n times equation (7) in respect to u, after which we assume $u = 2k$:

$$\left\{\left[\frac{\partial^n p}{\partial u^n}\right]_{u=2k}\right\}''_{tt} - 4k^2\left\{\left[\frac{\partial^n p}{\partial u^n}\right]_{u=2k}\right\}''_{zz} + \frac{4k}{z}\left\{\left[\frac{\partial^n p}{\partial u^n}\right]_{u=2k}\right\}'_{t} = H_n .$$

Here $H_n$ is the expression evidently depending on

$$\left[\frac{\partial^{n-1} p}{\partial u^{n-1}}\right]_{u=2k} \quad \text{and} \quad \left[\frac{\partial^{n-2} p}{\partial u^{n-2}}\right]_{u=2k} ;$$

$$H_n = 4kn\left\{\left[\frac{\partial^{n-1} p}{\partial u^{n-1}}\right]_{u=2k}\right\}''_{xz} + n(n-1)\left\{\left[\frac{\partial^{n-2} p}{\partial u^{n-2}}\right]_{u=2k}\right\}''_{zz} -$$

$$- \frac{4n}{z}\left\{\left[\frac{\partial^{n-1} p}{\partial u^{n-1}}\right]_{u=2k}\right\}'_{t} - \frac{n(n-1)}{kz}\left\{\left[\frac{\partial^{n-2} p}{\partial u^{n-2}}\right]_{u=2k}\right\}'_{t} .$$

In this manner we may consider that in obtaining

$$\left[\frac{\partial^n p}{\partial u^n}\right]_{u=2k}$$

the value $H_n$ appears as a fully known function of z and t.

The above obtained relation for

$$\left[\frac{\partial^n p}{\partial u^n}\right]_{u=2k}$$



Declassified in Part - Sanitized Copy Approved for Release 2012/03/12 : CIA-RDP82-00039R000100190014-6

Declassified in Part - Sanitized Copy Approved for Release 2012/03/12 : CIA-RDP82-00039R000100190014-6

appears as an equation of the form (8), that is,

$$\left[\frac{\partial^n p}{\partial u^n}\right]_{u=2k}$$

equal to the general solution of s of equation (8) when $H = H_n$.

Consequently we have demonstrated the method for obtaining further coefficients in series (10). Not touching at present the question of the interval of convergence of this series, let us consider that we have found the general solution of equation (7).

Up to now we have spoken only of general solutions. That is why the obtained expressions carried arbitrary functions. Let us show how these functions are determined according to one type of boundary conditions.

First let us consider equation (8) and its general solution (9). Let the coundary condition be of the following form:

$$S\Big|_{z=\epsilon} = A(t), \quad S'_z\Big|_{z=\epsilon} = B(t).$$

Then, directly from (9), supposing $z = \epsilon$ and $t = \xi$, we obtain:

$$A(\xi) = \epsilon\varphi(\epsilon + 2k\xi); \quad \varphi(k) = \frac{1}{\epsilon} A\left(\frac{k-\epsilon}{2k}\right).$$

Further differentiating the equality (9) in respect to z and then assuming $z = \epsilon$, we obtain:

$$B(t) = \frac{\epsilon}{2k} f\frac{(\epsilon - 2kt)}{\epsilon^2} + \frac{1}{\epsilon} A(t) + \frac{1}{2k} A'(t);$$

$$f(k) = -2kA\left(\frac{\epsilon-k}{2k}\right) - \epsilon A'\left(\frac{\epsilon-k}{2k}\right) + 2k\epsilon B\left(\frac{\epsilon-k}{2k}\right).$$



Declassified in Part - Sanitized Copy Approved for Release 2012/03/12 : CIA-RDP82-00039R000100190014-6

Declassified in Part - Sanitized Copy Approved for Release 2012/03/12 : CIA-RDP82-00039R000100190014-6

Let us substitute the found values for g(x) and f(x) in expression (9) for s:

$$S = -\frac{z}{4\kappa^2}\int_{\epsilon}^{z}\frac{d\alpha}{\alpha^2}\int_{\epsilon}^{\alpha}\beta H\left(\beta, \frac{\beta-2\alpha+z+2\kappa t}{2\kappa}\right)d\beta + \\ + \epsilon z\int_{\epsilon}^{z}\frac{B\left(\frac{\epsilon+z+2\kappa t-2\alpha}{2\kappa}\right)}{\alpha^2}d\alpha - z\int_{\epsilon}^{z}\frac{A\left(\frac{\epsilon+z+2\kappa t-2\alpha}{2\kappa}\right)}{\alpha^2}d\alpha - \\ - \frac{z\epsilon}{2\kappa}\int_{\epsilon}^{z}\frac{A'\left(\frac{\epsilon+z+2\kappa t-2\alpha}{2\kappa}\right)}{\alpha^2}d\alpha + \frac{z}{\epsilon}A\left(\frac{z+2\kappa t-\epsilon}{2\kappa}\right). \tag{11}$$

Now let us turn to the system of equations (6). Let us consider the following boundary conditions for this system:

$$\varphi\Big|_{z=\epsilon} = F(t), \quad p\Big|_{z=\epsilon} = \Phi(t). \tag{12}$$

The functions F(t) and $\Phi$ (t) may also depend on u and k.

Utilizing (6) from the conditions (12) we obtain boundary conditions for equation (7):

$$p\Big|_{z=\epsilon} = \Phi(t), \quad p'_z\Big|_{z=\epsilon} = -F'(t). \tag{13}$$

With the aid of (13) we can without difficulty determine the



Declassified in Part - Sanitized Copy Approved for Release 2012/03/12 : CIA-RDP82-00039R000100190014-6

Declassified in Part - Sanitized Copy Approved for Release 2012/03/12 : CIA-RDP82-00039R000100190014-6

arbitrary functions entering into the expression of coefficients of series (10).

The coefficients of series (10) appear already determined in a quite singular fashion. Namely.

$$\left[\frac{\partial^n p}{\partial u^n}\right]_{u=2k}$$

equal to s in expression (11) under the conditions:

$$H(z,t)=H_n\ ;$$

$$A(t)=\left[\frac{\partial^n}{\partial u^n}\Phi(t)\right]_{u=2k}\ ;\ B(t)=-\left[\frac{\partial^n}{\partial u^n}F'(t)\right]_{u=2k}\ . \tag{14}$$

In such a manner it is possible to consider found the unknown function p.

After this the second unknown $\varphi$ is found without difficulty. Actually, in accordance with (6) we have:

$$\varphi=F(t)-\frac{1}{u^2}\int_{\epsilon}^{z}p_t\,dz-\frac{1}{k}\int_{\epsilon}^{z}\frac{p}{z}\,dz. \tag{15}$$

If in the expression, the value p in the form of a series will be limited only by a definite end number of members, then we will obtain the value of $\varphi$, which interests us, in the area of conditions within the limits made in paragraph 2; the expression will fully satisfy any kind of computation. As to the number of members



Declassified in Part - Sanitized Copy Approved for Release 2012/03/12 : CIA-RDP82-00039R000100190014-6

Declassified in Part - Sanitized Copy Approved for Release 2012/03/12 : CIA-RDP82-00039R000100190014-6

in the above-mentioned infinite series with which we may limit ourselves in order to obtain a practically adequate accuracy, even though we cannot prove this strictly enough, we may assume that three members will turn out to be fully sufficient.

Actually, the usual multiple computations which up to now have been made for problems of a like type, depended in fact (directly or indirectly) on the assumption that $\varphi$ and p were not immediately dependent on the value u (the relationship between $\varphi$, p and u was taken into account only through the value $k_\gamma$). Such an assumption in our scheme actually means that we have limited ourselves only by the first member in series (10). As is known, computations based on such an assumption come to more-or-less acceptable results. Adding to the first member another two, we certainly define the resultant considerably. There will hardly ever be a necessity to consider a greater number of members.

In such a manner the results obtained may be effectively used for the computation of a whole series of problems. The use of this method (based on the solution of a hyperbolic equation) is especially pertinent to the study of processes near the space-time limits of distribution of transportable substance.

E N D



Declassified in Part - Sanitized Copy Approved for Release 2012/03/12 : CIA-RDP82-00039R000100190014-6

Declassified in Part - Sanitized Copy Approved for Release 2012/03/12 : CIA-RDP82-00039R000100190014-6

# A SPECTROGRAPHIC STUDY OF THE TRANSPARENCY OF THE ATMOSPHERE FOR ULTRA-VIOLET RADIATION OF THE SUN

Ye. A. Polyakova

The investigation of spectral transparency of the atmosphere for ultra-violet radiation of the sun is the basic method employed in studying atmospheric ozone.

Located beyond the belt of absorption by ozone, in the extreme ultra-violet portion of the spectrum ( $\lambda < 2200$ Angstroms) is the belt of absorption by oxygen.

That is why the study of the transparency of the atmosphere in this area of the spectrum may appear as one of the methods of study of atmospheric oxygen (1).

But the value of investigating the transparency of the atmosphere for ultra-violet radiation does not rest solely upon its importance to the study of atmospheric ozone and oxygen.

The transparency of the atmosphere is determined not only by selective absorption but also by extinction as a result of dispersion.

Inasmuch as dissipation is increased with the decrease of the wave length, it is most pronounced in the ultra-violet portion of the spectrum. Therefore, the study of the transparency of the atmosphere for this portion of the spectrum has an important value for the study of the process of dispersion in the actual atmosphere.



Declassified in Part - Sanitized Copy Approved for Release 2012/03/12 : CIA-RDP82-00039R000100190014-6

Declassified in Part - Sanitized Copy Approved for Release 2012/03/12 : CIA-RDP82-00039R000100190014-6

The long-wave portion of the ultra-violet spectrum ( $\lambda > 3200$ Ångströms) appears as that area in which extinction as a result of dispersion dominates, inasmuch as absorption by the ozone here is small. In this manner, this area is nearly free from selective absorption and is convenient for investigating the dispersion in the aerosols.

Very little work specially devoted to the problem of transparency of aerosols for ultra-violet radiation has been done.

This problem was touched upon in the thesis on atmospheric ozone since the generally accepted method for the determination of the amount of ozone is based on the assumption of the non-selective nature of extinction in aerosols.

As a basis for the present work are the measurements of intensity of separate portions of the spectrum of the ultra-violet radiation of the sun, taken by means of a quartz spectrograph.

The instrument with which we obtained all the data is Hilger's spectrograph with quartz optical elements. Its illuminating power is about 1:7; the linear dispersal is about 45 Ångströms for 1 millimeter near 3000 Ångströms. On each plate, in addition to a full series of comparative spectra, auxiliary spectra were taken for the construction of characteristic curves.

In order to obtain these auxiliary spectra, we employed the method for altering the intensity by using diaphragms of various sizes which were inserted with a barite shield.

Observations were made principally at two points: in August 1940 in Pavlovsk and during September 1940 in Sevastopol'. The observations in Sevastopol' were made on the shore of the bay near the center of the city; therefore, dust and smoke from the city, as well as smoke from ships, may have influenced the results obtained, although we made photographs only in those moments when no smoke near the sun could be observed by eye.

In order to evaluate to a certain degree the influence of city conditions, we conducted observations for several days outside



Declassified in Part - Sanitized Copy Approved for Release 2012/03/12 : CIA-RDP82-00039R000100190014-6

Declassified in Part - Sanitized Copy Approved for Release 2012/03/12 : CIA-RDP82-00039R000100190014-6

the city limits in Uchkuyevka; Uchkuyevka is four kilometers northeast of the city on the shores of the open sea.

Observations were made only on clear days. In Pavlovsk there were seven days of observation; in Sevastopol', six days; and in Uchkuyevka three days. In this manner we obtained data from 16 days of observation, and for each day of observation a series of photographs was made on the same plate. In all a total of 300 spectra were processed.

All spectrograms were processed by obtaining microphotometric registrations with the aid of a registering microphotometer.

On the basis of the material processed from observation, coefficients of transparency of the atmosphere for sections of the spectrum with the following values of wave lengths at the center of each section were determined: 3095, 3109, 3171, 3204, 3295, 3399, 3502, 3590 (in Ångström units).

The determination of spectral coefficients of transparency ($p_\lambda$) was done graphically, using lines for monochromatic evolution of light by the logarithmic relationship between the intensity of radiation and the atmospheric mass for each day of observation for each one of the eight selected spectral portions.

The value $d = -\lg p_\lambda$ we will in the future call the optical density of the atmosphere.

The consideration of the measured coefficients of transparency for the above mentioned wave lengths (from 3090 to 3600 Ångströms) showed that the spectral coefficients of transparency



Declassified in Part - Sanitized Copy Approved for Release 2012/03/12 : CIA-RDP82-00039R000100190014-6

Declassified in Part - Sanitized Copy Approved for Release 2012/03/12 : CIA-RDP82-00039R000100190014-6

of the atmosphere in the ultra-violet portions of the sun's spectrum are subject to considerable fluctuations from day to day -- fluctuations much greater than the coefficients of transparency for the integral flow of radiation. This same result was obtained by us through spectrographic observations in 1936 in Karadag (Crimea, on the Black Sea coast) and in 1937 in Berdyansk (Azov Sea coast). We were able to establish that in Karadag these fluctuations were related to the direction of the wind; for instance, at winds from shore, comparatively low values of atmospheric transparency coefficients in the ultra-violet portion of the spectrum were observed. This fact points to the considerable role played by atmospheric aerosols in the weakening of the ultra-violet portion of solar radiation.

With the aim of obtaining a more detailed study of the question concerning the factors determining the transparency of the atmosphere for ultra-violet radiation, the influence of separate components of the atmosphere on the extinction of ultra-violet radiation was investigated.

As is known, the transparency of the atmosphere for this portion of the spectrum is determined by three factors: molecular dispersion, absorption by the ozone, and extinction as a result of dispersion by aerosols.

Therefore, optical density specified for each of these factors was computed separately.

The computation of optical density in the given case is more convenient than the computation of coefficients of transparency,



Declassified in Part - Sanitized Copy Approved for Release 2012/03/12 : CIA-RDP82-00039R000100190014-6

Declassified in Part - Sanitized Copy Approved for Release 2012/03/12 : CIA-RDP82-00039R000100190014-6

because the total value of optical density of the atmosphere for the given wave length is equal to the sum of the optical densities of the separate components.

When computing optical density dependent on molecular dispersion ( $\beta_\lambda$ ) a correction allowing for anisotropy of molecules was introduced.

In order to account for absorption by the ozone it is necessary to know its coefficient of absorption.

Coefficients of absorption by the ozone for the intervals of wave lengths which interest us ($\lambda > 3050$ Ångströms) are determined reliably enough.

The coefficients of absorption by the ozone may be stated for the intervals of wave lengths 2900 to 3300 Ångströms by the empirical formula according to Fabry and Buisson (3):

$$\log \alpha_\lambda = 17.58 - 0.00564\lambda \quad (\lambda \text{ in Ångströms})$$

in which the value $\alpha_\lambda$ is introduced by the relation:

$$I_\lambda = I_{o\lambda}\, 10^{-\alpha_\lambda x}$$

where $I_{o\lambda}$ is the intensity of falling radiation of the given wave length; $I_\lambda$ is the intensity of radiation passed through the ozone; x is the thickness of the ozone layer brought to normal conditions (0 degrees and 760 millimeters mercury).



Declassified in Part - Sanitized Copy Approved for Release 2012/03/12 : CIA-RDP82-00039R000100190014-6

Declassified in Part - Sanitized Copy Approved for Release 2012/03/12 : CIA-RDP82-00039R000100190014-6

As is evident from the latter formula, the optical density of the ozone is equal to the value $\alpha_\lambda \chi$ .

Further, we considered the values of $\alpha_\lambda$ , which were given by the investigators working after Fabry and Buisson (3), and stopped at the coefficients given by the Chinese investigators Ni-Tsi-Ze and Choong-Shin-Piao (4).

All further computations were conducted using the values for $\alpha_\lambda$ given by Fabry and Buisson (3), as well as those given by Ni-Tsi-Ze and Choong-Shin-Piao (4); the results obtained by using either of the coefficients differ little from each other.

It is necessary to know the value $\chi$ for the computation of optical density of the ozone ( $\alpha_\lambda \chi$ ). The quantity of the ozone in the atmosphere is not known for each day; therefore, we decided to use the mean value $\chi$ for the given month and latitude.

Inasmuch as the absorption by the ozone within the area of the wave length considered by us is small, the use of mean values will not result in large errors.

Furthermore, computations for extreme values for quantity of ozone for each point were also made. According to Dobson (5) we determined the following mean values for quantity of ozone at the observation points.

Basing on the same graph of Dobson, the minimum values of $\chi$ for all points was .20 centimeters; maximum for Pavlovsk was .36 centimeters and the maximum for the rest was .30 centimeters.



Declassified in Part - Sanitized Copy Approved for Release 2012/03/12 : CIA-RDP82-00039R000100190014-6

Declassified in Part - Sanitized Copy Approved for Release 2012/03/12 : CIA-RDP82-00039R000100190014-6

TABLE I

| Place of observation | Latitude | Month of observation | Mean value of x, brought to normal conditions, cm |
|---|---|---|---|
| Pavlovsk. . . . . | 59° 41' | August | 0.27 |
| Sevastopol' and Uchkuyevka . . . | 44° 37' | September | 0.23 |
| Matsesta. . . . . | 43° 34' | August | 0.25 |

Optical planes of the ozone ( $\alpha_\lambda x$ ) for each of these values of x were determined for the wave lengths selected and optical densities defined by molecular dispersion were added to these.

Values for the residual optical density, the optical density of the aerosols ( $\delta_\lambda$ ), were obtained by subtracting the sum from the values of optical density for all of the atmosphere (from values of $\alpha_\lambda$).

In such a manner values of optical density of the aerosols corresponding to the three values for the amount of ozone (maximum, mean, and minimum) for each day were obtained. Whereupon, in each case, computations were made with the aid of the coefficients of Fabry and Buisson as well as with those of No-Tsi-Ze and Choong-Shin-Piaw.

The optical density of the aerosols ( $\delta_\lambda$ ) comprises a considerable portion of all of optical density. This is evident from Table II.



Declassified in Part - Sanitized Copy Approved for Release 2012/03/12 : CIA-RDP82-00039R000100190014-6

Declassified in Part - Sanitized Copy Approved for Release 2012/03/12 : CIA-RDP82-00039R000100190014-6

TABLE II

| Wave length in A | Relation of $\frac{\delta\lambda}{d\lambda}$ in percentage | | |
|---|---|---|---|
| | Pavlovsk | Sevastopol' | Uchkuyevka |
| 3095 | 26 | 34 | 31 |
| 3109 | 28 | 28 | 25 |
| 3171 | 26 | 36 | 28 |
| 3204 | 28 | 36 | 30 |
| 3295 | 40 | 48 | 40 |
| 3399 | 43 | 48 | 45 |
| 3502 | 43 | 53 | 48 |

In this table mean values of the relation of optical density of the aerosols in percentage to the corresponding value of the optical density of the atmosphere ($\frac{\delta\lambda}{d\lambda}$ 100) are given. These relations are obtained for average amounts of ozone and coefficients of absorption given by Ni-Tsi-Ze and Choong-Shin-Piaw.

Figure 1. Relation of optical density of the aerosols and the wave length. Pavlovsk.

Figure 2. Relation of optical density of the aerosols and the wave length. Sevastopol'.



Declassified in Part - Sanitized Copy Approved for Release 2012/03/12 : CIA-RDP82-00039R000100190014-6

Declassified in Part - Sanitized Copy Approved for Release 2012/03/12 : CIA-RDP82-00039R000100190014-6

We see that at these points, especially at Sevastopol', the weakening in the atmosphere of 3300 to 3500 Ångströms wave length radiation, that is, not quite absorbed by the ozone, is about 50 percent of the specified extinction in the aerosols. But, as Table II shows, the extinction of shorter wave lengths, noticeably absorbed by the ozone, is determined by the aerosols to a considerable degree (30 percent).

The question of the dependence of optical density of the aerosols, in other words of the extinction in the aerosols, upon the wave length presents great interest.

Let us consider the results obtained from the use of the coefficients of Fabry and Buisson.

Optical densities of the aerosols, obtained with the aid of these coefficients for the mentioned mean values of ozone quantities for each day of observation, were plotted on a graph in a relation to the wave length. Whereupon, for all the days of observation at all three points -- Pavlovsk, Sevastopol', and Uchkuyevka -- curves of the same type were obtained. In this manner, a nearly horizontal movement of the curve at $\lambda >$ 3000 Ångströms is obtained in all cases; then a short minimum in the vicinity of 3200 Ångströms, after which, in the section $\lambda <$ 3100 Ångströms, a rise in the curve with a decrease in the wave length is observed.

Figure 3. Relation of optical density of the aerosols to the wave length. Uchkuyevka.



Declassified in Part - Sanitized Copy Approved for Release 2012/03/12 : CIA-RDP82-00039R000100190014-6

Declassified in Part - Sanitized Copy Approved for Release 2012/03/12 : CIA-RDP82-00039R000100190014-6

In view of the fact that all of these curves show the same type of relation of the optical density to the aerosols and the wave length, we considered it logical to construct curves from the average of all days of observation for each point. Moreover, since we had used the mean value of the amount of ozone, such an average curve would appear as more reliable than curves for separate days.

For the construction of average curves we accepted as 100 percent of the optical density the spectral portion $\lambda = 3295$ Ångströms.

The mean curves obtained by such a method are shown by solid lines of the three graphs (Figures 1, 2, 3) corresponding to the three points of observation. On the axis of the abcissa the wave length in Ångströms is shown, and on the axis of the ordinate are the mean values of optical density in the above-mentioned relative magnitudes.

Comparing the curves of these three graphs (we are considering as yet only the solid line curves), we notice that at all points the dependence of optical density of the aerosols on the wave length remains the same.

This means that the relationship obtained is not the result of some specific local condition, but signifies a law of a more general character. The curves under consideration show that the extinction in the aerosols is not selective in the area of 3300 to 3600 Ångströms, and in the area of 3120 to 3300 Ångströms it has a small minimum (this corresponds to the maximum of



Declassified in Part - Sanitized Copy Approved for Release 2012/03/12 : CIA-RDP82-00039R000100190014-6

Declassified in Part - Sanitized Copy Approved for Release 2012/03/12 : CIA-RDP82-00039R000100190014-6

transparency), and then on the side of shorter wave lengths, a sharp rise is observed.

This rise is so considerable (60 to 80 percent) that it is difficult to doubt its reality.

It may be allowed that the increase of optical density of the aerosols with a decrease of the wave length at $\lambda <$ 3120 Ångströms appears as a result of having selected values too low for the average amount of ozone. Therefore, we made a computation for the maximum amount of ozone (.35 centimeters for Pavlovsk and .30 centimeters for the southern points).

In order to obtain a more complete picture, computations of the optical density for the minimum amounts of ozone (.20 centimeters) were also made.

On the graphs (Figures 1, 2, 3) the broken lines represent the amount of ozone corresponding to each curve shown on the graph.

Let us consider the curves obtained for the maximum value of quantity of ozone. On these curves, in comparison to the curves drawn with a solid line, the minimum (20 to 30 percent) is more strongly expressed, whereas the rise (30 to 50 percent) is weaker. In this manner, even when granting existence of exceptionally great quantities of ozone together with the assumption concerning the narrow section of anomalistic transparency of the aerosols in the portion 3170 to 3300 Ångströms, the rise in the interval $\lambda <$ 3100 Ångströms does not disappear.



Declassified in Part - Sanitized Copy Approved for Release 2012/03/12 : CIA-RDP82-00039R000100190014-6

Declassified in Part - Sanitized Copy Approved for Release 2012/03/12 : CIA-RDP82-00039R000100190014-6

The curves corresponding to .20 centimeters of ozone on all graphs differ little from the curves for average quantities of ozone (shown by solid lines); for them, as it should be, the rise in the area of short wave lengths is even steeper.

In order to be completely convinced of the reality of the curve's rise in the area of short wave lengths, we utilized the results of the work conducted by us in August 1938 in Matsesta (5), on the Black Sea coast of the Caucasus.

The observations were conducted with the aid of the same spectrograph that was used for the observations of 1940. But the method of measuring the intensity differed somewhat from the method that we employed in 1940. Specifically, during observations in Matsesta diaphragms were not used; the scale of auxiliary spectra was obtained by changing the time of exposure. This manner of obtaining the scale cannot be considered reliable. Even though corrections for Schwartschild's effect were introduced, the extent of the influence of this effect on ultra-violet radiation could be only approximated; therefore, in the final values there may be systematic errors as a result of this method.

According to the observations at Matsesta, coefficients of transparency for the following spectral portions were determined: 3095, 3061, 3051 Ångströms. This permits the curve under consideration to be extrapolated for shorter wave lengths ($\lambda$ shorter than 3095 Ångströms).

The data from the observations in Matsesta, compared to the



Declassified in Part - Sanitized Copy Approved for Release 2012/03/12 : CIA-RDP82-00039R000100190014-6

Declassified in Part - Sanitized Copy Approved for Release 2012/03/12 : CIA-RDP82-00039R000100190014-6

general average curve -- obtained from the curves for Pavlovsk, Sevastopol', and Uchkuyevka by averaging and taking into consideration the number of observations at each point -- indicate a considerable increase in optical density with a decrease in the wave length (for $\lambda < 3100$ Ångströms); this fact, according to our opinion, leaves no doubt that the rise of the curve in this area of the ultra-violet spectrum reflects actual conditions.

Employing the coefficients of Ni-Tsi-Ze and Choong-Shin-Piaw, we conducted analogous computations. Using observational data from all points (Pavlovsk, Sevastopol', Uchkuyevka, and Matsesta), and taking into account the mean amounts of ozone, a mean graph (Figure 4) was constructed. The general nature of the function between optical density of the aerosols and the wave length remains the same whether the coefficients of Ni-Tsi-Ze and Choong-Shin-Piaw or those of Fabry and Buisson are employed: in the area 3300 to 3600 Ångströms, within the limits of accuracy of measurements, there is a horizontal movement; in the area 3120 to 3300 Ångströms, a minimum; and then for $\lambda < 3100$ Ångströms, a sharp rise.

Figure 4. Relationship of the optical density of aerosols to wave length. The curve is plotted from observational data taken at Pavlovsk, Sevastopol', and Uchkuyevka (the broken line on observations in Matsesta).



Declassified in Part - Sanitized Copy Approved for Release 2012/03/12 : CIA-RDP82-00039R000100190014-6

Declassified in Part - Sanitized Copy Approved for Release 2012/03/12 : CIA-RDP82-00039R000100190014-6

Differences between the curves plotted from the coefficients of Ni-Tsi-Ze and Choong-Shin-Pian and the corresponding curves from the coefficients of Fabry and Buisson are found only in the details.

Summing up the results for all of the stated, the following conclusions may be drawn:

1. In the investigated interval of the wave lengths 3050-3600 Angstroms, the extinction in the aerosols may be considered as non-selective only in those intervals between 3300 and 3500 Angstroms.

2. Further in the direction of the shorter wave lengths this extinction has a sharply expressed selective character: in the area 3120-3300 Angstroms there is a somewhat large maximum of transparency with the center at about 3170 Angstroms, after which there is a sharp increase of extinction in the aerosols (decrease of transparency of the aerosols) as the wave lengths decrease.

It is necessary also to point out that the somewhat large minimum of optical density of the aerosols in the area of 3120-3300 Angstroms (maximum of transparency) becomes even more weakly expressed if we assume that Dobson's average values of ozone which we employed are too large. This assumption develops from the fact that under the usual allowances in computing amounts of ozone the property of extinction in the aerosols is non-selective, that is, the fact that extinction increases as the wave lengths decrease in the short wave length portion of the spectrum perhaps resulting in an increased value for the amount of ozone under great turbidity, is not taken into consideration.



Declassified in Part - Sanitized Copy Approved for Release 2012/03/12 : CIA-RDP82-00039R000100190014-6

Declassified in Part - Sanitized Copy Approved for Release 2012/03/12 : CIA-RDP82-00039R000100190014-6

This result may be compared to the result of Borne's (6) laboratory work on the investigations of transparency of various synthetic smokes. Comparing these with the obtained relation between the extinction of atmospheric aerosols and the wave length may indicate that Borne's curves have the same character as the obtained curves with the difference that on the latter curve, the minimum lies somewhat farther in the direction of greater wave lengths. Borne's minimum is about 3000 Ångströms, and thus a sharp increase of optical density with the decrease in the wave length takes place.

In this comparison it is interesting that the results of the laboratory investigations are consistent with the results of the study made by us concerning the extinction of ultra-violet radiation in the atmosphere.

Our results may be compared to the results of the work of A. and E. Vassy (7). The results of the study made by them concerning the transparency of the lower layers of the atmosphere for ultra-violet radiation presents great interest.

As the authors point out, the results of their spectrographic investigations on the transparency of the atmosphere in the area of 3000 to 4000 Ångströms do not differ greatly from the results of experiments in the visible part of the spectrum so far as distances are concerned. The measurements, moreover, were made in the course of three days.

The results of their measurements show that in the area of



Declassified in Part - Sanitized Copy Approved for Release 2012/03/12 : CIA-RDP82-00039R000100190014-6

Declassified in Part - Sanitized Copy Approved for Release 2012/03/12 : CIA-RDP82-00039R000100190014-6

3300 to 3600 Ångströms the optical density in the lower layers of the atmosphere do not depend on the wave lengths, and, beginning with 3300 Ångströms a rapid rise in the curve, that is, a sharp increase in optical density with a decrease in wave length is observed.

The authors themselves offer no explanation of the above mentioned relationship. In the lower layers of the atmosphere, selective absorption by the ozone is practically non-existent; therefore, the peculiarity of the course of the curves may be explained only by the selective character of the extinction in the aerosols in this portion of the spectrum.

The path of Vassy's curve in the section of the spectrum under investigation, in its basic features, is similar to the path of our curve, which represents a dependence of the optical density of the aerosols on the wave length. But in comparing it is necessary to take into account that the Vassys give a general value to optical density, not excluding from it parts of the arbitrary molecular dispersion. Therefore, in order to compare their curve with our data, a graph showing the relationship of optical density, conditioned by all dispersions (molecular and aerosolic) and the wave length has been plotted. This graph, shown in Figure 5, is plotted analogously to the graph in Figure 4.

The difference is found in that the original values for optical densities for each observation were obtained by subtracting the optical density of atmospheric ozone from the total



Declassified in Part - Sanitized Copy Approved for Release 2012/03/12 : CIA-RDP82-00039R000100190014-6

Declassified in Part - Sanitized Copy Approved for Release 2012/03/12 : CIA-RDP82-00039R000100190014-6

optical density of the atmosphere.

The curve thus obtained, shown in Figure 5, as opposed to the curve of optical densities of the aerosols (Figure 4) lacks the minimum which the latter curve has.

Figure 5. Optical density of the atmosphere conditioned by dispersion. According to observations at all points (taking into account the number of observations at each point).

The path of the curve in Figure 5 is analogous to the path of Vassy's curve in the corresponding interval of wave lengths. All the differences between them arise from the fact that the change from the horizontal portion of the curve to the sharp increase of optical density with a decrease in the wave length occurs on Vassy's curve at about 3300 Ångströms, whereas according to our observations this break in the path of the curve occurs at about $\lambda = 3150$ Ångströms.

Even so, the character of the obtained relation between the extinction in the aerosols and the wave length is consistent with the results of the work of Vassy as well as the previously mentioned work of Borne.

Common to the conditions under which our results were obtained and the results of the work with which the comparison is being made,



Declassified in Part - Sanitized Copy Approved for Release 2012/03/12 : CIA-RDP82-00039R000100190014-6

Declassified in Part - Sanitized Copy Approved for Release 2012/03/12 : CIA-RDP82-00039R000100190014-6

is the fact that in each of the cases considered there are certain dispersive particles, perhaps absolutely different according to their nature and comparable only in regard to their size and amount. It follows, therefore, that the agreement between the results obtained by me and the results of the studies of the transparency of the lower atmospheric layers, as well as of the transparency of synthetic smokes, confirms the fact that the established law represents precisely a law of the dispersion for atmospheric aerosols at the given portion of the spectrum.

E N D



Declassified in Part - Sanitized Copy Approved for Release 2012/03/12 : CIA-RDP82-00039R000100190014-6

Declassified in Part - Sanitized Copy Approved for Release 2012/03/12 : CIA-RDP82-00039R000100190014-6

# DYNAMICS OF CLIMATE IN CONNECTION WITH CHANGES IN SOLAR ACTIVITY

P. P. Predtechenskiy

1. At the present time, climatology has become a nodal discipline in which achievements and, to a considerable degree, the interests in further developments of a series of related disciplines such as meteorology, forecasting, agrometeorology, soil science, hydrology, geographical sciences, as well as remote disciplines such as astronomy and astrophysics, geology with its sciences, botany with its history of flora, history, archeology, and medicine are all closely tied together. The latest fluctuations in climate, of which we appear as the witnesses, force us to reconsider the basic conditions of our science, force us to utilize the achievements of related disciplines, and to propound to them a series of questions that should be answered without delay.

The broad and fruitful work on classical climatology accumulated materials for statistics of climate which may be reliably considered as clear in detail. However, we are only beginning to study the dynamics of climate. The present article sums up the work accomplished by the author and is not the final mastery of a new field, but only a prospecting journey into it.

2. Geological profiles of any territory give undisputed evidence of great climatic changes evidenced not only by animal and plant life, but also by the changes in the type of soil-producing processes. These changes occur in great intervals of time, not steadily, but developing by leaps and bounds, accelerating and decelerating



Declassified in Part - Sanitized Copy Approved for Release 2012/03/12 : CIA-RDP82-00039R000100190014-6

Declassified in Part - Sanitized Copy Approved for Release 2012/03/12 : CIA-RDP82-00039R000100190014-6

with retrogressions to phases already covered. Great and small fluctuations confuse geological records and at times make them illegible in parts (1). These properties of the development of climate we readily see in the history of post ice-age climate of Eurasia and America. Pollen analysis, a powerful investigative weapon acquired during the present century, everywhere points to the complicated play of climatic changes (1, 10). A series of such fluctuations make up immense contrasts in climate, whereupon only the most recent in the total give the direction and the gradual shift of climate. It is possible to make a reasonable assumption as to the unity of causes which determine the development of weather and the development of climate. A counter assumption would have demanded an admission, special for this case, of a series of complex formations similar to Ptolemaic epicycles. We have the right to accept a certain natural hierarchy genetically binding the appearance of various ranks of values: weather processes, seasonal weather, cycle of development of the general circulation of the earth's atmosphere, the climate of several dozen years, climatic fluctuations limited to a single direction, climatic change, a group of climatic changes, geological epoch of climatic changes.

Through geological experiments of the post glacial period we may make judgments on the velocities, amplitudes, and territorial range of climatic changes and groups of climatic fluctuations composing the latter. Archeology and history give a living account of distinct climatic fluctuations. Climate itself in a statistical version embraces the conditions or the regime of the weather for a portion of time not greater than 2 or 3 centuries: from the eighteenth century onward, that is, for that portion in which reliable instrument observations have been made of the weather. This portion, in the



Declassified in Part - Sanitized Copy Approved for Release 2012/03/12 : CIA-RDP82-00039R000100190014-6

Declassified in Part - Sanitized Copy Approved for Release 2012/03/12 : CIA-RDP82-00039R000100190014-6

scale of climatic changes, is small, and because of this the working hypothesis on the non-change-ability of climate was adopted. This hypothesis, in its practical application, gave valuable results; but from the second quarter of this century it has already slowed down the further development of climatology.

3. Weather and climate are two different aspects of the development of the same process. With necessary reservations it is permissible to speak of the weather of the nineteenth century and of the climate, say, of last year. Where weather ends and climate begins is a question which is determined in each separate case by those simplifications or precisions which are called for in practice.

A final and thorough determination of climate and its connections with weather is not be be had to this day, and even though no one denies the genetic relationship between climate and weather, in practice, as a rule, these conceptions are separated by a Chinese wall. But it is impossible to conceive of changes in climate without initially directed changes in weather. Therefore, speaking of climatic changes, we necessarily speak of definite systematic changes in weather. Conversely, if we state successive changes in weather, we have by this precisely determined the direction of climatic change.

The question of studying the development of climate may be brought to the undoubtedly more scientific and more understandable question regarding the changes and development of weather processes, that is, more specifically, to the question on the development of general circulation of the earth's atmosphere and the particular circulations entering into it.



Declassified in Part - Sanitized Copy Approved for Release 2012/03/12 : CIA-RDP82-00039R000100190014-6

Declassified in Part - Sanitized Copy Approved for Release 2012/03/12 : CIA-RDP82-00039R000100190014-6

However, in the investigations of the development of climate, this point of view is in greater part disregarded, and, as a rule, explanations for the observed facts are sought in catastrophes especially invented for each change. Even if we consider catastrophes in the history of the world and of the solar system possible, we still cannot expect their appearance to have been as frequent as necessary to use them as the explanation of the earth's climates detected so far by history.

4. The first group of causes, manifested in its effect on climate, is related to the change in the flow of heat from the sun to the earth. Actually, weather and climate both must depend on the balance of heat between an arbitrarily selected point on the earth's surface and the atmosphere over it.

The most attractive hypothesis of this group is the one established by Simpson (2) in the early Thirties of this century. Its aim is to explain the history of Quaternary glaciation. This aim was, and to this day is, a stimulus of many, if not all, dynamic-climatological researchers. Actually not one theory of climatic changes may be considered complete if it cannot point to the cause of the appearance, development, and liquidation of the last great glaciation.

Simpson admitted the possibility of fluctuations in the general illumination of the sun, but did not state their causes. The increase in the flow of solar radiation must cause, in the first place, a change in the regime of condensation of water vapor in the earth's atmosphere as a result of the increased evaporation of water from land and ocean upon the initial rise in temperature. Condensation would lead to an increase in cloudiness, and, as a result, to the



Declassified in Part - Sanitized Copy Approved for Release 2012/03/12 : CIA-RDP82-00039R000100190014-6

Declassified in Part - Sanitized Copy Approved for Release 2012/03/12 : CIA-RDP82-00039R000100190014-6

increase in the coefficient of reflection of the earth's atmosphere (albedo) and a decrease in the inflow of heat to the lower layers of the atmosphere. The albedo, due to the increase of solar radiation, initially will increase and will continue to increase with the radiation increase until it reaches a certain critical value; then it will rapidly fall and reach a value smaller than it had at the start of the process. Together with a great inflow of solar radiation, this will establish in the center of the wave of change in solar illumination, on its crest, a period of humid and warm climate, and on the fringes of the wave there will be periods of glaciation (Figure 1).

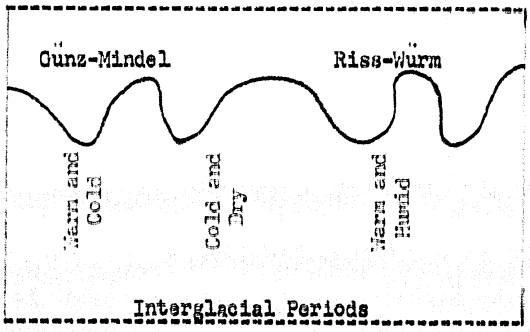


Figure 1. Development of metoorologic factors under changes in the general luminosity of the sun (according to Simpson).
The curves from top to bottom show the path of luminosity of the sun (I), the temperature of the lower troposphere (II), sum of precipitation (III), accumulation of snow in subpolar regions (IV) and sequential advances of Quaternary glaciation (V).

This hypothesis, valuable for its comparison of solar activity with the course of condensation processes in the earth's atmosphere,



Declassified in Part - Sanitized Copy Approved for Release 2012/03/12 : CIA-RDP82-00039R000100190014-6

Declassified in Part - Sanitized Copy Approved for Release 2012/03/12 : CIA-RDP82-00039R000100190014-6

was not verified by weather forecasts and remained an academic attempt at providing a solution to a purely climatological problem by which the appearance, development, and liquidation of Quaternary glaciation is explained. In the history of the latter, which took about one million years, there were actually four glaciations (at least in Western Europe) united in pairs: Günz, Mindel and Riss, Würm. They are divided, fully according to Simpson, into dry and warm interglacial periods: Günz-Mindel, Mindel-Riss and Riss-Würm. The central of these is the most dry and least warm; it is twice as long as the two on the extremities, which were about the same. The main objection to this hypothesis is the impossibility of permitting any appreciable fluctuations in the illumination of the sun (2). Besides, the hypothesis demands similarity in the development of glacial phenomena over the whole world. We have, however, considerable contradictions: glaciation on all continents was not synchronous; it developed by various paths and differed in intensity.

The main merit of Simpson's work is that it constituted the first attempt at comparing condensation processes of the earth's atmosphere with changes in the sun's activity. Its second is the idea, not stated by him, but definitely appearing to the reader, concerning the close and inseparable relation of climatic change with weather development.

5. Simpson did not explain why glaciations appear in the Quaternary epoch, and do not appear in the immediately preceding Tertiary and Cretaceous epochs which are characterized by their steadily mild climates over great territories. Research data indicate the regular change in climatic optimums with like conditions over great areas and



Declassified in Part - Sanitized Copy Approved for Release 2012/03/12 : CIA-RDP82-00039R000100190014-6

Declassified in Part - Sanitized Copy Approved for Release 2012/03/12 : CIA-RDP82-00039R000100190014-6

climatic pessimums with exaggerated climatic conditions in countless small provinces. Climatology cannot dismiss these factors, inasmuch as without understanding prehistory, it is impossible to understand the contemporary stage in the development of climate, or, what is more, to determine correctly and to evaluate its future changes.

From this point of view, the mathematical theory of climate, published by M. Milankovich in the beginning of the Twenties, is also not without faults (3). He sees the reason for climatic development in the regular change in the elements of the earth's orbit: an eccentricity, longitude of the perihelion, and the inclination of the axis of rotation of the planet to the plane of the orbit. These three elements actually do periodically fluctuate within strongly defined limits, but in unequal periods. Therefore, their joint action is either directed into one direction or is mutually weakened. As a result of the change in the longitude of the perihelion occurring during a period of 21,000 years, either the southern or the northern hemisphere falls into more favorable climatic conditions. In the hemisphere with favorable climate summer occurs in the aphelion and winter in the perihelion. Due to this the period of the warm portion is longer by a few days than the cold period; summer temperatures are mild as well as the winter temperatures, that is, the annual contrast between summer and winter temperature is lessened. In the unfavorable hemisphere, exactly the opposite conditions occur. Changes in the eccentricity of the earth's orbit, having a period of about 92,000 years, either decrease or increase the inequality in the inflow of heat during the epoch of aphelion or in the epoch of perihelion. Changes in the inclination of the axis of the planet to the plane of the orbit, with a period of about 40,000 years determine



Declassified in Part - Sanitized Copy Approved for Release 2012/03/12 : CIA-RDP82-00039R000100190014-6

Declassified in Part - Sanitized Copy Approved for Release 2012/03/12 : CIA-RDP82-00039R000100190014-6

the location of climatic belts and their mean insolation.

All of these considerations are without argument. Actually, the elements of the orbit do change, and their changes influence the climate of the earth as a whole as well as local climates. However, we may not give a definitive value to the changes in these elements. Contrary to Milankovich's theory stand direct observations: contemporary fluctuations in climate, as well as other historically investigated fluctuations, embrace both hemispheres in a like manner and at the same time; the periods of these fluctuations are small and do not depend upon astronomically long periods of changes in the elements. Besides, the calculations conducted by Milankovich himself, covering a period of 600,000 years previous to 1800, irreparably diverge from the geological scale of climatic changes based on direct calculations from clay stratification and on data from pollen analysis.

Not contradicting the climatic influences of the elements of the orbit, it is not possible to give them the decisive value for one more reason: the given hypothesis cannot explain the occurrence of long periods of climatic optimums -- Cretaceous, Paleocene and Devonian, Carboniferous.

6. As an explanation of the history of climates, and at the same time flora, the hypothesis of Kreykhgauer, Vegener, and Keppen was put forward, according to which the attitude of the earth's axis does not remain as a constant in the geoid. This forms the premise of the continental shift in the isostatic layer in the direction of the equator. Continental blocks, accordingly, break, and the blocks broken off have an autonomous movement and separate with time. According to this hypothesis, there was a single continental block



Declassified in Part - Sanitized Copy Approved for Release 2012/03/12 : CIA-RDP82-00039R000100190014-6

Declassified in Part - Sanitized Copy Approved for Release 2012/03/12 : CIA-RDP82-00039R000100190014-6

before the Carboniferous, and its broken-off portions now form our contemporary continents.

At the present time, this hypothesis is in use by botanists (4) and paleontologists; however, it encounters definite objection (5). It is especially necessary to note that the ~~shifts~~ displacements of the axis of rotation at the present time occur in a non-directional manner. ~~are being accomplished not incorrectly~~. The path of the rotation pole from 1890 to 1932 may be inscribed in a square with a side of 11 meters. The data on the velocity of shifts of the poles of rotation are sufficiently accurate. Observations are being made at many astronomical observatories of the International Latitude Service.

In so far as can be judged, the position of the axis of rotation changes under the influence of the annual rhythm of solid deposits and the epochal course of redistribution of masses inside the earth. Even taking into consideration the conditions of the glacial periods with local overloading by ice sheets, we could hardly accept the change in the position of the axis of rotation as is permitted by this hypothesis. From the Carboniferous to the end of the Tertiary epoch the pole traveled a distance from about the isthmus of Panama to the southern coast of Alaska. This route was covered in about 260 million years. From the end of the Tertiary epoch to the present time, less than 1½ million years, the North Pole apparently shifted according to a complex curve from the southern shores of Alaska to its present position and after this acquired its contemporary negligible velocities. From the mechanical point of view this is simply absurd.

Just as absurd appears to be the shift of continental blocks.



Declassified in Part - Sanitized Copy Approved for Release 2012/03/12 : CIA-RDP82-00039R000100190014-6

Declassified in Part - Sanitized Copy Approved for Release 2012/03/12 : CIA-RDP82-00039R000100190014-6

Thus, Australia, from the end of the Cretaceous epoch to our day, should have traveled from 8 to 13 thousand kilometers. About the same sort of record should have been set by Hindustan. But at the present time the velocities of relative shifts of continental blocks are measured in centimeters per century. Accordingly, here too there should have been periods of catastrophic accelerations releasing immense forces necessary for all of these shifts and which later completely disappeared. Even though this theory is called upon to explain the development of climate by a single cause or a group of causes, in actuality it demands the acceptance of a series of catastrophes whose causes remain completely unexplained.

7. For the explanation of the appearance of the glacial periods, Nel'ke permitted the appearance of a dark cosmic cloud with an unequal density, through which the solar system passed during the glacial epoch. Dust particles of the cloud screened the sun's rays, and, thanks to this, the earth did not receive a sufficient amount of light and heat.

In order that the substance of the cosmic cloud would be able to screen the sun's rays it should have a density of about $10^{-19}$ grams per cubic centimeter; under such a density the travel of the planetary system would have caused a disturbance in the movement of planets, the traces of which would have remained to our days. However, we do not find these traces. Further, a cosmic cloud with uneven densities could not remain stable. Accordingly, the hypothetical cloud that caused the climatic catastrophe must have itself experienced some sort of catastrophe shortly before its meeting with the solar system.

The relative velocity of the sun in the local system of stars is about 20 kilometers per second. Accordingly, in the 10,000 years



Declassified in Part - Sanitized Copy Approved for Release 2012/03/12 : CIA-RDP82-00039R000100190014-6

Declassified in Part - Sanitized Copy Approved for Release 2012/03/12 : CIA-RDP82-00039R000100190014-6

that passed since the last glaciation, we could have not yet lost sight of such an immense and unregulated cloudiness, through which, according to this hypothesis, we have just passed. Contemporary astronomy knows of no similar cosmic neighbors. On the other hand, the screening action of a cloud still remains unknown. All of these bodies and particles would have been acted upon by the sun and then would have retransmitted the sun's rays in the infra-red spectrum. It is possible that the total action of these small particles would have not merely compensated the screening of the sun's radiation, but even intensified the inflow of heat to the planets. All of these obscurities and innacuracies of Nel'ke's theories, particularly the unstated but clearly necessary series of catastrophes, force us to reject his reasoning.

8. If we do not call upon especially created catastrophes, whose frequency in the cosmos is negligibly small, then the explanation of the history of climate must be based on permanent and regular causes always present in the earth-sun system. In this system catastrophes are, of course, possible, but these can be only local and infrequent phenomena. Besides, in the history of climate, a certain rhythm is noticeable: Quaternary glaciation is analogous to the Carboniferous-Permian and Cambrian glaciation, the traces of which have been preserved by geological signs. Further, the Cretaceous-Paleogene optimum is definitely analogous to the Devonian-Carboniferous optimum. The glacial epochs have left us traces of immense continental ice sheets and fossil flora, clearly separated by small physico-geographic areas. Climatic optimums left traces of an even and mild climate from the equator to the 70 degree latitudes with a similar flora occupying all of this area in both hemispheres. Under



Declassified in Part - Sanitized Copy Approved for Release 2012/03/12 : CIA-RDP82-00039R000100190014-6

Declassified in Part - Sanitized Copy Approved for Release 2012/03/12 : CIA-RDP82-00039R000100190014-6

glaciation the appearance of deserts was greatly developed. Under climatic optimums we encounter only traces of drought-resisting plant areas.

Besides glacial periods and climatic optimums, there are other particular climates of the Triassic and upper Cambrian with the Ordovician epochs. During these epochs warm and dry climates together with a limited development of deserts are found. Diversified climates, at first glance, develop regularly, but not steadily. In them fluctuations appear constantly, establishing in the history of climate sub-periods which give rapid and contrasting fluctuations in climate. The post-glacial epoch thus produced, over a period of ten thousand years, four important climatic changes and an innumerable number of small fluctuations attested to by pollen analysis and stratification of ribbon clay.

9. The causes determining the development of climate in the past epoch must be in force also in our days. Changes in climate point to changes in the energy balance of all, without exception, territories of the earth. The only acting group of causes in our days which determine the changes of the everyday energy balance, not counting the rhythmical, monotonously changing, and easily followed variations in the elements of the earth's orbit, are covered in the general circulation of the earth's atmosphere. We consider the basic cause of the earth's climatic changes to be found in the changes in the general circulation of the earth's atmosphere. Accordingly, a permanently acting cause of the development of the general circulation of the earth's atmosphere must exist; and it must act with ceaseless fluctuations either stressing or diminishing its epochal development.



Declassified in Part - Sanitized Copy Approved for Release 2012/03/12 : CIA-RDP82-00039R000100190014-6

Declassified in Part - Sanitized Copy Approved for Release 2012/03/12 : CIA-RDP82-00039R000100190014-6

The single process answering these demands, which we know at the present time, is the change in the sun's activity.

10. If this assumption is to be accepted, we must have proof in the everyday processes of change in the general circulation, and for greater periods of time -- in the climatic processes. The portion of time illuminated by instrument observation is small. Therefore, it is necessary for us to utilize and consider historical archeological and geological data.

The latest fluctuation of climate is taking place before us (10, 11). It still has not gone very far. The previous fluctuation in climate is noted from the Eighth to the Fifteenth centuries. Its beginning, due to the cultural collapse of the Middle Ages, was not fixed in the historical documents of the era.

From the Eighth Century onward we have undisputed proof of the mildness of the climate of Europe and the North Atlantic. Iceland and Greenland were free of the ice blockade. Greenland lived up to the name it received at that time (green land). The Newfoundland bank and Davis Strait were free of icebergs, and the islands off the southern extremity of Greenland, now welded by ice to the mainland, were bathed by the open sea at that time. It is especially important that the ice sheet covering Greenland at that time was in retrogression, and in the retreat it opened a large sea-coast on which agriculture and animal husbandry were possible (13).

From the Twelfth to the Fifteenth centuries AD, a sharp and rapid worsening of the climate is noted: an ice re-blockading of Greenland and Iceland, an advance of the Greenland ice sheet, reappear-



Declassified in Part - Sanitized Copy Approved for Release 2012/03/12 : CIA-RDP82-00039R000100190014-6

Declassified in Part - Sanitized Copy Approved for Release 2012/03/12 : CIA-RDP82-00039R000100190014-6

ance of icebergs in the North Atlantic. The worsening of the climate was not only local, but also embraced all of Eurasia, appearing in the form of extremely hard winters and droughts. In northern Scandinavia it forced the cessation of agriculture, which was not resumed until the end of the Sixteenth and the beginning of the Seventeenth centuries. In Central Asia the worsening of the climate brought about (6) an increase in desert area and a decrease in the irrigated lands. In the same way increased droughts are also noted in the southern hemisphere. Thus, in the territory of Peru, due to water shortages, there was a sharp decrease in the amount of irrigated agriculture and in the amount of forest area.

B. P. Mal'tanovskiy (7) admits the impossibility of explaining this chapter in the history of climate, as it has remained in the circle of synoptic meteorology.

11. Archeological data show that at the end of the Bronze Age, from the Eighteenth to the Fifteenth centuries BC, there was a similar worsening in the climate and just as rapid and as deep. As with the more recent pessimums noted in our chronicles, it was accompanied in Northern Europe by extreme winter, hurricanes, and storms; in the pre-Atlantic seas fierce storms were set off, changing the outline of the coasts.

In the scheme of development of these particular climatic optimums and pessimums there are evident manifestations of redistribution of the constant inflow of solar energy. All observations and data speak of the fact that the solar constant is indeed a constant. The general luminosity of the sun undoubtedly changes with age, slowly



Declassified in Part - Sanitized Copy Approved for Release 2012/03/12 : CIA-RDP82-00039R000100190014-6

Declassified in Part - Sanitized Copy Approved for Release 2012/03/12 : CIA-RDP82-00039R000100190014-6

in our conception of time. Besides these, only gradual fluctuations of luminosity with great periods and small amplitudes may be permitted. The sun is a normal diminutive star of the spectral class G. It may become a variable star only under a real threat of a grave catastrophe.

12. Fluctuations in climate, of which we are witnesses, are characterized, first of all, by the fact that we do not discover any changes in the luminosity of the sun -- much less any systematic changes. Then the warming of the polar zones began simultaneously in the northern and southern hemispheres of the earth; the temperatures in the cold portion of the year especially are rising. The warming process is proceeding rapidly and evidently with self induction. At the same time, it is developing with constant fluctuations, with retrogressions to phases already covered, but still it develops further and further. It is necessary to stress that the annual temperatures of the earth have not changed, although in separate circulatory areas sharp changes have been observed, and in the future greater ones are expected.

In the equatorial-tropical zone the mean temperatures saw a decrease of about one to two degrees, and in the temperature of the Arctic there was an increase of several degrees (8).

Only one explanation can be given to the observed facts: the contemporary climatic fluctuation, and accordingly all general climatic fluctuations and their component climatic variations, are conditioned upon changes in the distribution of a practically unchanging inflow of solar radiation. In other words, all fluctuations and changes in climate are determined by the changes in the general cir-



Declassified in Part - Sanitized Copy Approved for Release 2012/03/12 : CIA-RDP82-00039R000100190014-6

Declassified in Part - Sanitized Copy Approved for Release 2012/03/12 : CIA-RDP82-00039R000100190014-6

culation of the earth's atmosphere.

Through this the problem is simplified: changes in the general circulation occur under the influence of changes in solar activity, as we know by experience. Those reactions of the general circulation on the changes in solar activity which we had mentioned thus far must necessarily enter as component parts of a mechanism still unknown to us -- a mechanism which activates the development of the general circulation. The following occur upon the strengthening of solar activity: (1) strengthening of the general circulation; (2) growth of meridional barometric gradients and decrease of thermal gradients between the equator and the poles; (3) shifts of sub-tropical maximums of pressure toward the respective poles and widening of the equatorial tropical zone; (4) strengthening of sub-tropical maximums of pressure and polar zones with a successive simultaneous advance by them upon their respective temperate latitudes; (5) increase in the area of the equatorial-tropical circulatory zone; (6) decrease in the area of temperate zone circulation with an increasing dependence by them upon the circulation of their active neighbors.

13. In the main, the general circulation is composed of two transferables -- east-west and meridional (by which we mean the eastern type of circulation of G. Ya. Vangengeym). The first is dependent on the rotation of the planet, the second on meridional baric gradients. The pressure and rhythm of both main transferables depend on the condition of the redistribution of energy in the atmosphere and hydrosphere.

At the present time these transferables are antagonistic: if under the given pressure of general circulation one of them is strengthened, then the other correspondingly weakens. In this manner the



Declassified in Part - Sanitized Copy Approved for Release 2012/03/12 : CIA-RDP82-00039R000100190014-6

Declassified in Part - Sanitized Copy Approved for Release 2012/03/12 : CIA-RDP82-00039R000100190014-6

strengthening or weakening of the general circulation is accomplished by a complex dual mechanism, about which there are arguments yet to be settled; what precisely to consider as a sign of strengthening -- agitation in the east-west transferable, or strengthening of the meridional. We believe that the argument here is about words and not about the substance of the phenomenon.

Judging the problem on the strengthening and weakening of general circulation, it is necessary to take into consideration its state of regularity. The more complicated the given process the more important is its state of regularity. The greater the latter, the more rapid and more effective is the process.

By the state of regularity of the general circulation we understand the greater or lesser regularity in a time-space distribution of homogeneous meteorological processes.

On this state of regularity depends the velocity of the exchange of air masses and, accordingly, the effectiveness of the redistribution of energy. It is necessary to distinguish the velocity of the movement of the baric systems and the velocity of transfer of air masses. Often, at slow transfer velocities of baric bodies, we observe great transfer velocities of air masses. Sometimes, however, at great velocities of movement of baric systems, we ascertain slow velocities of transfer of air masses.

The following are factors which disturb the state of regularity of the general circulation: (1) structure of the earth's surface, (2) interzonal exchange, and (3) local circulation. The regulatory factor is the sun's activity. Thus we have a period of considerable regularity between 1933 and 1944; there is more regularity than in the previous



Declassified in Part - Sanitized Copy Approved for Release 2012/03/12 : CIA-RDP82-00039R000100190014-6

Declassified in Part - Sanitized Copy Approved for Release 2012/03/12 : CIA-RDP82-00039R000100190014-6

cycles of solar activity.

The most regular portion of the contemporary general circulation of the earth's atmosphere is the trade wind circulation. Here the antagonism between the main components is resolved: trade winds provide a synthesis to the west-east and meridional transfers with the undoubted predominance of the latter. Here it is necessary to note especially that during the course of an 11-year cycle with a strengthening in solar activity there is also an acceleration in the trade winds (up to 10 percent in relation to the velocity at the minimum period) and an increase in the trade wind area of circulation.

The undoubted fact of the influence of solar activity upon meteorological processes is explained by the interference of active ultra-violet radiation of the sun in the condensation processes of the earth's atmosphere. As a result of the changes in the number or increase in the activity of condensation nuclei, induced by each impulse of solar activity, there sets in the compulsory resolution of the mature humidity-labile conditions. By mature humidity-labile conditions we mean those with a relative humidity over 80 percent. The forced resolution of the latter moves in the rhythm of the development of solar activity, and at each separate time occurs practically simultaneously over the entire globe. This rhythm is superposed over the macrometeorological process and determines it.

Humidity-labile equilibriums, in the absence of solar activity, are resolved not in rhythm but in confusion. With the strengthening of solar activity the number of resolution of humidity-labiles falls rapidly. The overwhelming majority of condensation processes, which determine the rhythm and distribution of the macrometeorological process, submit to the rhythm of impulses; and the general circulation,



Declassified in Part - Sanitized Copy Approved for Release 2012/03/12 : CIA-RDP82-00039R000100190014-6

Declassified in Part - Sanitized Copy Approved for Release 2012/03/12 : CIA-RDP82-00039R000100190014-6

having been regulated, becomes more rapid (11). With the weakening of solar activity, the condensation processes become less regulated insofar as the resolution of humidly non-stables becomes more elemental. A considerable portion of energy of all circulations is wasted unproductively upon the weakening of solar activity, and the general circulation is decelerated.

The strengthening of general circulation is formed simultaneously with the strengthening of each of the two main transferables. However, at the present time one of them is strengthening more than the other. The meridional transferable strengthens relatively more often; exceptions appear only in the case of sectional separation of the general circulation by the dynamic-monsoon processes in the Atlantic and Pacific Ocean sectors.

With the weakening of the general circulation, both main transferables weaken simultaneously, however the meridional weakens relatively more. In this case the relative predominance is held by the west-east transferable.

With the weakening of the general circulation, the quasi-stationary processes receive considerable development -- for example, from 1898 to 1902. With the strengthening of the general circulation, the percentage of quasi-stationary processes is lowered and the overwhelming predominance is held by advective processes. Thus, in the period from 1936 to 1939, quasi-stationary processes were observed only singly.

Upon the regulation of the circulation, the outflow of heat from the equatorial-tropical zone and the two zones of sub-tropical maximums is strengthened.. That is, the temperatures of the equatorial-



Declassified in Part - Sanitized Copy Approved for Release 2012/03/12 : CIA-RDP82-00039R000100190014-6

Declassified in Part - Sanitized Copy Approved for Release 2012/03/12 : CIA-RDP82-00039R000100190014-6

tropical zones fall with the strengthening in the general circulation and rise with its weakening.

14. All local circulations enter into the general circulation as components. The most important of them are ocean circulations. They condition the transfer of immense reserves of heat in ocean currents. The action of these reserves, with known after-effects, influences the development of the general circulation.

Evidently, the influence of ocean circulation conditions, in the main, the inertia of the general circulation. In the northern hemisphere the joint action of the Atlantic and Pacific Ocean circulations, due to their synchronous or asynchronous strengthening and weakening, establish a certain kind of pulsation, as yet not sufficiently studied.

Monsoon circulation appears as the main backbone of the general circulation. By the former we understand any kind of local circulation established because of diverse thermal regimes of adjoining physico-geographic areas. The leveling of the thermal regime of generally all areas, upon the strengthening of the general circulation, destroys monsoon circulation. Conversely, the weakening of the general circulation aids in the development of monsoons. However, with the strengthening of the general circulation and especially upon the strengthening of meridional circulation, areas of stable baric maximums and depressions, fully imitative of monsoon phenomena, are sometimes established. Any flow of air forms to the right of it a pressure area, and to the left -- an area of discharge. In case of stable localized and sufficiently intensive circulation, areas of dynamic maximums and depressions become important local members of circulation,



Declassified in Part - Sanitized Copy Approved for Release 2012/03/12 : CIA-RDP82-00039R000100190014-6

Declassified in Part - Sanitized Copy Approved for Release 2012/03/12 : CIA-RDP82-00039R000100190014-6

and while the direction and territorial stability of the process are conserved, their development progresses with a certain self-induction. Like processes must be placed in an independent group of dynamic-monsoon phenomena.

The similarity between these dynamic formations and monsoons makes it difficult to differentiate them from purely monsoon phenomena. The difference can be accurately ascertained if the history of such formations is studied. Real monsoon phenomena follow the semi-annual rhythm of the life of the atmosphere which influences the formation of winter and summer monsoons. Dynamic-monsoon phenomena do not follow the semi-annual rhythm. With certain territorial shifts, their existence lasts more than one ~~season~~ half year. Thus, the winter dynamic Siberian anti-cyclone continues to exist in the form of a summer dynamic Kazakhstanian anti-cyclone. The dynamic-monsoon American winter anti-cyclone exists in the summer in the form of the American-Canadian summer anti-cyclone.

15. The main divisions of the general circulation are formed by zonal boundaries. The latter do not follow geographic parallels but depart from them under the influence of the structure of the surface underneath, the time of the year, and the tension of the general circulation. Upon the joint action of two neighboring local circulations, one of them remains unchanged in principle, while the other is reformed under the influence of the first. We call these phenomena active and passive circulations.

The main zones of general circulation of the earth's atmosphere are: equatorial-tropical, the two zones of sub-tropical maximums of



Declassified in Part - Sanitized Copy Approved for Release 2012/03/12 : CIA-RDP82-00039R000100190014-6

Declassified in Part - Sanitized Copy Approved for Release 2012/03/12 : CIA-RDP82-00039R000100190014-6

pressure, two zones of temperate latitude, and two polar zones.

The main active circulation zone is the equatorial-tropical zone, which has the largest area and the greatest energy resources. It directly determines the regimen of the sub-tropical maximums and the polar zones which it supplies with air. The latter two zones are equally active in relation to the temperate latitude zones, the circulation of which they determine jointly.

With the strengthening of general circulation, the boundaries of the main zones shift; the boundaries of the equatorial-tropical zone and the areas of sub-tropical maximums shift toward the poles, and the polar zones shift in the direction of the lower latitudes. In this manner the zones of the temperate latitudes are attacked by their neighbors, active by comparison..

The strengthening in the general circulation is composed of the strengthening of generally all transferables. For this reason, climatic contrasts are leveled out: temperatures of the equatorial-tropical zone and the sub-tropical maximums fall somewhat, temperatures of the polar zones rise considerably; and the temperatures of the temperate zones, assuming a passive attitude in the exchange of energy, rise slowly. In total the mean temperature of the earth remains unchanged.

With the weakening of the general circulation, composed of the weakened overwhelming majority of air-mass transferables, the area of the temperate latitude zones increases, whereas the areas of all the main zones decrease; the sub-tropical maximums approach the equator; the interzonal exchanges decrease and the climatic contrasts are sharpened.



Declassified in Part - Sanitized Copy Approved for Release 2012/03/12 : CIA-RDP82-00039R000100190014-6

Declassified in Part - Sanitized Copy Approved for Release 2012/03/12 : CIA-RDP82-00039R000100190014-6

With the west-east transferable the boundaries of the circulatory zone are sharply delineated, and interzonal exchange becomes rather difficult. Meridional transfer strengthens interzonal exchange and, diminishing the difference in the regimen, makes the zonal boundaries less definite. The shift of zonal boundaries and their existence under definite conditions depends mainly, as far as can be judged, on the development of meridional transfer.

16. The changes in the general circulation, influencing the type and tension of redistribution of the constant in accordance with the size of the energy inflow, determine the development of climate. The development of climate according to geologic history indicates the continual development of the general circulation not experiencing planet-wide catastrophes. It is not possible to point out a different cause for this lengthy and directed development other than the development of solar activity. Helio-physics indicates the epochal development of activity during the Nineteenth and Twentieth centuries, reflected in and determining the development of contemporary fluctuations of climate. We know of no other cause for the observed process in the development of climate. The action of this causal interrelation we can apply to all climatic developments.

Analyzing the conditions in the epochs of climatic optimums, we see the surprising similarity of the climate from the equator to the 70 and 80 degrees North and South latitudes. We can follow this similarity in conditions by the distribution of flora. Both optimums, Devonian-Carboniferous and Cretaceous-Paleocene, give the same picture. A considerable similarity in flora is found in all layers, with the absolute impossibility of subdividing them into separate floral areas (5). One and the same kind of plants are found in deposits in



Declassified in Part - Sanitized Copy Approved for Release 2012/03/12 : CIA-RDP82-00039R000100190014-6

Declassified in Part - Sanitized Copy Approved for Release 2012/03/12 : CIA-RDP82-00039R000100190014-6

Greenland, Spitzbergen, Bear Islands, Canadian Archipelago, Canada and the United States, Western Europe, all of the USSR, Australia, the Antarctic, South America, and Africa. In connection with the absence of special forms conditioned to narrow limits, this illustrates the considerable similarity of conditions. At the same time the predominance of ligneous forms in the flora of the optimums -- which is characteristic for the tropical flora now -- speaks of the considerably higher average temperatures in the above mentioned higher latitudes, which is being observed now.

At the same time, undoubtedly, there were xerothermic areas, where xerophytic flora of the forest-steppe abounded, and which subsequently were further developed with the worsening in the climate. Generally, however, it is necessary to stress that at the time of climatic optimums there were no actual deserts nor desert-steppes.

Optimums influenced rapid development of plants. In the Devonian, water plants adapted themselves to land, giving birth to land flora. In the Cretaceous epoch angiosperms, originating in the Jurassic epoch, quickly developed over the whole earth.

17. If the link between climate and weather, and accordingly between the general circulation of the earth's atmosphere, took place in the past, then the climatic optimums answer certain definite and rather stable (in time) conditions of general circulation. On the basis of contemporary relations it can be stated that the distribution of climatic zones at that time ~~were~~ was different and that the zonal boundaries were not definite, as if half obliterated. The equatorial-tropical zone and the sub-tropical maximums within the limits of plus



Declassified in Part - Sanitized Copy Approved for Release 2012/03/12 : CIA-RDP82-00039R000100190014-6

Declassified in Part - Sanitized Copy Approved for Release 2012/03/12 : CIA-RDP82-00039R000100190014-6

and minus 65 degrees latitude were covered with evergreen plants. From these boundaries extended areas which were composed of deciduous flora with a considerable mixture of evergreens. In all, there were five circulatory zones: equatorial-tropical, closely linked to the bordering sub-tropical maximums, and two polar zones. Inter-zonal exchange was accomplished with incomparably more ease than now. The temperate latitude zones in these epochs were not present.

The general circulation in the epochs of climatic optimums should have developed under an undoubted predominance of the meridional transfer and under conditions of great regularity. This explains the regimen of circulation zones, the similarity of their weather characteristics, absence of deserts, the appearance of heat-resisting deciduous forests in the high latitudes, the absence of distinct floral areas.

The general circulation of these epochs is constructed in such a manner that it assures a rapid and stable redistribution of heat which is obtained in the low latitudes. This is attested to also by the fact that the role of local circulations is brought down to zero.

The duration of each optimum is put at about 40 million years. Accordingly, the stability of circulation was assured by a continuously active and very strong cause. Inasmuch as the development of the general circulation observed by us now is conditioned by the path of solar activity, it would not be erroneous to conclude that solar activity provided long and stable maximums of activity during those epochs.

The belief has been repeatedly expressed that the rise in the content of carbon dioxide in the atmosphere would tend to better the



Declassified in Part - Sanitized Copy Approved for Release 2012/03/12 : CIA-RDP82-00039R000100190014-6

Declassified in Part - Sanitized Copy Approved for Release 2012/03/12 : CIA-RDP82-00039R000100190014-6

climate of the Devonian-Carboniferous and Cretaceous-Paleocene optimums type. Based on the course of soil-forming processes and on the type of wind erosion, it is possible to state with great certainty that the first of the optimums actually possessed a very great reserve of carbon dioxide in the atmosphere which only subsequently was exhausted by organic flora and fauna. However, this condition did not play a decisive role: the Cretaceous-Paleocene climatic optimum appeared under carbon dioxide conditions very similar to the present. On the other hand, the first of the known climatic pessimums -- Cambrian -- developed under an exhausted supply of carbon dioxide, even more so than during the Devonian-Carboniferous optimum.

18. With the rise of the temperature background, the thermal differences between separate regions of circulation recede, particularly between cyclones and anti-cyclones making up the separate baric systems. Nonetheless the circulation moves intensively as present equatorial-tropical circulations show. "Baric bodies" as working wheels effect the general circulation, but they also slow it down. The contemporary trade wind circulation shows that under a regulated process and a lowering of thermal contrasts the cyclones and anti-cyclones do not appear to be necessary components of the realization of air-mass exchange.

Within the limits of development, the meridional transferable must provide a strongly stable distribution of meridional loss, taking into consideration the deviating force of the earth's rotation. It is linked with and influenced by the hydrological condition of the oceans. Velocity of the currents depends on the velocities of



Declassified in Part - Sanitized Copy Approved for Release 2012/03/12 : CIA-RDP82-00039R000100190014-6

Declassified in Part - Sanitized Copy Approved for Release 2012/03/12 : CIA-RDP82-00039R000100190014-6

air exchanges, but the velocities of the currents in a greater or lesser degree also determine the velocities and stability of the territorial distribution of air transfer. This dialectical unity becomes the deciding moment of the general circulation after reaching a certain level of regulation. Up to this level, however, both members of the unity develop more or less contradictorily. In the established circulation, as this is found in trade winds, it is necessary to speak of the harmonious circulation of the atmo-hydrosphere.

The strengthening of the meridional transfer stimulates the acceleration of ocean currents which level off the thermic conditions of the atmo-hydrosphere, and the process continues with self-induction and auto-regulation, as we observe it in our day. The inertia of the process of the hydrosphere spills over into the general harmonized stability of the atmo-hydrospheric circulation. Precisely because of this the high levels of solar activity provide a stable and regulated circulation, developing upon lowered thermic gradients of the equator to the pole, and free of chance changes because of the absence of unproductive expenditures of energy in chaotic movements. This is a geophysical interpretation of the initial determining moment of regulation of solar activity. Low levels of activity provide an unregulated and unstable circulation. Low levels of solar activity at the end of the Nineteenth and beginning of the Twentieth centuries (from 1878 to 1913) gave birth to an enthusiasm in climatology and meteorology for average values and the unselective application of statistical analysis without taking physical laws into consideration.

In epochs of climatic optimums the regulated circulation of



Declassified in Part - Sanitized Copy Approved for Release 2012/03/12 : CIA-RDP82-00039R000100190014-6

Declassified in Part - Sanitized Copy Approved for Release 2012/03/12 : CIA-RDP82-00039R000100190014-6

the trade wind type, as far as can be judged, embraces great territories described by warm-climate evergreen flora. At the present time, trade winds in part are masked by monsoons of continental circulation, but with the strengthening of the general circulation the influence of monsoons can hardly conserve the value of the determining moment. Trade wind circulation at the present time is observed in the majority of cases over oceans, and there it carries moisture-saturated air masses. Over continents, due to the strong development of deserts and semi-deserts, dry air masses are carried. In the region of the proper-equatorial circulation, over tropical forests, trade winds are saturated with moisture, the same as over oceans. Therefore, if we accept, based on the distribution of Jurassic flora, the distribution prior to the beginning of the Cretaceous period along all of the tropical and sub-tropical regions of hygrophyllic forest growth, then it is necessary to accept that in epochs of a climatic optimum the trade winds over continents carry air just as humid as over oceans.

At the present time, on the strength of the determining value of sub-tropical stationary anti-cyclones in the region of the trade winds, precipitation in general is adapted to the western regions of the oceans. The eastern regions of the oceans receive moisture, in general, because of fog, as in the region of Makaronezïya (archipelagoes of the Atlantic).

Upon the regulation of the circulation, the differences between the eastern and western regions of ocean trade winds level off because of a considerable weakening of continental xerothermic regions. However, Cretaceous flora still show that the adaptation of plants to dry and warm climates is going on in many regions of



Declassified in Part - Sanitized Copy Approved for Release 2012/03/12 : CIA-RDP82-00039R000100190014-6

Declassified in Part - Sanitized Copy Approved for Release 2012/03/12 : CIA-RDP82-00039R000100190014-6

the earth.

Trade wind circulation, thanks to its regulation, develops intensively upon the lowering of meridional baric gradients under which cyclone and anti-cyclone circulation, similar to contemporary circulation of the temperate latitudes, would have ceased on the strength of expenditures on unregulated movements.

Precisely due to the development of circulation of a trade wind type, upon the supression of monsoon circulation, the lowering of the equator-pole thermic gradient -- attained in the epoch of climatic optimums -- did not paralyze the general circulation, inasmuch as the meridional baric gradients of the atmo-hydrosphere are constantly maintained on a sufficiently high level.

19. After each climatic optimum, there followed, with some fluctuations, gradual and regular worsening in the climate, conditioning the appearance of floral regions and, particularly, desert-steppes and subsequently deserts. Two cases presented by the geologic chronicle show a similarly-acting picture, down to details: the Carboniferous-Permian and Tertiary climatic worsenings. The boundaries of circulation zones become more and more definite; the region of regulated trade wind circulation becomes smaller and the resultant region of circulation of the temperate latitudes continually grows. The redistribution of energy becomes less and less complete and for the Pliocene we have a sharply defined polar circulation, a circulation of the temperate latitudes, a sub-tropical maximum, an equatorial-tropical zone. The gradual development of the climate in this epoch shows the ever increasing role of the



Declassified in Part - Sanitized Copy Approved for Release 2012/03/12 : CIA-RDP82-00039R000100190014-6

Declassified in Part - Sanitized Copy Approved for Release 2012/03/12 : CIA-RDP82-00039R000100190014-6

west-east transfer and the ever decreasing regulating of the general circulation. The role of the meridional transfer is continually suppressed and, in the transitional period of the climatic pessimums, both transfers become equally strong. The general circulation receives a limiting instability, under which its development is determined by chance events of local circulations.

The transitional condition of climatic pessimums is stressed, on the one hand, by the numerous advances of glaciation in each of these epochs and, on the other hand, the short duration of these glaciations which embraced an interval of about one million years in each of the pessimums. The only explanation for this, from our point of view, can be the instability of the general circulation in these epochs, instability which influenced the appearance and development of stable local circulations, initially bringing about worsening in local climates. As a measure in the development of the process, the latter spill over into occurrences having a planet-wide significance determining the general circulation. It is necessary to note that the trade wind circulation during this time continues to exist within limited boundaries, determining the relative stability of the equatorial-tropical zone climate. The worsening of the climate in the epoch of the pessimum disturbs the polar and temperate latitude zones.

In the regions of positive balances of solid precipitation, snow drifts, firns, and glaciers developed with time. Due to the strengthening of the magnitude of local circulations, the glaciers spilled over into surface glaciation which further determined the circulation of the given region. The contemporary residue of surface glaciation -- the Antarctic and Greenland shields (especially the



Declassified in Part - Sanitized Copy Approved for Release 2012/03/12 : CIA-RDP82-00039R000100190014-6

Declassified in Part - Sanitized Copy Approved for Release 2012/03/12 : CIA-RDP82-00039R000100190014-6

former) -- influence the definitely expressed local circulation as well as the development of general circulation.

In regions not suitable to the accumulation of solid precipitation, permafrost was developed. The lessening in the strength of surface glaciation from west to east indicates the considerable development of west-east transfer during Quaternary glaciation. Lessening in glaciation from west to east is observed in the present epoch, and is due to the growth of dry climate influenced by the predominance of west-east transfer.

The conditions of Quaternary glaciations, clarified incomparably ~~sufficiently~~ more fully than the conditions of the Carboniferous-Permian glaciation, indicate the causes for the formation of climatic pessimums. The latter appear only under extreme instability of the general circulation when the west-east and the meridional transfers are equally strong, not extensive, and often of accidental circulation, but sufficient to reconstruct the general circulation in the non-tropical zones.

At the time of climatic pessimums, polar zones and temperate latitudes participate in glaciations. At such time the equatorial-tropical zone and the sub-tropical maximums evoke only separate reactions on the effect of regions of glaciation. Thus the increasing humidity in the region of the northern sub-tropical maximum during this epoch was so great that in Northern Africa, in the present Sahara, there was a strong and widely developed river system which appeared in the epoch of the optimum. Of the numberless rivers and streams, only dry beds have been preserved. Man inhabiting these regions left for us paintings on stone depicting hunting scenes,



Declassified in Part - Sanitized Copy Approved for Release 2012/03/12 : CIA-RDP82-00039R000100190014-6

Declassified in Part - Sanitized Copy Approved for Release 2012/03/12 : CIA-RDP82-00039R000100190014-6

the subjects of which were animals that at the present time have retreated far to the south under the influence of the developing climatic deserts.

In direct connection with surface glaciation, regions of arctic semi-deserts developed, which also show the great stability of the general circulation. Glaciations embraced the junction of the arctic and temperate latitude zones at a time when the high Arctic was free of ice. The regulation of the general circulation reaches a minimum in this epoch and the meridional baric gradients depend on local circulations.

20. With the further efforts of the west-east transfer, under the influence of weakened solar activity, the boundaries of zonal circulations become more and more definite and real deserts are formed, the climate of which is more severe according to the development of the west-east transfer; meridional baric gradients increase, and the circulation, begun by shifts of cyclones and anti-cyclones, strengthens. The regulation of the general circulation, suppressed due to the weakening of the meridional transfer, begins to increase because of the increasing importance of the role of the west-east transfer. This explains the climatic conditions of the Triassic epoch. Geological chronology shows that the duration of the development of this second maximum of stability of the general circulation embraced an interval of about 10 to 12 million years. Therefore, the second maximum of stability is conditioned, as the first, by powerful and long-lasting causes.

The unity of development in the general circulation, appearing in our day, indicates that the appearance and existence of the



Declassified in Part - Sanitized Copy Approved for Release 2012/03/12 : CIA-RDP82-00039R000100190014-6

Declassified in Part - Sanitized Copy Approved for Release 2012/03/12 : CIA-RDP82-00039R000100190014-6

second maximum of stability are conditioned by a nearly complete break in the influence of solar activity. In this manner, from the first maximum of stability in the general circulation -- from the climatic optimum of the First class, when the limit of development of solar activity determines the limit of development of the meridional transfer, and to the second maximum of stability, when solar activity falls to zero forming a climatic optimum of the Second class with the full predominance of west-east transfer -- solar activity travels a half wave-length of its development, determining a half wave-length of climatic development.

21. From the second maximum of stability in the general circulation of the earth's atmosphere, on the ascending branch of the development of solar activity and climate, the processes flow more quickly. The role of participation of the west-east transfer gradually decreases, and the participation of the meridional transfer increases. On the ascending arm of the curve of the development process, again a period of equal influence of both main transfers is met, and accordingly the extreme instability in the general circulation results. However, these epochs do not form climatic pessimums, thanks to the rapid tempo in the development of the process. The period of instability of the general circulation has too short a duration, interfering in the accumulation of glaciation, in the development of which time plays the determining role.

The principal reconstruction of the general circulation of the earth's atmosphere in epochs of its extreme instability, leads to the change in distribution of air masses and water masses on the globe. This reconstruction is apparent not only in the life of the



Declassified in Part - Sanitized Copy Approved for Release 2012/03/12 : CIA-RDP82-00039R000100190014-6

Declassified in Part - Sanitized Copy Approved for Release 2012/03/12 : CIA-RDP82-00039R000100190014-6

atmosphere, but also, evidently, in the life of the magmatic layer. In any case, all epochs of mountain formations are timed with those reconstructions, and particularly with those reconstructions on the ascending arm of development in the general circulation when surface glaciations are absent.

The mildness of the climate quickly increases on the ascending arm of the development of general circulation. Desert phenomena lessen and boundaries of floral regions are slowly erased; forests move farther toward the poles, and, finally, deciduous forests embrace the polar zone. On a small scale we see a similar fluctuation in climate in the history of post-glacial Quaternary flora. The end of the last great glaciation is dated with great certainty at more than 8,000 years before our era. During the time from the end of the last glaciation to the present, there were two betterings and two worsenings of climate. These fluctuations of climate left ineradicable traces, its own type of climatic passport, in the form of plant pollen buried in the deposits of these epochs.

22. In summation, it can be said that the entire history of the development of climate, supported by deposits of surface flora, etc., from the time of the Devonian to the present day, speaks of the unity of causes acting during the whole of this interval of time, and of the regularity of development of climate. This development is not effected unvaryingly but with continual fluctuations and regressions to already covered phases; moreover, if we set aside fluctuations, the development of climate shows the existence of a certain cyclic form which must also be characteristic of the cause on which this development depends.



Declassified in Part - Sanitized Copy Approved for Release 2012/03/12 : CIA-RDP82-00039R000100190014-6

Declassified in Part - Sanitized Copy Approved for Release 2012/03/12 : CIA-RDP82-00039R000100190014-6

Those changes which occur in front of our eyes are dependent on the development of solar activity. With great certainty we extrapolate this dependence on the past development of climate and similarly on its future changes. The maximum of stability of the First class, coinciding with the climatic optimum of the Cretaceous-Paleocene type, is conditioned by the limit of development of solar activity and, correspondingly, by the limit of development of the meridional transfer in the atmosphere. At this time local circulations are suppressed and the general circulation is determined by the meridional transfer. Meridional thermic and baric gradients at this time reach a minimum, but the general regulation of the circulation, developing on the trade wind type, allows it to act without hindrance. The fluctuations proper of the earth's atmosphere at this time are completely suppressed and are substituted by the meridional transfer.

With the weakening of solar activity and the strengthening of the west-east transfer, the general circulation again becomes stabilized and attains the second maximum of stability under the absolute predominance of the west-east transfer. At this time the climatic optimum of the Second class develops, observed for the last time in the Triassic era. The general circulation in this period is completely regulated and develops without participation of solar activity. The stabilizing moments are the fluctuations proper of the earth's atmosphere.

The rising arm of the climatic development, according to the measure of strengthening in solar activity and weakening in west-east transfer, again permits the appearance of the meridional transfer, the strength of which grows with time. And here the breaking



Declassified in Part - Sanitized Copy Approved for Release 2012/03/12 : CIA-RDP82-00039R000100190014-6

Declassified in Part - Sanitized Copy Approved for Release 2012/03/12 : CIA-RDP82-00039R000100190014-6

point occurs when the growing instability of the general circulation attains a maximum and then begins to recede with the growing role of the meridional transfer.

On the descending arm of the development of climate a similar period of instability of general circulation forms a climatic pessimum with extensive surface glaciations, in the development of which the determining role is the factor of time. On the ascending arm of climatic development the period of instability does not establish climatic pessimums in view of the rapidity in the development of the process.

23. In this manner, we accept the existence of regular fluctuations in the development of solar activity, with enormous periods and relatively great amplitudes. The history of the earth's climate is a witness to this fluctuation. It gives a chronological background to the processes. Using uranium clocks, we may evaluate the duration of geological epochs in millions of years, which evaluation is given in Table I.

Table I

DURATION OF GEOLOGICAL EPOCHS IN MILLIONS OF YEARS

| | | | | | | | |
|---|---|---|---|---|---|---|---|
| Cambrian | 74.7 | Carboniferous | 60.7 | Jurassic | 50.2 | Paleogene | 38.0 |
| Ordovician | 44.6 | Permian | 38.6 | Cretaceous | 36.4 | Neogene | 31.7 |
| Silurian | 34.3 | Triassic | 34.4 | | | | |
| Devonian | 31.6 | | | | | | |
| | 185.2 | | 133.7 | | 86.6 | | 69.7 |
| | | | | | 475.2 | | |



Declassified in Part - Sanitized Copy Approved for Release 2012/03/12 : CIA-RDP82-00039R000100190014-6

Declassified in Part - Sanitized Copy Approved for Release 2012/03/12 : CIA-RDP82-00039R000100190014-6

Even though the reliability of this scale of time is none too great, the order of values it gives is sufficiently accurate. Using this table we constructed a second graph where on the axis of the abscissa the duration of geological epochs is shown, calculated according to the uranium clock in millions of years, and on the axis of the ordinate, the conventional tension of solar activity (Figure 2).

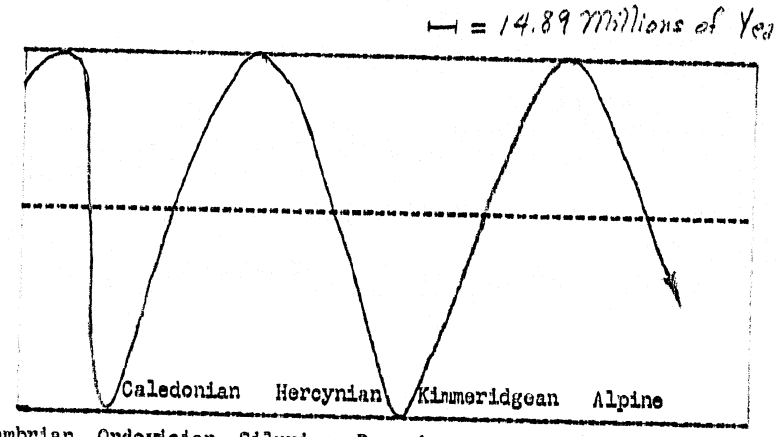


Figure 2. A smoothed curve of solar activity according to geologic chronicle. The curve gives an assumed path of solar activity expressed in conventional values.

The scale of the ordinate is deliberately reduced, as is shown by contemporary relation of tension of solar activity in the epochs of maximums and minimums of 11-year cycles. A correct relation to the ordinates should give values twice as large as is shown on the graph. The upper straight line limiting the graph gives the epochal change in the liminosity of the sun expressed in the changes of its activity. According to our calculations the over-all luminosity of



Declassified in Part - Sanitized Copy Approved for Release 2012/03/12 : CIA-RDP82-00039R000100190014-6

Declassified in Part - Sanitized Copy Approved for Release 2012/03/12 : CIA-RDP82-00039R000100190014-6

of the sun from the Carboniferous to the Cretaceous was lowered by 0,69 percent. At any rate these calculations are approximate.

Beginning with the Devonian to our time the curve in the change of solar activity is fixed according to climatic changes based on paleobotanic data. From the Devonian back to the Proterozoic era this curve is extrapolated. Therefore it is not possible to guarantee the invariability of the length of the period of change in the solar activity and climate. The last wave from the Devonian-Carboniferous optimum to the Cretaceous-Paleocene took about 220 million years.

Vertical dots denote the epoch of instability of the general circulation with the accompanying development of surface glaciation. The first — Cambrian — left traces over the whole of the earth, and the second - - Permian - - embraced, in the main, the southern hemisphere. Evidently, this is conditioned by the distribution of land and sea. The Quaternary glaciation embraced equally both hemispheres.

Periods of mountain formations, connected to the reconstruction in the type of circulation, are shown below by horizontal dashes. These are the Caledonian, Hercynian, Kimmeridgean and Alpine folds. Mountain formations of the Cambrian glaciation are marked arbitrarily.

24. Evaluating the present state of evolution of climate and using the second graph, we may with great certainty state that the glacial period is an accomplished phase in climatic history and that subsequently there will emerge a lengthy climatic development in the direction of an ever-increasing state of regularity of the general circulation, an increase in the role of west-east transfer, and the gradual formation of a climatic optimum of the Second class.



Declassified in Part - Sanitized Copy Approved for Release 2012/03/12 : CIA-RDP82-00039R000100190014-6

Declassified in Part - Sanitized Copy Approved for Release 2012/03/12 : CIA-RDP82-00039R000100190014-6

However, this process continues with incessant fluctuations, one of which, being experienced now by us, influences the return of the general circulation to a phase already covered, namely, to the relatively greater value of meridional transfer in the activity of the general circulation and to the lessening of climatic contrasts in the circulation zones. The interval of time separating us from the middle of the coming optimum of the Second class can be estimated at 58 million years.

- E N D -



Declassified in Part - Sanitized Copy Approved for Release 2012/03/12 : CIA-RDP82-00039R000100190014-6

Declassified in Part - Sanitized Copy Approved for Release 2012/03/12 : CIA-RDP82-00039R000100190014-6

# VERTICAL MOVEMENT OF THE AIR AND COSMIC DUST

L. R. Rakipova

In 1899 Teyseran-de-Bor discovered an interesting fact concerning the division of the atmosphere into two main layers: troposphere and stratosphere.

The initial concept held that in the stratosphere only horizontal movement of air and diffusive equilibrium of air took place. Actually, the conditions of vertical stability, influenced by isometric distribution of the temperature in the stratosphere omit, it would seem, the possibility of the existence here of vertical movement of air. Such ideas resulted in the well known calculations of the chemical properties of this portion of the atmosphere by Gemfris and Chempen as well as in its name itself.

But during the last 10 to 20 years the error of the original ideas has been demonstrated.

The chemical composition of the air in the stratosphere is sufficiently constant up to the ionosphere. This follows from the direct analysis of air samples taken on the flights by Soviet stratosphere observers up to a height of 20 to 22 kilometers, on the release of balloon soundings by Regener, Pennet, and Glyukauf from a height of 25 to 30 kilometers. The lines of emission of nitrogen and carbon dioxide were discovered by Vegard, MacLennak, and others in the spectra of northern lights and luminosity of the nocturnal sky.

The movement of meteoric trails, silver clouds, point to the existence of a stratospheric circulation composed of the



Declassified in Part - Sanitized Copy Approved for Release 2012/03/12 : CIA-RDP82-00039R000100190014-6

Declassified in Part - Sanitized Copy Approved for Release 2012/03/12 : CIA-RDP82-00039R000100190014-6

general system of stratospheric trade winds and anti-trade winds and disturbing local systems of a cyclonic type; the latter appear in the day and are destroyed at night /17. Sometimes observations of the movement of meteoric trails point to the direct vertical current of air in those layers.

What can be the cause for the mixing of air and the appearance of local circulation systems in the stratosphere compatible with the stable stratification of the latter?

As one of the causes, whose action is distributed over the whole stratosphere, it seems possible to assume the heating of the air by dust absorbing solar radiation. Actually, the appearance here of non-adiabatic vertical transfers of air may not be accompanied by its cooling to a lower temperature than the surrounding stratosphere. For this it is sufficient that upon rising, the air receive a quantity of heat from dust, compensating its cooling as a result of expansion. In this manner the vertical stability of the stratosphere (in the usual sense) on the one hand, and the vertical movement of air in it on the other hand, will not be mutually exclusive phenomena, and the problem of "mixed" atmosphere will appear solved.

As to dust, it can be assumed that it must be predominantly of cosmic origin. Volcanic dust is carried to the stratosphere comparatively rarely and usually obstructs only the lower layers -- up to 30 kilometers. Besides, the particles of volcanic dust are probably too large to remain in the air sufficiently long and show any kind of durable effect on its thermic condition. According to the radius of Bishop's rings observed after volcanic



Declassified in Part - Sanitized Copy Approved for Release 2012/03/12 : CIA-RDP82-00039R000100190014-6

Declassified in Part - Sanitized Copy Approved for Release 2012/03/12 : CIA-RDP82-00039R000100190014-6

eruptions (1883, Krakatoa, Sunda Islands), it is possible to determine that the size of particles was 1.8 microns, and if among the erupted products there were some gaseous substances, then they must have condensed in the form of elongated needles 1.5 microns thick [2]. The size of cosmic particles is smaller. This is borne out by spectra of the air reflected from clouds of volcanic dust and silver clouds. In the second case the maximum of brightness in the spectrum is shifted more to the short-wave portion than in the first. From the fact that silver clouds representing, according to Kulik, products of the sublimation of meteoric bodies [3], float at an altitude of 80 kilometers, it follows that the size of the particles of which they are composed is not greater than $10^{-5}$ centimeters [4].

The following examples can substantiate the conclusion that dust actually influences the thermic condition of the air.

According to the calculations of Kostrov, during periods of aridity, usually accompanied by dry fogs, the air is warmed on account of the absorption by particles of mist of direct solar radiation, by 5 degrees, and of diffused radiation, by another 2 degrees. But inasmuch as mist reduces the inflow of radiation to the surface of the earth, as well as the flow of heat from the latter to the air, the warming of the air by mist does not go beyond 1 to 2 degrees [5].

Durst, on the basis of an analysis of the data concerning temperature, concluded that the dust-filled air of Arabia is warmer than dust-free air [17].



Declassified in Part - Sanitized Copy Approved for Release 2012/03/12 : CIA-RDP82-00039R000100190014-6

Declassified in Part - Sanitized Copy Approved for Release 2012/03/12 : CIA-RDP82-00039R000100190014-6

In the "Dark Sea" (near the western shores of North Africa) trade wind dust systematically separates out; warm air and dry fog during the day, dew during the night are signs of dust separation [6].

At the time of one of the "black storms" in the Ukraine (April 1928), 15 million black-soil dust particles from an area of one million square kilometers were lifted into the air; the temperature rose from 1 to 2 degrees and the velocity of the wind from 7 to 19 meters per second [7].

At the time of a strong dust fog in Semipalatinsk from 16 to 18 February 1856, the temperature rose, in the 24 hours from the 15th to the 16th, from -20.5 to -8.0 degrees [6].

Astronomical observers have noticed on several occasions that if upon the appearance of a meteor, a telescope is directed to the corresponding point in the sky, the appearance of stars and planets through the telescope seems distorted by air whirls caused by the passing meteor [9].

In order to show the possibility of vertical movements of air in the stratosphere caused by thermic action of dust, it should be necessary to evaluate the concentration of dust necessary on the one hand, for such movements, and possible, on the other hand, in the conditions of the stratosphere.

Let us assume that the amount of radiation falling on a dust particle is determined by the law of geometric shielding. If $I_0$ is the amount of radiation falling on 1 square centimeter



Declassified in Part - Sanitized Copy Approved for Release 2012/03/12 : CIA-RDP82-00039R000100190014-6

Declassified in Part - Sanitized Copy Approved for Release 2012/03/12 : CIA-RDP82-00039R000100190014-6

of surface during a unit of time, then for N dust particles of radius r contained in 1 square centimeter of air, this comes to $\pi r^2 I_0 N$, where of this quantity $a\pi r^2 I_0 N$ is absorbed, and the rest diffused.

In general for particles whose size is smaller than the wave length of falling radiation, the quantity of falling energy is proportional to $r^n$, where $n \neq 2$, because it is determined by diffractional phenomena and not by geometric shielding. But inasmuch as the numerical value of n for small particles of various sizes is not established accurately, let us assume that $n = 2$.

The coefficient of absorption of the radiation by dust is less than 1. Because a together with $r^2$ appears as the multiplier in the evaluated concentration N in all expressions where the latter enters, as will become evident from the following, for simplicity and convenience of calculating let us accept $a = 1$. Upon the corresponding selection of a and n, it is necessary to multiply all of the numerical values of N obtained below by the value of the inverse product $a \cdot r^{n-2}$, in order to make them more accurate.

Let us assume further that the transfer of heat from dust to air is effected by way of molecular thermoconductivity.

Actually, heat transfer by radiation is impossible. Air containing no water vapor transmits long wave radiation by means of dust particles. Thermal conductivity by turbulence, evidently, is not possible, because eddies, generated by the surface of small dust particles, comparable in size to the length of a light wave, must themselves be submicroscopic. As to the influence of turbulence



Declassified in Part - Sanitized Copy Approved for Release 2012/03/12 : CIA-RDP82-00039R000100190014-6

Declassified in Part - Sanitized Copy Approved for Release 2012/03/12 : CIA-RDP82-00039R000100190014-6

effected by some kind of outside cause (in the given case such an 'outside' influence may be the difference in density between neighboring small volumes of air-masses because of their different dust content) upon the heat transfer between particles and gas , it has been established experimentally that this phenomenon decreases as the size of the particles decreases. Moreover, all of this must be related to the evaluated particles.

The amount of heat Q, transferred by the particles to the air, is determined thus:

$$Q = (1-b)\pi r^2 I_0.$$

Here $I_0$ is the size of the radiation balance for the particle. Having evaluated the coefficient of thermal conductivity from the particle to the air and the differences of temperatures between the particle and air, it is possible to show that the value b, the portion of energy necessary to heat the particle, is very small (on the order of $10^{-6}$). Therefore, without loss to the accuracy of end expression T, p, $\rho$ of the moving air, in future calculations we will accept the amount of heat transferred by the particle to the air as equal to $\pi r^2 I_0$. In other words, we may consider that the particle is found in a thermal balance with the surrounding medium, inasmuch as the amount of heat transferred by it to the surrounding air is equal to that amount which is received by it from the sun. Actually the temperature of the particle changes in accordance with the size of b, and this change is easily computed: when $b = 10^{-6}$, we obtain:

$$\frac{dT_n}{dt} = 0.5 \times 10^{-4} \text{ grams/second}$$



Declassified in Part - Sanitized Copy Approved for Release 2012/03/12 : CIA-RDP82-00039R000100190014-6

Declassified in Part - Sanitized Copy Approved for Release 2012/03/12 : CIA-RDP82-00039R000100190014-6

Now let us go to the problem of vertical movements of dust-filled air.

The condition necessary for such movements is that the temperature in the rising air must remain higher than the temperature of the surrounding atmosphere. Let us consider the stratosphere as isothermic, at least for a distance of several hundred meters. Then, for the rising air there must be:

$$\frac{\partial T}{\partial z} \geqslant 0.$$

Let us consider two schemes of vertical movement of air: under low and under high initial velocities of rise.

The first scheme: If the vertical velocity of the air is low then it is possible to consider that the pressures of the rising air and of the surrounding atmosphere are able to equalize.

The problem is solved by the following simplifying assumptions:

1. The process is stationary; if the movements begin on one and the same level under one and the same initial conditions, then they are fully identical.

2. Only the vertical component of the movement is considered; the vertical movement is the primary and the most characteristic in the process of free convection; horizontal movements are secondary effects.



Declassified in Part - Sanitized Copy Approved for Release 2012/03/12 : CIA-RDP82-00039R000100190014-6

Declassified in Part - Sanitized Copy Approved for Release 2012/03/12 : CIA-RDP82-00039R000100190014-6

3. The horizontal temperature gradient inside the rising air is taken as equal to 0, which is close to actuality in the central regions of a dust-laden air mass under a sufficient horizontal extent of the latter.

It is necessary to determine the temperature T, the density p, and velocity w of the moving air. Let us state the following equations:

Equation of the first source of thermodynamics:

$$\frac{\pi r^2 I_0}{\rho} N(z) = c_p \frac{dT}{dt} - \frac{A}{\rho} \frac{dp}{dt}. \qquad (1)$$

The member in the left part of the equation gives the inflow of heat per unit of air mass containing N dust particles per 1 cubic centimeter; N should be considered as dependent on the magnitude of vertical displacement.

Equation of continuity:

$$\frac{\partial}{\partial z}(\rho w) = 0 \quad \text{or} \quad \rho w = \rho_0 w_0 = B. \qquad (2)$$

Equation of condition:

$$p = \rho R T. \qquad (3)$$



Declassified in Part - Sanitized Copy Approved for Release 2012/03/12 : CIA-RDP82-00039R000100190014-6

Declassified in Part - Sanitized Copy Approved for Release 2012/03/12 : CIA-RDP82-00039R000100190014-6

Since

$$\frac{dT}{dt} = w\frac{\partial T}{\partial z} \quad \text{and} \quad \frac{dp}{dt} = w\frac{\partial p}{\partial z},$$

we obtain from (2) and (3):

$$\frac{I_0 \pi r^2}{\rho} N(z) = c_p \frac{B}{\rho}\frac{\partial T}{\partial z} - \frac{AB}{\rho^2}\frac{\partial p}{\partial z}.$$

But

$$\frac{\partial p}{\partial z} = \frac{\partial p_a}{\partial z} = -g\rho_a,$$

where $\rho_a$ is the density of the atmosphere. Therefore,

$$I_0 \pi r^2 N(z) = c_p B \frac{\partial T}{\partial z} + AB g \frac{T}{T_a}.$$

For T we obtain a differential equation of the 1st order, linear and heterogeneous.

Its solution

$$T = e^{-\int_0^z P dz}\left(T_0 - \int_0^z Q(z) e^{\int_0^z P dz} dz\right). \qquad (4)$$

Here

$$P = \frac{Ag}{c_p T_a} \quad \text{and} \quad Q(z) = -\frac{I_0 \pi r^2}{c_p B} N(z). \qquad (5)$$



Declassified in Part - Sanitized Copy Approved for Release 2012/03/12 : CIA-RDP82-00039R000100190014-6

Declassified in Part - Sanitized Copy Approved for Release 2012/03/12 : CIA-RDP82-00039R000100190014-6

Let us assume that the concentration of dust in the rising air changes with altitude in the following manner:

$$N(z) = N_0 e^{-\kappa z}$$

Then

$$T = \left(T_0 - \frac{a}{p-\kappa}\right) e^{-pz} + \frac{a}{p-\kappa} e^{-\kappa z}. \qquad (6)$$

Here

$$a = \frac{I_0 \pi r^2 N_0}{c_p B}. \qquad (7)$$

Let us calculate for a height of 30 kilometers: $T_0 = 230^0$, $p_0 = 10$ mb, $\rho_0 = 1.5 \times 10^{-5}$ grams per cubic centimeter.

Let $N_0 = 5 \times 10^3$, $r = 10^{-6}$ cm., $\kappa = 10^{-6}$. Then for $z = 1$ km, $I = 241^0$ at $B = 10^{-5}$ ($w_0 \approx 1$ cm/sec).

For an altitude of 75 kilometers $T_0 = 275^0$, $p_0 = 6.4 \times 10^{-6}$ mb, $\rho_0 = 0.8 \times 10^{-7}$ gm/cm$^3$. For $N_0 = 50$, $r = 10^{-6}$ cm, $\kappa = 10^{-6}$ and for $z = 1$ km $T = 288^0$ at $B = 10^{-7}$ ($w_0 \approx 1$ cm/sec).

For $N_0$ taken on a smaller order, the temperature drops with altitude and vertical movements of air are impossible.

That condition is characteristic, that the temperature of the rising air increases also in the case of diminution of N(z) with altitude. And in this condition the cooling due to expansion of the air appears to be less than the heating due to the inflow of heat from dust.



Declassified in Part - Sanitized Copy Approved for Release 2012/03/12 : CIA-RDP82-00039R000100190014-6

Declassified in Part - Sanitized Copy Approved for Release 2012/03/12 : CIA-RDP82-00039R000100190014-6

The value $w_o$ was selected on the basis of the following considerations. During movements, the order of w is conserved, which is evident from the examples shown. And during movement in the troposphere, in regards to which it is usually assumed that $\rho = \rho_a$, the magnitude of vertical velocity, as a rule, is within the limits of several centimeters per second. For example, theoretical calculations give for vertical velocities of air heated through absorption of radiation by water vapor or in trade wind regions, 10 centimeters per second and 1 to 5 centimeters per second, respectively [10, 15]. Accordingly, in the case under consideration it may be assumed that the velocity, in the beginning of the movement, as well as later, must have a magnitude in the order of not less than several centimeters per second. In the calculations shown $w \approx 1$ cm/sec is taken. Concerning the other basis of distribution of values $w_o$ with altitude, connected with the velocity of molecular diffusion, we shall speak later.

Owens speaks of the instance of vertical movement of thistle fluff in completely still air warmed by the sun's rays with complete absence of wind. This could serve as experimental proof for the scheme under consideration.

The second scheme: The pressure inside a rising air movement is less than in the surrounding atmosphere, which is possible, evidently, at vertical velocities greater than those just considered.

The simplifying equations here are the same as in the first scheme, but to the initial three equations the following equation



Declassified in Part - Sanitized Copy Approved for Release 2012/03/12 : CIA-RDP82-00039R000100190014-6

Declassified in Part - Sanitized Copy Approved for Release 2012/03/12 : CIA-RDP82-00039R000100190014-6

of vertical air movement is added:

$$\frac{dw}{dt} = -\frac{1}{\rho}\frac{\partial p}{\partial z} - g. \tag{8}$$

Solving this equation system, neglecting small members, we obtain:

$$\rho = \rho_0 e^{-\int_0^z \frac{R\frac{\partial T}{\partial z} + g}{RT} dz}; \tag{9}$$

$$p = p_0 e^{\left(\frac{c_p}{AR}\ln\frac{T}{T_0} - \frac{Q}{ABR}\int\frac{N dz}{T}\right)} \tag{10}$$

Accordingly,

$$T = \frac{p_0}{R\rho_0} e^{\left(\frac{c_p}{AR}\ln\frac{T}{T_0} - \frac{Q}{ABR}\int\frac{N dz}{T} + \int\frac{R\frac{\partial T}{\partial z} + g}{RT} dz\right)} \tag{11}$$

and

$$w = B\rho_0 e^{\int\frac{R\frac{\partial T}{\partial z} + g}{RT} dz}. \tag{12}$$



Declassified in Part - Sanitized Copy Approved for Release 2012/03/12 : CIA-RDP82-00039R000100190014-6

Declassified in Part - Sanitized Copy Approved for Release 2012/03/12 : CIA-RDP82-00039R000100190014-6

Here $Q = \pi r^2 I_0$.

Evidently, the order $w_0$ here must be not less than 10 centimeters per second.

Let us determine the initial concentration $N_0$ of dust necessary, for example, for the temperature of the air to increase by 1 degree at the displacement upward of 1 kilometer, as well as the difference of pressure $\Delta p = p_a - p$, resulting from this displacement.

At first let us calculate for an altitude of 30 kilometers: $T_0 = 230^\circ$, $p_0 = 10$ mb., $\rho_0 = 1.5 \times 10^{-5}$ gms/cm$^3$; $231 = 230\, e^y$; $y \approx 0$.

If we consider that the temperature T and the gradient $\frac{\partial T}{\partial z}$ may be substituted by the average values $T_c$ and $\left(\frac{\partial T}{\partial z}\right)_c$ for a layer of thickness z, then

$$y = \frac{c_p}{AR} \ln \frac{T}{T_0} - \frac{Q}{ABRT_c} \int N dz + \frac{R\left(\frac{\partial T}{\partial z}\right)_c + g}{RT_c} z .$$

Let us introduce the symbol

$$L = \frac{Q \int N dz}{ABR} .$$

Then

$$0 = -\frac{L}{230.5} + \frac{2.87 \times 10^6 \times 10^{-5} + 0.98 \times 10^3}{2.87 \times 10^6 \times 230.5}; \quad L = 35.$$



Declassified in Part - Sanitized Copy Approved for Release 2012/03/12 : CIA-RDP82-00039R000100190014-6

Declassified in Part - Sanitized Copy Approved for Release 2012/03/12 : CIA-RDP82-00039R000100190014-6

When $k=10^{-6}$ and $r=10^{-6}$ cm, $N_0 = 5 \times 10^2$ for $B=10^6$ ($w \sim 10$ cm/sec) $x = -0.127$.

$$p_1 = 5.3 \times 10^{-2}\ mb,\ p_2 = 6 \times 10^{-2}\ mb,\ \Delta p = 0.007\ mb,\ \frac{\partial p}{\partial R} = 7 \times 10^{-7}\ dyn/cm^3.$$

A study of a series of photographs of silver clouds observed on 29 June 1936, permitted the discovery of cyclonic rotating movement of the air at heights of 70 to 80 kilometers embracing an area of $5.10^4$ square kilometers [11], a velocity of rotation of 29 to 34 meters per second. Movement of luminous meteoric trails also point to the existence of local systems of air currents, whereupon the latter usually are destroyed toward the end of the night. Therefore, V. V. Fedynskiy [1] assumed that these air currents are a consequence of the action of solar radiation.

May there appear similar cyclonic systems as a consequence of the movement of the air as considered in the second scheme?

In order to solve this question, however approximately, there should be a comparison between the above-calculated horizontal gradients of pressure and gradients corresponding to the velocity of rotation.

Radius $R'$ of the cyclone in the above example is $10^7$ centimeters. The velocity $C$ is of the order $3.10^3$ centimeters per second. The gradient of pressure for the cyclone may be determined from the relation:

$$\frac{C^2}{F'} + fc - \frac{1}{\rho}\frac{\partial p}{\partial R'} = 0.$$



Declassified in Part - Sanitized Copy Approved for Release 2012/03/12 : CIA-RDP82-00039R000100190014-6

Declassified in Part - Sanitized Copy Approved for Release 2012/03/12 : CIA-RDP82-00039R000100190014-6

If

$$N = N_0 e^{-kz}$$

then

$$N_0 = \frac{4\pi ABkr}{Q(1-e^{-kr})} \cdots$$

When $k = 10^{-6}$ and $r = 10^{-5}$ cm, we obtain: $N_0 = 5.10^4$ for $B = 10^{-4}$ ($w_0 \approx$ 10 cm/sec).

Let us solve for

$$p_1 = p_0 e^{\chi},$$

where

$$\chi = \frac{c_p}{AR} \ln \frac{T}{T_0} - \frac{QN_0(1-e^{-kr})}{4\pi ABRT_0 k} = -\frac{L}{T_0} = -0.15.$$

$p_1 = 10 e^{-0.15} = 8.3$ mb. In the stratosphere at an altitude of 31 kilometers $p_0 = 9.5$ mb. Therefore, the fall of pressure toward the center of the region of dust congestion is $\Delta p = 3.2$ mb. In the radius of this region $R = 10^7$ cm, the horizontal gradient of pressure: $\frac{\partial p}{\partial R} = 32 \times 10^{-5}$ dyn/cm$^3$.

Let us make the same calculations for an altitude of 75 kilometers: $T_0 = 275°$, $p_0 = 6.4 \times 10^{-2}$ mb, $\rho_0 = 0.8 \times 10^{-7}$ gms/cm$^3$, $\gamma = 0$, $L = 55$.



Declassified in Part - Sanitized Copy Approved for Release 2012/03/12 : CIA-RDP82-00039R000100190014-6

Declassified in Part - Sanitized Copy Approved for Release 2012/03/12 : CIA-RDP82-00039R000100190014-6

Here $l = 2\omega \sin\varphi$, where $\omega$ is the angular velocity of rotation of the earth, $\varphi$ is the geographic latitude of the point of observation. When $\varphi = 30^\circ$ $l = 10^{-4}$ sec.$^{-1}$.

For an altitude of 30 kilometers $\frac{\partial p}{\partial R} = 10^{-5}$ dyn/cm$^3$, for an altitude of 75 kilometers $\frac{\partial p}{\partial R} = 10^{-7}$ dyn/cm$^3$.

Accordingly, in the examples considered, the gradient of pressure is 30 times greater than is / from the data of observations the one obtained for the 30 kilometer altitude and 5 times greater for the 75 kilometer altitude. Such gradients appear with the movement of air at 1 kilometer; with further moving they must become even more considerable.

Undoubtedly, thanks to the irregular pattern of horizontal movements, gradients of pressure are established that are less than those obtained. But if we consider them to be sufficient for enough that the velocities of the wind in the cyclones of the second scheme will be of the order observed, then the latter may explain cyclones observed in the stratosphere. For this we must only propose the possibility of the existence in the stratosphere of sufficiently large areas of dust. Then we can consider that silver clouds found in the uppermost portion of such a region, embraced by cyclonic rotation, expose it with its movement. We must note that under such an explanation of causes of local currents in the stratosphere, their diurnal periodicity, discovered on observation, become absolutely natural.

Let us return to the question of initial vertical velocities $w_0$ of movement of dust-laden air. Is it possible to establish a connection between the level in the atmosphere on



Declassified in Part - Sanitized Copy Approved for Release 2012/03/12 : CIA-RDP82-00039R000100190014-6

Declassified in Part - Sanitized Copy Approved for Release 2012/03/12 : CIA-RDP82-00039R000100190014-6

which the movement begins, and the value of $w_0$? In other words, is it possible to state something about the distribution of movements in the atmosphere according to height, movements given in the schemes considered?

For heights greater than 60 kilometers, $w_0$ of the order of $10^2 - 10^3$ centimeters per second may be denoted in the following manner. We may not assume that a distinction exists between the velocity of mixing of various particles of gas as a result of diffusion and the velocity of the initial regulated convectional movement of the same particles of gas. Therefore, at a height of 75 to 80 kilometers, $w_0$ must be on the order of several meters per second. Actually, the velocity of expansion of gaseous meteoric trails, where the diffusion "in itself" becomes visible because of the presence of stimulated molecules, is 2 to 10 meters per second [1]. But the velocity of diffusion is proportional to the coefficient of diffusion, and the latter is inversely proportional to the density of the air. This follows directly from the expression for the coefficient of diffusion "in itself" according to Enskog [1]:

$$D = \frac{3\sqrt{R}}{32\pi} \cdot \frac{\sqrt{T}}{N_L} \cdot \frac{1}{\sqrt{\mu}\, 2\rho\psi}.$$

Here $\rho$ is the density of the gas; $\mu$ is its molecular weight; $N_L$ is Avogadro's number; function $\psi$ depends on the interacting forces between molecules. Accordingly, for any two heights in the stratosphere, where $T_1$ and $T_2$ have one and the same order:

$$D_2 = D_1 \frac{\rho_1}{\rho_2}.$$



Declassified in Part - Sanitized Copy Approved for Release 2012/03/12 : CIA-RDP82-00039R000100190014-6

Declassified in Part - Sanitized Copy Approved for Release 2012/03/12 : CIA-RDP82-00039R000100190014-6

If at an altitude of 75 kilometers $\rho_1 \approx 10^{-7}$ gm/cm$^3$ and $w_0$ is equal to several meters per second, and at an altitude of 30 kilometers $\rho_2 \approx 10^{-5}$ gm/cm$^3$, then at the latter altitude $w_0$ has the order of several centimeters per second.

Accordingly, the movements of the first scheme may take place in the lower portion of the stratosphere (20 to 60 kilometers), and movements of the second scheme, in the upper stratosphere (60 to 80 kilometers), where, besides the necessary value of w, there is an even greater drop in temperature with altitude, which also makes for the development of convection.

Such a conclusion is not contradicted by the fact that local circulation systems are discovered only in the upper stratosphere. For the lower stratosphere, it seems, there are no observations which would point to the existence in it of like systems. The longer existence of dust trails (up to 5 or 6 hours) as compared to luminous trails [12] can also be explained by the assumption of small velocities in vertical displacements of the air in the lower stratosphere.

It is necessary to note that the formulas of both schemes give only average values for T, $\rho$, $\rho_2$, w, which must be related to final and sufficiently long intervals of time and displacements. These formulas describe the macromovement and do not give instantaneous values to the corresponding physical values describing the macromovements. The latter we related to the thermic heterogeneity in the moving air, which, of course, should be assumed, because the dust cannot fill a given air mass uniformly.



Declassified in Part - Sanitized Copy Approved for Release 2012/03/12 : CIA-RDP82-00039R000100190014-6

Declassified in Part - Sanitized Copy Approved for Release 2012/03/12 : CIA-RDP82-00039R000100190014-6

Let us now consider the movement of the air heated by dust inside a dust cloud. In order to separate these micromovements from the movements of the cloud itself, let us solve a fixed problem. As previously, the stratification of the stratosphere is assumed to be isometric; velocity changes, temperature and pressure changes we considered on the plane of x, z. The influence of thermoconductivity on the temperature and vertical velocity of air is determined below.

We consider the upper and lower limits of the cloud as being plane. The distribution of dust in the cloud we shall set so that at the lower limit of the cloud ($z=0$), on the upper limit of the cloud ($z=H$) and on both side limits ($x=L$), and the concentration of dust $N=0$. In simplest form this can be stated as follows:

$$N = N_0 \frac{z(H-z)(1-bx^2)}{H^2}. \qquad (13)$$

Here $bx=1$ when $x=L$.

The greatest concentration of dust will be in the center of the cloud:

$$N_{max} = \frac{N_0}{4}$$

Then, the amount of heat flowing into a unit of air mass per unit of time from the dust, whose concentration in cubic centimeters is equal to N,

$$Q = \frac{\pi r^2 I_0 N_0}{\rho H^2} z(H-z)(1-bx^2). \qquad (14)$$



Declassified in Part - Sanitized Copy Approved for Release 2012/03/12 : CIA-RDP82-00039R000100190014-6

Declassified in Part - Sanitized Copy Approved for Release 2012/03/12 : CIA-RDP82-00039R000100190014-6

It is necessary to solve the following system of equations.

Equations of movement:

$$u\frac{\partial u}{\partial x} + w\frac{\partial u}{\partial z} - lv = -\frac{1}{\rho}\frac{\partial p}{\partial x}; \qquad (15)$$

$$u\frac{\partial v}{\partial x} + w\frac{\partial v}{\partial z} + lu = 0; \qquad (16)$$

$$w\frac{\partial w}{\partial z} = -\frac{1}{\rho}\frac{\partial p}{\partial z} - g. \qquad (17)$$

Equation of continuity:

$$\frac{\partial u}{\partial x} + \frac{\partial w}{\partial z} = 0. \qquad (18)$$

Equation of inflow of heat:

$$u\frac{\partial \theta}{\partial x} + w\frac{\partial \theta}{\partial z} + \Gamma w = \frac{Q(x,z)}{c_p}. \qquad (19)$$

Here $u, v,$ w are components of velocities of the air; $\theta$ is the deflection of the temperature from the non-disturbed sections of dust values; $\Gamma = \gamma_a$ upon isometric stratification, where $\gamma_a$ is the adiabatic gradient of temperature; $c_p$ the conventional thermal capacity of the air under constant exchange.

Let us solve for the distribution of vertical velocity w. It is known that under thermal heterogeneity in a horizontal direction, a vertical movement of the air appears in the atmosphere, and inside a dust cloud the air is found to be precisely under thermic heterogeneous conditions. Evidently, at a certain level



Declassified in Part - Sanitized Copy Approved for Release 2012/03/12 : CIA-RDP82-00039R000100190014-6

Declassified in Part - Sanitized Copy Approved for Release 2012/03/12 : CIA-RDP82-00039R000100190014-6

(and also at a certain second level located upon the cloud and above it,) located near the cloud and below it, there are no vertical movements of air. These movements outside the cloud we shall consider insignificant compared with movements inside the cloud. Therefore, let us relate w=0, kz= 0, and z= H, and let us not consider movements of the air outside the cloud. Let us assume that w does not depend on x, that is, our calculations will be right for parts of the cloud, at a distance from its side limits.

Distribution according to altitude w and N are similar. Then

$$w = az(H-z). \tag{20}$$

Here a is a certain constant determining the velocity, which must be found.

Having accepted the given boundary conditions for w, it is evident, we must assume, that the thermic heterogeneity is absent at the upper and lower limits of the cloud.

Thus, the problem is solved under the following boundary conditions:

$$z = 0;\ w = Q = \theta = 0;$$
$$z = H;\ w = Q = \theta = 0.$$



Declassified in Part - Sanitized Copy Approved for Release 2012/03/12 : CIA-RDP82-00039R000100190014-6

Declassified in Part - Sanitized Copy Approved for Release 2012/03/12 : CIA-RDP82-00039R000100190014-6

For various values of $N_{max}$ let us determine the corresponding values: a, u, v, $\theta$ and $\rho$. Further, let us evaluate x=L, under which the upper limit of the cloud may still be considered as flat. Evidently, the distribution of velocities, temperatures and pressures in the cloud will be stationary until changes in its dust distribution take place, that is, until a considerable deformation of the cloud takes place. Let us evaluate the interval $\Delta t$, during which the cloud may be considered as not deformed and the distribution of elements in it as stationary. In this manner, we shall determine the conditions under which the above assumptions are right.

Let us begin the solution of the problem:

Let us find u from (16):

$$u = -\int \frac{\partial w}{\partial z}\, dx = -ax(H-2z) + \varphi(z).$$

When $x = 0$, $u = \varphi(z) = 0$.

Thus

$$u = -ax(H-2z). \tag{21}$$

Horizontal component of velocity u in the lower and upper halves of the cloud has contrary directions and attains the greatest values when $z = 0$ and $z = H$.



Declassified in Part - Sanitized Copy Approved for Release 2012/03/12 : CIA-RDP82-00039R000100190014-6

Declassified in Part - Sanitized Copy Approved for Release 2012/03/12 : CIA-RDP82-00039R000100190014-6

From (19) let us find $\theta$ :

$$\frac{\partial \theta}{\partial z} - \frac{x(H-2z)}{z(H-z)} \frac{\partial \theta}{\partial x} + \Gamma = \frac{\alpha(1-bx^2)}{ac_p};$$

$$\alpha = \frac{\pi r^2 I_0 N_0}{\rho H^2}$$

The integrals of this equation are:

$$C_1 = xz(H-z);$$

$$\theta + C_2 = \left(\frac{\alpha}{ac_p} - \Gamma\right) \cdot z + \frac{2\alpha b}{ac_p H^3} x^2 z^2 (H-z)^2 \ln\left(\frac{H}{z} - 1\right) +$$

$$+ \frac{\alpha b}{ac_p H^2} x^2 z (H-z)(H-2z).$$

From the condition that $\theta = 0$ when $z = 0$ it follows that $C_2 = 0$.

Because $\theta = 0$ when $z = H$, then

$$\frac{\alpha}{ac_p} - \Gamma = 0. \qquad (22)$$

Hence

$$a = \frac{\alpha}{\Gamma c_p}.$$



Declassified in Part - Sanitized Copy Approved for Release 2012/03/12 : CIA-RDP82-00039R000100190014-6

Declassified in Part - Sanitized Copy Approved for Release 2012/03/12 : CIA-RDP82-00039R000100190014-6

Evidently, under any other law concerning the change of w with altitude, but under the same boundary conditions and conditions of similar changes with altitude of w and N, we shall obtain the same expression for a.

Actually, let $w = af(z)$ and $Q = df(z)(1-bx^2)$. Then $u = af'(z)x$ and the equation for $\theta$ has the following form:

$$\frac{\partial\theta}{\partial z} - \frac{f'(z)}{f}\frac{\partial\theta}{\partial x} + \Gamma = \frac{\alpha(1-bx^2)}{ac_p}.$$

The integrals of this equation are:

$$f \cdot x = C_1$$

and

$$\theta + C_2 = \left(\frac{\alpha}{ac_p} - \Gamma\right)z - b\int\frac{C_1^2}{f^2}dz.$$

The integral contained herein converts to 0 when $z = 0$ and $z = H$.

Therefore, from condition $\theta = 0$ when $z = 0$, it follows that $C_2 = 0$, and from conditions $\theta = 0$ when $z = H$ it follows that

$$\frac{\alpha}{ac_p} - \Gamma = 0.$$

It is just as easy to show that under any possible profile of vertical velocity, which under the stated boundary conditions in general form can be expressed thus:

$$w = az^m(H-z)^n$$



Declassified in Part - Sanitized Copy Approved for Release 2012/03/12 : CIA-RDP82-00039R000100190014-6

Declassified in Part - Sanitized Copy Approved for Release 2012/03/12 : CIA-RDP82-00039R000100190014-6

and under conditions of similarity N(z) and w, the maximum value of the vertical velocity $w_{max}$ will be one and the same in the given cloud.

Evidently

$$a_{(m,n)} = \frac{\pi r^2 I_0 N_{0(m,n)}}{\rho \cdot H^{m+n}}.$$

When

$$a_{(1,1)} = \frac{\pi r^2 I_0 N_{0(1,1)}}{\rho \cdot H^2}$$

Let us formulate a relation:

$$\frac{a_{(m,n)}}{a_{(1,1)}} = \frac{a_{(m,n)}}{a_{(1,1)}} = \frac{1}{H^{m+n-2}} \cdot \frac{N_{0(m,n)}}{N_{0(1,1)}}.$$

Relation of maximum velocities:

$$\frac{w_{(m,n)max}}{w_{(1,1)max}} = \frac{1}{H^{m+n-2}} \cdot \frac{N_{0(m,n)}}{N_{0(1,1)}} \cdot \frac{z^m (H-z)^n \Big|_{z\ max(m,n)}}{z(H-z) \Big|_{z\ max(1,1)}}.$$

But

$$N_{0(m,n)} = N_{max} \cdot \frac{H^{m+n}}{z^m (H-z)^n \Big|_{z\ max(m,n)}};$$

$$N_{0(1,1)} = N_{max} \cdot \frac{H^2}{z(H-z) \Big|_{z\ max(1,1)}}$$



Declassified in Part - Sanitized Copy Approved for Release 2012/03/12 : CIA-RDP82-00039R000100190014-6

Declassified in Part - Sanitized Copy Approved for Release 2012/03/12 : CIA-RDP82-00039R000100190014-6

Under the given dust-filling of the cloud, that is, under one and the same $N_{max}$:

$$w_{(m,n)max} = w_{(1,1)max} = const.$$

Accordingly, under any possible profile of vertical velocity $w_{max}$, and value of the order w, the following has one and the same value in the given dust cloud:

$$w_{max} = \frac{1}{c_p \Gamma} \frac{\pi r^2 I_0}{\rho} N_{max}. \qquad (23)$$

As we should have expected, the vertical velocity of the air in the cloud is determined by the amount of dust in the cloud, stratification of the atmosphere, and density of the air. The latter condition is fully in accord with the earlier obtained conclusion on the height distribution of vertical velocities of movement of dust air masses in the atmosphere.

Physically it is completely clear that the form of solution for N(z), differs from w, and under the same boundary conditions and the same value of $N_{max}$, cannot influence the value w to a considerable degree.

Let us continue the solution of our problem. Substituting $\frac{\varkappa}{ac_p}$ through $\Gamma$, we shall obtain the temperature of the air:

$$\theta = \frac{2\Gamma b}{H^3} x^2 z^2 (H-z)^2 \ln\left(\frac{H}{z} - 1\right) + \frac{\Gamma b}{H} x^2 z (H-z)(H-2z).$$



Declassified in Part - Sanitized Copy Approved for Release 2012/03/12 : CIA-RDP82-00039R000100190014-6

Declassified in Part - Sanitized Copy Approved for Release 2012/03/12 : CIA-RDP82-00039R000100190014-6

Accepting $\Gamma = \gamma_a = 10^{-4}$ gm/cm and $k = 1$, we shall obtain the following distribution of $\theta$ according to altitude:

| $z$: | 0 | $\frac{1}{4}H$ | $\frac{1}{2}H$ | $\frac{3}{4}H$ | $H$ |
|---|---|---|---|---|---|
| $\theta$: | 0 | +0.25° | 0 | −0.25° | 0 |

If $x = 0$, then $\theta = 0$.

The distribution of temperature inside the cloud depends only on the stratification of the atmosphere ($\Gamma$); the horizontal dimension of the cloud (b) and the distance from the center of the cloud; the concentration of dust ($\alpha$) does not influence $\theta$.

The thermal heterogeneity in the cloud intensifies in the direction of its side boundaries, whereas in the lower half of the cloud, the deviation of the temperature from the non-disturbed value is positive while in the upper half it is negative, which should have been expected, because the acceleration of air

$$\frac{du}{dt} = u\frac{\partial u}{\partial x} = a^2 z(H-z)(H-2z)$$

in the lower half of the cloud is positive and in the upper, negative. That $\theta = 0$, when $z = \frac{H}{2}$ and at any x, corresponds to the fact that here the acceleration of particles of air is equal to 0, because the velocity approaches its greatest magnitude.

From (16) let us find v:

$$\frac{\partial v}{\partial x} - \frac{z(H-z)}{k(H-2z)}\frac{\partial v}{\partial z} + l = 0.$$



Declassified in Part - Sanitized Copy Approved for Release 2012/03/12 : CIA-RDP82-00039R000100190014-6

Declassified in Part - Sanitized Copy Approved for Release 2012/03/12 : CIA-RDP82-00039R000100190014-6

Integrals of the equation:

$$C_1 = xz(H-z);$$

$$C_2 = x + \frac{v}{l};$$

$C_2 = 0$, because $v = 0$ when $x = 0$. Hence, Fromwhere

$$v = -lx + mxz(H-z). \tag{24}$$

The constant m we determine by differentiating (15) in respect to z and (17) in respect to z and eliminating excluding $\frac{\partial^2 p}{\partial x \partial z}$ from them,

$$\frac{\partial u}{\partial x}\frac{\partial u}{\partial x} + u\frac{\partial^2 u}{\partial x \partial z} + \frac{\partial w}{\partial z}\frac{\partial u}{\partial z} - l\frac{\partial v}{\partial z} = 0.$$

Hence
Fromwhere

$$m = -\frac{2a^2}{l} \tag{25}$$

The pressure p we shall find from equations (15) and (17).



Declassified in Part - Sanitized Copy Approved for Release 2012/03/12 : CIA-RDP82-00039R000100190014-6

Declassified in Part - Sanitized Copy Approved for Release 2012/03/12 : CIA-RDP82-00039R000100190014-6

Evidently

$$dp = \frac{\partial p}{\partial z}\,dz + \frac{\partial p}{\partial x}\,dx$$

or

$$p = \int_H^z \frac{\partial p}{\partial z}\,dz + \int_0^x \frac{\partial p}{\partial x}\,dx + C. \qquad (26)$$

Here C is the pressure of the atmosphere for the upper surface of the cloud.

If we consider that p does not depend on z within the limits of the cloud, then

$$\int_H^z \frac{\partial p}{\partial z}\,dz = -\rho g (z - H) - \rho \frac{a^2 z^2 (H-z)^2}{2}; \qquad (27)$$

$$\int_0^x \frac{\partial p}{\partial x}\,dx = \rho \int_0^x \left(k w - u \frac{\partial u}{\partial x} - w \frac{\partial u}{\partial z}\right) dx =$$

$$= \rho \left[\frac{k a z (H-z) - k^2}{2} - \frac{a^2 (H-2z)^2}{2} - a^2 z (H-z)\right] x^2. \qquad (28)$$

Now we may evaluate the distance L in a horizontal direction upon which the upper boundary of the cloud may be considered flat. L must satisfy the condition:

$$p\Big|_{H,L} = \int_0^L \frac{\partial p}{\partial x}\,dx\Big|_{z=H} + C \approx C$$



Declassified in Part - Sanitized Copy Approved for Release 2012/03/12 : CIA-RDP82-00039R000100190014-6

Declassified in Part - Sanitized Copy Approved for Release 2012/03/12 : CIA-RDP82-00039R000100190014-6

or

$$\left| \int_0^L \frac{\partial p}{\partial x}\, dx \right|_{z=H} \Bigg| < C.$$

But when calculating we do not disregard the pressure by values of the order of $\rho g H$. Accordingly

$$\left| \int_0^L \frac{\partial p}{\partial x}\, dx \right|_{z=H} \Bigg| < \rho g H$$

and

$$\left( \frac{L^2}{2} + \frac{a^2 H^2}{2} \right) L^2 < g H.$$

If the cloud is located at an altitude of 30 kilometers then $\rho = 2.2 \cdot 10^{-6}$ gm/cm$^3$ when $N_0 = 10^3$, $r = 10^{-4}$ cm, and $H = 10^5$ cm, we obtain $a = 6.4 \times 10^{-11}$ and $L < 10^8$ cm.

The member depending on H may be disregarded in comparison with the member depending on $L$ for a concentration of dust, even as $10^2$ and $10^3$ times greater than the selected, and the value L is determined by Coriolis force and height of the cloud:

$$L < \sqrt{\frac{2gH}{f^2}}. \qquad (29)$$



Declassified in Part - Sanitized Copy Approved for Release 2012/03/12 : CIA-RDP82-00039R000100190014-6

Declassified in Part - Sanitized Copy Approved for Release 2012/03/12 : CIA-RDP82-00039R000100190014-6

Let us calculate w and u for a dust cloud, the dimensions and dust content of which we must solve for, and we must also evaluate the interval of time during which such a cloud may be considered not deformed and the processes in it as stationary.

Let $H = 5 \times 10^4$ cm, $L = 10^5$ cm and the cloud be located at a height of 30 kilometers

$$N_{max} = 2500 \quad (N_0 = 10^4),$$

$$a = 1.6 \times 10^{-10},$$

$$w = 0.3 \times 10^{-1} \text{ cm/sec for } z = 10^{-1} H,$$

$$w = 0.9 \times 10^{-1} \text{ cm/sec for } z = \frac{1}{2} H,$$

$$|u| = 0.7 \text{ cm/sec for } z = 0,\ z = H \text{ and } x = L.$$

If $N_{max}$ from height $z = \frac{H}{2}$ is displaced to height $z = \frac{H}{2} + \Delta z$ then we shall consider that the distribution of dust in a vertical direction did not change if $\Delta z = 10^{-1} H$ ( $\Delta z$ for other z will be less). This will occur in $\Delta t_1 = 16$ hours.

If the displacement of side boundaries of the cloud in a horizontal direction is $10^{-1} L$, then we shall consider that the distribution of dust in a horizontal direction is also unchanged. This will occur in $\Delta t_2 = 4$ hours.

Accordingly, in the course of several hours of the daylight half of a 24-hour period, when the considered movements are only



Declassified in Part - Sanitized Copy Approved for Release 2012/03/12 : CIA-RDP82-00039R000100190014-6

Declassified in Part - Sanitized Copy Approved for Release 2012/03/12 : CIA-RDP82-00039R000100190014-6

possible, the latter may be considered as stationary when $N_{max} \approx 10^3$, and all values calculated in the given problem will be correct for them.

It is possible to show that the viscosity changing the distribution of temperature according to height does not influence the magnitude of the vertical velocity of the air. Therefore, when considering the vertical movement of air warmed by dust, it does not have to be taken into account.

We would expect that with the course of time the dust cloud will deform so that the horizontal dimensions of its lower half become smaller, and the concentration of dust in it becomes greater; whereas the horizontal dimensions of the upper half become greater and the concentration of dust in it becomes smaller. Therefore, in the lower half of the cloud velocities will increase with time, and in the upper, they will decrease.

In 24 hours the air in the cloud displaces upward by several tens of meters at an altitude of 30 kilometers when $N \approx 10^3$. With an increase in altitude and a decrease in density, air velocities, meaning the diurnal displacement of air, increase.

With the increase of the dust content of a cloud, the vertical velocities in it increase; therefore the time decreases during which the movement processes may be considered as stationary.



Declassified in Part - Sanitized Copy Approved for Release 2012/03/12 : CIA-RDP82-00039R000100190014-6

Declassified in Part - Sanitized Copy Approved for Release 2012/03/12 : CIA-RDP82-00039R000100190014-6

From the comparison of the results of calculations of the first two schemes and the latter, the conclusion may be drawn that taking horizontal currents into account decreases the magnitude of vertical velocity by one fifth.

The result of the whole aggregate of vertical macro- and micro-movement may be the mixing of the air in the stratosphere, which impedes the established diffusive equilibrium.

In this manner the stated considerations on the connections between cosmic dust warmed by the sun and its surrounding air may in themselves result in the explanation of characteristic peculiarities of the stratosphere which as yet remain unclear.

Now let us ask the question: are the concentrations of dust necessary for the considered processes possible in the stratosphere?

In what quantities and of what size can dust remain in a constant state of suspension in the air, forming, as it were, its own "dust atmosphere"?

We may show that the lower limit for the concentration of dust constantly penetrating the atmosphere is $10^3$ if the size of the dust particles is $10^{-6}$ centimeters. Let us make two basic assumptions: in the first place, particles of the $10^{-6}$ centimeter size are mixed in the atmosphere below the 60-kilometer level, because here Stoke's velocity for them is lower than the Brownian movement (both velocities are calculated taking into account corrections for Cunningham's slide); in the second, the density of the



Declassified in Part - Sanitized Copy Approved for Release 2012/03/12 : CIA-RDP82-00039R000100190014-6

Declassified in Part - Sanitized Copy Approved for Release 2012/03/12 : CIA-RDP82-00039R000100190014-6

dust in the outer portions of the stratosphere may not be less than the density in interplanetary space. Both assumptions are physically fully natural. In general, as is known, the level of 80 kilometers appears ideal from several points of view: the lower levels of northern lights, the second crepuscular arch, the lower limit of the Heaviside layer correspond to this level; here ends the ionization trails of meteors and begins the dust, and so forth. Now it is important to note that dust particles may not be found in a suspended condition higher than this level. This conclusion is proved by the following facts: observations of meteors have shown that an 80 kilometer altitude is the limit above which the density of the air falls sharply; above this level silver clouds are never observed.

Thus, let the mean concentration of particles, suspended in the atmosphere below 80 kilometers and not settling on the surface of the earth, with a size of $10^{-6}$ centimeters, be equal to $10^3$.

Then the mean density of this dust in the atmosphere is $\rho = 1.2 \times 10^{-14}$ g/cm$^3$ under a density of dust matter of 3 g/cm$^3$. The total amount of dust B in the considered layer with a volume of $3.7 \times 10^{25}$ cm$^3$ is equal to $4.5 \times 10^5$ t.

Let the total diurnal inflow A of cosmic matter brought in by meteoric bodies into the atmosphere remain constant with time. According to the latest data, it makes up about 6 t [13]. If the time of the existence of the earth is $3 \times 10^9$ years (according to the radiometric method), the total amount M of meteoric substance



Declassified in Part - Sanitized Copy Approved for Release 2012/03/12 : CIA-RDP82-00039R000100190014-6

Declassified in Part - Sanitized Copy Approved for Release 2012/03/12 : CIA-RDP82-00039R000100190014-6

entering the atmosphere during this period is equal to $6.6 \times 10^{12}$ t. The portion $\alpha$ of the amount of cosmic substance B, not settled on the surface of the earth, of the total amount M will not be more than $10^{-7}$.

Now let us consider the question of the density of dust in the layer 160 to 80 kilometers. Inasmuch as here the velocity of the Brownian movement is less than Stoke's velocity C for particles of size $10^{-6}$ centimeters, then they settle with a velocity of $10^2$ centimeters per second (at an altitude of 100 kilometers C = 8 centimeters per second; at an altitude of 120 kilometers, C = 110 centimeters per second). Then the path from the 160 kilometer level to the 80 kilometer level will be covered by the particles during a time period $T$ of the order of 24 hours.

Evidently, the total amount of dust in this layer is

$$B' = T\alpha \cdot A = \alpha \cdot 6 \cdot 10^6 \text{ grams}$$

Because the volume of the layer is equal to $7.10^{25}$ cm$^3$, the density of the dust in it is

$$\rho = \alpha \cdot 0.6 \cdot 10^{-20} \text{ gms/cm}^3$$

It is known that the density of cosmic dust in space is $10^{-21}$ to $10^{-26}$ grams per cubic centimeter. In the earth's atmosphere it cannot be less than this value.

Accordingly, the above obtained value of $\alpha$, equal to $10^{-7}$,



Declassified in Part - Sanitized Copy Approved for Release 2012/03/12 : CIA-RDP82-00039R000100190014-6

Declassified in Part - Sanitized Copy Approved for Release 2012/03/12 : CIA-RDP82-00039R000100190014-6

is the smallest possible in the atmosphere. Correspondingly, the concentration of particles taken by us, $10^3$, suspended in the atmosphere, is the smallest. The actual values of $\alpha$, and, accordingly the concentration, must be considerably greater.

Dust cannot be equally distributed in the atmosphere. Deviations from the mean values must be both spatial and temporal. Actual observations of silver clouds show that the surface brightness of the latter sometimes changes sharply and suddenly, which evidently indicates the same changes of concentration of dust in them. Sometimes it even seems that a shadow appears and just as quickly disappears on and off the cloud, so rapidly does the intensity of their luminosity vary [4]. Usually the brightness of the clouds changes 10 to 15 times in several minutes [3]. But there exist more lengthy disturbances in the clouding of the atmosphere.

In 1944, N. N. Kalitin conducted an investigation of year-long actinometric observations at a series of stations in order to ascertain whether there may be a connection between these variations in luminosity and the flow of "Perseid" [14]. It developed that there is a minimum and it begins simultaneously for all observation points from Pavlovsk to Yakutsk, whereupon its magnitude is of the same order, even though the points of location are under varying climatic conditions. From here, the conclusion was drawn that the cause for the August minimum is the same and not of the earth's origin. The ~~transverse~~ diameter of the accumulation of cosmic dust should have a size of 70 million kilometers with whereupon the absorbent mass in it is not distributed evenly. The maximum



Declassified in Part - Sanitized Copy Approved for Release 2012/03/12 : CIA-RDP82-00039R000100190014-6

Declassified in Part - Sanitized Copy Approved for Release 2012/03/12 : CIA-RDP82-00039R000100190014-6

of absorption extends from the front boundary of the accumulation for a distance of 26 million kilometers; the second part of the accumulation is more dense than the first. The earth enters the dust cloud on 8 August and leaves it on 5 September.

Preliminary processing of the material showed that in addition to the August minimum there is also an April minimum which could be attributed to the influence of the meteoric inflow "Lirid." In 1925, upon studying the annual transparency of the atmosphere at Pavlovsk, it was revealed that the transparency in April is less than what it should be according to the annual values.

These data support the assumption that the earth on its orbit encounters dust accumulations of various extents and various concentrations.

And, evidently, during the time of entry of cosmic dust concentrations that cause anomalies in the transparency of the atmosphere, there are especially sharp deviations from the mean value of dust content in the atmosphere [14, 15].

In this manner, we may expect that the conditions necessary for the considered processes of vertical air movements will always occur in the stratosphere between 20 and 60 kilometers, where there is a sufficient quantity of dust for this, and vertical velocities attain sufficient magnitudes. Above 60 kilometers temperature drops with altitude, which also furthers the mixing of air in that region.



Declassified in Part - Sanitized Copy Approved for Release 2012/03/12 : CIA-RDP82-00039R000100190014-6

Declassified in Part - Sanitized Copy Approved for Release 2012/03/12 : CIA-RDP82-00039R000100190014-6

During periods when great concentrations of cosmic dust enter the atmosphere, there will be more intense mixing of air and local cyclonic systems.

In conclusion, let us evaluate the possible order of diurnal fluctuations of air temperatures in the stratosphere, called forth by the heating effect of dust contained in it. Let us assume that air layers in a horizontal direction contain dust so homogeneously distributed that vertical currents may not begin.

Let us consider the equation of heat inflow related as previously to a unit of air mass occupying a given volume v:

$$\pi r^2 I_0 v N = c_p \frac{dT}{dt} - Av \frac{dp}{dt} . \qquad (30)$$

Inasmuch as in the given case the volume of air expands upon heating without being displaced, then

$$\frac{dT}{dt} = \frac{\partial T}{\partial t} \quad and \quad \frac{dp}{dt} = 0.$$

Therefore,

$$\ln \frac{T}{T_0} = \frac{\pi r^2 I_0 R}{c_p p} N (t - t_0) \qquad (31)$$

Let us compute the variations of temperature in the course of one day.



Declassified in Part - Sanitized Copy Approved for Release 2012/03/12 : CIA-RDP82-00039R000100190014-6

Declassified in Part - Sanitized Copy Approved for Release 2012/03/12 : CIA-RDP82-00039R000100190014-6

Let the time from sunrise to sunset, $t - t_0 = 12$ hours.

The mean concentration of dust $N = 10^3$ (in the upper half of the stratosphere, $10^2$; in the lower half, $10^4$).

At a level of 30 km: $T_0 = 230°$, $p_0 = 10$ mb, $\Delta T = 13°$.

At 75 km: $T_0 = 275°$, $p_0 = 6.4 \cdot 10^{-2}$ mb, $\Delta T = 24.5°$.

If we take here $N = 10^3$, then $\Delta T = 370°$ and coincides with the value of the diurnal ~~path~~ cycle (in order), which is obtained according to the hypothesis of "pulsating" atmosphere.

At 5 km: $T_0 = 250°$, $p = 500$ mb, $\Delta T = 0.3°$.

In this manner, according to altitude the diurnal ~~path~~ cycle of temperature should grow. In layers of inversion, for example, in the tropopause, dust content must deviate from mean conditions, and the diurnal ~~path~~ cycle must be correspondingly larger than the upper layers adjoining the inversion.

In this connection it should be noted that upon the processing of aerological observations, the increase of the diurnal ~~path~~ cycle of temperature with altitude in the upper atmosphere is established. And such phenomena as the differences in the height of day and night polar lights, differences in the intensity of evening and morning twilight [16] compel us to accept the hypothesis of "pulsating" atmosphere, which means also that we must assume a considerable diurnal course in temperature in the upper layers (~~because~~ because it is natural to consider that the pulsations are the results of dynamic as well as thermal causes).



Declassified in Part - Sanitized Copy Approved for Release 2012/03/12 : CIA-RDP82-00039R000100190014-6

Declassified in Part - Sanitized Copy Approved for Release 2012/03/12 : CIA-RDP82-00039R000100190014-6

Accordingly, the assumption of a "dusty" atmosphere, predominantly of cosmic origin, which in itself does not seem impossible, allows us to construct a physically simple and natural picture uniting the various phenomena of the stratosphere, to which as yet no contradictory reasoning has been found. This condition, in turn, may serve as an indirect proof of the probability of the assumptions made. First of all the problem of the "mixed" atmosphere appears as possible for solution.



Declassified in Part - Sanitized Copy Approved for Release 2012/03/12 : CIA-RDP82-00039R000100190014-6

Declassified in Part - Sanitized Copy Approved for Release 2012/03/12 : CIA-RDP82-00039R000100190014-6

# CERTAIN CONCLUSIONS FROM THE KOLTUSHA OBSERVATION STATION ON THE PHYSICS OF THE SURFACE LAYER OF AIR

S. A. Sapozhnikova

The interaction of the atmosphere with the underlying surface, the complex characteristics of which give the heat balance of the active surface, appears as the basic problem of physics of the surface layer.

The importance of the problem of the study of the heat balance and its components was formulated accurately by A. I. Voyeykov in 1884 (1). His ideas found their reflection in the works of D. A. Rymoslavskiy (2) and V. A. Mikhelson (3) and other investigators.

In the last few years, a series of works of the main geophysical laboratory was devoted to the question of the heat balance of the active surface (2, 3, 4, 5). In the greater number of cases, the computation of the heat balance was done approximately, often utilizing indirect methods (effective radiation was computed by temperature, humidity, and cloudiness; the radiation balance, by the height of the sun; vaporization, by precipitation and flow, etc); because of this it was necessary to limit oneself to mean, long standing seasonal, and even annual values, and characteristics of geographic distribution were applied only by zones (5-6 zones for the USSR). But experience shows that zonal characteristics (forest, steppe and others) do not have a great practical value.

A series of productive problems, ~~(especially ameliorations)~~ especially of legislative enactment, directed toward changes in climate, and primarily, the grandiose plan of remaking nature envisaged by the governmental decree of October 1948, concerning land conservation, forest planting, and other



Declassified in Part - Sanitized Copy Approved for Release 2012/03/12 : CIA-RDP82-00039R000100190014-6

Declassified in Part - Sanitized Copy Approved for Release 2012/03/12 : CIA-RDP82-00039R000100190014-6

measures in the struggle against drought and dry scorching winds, require an analysis of the heat balance of the active surface.

Moreover, the necessity of detailed daily characteristics appears in connection with the statement of the question on the utilization of the components of the heat balance in current forecasts.

In this connection, a problem arose concerning the establishment of stationary daily observations of heat balance components and the parallel development of methods in processing the observations themselves as well as necessary computations.

Considering the importance of the problem, the Department of Atmospheric Physics, etc., organized a station on the physics of the surface air layer.

In the selection of the site, special consideration was given to the characteristics of its location. The basic observations must be made on an open level place in order, on the one hand, that comparisons with analogous observations under other climatic conditions (at other observatories) might be assured, and on the other, to obtain criteria upon comparison with which it will be possible to determine the influence of local conditions (relief, cover, etc) under microclimatic homogeneity.

The site considered for the station should be open and level.

An open and level location is necessary in order that air and turbulence exchange connected therewith not be disturbed. For the purpose of checking the non-disturbance of the air flow, variations in the velocity of the wind in the 1 to 5 meter layer, under



Declassified in Part - Sanitized Copy Approved for Release 2012/03/12 : CIA-RDP82-00039R000100190014-6

Declassified in Part - Sanitized Copy Approved for Release 2012/03/12 : CIA-RDP82-00039R000100190014-6

different wind directions, were compared. It developed that the vertical profile of the wind under adiabatic conditions remains constant, independent of the direction and relative velocities at a height of 5 and 1 meters during the summer on the order of 1.40 and in the winter, 1.10. This is normal for an open and level place having grasses in summer and smooth snow surface in winter.

The soil at the site is sandy loam, and with the exception of a special bare spot measuring 3 by 3 square meters, is covered with various grasses and mowed periodically.

In the beginning of August 1948, the weight of the green mass of grass on the anemometric and soil platforms equalled 247 grams per square meter before drying and 1.2 after drying, with a gross height of 5 to 7 centimeters. On the plot of the psychrometric observations, the length of the unmowed grass was 30 centimeters and the weight of the green mass before drying was 542 grams per square meter and 235 grams per square meter after drying. According to the character of the plant cover, the plot is typical for a dry plain. The ground is well drained. The level of ground water is not established, but the humidity of the soil in the upper 20 centimeter layer, in the summer of 1948, fluctuated with 7 to 15 percent under grass and 10 to 20 percent fallow. As was stated above, the station site has a plot devoid of growth. This is a control area for determining the role of grass in the formation of the radiation balance and heat exchange in the soil.

In observing the characteristics of radiation balance as a whole as well as in particular components, a series of actinometric instruments are used, including self-recording instruments (Krov-Savinov's



Declassified in Part - Sanitized Copy Approved for Release 2012/03/12 : CIA-RDP82-00039R000100190014-6

Declassified in Part - Sanitized Copy Approved for Release 2012/03/12 : CIA-RDP82-00039R000100190014-6

actinograph, Kobtch's pyronograph, Yanishevskiy's balanceograph, Aykhel'son's actinometer, Savinov's pyrogeometer, Yanishevskiy's pyranometer and others).

For the characteristics of heat exchange in the soil, systematic observations of the temperature of the soil are being conducted. In the summer period the temperature of the soil is measured by Savinov thermometers at two locations; at the bare spot and at the grass covered spot. The temperature of the surface of the soil is measured by a standard thermometer. In order to increase the accuracy of observations at each of the locations, the thermometers were installed with a two-stage frequency.

Since 1 July 1948, resistance thermometers designed by V. P. Tretyakov were installed at the grass location. Their receiving part consists of a copper resistance bar in a glass tube.

A verifying graduation showed the stability of their conversion factors. Resistance thermometers installed in the winter of 1 48/49 were placed at the following depths: 5, 10, 15, 20, 40, 60 and 80 centimeters and on the surface.

Besides observations on the temperature of the soil beginning June 1948, observations have been conducted every ten days of the humidity of the soil at depths of 5, 20, 40, 60 and 80 centimeters by the commonly used weight method, as well as by periodic determination of the weight of the volume of soil.

Observations at various heights conducted by electric anemometers of N. Z. Sternzat's system and Assmen's psychrometer, the design of which is changed somewhat for heights above 2 meters, serve for com-



Declassified in Part - Sanitized Copy Approved for Release 2012/03/12 : CIA-RDP82-00039R000100190014-6

Declassified in Part - Sanitized Copy Approved for Release 2012/03/12 : CIA-RDP82-00039R000100190014-6

puting the direct thermal exchange between the air and soil and for latent exchange through vaporization, as well as for the characteristics of vertical stratification of the wind, temperature, and humidity in the surface air layer (see below).

Readings of Sternzat's contact electric anemometers installed at heights of 0.5, 1, 2, 5.1, 7.5, and 15.9 meters (the 3 latter on a portable metal tower), are registered with the aid of a 6-point chronograph with a clock-wound drum. During operation covering 1½ years, Sternzat's anemometers fully justified themselves in regard to calibration curves and accuracy (from 0.3--0.5 meters per second) as well as the comparatively simplified handling and maintenance.

The matter of recording air temperature and humidity is not so easily solved. Our investigations in the area of utilization of electric apparats for measurement of air temperatures have not as yet been crowned with success due to certain technical difficulties. As a result of this, measurement of temperature and humidity were conducted, as was already noted, with the aid of Assman's psychrometer, which gave some distortions of temperature gradients below 1 meter and was inconvenient for use at heights over 2 meters. In connection with the latter, systematic observation of temperature and humidity during the total time of operation of the station were conducted at heights of 0.2, 0.5, and 1.5 meters. In the summer of the current year, additional readings were made at 2.6, 2.3, and 10.5 meters.

Psychrometric readings at heights of 2.6 and 5.2 meters were made through a 27 x leveling instrument especially set up on a pole in a horizontal axis position at a distance of 10 meters from the second pole, on which psychrometers with electrically-controlled ventilation were installed. In order



Declassified in Part - Sanitized Copy Approved for Release 2012/03/12 : CIA-RDP82-00039R000100190014-6

Declassified in Part - Sanitized Copy Approved for Release 2012/03/12 : CIA-RDP82-00039R000100190014-6

to insure the wetting of the psychrometer from the side, an arrangement with water was attached, into which the end of the wetted thermometer was immersed, similar to what is done with August's thermometer. During night observations the thermometers were illuminated by a light fastened in back of the psychrometer.

At a height of 10.5 meters the temperature was read with the aid of a tilting psychrometer of Zubov's system, manufactured by the State Hydrologic Institute. The latter is an Assman's psychrometer encased in a special mounting in which the psychrometer at the needed moment tilts upward by the reservoir of its thermometers. Instead of the usual thermometers, special thermometers of the depth type with a detachable mercury column and scale were installed. The scale was inscribed from the end of the capillary opposite the reservoir.

The presence of uniform temperatures in regard to sensitivity and inertia of the thermometers at all heights permitted obtaining on particular days undistorted profile of temperatures for the entire 10-meter layer.

Besides the above mentioned apparatuses there was a complete set of equipment for a network station. Wild's wind vane was inefficient and wind direction was determined by Tret'yakov's anemometer at a height of 2 meters.

It can be stressed with satisfaction that all of the special equipment, with some rare exceptions, was designed by Soviet meteorologists, principally, by the meteorologists of the main Geophysical Observatory (S. I. Savinov, Yu. D. Yanishevski, V. D Tret'yakov, N. S. Sternzat.)

Observations were conducted at varying intervals, up to hourly,



Declassified in Part - Sanitized Copy Approved for Release 2012/03/12 : CIA-RDP82-00039R000100190014-6

Declassified in Part - Sanitized Copy Approved for Release 2012/03/12 : CIA-RDP82-00039R000100190014-6

depending on particular concrete problems and technical possibilities. Compulsory in all cases were two periods -- 00 and 12 hours.

Observations at the station permitted the independent computation of each component of the heat balance of the active surface, that is, the radiation balance, heat exchange in the soil, heat exchange between soil and air, and expenditure of heat for vaporization.

Not stopping with the methods of computing components of heat balance, inasmuch as they are published in the transactions of the GGO and *others* (3 -- 12), let us go on to the consideration of certain results of the investigations.

The considerable material of the station is now in the processing state. Therefore, we will limit ourselves to the consideration of separate problems, in order to show according to factual material the practical and theoretical value of the investigations conducted by the station.

Of the questions connected with the radiation balance, let us ~~dwell upon~~ the dependence of the tension of the radiation balance upon general and lower clouds in summer near-noon hours, utilizing for this the observations in July and August 1940. For comparison, August data were placed with July 15 taking into account that under other similar conditions



Declassified in Part - Sanitized Copy Approved for Release 2012/03/12 : CIA-RDP82-00039R000100190014-6

Declassified in Part - Sanitized Copy Approved for Release 2012/03/12 : CIA-RDP82-00039R000100190014-6

the intensity of radiation is approximately proportional to the height of the sun (4).

The dependence of the mean hourly tension of the radiation balance in the near-noon hours (11 to 13 hours) on cloudiness is shown in Figures 1 and 2.

The general cloudiness gives a great dispersion of points at so called cloudy skies (8 to 10 balls). During this interval a maximum tension (0.9 calories per minute per square centimeter) enters, also the minimum (0.04 calories per minute per square centimeter). At a cloudiness of less than 8 balls the tension of the radiation balance is maintained approximately at the same level, 0.7 to 0.8 calories per minute per square centimeter, that is if we do not consider a cloudiness of 7, under which the radiation intensity varies as under a cloudy sky. Within the limits of cloudiness accepted in climatology, we obtain the following mean value for intensity of radiation. At a cloudiness of 0 to 2 -- 0.75, cloudiness of 3 to 7 -- 0.64, and of 8 to 10, -- 0.30 calories per minute per square centimeter.

In comparing the intensity of radiation with the lower overcast, the dispersion of the point within the "cloudy"gradation is considerably smaller, and the average intensity is naturally less -- 0.21 calories per minute per square centimeter. The average intensity in the other two groups was changed comparatively insignificantly -- 0.72 and 0.64 calories per minute per square centimeter respectively. The lower overcast of 7 cloudiness, as the general,according to its characteristic intensity of radiation,is closer to the gradation "cloudy".

If we carry the 7 cloudiness over to the "cloudy" gradation,



Declassified in Part - Sanitized Copy Approved for Release 2012/03/12 : CIA-RDP82-00039R000100190014-6

Declassified in Part - Sanitized Copy Approved for Release 2012/03/12 : CIA-RDP82-00039R000100190014-6

than the "variable cloudiness" gradation (within 3 to 6) will have an average intensity for the lower overcast of 0.70 and for the general, 0.78 calories per minute per square centimeter, that is, the same or even greater than under a cloudiness of 0 to 2. From a physical point of view this is quite understandable, because under a presence of direct radiation, the increase of cloudiness increases the intensity on account of the increase of dispersion of radiation as well as the decrease of the effective radiation.

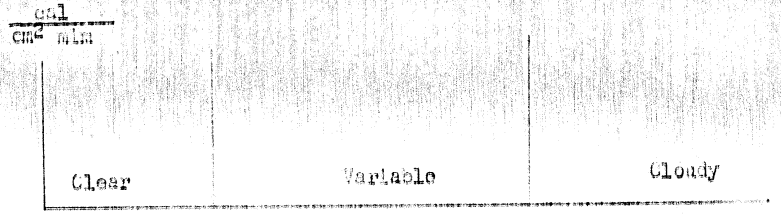


Figure 1. Dependence of the intensity of radiation on general cloudiness during near-noon hours. 1 -- July; 2 -- August.

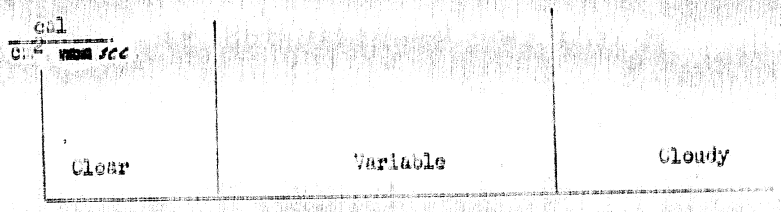


Figure 2. Dependence of the intensity of radiation on lower overcast during near-noon hours. 1 -- July; 2 -- August.

Due to the fact that cloudiness, as a climatic characteristic, is



Declassified in Part - Sanitized Copy Approved for Release 2012/03/12 : CIA-RDP82-00039R000100190014-6

Declassified in Part - Sanitized Copy Approved for Release 2012/03/12 : CIA-RDP82-00039R000100190014-6

used as an indirect index of the radiation conditions, the above stated nearness of the intensity of radiation at a 7 cloudiness to the "cloudy" gradation, supported in mass data which took into account diurnal and annual paths, should be taken into consideration in the grouping of cloudiness ~~and~~ by gradation, ~~which~~ and, possibly, may ~~call forth~~ necessitate a reconsideration ~~in the grouping~~ of the existing gradation.

This conclusion shows what value the observations of the station may have in the physics of the surface air layer for the solution of methodological problems even in matters of climatography.

Subsequent analysis of the materials on the radiation balance and its connections with cloudiness, as well as the radiation characteristics of the active surface will permit an all-round study of this leading component of heat balance of the active surface, which is of interest not only as a weather- and climate-forming factor, but as one directly important for the practice of sanatoria construction, agriculture, peat industry and so forth.

The systematic observations conducted at the station on the changes of the velocity of the wind gave empirical proof for the theory of D. L. Laykhtman on the vertical profile of the wind and turbulence of the surface layer (12).

left hours

Figure 3. Profile of the wind in semi-logarithmic coordinates on a 10-day average in July 1943

Earlier observations as a result of inaccuracies of instruments (Fuss's anemometer) and of their limited sensitivity (from 1 meter



Declassified in Part - Sanitized Copy Approved for Release 2012/03/12 : CIA-RDP82-00039R000100190014-6

Declassified in Part - Sanitized Copy Approved for Release 2012/03/12 : CIA-RDP82-00039R000100190014-6

per second) as well as the insufficient uniformity of the underlying surface, permitted certain investigators (13) to affirm that in a layer of several centimeters up to 5 and more meters, a logarithmic law on the changes of wind with height is maintained, independent of the stability of the atmosphere.

Only by utilizing Starmast's anemometers under conditions of the uniform cover at the station were we able to obtain complete materials on the mean profile of the wind in the interval from 0.5 to 15.9 meters.

The curves shown on Figure 3 are constructed according to hourly data on an average of ten day full diurnal observations in July 1948.

The graph is constructed in semi-logarithmic coordinates (log z, u). In a logarithmic distribution, the profile of the wind of such coordinates is a straight line. But only the profile at 6, 18 and 20 hours corresponds to a straight line. In all other cases the profile is a curve, convex in relation to the abcissa at night and concave in the day. The curvature is seen clearly if we draw a straight line through the points corresponding to 0.5 and 1 meter. In particular instances the deviation of the actual velocity at a height of 5 meters from that which would have been in a logarithmic law, approach ~~es to~~ 0.5 meters per second, and at a height of 15.9 meters -- nearly ~~up to~~ 1 meter per second. A similar deviation from the straight line of the wind velocity profile is possible under the condition that at night, in a temperature inversion, the increase of turbulence exchange with altitude occurs non-proportionally to the height, that is, not as under an equilibrium of conditions, but more slowly; during the day, however, in thermal convections, it is reversed, speeded up; that is taken into condideration by D. L. Laykhtman's formula.

T. A. Ogneva, utilizing D. L. Laykhtman's method, on the



Declassified in Part - Sanitized Copy Approved for Release 2012/03/12 : CIA-RDP82-00039R000100190014-6

Declassified in Part - Sanitized Copy Approved for Release 2012/03/12 : CIA-RDP82-00039R000100190014-6

basis of diurnal observations in the surface air layer of verticle profiles, computed annual cycles of daylight and night values of turbulence coefficients (Table I).

Table I

Annual path of the coefficient of turbulence in $m^2$/sec for day and night at a height of 1 m ($K_1$)

| | I | II | III | IV | V | VI | VII | VIII | IX | X | XI | XII |
|---|---|---|---|---|---|---|---|---|---|---|---|---|
| Day... | 0.04 | 0.05 | 0.06 | 0.08 | 0.12 | 0.14 | 0.15 | 0.15 | 0.16 | 0.13 | 0.18 | 0.04 |
| Night.. | 0.04 | 0.04 | 0.03 | 0.02 | 0.02 | 0.02 | 0.01 | 0.01 | 0.02 | 0.03 | 0.03 | 0.02 |

Day and night coefficient values have an annual cycle, but at that time when the day values rise sharply in the move from winter to summer, the night values are reversed and diminish. The noted peculiarities are determined by the nature of the day and night turbulence itself; their connection with the general weather conditions, shown in Table II.

Table II

Variations in the coefficient of turbulence ($K_1$) in relation to the velocity of the wind ($u_1$) and cloudiness in summer and winter, during the day and during the night.

| $u_1$ m/sec | Less than 1 | | 1 to 3 | | 4 to 6 | |
|---|---|---|---|---|---|---|
| Cloudiness | day | night | day | night | day | night |
| Warm part of the year | | | | | | |
| 0-2 | 0.20 | 0.005 | 0.20 | 0.02 | 0.25 | 0.05 |
| 8-10 | 0.10 | 0.01 | 0.15 | 0.05 | 0.20 | 0.10 |
| Cold part of the year (snow cover) | | | | | | |
| 0-2 | 0.005 | | 0.02 | | 0.05 | |
| 8-10 | 0.005 | | 0.03 | | 0.10 | |



Declassified in Part - Sanitized Copy Approved for Release 2012/03/12 : CIA-RDP82-00039R000100190014-6

Declassified in Part - Sanitized Copy Approved for Release 2012/03/12 : CIA-RDP82-00039R000100190014-6

As is evident in table No. 11, the daily turbulence during the warm period of the year in clear skies (that is, under great intensity of radiation), is nearly independent of wind velocity, and only during cloudy weather does it double at an increase of wind velocity from 1 meter per second to 4 - 6 meters per second. Night turbulence at like wind velocities increases 10 times. Whereupon, if the day turbulence decreases with the increase of cloudiness (weakening of convection), the night turbulence, on the contrary, increases (decrease of temperature inversion).

The yearly cycles of cloudiness and wind, their changes from winter to summer, determine the character of the yearly cycles of night and day turbulence.

Special attention should be given to the fact of reduced turbulence, that is, greater standstill of air, in summer nights in comparison to winter nights. The property of dependence between the day and night turbulence and wind/ velocity should be considered in all kinds of measures connected with the regulation of wind velocity. The decrease of wind velocity will influence night turbulence especially strongly, and day turbulence less strongly. The regulation of the velocity of the wind in the day hours will still show a determinant value on the processes embracing the diurnal periods, and the phenomena connected therewith, for example, the diurnal total of heat exchange between soil and air, because even small percentage-wise variations of day-hour turbulence in an absolute magnitude surpass the corresponding changes of turbulence during night hours.

Heat exchange in the soil, especially in the northern regions, where the low temperature condition of the soil may retard the success of agricultural crops, is of great practical interest.



Declassified in Part - Sanitized Copy Approved for Release 2012/03/12 : CIA-RDP82-00039R000100190014-6

Declassified in Part - Sanitized Copy Approved for Release 2012/03/12 : CIA-RDP82-00039R000100190014-6

Moreover, the soil, as a particular accumulator of day warmth, regulates the cooling of the lower layers of air at night; this must be taken into account when forecasting early autumn frosts.

In accordance with the investigations of G. A. Voloshinova, the temperature conductivity of our soil in the 5 to 15 centimeter layer during July 1948, fluctuated near 0.003 - 0.005 square centimeters per second; on only 1 August it approached 0.007 square centimeters per second. Comparing the cycle of temperature conductivity with the cycle of humidity (triple repetition) at a depth of 5 and 20 centimeters (figure 4), we arrive at the conclusion that a full agreement between the mentioned elements does not appear, and a sharp jump of temperature conductivity from 13 to 14 July (from 0.0035 to 0.0051) is accompanied even by a certain decrease in humidity, which is supported in the general course of weather conditions. There may be two reasons for this phenomenon: either the noted fluctuation of the coefficient of temperature conductivity lies within the limits of permissible errors in the computation of the coefficient, or its actual connections with the average humidity of the layer may be overcome by other factors. One or the other is fully possible. The transfer of heat into the soil, of course, is not only molecular, but also by means of water migration and, what is especially important, by means of a concomitant transfer of heat from a gaseous form into liquid and vice-versa. Concerning migration of water particularly, the well-known diurnal cycle of humidity of the upper layer of soil serves as a witness.



Declassified in Part - Sanitized Copy Approved for Release 2012/03/12 : CIA-RDP82-00039R000100190014-6

Declassified in Part - Sanitized Copy Approved for Release 2012/03/12 : CIA-RDP82-00039R000100190014-6

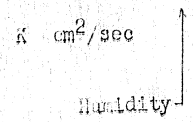


Figure 4. Cycle of humidity and temperature conductivity of the soil. July.

1 - temperature conductivity; 2 - humidity of the soil in percent at per 10 cm;

3 - humidity of the soil in percent at per 5 cm.

In determining the temperature conductivity of the soil in its variation during the period of vertical profile of temperature, on which the method of M. I. Laykhtman and the previous methods of amplitude are based, we actually take into consideration the final, summary effect. In this there are advantages and disadvantages. The advantages lies in the fact that in the end total we precisely need the summary temperature conductivity; the disadvantage lies in the difficulty of determining the regularity and correlation of heat characteristics. Furthermore, the possibilities here of additional sources of heat (for example, from condensation of water vapor for a specific depth) are ignored.

Temperature conductivity of the surface layer from 0 to 5 centimeters is less. In the soil near the grass cover, it equals 0.014 square centimeters per second, and on plowed fallow earth -- 0.023 square centimeters per second.

Because the temperature of the surface is determined by a mercury thermometer, which, as is known (4), records the diurnal amplitude of the temperature of the surface of the soil as lower than the actual, the error of observations may have had a bearing only on the coefficient of temperature conductivity. The



Declassified in Part - Sanitized Copy Approved for Release 2012/03/12 : CIA-RDP82-00039R000100190014-6

Declassified in Part - Sanitized Copy Approved for Release 2012/03/12 : CIA-RDP82-00039R000100190014-6

especially small temperature conductivity of the soil under a grassy cover is determined by the existence of sod, a thermoinsulator of a kind. The effect of divergence of heat chacteristics is visually illustrated by the diurnal cycle of temperature on the surface and at a depth of 5 centimeters at both sites during one of the dry clear days, 9 July (Figure 5).

hours

Figure 5. The diurnal path of temperature of the soil on 9 July 1946.

1 - fallow; 2 - grass

During the day, on the surface of the grass-covered soil, the temperature is higher than in the fallow soil; and at 5 centimeters, on the contrary, it is lower by more than 3 degrees during noon hours. During the night, the reverse is observed.

A surface temperature on grass-covered soil higher than that over fallow soil does not appear as something exceptional. Particularly at the Pavlovsk observatory, the temperature of the so-called natural surface, that is, grass cover, very often was greater than the temperature of open sand (15). This phenomenon, when it is accompanied by an increase of day heat of the entire soil, may be explained by a weakening of heat transfer into the air, by standstill of hot air over grassy vegetation. But in the given case, the role of heat conductivity in the upper layer of the surface itself is reduced because, beginning with 5 centimeters, the day temperature of the soil under grass is lower than that under plowed fallow, and, nothwithstanding the uniformity of thermal constants of the underlying layer of soil, the diurnal amplitude at a depth of 20 centimeters under plowed fallow is 3.3 degrees and under grass is only 1.1 degrees.

Table III shows the diurnal cycle of the intensity of heat ex-



Declassified in Part - Sanitized Copy Approved for Release 2012/03/12 : CIA-RDP82-00039R000100190014-6

Declassified in Part - Sanitized Copy Approved for Release 2012/03/12 : CIA-RDP82-00039R000100190014-6

change in the grass-covered soil during 2 clear days and one cloudy day, and in plowed fallow soil during one clear day.

In all of these cases, the flow of heat into the soil begins around 5 A.M. The flow of heat stops around 16 -- 17 hours, that is, a long time before sunset. The diurnal cycle of the heat flow intensity in cloudy weather is distorted due to clearing up during the separate hours of the day, and therefore we shall not discuss it. We shall only note that during cloudy weather, the intensity of positive as well as negative flow of heat fluctuated between 0.02 to 0.04 calories per second per square centimeter, and only during the four noon hours increased as much as from 0.06 to 0.08. At the same time it should be noted that the wind velocity at a height of 2 meters was on an average 2.1 meters per second during the period from 20 hours to 4 hours and 4.4 meters per second during the period from 5 hours to 19 hours.

Table 11

Tension of heat exchange in the soil in cal/cm² min x $10^{-2}$ (+ denotes the flow of heat is directed toward the surface of the soil)

| hours | calories |
|---|---|
| | *Meadow* |
| 1-2 July, overcast at night $u_2$=2.1, in day $u_2$=4.4... | |
| 2-3 July clear (cloudy 3) at night $u_2$=2.1, in day $u_2$=4.9... | |
| 31 July -- 1 August clear (cloudy 0%) | |



Declassified in Part - Sanitized Copy Approved for Release 2012/03/12 : CIA-RDP82-00039R000100190014-6

Declassified in Part - Sanitized Copy Approved for Release 2012/03/12 : CIA-RDP82-00039R000100190014-6

at night $u_2$=0.9, in day $u_2$=3.6.
at night fo2...

plowed fallow

5-9 July clear

---

In clear weather the intensity of heat flow is considerably greater, especially during the day hours. The maximum of day intensity occurs from 9 to 12 hours; it reached 0.08 to 0.09 at a wind velocity of 4 meters per second and 0.12 to 0.13 at a wind velocity of 4 meters per second. The intensity of heat flow of heat to the surface of the soil does not show a sharply expressed occurrence even during clear nights. The general tendency to a diminished intensity of heat flow increases with the decrease of wind. This inverse relationship is well illustrated in Figure 6, which is constructed on the data of four clear nights (from 24 hours to 2 hours). The intensity of flow decreases by one half when the wind velocity increases from 0 to 3 meters per second.

As could be anticipated, the heat exchange in plowed fallow soil proceeds much more intensely and reaches 0.13 calories per minute per square centimeters during night hours and 0.16 during the day, that is, almost twice as much as during the same day on soil covered with grass.

Given in the last column of Table 11 are over-all figures of the quantity of calories which enter the ground during the period of its warming and leave during the period of its cooling. These figures give the clear evaluation of the role of weather conditions as well as the vegetation cover. In the final [illegible] --



Declassified in Part - Sanitized Copy Approved for Release 2012/03/12 : CIA-RDP82-00039R000100190014-6

Declassified in Part - Sanitized Copy Approved for Release 2012/03/12 : CIA-RDP82-00039R000100190014-6

the diurnal increase of heat -- they are all near each other, but the diurnal amplitude of heat exchange changes considerably, whereupon the influence of vegetation cover superimposes corresponding effects on weather conditions.

These results fully correspond to the evaluation of the role of grass cover in the annual heat formation, which was stated by G. A. Lyuboslavskiy 40 years ago (2).

The stated characteristics are fully understood from the point of view of physics, but not all of them are taken into account in actual conclusions with regard to soil climate, its melioration, nor in the calculation of the heat exchange of the soil when making forecasts of first autumn frosts. First of all, the leading role played by the type of soil in heat exchange of the soil should be understood. Even such an insignificant amount of cover (height 5 to 7 centimeters, weight of the green mass 0.2 kilograms per square meter) with sod, decreased the intensity of the heat exchange by 2/3 to 1/2 during the night hours. Considerably greater effect should be expected from vegetation cover with a green mass of 1 to 3 kilograms per square meter, which is common to our fields and meadows. The deciding influence of grasses upon the condition of the soil is confirmed by many surveys (16, 17, 18, etc).

$\frac{cal}{cm^2\ min}$ ——————— m/sec

Figure 6. Variation in the intensity of heat exchange in the soil in relation to the velocity of the wind during clear days: 4-5, 8-9 13-14 of July and 31 July -- 1 August 1948. (from 20 to 2 hours).



Declassified in Part - Sanitized Copy Approved for Release 2012/03/12 : CIA-RDP82-00039R000100190014-6

Declassified in Part - Sanitized Copy Approved for Release 2012/03/12 : CIA-RDP82-00039R000100190014-6

Taking into consideration that the variations in the heat exchange in relation to the humidity of the soil regulate its temperature conductivity in natural conditions of the same order (Figure 4), we arrive at the conclusion that upon the determination (as well as the forecasting) of soil heat exchange, in particular the forecasting of first autumn frosts, it is necessary to take into consideration not only, or possibly not so much, the soil humidity, as is assumed by certain investigators (10) but the type of soil cover as well.

The above-mentioned data make it possible to arrive at certain conclusions in regard to the role of weather conditions. Side by side with the radiation cycle, the big role in the formation of thermal conditions of the soil is played by the wind, which increases the heat exchange between the soil and the air because of the decrease of heat exchange in the soil itself. The role of the wind was practically neglected up to very recently. Only certain of our works give some corresponding indications.

Thus, S. M. Nikhaylovskaya (19), analyzing the temperature of the soil at a depth of 20 centimeters on the slopes of different exposures, discovered the influence of wind velocity; because of this influence similarly located slopes had different soil temperatures depending upon the degree of protection from the wind. Because of the fact that the wind diminishes heat exchange in the soil during the day as well as the night, there occur reciprocal compensations in many cases, and the influence of wind may not change the average diurnal temperatures. Because of this, the fact that the role of wind has been up to now ignored in the



Declassified in Part - Sanitized Copy Approved for Release 2012/03/12 : CIA-RDP82-00039R000100190014-6

Declassified in Part - Sanitized Copy Approved for Release 2012/03/12 : CIA-RDP82-00039R000100190014-6

analysis of heat conditions of the soil can readily be understood.

The calculation of
A the role of the wind is of exceptional value from the point of view of the artificial increase in the temperature of the soil and the adjacent air layers. If the increase of wind velocity at night together with a decrease in the cooling of the soil is still technically difficult ~~to realization~~ to bring about, the decrease of day-time wind velocity by means of wind-break installations is entirely possible. But wind-break installations should be used only during the day; at night they should be rolled up.

Similar measures should be of great material aid to grape culture, berry growing, and the cultivation of other plants which demand warmth in regions which have relatively cold summers and which are transitional between open and protected soil. The greatest thermal effectiveness should be expected in elevated regions with higher wind velocities, especially in the upper regions of southern slopes.

The problems discussed show the practical value of investigations into the field of heat balance of the active surface as applied to climate service, weather service, and measures for meliorative work on the climate of the surface air layer.

For the successful development of these problems a thorough analysis of phenomena is necessary. This analysis is possible only under the joint study of meteorologist-theoreticians, experimenters, and climatologist-geographers, because the required accuracy of decisions for the practice not in general terms, but under concrete conditions of weather and locality, sometimes very complex, can be secured only by developing better obser-



Declassified in Part - Sanitized Copy Approved for Release 2012/03/12 : CIA-RDP82-00039R000100190014-6

Declassified in Part - Sanitized Copy Approved for Release 2012/03/12 : CIA-RDP82-00039R000100190014-6

vation methods, improving interpretation of the physical nature of phenomena, and increasing the knowledge of characteristics of the active surface (soil, vegetation).

The more concrete the work is in the sense of its practical utilization, the greater will be the role of experience in the quantitative formulation of its decisions. The proper application of this experience without the knowledge of all the correlation of natural conditions is impossible.

In conclusion, it should be stressed that the organization of the station, which as a matter of fact was not foreseen by the budget nor by the preliminary plan of construction of the experimental base of the Main Geophysical Observatory, was possible only because of the enthusiasm of the workers of the department of physics of the surface air layer: Junior Scientific Workers Z. I. Pivovarova, T. A. Ogneva, G. A. Voloshinova and Senior Technicians A. I. Andreyeva and I. A. Golodenova. Professor D. L. Laykhtman and candidate of Physics and Mathematical Sciences M. P. Timofeyev took direct part in the management of the station. The installation of instruments and necessary structural improvements were supervised by Candidates of Physics and Mathematical Sciences V. D. Tret'yakov and A. V. Kucherov. Senior Scientific Worker of the Actinometric Laboratory Yu. D. Yanishevskiy assisted with instruments and consultations in actinometric observations.



Declassified in Part - Sanitized Copy Approved for Release 2012/03/12 : CIA-RDP82-00039R000100190014-6

Declassified in Part - Sanitized Copy Approved for Release 2012/03/12 : CIA-RDP82-00039R000100190014-6

# ON AN APPROXIMATE METHOD OF SOLVING CERTAIN PROBLEMS OF GEOPHYSICS AND AEROHYDROMECHANICS

M. Ye Shvets

1. Problems of geophysics and hydromechanics formulated for conditions close to the actual, are found to be exceptionally arduous for a mathematical study and in most instances can be solved only by approximation.

For the study of problems under consideration in the present work there is utilized an approximate method of integration of a class of differential equations of the parabolic type; this includes many important aspects of mathematical physics.

This method consists of a combination, in a special manner, of boundary layer methods and of consecutive approximations, and possesses a number of important advantages over other methods utilized in hydromechanics (methods of Oseen, Karman, integral correlations, and others) and recently also in geophysics. It makes it possible to solve, with sufficient accuracy, in a wholly uniform and, in our opinion, the most simple manner, a series of problems of mathematical physics.

The successful application of this method to the study of a number of problems of hydromechanics and geophysics characterizes it as a tool for solving a great number of practical problems encountered also in other scientific fields (the study of heat exchange, chemical hydromechanics, etc.). Nevertheless it must still be determined under what conditions it obtains.



Declassified in Part - Sanitized Copy Approved for Release 2012/03/12 : CIA-RDP82-00039R000100190014-6

Declassified in Part - Sanitized Copy Approved for Release 2012/03/12 : CIA-RDP82-00039R000100190014-6

The gist of the evolved method is apparent from the problems considered hereinafter.

The designations adopted are: A -- coefficient of turbulent exchange; K -- coefficient of thermoconductivity (or diffusion); Pr -- Prandle's number; q -- concentration; Re -- Reynold's number; t -- time; T -- temperature; u -- longitudinal velocity component; v -- transversal velocity component; x and y -- horizontal coordinates; z -- vertical coordinate; $\delta$ -- thickness of boundary layer; $\theta$ -- non-dimensional temperature; $\mu$ -- dynamic viscosity; $\nu$ -- kinematic viscosity; $\rho$ -- density.

Other designations are introduced as the need arises.

Differentiation with respect to x (or to t) is denoted for the sake of brevity by a dot placed over the differentiated quantity.

## CHAPTER I

## APPROXIMATE SOLUTION OF HEAT CONDUCTIVITY EQUATION

2. Let us consider the heat conductivity equation with a variable coefficient of temperature conductivity frequently encountered in geophysical problems:

$$\frac{\partial T}{\partial t} = \frac{\partial}{\partial z} z^{1-\epsilon} \frac{\partial T}{\partial z} \qquad (1)$$

and let us find the approximate solution of this equation which



Declassified in Part - Sanitized Copy Approved for Release 2012/03/12 : CIA-RDP82-00039R000100190014-6

Declassified in Part - Sanitized Copy Approved for Release 2012/03/12 : CIA-RDP82-00039R000100190014-6

satisfies the following limit conditions:

$$\lim_{z\to 0} z^{1-\epsilon}\left(\frac{\partial T}{\partial z}\right) = q(t);$$

$$T(z,0)=0, \quad T(\infty,t)=0. \tag{2}$$

as is known, the accurate solution of equation (1), which satisfies conditions (2), has the following form:

$$T = \frac{(1+\epsilon)^{-\frac{z}{1+\epsilon}}}{\Gamma\left(\frac{2+\epsilon}{1+\epsilon}\right)} \int_0^t \frac{q(\tau)\exp\left[\frac{z^{1+\epsilon}}{(1+\epsilon)^2(t-\tau)}\right]d\tau}{(t-\tau)^{2-\frac{\epsilon}{1+\epsilon}}},$$

where $\Gamma$ is a function.

If

$$\Gamma\left(\frac{2+\epsilon}{1+\epsilon}\right)(1+\epsilon)^{\frac{2}{1+\epsilon}} = A,$$

then the temperature on the surface $z=0$, will be, as is readily apparent, equal to:

$$T(0,t) = \frac{1}{A}\int_0^t \frac{q(\tau)\,d\tau}{(t-\tau)^{2-\frac{\epsilon}{1+\epsilon}}}.$$



Declassified in Part - Sanitized Copy Approved for Release 2012/03/12 : CIA-RDP82-00039R000100190014-6

Declassified in Part - Sanitized Copy Approved for Release 2012/03/12 : CIA-RDP82-00039R000100190014-6

If, on the other hand, the temperature T (o, t) is given, then the rate of heat emission is

$$q = \frac{A}{\pi} \sin \pi \frac{\epsilon}{1+\epsilon} \frac{d}{dt} \int_0^t \frac{T(0,\tau)\, d\tau}{(t-\tau)^{1-\frac{\epsilon}{1+\epsilon}}} .$$

If $T(o,t) = T = \text{const}$, then,

$$q = \frac{AT_o}{\pi} \sin \frac{\pi\epsilon}{1+\epsilon} \frac{1}{t^{\frac{\epsilon}{1+\epsilon}}} .$$

Consider the approximate solution of equation (1); to simplify the results we will confine ourselves to the following simple limit conditions:

$$T(0,t) = 1;\ T(\infty,t) = 0;\ \ T(z,0) = 0.$$

We will introduce the "thickness of heat penetration" $\delta$, (thickness of boundary layer), and determine it as a value of z, where

$$\left(\frac{\partial T}{\partial z}\right)_{z=\delta} = 0.$$

We will determine T by means of consecutive approximations.

For zero approximation it is assumed that the left part of (1) is equal to zero.

Let $T_0$ be a function determined by the differential equation:



Declassified in Part - Sanitized Copy Approved for Release 2012/03/12 : CIA-RDP82-00039R000100190014-6

Declassified in Part - Sanitized Copy Approved for Release 2012/03/12 : CIA-RDP82-00039R000100190014-6

$$\frac{\partial}{\partial z} z^{1-\epsilon} \frac{\partial T_0}{\partial z} = 0$$

and by all the limit conditions of the problem.

For the next approximation we assume $T = T_0 + T_1$, where $T_1$ satisfies the equation:

$$\frac{\partial}{\partial z} z^{1-\epsilon} \frac{\partial T_1}{\partial z} = \frac{\partial T_0}{\partial t}$$

and here also, all the limit conditions.

Considering this approximation, we have:

$$T = T_0 + T_1 = 1 - \left(\frac{z}{\delta}\right)^{\epsilon} + \frac{\epsilon}{1+\epsilon}\left[\left(\frac{z}{\delta}\right)^{2\epsilon+1} - \left(\frac{z}{\delta}\right)^{\epsilon}\right].$$

For determination of $\delta$ we have the equation:

$$\delta \delta^{\epsilon} = 2\epsilon + 1 .$$

from which

$$\delta = \left[(2\epsilon+1)(\epsilon+1)t\right]^{\frac{1}{1+\epsilon}} .$$

The rate of heat emission is thus equal to:



Declassified in Part - Sanitized Copy Approved for Release 2012/03/12 : CIA-RDP82-00039R000100190014-6

Declassified in Part - Sanitized Copy Approved for Release 2012/03/12 : CIA-RDP82-00039R000100190014-6

$$q = \lim_{z \to 0} z^{1-\epsilon} \left( \frac{dT}{dz} \right) = \frac{\epsilon (1+2\epsilon)^{\frac{1}{1+\epsilon}}}{(1+\epsilon)^{\frac{2\epsilon+1}{1+\epsilon}} t^{\frac{\epsilon}{1+\epsilon}}}$$

In the second approximation we have:

$$T = 1 + \frac{\epsilon(2\epsilon+1)(3\epsilon+2)}{(1+\epsilon)^2} \left[ \frac{\xi^{2\epsilon+1}}{2\epsilon+1} - \frac{\xi^{3\epsilon+2}}{2(3\epsilon+2)} - \frac{\xi^{\epsilon}}{2\epsilon} \right];$$

$$\delta = \left[ (3\epsilon+2)(\epsilon+1)t \right]^{\frac{1}{1+\epsilon}};$$

$$q = - \frac{\epsilon(2\epsilon+1)(3\epsilon+2)^{\frac{1}{1+\epsilon}}}{2(1+\epsilon)^{\frac{2+3\epsilon}{1+\epsilon}} t^{\frac{\epsilon}{1+\epsilon}}}.$$

In the case of a constant heat conductivity coefficient ($\epsilon = 1$), we have in the first approximation:

$$T = 1 - 1.5\xi + 0.5\xi^3 \left( \xi = \frac{z}{\sqrt{6k}} \right). \qquad (3)$$

and in the fourth approximation:



Declassified in Part - Sanitized Copy Approved for Release 2012/03/12 : CIA-RDP82-00039R000100190014-6

Declassified in Part - Sanitized Copy Approved for Release 2012/03/12 : CIA-RDP82-00039R000100190014-6

$$T = 1 - \frac{315}{128}\xi + \frac{315}{32}\left[\frac{\xi^3}{3} + \frac{\xi^7}{7} - \frac{\xi^9}{36} - \frac{3\xi^5}{10}\right]; \quad (3')$$

$$\delta^2 = 18t, \left(\frac{\partial T}{\partial z}\right)_0 = -\frac{0.580}{\sqrt{t}}.$$

The exact solution gives $\left(\frac{\partial T}{\partial z}\right)_0 = -\frac{0.565}{\sqrt{t}}$.

Figure 1 shows graphs of T, calculated on the basis of the exact formula, and of the approximate formula (3'), respectively.

Figure 1. 1 - Approximate solution; 2 - Exact solution.

In Table I are given, for comparison, the exact and approximate values of q for some of the values of $\epsilon$.

Table I

| $\epsilon$ | q in first approximation | q in second approximation | Exact value of q |
|---|---|---|---|
| 0.10 | 0.106 | 0.104 | 0.104 |
| 0.25 | 0.265 | 0.251 | 0.249 |
| 0.50 | 0.462 | 0.447 | 0.427 |
| 0.75 | 0.569 | 0.546 | 0.523 |
| 1.00 | 0.612 | 0.592 | 0.564 |

We note that the above-described method is an effectual means of solving problems which can be reduced to a heat transfer equation and boundary conditions postulated on changeable limits.



Declassified in Part - Sanitized Copy Approved for Release 2012/03/12 : CIA-RDP82-00039R000100190014-6

Declassified in Part - Sanitized Copy Approved for Release 2012/03/12 : CIA-RDP82-00039R000100190014-6

Cooling of Half-Space in the Case of Heat Conductivity and Heat Capacity is Dependent on the Temperature

3. When thermal conductivity $\lambda$, and thermal capacity C, depends on the temperature, the heat conductivity equation assumes the form:

$$\kappa(T)\frac{\partial^2 T}{\partial z^2}=\frac{\partial T}{\partial t}-\frac{1}{c(T)}\frac{d\lambda}{dT}\left(\frac{dT}{dz}\right)^2. \qquad (4)$$

We divide both sides of the equation by k (T) and adopt the following designation:

$$\frac{1}{\kappa(T)}F(T),\ \frac{1}{c\kappa}\frac{d\lambda}{dT}=\Phi(T).$$

Then in lieu of (4) we have:

$$\frac{\partial^2 T}{\partial z^2}=F(T)\frac{\partial T}{\partial t}-\Phi(T)\left(\frac{\partial T}{\partial z}\right)^2. \qquad (4')$$

Assuming, for the sake of definiteness, that limit conditions are given as:

$$\left.\begin{aligned} T(t,0)&=0;\\ T(t,\delta)&=1;\\ T(0,z)&=0. \end{aligned}\right\} \qquad (5)$$

The solution of this problem can be effected in the same manner as that of the foregoing.

As a zero approximation we have:

$$T_0=\frac{z}{\delta}=\xi.$$



Declassified in Part - Sanitized Copy Approved for Release 2012/03/12 : CIA-RDP82-00039R000100190014-6

Declassified in Part - Sanitized Copy Approved for Release 2012/03/12 : CIA-RDP82-00039R000100190014-6

The first approximation is determined from the equation:

$$\frac{\partial^2 T}{\partial \xi^2} = -\delta\delta\xi F(\xi) - \Phi(\xi).$$

If it is assumed that $\delta = \alpha\sqrt{t}$ , we then have:

$$T = T_0 + T_1 = \xi - \alpha^2\left[\int_0^{\xi}\eta(\xi-\eta)F(\eta)d\eta - \xi\int_0^{1}\eta(1-\eta)F(\eta)d\eta\right] -$$

$$-\left[\int_0^{\xi}\Phi(\eta)(\xi-\eta)d\eta - \xi\int_0^{1}\Phi(\eta)(1-\eta)d\eta\right].$$

Coefficient $\alpha$ is found from:

$$\left.\frac{\partial T}{\partial \xi}\right|_{\xi=1} = 0;$$

on simple transformations, we have

$$\alpha = \sqrt{\frac{2+2\int_0^1\Phi\eta\,d\eta}{\int_0^1\eta^2F(\eta)d\eta}}.$$

Thus, the solution of equation (4) has the following form:

$$T = f\left(\frac{x}{\alpha\sqrt{t}}\right).$$

An approximate solution of the non-linear equation of thermal conductivity can be attained in a somewhat different manner.

In place of equation (4) consider the thermal conductivity equation, written as follows:

$$c(T)\frac{\partial T}{\partial t} = \frac{\partial}{\partial z}\lambda(T)\frac{\partial T}{\partial z}. \qquad (4'')$$



Declassified in Part - Sanitized Copy Approved for Release 2012/03/12 : CIA-RDP82-00039R000100190014-6

Declassified in Part - Sanitized Copy Approved for Release 2012/03/12 : CIA-RDP82-00039R000100190014-6

We introduce a new function $\Phi$ in accordance with:

$$P = \int \lambda(T)\, dT,$$

then,

$$\frac{\partial P}{\partial z} = \lambda(T)\frac{\partial T}{\partial z} \quad \text{and} \quad \frac{\partial P}{\partial t} = \lambda(T)\frac{\partial T}{\partial t}$$

and, in lieu of equation (4') we have:

$$\frac{\partial^2 P}{\partial z^2} = a(P)\frac{\partial P}{\partial t}, \qquad (4'')$$

wherein $a = \lambda c$.

If $P_1$ (t) is the value of $P_0$ on surface $z = 0$, and $P_0 =$ const. the value of P at infinity, then on assuming

$$\theta = \frac{P - P_1}{P_0 - P_1},$$

in place of (4''') we have:

$$\frac{\partial^2 \theta}{\partial z^2} = \tilde{a}(\theta)\left[\frac{\partial \theta}{\partial t} - (\theta - 1)\frac{d}{\partial t}\ln(P_1 - P_0)\right].$$

The limit conditions for $\theta$ are:

$$\theta = 0 \text{ when } z = 0;\ \theta = 1 \text{ when } y = \infty.$$

The solution of the last equation can be effected in the same manner as that of equation (4').

Stationary Diffusion; Stream Velocity and Diffusion Coefficient Depend on Distance

4. In the solution of a number of geophysical problems one is confronted with a diffusion equation which contains instead of



Declassified in Part - Sanitized Copy Approved for Release 2012/03/12 : CIA-RDP82-00039R000100190014-6

Declassified in Part - Sanitized Copy Approved for Release 2012/03/12 : CIA-RDP82-00039R000100190014-6

a constant diffusion coefficient, the so-called coefficient of turbulent transfer A. Under stationary conditions it is dependent on distance z.

Without considering the question relative to the nature of dependence of coefficient of turbulent transfer on the distance, we will confine ourselves to developing the first approximation which is amply sufficient for practical purposes.

We multiply both sides of the diffusion equation

$$u(z)\frac{\partial q'}{\partial x} = \frac{\partial}{\partial z} A(z) \frac{\partial q'}{\partial z} \qquad (6)$$

by A(z), introduce a new variable $\eta = \int_0^z \frac{dz}{A}$, and designate $ux = \Phi(\eta)$, then equation (6) assumes the form:

$$\Phi(\eta)\frac{\partial q'}{\partial x} = \frac{\partial^2 q'}{\partial \eta^2} \qquad (6')$$

If the limit and initial conditions are:

when $z = 0$: $q' = q_0$;

when $z = \infty$: $q' = 0$;

when $x = 0$: $q' = 0$.

To simplify the limit conditions we assume $q' = q_0 q$, then when $z = 0$: $q = 1$.

We postulate $q = 0$ at the limit of boundary layer $\delta$, that is, $q(\delta) = 0$. The zero approximation is of form:

$$q = 1 - \frac{\eta}{\delta},$$

First approximation is equal to:



Declassified in Part - Sanitized Copy Approved for Release 2012/03/12 : CIA-RDP82-00039R000100190014-6

Declassified in Part - Sanitized Copy Approved for Release 2012/03/12 : CIA-RDP82-00039R000100190014-6

$$q = 1 - \frac{\eta}{\delta} + \frac{\dot{\delta}}{\delta}\left[\int_0^{\eta} y(\eta - y)\Phi\, dy - \frac{\eta}{\delta}\int_0^{\delta} y(\delta - y)\Phi\, dy\right].$$

wherefrom,

$$\frac{\partial q}{\partial \eta} = -\frac{1}{\delta} + \frac{\dot{\delta}}{\delta^2}\left[\int_0^{\eta} y\Phi\, dy - \frac{1}{\delta}\int_0^{\delta} y(\delta - y)\Phi\, dy\right].$$

On determining thickness of boundary layer on the basis of $\left(\frac{\partial q}{\partial \eta}\right)_{\delta} = 0$, the following equation is obtained:

$$\dot{\delta}\int_0^{\delta} y^2\Phi\, dy = \delta^2. \qquad (7)$$

Following determination of value $\delta$, stream $\left(\frac{\partial q}{\partial \eta}\right)_0$ is determined from the formula:

$$-\left(\frac{\partial q}{\partial \eta}\right)_0 = \frac{1}{\delta} + \frac{\dot{\delta}}{\delta^3}\int_0^{\delta} y(\delta - y)\Phi\, dy.$$

In accordance with (7) this expression can be transformed to give:

$$-\left(\frac{\partial q}{\partial \eta}\right)_0 = \frac{\int_0^{\delta} y\Phi\, dy}{\int_0^{\delta} y^2\Phi\, dy}$$

We note that on using the expression (7), a simpler expression



Declassified in Part - Sanitized Copy Approved for Release 2012/03/12 : CIA-RDP82-00039R000100190014-6

Declassified in Part - Sanitized Copy Approved for Release 2012/03/12 : CIA-RDP82-00039R000100190014-6

is obtained for concentration:

$$q = 1 + \frac{\int_0^\eta y(\eta - y)\Phi\, dy}{\int_0^\delta y^2 \Phi\, dy} - \eta \frac{\int_0^\delta y\Phi\, dy}{\int_0^\delta y^2 \Phi\, dy}.$$

If $q_1$ -- concentration on the surface -- is a function of x, and $q_0 =$ const. the concentration at infinity, then on assuming

$$\theta = \frac{q - q_1}{q_0 - q_1}$$

we have, in lieu of (6):

$$\Phi(\eta)\left[\frac{\partial \theta}{\partial x} + (\theta - 1)\frac{d \ln(q_1 - q_0)}{dx}\right] = \frac{\partial^2 q}{\partial \eta^2}.$$

Limit conditions for $\theta$ are:

$$\theta = 0 \text{ when } \eta = 0;\ \theta = 1 \text{ when } \eta = \delta.$$

Omitting all the calculations, we give the expression for q in the first approximation:

$$q = \frac{\eta}{\delta} - \frac{\dot{\delta}}{\delta^2}\left[\int_0^\eta \Phi y(\eta - y)\, dy - \frac{\eta}{\delta}\int_0^\delta \Phi y(\delta - y)\, dy\right] +$$

$$+ \frac{d}{dx}\ln(q_1 - q_0)\left[\int_0^\eta \Phi\left(\frac{y}{\delta} - 1\right)(\eta - y)\, dy - \frac{\eta}{\delta}\int_0^\delta \Phi\left(\frac{y}{\delta} - 1\right)(\delta - y)\, dy\right].$$

For the determination of $\delta$ we have equation:



Declassified in Part - Sanitized Copy Approved for Release 2012/03/12 : CIA-RDP82-00039R000100190014-6

Declassified in Part - Sanitized Copy Approved for Release 2012/03/12 : CIA-RDP82-00039R000100190014-6

$$I = \frac{\dot{\delta}}{\delta^2}\int_0^{\delta} y^2 \Phi\, dy - \frac{a}{dx}\ln(q_1 - q_0)\int_0^{\delta} \Phi y\left[\frac{y}{\delta} - 1\right] dy.$$

## CHAPTER II

## METHOD FOR APPROXIMATE COMPUTATION OF STEADY PLANE MOTION IN LAMINARY BOUNDARY LAYER

### Flow Along a Flat Plate in an Incompressible Liquid

5. Forty years ago G. Blasius /2/ developed the theory of flow around a flat plate. This theory was the starting point of a number of aerodynamic investigations.

The work of Blasius is well known, hence there is no need to expound it. We may point out, however, that it is fairly complex from a mathematical standpoint.

We shall show here that the results of Blasius can be attained, with great accuracy, by means of the approximate method.

Let the flat plate progress at a constant velocity U.

Equations of motion and continuity in a laminary boundary layer are of the form:

$$u'\frac{\partial u'}{\partial x'} + v'\frac{\partial u'}{\partial y'} = \nu\frac{\partial^2 u'}{\partial y'^2}; \qquad (1)$$



Declassified in Part - Sanitized Copy Approved for Release 2012/03/12 : CIA-RDP82-00039R000100190014-6

Declassified in Part - Sanitized Copy Approved for Release 2012/03/12 : CIA-RDP82-00039R000100190014-6

$$\frac{\partial u'}{\partial x'} + \frac{\partial v'}{\partial y'} = 0. \qquad (2)$$

Eliminating from (1), by means of the continuity equation, the vertical component of velocity v, we have:

$$\nu \frac{\partial^2 u'}{\partial y'^2} = u' \frac{\partial u'}{\partial x'} - \frac{du'}{dy'} \int_0^{y'} \frac{\partial u'}{\partial x'} dy' \qquad (3)$$

Introducing non-dimensional values from formulas:

$$x' = lx, y' = \frac{l}{\sqrt{Re}} y, \; v' = \frac{U}{\sqrt{Re}} v, \; u' = Uu,$$

where $l$ is the length of the plate, and Re is Reynold's number.

Thus, in place of equation (3) we have:

$$\frac{\partial^2 u}{\partial y^2} = u \frac{\partial u}{\partial x} - \frac{\partial u}{\partial y} \int_0^{y} \frac{\partial u}{\partial x} dy. \qquad (4)$$

Solution of equation (4) must satisfy the conditions:

$$\left.\begin{array}{l} \text{when } y = 0; \quad u = 0; \\ \text{when } y = \delta; \quad u = 1. \end{array}\right\} \qquad (5)$$

here $\delta$ is the thickness of the boundary layer, which must be determined.

Zero approximation is found by solving equation $\frac{\partial^2 u}{\partial y^2} = 0$ at limit conditions (5). This approximation is of the form:

$$u = \frac{y}{\delta}.$$



Declassified in Part - Sanitized Copy Approved for Release 2012/03/12 : CIA-RDP82-00039R000100190014-6

Declassified in Part - Sanitized Copy Approved for Release 2012/03/12 : CIA-RDP82-00039R000100190014-6

Substituting the value of u, thus obtained, in the right hand side of equation (4), we obtain the first approximation:

$$u = \frac{y}{\delta} + \frac{\delta y}{24}\left(1 - \frac{y^3}{\delta^3}\right) \qquad (6)$$

As is shown by the calculations, a second approximation gives a negligible correction, and therefore the first approximation is sufficient.

On determining the value of $\delta$, from condition $\left(\frac{\partial u}{\partial y}\right)_\delta = 0$ we have:

$$\delta = 4\sqrt{\nu}.$$

Friction intensity on the plate $\tau_0$ is obtained from (6):

$$\tau_0 = \left(\frac{\partial u}{\partial y}\right)_0 = \frac{1}{\delta} + \frac{\delta}{24} = \frac{0.333}{\sqrt{\nu}},$$

and the dimensional friction intensity $\tau_0'$ is:

$$\tau_0' = \sqrt{\mu\rho U^3}\,\frac{0.333}{\sqrt{\nu}}.$$

The exact value of friction intensity, according to Blasius, is equal to:

$$\tau_0' = \sqrt{\mu\rho U^3}\,\frac{0.332}{\sqrt{\nu}}.$$

Thus, the relative error is equal to 1/3 percent. On substituting the value of $\delta$ in (6), the expression of velocity is obtained:

$$u = \frac{1}{3}\xi - \frac{1}{768}\xi^4 \left(\xi = \frac{y}{\sqrt{\nu}}\right). \qquad (7)$$

The vertical component of velocity is determined from the



Declassified in Part - Sanitized Copy Approved for Release 2012/03/12 : CIA-RDP82-00039R000100190014-6

Declassified in Part - Sanitized Copy Approved for Release 2012/03/12 : CIA-RDP82-00039R000100190014-6

continuity equation.

Following simple transformations we have:

$$v = \frac{1}{12\sqrt{k}}\left[\xi^2 - \frac{1}{160}\xi^5\right] \qquad (8)$$

For comparison, Table II shows the exact values of u, and also the values obtained by means of formula (6), for various values of $\xi$.

TABLE II

| $\xi$ | 0.2 | 0.6 | 1.0 | 1.4 | 1.8 | 2.2 | 2.6 | 3.0 | 3.4 |
|---|---|---|---|---|---|---|---|---|---|
| u -- approximate | 0.0666 | 0.200 | 0.332 | 0.461 | 0.586 | 0.703 | 0.807 | 0.895 | 0.958 |
| u -- exact value | 0.0664 | 0.199 | 0.330 | 0.456 | 0.575 | 0.681 | 0.773 | 0.846 | 0.902 |

## Liquid Motion in a Laminar Boundary Layer in the Case of $U = cx^m$

6. If the velocity of the external stream is $U' = cx'^m$, then $U\frac{dU}{dx} = mc^2 x'^{2m-1}$. Introducing the non-dimensional variables:

$$x' = \left[\nu^m c\right]^{\frac{1}{1+m}} x, \quad k' = \left[\frac{\nu}{c}\right]^{\frac{1}{1+m}} k, \quad y' = \left[\frac{\nu}{c}\right]^{\frac{1}{1+m}} y,$$

Whereupon the equation of motion, and the limit conditions assume the form:

$$\frac{\partial^2 u}{\partial y^2} = -mx^{2m-1} + u\frac{\partial u}{\partial x} - \frac{\partial u}{\partial y}\int_0^y \frac{\partial u}{\partial x}\,dy \qquad (9)$$



Declassified in Part - Sanitized Copy Approved for Release 2012/03/12 : CIA-RDP82-00039R000100190014-6

Declassified in Part - Sanitized Copy Approved for Release 2012/03/12 : CIA-RDP82-00039R000100190014-6

when $y = 0$: $u = 0$;

when $y = \delta$: $u = U = x^m$

The exact solution of equation (9) can be found according to Falkner and Skan-Silvia /3/ on making

$$u' = U'\Phi'(\xi); \quad \xi = y'\sqrt{\frac{(m+1)cx'^{m-1}}{2\nu}}$$

For the determination of function $\Phi$ we obtain the equation:

$$\Phi''' + \Phi\Phi'' = \beta(\Phi'^2 - 1),$$

where

$$\beta = \frac{2m}{1+m}$$

Numerical solution of the latter equation, for various values of m, was obtained by Hartree /4/. This solution obviously depends on $\beta$ and $\xi$.

In 1942, N. Ye. Kochin and L. G. Loitsyanskiy /1/, have used Hartree's function for approximate computation of laminar layer for any function U(x).

The approximate solution of this problem follows.

Here again the zero approximation is:

$$u_0 = x^m\xi = U\xi \quad \left(\xi = \frac{y}{\delta}\right).$$

On substituting this expression in the right hand side of (9), we have for the determination of the first approximation, the equation:

$$\frac{\partial^2 u_1}{\partial \xi^2} = -mx^{2m}\delta^2 + \frac{x^{2m}\xi^2}{2}\left[mx^{-1}\delta^2 - \dot{\delta}\delta\right].$$



Declassified in Part - Sanitized Copy Approved for Release 2012/03/12 : CIA-RDP82-00039R000100190014-6

Declassified in Part - Sanitized Copy Approved for Release 2012/03/12 : CIA-RDP82-00039R000100190014-6

It is readily found that

$$u = u_0 + u_1 = \kappa^m \xi - \frac{m\kappa^{2m-1}\delta^2}{2}\xi^2 + \frac{\kappa^{2m}\xi^4}{24}\left[m\kappa^{-1}\delta^2 - \dot{\delta}\delta\right] + C\xi. \quad (10)$$

Arbitrary integration constant C, determined from limit conditions, is found to be equal to:

$$C = \frac{\delta\kappa^{2m}}{24}\left[\dot{\delta} + \frac{11m\delta}{\kappa}\right]$$

Thickness of boundary layer, determined from

$$\left.\frac{\partial u}{\partial \xi}\right|_{\xi=1} = 0,$$

is found to be:

$$\delta = \alpha\kappa^{\frac{1-m}{2}} \left(\alpha = \frac{4}{\sqrt{1+5m}}\right).$$

wherefrom,

$$\dot{\delta} = \frac{1-m}{2}\frac{\delta}{\kappa}.$$

From the latter expressions it follows that the solution found occurs when $m > -0.2$.

On substituting the values found for $\delta$ and $\dot{\delta}$ in (10) we have the following expression for the velocity:

$$\frac{u}{U} = \xi\left[1 - \frac{m}{2}\alpha^2(\xi-1) + \frac{\alpha^2}{48}(3m-1)(\xi^3-1)\right]$$



Declassified in Part - Sanitized Copy Approved for Release 2012/03/12 : CIA-RDP82-00039R000100190014-6

Declassified in Part - Sanitized Copy Approved for Release 2012/03/12 : CIA-RDP82-00039R000100190014-6

or,

$$\frac{u}{U} = \xi\left[1 - \frac{8m}{1+5m}(\xi - 1) + \frac{3m-1}{3(1+5m)}(\xi^3 - 1)\right].$$

On assuming in this expression $m = 0$, we obtain the solution of Blasius' problem:

$$u = \xi\left[\frac{4}{3} - \frac{1}{3}\xi^3\right]$$

Friction intensity $\tau_0$ is found to be:

$$\tau_0 = \left(\frac{\partial u}{\partial y}\right)_0 = \frac{1.333 + 12m}{4\sqrt{1+5m}}\, x^{\frac{3m-1}{2}}.$$

Table III gives values of $\tau_0$ calculated by means of this formula for various values of m, and for comparison the exact values of $\tau_0$ are also included.

It must be pointed out that solutions obtained for $m < 0$ are artificial since for negative m the velocity becomes infinite for $x = 0$.



Declassified in Part - Sanitized Copy Approved for Release 2012/03/12 : CIA-RDP82-00039R000100190014-6

Declassified in Part - Sanitized Copy Approved for Release 2012/03/12 : CIA-RDP82-00039R000100190014-6

TABLE III

| m | $\beta$ | Exact value of $\tau_0$ | $\tau_0$ Approximate |
|---|---|---|---|
| -0.074 | -0.16 | 0.130 | 0.141 |
| -0.065 | -0.14 | 0.164 | 0.167 |
| -0.048 | -0.10 | 0.220 | 0.218 |
| 0.000 | 0.00 | 0.332 | 0.333 |
| 0.053 | 0.10 | 0.426 | 0.438 |
| 0.110 | 0.20 | 0.512 | 0.534 |
| 0.176 | 0.30 | 0.594 | 0.629 |
| 0.250 | 0.40 | 0.675 | 0.723 |
| 0.333 | 0.50 | 0.758 | 0.817 |
| 0.429 | 0.60 | 0.842 | 0.913 |
| 0.667 | 0.80 | 1.022 | 1.120 |

Subsequent approximations, which we do not include here, considerably improve the results. Thus the values of $\tau_0$ derived from the second approximation do not exceed in any instance the exact values by more than 6 percent.

Liquid Motion in Laminar Boundary Layer at Linear Velocity Distribution within the External Flow.

7. This problem was studied by Howarth /5/. Howarth's method of solving it is most complex and necessitates extensive numerical computations.

The approximate solution of the problem is as follows.



Declassified in Part - Sanitized Copy Approved for Release 2012/03/12 : CIA-RDP82-00039R000100190014-6

Declassified in Part - Sanitized Copy Approved for Release 2012/03/12 : CIA-RDP82-00039R000100190014-6

If velocity distribution within the external flow is of the form

$$U' = b_0 - b_1 x .$$

Then the pressure gradient is equal to:

$$-\frac{\partial P'}{\partial x'} = \rho U' \frac{dU'}{dx'} = -b_1 (b_0 - b_1 x')\rho .$$

On introducing non-dimensional values by means of the correlations

$$x' = \frac{b_0}{b_1} x, \quad y' = \sqrt{\frac{\nu}{b_1}}\, y, \quad v' = \sqrt{\nu b_1}\, v, \quad u' = b_0 u,$$

the equations of motion, and limit conditions assume the form:

$$\frac{\partial^2 u}{\partial y^2} = (1-x) + u\frac{\partial u}{\partial x} - \frac{\partial u}{\partial y}\int_0^y \frac{\partial u}{\partial x}\, dy \qquad (11)$$

$$\left.\begin{array}{ll} \text{when } y = 0: & u = 0 \\ \text{when } y = \delta: & u = 1-x = U \end{array}\right\} \quad (12)$$

Let $\frac{y}{\delta} = \xi$. Zero approximation is found on solving equation $\frac{\partial^2 u}{\partial y} = 0$, for limit conditions (12). This approximation is of the form:

$$u = U\xi .$$

On substituting in the right hand side of (11), the value of u thus found, we have:

$$\frac{\partial^2 u}{\partial \xi^2} = U\delta^2\left[1 - \frac{\xi^2}{2}\left(1 + \frac{U\dot{\delta}}{\delta}\right)\right] . \qquad (13)$$



Declassified in Part - Sanitized Copy Approved for Release 2012/03/12 : CIA-RDP82-00039R000100190014-6

Declassified in Part - Sanitized Copy Approved for Release 2012/03/12 : CIA-RDP82-00039R000100190014-6

Wherefrom,

$$\frac{u}{U} = \xi + \delta^2 \left[ \frac{\xi^2 - \xi}{2} - \left( 1 + \frac{U\dot{\delta}}{\delta} \right) \frac{\xi^4 - \xi}{24} \right].$$

For determination of boundary layer thickness we obtain from $\left( \frac{\partial u}{\partial \xi} \right)_{\xi=1} = 0$, the equation:

$$\dot{\delta}\delta - \frac{3}{U}\delta^2 - \frac{8}{U} = 0. \qquad (14)$$

Equation (14) has an elementary solution. This solution, if one considers that when $x = 0$ the boundary layer only begins to develop, is:

$$\delta^2 = \frac{8}{3}\left[ (1-k)^{-6} - 1 \right] \qquad (15)$$

Friction intensity at the wall $\tau_0$ is equal to:

$$\tau_0 = \frac{1}{\delta}\left( \frac{\partial u}{\partial \xi} \right)\Big|_{\xi=0} = \frac{1-k}{3}\left[ \frac{4}{\delta} - \delta \right] \qquad (16)$$

For low values of $\delta$ the last two equations give:

$$\delta = 4\sqrt{k}\,; \quad \tau = \frac{0.333}{\sqrt{k}}$$

that is, we have correlations which were encountered in the problem



Declassified in Part - Sanitized Copy Approved for Release 2012/03/12 : CIA-RDP82-00039R000100190014-6

Declassified in Part - Sanitized Copy Approved for Release 2012/03/12 : CIA-RDP82-00039R000100190014-6

of flow along a plate in the absence of longitudinal pressure drop. Consequently, the solution obtained in the case of low values of x, proceeds in the same manner as that obtained by Blasius.

Reverting to expression (13), we have from (14):

$$U\dot{\delta}=3\delta+\frac{\theta}{\delta}\cdot$$

Substituting the value of $\dot{\delta}$ in (13) we obtain for the velocity an expression:

$$\frac{u}{U}=\frac{1}{3}\xi(4-\delta^2)+\frac{\xi^2}{2}\delta-\frac{\xi^4}{6}(2+\delta^2).$$

We pass to the determination of the coordinate of boundary layer separation point. As is known this coordinate is determined by condition $\left(\frac{\partial u}{\partial y}\right)_0=0.$

In the case under consideration, this condition gives $\delta^2=4$, from which the coordinate of the separation point is found to be $\kappa=0.14$ instead of the exact value $\kappa=0.12$.

Table IV gives the thickness of the boundary layer and the friction intensity for various values of x. For comparison the table also includes the values of friction intensity according to Howarth.



Declassified in Part - Sanitized Copy Approved for Release 2012/03/12 : CIA-RDP82-00039R000100190014-6

Declassified in Part - Sanitized Copy Approved for Release 2012/03/12 : CIA-RDP82-00039R000100190014-6

TABLE IV

| x | $\delta$ | $\frac{\tau_0}{1-x}$ | $\frac{\tau_0}{1-x}$ according to Howarth |
|---|---|---|---|
| 0.0125 | 0.457 | 2.764 | 2.773 |
| 0.0250 | 0.662 | 1.795 | 1.817 |
| 0.0375 | 0.829 | 1.332 | 1.360 |
| 0.0500 | 0.978 | 1.036 | 1.064 |
| 0.0625 | 1.123 | 0.813 | 0.843 |
| 0.0750 | 1.260 | 0.636 | 0.663 |
| 0.0875 | 1.399 | 0.467 | 0.503 |
| 0.1000 | 1.531 | 0.361 | 0.345 |
| 0.1125 | 1.666 | 0.245 | 0.184 |
| 0.1200 | 1.728 | 0.196 | 0.000 |

It is to be noted that the second approximation gives the value $x = 0.110$ for the coordinate of separation point.

6. Generally, equations of motion and the limit conditions are of the form:

$$u\frac{\partial u}{\partial x} - \frac{\partial u}{\partial y}\int_0^y \frac{\partial u}{\partial x}\,dy - U\frac{\partial U}{\partial x} = \frac{\partial^2 u}{\partial y^2} \qquad (17)$$

when $y = 0$: $u = 0$;

when $y = \delta$: $u = U$.



Declassified in Part - Sanitized Copy Approved for Release 2012/03/12 : CIA-RDP82-00039R000100190014-6

Declassified in Part - Sanitized Copy Approved for Release 2012/03/12 : CIA-RDP82-00039R000100190014-6

Solely on the basis of first approximation we find:

$$\frac{u}{U} = \frac{\dot{U}}{24}\delta^2(\xi^4 - 12\xi + 11\xi) - \frac{U\dot{\delta}\delta}{24}(\xi^4 - \xi) + \xi. \quad (18)$$

In order to determine thickness of boundary layer we obtain the equation

$$\frac{3}{8}\delta^2\dot{U} + \frac{U\dot{\delta}\delta}{8} = 1.$$

Assuming that when $x = 0$ $\delta = 0$, we have:

$$\delta^2 = 16U^{-6}\int_0^x U^5 dx. \quad (19)$$

Friction intensity at the wall is

$$\tau_0 = \left(\frac{\partial u}{\partial y}\right)_0 = \frac{1}{\delta}\frac{\partial u}{\partial \xi}\Big|_{\xi=0} = \frac{U}{3}\left[\frac{4}{\delta} + \delta\dot{U}\right]$$

or

$$\tau_0 = \frac{U^4}{3\sqrt{\int_0^x U^5 dx}}\left[1 + \frac{4\dot{U}}{U^6}\int_0^x U^5 dx\right] \quad (20)$$

The separation point of boundary layer (if separation takes place) we determine from



Declassified in Part - Sanitized Copy Approved for Release 2012/03/12 : CIA-RDP82-00039R000100190014-6

Declassified in Part - Sanitized Copy Approved for Release 2012/03/12 : CIA-RDP82-00039R000100190014-6

$$4\dot{U}U^{-6}\int_0^x U^5 dx = -1. \qquad (21)$$

If we introduce the parameter $\sigma = \delta^2 \dot{U}$, the velocity expression can be given the form:

$$\frac{u}{U} = \frac{\sigma}{6}\xi(\xi^3 - 3\xi + 2) - \frac{1}{3}\xi(\xi^3 - 4) \qquad (22)$$

The point of separation is given by the condition $\sigma = -4$.

Motion within Laminar Boundary Layer on a Body of Revolution

9. Let the velocity of undisturbed stream, U, be directed along the symmetry axis of the body of revolution, then liquid motion within the boundary layer of this body is characterized by:

(a) Equation of steady motion:

$$\frac{\partial^2 u}{\partial y^2} = u\frac{\partial u}{\partial x} + v\frac{\partial u}{\partial y} - U\frac{\partial U}{\partial x};$$

(b) Continuity equation:

$$\frac{\partial u}{\partial x} + \frac{\partial v}{\partial y} + \frac{u}{r_0}\frac{\partial r_0}{\partial x} = 0.$$

where x is distance from forward critical point, measured along the meridian arc on the body surface; y -- the distance along the normal to this surface; $r = r_0(x)$ -- the distance from section contour points to rotation axis of the body, the remainder of symbols being the same as before.

From the continuity equation it follows:



Declassified in Part - Sanitized Copy Approved for Release 2012/03/12 : CIA-RDP82-00039R000100190014-6

Declassified in Part - Sanitized Copy Approved for Release 2012/03/12 : CIA-RDP82-00039R000100190014-6

$$v = -\int_0^y \frac{\partial u}{\partial x}\,dy - \frac{\partial \ln r_0}{\partial x}\int_0^y u\,dy.$$

hence, the equation of motion can be written as follows:

$$u\frac{\partial u}{\partial x} - \frac{\partial u}{\partial y}\int_0^y \frac{\partial u}{\partial x}\,dy - \frac{du}{dy}\frac{\partial \ln r_0}{\partial x}\int_0^y u\,dy - U\frac{\partial U}{\partial x} = \frac{\partial^2 u}{\partial y^2},$$

Limit conditions are:

$$u = 0 \quad \text{when } y = 0;$$
$$u = U(x) \quad \text{when } y = \delta.$$

Solely on the basis of the first approximation, we have:

$$\frac{u}{U} = \xi + \delta^2\left[\frac{U}{24}(\xi^4 - \xi)\frac{\partial}{\partial x}\ln\frac{U}{\partial r_0} - \frac{\dot{U}}{2}(\xi^2 - \xi)\right] \qquad (23)$$

For determination of boundary layer thickness $\delta$, we have the ordinary linear equation:

$$1 + \delta^2\left[\frac{U}{\delta}\frac{\partial}{\partial x}\ln\frac{U}{\delta r_0} - \frac{\dot{U}}{2}\right] = 0, \qquad (24)$$

The solution of which is:

$$\delta^2 = \frac{16}{U^6 r_0^2}\left[\int_0^x U^5 r_0^2\,dx + C\right], \qquad (25)$$



Declassified in Part - Sanitized Copy Approved for Release 2012/03/12 : CIA-RDP82-00039R000100190014-6

Declassified in Part - Sanitized Copy Approved for Release 2012/03/12 : CIA-RDP82-00039R000100190014-6

where C is the integration constant, determined on the basis of condition at the critical point.

Using equation (24) we transform equation (23) to the following form:

$$\frac{u}{U} = \xi - \frac{\sigma}{2}(\xi^2 - \xi) + \frac{1}{3}\left(\frac{\sigma}{2} - 1\right)(\xi^4 - \xi) \quad (\sigma = \delta^2 \dot{U}). \quad (26)$$

## CHAPTER III

## FORCED CONVECTION IN LAMINAR BOUNDARY LAYER

10. Let us consider the problem of heat transfer in the laminar boundary layer, assuming the liquid to be incompressible and its physical constants independent of the temperature.

Disregarding heat influx due to friction and assuming the process steady, we have the thermal conductivity equation:

$$u' \frac{\partial T}{\partial x} - \frac{\partial T}{\partial y'} \int_0^{y'} \frac{\partial u'}{\partial x} dy' = \kappa \frac{\partial^2 T}{\partial y^2}. \quad (1)$$

Passing in this equation to the same non-dimensional values, as in Section 5, and introducing the non-dimensional temperature by means of correlation:

$$\theta = \frac{T_1 - T}{T_1 - T_0},$$

where $T_1$ (x) is the plate temperature, $T_0$ the temperature of liquid at boundary layer edge.

Thereafter equation (1) assumes the form:



Declassified in Part - Sanitized Copy Approved for Release 2012/03/12 : CIA-RDP82-00039R000100190014-6

Declassified in Part - Sanitized Copy Approved for Release 2012/03/12 : CIA-RDP82-00039R000100190014-6

$$u\frac{\partial\theta}{\partial x}-\frac{\partial\theta}{\partial y}\int_0^y\frac{\partial u}{\partial x}dy+u\frac{\theta-1}{T_1-T_0}\frac{\partial T_1}{\partial x}=\frac{\partial^2\theta}{\partial y^2},\qquad(1')$$

while limit conditions are:

$$\text{when } y=0:\ \theta=0;\qquad(2)$$
$$\text{when } y=\delta_*:\ \theta=1.$$

The question of velocity distribution in the boundary layer was considered in Section 9. Hence, assuming the distribution of velocities to be known, we will proceed with the solution of equation (1') by consecutive approximations, introducing into the study the thickness of temperature boundary layer $\delta_*$, and determining this thickness as that value of y at which

$$\left(\frac{\partial\theta}{\partial y}\right)_{y=\delta_*}=0.$$

Zero approximation for $\theta$ and u, which are obtained as a result of making the left-hand side of each equation (1') and (17) equal to zero, are of the form:

$$\theta=\eta\left(\eta-\frac{y}{\delta_*}\right);$$

$$u_0=U_\xi\left(\xi-\frac{y}{\delta}\right).$$

According to Section 9

$$\delta^2=16\,U^{-6}\int_0^x U^5\,dx.$$

Substituting $\theta_0$ and $u_0$ in the left hand side of equation (1')



Declassified in Part - Sanitized Copy Approved for Release 2012/03/12 : CIA-RDP82-00039R000100190014-6

Declassified in Part - Sanitized Copy Approved for Release 2012/03/12 : CIA-RDP82-00039R000100190014-6

we have

$$\frac{\partial^2\theta_1}{\partial\eta^2} = -\frac{U\delta_*^3 P_r}{2\delta}\left\{\eta^2\frac{d}{dx}\ln\frac{\delta_*^2 U}{\delta(T_1-T_0)^2} + 2\eta\frac{d}{dx}\ln(T_1-T_0)\right\}.$$

wherefrom

$$\theta = \theta_0+\theta_1 = \eta - \frac{U\delta_*^3 P_r}{2\delta}\left\{\frac{\eta^4-\eta}{12}\frac{d}{dx}\ln\frac{\delta_*^2 U}{\delta(T_1-T_0)^2} + \frac{1}{3}(\eta^3-\eta)\frac{d}{dx}\ln(T_1-T_0)\right\}. \quad (2')$$

On the basis of condition $\left(\frac{\partial\theta}{\partial\eta}\right)_{\eta=1} = 0$ we obtain for the determination of $\delta_*$ the equation:

$$\frac{d\delta_*^3}{dx} + \delta_*^3\frac{\partial}{\partial x}\left\{\ln\left[\left(\frac{U}{\delta}\right)^{3/2}(T_1-T_0)\right]\right\} = \frac{12\delta}{UP_r}.$$

If we consider that $\delta_*(0) = 0$, then the solution of this equation is:

$$\delta_*^3 = \frac{12}{P_r}\left(\frac{\delta}{U}\right)^{3/2}\frac{1}{T_1-T_0}\int_0^x\sqrt{\frac{U}{\delta}}(T_1-T_0)\,dx. \quad (3)$$

The rate of heat emission per surface unit at point x is equal to:



Declassified in Part - Sanitized Copy Approved for Release 2012/03/12 : CIA-RDP82-00039R000100190014-6

Declassified in Part - Sanitized Copy Approved for Release 2012/03/12 : CIA-RDP82-00039R000100190014-6

$$\left(\frac{\partial\theta}{\partial y}\right)_0 = \frac{1}{\delta_*}\left(\frac{\partial\theta}{\partial\eta}\right)_0 = \frac{1}{\delta_*}\left[\frac{4}{3} + \frac{U\delta_*^3 P_r}{18\delta}\frac{d}{dx}\ln(T_1 - T_0)\right]. \quad (4)$$

In an analogous manner a study can be made of heat transfer within the boundary layer of a revolving body. But in this case the square of velocity boundary layer thickness will be, in accordance with Section 10, equal to:

$$\delta^2 = \frac{16}{U^6 r_0^2}\int_0^x U^5 r_0^2\, dx.$$

11. Consider the specific instance when $U = x^m$ and $T_1 = T_0 + B x^\beta$ where $m$, $B$, $\beta$ are constants. According to (3) and (4) we have:

$$\delta_*^3 = \frac{48\alpha}{P_r[3(m+1)+4\beta]}x^{\frac{3(1-m)}{2}}\left(\alpha = \frac{4}{\sqrt{1+5m}}\right);$$

$$\left(\frac{\partial\theta}{\partial y}\right)_0 = \frac{2}{3}\left[1 + \frac{2\beta P_r}{[3(m+1)+4\beta]}\right]\sqrt[3]{\frac{3(m+1)+4\beta}{6\alpha}P_r}\, x^{\frac{m-1}{2}}. \quad (5)$$

This case was studied by Page and Feilmer /6/.

Assuming that in the boundary layer u varies in accordance



Declassified in Part - Sanitized Copy Approved for Release 2012/03/12 : CIA-RDP82-00039R000100190014-6

Declassified in Part - Sanitized Copy Approved for Release 2012/03/12 : CIA-RDP82-00039R000100190014-6

with the linear rule, they have integrated numerically the equations thus obtained for $\theta$ at Pr = 0.77 and certain values of m and $\beta$. The values of heat emission rate, thus obtained, are shown in Table V; which also includes, for comparison, the values of $\left(\frac{\partial\theta}{\partial y}\right)_0$, calculated by means of formula (5).

TABLE V

| m | $\beta$ | $\left(\frac{d\theta}{dy}\right)_0$ | |
|---|---|---|---|
| | | From Formula (5) | By Method of Fage and Falkner |
| 0 | 0.5 | 0.421 | 0.425 |
| | 0.4 | 0.397 | 0.406 |
| | 0.3 | 0.377 | 0.386 |
| | 0.2 | 0.356 | 0.369 |
| | 0.0 | 0.305 | 0.310 |
| 1 | 0.0 | 0.326 | 0.321 |

It can be assumed that values obtained by Fage and Falkner are somewhat too high.

Thus, in the case of a flat plate at constant temperature ($m = \beta = 0$) their computations give $\left(\frac{\partial\theta}{\partial y}\right)_0 = 0.310$ instead of the exact value 0.305.

As is readily apparent in the case of a flat plate at constant temperature the following correlations are obtained:



Declassified in Part - Sanitized Copy Approved for Release 2012/03/12 : CIA-RDP82-00039R000100190014-6

Declassified in Part - Sanitized Copy Approved for Release 2012/03/12 : CIA-RDP82-00039R000100190014-6

$$\theta = \frac{4}{3}\eta - \frac{1}{3}\eta^4; \left(\eta = \frac{y}{4\sqrt{\nu}\, Pr^{-\frac{1}{3}}}\right);$$

$$\left(\frac{\partial \theta}{\partial y}\right)_0 = \frac{0.333}{\sqrt{\nu}} \sqrt[3]{Pr}.$$

According to Pohlhausen /7/ for the interval $0.6 < Pr < 15.0$;

$$\left(\frac{\partial \theta}{\partial y}\right)_0 = \frac{0.332}{\sqrt{\nu}} \sqrt[3]{Pr}.$$

Thus our result differs from the accurate by 1/5 percent.

12. Results obtained in Section 11 can be transferred to diffusion problems because of the known analogy between diffusion and heat transfer processes. It is necessary, however, to differentiate one special case.

We have in mind the problem relating to diffusion near the surface from which evaporation of the liquid takes place, or which possesses the property that the substance being diffused, on reaching the surface, is absorbed or condensed.

As was shown by Nusselt /8/, at high concentrations of gas (or vapor) the velocity component perpendicular to the surface which absorbs (or vaporizes) the substance undergoing diffusion, does not become equal to zero on this surface, and consequently the analogy previously referred to no longer obtains.

According to Nusselt, the following correlation takes place on the surface.



Declassified in Part - Sanitized Copy Approved for Release 2012/03/12 : CIA-RDP82-00039R000100190014-6

Declassified in Part - Sanitized Copy Approved for Release 2012/03/12 : CIA-RDP82-00039R000100190014-6

$$v' = \frac{\kappa}{q_0'\left(\frac{p}{p_0}-1\right)}\left(\frac{\partial q'}{\partial y'}\right)_0, \qquad (6)$$

where $q'$ is the concentration of gas to which the surface is permeable; $q_0'$ -- concentration on the surface; $p_0$ -- the partial pressure of gas or vapor; $p$ -- total pressure. If evaporation takes place, then $v' > 0$; if condensation (or absorption of the gas) occurs, $v' < 0$.

We assume that the motion of the gas is of a laminar nature near the surface, and that at a distance from the surface, which for simplicity's sake we will assume to be flat, concentration and velocity of the stream are constant and equal to $q_1'$ and $U$ respectively.

The stationary diffusion process is defined by the following equations and limit conditions.

(a) equation of motion:

$$u'\frac{\partial u'}{\partial x'} + v'\frac{\partial u'}{\partial y'} = \nu\frac{\partial^2 u'}{\partial y'^2}; \qquad (7)$$

(b) continuity equation:

$$\frac{\partial u'}{\partial x'} = \frac{\partial v'}{\partial y'} = 0; \qquad (8)$$

(c) diffusion equation:

$$u'\frac{\partial q'}{\partial x'} + v\frac{\partial q'}{\partial y'} = \kappa\frac{\partial^2 q'}{\partial y'^2}; \qquad (9)$$

(d) limit conditions:

$$\left.\begin{aligned} u' = 0 \quad q' = q_0' \quad \text{when} \quad y' = 0; \\ u' = U \quad q' = q_1' \quad \text{when} \quad y' = \infty. \end{aligned}\right\} \qquad (10)$$



Declassified in Part - Sanitized Copy Approved for Release 2012/03/12 : CIA-RDP82-00039R000100190014-6

Declassified in Part - Sanitized Copy Approved for Release 2012/03/12 : CIA-RDP82-00039R000100190014-6

On introducing the non-dimensional values in accordance with formulas:

$$x' = lx,\quad y' = \frac{l}{\sqrt{Re}}y,\quad v' = \frac{U}{\sqrt{Re}}v,\quad u' = Uu,\quad c = \frac{q' - q'_0}{q'_1 - q'_0},$$

we have in lieu of (7) -- (9):

$$u\frac{\partial u}{\partial x} + v\frac{\partial u}{\partial y} = \frac{\partial^2 u}{\partial y^2}; \qquad (11)$$

$$\frac{\partial u}{\partial x} + \frac{\partial v}{\partial y} = 0; \qquad (12)$$

$$u\frac{\partial c}{\partial x} + v\frac{\partial c}{\partial y} = \frac{1}{Pr}\frac{\partial^2 c}{\partial y^2}; \qquad (13)$$

$$\left.\begin{aligned} &u = c = 0,\quad v = N'\left(\frac{\partial c}{\partial y}\right)_0 \text{ when } y = 0; \\ &\left(N' = -\frac{\kappa}{\nu}\frac{q'_1 - q'_0}{q'_0\left(\frac{\rho}{\rho_0} - 1\right)}\right); \\ &u = 1 \text{ when } y = \delta,\quad c = 1 \text{ when } y = \delta_*. \end{aligned}\right\} \qquad (14)$$

From the continuity equation, we have:

$$v = N'\left(\frac{\partial c}{\partial y}\right)_0 - \int_0^y \frac{\partial u}{\partial x}\,dy.$$

On substituting this expression in equations (11) and (13) we obtain the first approximation:

$$u = \xi + \frac{N'}{2}\beta(\xi^2 - \xi) - \frac{\delta\dot{\delta}}{24}(\xi^4 - \xi); \qquad (15)$$



Declassified in Part - Sanitized Copy Approved for Release 2012/03/12 : CIA-RDP82-00039R000100190014-6

Declassified in Part - Sanitized Copy Approved for Release 2012/03/12 : CIA-RDP82-00039R000100190014-6

$$c = \eta + \frac{N' Pr}{2}(\eta^2 - \eta) - \frac{\delta \dot{\delta}}{24}(\eta^4 - \eta), \qquad (16)$$

where

$$\xi = \frac{y}{\delta}, \quad \eta = \frac{y}{\delta_*}, \quad \beta = \frac{\delta}{\delta_*}.$$

values of $\delta$ and $\beta$ are found from conditions:

$$\left.\frac{\partial u}{\partial \xi}\right|_{\xi=1} = 1 + \frac{N'\beta}{2} - \frac{\delta \dot{\delta}}{8} = 0;$$

$$\left.\frac{\partial c}{\partial \eta}\right|_{\eta=1} = 1 + \frac{N' Pr}{2} - \frac{\delta \dot{\delta}}{8}\frac{Pr}{\beta^3} = 0.$$

Wherefrom

$$\delta = 4\sqrt{\left(1 + \frac{N'\beta}{2}\right)\varkappa},$$

and $\beta$ is found by means of the equation:

$$\frac{Pr}{\beta^3} - 1 + \frac{N' Pr}{2}\left(\frac{1}{\beta^2} - 1\right) = 0.$$

The values of $\beta$ for some values of Pr and $\Pi = N'\beta$ are shown in Table VI



Declassified in Part - Sanitized Copy Approved for Release 2012/03/12 : CIA-RDP82-00039R000100190014-6

Declassified in Part - Sanitized Copy Approved for Release 2012/03/12 : CIA-RDP82-00039R000100190014-6

TABLE VI

| Pr \ N | -1 | 0 | 1 | 2 | 3 | 4 |
|---|---|---|---|---|---|---|
| 1 | 1.00 | 1.00 | 1.00 | 1.00 | 1.00 | 1.00 |
| 2 | 2.00 | 1.26 | 1.10 | 1.16 | 1.12 | 1.08 |
| 5 | -- | 1.71 | 1.17 | 1.33 | 1.23 | 1.14 |
| 8 | -- | 2.00 | 1.20 | 1.39 | 1.26 | 1.16 |
| 10 | -- | 2.15 | 1.21 | 1.42 | 1.27 | 1.17 |

Expressions (15) and (16) can be transformed to forms:

$$u = \xi + \frac{N'\beta}{2}(\xi^2 - \xi) - \frac{1}{3}\left(1 + \frac{N'\beta}{2}\right)(\xi^4 - \xi); \qquad (15')$$

$$c = \eta + \frac{N'Pr}{2}(\eta^2 - \eta) - \frac{1}{3}\left(1 + \frac{N'Pr}{2}\right)(\eta^4 - \eta). \qquad (16')$$

It follows from (15') and (16'):

$$\left(\frac{\partial u}{\partial y}\right)_0 = \frac{4 - N'\beta}{12\sqrt{\left(1 + \frac{N'\beta}{2}\right)\kappa}};$$

$$\left(\frac{\partial c}{\partial y}\right)_0 = \frac{4 - N'Pr}{12\sqrt{\left(1 + \frac{N'\beta}{2}\right)\kappa}}\beta.$$

For $N' = 0$ we have the previously obtained results:

$$\left(\frac{\partial u}{\partial y}\right)_{y=0} = \frac{0.333}{\sqrt{\kappa}}; \quad \left(\frac{\partial c}{\partial y}\right)\Big|_0 = \frac{0.333}{\sqrt{\kappa}}\sqrt[3]{Pr}.$$

Figure 2 shows graphs of u for Pr = 1 and various $N = N'\beta$.



Declassified in Part - Sanitized Copy Approved for Release 2012/03/12 : CIA-RDP82-00039R000100190014-6

Declassified in Part - Sanitized Copy Approved for Release 2012/03/12 : CIA-RDP82-00039R000100190014-6

# ON THE THEORY OF LIGHT SCATTER IN THE ATMOSPHERE

K. S. SHIFRIN

## 1. Introduction

Propagation of electromagnetic waves in the atmosphere is accompanied by their scattering and absorption. ~~The theory of these phenomena is of great importance.~~ Since these phenomena are involved in a vast number of meteorological problems their theory is of great importance. Among these are combinations of various optical factors, and also problems relating to propagation of radio waves, long-wave terrestrial and air-gas radiations. The theory under consideration is also of great importance in its purely practical applications.

Thus its development is closely associated with those of aerial photography and searchlight utilization, the determination of limits of visual or photographic observations of remote objects, and with many other practical considerations.

Especially must be stressed the part played by optical phenomena in local forecasts of atmospheric conditions and in atmosphere sounding.

Over the hundred-year period during which the Central Geophysical Observatory has been in existence, various theoretical and practical aspects of the above-indicated problems have undergone substantial development within its walls. There could be mentioned a number of outstanding scientists -- collaborators of the Central Geophysical Observatory; but since this is not one of the purposes



Declassified in Part - Sanitized Copy Approved for Release 2012/03/12 : CIA-RDP82-00039R000100190014-6

Declassified in Part - Sanitized Copy Approved for Release 2012/03/12 : CIA-RDP82-00039R000100190014-6

of the present paper I will mention only two: P. I. Brounov and N. N. Kalitin.

The work of P. I. Brounov includes /1/ a great number of observations relative to various optical phenomena connected with weather elements.

In the numerous papers of N. N. Kalitin, a synopsis of which is given in his monograph /3/, the spectral components of radiation fluxes reaching the earth, and their geographical variations were studied. The work on the study of radiance emitted by the immediate surroundings of the sun, conducted by N. N. Kalitin /3/, shows that in accordance with the effect of G. Mie, a sharp increase in radiance intensity occurs with decreasing angle of direction toward the sun.

Study of this phenomenon makes it possible to evaluate the amount and the physical nature of atmospheric admixtures. Here we deal with a special form of optical sounding wherein the source of illumination is the sun.

In the present paper we will confine ourselves to processes the occurrence of which in the atmosphere is due to extraneous particles, that is, to admixtures, omitting those processes which take place in a pure gaseous medium. We will further limit our considerations to the problem of scatter by a single admixture particle. Strictly speaking the results thus obtained will pertain to infinitely diluted systems. It is known, however, that in a great many important problems, limiting them by taking into account scatter of the first order constitutes a good approximation of actual conditions.



Declassified in Part - Sanitized Copy Approved for Release 2012/03/12 : CIA-RDP82-00039R000100190014-6

Declassified in Part - Sanitized Copy Approved for Release 2012/03/12 : CIA-RDP82-00039R000100190014-6

The problem of electromagnetic waves scattered by a sphere of arbitrary radius a, the electric properties of which are characterized by macroscopic constants $\epsilon$, $\mu$, $\sigma$ ($\epsilon$ is the dielectric constant, $\mu$ -- magnetic permeability, $\sigma$ -- electric conductivity), was fully solved by G. Mie /11/. The solution of G. Mie, however, is impaired by two material defects. First, it is most cumbersome, especially in the case of large spheres, and second, the method utilized by G. Mie cannot be expanded to apply to particles of irregular shape.

The cumbrous formulas given by G. Mie have compelled a number of investigators to seek other, even though approximate, solutions to the same problem. Here should be mentioned the work of Rocard /12/ who obtained a simple formula for the intensity of scattered light by assuming that the field within the light-scattering particle coincides with the external field.

To support such an assumption Rocard refers to the theoretical studies of Mallemann /13/ who in the opinion of Rocard has proved that the electric field within the sphere does coincide with the external field.

Actually, however, in his two notes Mallemann merely shows that in a static case the effective field, acting upon the molecules within the sphere, coincides with the external field. This, generally speaking, correct assertion (see below, paragraph 6) can by no means be applied to the case of a field dependent on time. Insofar as the static field is concerned, where Rocard's assumption is correct, it corresponds in our problem to the instance where dimensions of the particle are infinitely small in comparison with the wave length



Declassified in Part - Sanitized Copy Approved for Release 2012/03/12 : CIA-RDP82-00039R000100190014-6

Declassified in Part - Sanitized Copy Approved for Release 2012/03/12 : CIA-RDP82-00039R000100190014-6

( $\frac{a}{\lambda} = 0$ ) (In this case the field hardly changes over the length of the particle, that is, we can consider the particle as being located in a constant field which oscillates periodically in time.), in which case we have the solution of Rayleigh.

But applying Rayleigh's solution to a case where $\frac{a}{\lambda} \neq 0$ has physically no foundation, and the solution of Rocard, in the form published by him, is incorrect.

Here we propose a new method for the solution of the problem of light scattering by the admixture particle. Similar to the method utilized by G. Mie, the new method makes it possible, in principle, to obtain an accurate solution of the problem. Essentially it consists in formulating the problem as a system of integral equations in lieu of seeking the solution of a system of differential equations. Such a substitution is found to be rational because in so doing it becomes apparent that solution of the problem is essentially dependent upon a certain parameter, which in a number of cases -- important under conditions prevailing in the atmosphere and hydrosphere -- is found to be small. It is natural that in such cases the scattered field is sought for in the form of a series of this small parameter. This makes it possible to obtain, fairly simply, the solution for spheric particles, and, what is of special importance, the new method can be readily applied to particles of arbitrary form.

In the paper published previously, we have already applied this method to rod-like and disk-shaped particles /4/. In the present article we present derivations of formulas referred to in our preliminary communication /5/, and study the solution of the



Declassified in Part - Sanitized Copy Approved for Release 2012/03/12 : CIA-RDP82-00039R000100190014-6

Declassified in Part - Sanitized Copy Approved for Release 2012/03/12 : CIA-RDP82-00039R000100190014-6

of the problem in the case of a sphere, the dimensions of which are commensurate with the wave length of light. We will show that the formula obtained by Rocard is a correct first approximation of the solution of the problem, and we will evaluate the range of its applicability. We will also calculate the subsequent approximations.

In order to characterize the method fully, we will also present here a number of results from the paper /4/ pertaining to non-spherical particles.

## 2. STATEMENT OF THE PROBLEM -- DERIVATION OF THE PRIMARY INTEGRAL EQUATION

If a plane-polarized, monochromatic, electromagnetic wave $\vec{E} = \vec{E}_0 e^{i(\vec{\varkappa}\vec{r} - \omega t)}$ strikes the particle, the field within and outside the particle will satisfy Maxwell's equations, which in the case of non-magnetic bodies (magnetic permeability equal to one) and in the absence of free charges are of the form:

$$\operatorname{div}\vec{D} = 0;$$

$$\operatorname{div}\vec{H} = 0;$$

$$\operatorname{rot}\vec{E} + \frac{1}{c}\frac{\partial \vec{H}}{\partial t} = 0;$$

$$\operatorname{rot}\vec{H} - \frac{1}{c}\frac{\partial \vec{D}}{\partial t} = \frac{4\pi}{c}\vec{j}.$$

Introducing, in the usual manner, linear correlations between fields, inductions, and current, we have:



Declassified in Part - Sanitized Copy Approved for Release 2012/03/12 : CIA-RDP82-00039R000100190014-6

Declassified in Part - Sanitized Copy Approved for Release 2012/03/12 : CIA-RDP82-00039R000100190014-6

$$\vec{D} = \epsilon \vec{E} = \vec{E} + 4\pi \vec{P}; \quad P = \kappa \vec{E};$$

$$\vec{j} = \sigma \vec{E}.$$

It should be noted that in the general case the dielectric constant $\epsilon$ and electrical conductivity $\sigma$ are functions of frequencies. They may also assume complex values.

We will try to find the solution of the problem in the form of periodical functions of time

$$\vec{E} = \vec{E}(\vec{r}) e^{-i\omega t}, \quad \vec{H} = \vec{H}(\vec{r}) e^{-i\omega t}.$$

We introduce the electromagnetic potentials $\vec{A}$ and $\varphi$ in accordance with formulas:

$$\vec{H} = \operatorname{rot} \vec{A};$$

$$\vec{E} = -\nabla \varphi - \frac{1}{c} \frac{\partial \vec{A}}{\partial t} = -\nabla \varphi + \frac{i\omega}{c} \vec{A}.$$

As is known, the four Maxwell equations are now reduced to the following two equations of potentials:

$$\Delta \vec{A} + \frac{\omega^2}{c^2} \vec{A} = +i\omega \frac{4\pi}{c} \vec{I};$$

$$\Delta \varphi + \frac{\omega^2}{c^2} \varphi = 4\pi \operatorname{div} \vec{I},$$

where

$$\vec{I} = \kappa \vec{E}, \quad \text{and} \quad \kappa = \frac{\epsilon - 1}{4\pi} + i \frac{\sigma}{\omega}.$$



Declassified in Part - Sanitized Copy Approved for Release 2012/03/12 : CIA-RDP82-00039R000100190014-6

Declassified in Part - Sanitized Copy Approved for Release 2012/03/12 : CIA-RDP82-00039R000100190014-6

The potentials $\vec{A}$ and $\varphi$ are also correlated by the calibration equation

$$\operatorname{div}\vec{A} - \frac{i\omega}{c}\varphi = 0.$$

The last equation permits us to pass to a single unknown vector function $\vec{z}$ -- Hertz's vector. Assuming,

$$\vec{A} = -\frac{i\omega}{c}\vec{z};$$

$$\varphi = -\operatorname{div}\vec{z},$$

we find that Hertz's vector satisfies the equation:

$$\Delta\vec{z} + \frac{\omega^2}{c^2}\vec{z} = -4\pi\vec{I}.$$

Solution of the last equation, which decreases sufficiently rapidly at infinity, is, as known:

$$\vec{z}(\vec{r}) = \int \frac{\vec{I}(\vec{r}')e^{\frac{i\omega}{c}R}}{R}\,dv'.$$

Here $R = |\vec{r} - \vec{r}'|$ is the distance between point of observation and the location point of the source (volume element of particle polarized by electromagnetic wave). Integration is effected over the entire volume occupied by the sources (over the entire particle).

Electrical and magnetic field are expressed by means of Hertz's vector in the following manner.

$$\vec{H} = -\frac{i\omega}{c}\operatorname{rot}\vec{z};$$

$$\vec{E} = \nabla\operatorname{div}\vec{z} + \frac{\omega^2}{c^2}\vec{z}.$$

Using the above-indicated formulas we obtain readily from the last equation, for the electrical field created by the polarized volume elements:



Declassified in Part - Sanitized Copy Approved for Release 2012/03/12 : CIA-RDP82-00039R000100190014-6

Declassified in Part - Sanitized Copy Approved for Release 2012/03/12 : CIA-RDP82-00039R000100190014-6

$$\vec{E}(\vec{r}) = rot\ rot \int \frac{\vec{I}(\vec{r}')e^{ikR}}{R} dv - 4\pi \vec{I}(\vec{r}).$$

For the whole electrical field, outside as well as within the sphere, we obtain the following integral equation:

$$\vec{E}(\vec{r}) = \vec{E}_0 e^{i\vec{k}\vec{r}} + rot\ rot \int \frac{\kappa(\vec{r}')\vec{E}(\vec{r}')e^{ikR}}{R} dv' - \qquad (1)$$

$$- 4\pi\kappa(\vec{r})\vec{E}(\vec{r}).$$

We will determine the electrical field as the solution of this integral equation. Its physical meaning is very simple. It is known that an electric field created by a dipole of moment $\vec{p}$ at a point located at a distance R from the dipole, is:

$$\vec{E} = rot\ rot \frac{\vec{p}}{R}.$$

$\kappa \vec{E} dv'$ is the dipole moment of the volume element polarized by the electromagnetic wave. Thus, according to equation (1) the electric field at some point of space is the sum of the field created by external bodies (sources of light) $\vec{E}_0 e^{i\vec{k}\vec{r}}$, the field of polarized particle elements

$$\int rot\ rot \frac{\kappa \vec{E} e^{ikR}}{R} dv'$$

(The multiplier $e^{ikR}$ is due to lag)

and the field of screening (assumed) charges on the surface of the particle: $- 4\pi\kappa\vec{E}$.



Declassified in Part - Sanitized Copy Approved for Release 2012/03/12 : CIA-RDP82-00039R000100190014-6

Declassified in Part - Sanitized Copy Approved for Release 2012/03/12 : CIA-RDP82-00039R000100190014-6

We obtained integral equation (1) as a result of Maxwell's differential equations. Actually, however, it is not a result of these equations. It may be considered as directly derived from experiment, in a manner similar to that we have used in connection with Maxwell's equations.

In solving differential equations it is necessary to satisfy, in addition to the equations, the limit conditions as well. On surfaces of discontinuity of electrical constants these conditions require that for all volume elements, even those comprising areas of such surfaces of electric constants discontinuity, the equations of Maxwell must be satisfied. At infinity the field must satisfy the radiation principle.

In the solution of such integral equations the corresponding prerequisites are automatically satisfied. In our case, for example, we have already found that the electric field is a superposition of the external field and the fields of dipoles which fill up the scattering particle. Since each member of this sum satisfies Maxwell's equations throughout, the sum also satisfies them everywhere. Insofar as radiation principle is concerned it is provided for by utilization of lagging potentials.

In view of considerations which will be made apparent hereinafter (see paragraph 6), in lieu of the differential equation (1), for the mean electric field, it is more convenient to study the integral equation derived therefrom for the effective electric field $\vec{E}_{eff}$. The latter we introduce in accordance with formula:



Declassified in Part - Sanitized Copy Approved for Release 2012/03/12 : CIA-RDP82-00039R000100190014-6

Declassified in Part - Sanitized Copy Approved for Release 2012/03/12 : CIA-RDP82-00039R000100190014-6

$$\vec{E}_{eff} = \vec{E} + \frac{4\pi}{3}\vec{I} = \vec{E}\left(1 + \frac{4\pi}{3}\chi\right).$$

wherefrom we readily obtain also.

$$\vec{I} = \alpha E_{eff},$$

where

$$\alpha = \frac{\chi}{1 + \frac{4\pi}{3}\chi}, \qquad (2)$$

while

$$\chi = \frac{\epsilon - 1}{4\pi} + i\frac{\sigma}{\omega}; \qquad (3)$$

$$\vec{E}_{eff}(\vec{r}) = \vec{E}_0 e^{i\vec{\kappa}\vec{r}} + \alpha\, rot\, rot \int \vec{E}_{eff}(\vec{r}') \frac{e^{i\kappa R}}{R} d\omega' - \frac{8\pi}{3}\alpha \vec{E}_{eff}. \qquad (4)$$

Equation (4) is the very basic equation of our problem. We note that outside of the particle the effective field coincides with the mean field.

## 3. PARAMETER OF SMALLNESS; CONSECUTIVE APPROXIMATIONS OF THE SOLUTION

Parameter $\alpha$ which appears in integral equation (4), is actually a very small quantity in all cases of practical interest. In Table I we show the values of modulus $\alpha$ for various substances; it being understood that the dielectric constant as well as electric conductivity comprises only their electronic portion.



Declassified in Part - Sanitized Copy Approved for Release 2012/03/12 : CIA-RDP82-00039R000100190014-6

Declassified in Part - Sanitized Copy Approved for Release 2012/03/12 : CIA-RDP82-00039R000100190014-6

TABLE I

Electric Properties of Admixtures

| | In Atmosphere | | | |
|---|---|---|---|---|
| | $\epsilon = n^2$ | $\frac{\epsilon - 1}{4\pi}$ | $\sigma$ | $\alpha$ |
| Water | 1.77 | 0.061 | 0 | 0.048 |
| Ice | 1.71 | 0.056 | 0 | 0.045 |
| HCl | 1.56 | 0.044 | 0 | 0.037 |
| | In Hydrosphere | | | |
| Air | 0.56 | 0.35 | 0 | 0.030 |

The ionic portion of conductivity and constant dipole moments of the molecules are omitted from consideration, since neither ions nor, so much the more, molecules will be able to follow oscillations of the rapidly alternating field of the light wave.

In addition to water, ice, droplets of various ionic solutions (the table shows hydrochloic acid as one such solution), solid dust particles are encountered in the atmosphere. The refractive index of the latter is usually unknown. Assuming that in this case $\left|\frac{n^2 - 1}{4\pi}\right| \ll 1$, in this instance also $\alpha$ will be much smaller than one, since the electronic conductivity of such particles is usually less than $10\ \Omega^{-1}\ cm^{-1}$ (semi-conductors), and $\frac{\sigma}{\omega} < 10^{-2}$, for $\omega \cong 10^{15}\ \frac{1}{sec.}$. The same applies to smoke particles.

Let us find the solution of integral equation (4) as a series of $\alpha$. Assuming

$$\vec{E}_{eff} = \vec{E}^{(0)}_{eff} + \alpha \vec{E}^{(1)}_{eff} + \alpha^2 \vec{E}^{(2)}_{eff} + \cdots \qquad (5)$$



Declassified in Part - Sanitized Copy Approved for Release 2012/03/12 : CIA-RDP82-00039R000100190014-6

Declassified in Part - Sanitized Copy Approved for Release 2012/03/12 : CIA-RDP82-00039R000100190014-6

From equation (4) we thus have:

$$\vec{E}_{eff}^{(0)} = E_0 e^{i\vec{\kappa}\vec{r}}; \qquad (6)$$

$$\vec{E}_{eff}^{(1)} = rot\ rot \int \vec{E}_0 \frac{e^{i(\kappa R + \vec{\kappa}\vec{r}')}}{R} dv' - \frac{8\pi}{3}\vec{E}_0 e^{i\vec{\kappa}\vec{r}}; \qquad (7)$$

$$\vec{E}_{eff}^{(2)} = rot\ rot \int \vec{E}_{eff}^{(1)} \frac{e^{i\kappa R}}{R} dv' - \frac{8\pi}{3}\vec{E}_{eff}^{(1)} \qquad (8)$$

and so forth.

If we have $\vec{E}_{eff}$ we can determine also the mean electric field $\vec{E}$, and then the magnetic field $\vec{H}$.

It is apparent that the magnetic field as well will be obtained as a series of $\alpha$:

$$\vec{H} = \vec{H}^0 + \alpha\vec{H}^{(1)} + \alpha\vec{H}^{(2)} + \cdots \qquad (9)$$

For $\vec{H}^{(i)}$ we have:

$$\vec{H}^{(i)} = \frac{1}{i\kappa} rot\, \vec{E}^{(i)}. \qquad (10)$$

Integral equation (4) determines $\vec{E}_{eff}$ within the entire space, that is outside as well as inside the sphere. In the latter case the equation can be simplified, since the field outside the sphere is usually measured at distances considerably in excess of the sphere radius $(R \gg a)$. In general, on differentiating in equation (4) with respect to the parameter, we have:



Declassified in Part - Sanitized Copy Approved for Release 2012/03/12 : CIA-RDP82-00039R000100190014-6

Declassified in Part - Sanitized Copy Approved for Release 2012/03/12 : CIA-RDP82-00039R000100190014-6

$$rot\ rot \int \vec{E}_{eff} \frac{e^{i\varkappa R}}{R} dv' = \int \vec{E}_{eff}\ rot\ rot \frac{e^{i\varkappa R}}{R} dv' =$$

$$= \int \left\{ \frac{3\vec{R}_0(\vec{R}_0\vec{E}_{eff}) - \vec{E}_{eff}}{R^3} - i\varkappa \frac{3\vec{R}_0(\vec{R}_0\vec{E}_{eff}) - \vec{E}_{eff}}{R^2} - \varkappa^2 \frac{\vec{R}_0(\vec{R}_0\vec{E}_{eff}) - \vec{E}_{eff}}{R} \right\} e^{i\varkappa R} dv'.$$

Here $\vec{R}_0$ is a unitary vector, directed from source ( $\vec{r}'$ ) to observation point ( $\vec{r}$ ). At large R values ( $R \gg a$ ), disregarding members containing $R^3$ and $R^2$ in the denominator, we have for the field of scattered wave:

$$\vec{E}_{scat.} = \frac{-\alpha\varkappa^2}{r_0} \int \left\{ \vec{R}_0(\vec{R}_0\vec{E}_{eff}) - \vec{E}_{eff} \right\} e^{i\varkappa R} dv. \quad (11)$$

In so doing we have taken outside the sign of integration the slowly changing factor $\frac{1}{R}$ at its mean value $\frac{1}{r_0}$ ($r_0$ is the distance from observation point to the center of the sphere).

The scattered wave field is also given as a series of $\alpha$ .

$$\vec{E}_{scat.} = \vec{E}^{0}_{scat.} + \alpha\vec{E}^{(1)}_{scat.} + \alpha^2\vec{E}^{(2)}_{scat.} + \cdots \quad (12)$$

Naturally, in the resolution $\vec{E}_{scat}$ the zero member, that is $\vec{E}^{0}_{scat.} = 0$ must be absent. (More precisely what we are measuring in the form of scattered wave field is $\vec{E}_{scat} - \vec{E}^{0}_{scat.}$ ).

In accordance with formulas (5) and (11) we have:



Declassified in Part - Sanitized Copy Approved for Release 2012/03/12 : CIA-RDP82-00039R000100190014-6

Declassified in Part - Sanitized Copy Approved for Release 2012/03/12 : CIA-RDP82-00039R000100190014-6

$$\vec{E}^{(1)}_{scat.} = -\frac{\kappa^2}{r_0}\int\left\{\vec{R}_0(\vec{R}_0\vec{E}^{0}_{eff}) - \vec{E}^{0}_{eff}\right\} e^{i\kappa R}\, dv'; \qquad (13)$$

$$\vec{E}^{(2)}_{scat} = -\frac{\kappa^2}{r_0}\int\left\{\vec{R}_0(\vec{R}_0\vec{E}^{(1)}_{eff}) - \vec{E}^{(1)}_{eff}\right\} e^{i\kappa R}\, dv' \qquad (14)$$

and so forth.

On final analysis we are here interested in the components of scattered field along the spherical axes $\theta$ and $\varphi$. Thus the first member of expressions $\vec{E}^{(i)}_{scat.}$, containing $\vec{R}_0$ naturally is eliminated.

Let us denote by $\vec{i}_\theta$ and $\vec{i}_\varphi$ the unitary vectors of axes $\theta$ and $\varphi$ of the spherical system of coordinates. For the projections of the scattered field on these axes we have:

$$E_{scat\,\theta} = (\vec{E}_{scat}\,\vec{i}_\theta) = \alpha\frac{\kappa^2}{r_0}\int(\vec{E}_{eff}\,\vec{i}_\theta)e^{i\kappa R}\,dv = \frac{\alpha\kappa^2}{r_0}(\vec{A},\vec{i}_\theta); \qquad (15)$$

$$E_{scat\,\varphi} = (\vec{E}_{scat}\,\vec{i}_\varphi) = \alpha\frac{\kappa^2}{r_0}\int(\vec{E}_{eff}\,\vec{i}_\varphi)e^{i\kappa R}\,dv = \frac{\alpha\kappa^2}{r_0}(\vec{A},\vec{i}_\varphi). \qquad (16)$$

Here $\vec{A}$ designates the following vector:

$$\vec{A} = \int\vec{E}_{eff}\,e^{i\kappa R}\,dv. \qquad (17)$$

It is apparent that vector $\vec{A}$ can also be formulated as a series of $\alpha$, analogous to the series of $\vec{E}_{eff}$.

$$\vec{A} = \vec{A}^{(0)} + \alpha\vec{A}^{(1)} + \alpha^2\vec{A}^{(2)} + \cdots \qquad (18)$$

It is clear without further calculations, that smallness of $\alpha$ is insufficient for convergence of the formulated series here.



Declassified in Part - Sanitized Copy Approved for Release 2012/03/12 : CIA-RDP82-00039R000100190014-6

Declassified in Part - Sanitized Copy Approved for Release 2012/03/12 : CIA-RDP82-00039R000100190014-6

Smallness of $\alpha$ is physically due to the fact that the external field excites small electric moments in the molecules. The field created by the molecules, however, will be small only when the number of the molecules is sufficiently small. Therefore in the case of large spheres, the series given above can diverge. This divergence will occur the more belatedly, the lesser is the value of $\alpha$. In view of the above-indicated small value of $\alpha$, it can be assumed that the application range of the proposed method will be found to be sufficiently large.

## 4. FIRST APPROXIMATION FOR FIELD SCATTERED BY A SPHERE

### a. Effective Field Within the Sphere

To calculate the first approximation of the scattered field, we must take zero approximation for the effective field.

By assuming

$$\vec{E}_{eff} = \vec{E}_0 e^{i(\vec{\kappa}\vec{r} - \omega t)}, \tag{19}$$

that is, to the field of incident wave.

### b. Scattered Field

According to (13) we have

$$\vec{E}_p^{(1)} = + \frac{\kappa^2}{r_0} \vec{E}_{0\perp} f'(\beta). \tag{20}$$

Here,

$$\vec{E}_{0\perp} = \vec{E}_0 - \vec{R}_0 (\vec{R}_0 \vec{E}_0) \tag{21}$$

is the component amplitude of the incident field in the direction



Declassified in Part - Sanitized Copy Approved for Release 2012/03/12 : CIA-RDP82-00039R000100190014-6

Declassified in Part - Sanitized Copy Approved for Release 2012/03/12 : CIA-RDP82-00039R000100190014-6

perpendicular to $\vec{\mathcal{R}}_0$ in the plane of vectors $\vec{E}_0$ and $\vec{\mathcal{R}}_0$ .

Further

$$f'(\beta) = \int e^{i(\vec{\varkappa}\vec{r}' + \varkappa R)} dv' \qquad (22)$$

By $\beta$ we denote, here and thereafter, the dispersion angle;
$\beta = (\vec{\varkappa}, \widehat{\ } \vec{\mathcal{R}}_0)$.

Vector $\vec{A}$ in this approximation is,

$$\vec{A}_0 = \vec{E}_0 f'(\beta) \qquad (23)$$

reverting to determination of the integral representing function $f'(\beta)$.

We note that the function in $f'(\beta)$, within the sign of integration, is dependent only on two vectors: $\vec{\varkappa}$ and $\vec{\mathcal{R}}_0$ . Extending the coordinate plane xz through the plane of vectors $\vec{\varkappa}$ and $\vec{\mathcal{R}}_0$, and selecting axis X so that it divides angle $(\vec{\varkappa}, \vec{\mathcal{R}}_0) = \beta$ into two equal parts (Figure 1), we have:

$$\vec{\varkappa}\vec{r}' + \varkappa R = \varkappa_x X + \varkappa_z Z + \varkappa R .$$

R is the distance from the variable point of sphere M to the infinitely remote point of observation, located in the direction $\vec{\mathcal{R}}_0 = \frac{\vec{\mathcal{R}}}{\mathcal{R}}$ .

From Figure 1 it is apparent that

$$R = r_0 - d$$

where $r_0$ is the distance from the observation point to the center of the sphere, while d is the distance from point M to the plane, passing through the center of the sphere, perpendicularly to $\vec{\mathcal{R}}_0$ (plane AA).



Declassified in Part - Sanitized Copy Approved for Release 2012/03/12 : CIA-RDP82-00039R000100190014-6

Declassified in Part - Sanitized Copy Approved for Release 2012/03/12 : CIA-RDP82-00039R000100190014-6

The equation of this plane surface is:

$$xR_{0x} + zR_{0z} = 0$$

and consequently

$$d = xR_{0x} + zR_{0z} .$$

It is readily apparent that

$$R_{0x} = \cos\frac{\beta}{2}; \quad R_{0z} = -\sin\frac{\beta}{2}; \quad \varkappa_x = \varkappa\cos\frac{\beta}{2}; \quad \varkappa_z = \varkappa\sin\frac{\beta}{2} .$$

Therefore,

$$\vec{\varkappa}\vec{r} + \varkappa R = \varkappa\left(R_0 + x\cos\frac{\beta}{2} + z\sin\frac{\beta}{2} - x\cos\frac{\beta}{2} + \right.$$

$$\left. + z\sin\frac{\beta}{2}\right) = \varkappa\left(R_0 + 2z\sin\frac{\beta}{2}\right) .$$

We now have for f' ( $\beta$ ):

$$f'(\beta) = \int e^{i\varkappa\left(r_0 + 2z\sin\frac{\beta}{2}\right)}\, dx\, dy\, dz = \int_{-a}^{+a} \pi(a^2 - z^2)\, e^{i\varkappa r_0} \cdot e^{i\varkappa 2z\cdot\sin\frac{\beta}{2}}\, dz .$$

Integrating with respect to z, we have:

$$f'(\beta) = e^{i\varkappa r_0} v \frac{3}{q^3}\left\{\sin q - q\cos q\right\} \qquad (24)$$

where

$$q = 2a\varkappa\sin\frac{\beta}{2} . \qquad (25)$$

$v = \frac{4}{3}\pi a^3$ is the volume of the sphere.

Finally, sphere-scattered field at first approximation is:



Declassified in Part - Sanitized Copy Approved for Release 2012/03/12 : CIA-RDP82-00039R000100190014-6

Declassified in Part - Sanitized Copy Approved for Release 2012/03/12 : CIA-RDP82-00039R000100190014-6

$$\vec{E}_{scat} = \alpha \frac{4\pi^2}{\lambda^2 r_0} \cdot v e^{i(\kappa r_0 - \omega t)} \vec{E}_{\perp} f(q), \qquad (26)$$

whereby f (q) we denote the quantity:

(27)

For computation it is expedient to keep in mind that

$$f(q) = \frac{3}{q^{3/2}} \sqrt{\frac{\pi}{2}} J_{3/2}(q), \qquad (28)$$

where $J_{3/2}$ is Bessel's function of the order 3/2. The values of this function usually given in tables are not sufficient in our case. For our purposes the values $J_{3/2}$ from 0 to 10, at 0.02 intervals, have been calculated by utilizing the known recurrent correlation $J_{3/2} = \frac{1}{\chi} J_{1/2} - J_{-1/2}$. Also, we have used the particular values of $J_{1/2}$ and $J_{-1/2}$ given in /6/. Using the $J_{3/2}$ table we prepared a table of function f (q), for q from 0 to 10, at 0.02 intervals, and from 10 to 40 at intervals of 1. This table appears below.

Graph of function f (q) is shown in Figure 2. At small values of q it is convenient approximately to replace f (q) by a polynomial. To do this we note that on the basis of the $J_{3/2}$ (q) series it can be readily shown that f (q) can be represented as the following series:

$$f(q) = 3 \sum_{k=0}^{\infty} (-1)^k \frac{(q^2)^k}{k!\, 2^k (2k+3)!!} = 1 - \frac{q^2}{10} + \frac{q^4}{280} - \frac{q^6}{15120} + \cdots \qquad (29)$$

when $a\kappa \leqslant 1$, q is $\leqslant 2$. Thus within an error not exceeding 6 percent we have



Declassified in Part - Sanitized Copy Approved for Release 2012/03/12 : CIA-RDP82-00039R000100190014-6

Declassified in Part - Sanitized Copy Approved for Release 2012/03/12 : CIA-RDP82-00039R000100190014-6

$$f(q) = 1 - \frac{q^2}{10}. \qquad (30)$$

For high q values we have, approximately:

$$f(q) = -\frac{3}{q^2}\cos q \qquad (31)$$

This formula adequately defines f (q) anywhere except at those points where cos q = 0. Here the formula yields the highest error (the relative error being equal to 1). Its absolute value is $\sim \frac{3}{q^3}$.

In the case of very small spheres $q \ll 1, f(q) \cong 1$, and formula (26) becomes the formula given by Rayleigh.

c. Indicatrix of Scatter

Indicatrix of scatter denotes the flux of scattered energy per unit of solid angle in the given direction. The energy flux through section $\Delta S$ perpendicular to $\vec{R}_0$ is $\vec{P}\Delta S$, where $\vec{P}$ is the vector of Poynting-Umov:

$$\vec{P} = \frac{cE^2}{4\pi}\vec{R}_0$$

Section $\Delta S$ spans solid angle $\Delta\omega = \frac{\Delta S}{r_0^2}$. Thus, $\Delta S = r_0^2 \Delta\omega$ and we have for the indicatrix of scatter I:

$$I = \frac{P\Delta S}{\Delta\omega} = \frac{cE^2}{4\pi} r_0^2. \qquad (32)$$

In the case of scattering of linearly polarized light, we have from formula (26):

$$I_1 = I_0 |\alpha|^2 \frac{16\pi^4}{\lambda^4} v^2 (1 - \sin^2\beta \cos^2\varphi) f^2(q). \qquad (33)$$

Here, $I_0 = \frac{cE_0^2}{4\pi}$ is the vector of Poynting-Umov (intensity) of



Declassified in Part - Sanitized Copy Approved for Release 2012/03/12 : CIA-RDP82-00039R000100190014-6

Declassified in Part - Sanitized Copy Approved for Release 2012/03/12 : CIA-RDP82-00039R000100190014-6

incident radiation; $\varphi$ the angle between direction of polarization ( $\vec{E}_0$ ) and projection of $\vec{R}_0$ , on a plane perpendicular to $\vec{\kappa}$ (Figure 3).

Factor $(1 - \sin^2\beta \cos^2\varphi)$ appears in I because of $E_{0\perp}^2$, since

$$E_\perp^2 = E_0^2(1 - \sin^2\beta\cos^2\varphi).$$

Because of the smallness of $\alpha$ we have

$$|\alpha|^2 \simeq |\kappa|^2 \cong \kappa^2 + \frac{\sigma^2}{\omega^2}.$$

It is pointed out that in the case of bodies in which electric conductivity plays a more important part than polarization, that is if $\frac{\sigma}{\omega} \gg \kappa$ , we have $I_1 \sim \frac{1}{\lambda^2}$ , and not $\sim \frac{1}{\lambda^4}$ as usually.

To formula (33) corresponds the following distribution of scattered light within different planes.

1. In the plane perpendicular to the direction of incident ray, that is, at $\beta = 90^\circ$ :

$$I_1 \infty \sin^2\varphi f^2(q_0),$$

where

$$q_0 = \frac{2\sqrt{2}\pi a}{\lambda}$$

2. In the plane formed by the direction of incident ray and the magnetic vector, that is, with $\varphi = 90^\circ$ ,

$$I_1 \infty f^2(q).$$



Declassified in Part - Sanitized Copy Approved for Release 2012/03/12 : CIA-RDP82-00039R000100190014-6

Declassified in Part - Sanitized Copy Approved for Release 2012/03/12 : CIA-RDP82-00039R000100190014-6

3. In the plane formed by the incident ray and the electric vector ( $\varphi = 0$, or $\pi$ ):

$$I_1 \infty \cos^2\beta f^2(q).$$

Scatter indicatrix of natural light, obviously is obtained from (33) by averaging with respect to $\varphi$ . On so doing we have:

$$I_1 = I_0 |a|^2 \frac{16\pi^4}{\lambda^4} v^2 \left(\frac{1+\cos^2\beta}{2}\right) f^2(q). \qquad (34)$$

After averaging, planes 2 and 3 obviously coincide, and we have a distribution of natural scattered light intensity as follows:

a. In a plane perpendicular to the direction of incident ray:

$$I_1 \infty \frac{1}{2} f^2(q_0) \text{ circumference};$$

b. In any plane passing through the direction of incident ray:

$$I_1 \infty \left(\frac{1+\cos^2\beta}{2}\right) f^2(q).$$

With spheres the dimensions of which are commensurate with the wave length, that is, in the case of [redacted] $xa \leq 1$ , on replacing f (q) by its approximate expression (30), we obtain the following approximate formula of scattered intensity:

$$I_1 = I_0 |\alpha|^2 \frac{16\pi^4 v^2}{\lambda^4} \left(\frac{1+\cos^2\beta}{2}\right) \left[1 - \frac{4}{5}(ax)^2 \sin^2\frac{\beta}{2} + \frac{4}{25}(ax)^4 \sin^4\frac{\beta}{2}\right]. \qquad (35)$$

when $ak \leq 1$, $I_1$ calculated on the basis of this formula, diverges from values of $I_1$ obtained by means of formula (34) by not more than 8 percent.



Declassified in Part - Sanitized Copy Approved for Release 2012/03/12 : CIA-RDP82-00039R000100190014-6

Declassified in Part - Sanitized Copy Approved for Release 2012/03/12 : CIA-RDP82-00039R000100190014-6

To illustrate the formulas derived, we have plotted, in accordance therewith, the indicatrixes for each of the following four cases.

$$1)\ \frac{2\pi a}{\lambda} = 0.4;\quad 2)\ \frac{2\pi a}{\lambda} = 0.8;\quad 3)\ \frac{2\pi a}{\lambda} = 1.6;\quad 4)\ \frac{2\pi a}{\lambda} = 4.$$

Each of these indicatrixes, not to scale, are shown in Figure 4.

From Figure 4 it is apparent that with increasing dimensions of the particle the portion of light scattered onward increases sharply.

d. Polarization

The degree of polarization of scattered light is given by the formula:

$$p = \frac{I_\perp - I_\parallel}{I_\perp + I_\parallel} = \frac{I_\perp - I_\parallel}{I} \qquad (36)$$

where $I_\perp$ and $I_\parallel$, respectively, are the intensities of the perpendicular and parallel plane sight components of scattered light, and I is the total intensity. For the scattering of natural light we readily obtain from formula (35):

$$p_1 = \frac{\sin^2\beta}{1+\cos^2\beta}. \qquad (37)$$

Thus in the first approximation polarization of scattered light is that of Rayleigh.

e. Coefficient of Scatter

Scatter coefficient, referring to a single particle, is equal to the full amount of energy scattered by the particle (in parts of



Declassified in Part - Sanitized Copy Approved for Release 2012/03/12 : CIA-RDP82-00039R000100190014-6

Declassified in Part - Sanitized Copy Approved for Release 2012/03/12 : CIA-RDP82-00039R000100190014-6

incident flux). To determine it one must integrate the scattered flux in all directions:

$$\Pi = \int_0^{2\pi} d\varphi \int_0^{\pi} \sin\beta I(\varphi,\beta)\, d\beta. \qquad (38)$$

In doing this it is obviously immaterial which one of the formulas for $I_1$, (33) or (34), is used to effect the substitution. (Actually (34) differs from (33) in this, that $I_1$ is integrated with respect to $\varphi$ and is divided by $2\pi$. On integration of $\Pi$ we will have to multiply $I_1$ in accordance with (34) by $2\pi$).

Substituting (33) in $\Pi$, we have $\Pi_1 = \Pi' \Phi$, where $\Pi'$ designates the coefficient independent of the angles:

$$\Phi = \int_0^{2\pi}\int_0^{\pi} f^2(q)(1-\sin^2\beta\cos^2\varphi)\sin\beta\, d\beta\, d\varphi = 2\pi\Phi_1 - \pi\Phi_2;$$

$$\Phi_1 = \frac{16}{z^2}\int_0^{\frac{z}{2}} f^2(q)\, q\, dq;$$

$$\Phi_2 = \frac{16^2}{z^4}\int_0^{\frac{z}{2}} f^2(q)\, q^3\left(1-\frac{4q^2}{z^2}\right) dq.$$

Here

$$z = \frac{8n\alpha}{\lambda} \qquad (39)$$

On effecting integration with respect to q we have:

$$\Phi_1 = \frac{16}{z^2}\, 9\left[-\frac{2}{z^4} - \frac{1}{z^2} + \frac{2\cos z}{z^4} + \frac{2\sin z}{z^4}\right]_0^z;$$

$$\Phi_2 = \frac{16^2}{z^4}\left\{9\left[-\frac{1}{z^2} + \frac{1}{2}\ln z + \frac{\cos z}{z^2} + \frac{\sin z}{z} - \frac{1}{2}Ciz\right]_0^z - \right.$$

$$\left. - \frac{4}{z^2}\frac{9}{2}\left[\ln z - Ciz + \frac{z^2}{8} + \frac{z\sin z}{4} + \frac{5}{4}\cos z\right]_0^z\right\}.$$



Declassified in Part - Sanitized Copy Approved for Release 2012/03/12 : CIA-RDP82-00039R000100190014-6

Declassified in Part - Sanitized Copy Approved for Release 2012/03/12 : CIA-RDP82-00039R000100190014-6

Wherein Ciz denotes the integral cosine of z:

$$Ciz = -\int_{z}^{\infty} \frac{\cos t}{t}\, dt.$$

A table of functions of Ciz is given in /7/.

Substituting limits in $\Phi_1$ and $\Phi_2$ we have finally for the expression:

$$\Pi_1 = I_0 \pi a^2 |\alpha|^2 F_1(z) \qquad (40)$$

where

$$F_1(z) = \frac{2\pi}{z^2}^2 \left\{ 14(\cos z - 1) - 2z \sin z + (4z^2 - 16)(Ciz - \ln z - C) + \right. \qquad (41)$$
$$\left. + 5z^2 + \frac{z^4}{4} \right\},$$

and C is Eiler's constant. C = 0.577...

Coefficient of scatter is given by the formula:

$$K_1 = \frac{\Pi}{I_0} = \pi a^2 |\alpha|^2 F_1(z) \qquad (42)$$

For small values of z (Rayleigh's case) we have:

$$F_1(z) = 2\pi^2 \left( \frac{1}{108} z^4 - 0.00026 z^6 \right) \simeq 0.183 z^4; \qquad (43)$$

$$K_1 = \pi a^2 |\alpha|^2 \cdot 0.183 z^4. \qquad (44)$$

Coefficient of scatter is here proportional to $\sim \frac{1}{\lambda^4}$.



Declassified in Part - Sanitized Copy Approved for Release 2012/03/12 : CIA-RDP82-00039R000100190014-6

Declassified in Part - Sanitized Copy Approved for Release 2012/03/12 : CIA-RDP82-00039R000100190014-6

For large values of z

$$F_1(z) \cong \frac{\pi^2}{2} z^2, \tag{45}$$

$$K_1 = \pi a^2 |\alpha|^2 \frac{z^2}{2} \pi^2 \tag{46}$$

and consequently in first approximation the coefficient of scatter, with increasing z, increases without bounds (in proportion to $\sim \frac{a^4}{\lambda^2}$).

Function $F_1(z)$ has been tabulated by us. Its values for z, from 0 to 20, are given in Table III. For large values of z the asymptotic formula (45) can be used.

TABLE III

| z | $F_1(z)$ | z | $F_1(z)$ | z | $F_1(z)$ | z | $F_1(z)$ | z | $F_1(z)$ |
|---|---|---|---|---|---|---|---|---|---|
| 0.0 | 0.000 | 2.6 | 7.106 | 3.5 | 20.391 | 5.9 | 102.407 | 9.0 | 285.508 |
| 1.0 | 0.178 | 2.8 | 9.277 | 3.6 | 22.463 | 6.0 | 106.927 | 10.0 | 365.570 |
| 1.2 | 0.375 | 3.0 | 11.883 | 3.7 | 24.654 | 6.1 | 111.368 | 11.0 | 463.141 |
| 1.4 | 0.651 | 3.1 | 13.363 | 3.8 | 26.944 | 6.2 | 116.224 | 12.0 | 571.884 |
| 1.6 | 1.145 | 3.14 | 14.015 | 3.9 | 29.372 | 6.28 | 120.054 | 13.0 | 691.089 |
| 1.8 | 1.757 | 3.2 | 14.920 | 4.0 | 31.938 | 6.4 | 125.956 | 14.0 | 818.506 |
| 2.0 | 2.665 | 3.3 | 16.640 | 4.5 | 46.545 | 7.0 | 158.012 | 15.0 | 956.147 |
| 2.2 | 3.810 | 3.4 | 18.456 | 5.0 | 64.093 | 8.0 | 217.111 | 20.0 | 1794.59 |
| 2.4 | 5.290 | | | | | | | | |

Graph of function $F_1(z)$ is shown in Figure 5.

For comparison there is also shown the graph of Rayleigh's function, that is, the function $0.183z^4$.



Declassified in Part - Sanitized Copy Approved for Release 2012/03/12 : CIA-RDP82-00039R000100190014-6

Declassified in Part - Sanitized Copy Approved for Release 2012/03/12 : CIA-RDP82-00039R000100190014-6

Decreasing rate of growth of $F_1(z)$ with increasing dimensions of the particle is physically due to mutual damping of fields of various portions of the sphere occurring as a result of phase differences between these fields.

Quantity $\Pi_0 = I_0 \pi a^2$ can be designated as the amount of energy having reached the particle, then $\frac{\Pi_1}{\Pi_0} = |\alpha|^2 F_1(z)$ is the portion of energy scattered by the particle. Generally speaking, this quantity can be greater than unity. Due to continuity conditions of the electromagnetic field the particle not only scatters the flux actually reaching it, but also disturbs the field beyond it. The problem of coefficient of scatter in the case of large particles has been extensively studied in our paper /8/. There it was shown that because of the fact that when $\frac{a}{\lambda} \longrightarrow \infty$ transition to geometrical optics, contrary to common conceptions, generally does not take place, the value $\frac{\Pi_1}{\Pi_0}$, in the case of a large particle, differs from the unit value corresponding to geometrical optics. In this instance $1 \leqslant \frac{\Pi_1}{\Pi_0} \leqslant 2$.

We obtain on first approximation for large particles:

$$\frac{\Pi_1}{\Pi_0} = |\alpha|^2 \frac{\pi^2}{2} z^2.$$

Since actually $\frac{\Pi_1}{\Pi_0} \infty 1$ or 2, the upper limit of values $z = \frac{8\pi a}{\lambda}$, beyond which one may no longer use first approximation, is given by the condition

$$|\alpha|^2 F_1(z) \infty 1 \text{ or } 2. \qquad (47)$$

Using Tables I and III we readily obtain, in the case of a water droplet in air, a result showing that first approximation is



Declassified in Part - Sanitized Copy Approved for Release 2012/03/12 : CIA-RDP82-00039R000100190014-6

Declassified in Part - Sanitized Copy Approved for Release 2012/03/12 : CIA-RDP82-00039R000100190014-6

not applicable for values

$$\frac{2\pi a}{\lambda} > 3.5-5, \tag{48}$$

and in the case of an air bubble in water for values

$$\frac{2\pi a}{\lambda} > 4-5.5. \tag{49}$$

It must be stressed that the limits here indicated are of an integral nature, that is, they relate to values of a fully scattered flux.

## 5. CORRELATION OF FIRST APPROXIMATION THEORY WITH DIFFRACTION THEORY OF KIRCHHOFF

Computation of scattered field at first approximation, amounts to summation of fields emitted by dipoles, uniformly filling the sphere. This problem is analogous with the usual diffraction problem. The difference is only this, that here we have a volume "aperture." Moreover since excitation intensity of the dipoles is set by a flat wave, while the observation point is located at a distance $R \gg a$, the problem under consideration is the Fraunhofer's problem of diffraction theory (Source and receiving screen at infinity) in Kirchhoff approximation.

It is known that the theory of diffraction developed by Kirchhoff is an approximate theory which takes into account members of the first order in $\frac{\lambda}{a}$ (a -- dimensions of bodies, apertures etc). Therefore in order to connect our formulas of first approximation with the theory of Kirchhoff we must consider the limit form of our formulas in the case of large spheres. We will show, presently, that in this



Declassified in Part - Sanitized Copy Approved for Release 2012/03/12 : CIA-RDP82-00039R000100190014-6

Declassified in Part - Sanitized Copy Approved for Release 2012/03/12 : CIA-RDP82-00039R000100190014-6

limit case our results are (actually only somewhat) correlated with the results of Kirchhoff's theory. We will discuss here two basic problems: the question of scattering indicatrix deformation with increasing a, and the question of scattering coefficient changes on increase of a.

Let us first consider deformation of scatter indicatrix. We have indicated already that with increasing radius of the sphere the indicatrix of scatter acquires more and more forward elongation. This elongation leads to the result that in the case of large particles, practically all of the scattered energy is directed only forward. Waves in lateral directions and rearward are extinguished as a result of mutual interference. Elongation of the indicatrix in the forward direction must be considered in conformity with the known result of the diffraction theory proving the rectilinear propagation of light. In the diffraction theory this result is attained by means of plotting Fresnal's zones. Deviation of the indicatrix from a symmetrical form and its forward elongation with increasing size of the particles is known as the Mie effect. Thus the physical nature of the Mie effect consists in this, that with increasing size of the particles, the indicatrix undergoes deformation so as to ensure, in the case of an infinite space, the transition to the rectilinear propagation of light. These considerations relate to the cases of $\alpha \longrightarrow 0$ and $\frac{a}{\lambda} \to \infty$, so that $|\alpha| \frac{a}{\lambda} \longrightarrow$ const.

Let us now consider the expression given for the scatter coefficient /formula 42/. We have already indicated that in the case of large particles our formula yields a physically paradoxical result — the scatter coefficient increases proportionally to the fourth power of the radius (in lieu of the correct, second power). This result apparently is due to the approximate computation method. Formula (42) is obtained by first approximation. In its derivation we have also made the assumption



Declassified in Part - Sanitized Copy Approved for Release 2012/03/12 : CIA-RDP82-00039R000100190014-6

Declassified in Part - Sanitized Copy Approved for Release 2012/03/12 : CIA-RDP82-00039R000100190014-6

that $R \gg a$. Now we are considering a case where $a \gg \lambda$. It is clear, however, that both inequalities are conjoined, and with $R \gg a$ we can have $a \ll \lambda$, as well as $a \gg \lambda$. In the calculation of $\vec{E}_{scat.}$ we retained only members proportional to $\frac{a}{R}$. It is readily apparent, however, that inclusion of succeeding members of the resolution in $\frac{a}{R}$, does not alter the formula giving the scatter coefficient. In fact taking these members into consideration corresponds to a transition from the Fraunhofer's case of Kirchhoff's theory, to that of Fresnal.

In so doing intensity of the scattered field is made to include members of the order of $\frac{a^3}{R^3}$; and the coefficient of scatter, members of the order of $\frac{a}{R}$. This means that the expression giving the coefficient of scatter will not be altered.

Paradoxicalness of formula (42) is due to the fact that we were concerned with the first approximation, which, as noted previously (see paragraph 4), is not applicable to the case of $a \gg \lambda$. When $\frac{a}{\lambda} \gg 1$, in order to obtain the correct result it is imperative that the mutual relationship of the radiating dipoles be taken into account. It must be merely accepted as factual, that the system of non-interacting dipoles, which uniformly fill the sphere, is excited in accordance with the rule $e^{i\vec{\kappa}\vec{r}}$ ($\vec{r}$ being the coordinates of the dipole) and radiates energy into space in proportion to the fourth power of the sphere's radius.

We will show that this fact is correlated with (to a certain extent) the theory of Kirchhoff. To do so it must be recalled that light intensity at the center of the diffraction spot in Fraunhofer's diffraction through a circular aperture is given by the formula:



Declassified in Part - Sanitized Copy Approved for Release 2012/03/12 : CIA-RDP82-00039R000100190014-6

Declassified in Part - Sanitized Copy Approved for Release 2012/03/12 : CIA-RDP82-00039R000100190014-6

$$I = I_0 \frac{a^4 \pi^2}{\lambda^2} \qquad (50)$$

where $I_0 = \frac{c E_0^2}{4\pi}$ is the intensity of incident light.

Pursuing the analogy between diffraction of light on passing through a circular aperture in an opaque screen, and diffraction of light in a drop, we note that if formation of a diffraction image in the first instance is due to $\vec{E}$ in the aperture differing from zero, in the second instance it is due to the fact that $\vec{E} = \epsilon \vec{E}_0$ within the sphere differs from $\vec{E}_0$ in the surrounding space. Therefore, if in the case of diffraction in an aperture we have

$$I_0 = \frac{c(E_0 - 0)^2}{4\pi}$$

then, in the instant case we must have:

$$I_0 = \frac{c(\epsilon E_0 - E_0)^2}{4\pi} = \frac{c E_0^2}{4\pi}(\epsilon - 1)^2 = \frac{c E_0^2}{4\pi}(4\pi)^2 \alpha^2. \qquad (51)$$

Hence light intensity in the direction of the wave vector is:

$$I = I_0 \frac{a^4 \pi^2}{\lambda^2} = \frac{c E_0^2}{4\pi} \alpha^2 \pi a^2 \left(\frac{4\pi a}{\lambda}\right)^2 \pi. \qquad (52)$$

Total scattered flux is derived therefrom on multiplying I by the value of the solid angle within which scatter takes place. Since, as previously noted, light is scattered essentially forward, this solid angle is equal in order of magnitude to $2\pi$. Thus we have:



Declassified in Part - Sanitized Copy Approved for Release 2012/03/12 : CIA-RDP82-00039R000100190014-6

Declassified in Part - Sanitized Copy Approved for Release 2012/03/12 : CIA-RDP82-00039R000100190014-6

$$\Pi = 2\pi I = I|\alpha|^2 \pi a^2 \left(\frac{8\pi a}{\lambda}\right)^2 \frac{\pi^2}{2}; \qquad (53)$$

$$K = \pi a^2 |\alpha|^2 z^2 \frac{\pi}{2},$$

that is, exactly the formula (46) given above. (Strictly speaking, there should be introduced a coefficient $\beta 2\pi$, wherein $0<\beta\leqslant 1$. However, taking into account the "volume" of aperture (in contrast to the usual case every direction here is the direction of disk axis even though it is not parallel to $\vec{\kappa}$) -- shows that $\beta = 1$ ).

Thus a sphere of non-interacting dipoles emits in all directions within angle $2\pi$ on the average, the same amount of light as is emitted only forward by the ordinary sphere. (In our paper /8/ it is shown that the amount of light scattered forward by a large sphere is exactly determined by formula (50)). This is the very reason why the scatter coefficient in first approximation differs from the value $2\pi a^2$.

## 6. SECOND APPROXIMATION FOR A SPHERE THE DIMENSIONS OF WHICH ARE COMMENSURABLE TO THE WAVE LENGTH

In this paragraph we will effect computations in second approximation, that is taking into account in the field of scattered wave, members proportional to $|\alpha|^2$. In doing this we will limit ourselves to the case of a sphere the dimensions of which are commensurable to the wave length, that is,

$$\frac{2\pi a}{\lambda} < 1.$$



Declassified in Part - Sanitized Copy Approved for Release 2012/03/12 : CIA-RDP82-00039R000100190014-6

Declassified in Part - Sanitized Copy Approved for Release 2012/03/12 : CIA-RDP82-00039R000100190014-6

a. Effective Field Within the Sphere

In order to calculate the members $\sim |\alpha|^2$ of the scattered field, we must take into account the members $\sim |\alpha|$ of the effective field.

Amplitude of the effective field within the sphere on first approximation is determined by means of formula (7):

$$\vec{E}^{(1)}_{eff} = rot\ rot \int \vec{E}_0 \frac{e^{i(\kappa R + \vec{\kappa}\vec{r}')}}{R} dv' - \frac{8\pi}{3} E_0 e^{i\vec{\kappa}\vec{r}}.$$

The problem is thus reduced to determining the following integral over a sphere:

$$I = \int \frac{e^{i(\kappa R + \vec{\kappa}\vec{r}')}}{R} dv'. \qquad (54)$$

Then,

$$\vec{E}^{(1)}_{eff} = rot\ rot\, I\vec{E}_0 - \frac{8\pi}{3}\vec{E}_0 e^{i\vec{\kappa}\vec{r}}. \qquad (55)$$

Here $\vec{R} = \vec{r} - \vec{r}'$ (both points, point of observation ( $\vec{r}$ ) and source ( $\vec{r}'$ ), are located inside the sphere). Having calculated I, we will have a complete solution of the problem in second approximation (taking into account mutual polarization of sphere elements). We will perform here the computation of I in the case of a sphere the dimensions of which are commensurable to the wave length ( $\frac{2\pi a}{\lambda} \sim 1$ ).

I is a dimensional value. On passing to the non-dimensional coordinates within the sphere we have:

$$I = a^2 \int \frac{e^{ia(\kappa 2 + \vec{\kappa}\vec{r}')}}{R} dv. \qquad (56)$$



Declassified in Part - Sanitized Copy Approved for Release 2012/03/12 : CIA-RDP82-00039R000100190014-6

Declassified in Part - Sanitized Copy Approved for Release 2012/03/12 : CIA-RDP82-00039R000100190014-6

Here integration is effected over a sphere of unitary radius. Since, however, on calculating $\vec{E}_{eff}$ we must differentiate I twice, the sphere radius will not, of course, appear in the expression giving the field. Therefore, to simplify the writing let us omit the factor $a^2$ in I, keeping in mind meanwhile that coordinates appearing in our expressions of I and $\vec{E}_{eff}$ relate to a sphere of unitary radius.

It is natural to compute I for $\frac{2\pi a}{\lambda} \lesssim 1$ developing $e^{i(\kappa R + \kappa \vec{r}')}$ as a series. (Here and henceforth $\kappa = \frac{2\pi a}{\lambda}$). This method, however, results in cumbersome calculations. A series for I can be obtained directly, on observing that within the sign of integration, in (54), we have the product of plane and spherical waves.

It is known (see /9/) that these waves can be formulated in the form of the following series:

$$e^{i\kappa r' \cos\theta'} = \sum_{n=0}^{\infty} (2n+1) i^n \psi_n(\kappa r') P_n(\cos\theta');$$

$$\frac{e^{i\kappa R}}{R} = i\kappa \sum_{m=0}^{\infty} (2m+1) \psi_m(\kappa r) \zeta_m^{(2)}(\kappa r') P_m(\cos\theta\cos\theta' + \sin\theta\sin\theta'\cos\varphi').$$

Here it is assumed that $r, \theta, \varphi = 0$ are coordinates of the observation point; $r', \theta', \varphi'$ are coordinates of the "luminescent" point; R is the distance between them; $P_n(\kappa)$ is the polynomial of Legendre; $\psi_n(\kappa)$ and $\zeta_n^{(2)}(\kappa)$ are specifically normalized Bessel's functions and Hankel's functions of the first kind, namely:

$$\psi_n(\kappa) = \sqrt{\frac{\pi}{2\kappa}} J_{n+\frac{1}{2}}(\kappa);$$

$$\zeta_n^{(2)}(\kappa) = \sqrt{\frac{\pi}{2\kappa}} H_{n+\frac{1}{2}}^{(2)}(\kappa),$$



Declassified in Part - Sanitized Copy Approved for Release 2012/03/12 : CIA-RDP82-00039R000100190014-6

Declassified in Part - Sanitized Copy Approved for Release 2012/03/12 : CIA-RDP82-00039R000100190014-6

where $J_{n+1/2}(\chi)$ and $H^{(1)}_{n+1/2}(\chi)$ are functions with half-integer indices.

In accordance with the known theorem on the addition of Legendre's polynomials, the polynomial $P_m$, appearing in the development of the spherical wave, can be written in the form:

$$P_m = \sum_{e=0}^{m} \frac{(m-e)!}{(m+e)!} \frac{2}{\delta_e} P_m^e(\cos\theta') P_m^e(\cos\theta) \cos e\varphi;$$

$$\delta_e = 2 \text{ when } e = 0;$$

$$\delta_e = 1 \text{ when } e > 0.$$

Substituting this expression in the development of $\frac{e^{i\kappa R}}{R}$, and then the development of $\frac{e^{i\kappa R}}{R}$ and $e^{i(\vec{\kappa}, \vec{r}')}$, in I, we have, following integration with regard to $\varphi'$ and $\theta'$:

$$I = 4\pi\kappa \sum_{n=0}^{\infty} (2n+1) i^{n+1} P_n(\cos\theta) \left\{ \psi_n(\kappa r) \int_r^1 \zeta_n^{(1)}(\kappa\rho) \psi_n(\kappa\rho) \rho^2 d\rho + \right. \tag{57}$$

$$\left. + \zeta_n^{(1)}(\kappa r) \int_0^r \psi_n^2(\kappa\rho) \rho^2 d\rho \right\}.$$

Two members are within braces because it was necessary to resort to different developments of $\frac{e^{i\kappa R}}{R}$ for $r' < r$ and for $r' > r$.

Developing cylindrical functions as series, multiplying and integrating, we can write I in the form:

$$I = 4\pi \sum_{n=0}^{\infty} (2n+1) i^n P_n(\cos\theta) \left\{ a_n + b_n + c_n \right\}. \tag{58}$$



Declassified in Part - Sanitized Copy Approved for Release 2012/03/12 : CIA-RDP82-00039R000100190014-6

Declassified in Part - Sanitized Copy Approved for Release 2012/03/12 : CIA-RDP82-00039R000100190014-6

Here the assumption is:

$$\left(\kappa = \frac{2\pi a}{\lambda}\right);$$

$$1.\quad a_n = i\kappa^{3n+1} r^n \sum_{e=0}^{\infty} (-1)^e \kappa^{2e} 2^{-e} c_e , \tag{59}$$

wherein

$$c_e = \sum_{u=0}^{e} \frac{A_u}{(e-u)!\,[2(n+e-u)+1]!!\,[2(n+u)+3]} ,$$

where

$$A_u = \sum_{r=0}^{u} \frac{1}{(u-r)!\,r!\,[2(n+r)+1]!!\,[2(n+u-r)+1]!!} .$$

$$2.\quad b_n = (-1)^n \frac{\sqrt{\pi}}{2} \kappa^n (2r)^n \sum_{f=0}^{\infty} (-1)^f \kappa^{2f} 2^{-f} M_f , \tag{60}$$

where

$$M_f = \sum_{t=0}^{f} \frac{r^{2(f-t)}\left[1 - r^{2(t+1)}\right] B_t}{(f-t)!\,(t+1)\,[2(n+f-t)+1]!!} ,$$

where

$$B_t = \sum_{s=0}^{t} \frac{2^{-s}}{s!\,(t-s)!\,[2(t-s+n)+1]!!\,\Gamma\left(-n+s+\frac{1}{2}\right)}$$

$$3.\quad c_n = (-1)^n \sqrt{\pi}\, 2^n \kappa^n r^{n+2} \sum_{v=0}^{\infty} (-1)^v \left(\frac{\kappa r}{2}\right)^{2v} D_v , \tag{61}$$

where

$$D_v = \sum_{s=0}^{v} \frac{E_s 2^s}{(v-s)!\,(2n+2s+3)\,\Gamma\left(-n+v-s+\frac{1}{2}\right)} ,$$



Declassified in Part - Sanitized Copy Approved for Release 2012/03/12 : CIA-RDP82-00039R000100190014-6

Declassified in Part - Sanitized Copy Approved for Release 2012/03/12 : CIA-RDP82-00039R000100190014-6

where

$$E_s = \sum_{r=0}^{s} \frac{1}{r!(s-r)![2(n+r)+1]!![2(n+s-r)+1]!!}$$

These formulas have a cumbersome appearance. But actually successive approximations of I can be easily determined by their use. On utilizing them it is convenient to bear in mind the following quadratic tables, which specify the power of K in the member comprising the given pair (n, e), (n, f) or (n, v):

For $a_n$

| n \ e | 0 | 1 | 2 | 3 |
|---|---|---|---|---|
| 0 | 1 | 3 | 5 | 7 |
| 1 | 4 | 6 | 8 | 10 |
| 2 | 7 | 9 | 11 | 13 |

For $b_n$ and $c_n$

| n \ v,f | 0 | 1 | 2 | 3 | 4 |
|---|---|---|---|---|---|
| 0 | 0 | 2 | 4 | 6 | 8 |
| 1 | 1 | 3 | 5 | 7 | 9 |
| 2 | 2 | 4 | 6 | 8 | 10 |
| 3 | 3 | 5 | 7 | 9 | 11 |
| 4 | 4 | 6 | 8 | 10 | 12 |
| 5 | 5 | 7 | 9 | 11 | 13 |

These tables should be used as follows. Let us assume that we wish to calculate member $I_r$, the member proportional to $k^r$. We find in our tables the values of r, and determine in the left-hand vertical and upper horizontal lines that pair of indexes (n, e), (n, f) and (n, v), which must be taken into account for the given r. Thus for r = 3, we find in the table for $a_n$ that it occurs but once, when n = 0 and e = 1; and in the table for $b_n$ and $c_n$, twice, when n = 1 v,f = 1 and when n = 3 v,f = 0. Now to calculate $I_3$, in the sum for $a_n$, we take the member wherein n = 0 and e = 1, and in the sums for $b_n$ and $c_n$, members wherein



Declassified in Part - Sanitized Copy Approved for Release 2012/03/12 : CIA-RDP82-00039R000100190014-6

Declassified in Part - Sanitized Copy Approved for Release 2012/03/12 : CIA-RDP82-00039R000100190014-6

n = 1 v,f = 1, and n = 3 v,f = 0. Thus we readily obtain the following expressions for $I_0$, $I_1$, $I_2$, $I_3$, $I_4$:

1. For the zero member (not containing k):

$$a_0 = 0$$

$$b_0 = \frac{1-r^2}{2} \quad (n=0,\ f=0),$$

$$c_0 = \frac{r^2}{3} \quad (n=0,\ t=0).$$

Therefrom

$$I_0 = 2\pi\left(1 - \frac{r^2}{3}\right). \tag{62}$$

2. For member proportional to k:

$$a_1 = \frac{ik}{3} \quad (n=0,\ e=0);$$

$$b_1 = -\frac{kr}{18}(r^2-1) \quad (n=1,\ f=0);$$

$$c_1 = \frac{kr^2}{45} \quad (n=1,\ v=0).$$

Therefrom

$$I_1 = \frac{4\pi}{3} ik\left\{1 + \cos\theta\, \frac{5r-3r^3}{10}\right\}. \tag{63}$$

3. Members proportional to $k^2$, $k^3$, and $k^4$, are analogously:

$$I_2 = -\frac{2\pi k^2}{3}\left\{1 + r^2\frac{4+3\cos^2\theta}{10} - r^4\frac{2+15\cos^2\theta}{70}\right\}. \tag{64}$$

$$I_3 = \frac{-22\pi i k^3}{45}\left\{1 - \frac{3}{11}r\cos\theta + \frac{3r^3}{77}\left(2\cos\theta + \frac{5}{2}\cos^3\theta\right) - \frac{r^5}{11}\left(\frac{\cos\theta}{7} + \frac{5}{6}\cos^3\theta\right)\right\} \tag{65}$$

$$I_4 = \frac{4\pi k^4}{45}\left\{1 - r\cos\theta + r^2\frac{36-3\cos^2\theta}{28} + r^4\frac{48+24\cos^2\theta+35\cos^4\theta}{336} - r^6\frac{16+60\cos^2\theta+315\cos^4\theta}{3696}\right\}. \tag{66}$$



Declassified in Part - Sanitized Copy Approved for Release 2012/03/12 : CIA-RDP82-00039R000100190014-6

Declassified in Part - Sanitized Copy Approved for Release 2012/03/12 : CIA-RDP82-00039R000100190014-6

Reverting now to the calculation of the effective field, let $\vec{i}$ be a unitary vector in the direction $\vec{E}_o$. In accordance with formula (55) we have:

$$\vec{E}^{(1)}_{eff} = E_0 \left\{ \nabla\left(\vec{i}\nabla l\right) - \vec{i}\Delta l - \vec{i}\frac{8\pi}{3} e^{i\vec{k}\vec{r}} \right\}. \qquad (67)$$



Declassified in Part - Sanitized Copy Approved for Release 2012/03/12 : CIA-RDP82-00039R000100190014-6

Declassified in Part - Sanitized Copy Approved for Release 2012/03/12 : CIA-RDP82-00039R000100190014-6

In the quasistatic case, that is, in the case of $\lambda \gg a$, assuming $\varkappa = 0$ and substituting in (67) for $I$ $I_0$, we have $\vec{E}^{(1)}_{eff} = 0$. Thus in the case of very small spheres, the effective field within the sphere exactly coincides with the external, since, if $\vec{E}^{(1)}_{eff} = 0$, then obviously $\vec{E}^{(2)} = \vec{E}^{(1)}_{eff} \ldots = 0$. as well. This condition obtains only in the case of effective field and not in that of the mean field. Its physical significance is that in the case of long waves the field of screening charges upon the surface exactly compensates the field created by the polarized elements of the sphere's volume. This compensation renders more convenient the calculation of successive approximations of the effective field than that of the mean field. It was the compelling reason for passing in paragraph 2 from a study of a solution of equation (1) to a study of solutions of equation (4) (that of the effective field). By means of our calculations of the values of $I$, in accordance with formula (67), we can readily determine $\vec{E}^{(1)}_{eff}$. Let $\vec{i}$ be the direction of axis X, and $\vec{k}$ the direction of axis Z. Then, omitting the factor $E_0$ we have, with an accuracy up to members $\sim \varkappa^2$

$$E^{(1)}_{eff\,x} = \frac{8\pi}{15} i\varkappa z + \frac{4\pi}{3}\varkappa^2\left(\frac{11}{10} - \frac{23x^2 + 31y^2 + 51z^2}{70}\right); \qquad (68)$$

$$E^{(1)}_{eff\,y} = \frac{16\pi\varkappa^2}{105} xy; \qquad (69)$$

$$E^{(1)}_{eff\,z} = \frac{-9\pi i\varkappa}{5} x + \frac{2\pi\varkappa^2}{105} 38xz. \qquad (70)$$



Declassified in Part - Sanitized Copy Approved for Release 2012/03/12 : CIA-RDP82-00039R000100190014-6

Declassified in Part - Sanitized Copy Approved for Release 2012/03/12 : CIA-RDP82-00039R000100190014-6

If we wish to effect calculation with an accuracy up to members $\sim \kappa^4$, then to the above expressions for components of $\vec{E}^{(1)}_{eff}$ must be added the expressions:

$$E^{(2)}_{eff\,x} = \frac{2\pi i\kappa^3}{105}\left\{31z - 17\kappa^2 z - \frac{59}{3}y^2 z - \frac{247}{9}z^3\right\} +$$

$$+ \frac{4\pi\kappa^4}{315}\left\{-\frac{69}{2} - 17y^2 - 9\kappa^2 - \frac{127}{4}z^2 + \frac{519}{44}\kappa^2 z^2 + \right.$$

$$\left. + \frac{591}{44}y^2 z^2 + \frac{21}{11}y^2\kappa^2 + \frac{13}{22}\kappa^4 + \frac{29}{22}y^4 + \frac{673}{44}z^4\right\}; \quad (71)$$

$$E^{(2)}_{eff\,y} = \frac{16\pi i\kappa^3}{315}\kappa yz + \frac{4\pi\kappa^4}{315}\left\{8\kappa y - \frac{18}{11}\kappa yz^2 - \frac{8}{11}\kappa^3 y - \frac{8}{11}\kappa y^3\right\}; \quad (72)$$

$$E'_{eff\,z} = -\frac{2\pi i\kappa^3}{315}\left\{12\kappa - 4\kappa^3 - 4\kappa y^2 - 47\kappa z^2\right\} +$$

$$+ \frac{8\pi\kappa^4}{315}\left\{5\kappa z - \frac{9}{11}\kappa y^2 z - \frac{9}{11}\kappa^3 z - \frac{161}{44}\kappa z^3\right\}. \quad (73)$$

b. Scattered Field.

To calculate projections of the scattered field, we first determine vector $\vec{A}^{(1)}$, in accordance with formulas (15) - (18). In doing this, as in the calculation of $\vec{A}^{(0)}$, we write $R = r_0 - d$, where $r_0$ is the distance from the observation point to the center of the sphere, while $d$ is the distance from source (point within



Declassified in Part - Sanitized Copy Approved for Release 2012/03/12 : CIA-RDP82-00039R000100190014-6

Declassified in Part - Sanitized Copy Approved for Release 2012/03/12 : CIA-RDP82-00039R000100190014-6

the sphere) to a plane perpendicular to $\vec{R}_0$ and passing through the center of the sphere.

$$\vec{A}^{(1)} = a^3 \int \vec{E}^{(1)}_{eff} e^{ikR} dv = e^{ikr_0} a^3 \int \vec{E}^{(1)}_{eff} e^{-ikd} dv.$$

In so doing we have passed here to non-dimensional coordinates so that the integrals appearing herein relate to a sphere, the radius of which is one. We now substitute in this expression the previously calculated values of the components of $\vec{E}^{(1)}_{eff}$. In addition we develop $e^{-ikd}$ as a series:

$$e^{-ikd} = 1 - ikd - \frac{d^2k^2}{2} + i\frac{d^3k^3}{6} + \frac{d^4k^4}{24} - \frac{id^5k^5}{120} - \dots$$

$$d = k \cdot \sin\beta\cos\varphi + y\sin\beta\sin\varphi + z\cos\beta.$$

Substituting these expressions within the sign of integration, we readily find that components of vector $\vec{A}^{(1)}$ proportional to $k$ and $k^3$ are equal to zero. With an accuracy up to the members of the $k^4$ order, we have:

$$A^{(1)}_k = ve^{ikr_0}\left\{k^2(m_1 + \mu_1\cos\beta) + k^4\left(-t_1 + t_2\cos\beta + t_3\cos^2\beta - \tfrac{t_4}{2}\sin^2\beta\cos^2\varphi\right)\right\}; \quad (74)$$



Declassified in Part - Sanitized Copy Approved for Release 2012/03/12 : CIA-RDP82-00039R000100190014-6

Declassified in Part - Sanitized Copy Approved for Release 2012/03/12 : CIA-RDP82-00039R000100190014-6

$$A_y^{(1)} = -ve^{ikr_0}k^4 t_4 \sin^2\beta\cos\varphi\sin\varphi; \tag{75}$$

$$A_z^{(1)} = -ve^{ikr_0}\left\{k^2\mu_2\sin\beta\cos\varphi + k^4(-t_5 + t_6\cos\beta)\sin\beta\cos\varphi\right\} \tag{76}$$

Here $v$ is the volume of the particle.

The constants appearing herein have the following values:

$$m_1 = \frac{16\pi}{15} = 3.351; \qquad t_3 = \frac{120\pi}{(105)^2} = 0.0342;$$

$$\mu_1 = \frac{8\pi}{75} = 0.335; \qquad t_4 = \frac{48\pi}{(105)^2} = 0.0137;$$

$$\mu_2 = \frac{4\pi}{25} = 0.502; \qquad t_5 = \frac{84\pi}{(105)^2} = 0.0240;$$

$$t_1 = \frac{7248\pi}{(105)^2} = 2.065; \qquad t_6 = \frac{228\pi}{(105)^2} = 0.0650.$$

$$t_2 = \frac{504\pi}{(105)^2} = 0.144;$$

Reintroducing the previously omitted factor $E_0$, we now have for the components of the scattered field:

$$E_\theta = S\cos\varphi\cdot\cos\beta\left\{f(q) + \alpha\left[k^2\left(m_1 + \mu_1\cos\beta + \mu_2\frac{\sin^2\beta}{\cos\beta}\right) + \right.\right.$$
$$\left.\left. + k^4\left(-t_1 + t_2\cos\beta + t_3\cos^2\beta + (t_6 - t_4)\sin^2\beta - t_5\frac{\sin^2\beta}{\cos\beta}\right)\right]\right\} \tag{77}$$

$$E_\varphi = -S\sin\varphi\left\{f(q) + \alpha\left[k^2(m_1 + \mu_1\cos\beta) + k^4(-t_1 + t_2\cos\beta + t_3\cos^2\beta)\right]\right\}. \tag{78}$$



Declassified in Part - Sanitized Copy Approved for Release 2012/03/12 : CIA-RDP82-00039R000100190014-6

Declassified in Part - Sanitized Copy Approved for Release 2012/03/12 : CIA-RDP82-00039R000100190014-6

$$S = \frac{\alpha k^2}{r_0} v e^{ikr_0} E_0 . \qquad (79)$$

3. Indicatrix of Scatter

Formulas (77) and (78) determine the amplitude and polarization of the field on scattering of linearly polarized wave. To determine the intensity of scatter of natural light it is necessary to average the squares of the field along all possible directions of electric vector of natural light, that is at all angles $\varphi$. Following such an averaging we have:

$$I_\theta = \overline{E_\theta^2} = \frac{S^2}{2}\cos^2\beta\left\{f^2(q) + 2\alpha f\left[k^2\left(m_1 + \mu_1\cos\beta + \mu_2\frac{\sin\beta}{\cos\beta}\right) + \right.\right.$$

$$\left.\left. + k^4\left(-t_1 + t_2\cos\beta + t_3\cos^2\beta + (t_6 - t_4)\sin^2\beta - t_5\frac{\sin^2\beta}{\cos\beta}\right)\right]\right\}; \qquad (80)$$

$$I_\varphi = \overline{E_\varphi^2} = \frac{S^2}{2}\left\{f^2(q) + 2\alpha f\left[k^2(m_1 + \mu_1\cos\beta) + k^4\left(-t_1 + t_2\cos\beta + t_3\cos^2\beta\right)\right]\right\} \qquad (81)$$

Taking in $I_\theta$ and $I_\varphi f,^2$ outside the braces, bearing in mind (20) and (25), and retaining members of order not exceeding $k^4$, we have



Declassified in Part - Sanitized Copy Approved for Release 2012/03/12 : CIA-RDP82-00039R000100190014-6

Declassified in Part - Sanitized Copy Approved for Release 2012/03/12 : CIA-RDP82-00039R000100190014-6

$$I_\theta = \frac{S^2}{2}\cos^2\beta f^2(q)\left\{1+2\alpha\kappa^2\left[\left(m_1+\mu_1\cos\beta+\mu_2\frac{\sin^2\beta}{\cos\beta}\right)-\right.\right. \tag{82}$$

$$\left.\left.-\kappa^2\left(\lambda_1+\lambda_2\cos\beta+\lambda_3\sin^2\beta-\lambda_4\frac{\sin^2\beta}{\cos\beta}\right)\right]\right\};$$

$$I_\varphi = \frac{S^2}{2}f^2(q)\left\{1+2\alpha\kappa^2\left[\left(m_1+\mu_1\cos\beta\right)-\kappa^2\left(\lambda_1+\lambda_2\cos\beta-\lambda_3'\sin^2\beta\right)\right]\right\}. \tag{83}$$

Constants appearing herein bear a simple relationship to those introduced before.

$$\lambda_1 = +t_1-\frac{m_1}{5}-t_3+\frac{\mu_1}{5}=\frac{25056\pi}{5(105)^2}=1.4279\ldots$$

$$\lambda_2 = -t_2-\frac{\mu_1}{5}+\frac{m_1}{5}=\frac{8064\pi}{5(105)^2}=0.45957\ldots$$

$$\lambda_3 = +t_3-\frac{\mu_1}{5}+t_4+\frac{\mu_2}{5}-t_6=\frac{268\pi}{5(105)^2}=0.015273\ldots$$

$$\lambda_4 = -t_6+\frac{1}{5}\mu_2=\frac{1344\pi}{5(105)^2}=0.074852\ldots$$

$$\lambda_3' = -t_3+\frac{\mu_1}{5}=\frac{576\pi}{5(105)^2}=0.032826.$$

For the scatter indicatrix we now have:



Declassified in Part - Sanitized Copy Approved for Release 2012/03/12 : CIA-RDP82-00039R000100190014-6

Declassified in Part - Sanitized Copy Approved for Release 2012/03/12 : CIA-RDP82-00039R000100190014-6

$$I_2 = I_\theta + I_\varphi = I_1 \left\{ 1 + 2\alpha\kappa^2 \left[ \left( m_1 + \mu_1 \cos\beta + \mu_2 \frac{\sin^2\beta\cos\beta}{1+\cos^2\beta} \right) - \right. \right. \tag{84}$$

$$\left. \left. - \kappa^2 \left( \lambda_1 + \lambda_2 \cos\beta - \frac{\sin^2\beta}{1+\cos^2\beta} \left( -\lambda_3 \cos^2\beta + \lambda_4 \cos\beta + \lambda_3' \right) \right) \right] \right\}.$$

wherein $I_1$, is the indicatrix of scatter at first approximation.

Numerical computation shows that the member containing $\lambda_3$, $\lambda_4$ and $\lambda_3'$, constitutes not more than 2.5 percent of the member containing $\lambda_1$ and $\lambda_2$.

Since these members in themselves introduce a certain correction, we can write:

$$I_2 = I_1 \left\{ 1 + 2\alpha\kappa^2 \left[ \left( m_1 - \lambda_1\kappa^2 \right) + \left( \mu_1 - \lambda_2\kappa^2 \right) \cos\beta + \right. \right. \tag{85}$$

$$\left. \left. + \mu_2 \frac{\sin^2\beta\cos\beta}{1+\cos^2\beta} \right] \right\}.$$

Or, in the case of small particles ( $\kappa \ll 1$ ), keeping in mind (30), we have:

$$I_2(\beta) = I_0 |\alpha|^2 \frac{16\pi^4 v^2}{\lambda^4} \left( \frac{1+\cos^2\beta}{2} \right) \left( 1 - \frac{2}{5}\kappa^2 \sin^2\frac{\beta}{2} \right)^2 \left\{ 1 + \tag{86}$$

$$+ 2\alpha\kappa^2 \left[ \left( m_1 - \lambda_1\kappa^2 \right) + \left( \mu_1 - \lambda_2\kappa^2 \right) \cos\beta + \mu_2 \frac{\sin^2\beta \cdot \cos\beta}{1+\cos^2\beta} \right] \right\}.$$

With $\kappa \sim 1$ this formula may give an error amounting to 6 percent, and it is better to calculate $I$ by means of formula (85), using the detailed $f(q)$ table compiled by us.



Declassified in Part - Sanitized Copy Approved for Release 2012/03/12 : CIA-RDP82-00039R000100190014-6

Declassified in Part - Sanitized Copy Approved for Release 2012/03/12 : CIA-RDP82-00039R000100190014-6

d. Polarization

The degree of polarization of scattered light is determined by means of formula (36) which in this case assumes the form:

$$p = \frac{I_\varphi - I_\theta}{I_\varphi + I_\theta} \qquad (87)$$

Using the previously derived expressions for $I_\varphi$ and $I_\theta$, we have:

$$I_\varphi - I_\theta = \frac{S^2}{2} f^2(q) \sin^2\beta \left\{1 + 2\alpha\kappa^2 \left[(m_1 + \mu_1 \cos\beta - \right.\right.$$

$$\left.\left. - \mu_2 \cos\beta) - \kappa^2(\lambda_1 + \lambda_2 \cos\beta - \lambda_3 \cos^2\beta + \lambda_4 \cos\beta - \lambda_3')\right]\right\}$$

For $p$ we have:

$$p_2 = p_1 \left\{1 - \frac{4\alpha\kappa^2 \cos\beta}{1 + \cos^2\beta} \left[\mu_2 + \kappa^2(\lambda_4 - (\lambda_3 + \lambda_3')\cos\beta)\right]\right\} \qquad (88)$$

where $p_2$ is the polarization of the scattered light, at first approximation /formula (37)/. We note that here the polarization maximum (in the case of small spheres) does not shift. It is equal to one when $\beta = 90°$.



Declassified in Part - Sanitized Copy Approved for Release 2012/03/12 : CIA-RDP82-00039R000100190014-6

Declassified in Part - Sanitized Copy Approved for Release 2012/03/12 : CIA-RDP82-00039R000100190014-6

e. Coefficient of Scattering

On second approximation we have for the value $\Pi$ :

$$\Pi_2 = 2\pi \int_0^{\pi} I_2(\beta)\cos\beta\, d\beta = \pi S^2 (A_1 + A_2 + A_3);$$

$$\pi S^2 A_3 = I_0 \pi a^2 |\alpha|^2 F_3(z);$$

$$A_2 = 2\alpha\kappa^2 \int_0^{\pi} \left(m_1 + \mu_1 \cos\beta + \mu_2 \frac{\sin^2\beta\cos\beta}{1+\cos^2\beta}\right)(1+\cos^2\beta)\sin\beta\, d\beta = 2\alpha\kappa^2 m_1 \frac{8}{3};$$

$$A_3 = -2\alpha\kappa^4 \int_0^{\pi} [\lambda_1(1+\cos^2\beta) + \lambda_2\cos\beta(1+\cos^2\beta) -$$

$$- \sin^2\beta(-\lambda_3\cos^2\beta + \lambda_4\cos\beta + \lambda_3')]\sin\beta\, d\beta -$$

$$- \frac{4}{5}\alpha\kappa^4 \int_0^{\pi} \left(m_1 + \mu_1\cos\beta + \mu_2 \frac{\sin^2\beta\cos\beta}{1+\cos^2\beta}\right) \cdot$$

$$(1-\cos\beta)(1+\cos^2\beta)\sin\beta\, d\beta = -2\alpha\kappa^4\left(\frac{8}{3}\lambda_1 + \frac{4}{15}\lambda_3 - \frac{4}{3}\lambda_3'\right) -$$

$$- \frac{4}{5}\alpha\kappa^4\left(\frac{8}{3}m_1 - \frac{16}{15}\mu_1 - \frac{4}{15}\mu_2\right).$$

The last member in the expression of $A_3$ originates from the development of $f^2(q)$ as a series. In so doing we have retained members proportional to $\kappa^4$ in the result.

Collecting all terms occurring in $\Pi_2$ , and following uncomplicated transformations, we have:



Declassified in Part - Sanitized Copy Approved for Release 2012/03/12 : CIA-RDP82-00039R000100190014-6

Declassified in Part - Sanitized Copy Approved for Release 2012/03/12 : CIA-RDP82-00039R000100190014-6

$$\Pi_2 = I_0 \pi a^2 |\alpha|^2 \{F_2(z) + \alpha(\gamma_2 z^6 - \gamma_3 z^8)\}, \qquad (89)$$

where $\gamma_2$ and $\gamma_3$ are:

$$\gamma_2 = \frac{\pi^3}{105} = 0.076558;$$

$$\gamma_3 = \frac{\pi^3 235106}{256(105)^2 675} = 0.0038264.$$

Using the develcement indicated in paragraph 4 for $F_2(z)$ at small values of $z$ /formula (43)/the last of the foregoing formulas can be written:

$$\Pi_2 = \Pi_1 \{1 + \alpha z^2 \gamma_1 (1 - \gamma_4 z^2)\} \qquad (90)$$

wherein $\Pi_1$ is determined on the basis of formula (40).

Constants $\gamma_1$ and $\gamma_4$ have the following values:

$$\gamma_1 = 0.4183$$

$$\gamma_4 = 0.02190.$$

Now the coefficient of scattering is given by the formula:

$$\kappa_2 = \frac{\Pi_2}{I_0} = \pi a^2 |\alpha|^2 F_2(z), \qquad (91)$$



Declassified in Part - Sanitized Copy Approved for Release 2012/03/12 : CIA-RDP82-00039R000100190014-6

Declassified in Part - Sanitized Copy Approved for Release 2012/03/12 : CIA-RDP82-00039R000100190014-6

where

$$F_2(z) = F_1(z)\left\{1 + \alpha z^2 \gamma_1 (1 - \gamma_4 z^2)\right\}$$

Function $F_1(z)$ is indicated by formula (41).

Values of function $F_2(z)$ for $z$ from 0 to 4 are shown in Table IV.

TABLE IV

| z | F2(z) | z | F2(z) | z | F2(z) |
|---|---|---|---|---|---|
| 0.00 | 0.000 | 2.40 | 5.835 | 3.40 | 21.704 |
| 1.00 | 0.182 | 2.60 | 7.944 | 3.50 | 24.082 |
| 1.20 | 0.386 | 2.80 | 10.502 | 3.60 | 26.708 |
| 1.40 | 0.671 | 3.00 | 13.630 | 3.70 | 29.486 |
| 1.60 | 1.201 | 3.10 | 15.434 | 3.80 | 32.359 |
| 1.80 | 1.864 | 3.14 | 16.229 | 3.90 | 35.452 |
| 2.00 | 2.866 | 3.20 | 17.341 | 4.00 | 38.709 |
| 2.20 | 4.145 | 3.30 | 19.452 | | |

## 7. COMPARISON WITH COMPUTATIONS OF OTHER RESEARCHERS

Although at present there is available a large number of experimental studies, conducted under laboratory as well as natural conditions, relative to light scattered by a turbid medium, nevertheless, in all instances involved the exact dimensions of the particles and their electric characteristics are very inadequately known. Hence, precise quantitative comparison with experimental



Declassified in Part - Sanitized Copy Approved for Release 2012/03/12 : CIA-RDP82-00039R000100190014-6

Declassified in Part - Sanitized Copy Approved for Release 2012/03/12 : CIA-RDP82-00039R000100190014-6

data is impossible. Insofar as a qualitative agreement is concerned, our computations tally quite satisfactorily with the experimental results.

We can evaluate the simple formulas of our derivation by comparing results obtained by calculations based thereon with results of computations in accordance with the formulas of Mie.

a. Indicatrix

For some specific instances Mie's formulas were compiled in tabular form by Blumer. /14/. We have computed the same cases by means of our formulas.

Values of $i_1$ and $i_2$ given in Blumer's tables are correlated with $I_\varphi$ and $I_\theta$ (intensities of scattered light crosswise and parallel to plane of vision) by the following relationships:

$$i_1 = \frac{4\pi^2}{\lambda^2} I_\varphi; \quad i_2 = \frac{4\pi^2}{\lambda^2} I_\theta; \tag{92}$$

$$i = i_1 + i_2 = \frac{4\pi^2}{\lambda^2}(I_\varphi + I_\theta) = \frac{4\pi^2}{\lambda^2} I.$$

Table 5 shows values of $\frac{4\pi^2}{\lambda^2}$ computed by us on the basis of formula (85) for small spheres of ice in cases where

$$(a) \quad \frac{2\pi a}{\lambda} = 0.4 \text{ and } (b) \quad \frac{2\pi a}{\lambda} = 0.8.$$



Declassified in Part - Sanitized Copy Approved for Release 2012/03/12 : CIA-RDP82-00039R000100190014-6

Declassified in Part - Sanitized Copy Approved for Release 2012/03/12 : CIA-RDP82-00039R000100190014-6

Blumer assumes in the case of ice $n = 1.25$ $\sigma = 0.1$

(In compiling Table I we have taken for ice n = 1.31):

$$K = \frac{n^2-1}{4\pi} = 4.47 \cdot 10^{-2} \text{ and } \alpha = \frac{K}{1+\frac{4\pi}{3}K} = 0.0377.$$

Columns 2 and 5 show Blumer's values. Columns 3 and 4 show results of computation in the case of a, first (i') and second approximation (i"), while columns 6 and 7 show the corresponding values in the case b. Angles 40, 50, 130, 140 are omitted by Blumer.



Declassified in Part - Sanitized Copy Approved for Release 2012/03/12 : CIA-RDP82-00039R000100190014-6

Declassified in Part - Sanitized Copy Approved for Release 2012/03/12 : CIA-RDP82-00039R000100190014-6

Table V

| β | a | | | b | | |
|---|---|---|---|---|---|---|
| | $10^3 i_{Bl}$ | $10^3 i_l'$ | $10^3 i_l''$ | $10^2 i_{Bl}$ | $10^2 i_l'$ | $10^2 i_l''$ |
| 0 | 0.107 | 0.102 | 0.107 | 0.746 | 0.654 | 0.733 |
| 10 | 0.105 | 0.101 | 0.105 | 0.732 | 0.641 | 0.719 |
| 20 | 0.100 | 0.096 | 0.100 | 0.692 | 0.607 | 0.680 |
| 30 | 0.0925 | 0.089 | 0.0926 | 0.632 | 0.553 | 0.621 |
| 40 | | 0.080 | 0.083 | | 0.488 | 0.549 |
| 50 | | 0.071 | 0.074 | | 0.421 | 0.474 |
| 60 | 0.0645 | 0.062 | 0.0646 | 0.411 | 0.360 | 0.404 |
| 70 | 0.057 | 0.055 | 0.057 | 0.352 | 0.308 | 0.346 |
| 80 | 0.0515 | 0.050 | 0.0519 | 0.309 | 0.272 | 0.305 |
| 90 | 0.0495 | 0.048 | 0.0498 | 0.285 | 0.252 | 0.282 |
| 100 | 0.050 | 0.049 | 0.050 | 0.279 | 0.247 | 0.275 |
| 110 | 0.054 | 0.0525 | 0.054 | 0.287 | 0.256 | 0.285 |
| 120 | 0.060 | 0.058 | 0.060 | 0.308 | 0.275 | 0.304 |
| 130 | | 0.065 | 0.067 | | 0.299 | 0.332 |
| 140 | | 0.072 | 0.075 | | 0.325 | 0.361 |
| 150 | 0.082 | 0.080 | 0.082 | 0.390 | 0.349 | 0.388 |
| 160 | 0.0875 | 0.085 | 0.0879 | 0.412 | 0.367 | 0.410 |
| 170 | 0.0915 | 0.089 | 0.0917 | 0.426 | 0.380 | 0.424 |
| 180 | 0.093 | 0.090 | 0.0930 | 0.431 | 0.384 | 0.428 |

The indicatrix calculated by us in the case of b is shown in Figure 6. It should be compared with curve 2 of Figure 4, showing the indicatrix of the same particle at first approximation.

On preparing Table V we have eliminated from Blumer's data the numerical error contained therein. As stated more in detail in



Declassified in Part - Sanitized Copy Approved for Release 2012/03/12 : CIA-RDP82-00039R000100190014-6

Declassified in Part - Sanitized Copy Approved for Release 2012/03/12 : CIA-RDP82-00039R000100190014-6

paper /10/, in the formulas used by Blumer in his calculations there is omitted the factor $\frac{1}{2}$, so that his figures are twice too high. An analogous error appears in all other publications in which the results of Mie's formulas are presented in tabular form.

In the case a, for angles larger than 20 degrees Blumer gives only two determinant figures, the third figure (5), supplied by us in the case of some of the angles, is the result of dividing by two. To attain accuracy of one percent in the case a Blumer found it necessary to take into account four partial oscillations -- 2 electric and 2 magnetic. Our calculations in this instance are conducted in accordance with formula (85) simplified by omitting members $\sim x^4$. (In second approximation) On comparing columns 3 and 4 with the second, it is apparent that in case a, even first approximation gives an error not exceeding 5 percent, while simplified calculation of the second approximation results in an error not exceeding 0.8 percent. Since divergence of our data from those of Blumer is less than the accuracy of his computations, there is no reason for conducting calculations with a greater degree of preciseness, and the indicated conformity may be considered as being a very good one.

In case b, first approximation gives values less than those of Blumer. Error does not exceed 12 percent and its relative magnitude is almost constant. In the second approximation deviations from Blumer's data do not exceed 1.8 percent and the error is also almost constant. We note that to attain the necessary accuracy in this case Blumer had to take into account six partial oscillations.



Declassified in Part - Sanitized Copy Approved for Release 2012/03/12 : CIA-RDP82-00039R000100190014-6

Declassified in Part - Sanitized Copy Approved for Release 2012/03/12 : CIA-RDP82-00039R000100190014-6

The two examples so far considered show that for particles having dimensions commensurable to the wave length $\left(\frac{2\pi a}{\lambda} \gtrsim 1\right)$, one may limit oneself to the simple formulas of our derivation, omitting (on second approximation) members of higher order. Computations on the basis of formula (85) are effected more simply and more rapidly than by means of the sums of Mie.

b. Coefficient of Scatter

For a drop of water ( $n = \frac{4}{3}$ ) Mie formulas giving the coefficient of scatter $K$ were tabulated by Stratton and Houghton [15]. In Figure 7 we show a portion of their curve (curve 2) ($x = \frac{2\pi a}{\lambda}$ ). Using our formulas, we have calculated $K$, for the same specific instance. Graph $K = K_1(x)$ (first approximation) is shown in Figure 7, (curve 1). For comparison there is also shown Rayleigh's coefficient for a drop of water (curve 3). It can be seen that taking into account the interference of dipole waves, which differentiates our first approximation from Rayleigh's solution, leads to a considerable amplification of the range of scattering coefficient formula. Our formula for $K = K_1(x)$, even at first approximation, gives $K$ within the interval of $x$ from $0$ to 0.6, and even at its highest, within the middle portion, the relative error does not exceed 20 percent.

Figure 7. Coefficient of Scatter with Function

Figure 7 substantiates considerations adduced at the end of paragraph 4, relative to particle dimensions for which formulas of first approximation may still be used in computing total magnitude of scattered flux. It is apparent that in the case of a drop of



Declassified in Part - Sanitized Copy Approved for Release 2012/03/12 : CIA-RDP82-00039R000100190014-6

Declassified in Part - Sanitized Copy Approved for Release 2012/03/12 : CIA-RDP82-00039R000100190014-6

water we have $\frac{2\pi a}{\lambda} < 5$. (Stratton and Houghton give $\frac{\pi}{\pi_0} = 2$ .)

c. On the Rocard's Indicatrix

We have noted previously that our formula for indicatrix of first approximation coincides with the indicatrix given by Rocard. Therefore everything previously set forth on accuracy of first approximation indicatrixes applies to the accuracy of the indicatrix of Rocard. In particular, even when $\frac{2\pi a}{\lambda} \sim 1$, the error along certain directions (for a small sphere of ice or water) will be equivalent to 12 percent.

Therefore extending Rocard's indicatrix to apply to particles of large dimensions (as done by Rocard) is faulty. Insofar as drops of water are concerned, wherein $\frac{2\pi a}{\lambda} > 5$, Rocard's indicatrix yields in such cases an incorrect angular distribution of scattered light intensity, and furthermore the total magnitude of the scattered flux when computed on the basis of Rocard's indicatrix will be an incorrect one.

To obtain an indicatrix with an accuracy of 2 percent, even in the case of a sphere (of ice or water) wherein $\frac{2\pi a}{\lambda} \sim 1$, it is necessary to effect calculations taking into account the second approximation, that is, in accordance with our formula (85).

3. Scattering by Non-Spherical Particles

We noted previously that a substantial advantage of the new method of solving the problem of scattering is its ready adaptability to particles of arbitrary shape. Next in importance to particles of spherical shape are particles elongated and compressed



Declassified in Part - Sanitized Copy Approved for Release 2012/03/12 : CIA-RDP82-00039R000100190014-6

Declassified in Part - Sanitized Copy Approved for Release 2012/03/12 : CIA-RDP82-00039R000100190014-6

-- rods and disks. These may be ice rods and plates or particles of smoke and dust.

We will consider this problem at first approximation, and will approximate the rod-like and disk-like particles to rotation ellipsoids correspondingly elongated and compressed.

a. Field Scattered by Elongated Rotation Ellipsoid.

Let a monochromatic, linearly polarized wave strike a rotation ellipsoid, at an angle $\Delta$ to its longer axis (Figure 8).

$$\vec{E}=\vec{E}_0 e^{i(\vec{\kappa}\vec{r}-\omega t)}$$

In accordance with paragraph 4, the field scattered by the ellipsoid in some direction $\vec{R}_0$ is determined by formula:

$$E_{scat}=\alpha\frac{\kappa^2}{r_0}\vec{E}_{0\perp}f'(\vec{R}_0,\Delta). \qquad (93)$$

where

$$f'(\vec{R}_0,\Delta)=\int e^{i(\vec{\kappa}\vec{r}'+\kappa R)}dv;$$

wherein the integral is extended over the volume of the ellipsoid and all other quantities have the previous significance. Function $f'(\vec{R}_0,\Delta)$ can be calculated. It is found to be

$$f'(\vec{R}_0,\Delta)=v\cdot e^{i\kappa r_0}F(\Delta,\beta), \qquad (94)$$



Declassified in Part - Sanitized Copy Approved for Release 2012/03/12 : CIA-RDP82-00039R000100190014-6

Declassified in Part - Sanitized Copy Approved for Release 2012/03/12 : CIA-RDP82-00039R000100190014-6

where

$$F(\Delta,\beta) = \frac{3}{q^3}\left[\frac{1-\epsilon^2}{1-\epsilon^2+\alpha_{13}^2(1-\alpha_{13}^2)\epsilon^4}\right]^{3/2}\left\{\left[1+q^2\frac{\alpha_{13}^2(1-\alpha_{13}^2)\epsilon^4}{2(1-\epsilon^2)}\right]\sin q - q\cos q\right\}. \tag{95}$$

wherein $\beta$ is the angle of scatter; and $\epsilon$ the eccentricity of the ellipsoid.

$$\alpha_{13} = \frac{\cos\Delta - R_{0x}}{2\sin\frac{\beta}{2}}, \tag{96}$$

$$q = \frac{4\pi b}{\lambda}\frac{1}{\sqrt{1-\alpha_{13}^2\epsilon^2}}\sin\frac{\beta}{2}. \tag{97}$$

$R_{0x}$ is the cosine of the angle formed by direction $\vec{R}_0$ and the direction of the long axis; $b$ is the short half-axis. When $\epsilon \to 0$ the ellipsoid becomes a sphere. In that case

$$q \to \frac{4\pi b}{\lambda}\sin\frac{\beta}{2}, \text{ while } F \to \frac{3}{q^3}(\sin q - q\cos q).$$

Thus the scattered field also becomes exactly that of the expression representing the field scattered by a sphere /formula (26)/. We have seen already that for particles the dimensions of which are commensurable to the wave length, first approximation gives fairly accurate results: indicatrixes computed by us, using the above-given formulas, in the case where the long axis is ten



Declassified in Part - Sanitized Copy Approved for Release 2012/03/12 : CIA-RDP82-00039R000100190014-6

Declassified in Part - Sanitized Copy Approved for Release 2012/03/12 : CIA-RDP82-00039R000100190014-6

times the length of the short one, and where $\frac{2\pi}{\lambda}\sqrt[3]{\frac{3v}{4\pi}} = 1$ , are shown in Figure 9. Curve a corresponds to the indicatrix of scatter when the light comes in the direction of the long axis, while curve b is the indicatrix of scatter of the same ellipsoid when the light comes in the direction perpendicular to the long axis. This indicatrix is plotted upon the plane surface formed by the long axis of the particle and the incident ray.

The formulas can be simplified on transition to the case of a small particle, that is, on assuming

$$\frac{2\pi}{\lambda}\sqrt[3]{\frac{3v}{4\pi}} \ll 1.$$

We have then

$$F = \left[\frac{1-\epsilon^2}{1-\epsilon^2+\alpha_{13}^2(1-\alpha_{13}^2)\epsilon^4}\right]^{3/2}\left\{1+\frac{3}{2}\,\frac{\alpha_{13}^2(1-\alpha_{13}^2)\epsilon^4}{1-\epsilon^2}\right\}. \qquad (98)$$

Dependence on the angle of scattering $\beta$ is here introduced only by $\alpha_{13}$. Study of this case makes apparent a very important characteristic of Rayleigh's indicatrix of scatter. It is usually found that if the shape of the particle deviates but little from the spherical, the indicatrix of scatter differs but little from Rayleigh's. Thus in Figure 10, there is shown the indicatrix of scatter, along the longer axis, of a small ellipsoid, the long axis of which is 2.3 times longer than the short one (inner curve).



Declassified in Part - Sanitized Copy Approved for Release 2012/03/12 : CIA-RDP82-00039R000100190014-6

Declassified in Part - Sanitized Copy Approved for Release 2012/03/12 : CIA-RDP82-00039R000100190014-6

The outer curve is Rayleigh's indicatrix. In the center of the figure are shown, for comparison, the scattering ellipsoid and a sphere. The property under consideration may be referred to as stability of Rayleigh's indicatrix. On two to threefold comparison the indicatrix of scatter of a small particle undergoes almost no change.

b. Mean Indicatrix at Various Orientations.

If the ellipsoid is strongly compressed, for example so that its short axis is about 10 times smaller than the long axis, then its indicatrix is altered appreciably. It assumes the shape of a flattened, horizontal, figure eight. In such a case, without change in volume, the total amount of scattered light will become less.

In the atmosphere we usually have to deal with a mean indicatrix of scatter, of a large agglomerate of chaotically distributed particles. Let us assume that size and shape of all particles are identical. If the assumption is made that distribution of the particles in space is completely chaotic, the question arises as to whether or not the mean indicatrix is that of a sphere, and what is the volume of this sphere. For small particles the first part of the question can be answered affirmatively. Insofar as the second part of the question is concerned, it is found that the more elongated is the particle, the smaller must be the volume $v^*$ of the sphere that is equivalent thereto. If $v$ is the volume of the ellipsoid, we have for $v^*$ :



Declassified in Part - Sanitized Copy Approved for Release 2012/03/12 : CIA-RDP82-00039R000100190014-6

Declassified in Part - Sanitized Copy Approved for Release 2012/03/12 : CIA-RDP82-00039R000100190014-6

$$v^* = \sqrt{\varphi(\epsilon)}\, v_0$$

where $\varphi(\epsilon)$ is the following function of eccentricity $\epsilon$ :

$$\lambda = \frac{\epsilon^4}{1-\epsilon^2};$$

$$\varphi(\epsilon) = \varphi^*(\lambda) = \frac{1}{32(\lambda+4)^2}\left\{-(43\lambda+148) + \right.$$

$$\left. + \frac{1}{2\sqrt{\lambda^2+4\lambda}}\left[(A_\lambda - C_2^2 B_\lambda)\frac{2}{C_2}\arctan\frac{1}{C_2} + (A_\lambda + C_1^2 B_\lambda)\frac{1}{C_1}\ln\frac{C_1+1}{C_1-1}\right]\right\}. \qquad (99)$$

Here we have

$$A_\lambda = 41\lambda^2 + 363\lambda + 660; \quad B_\lambda = 21\lambda^2 + 72\lambda;$$

$$C_1 = \sqrt{\frac{\sqrt{\lambda+4} + \sqrt{\lambda}}{2\sqrt{\lambda}}};$$

$$C_2 = \sqrt{\frac{\sqrt{\lambda+4} - \sqrt{\lambda}}{2\sqrt{\lambda}}}.$$

A table of function $\varphi^*(\lambda) = \varphi_1(m)$ , wherein $m$ is the ratio of long to short axes, is given in /4/ [redacted] (In /4/ there is an error which incidentally affects neither the formulas nor the text. On page 18 $m = \frac{b}{a}$ is printed by error instead of $m = \frac{a}{b}$.)

Graph of $\varphi(m)$ is shown in Figure 11. When $\lambda \to \infty$ the function $\varphi^*(\lambda)$ has a simple asympotic expression, namely:



Declassified in Part - Sanitized Copy Approved for Release 2012/03/12 : CIA-RDP82-00039R000100190014-6

Declassified in Part - Sanitized Copy Approved for Release 2012/03/12 : CIA-RDP82-00039R000100190014-6

$$\varphi^*(\lambda) = \frac{1}{32\lambda}\left\{\frac{41}{2}\pi\sqrt{\lambda} + 31\ln 4\lambda - 43\right\} \qquad (100)$$

that is, when $\lambda \to \infty$ the function slowly decreases as $\frac{41\pi}{64\sqrt{\lambda}}$.

c. Disk-Like Particles.

What has been said relative to rod-like particles can be analogously restated for disk shaped particles. In this instance we have to deal with rotation ellipsoids, the transversal axis $b$ of which is longer than the axis of rotation $a$. In such a case eccentricity $\epsilon^*$ is determined by means of the following formula:

$$\epsilon^{*2} = \frac{b^2 - a^3}{b^2}.$$

Since in $F(\beta, \Delta)$, $\epsilon$ appears only as $\frac{\epsilon^4}{1-\epsilon^2}$, and that expression is equal to $\frac{\epsilon^{*4}}{1-\epsilon^{*2}}$, we now can simply replace in expression F, $\epsilon$ by $\epsilon^*$. Insofar as $q$ is concerned, it is now expressed by the formula:

$$q = \frac{4\pi a}{\lambda}\frac{\sin\frac{\beta}{2}}{\sqrt{1-\epsilon^{*2}(1-\alpha_{13}^2)}}, \qquad (101)$$

wherein $\alpha_{13}$ has the same significance as before.



Declassified in Part - Sanitized Copy Approved for Release 2012/03/12 : CIA-RDP82-00039R000100190014-6

Declassified in Part - Sanitized Copy Approved for Release 2012/03/12 : CIA-RDP82-00039R000100190014-6

In the instant case, with the same volume and ratio of axes as those of the previously considered example, we find that case *a* (Figure 9) corresponds to the indicatrix of scattering of light incident across the axis, while in case *b* to that of light incident lengthwise thereof. Thus the strongly compressed particle displays a behavior opposite to that of a strongly elongated rod. Polarization of scattered light in all instances here considered will be that of Rayleigh (first approximation).

## SUMMARY

Some of the overall results are as follows:

1. There is developed in the present paper a new method of solving the problem of light-scatter in the atmosphere by an admixed particle. The method is based on substituting for a system of differential equations a system of integral equations, the solution of which is determined as a series of a certain parameter $\alpha$. This parameter characterizes the degree of deviation of electrical properties of the scattering particle from properties of surrounding medium.

2. It is shown that electric properties of admixtures in atmosphere and hydrosphere are usually within the domain of applicability of the new method.

3. Solution is given of the problem of light scatter by a sphere, the dimensions of which are commensurable to the length of the wave scattered, taking into account mutual polarization.



Declassified in Part - Sanitized Copy Approved for Release 2012/03/12 : CIA-RDP82-00039R000100190014-6

Declassified in Part - Sanitized Copy Approved for Release 2012/03/12 : CIA-RDP82-00039R000100190014-6

4. Comparison is made of results computed on the basis of our formulas with results of tabulation of Mie's formulas, and an evaluation is given of the accuracy of various approximations, and particularly of Rocard's formula.

5. There is indicated a solution, in first approximation, of the problem as applied to rod-like and disk-like particles, and a study is made of the question relative to a "mean" indicatrix of scatter in the case of a chaotic distribution of particles.

6. It is established that the simple formulas of our derivation represent with a good degree of accuracy scatter of light by a small sphere of ice (or water), the dimensions of which are commensurable to the wave length. Simplicity of final formulas obtained is the essential attainment of the work.



Declassified in Part - Sanitized Copy Approved for Release 2012/03/12 : CIA-RDP82-00039R000100190014-6

Declassified in Part - Sanitized Copy Approved for Release 2012/03/12 : CIA-RDP82-00039R000100190014-6

4. Comparison is made of results computed on the basis of our formulas with results of tabulation of Mie's formulas, and an evaluation is given of the accuracy of various approximations, and particularly of Rocard's formula.

5. There is indicated a solution, in first approximation, of the problem as applied to rod-like and disk-like particles, and a study is made of the question relative to a "mean" indicatrix of scatter in the case of a chaotic distribution of particles.

6. It is established that the simple formulas of our derivation represent with a good degree of accuracy scatter of light by a small sphere of ice (or water), the dimensions of which are commensurable to the wave length. Simplicity of final formulas obtained is the essential attainment of the work.



Declassified in Part - Sanitized Copy Approved for Release 2012/03/12 : CIA-RDP82-00039R000100190014-6

Declassified in Part - Sanitized Copy Approved for Release 2012/03/12 : CIA-RDP82-00039R000100190014-6

# SOME PROBLEMS OF THE THEORY OF METEOREOLOGICAL FIELDS

M. I. Yudin

## 1. SIMILARITY OF TURBULENT MOTIONS AND PHYSICAL AVERAGING

Study of turbulent flow begins, as is known, with averaging, leveling of motion element fields. In so doing very important questions immediately arise: how should the averaging be effected; to what degree is this basic operation a matter of judgment; and to what extent does a change of averaging method alter the properties of physically-evolved motions, and fields of mean and fluctuant motions. More than fifty years ago, O. Reynolds raised these problems and supplied the first solution, basing it on the hypothesis of a qualitative difference between mean and fluctuant motion.

In the light of modern knowledge of turbulent flow structure, the solution of the averaging problem proposed by Reynolds can no longer be recognized as a satisfactory one. It has been found that averaging in time and space does not satisfy the basic postulate of averaging, that is to put it differently, spatial and time averages do not possess properties of probable averages (see /2/ paragraph 4). Hence there arises the need of an averaging method different in principle; an averaging with respect to multiple physical conditions of the fluid, satisfying definite conditions, which hereafter will be referred to as equivalence conditions. These conditions were defined in my publications /2/, /3/, and the indicated averaging



Declassified in Part - Sanitized Copy Approved for Release 2012/03/12 : CIA-RDP82-00039R000100190014-6

Declassified in Part - Sanitized Copy Approved for Release 2012/03/12 : CIA-RDP82-00039R000100190014-6

method was designated as physical averaging.

The meaning of equivalence conditions is very readily ascertained by considering an experimental investigation of turbulent flow. In this instance equivalence conditions signify identity of all experimental conditions, so that each individual experiment is a variation of one repeatedly performed experiment.

Nevertheless the momentary significances of motion elements at a given point of space are found to differ in each instance, and the process of motion acquires the nature of a fortuitous process. Thus the conditions of equivalence differ substantially from conditions of univalence (a concept introduced by academician M. V. Kirpichev and A. A. Gukhman /4/ in the derivation of adequate conditions of existent similarity).

Simultaneously, fulfillment of equivalence conditions ensures that in each experiment one chance variation is reproduced of a definite regularly occurring process of motion, and the regular occurrence of the process can be fully revealed by averaging a sufficient number of equivalent states.

From a mathematical standpoint physical averages may be considered as conditional mathematical expectations. Operation of physical averaging does not require introduction of any new mathematical apparatus, and fits entirely into the classic schemes of the theory of probability. But from a viewpoint of the physics of the phenomena, matters are much more complex. Determination of equivalence conditions in each instance is connected with a concrete physical analysis of characteristics of the process studied. In



Declassified in Part - Sanitized Copy Approved for Release 2012/03/12 : CIA-RDP82-00039R000100190014-6

Declassified in Part - Sanitized Copy Approved for Release 2012/03/12 : CIA-RDP82-00039R000100190014-6

fact, on repeating each physical experiment, it is necessary to define clearly what initial and limit conditions are to be reproduced. On correct selection of these conditions, repetition of a sufficiently large number of experiments must disclose definite laws of distribution of all elements of motion and identical values of all kinds of correlative momenta. But upon poor selection of conditions, omission of some factor determining the character of the motion, differences of empirical curves of distribution in several arbitrary series of experiments of sufficiently large scope will no longer be chance differences, and cannot then be described by general laws of the theory of probability (particularly the law of large numbers).

What has been said hereinbefore, is readily applicable to the case of an ideal experiment or to the instance where a selection is made of equivalent conditions from the sum total of observed states of motion (the latter case is most characteristic of the study of atmospheric motions). In these instances the basic problem involved with performing the physical averaging consists in the selection of equivalent conditions of fluid states, determined by physical characteristics of the process studied.

A good illustration of the significance of physical analysis in performing the averaging can be considered to be the problem, studied in papers /2/, and /3/, relating to various types of turbulent diffusion processes. At the same time these studies show how little, at present, the foundations of such physical analysis are developed. Hitherto not only no indication has been given of general rules which would make it possible to find the



Declassified in Part - Sanitized Copy Approved for Release 2012/03/12 : CIA-RDP82-00039R000100190014-6

Declassified in Part - Sanitized Copy Approved for Release 2012/03/12 : CIA-RDP82-00039R000100190014-6

conditions of equivalence in each problem, but also the basic principles of investigation have not yet even been formulated. The most elementary and initial concepts, such as the difference between diffusion of Richardson, and the classic process of turbulent transfer, are found to be novel. Thus, in the theory of averaging turbulent motion fields, ~~there~~ considerable difficulties still must be overcome. Averaging theory can however be very substantially advanced, if attention is devoted to the intimate connection of problems considered therein with the much better developed branch of hydromechanics concerned with problems of modeling.

With this purpose in view let us consider the class of motions derived from equivalent ones by means of arbitrary transformations of similarity. These motions are not similar in the strict meaning of the term. As is readily apparent, however, conventional definition of similarity/ loses its meaning altogether on study of turbulent motions; for instance, velocity fields of steady turbulent flow at two different points of time will not be similar to one another from the standpoint of this definition. Reverting again to the simplest case of experimental turbulent motion study, we reach the conclusion that it is only possible to speak of a reproduction on a different scale of all experimental conditions, that is, of a similarity of equivalent conditions. Thus we arrive at the above-cited class of motions, henceforth designated as being "summatively similar," and sometimes simply as similar, without further qualification, in full accordance with the practical use of this concept.



Declassified in Part - Sanitized Copy Approved for Release 2012/03/12 : CIA-RDP82-00039R000100190014-6

Declassified in Part - Sanitized Copy Approved for Release 2012/03/12 : CIA-RDP82-00039R000100190014-6

From the standpoint of classical theory of similarity, in order to determine recurring regularities appearing in a whole class of similar motions, a single, ideally accurate experiment is sufficient. The necessity of repeating experiments and averaging the results obtained is stipulated, from this viewpoint, only by the unknown errors of the single experiment. On experimental study of turbulent flow, the necessity of repeating experiments, and of physical averaging of results, is one of principle and is determined by basic properties of the motion. It is not at all indispensible, however, on repeating the experiments, to be limited by equivalent states. Averaging can be effected just as successfully for a series of experiments, in which conditions of summative similarity are maintained, following reduction of all measurement results to some set scale of motion (or even better to a non-dimensional form).

We can now materially generalize the determination of the physical average by defining it in the following words. Physical average is the average of adduced values of a given element for the aggregate of similar motions at corresponding points and at corresponding times.

The new formulation establishes directly the connection between theory of physical averaging and theory of similarity, and thus makes it possible to utilize a number of very important developments of the theory of similarity on the basis of this viewpoint.



Declassified in Part - Sanitized Copy Approved for Release 2012/03/12 : CIA-RDP82-00039R000100190014-6

Declassified in Part - Sanitized Copy Approved for Release 2012/03/12 : CIA-RDP82-00039R000100190014-6

Actually, the problem concerning the conditions of similarity of turbulent motions is solved in practice for many classes of motions which have important applications in aero-hydrodynamics and thermotechnics. In all these cases analysis of equivalence conditions, which presents, as previously stated, the greatest difficulties to performing the operation of physical averaging, has been effected by empirical means. This substantially simplifies further development of the theory of physical averaging.

At the same time it must be stressed that the problem relative to necessary and sufficient conditions of similarity of turbulent motions is far from being solved in its general aspects.

The basic question of initial conditions and conditions at fluid boundaries (condition $b$ of state equivalence, as formulated in my paper /2/) is reduced to the condition of identical kinematic development of streams by the originators of fundamental investigations in the field of similarity theory. Thus A. A. Gukhman (/5/, page 119) writes:

"If two streams are kinematically equally developed, we may assert that at the boundaries of the system there are established conditions, ensuring a similarity of kinematic state, even though we do not know in what specific quantities this state is characterized in an exhaustive manner...

"Thus kinematic development of the stream consists in a reproduction of all those conditions, upon which is dependent the kinematic picture at boundaries, at the initial moment. In practice, it is always possible to ascertain with sufficient



Declassified in Part - Sanitized Copy Approved for Release 2012/03/12 : CIA-RDP82-00039R000100190014-6

Declassified in Part - Sanitized Copy Approved for Release 2012/03/12 : CIA-RDP82-00039R000100190014-6

clarity what specific circumstances are the essential ones from this standpoint."

Consequently, A. A. Gukhman does not deny the lack of general rules for finding the necessary and sufficient conditions of motion similarity.

Thus he characterizes in the following manner the significance, in principle, of the problem under consideration (loc. cit. page 107):

"Meanwhile not having available precisely formulated univalence conditions, we are not in a position to apply to a full extent the apparatus of the theory of similarity. What is important is the fact that there are thus lost precisely those elements of research which are of greatest practical value. Not knowing the list of univalence conditions we are unable to answer the basic question as to the criteria sufficient for asserting the existence of similarity.

"But in such case it also does not appear possible to ascertain which of the criteria are determinant. And this means that correlating equations of the criteria cannot be formulated, - those fundamental equations which determine the general design of the experiment and the manner in which results are interpreted."

The cited statements appear to be indisputable if in them "conditions of equivalence" are substituted for "conditions of univalence." It follows that elucidation of the hitherto insufficiently determined concept of "kinematic development of the



Declassified in Part - Sanitized Copy Approved for Release 2012/03/12 : CIA-RDP82-00039R000100190014-6

Declassified in Part - Sanitized Copy Approved for Release 2012/03/12 : CIA-RDP82-00039R000100190014-6

stream" constitutes one of the most important problems of the theory of similarity. It appears to me that the clarification proposed here of fundamental concepts may substantially facilitate further investigations aiming at coordination and systematization of the vast experimental material pertaining to the theory of similarity, and the establishment of general rules for proper performance of experimental study of turbulent flow.



Declassified in Part - Sanitized Copy Approved for Release 2012/03/12 : CIA-RDP82-00039R000100190014-6

Declassified in Part - Sanitized Copy Approved for Release 2012/03/12 : CIA-RDP82-00039R000100190014-6

## 2. OPTIMUM CHARACTERISTICS OF AVERAGING IN TIME AND SPACE

The introduction of physical averaging as a basic method of averaging motion element fields by no means eliminates the necessity to study further the characteristics of space and time average quantities.

Such studies are necessary merely because, if for no other reasons, the readings of all our measuring instruments are quantities averaged to some degree in time and space. Moreover, very often some of the characteristics of state equivalence are reducible to conditions of equality of space and time averages. Thus, in studying flow in pipes an essential condition of state equivalence is the equality of discharge; in the study of wind distribution by altitude, the quality of geostrophic wind expressed by means of the average value of the horizontal gradient (that is, terminal difference) of pressure at a given altitude, and so forth.

Also there must be kept in mind the substantial practical significance of averaging in time and space when solving a number of important meteorological problems. This significance is most clearly formulated in the publications of L. B. Keller, /6/, /7/, who worked out many important results in the field of space-time averaging theory, as well as various applications of this operation.

Finally, of special importance are those instances where averaging in time and space may be considered as an empirical method of effecting physical averaging. Such a possibility arises in steady



Declassified in Part - Sanitized Copy Approved for Release 2012/03/12 : CIA-RDP82-00039R000100190014-6

Declassified in Part - Sanitized Copy Approved for Release 2012/03/12 : CIA-RDP82-00039R000100190014-6

mean motion, when it is expedient to perform averaging in time within the limits of one experiment. In the same manner under condition of independence of mean motion elements from one of the spatial coordinates, it is convenient to effect averaging with respect to this coordinate.

Considerations presented here indicate the existence of a definite correlation between characteristics of space and time average quantities, and the general characteristics of fields of turbulent motion.

Problems considered hereinafter are intended to render definite and to illustrate the nature of this correlation. From this standpoint they appear of sufficient interest, despite the elementary nature of the mathematical apparatus utilized.

Let us investigate first the question of most advantageous duration of meteorologic measurements.

Let a certain meteorological element be measured by a registering instrument over a length of time $\theta$ . Over the length of time T the meteorological station assumes the value of the given element f(t) to be equal to its mean value at the time of the last measurement, and supplies the corresponding information to the experimenters. (The conditions indicated are very frequently encountered in practice, this being especially true of aerologic observations.) It must be determined what is the optimum duration of averaging interval $\theta$ , for the given T, assuming the measure-



Declassified in Part - Sanitized Copy Approved for Release 2012/03/12 : CIA-RDP82-00039R000100190014-6

Declassified in Part - Sanitized Copy Approved for Release 2012/03/12 : CIA-RDP82-00039R000100190014-6

ment error as being negligibly small (in the solution of most of the problems, in practice, the measurement error must, of course be taken into account, which can be readily ascertained in each instance by means of the same computation methods).

Thus, the problem consists in finding the minimum error of a specific extrapolated forecast. Obviously the error of such a single forecast is an indefinite quantity, and, what is being considered is the minimum of some characteristic of distribution of a large number of forecasts under equal external conditions. From considerations equal in such cases, it follows that the most important characteristic is the average (physical) square of the error, the minimum of which we must determine.

It being agreed that time reckoning is to start from the moment of termination of the preceding measurement, the error due to replacement of the actual value of the element by the measured value is then equal to:

$$f(t) - \frac{1}{\theta}\int_{-\theta}^{0} f(\tau)\,d\tau.$$

On taking into account the fact that at any moment, from 0 until T, the value of the measured meteorological element may be needed, with equal degree of probability the average square of error assumes the form:



Declassified in Part - Sanitized Copy Approved for Release 2012/03/12 : CIA-RDP82-00039R000100190014-6

Declassified in Part - Sanitized Copy Approved for Release 2012/03/12 : CIA-RDP82-00039R000100190014-6

$$\psi_1(\theta,T)=\frac{1}{T}\int_0^T\overline{\left[f(t)-\frac{1}{\theta}\int_{-\theta}^{0}f(\tau)\,d\tau\right]^2}\,dt=$$

$$=\frac{1}{T\theta^2}\int_0^T dt\int_{-\theta}^{0}d\tau\int_{-\theta}^{0}\overline{[f(t)-f(\tau)][f(t)-f(\tau_1)]}\,d\tau_1\,. \qquad (1)$$

Our next problem is to express quantity $\psi_1$ by means of momentary characteristics of the chance function f(t). This question must be considered somewhat in detail. The "connection moments" introduced in the remarkable paper of A. A. Friedmann and L. V. Keller /25/ make possible a complete description of chance fields of motion elements.

In practice however utilization of connection moments can be done conveniently only in considering uniform fields of chance; this generally constitutes a fairly substantial limitation. Therefore a very great importance is acquired by the introduction in hydrodynamics and theoretical meteorology, of the concept of structural functions, contributed by academician A. N. Kolmogorov /8/. On divisional study of the fields of each element of motion the structural function is determined as the average square of difference between values of the given element at two different points at different moments.

$$b_f(\xi,\eta,\zeta,\tau)=$$

$$=\overline{\left[f\left(x+\frac{\xi}{2},y+\frac{\eta}{2},z+\frac{\zeta}{2},t+\frac{\tau}{2}\right)-f\left(x-\frac{\xi}{2},y-\frac{\eta}{2},z-\frac{\zeta}{2},t-\frac{\tau}{2}\right)\right]^2} \qquad (2)$$



Declassified in Part - Sanitized Copy Approved for Release 2012/03/12 : CIA-RDP82-00039R000100190014-6

Declassified in Part - Sanitized Copy Approved for Release 2012/03/12 : CIA-RDP82-00039R000100190014-6

Determination of structural function by means of formula (2) also expresses the most important characteristic of the structural function formulated by A. N. Kolmogorov in the form of a hypothesis of local uniformity of turbulent fields. This characteristic consists in the structural function being independent of the mean coordinates x, y, z, t, (naturally, within limits of a certain terminal region of the changes of these coordinates), but depends only on the relative coordinates $\xi, \eta, \zeta, \tau$. The hypothesis of local uniformity correctly reflects the actual characteristics of atmospheric motions, and is realized also in those instances when the mean square of the function proper depends essentially on coordinates and time; this was established on the basis of extensive investigations of the climatological section of GGO, conducted in the course of the last 15 years under the general direction of O. A. Drozdov /9/, 10/. For the field of mean monthly temperatures the characteristic of local uniformity was established back in 1922 by E. S. Rubinshtein /11/.

Hereafter the characteristic of local uniformity will be accepted throughout as correct, and all kinds of secondary moments will be expressed by means of structural function values. In those cases where some of the arguments of function $C_f$ become equal to zero, they will be omitted in the formulation of functional dependence.

Then: $C_f(0, 0, 0, \tau) = C_f(\tau)$.



Declassified in Part - Sanitized Copy Approved for Release 2012/03/12 : CIA-RDP82-00039R000100190014-6

Declassified in Part - Sanitized Copy Approved for Release 2012/03/12 : CIA-RDP82-00039R000100190014-6

We now transform the expression within the sign of integration in (1), using the equation:

$$2[\varphi(A)-\varphi(B)][\varphi(C)-\varphi(D)]=[\varphi(A)-\varphi(D)]^2+[\varphi(B)-\varphi(C)]^2-$$
$$-[\varphi(A)-\varphi(C)]^2-[\varphi(B)-\varphi(D)]^2, \qquad (3)$$

in which A, B, C, D are points within the four-dimensional space x, y, z, t.

We have then,

$$\psi_1(\theta,T)=\frac{1}{2T_1\theta^2}\int_0^T dt\int_{-\theta}^{0} d\tau\int_{-\theta}^{0}[b_f(t-\tau_1)+b_f(t-\tau)-b_f(\tau-\tau_1)]\,d\tau_1=$$
$$=\frac{1}{T_1\theta}\int_0^T dt\int_{-\theta}^{0} b_f(t-\tau)\,d\tau-\frac{1}{2\theta^2}\int_{-\theta}^{0} d\tau\int_{-\theta}^{0} b_f(\tau-\tau_1)\,d\tau_1. \qquad (4)$$

Thereafter it is expeditious to render more definite the form of function $b_f(\tau)$, although the problem concerning the minimum $\psi_1(\theta,T)$, as a function of averaging interval $\theta$, can obviously be solved for any given form of function $b_f(\tau)$, analytic or graphic. (In the latter case it is best first to transform the double integrals of (4) into simple integrals, and then to plot $\psi_1$ as a function of $\theta$).



Declassified in Part - Sanitized Copy Approved for Release 2012/03/12 : CIA-RDP82-00039R000100190014-6

Declassified in Part - Sanitized Copy Approved for Release 2012/03/12 : CIA-RDP82-00039R000100190014-6

Theoretical investigations of the field of wind have shown that the structural function of wind is very well described by the power law. For small intervals of time (more precisely, the laws indicated are obtained on investigating the spatial structure. For a determination of the dependence of structural function on time interval, the hypothesis of fluctuation transfer by mean stream is utilized, which tallies well with actual conditions) (microstructure) A. N. Kolmogorov /8/, and A. M. Obukhov /12/ obtained the known law:

$$b(\tau) \sim |\tau|^{2/3}$$

whereas, for considerable intervals of time (macrostructure) I obtained (/2/ paragraph 9) one of the first order:

$$b(\tau) \sim |\tau|$$

Both of these laws have been substantiated experimentally; the 2/3 law by the results of experiments by A. M. Obukhov /12/ and his interpretations of experimental data of Gedeke; the law of first power by the data of Ye. S. Seleznevoy /12/ and M. V. Zaverinoy /15/; and were successfully applied to the solution of a number of practical problems. It should be noted that the first power law is correct only under free atmosphere conditions. In the layer of air close to the ground the dependence of structural function on the time interval is of a more complex form, although



Declassified in Part - Sanitized Copy Approved for Release 2012/03/12 : CIA-RDP82-00039R000100190014-6

Declassified in Part - Sanitized Copy Approved for Release 2012/03/12 : CIA-RDP82-00039R000100190014-6

in some cases it can also be rendered by the power law.

In any case it is expedient to study in detail the dependence of the form

$$b(\tau) = \beta|\tau|^n, \tag{5}$$

considering n as a parameter determining the solution form of the minimum problem.

In such a case we have:

$$\psi_1(\theta,T) = \frac{\beta}{(n+1)(n+2)T}\left[\frac{(T+\theta)^{n+2} - T^{n+2}}{\theta} - T\theta^n - \theta^{n+1}\right]$$

or, on introducing a new variable

$$q = \frac{\theta}{T}$$

and the function

$$\Phi_1(q) = \frac{(n+1)(n+2)}{\beta T^n}\psi_1(\theta,T),$$



Declassified in Part - Sanitized Copy Approved for Release 2012/03/12 : CIA-RDP82-00039R000100190014-6

Declassified in Part - Sanitized Copy Approved for Release 2012/03/12 : CIA-RDP82-00039R000100190014-6

we have

$$\Phi_2(q) = \frac{1}{q}(1+q)^{n+2} - \frac{1}{q} - q^n - q^{n+1}. \qquad (6)$$

On studying the sign of the derivative function $\Phi_2(q)$ we readily find that:

$$\left.\frac{d\Phi_2(q)}{dq}\right|_{q=0} < 0; \quad \left.\frac{d\Phi_2(q)}{dq}\right|_{q\to\infty} > 0 \text{ for } 0<n<1$$

and

$$\frac{\partial\Phi_2(q)}{\partial q} > 0 \text{ for } q \geqslant 0 \text{ and for } n \geqslant 1.$$

It follows therefrom that at any n located between zero and one, there can be found an optimum interval of averaging, but when $n \geqslant 1$ the smallest error would be produced by the ideally precise momentary data.

Now, on elementary computation we find some values of $q = \frac{\theta}{T}$, at which function $\Phi_1(q)$ and hence also $\psi_1(\theta, T)$ attain a minimum (Table I).



Declassified in Part - Sanitized Copy Approved for Release 2012/03/12 : CIA-RDP82-00039R000100190014-6

Declassified in Part - Sanitized Copy Approved for Release 2012/03/12 : CIA-RDP82-00039R000100190014-6

TABLE I

Values of $\frac{\theta}{T}$ at which $\frac{1}{T}\int_0^T \left[f(t) - \frac{1}{\theta}\int_{-\theta}^{0} f(\tau)\,d(\tau)\right]^2 dt$ reaches a minimum

| $n$ | $1/10$ | $1/3$ | $2/3$ | $9/10$ | $\geqslant 1$ |
|---|---|---|---|---|---|
| $\frac{\theta}{T}$ | 2.5 | 0.22 | 0.033 | $1.4 \times 10^{-5}$ | 0 |

It is important that, with the form of structural function under consideration, optimum values of $\frac{\theta}{T}$ are found to be independent of absolute values of T (which actually was apparently beforehand). Thus values of $\frac{\theta}{T}$ shown in the table have the nature of certain constants reflecting the basic structure of the medium (power exponent n). Of special importance becomes the law of first power; this sharply segregates the class of motions, to which is appropriate an averaging of values of the meteorological element measured, from the class of motions for which results superior in principle are obtained by extrapolation of momentary values of the element (under conditons of absolute accuracy of measurements).

In order to evaluate the degree of generality of the solutions obtained, let us consider also another variant of practical utilization of meteorological data. In the solution of a number of applied problems it is necessary to reach a con-



Declassified in Part - Sanitized Copy Approved for Release 2012/03/12 : CIA-RDP82-00039R000100190014-6

Declassified in Part - Sanitized Copy Approved for Release 2012/03/12 : CIA-RDP82-00039R000100190014-6

clusion not concerning the momentary value of meteorological element f(t), but concerning its mean value. Problems of this nature are characteristic, for example, of aero-navigation, wherein the value of travel velocity or drift angle, obtained in the last measurement, is used as the mean value for time interval T, separating two consecutive measurements. Accordingly the mean square of extrapolation error assumes the form:

$$\psi_1(\theta, T) = \left[\frac{1}{T}\int_0^T f(\tau)\,d\tau - \frac{1}{\theta}\int_{-\theta}^{0} f(\tau)\,d\tau\right]^2 \qquad (7)$$

Transforming this expression in a manner analogous to the prior transformation of $\psi_1(\theta, T)$ by means of equation (3), we have

$$\psi_2(\theta,T) = \frac{1}{T\theta}\int_0^T d\tau \int_{-\theta}^{0} b_f(\tau-\tau_1)\,d\tau_1 -$$

$$-\frac{1}{2\theta^2}\int_{-\theta}^{0} d\tau \int_{-\theta}^{0} b_f(\tau-\tau_1)\,d\tau_1 - \frac{1}{2T^2}\int_0^T d\tau \int_0^T b_f(\tau-\tau_1)\,d\tau_1 . \qquad (8)$$



Declassified in Part - Sanitized Copy Approved for Release 2012/03/12 : CIA-RDP82-00039R000100190014-6

Declassified in Part - Sanitized Copy Approved for Release 2012/03/12 : CIA-RDP82-00039R000100190014-6

Now on comparing $\psi_2(\theta,T)$ and $\psi_1(\theta,T)$ /See (4)/ we find:

$$\psi_2(\theta,T)=\psi_1(\theta,T)-\frac{1}{2T^2}\int_0^T d\tau\int_0^T b_j(\tau-\tau_1)\,d\tau_1 \qquad (9)$$

From this the conclusion is reached directly that our minimum problem is reduced to the one already considered, and that all previously obtained results, including Table I, hold in the case of extrapolation of mean values. This conclusion, which could hardly be foreseen beforehand, shows that the determined optimum correlations between averaging interval of meteorological data and the time of their action, are not chance characteristics differing in each problem, but are stable characteristics of the structure of the medium.

An essential feature of the problem considered is that the result of measurement is compared with the future value of the meteorological element. On consideration of measurements intended to characterize only actual physical conditions (regardless whether momentary or average), no minimum problem is encountered. It is immediately apparent that in this very common case continuous registration of values of meteorological elements by objective instruments meets any kind of requirement (we must remember that the question of observation errors is not being considered here. If, however, transition is effected from averaging with respect to one variable, to spatial, or to the even more general space-time



Declassified in Part - Sanitized Copy Approved for Release 2012/03/12 : CIA-RDP82-00039R000100190014-6

Declassified in Part - Sanitized Copy Approved for Release 2012/03/12 : CIA-RDP82-00039R000100190014-6

averaging (which actually always takes place in performing the measurements), a new type of problem arises -- specifically, problems concerned with optimum correlations between averaging intervals with regard to different variables.

On passing to the consideration of the simplest problem of this type, let us recall as a preliminary, some postulates of the theory of space-time averaging.

The most general form of space-time averaging is given by the expression

$$(\omega)\overline{f(x_1,\ldots,x_4)} = \int_{-\infty}^{+\infty}\int\int\int f(x_1-y_1,\ldots,x_4-y_4)\,\omega(y_1,\ldots,y_4)\,dy_1,\ldots,dy_4, \qquad (10)$$

wherein indexes 1, 2, relate to horizontal axes; $x_3$ (and $y_3$) to altitude; $x_4$ (and $y_4$) denote time; index ($\omega$ ), to the left of the line, differentiates the averaging being performed from the physical. Function $\omega\ (y_1, y_2, y_3, y_4)$, called leveling function, or weight, is not negative for any values of independent variables, and as a rule is such that any of its moments is finite.

In addition, $\omega\ (y_1,\ldots.y_4)$ must satisfy normalizing condition:



Declassified in Part - Sanitized Copy Approved for Release 2012/03/12 : CIA-RDP82-00039R000100190014-6

Declassified in Part - Sanitized Copy Approved for Release 2012/03/12 : CIA-RDP82-00039R000100190014-6

$$\int_{-\infty}^{+\infty}\int\int\int \omega(y_1,\ldots,y_4)\,dy_1,\ldots,dy_4 = 1 . \qquad (11)$$

The simplest form of averaging, which we have already utilized repeatedly in the present paper, is readily generalized in the case of space and time averaging.

It suffices to assume:

$$\omega(y_1,\ldots,y_4) = \begin{cases} \dfrac{1}{S_1 S_2 S_3 S_4}, \text{ if } |y_j| \leq \dfrac{S_j}{2} \ (j=1,\ldots,4); \\ 0, \text{ if } |y_1| > \dfrac{S_1}{2} \text{ or } \ldots \text{ or } |y_4| > \dfrac{S_4}{2}. \end{cases} \qquad (12a)$$

L. V. Keller /7/ has evolved another very important class of leveling functions with a number of remarkable characteristics, analogous to the characteristics of the normal distribution law of the theory of probability and expressed by the probability density formula of this law:

$$\omega(y_1,\ldots,y_4) = \frac{1}{4\pi^2\sigma_1,\ldots,\sigma_4} \exp\left\{-\frac{y_1^2}{2\sigma_1^2}-\ldots-\frac{y_4^2}{2\sigma_4^2}\right\} \qquad (12b)$$



Declassified in Part - Sanitized Copy Approved for Release 2012/03/12 : CIA-RDP82-00039R000100190014-6

Declassified in Part - Sanitized Copy Approved for Release 2012/03/12 : CIA-RDP82-00039R000100190014-6

Averaging with leveling function (12b) is found in many instances very convenient in the course of theoretical investigations.

Both of the indicated classes of leveling functions have four available parameters for the number of independent variables. In particular, without excluding the possibility of conversion of one or several parameters $s_j$ and $\sigma_j$ to zero, which lead to a reduction of the number of measurements of averaging scope. (Although averaging by formula (12b) is effected over the entire infinite space, in practice values of $f(x_1 - y_1, \ldots, x_1 - y_4)$ at high values of arguments, do not affect the mean value. By analogy with (12a) we will hereafter designate by averaging scope of formula (12b) the quantity appearing in the denominator.)

The basic prerequisite which is naturally applied to space-time averaging may be formulated as follows: fields of mean values must reflect in the nearest possible manner the characteristics of non-averaged fields. If, for example, we agree to compare only different variants of averaging by equal scope, we see immediately that selection of values $s_j$ and $\sigma_j$ is far from being immaterial from this standpoint.

The most advantageous correlations of dimensions in different directions is determined, of course, by characteristics of the field being averaged, and only by these characteristics. To render this definition more precise we can say offhand that on using the principle of least squares, solution of minimum problem will



Declassified in Part - Sanitized Copy Approved for Release 2012/03/12 : CIA-RDP82-00039R000100190014-6

Declassified in Part - Sanitized Copy Approved for Release 2012/03/12 : CIA-RDP82-00039R000100190014-6

depend solely on the form of structural function.

Problems to be solved are formulated almost identically in the case of simple averaging with weight (12a) and in the case of averaging with leveling function (12b). Since in the consideration of the foregoing problem, simple averaging was used, it is desirable to demonstrate the solution of at least one problem by the utilization of weight (12b).

In so doing we will use spatial averaging and assume that the function under consideration depends on coordinates $x_1$, $x_2$, $x_3$ but not on time $x_4$. All the results that we will obtain can be automatically transferred to the general case of space-time averaging, but it must be kept in mind that the proposed formulation of the problem will be less well founded, physically, in the latter case.

Following these preliminary remarks let us pass onto the formulation of the problem proper. Let us find among the class of functions:

$$\omega(y_1, y_2, y_3) = \frac{1}{(2\pi)^{3/2}\sigma_1\sigma_2\sigma_3} \exp\left\{-\frac{y_1^2}{2\sigma_1^2} - \frac{y_2^2}{2\sigma_2^2} - \frac{y_3^2}{2\sigma_3^2}\right\}, \quad (12c)$$

connected by the condition of equality of averaging scope,

$$(2\pi)^{3/2}\sigma_1\sigma_2\sigma_3 = \Gamma = idem \quad (13)$$

the function is converted into minimum average (physical) square



Declassified in Part - Sanitized Copy Approved for Release 2012/03/12 : CIA-RDP82-00039R000100190014-6

Declassified in Part - Sanitized Copy Approved for Release 2012/03/12 : CIA-RDP82-00039R000100190014-6

of deviation of spatial average from actual value of function:

$$\psi_3(\sigma_1, \sigma_2, \sigma_3) = \overline{\left[\overset{\omega}{f}(x_1, x_2, x_3) - f(x_1, x_2, x_3)\right]^2} = \min. \tag{14}$$

We perform first of all a general transformation of expression (14). We have, in view of normalizing condition (11),

$$f(x_1, x_2, x_3) - \int_{-\infty}^{+\infty}\int\int f(x_1 - y_1, x_2 - y_2, x_3 - y_3)\,\omega(y_1, y_2, y_3)\,dy_1\,dy_2\,dy_3 =$$

$$= \int_{-\infty}^{+\infty}\int\int [f(x_1, x_2, x_3) - f(x_1 - y_1, x_2 - y_2, x_3 - y_3)]\,\omega(y_1, y_2, y_3)\,dy_1\,dy_2\,dy_3.$$

It follows therefore that:

$$\left[\overset{\omega}{f}(x_1, x_2, x_3) - f(x_1, x_2, x_3)\right]^2 = \int_{-\infty}^{+\infty}\int\int\int\int\int\int [f(x-y) - f(x)][f(x-z) -$$

$$- f(x)]\,\omega(y)\,\omega(z)\,dy\,dz.$$



Declassified in Part - Sanitized Copy Approved for Release 2012/03/12 : CIA-RDP82-00039R000100190014-6

Declassified in Part - Sanitized Copy Approved for Release 2012/03/12 : CIA-RDP82-00039R000100190014-6

Here have been introduced abbreviated designations, such as,

$$f(x-y) = f(x_1-y_1,\ x_2-y_2,\ x_3-y_3);$$

$$dz = dz_1\, dz_2\, dz_3.$$

using equation (3) we have on physical averaging:

$$\psi_3(\sigma_1, \sigma_2, \sigma_3) = \frac{1}{2}\int_{-\infty}^{+\infty}\int\int\int\int\int\int [b(y) + b(z) - b(z-y)]\, w(y)\, w(z)\, dy\, dz =$$

$$= \int_{-\infty}^{+\infty}\int\int\int b(y)\, w(y)\, dy - \frac{1}{2}\int_{-\infty}^{+\infty}\int\int\int\int\int\int b(z-y)\, w(y)\, w(z)\, dy\, dz.$$

(15)

It is very important that value $\psi_3$ does not depend on $x_1$, $x_2$, $x_3$. (This conclusion follows from characteristics of local uniformity of flow which formally should be extended in our case upon the entire infinite space. In practice, however, as follows from the foregoing considerations, it is sufficient to exact the fulfillment of local uniformity characteristics to the area of volume $\Gamma$, while only moderate limitations, which are always possible, are applied to the values of structural function outside this volume.) Due to this $\psi_3$ is found to be a representative characteristic of deviation of the leveled field of motion from the actual. We also note that expression (15) is correct for any



Declassified in Part - Sanitized Copy Approved for Release 2012/03/12 : CIA-RDP82-00039R000100190014-6

Declassified in Part - Sanitized Copy Approved for Release 2012/03/12 : CIA-RDP82-00039R000100190014-6

form of leveling function, if $\sigma_j$ are considered as arbitrary parameters characterizing the form of function. (Their number, of course, may differ from three.)

For the considered concrete form of leveling function given by formula (12c) the second integral of formula (15) permits an elementary transformation.

Introducing in lieu of variables yj and zj, new variables $y_j'$ and $z_j'$, by means of correlations:

$$\sqrt{2}\,y_j' = z_j - y_j;\quad \sqrt{2}\,z_j' = z_j + y_j,$$

we have

$$\int_{-\infty}^{+\infty}\int\int\int\int\int b(z-y)\,\omega(y)\,\omega(z)\,dy\,dz = \int_{-\infty}^{+\infty}\int\int\left[\int_{-\infty}^{+\infty}\int\omega\left(\frac{\sqrt{2}}{2}z' - \frac{\sqrt{2}}{2}y'\right)\omega\left(\frac{\sqrt{2}}{2}z' + \frac{\sqrt{2}}{2}y'\right)dz'\right] b(\sqrt{2}\,y')\,dy'.$$

In view of known characteristics of the normal law, integration of the expression within brackets is readily effected, whereupon we find that:



Declassified in Part - Sanitized Copy Approved for Release 2012/03/12 : CIA-RDP82-00039R000100190014-6

Declassified in Part - Sanitized Copy Approved for Release 2012/03/12 : CIA-RDP82-00039R000100190014-6

$$\psi_3(\sigma_1,\sigma_2,\sigma_3)=\frac{1}{(2\pi)^{3/2}\sigma_1\sigma_2\sigma_3}\int_{-\infty}^{+\infty}\iiint\exp\left\{-\frac{y_1^2}{2\sigma_1^2}-\frac{y_2^2}{2\sigma_2^2}-\frac{y_3^2}{2\sigma_3^2}\right\}\left[b(y_1,y_2,y_3)-\right. \tag{16}$$

$$\left.-\frac{1}{2}b(\sqrt{2}y_1,\sqrt{2}y_2,\sqrt{2}y_3)\right]dy_1\,dy_2\,dy_3.$$

We form now in accordance with the general rules of determining conventional extreme, the function

$$\Phi(\sigma_1,\sigma_2,\sigma_3)=\Gamma\psi_3(\sigma_1,\sigma_2,\sigma_3)+\lambda\left[(2\pi)^{3/2}\sigma_1\sigma_2\sigma_3-\Gamma\right] \tag{17}$$

and we bring to zero the derivatives of this function in $\sigma_j$ ($j = 1, 2, 3$). Then we have three equations:

$$\int_{-\infty}^{+\infty}\iiint\exp\left(-\frac{y_1^2}{2\sigma_1^2}-\frac{y_2^2}{2\sigma_2^2}-\frac{y_3^2}{2\sigma_3^2}\right)\frac{y_j^2}{\sigma_j^2}\left[b(y_1,y_2,y_3)-\right. \tag{18}$$

$$\left.-\frac{1}{2}b(\sqrt{2}y_1,\sqrt{2}y_2,\sqrt{2}y_3)\right]dy_1\,dy_2\,dy_3+\frac{\lambda\Gamma}{\sigma_j}=0.$$

We eliminate $\lambda$ and pass to non-dimensional variables

$$\eta_j=\frac{y_j}{\sigma_j}\ , \tag{19}$$



Declassified in Part - Sanitized Copy Approved for Release 2012/03/12 : CIA-RDP82-00039R000100190014-6

Declassified in Part - Sanitized Copy Approved for Release 2012/03/12 : CIA-RDP82-00039R000100190014-6

whereupon we have:

$$\iiint_{-\infty}^{+\infty} \eta_1^2 \exp\left(-\sum_{k=1}^{3} \frac{\eta_k^2}{2}\right) \left[b(\sigma_1\eta_1, \sigma_2\eta_2, \sigma_3\eta_3) - \right.$$

$$\left. - \frac{1}{2} b(\sqrt{2}\sigma_1\eta_1, \sqrt{2}\sigma_2\eta_2, \sqrt{2}\sigma_3\eta_3)\right] d\eta_1 d\eta_2 d\eta_3 =$$

$$\iiint_{-\infty}^{+\infty} \eta_2^2 \exp\left(-\sum_{k=1}^{3} \frac{\eta_k^2}{2}\right) \left[b(\sigma_1\eta_1, \sigma_2\eta_2, \sigma_3\eta_3) - \right.$$

$$\left. - \frac{1}{2} b(\sqrt{2}\sigma_1\eta_1, \sqrt{2}\sigma_2\eta_2, \sqrt{2}\sigma_3\eta_3)\right] d\eta_1 d\eta_2 d\eta_3 =$$

$$\iiint_{-\infty}^{+\infty} \eta_3^2 \exp\left(-\sum_{k=1}^{3} \frac{\eta_k^2}{2}\right) \left[b(\sigma_1\eta_1, \sigma_2\eta_2, \sigma_3\eta_3 - \right.$$

$$\left. - \frac{1}{2} b(\sqrt{2}\sigma_1\eta_1, \sqrt{2}\sigma_2\eta_2, \sqrt{2}\sigma_3\eta_3)\right] d\eta_1 d\eta_2 d\eta_3. \qquad (20)$$

Equations (20) determine optimum correlations between values $\sigma_1, \sigma_2, \sigma_3$. To find the absolute values $\sigma_1$, $\sigma_2, \sigma_3$ we must resort to (13).

Let us consider now one important specific form of structural function for which the solution is obtained especially readily. Let surfaces of equal values of structural function represent surfaces of similar ellipsoids

$$\frac{y_1^2}{L_1^2} + \frac{y_2^2}{L_2^2} + \frac{y_3^2}{L_3^2} = \zeta^2(B), \qquad (21)$$



Declassified in Part - Sanitized Copy Approved for Release 2012/03/12 : CIA-RDP82-00039R000100190014-6

Declassified in Part - Sanitized Copy Approved for Release 2012/03/12 : CIA-RDP82-00039R000100190014-6

where B is the value of structural function $B(y_1, y_2, y_3)$ on the given surface; $\zeta^2$ is a parameter monotonically increasing with increasing B. This increase is obviously limited, since the expressions appearing in equation (20) within the bracket are essentially positive. Obviously that values $L_1$, $L_2$, $L_3$ can be simultaneously increased or decreased in an arbitrary correlation with the corresponding change of values $\zeta^2$. Therefore we subject $L_1$, $L_2$, $L_3$ to the condition:

$$(2\pi)^{3/2} L_1, L_2, L_3 = \Gamma. \tag{22}$$

But now it is readily apparent that assuming

$$\sigma_j = L_j \ (j=1,2,3), \tag{23}$$

we satisfy equation (20) as well as normalizing condition (13). Indeed, in variables $\eta_1, \eta_2, \eta_3$ surfaces of equal values of structural function are found to be surfaces of spheres; introducing spherical coordinates, we find immediately that all the integrals in equation (20) are equal to each other.

Due to general characteristics of locally uniform field, increase of structural function with the distance occurs more slowly than in accordance with the quadratic law; that is, monotonically increasing function B /in this connection see formula (26) of next paragraph/.



Declassified in Part - Sanitized Copy Approved for Release 2012/03/12 : CIA-RDP82-00039R000100190014-6

Declassified in Part - Sanitized Copy Approved for Release 2012/03/12 : CIA-RDP82-00039R000100190014-6

Now on determining the signs of second derivatives of function $\psi_3(\sigma_1, \sigma_2, \sigma_3)$, it becomes readily apparent that half-axes of the ellipsoid, formed by the surface of equal values of structural function, actually have in the case under consideration, the desired minimum characteristics.

## 3. CHARACTERISTIC VALUES OF TERMINAL DIFFERENCES OF HORIZONTAL MOTION VELOCITY

It is known that simple averaging of derivatives of a certain function in time and space leads to a divided difference of the given function (that is, correlation of corresponding terminal difference and increase of independent variable). Thus:

$$\frac{1}{T}\int_{-\frac{T}{2}}^{\frac{T}{2}} f(t-\tau)\,d\tau = \frac{f\left(t+\frac{T}{2}\right)-f\left(t-\frac{T}{2}\right)}{T}. \qquad (24)$$

It follows that terminal differences of motion elements constitute a particular case of space and time averages and must be studied from this standpoint. There exist, however, additional important circumstances which determine special value of terminal differences. In the foregoing paragraph on considering the question of replacing physical averages by space-time averages there was established the the conditon under which such a replacement is justified. The gist of this condition, as is readily apparent, is the requirement



Declassified in Part - Sanitized Copy Approved for Release 2012/03/12 : CIA-RDP82-00039R000100190014-6

Declassified in Part - Sanitized Copy Approved for Release 2012/03/12 : CIA-RDP82-00039R000100190014-6

of a uniform chance field in relation to the corresponding coordinate (or several coordinates). Then it follows directly from the characteristic of local uniformity of fields of motion elements, that divided differences in many instances are found to be closely approximate to physical mean values of the derivatives. But then to each class of actual processes there corresponds a definite method of replacement of derivatives by terminal differences. Characteristics of the studied process determine elementary intervals of increase -- "steps" of independent variables and degree of approximation of terminal differences to the physical average values of derivatives.

It must be noted that decreasing the interval size of independent variable because of a desire to approach true values of derivatives constitutes no less an error than the selection of too large a step.

In the solution of a large number of problems pertaining to dynamic meteorology excessive detail of field of turbulent motion not only does not elucidate, but on the contrary obscures basic recurring regularities of the studied motion. Terminal differences of motion elements, determined for a group of equivalent states, will have a chance character when the step is unduly reduced and even when a large number of experiments have been performed, determination of the general trend of the process is found to be quite difficult. Thus incongruousness of space averaging and physical averaging results in great technical disadvantages, and there arises therefore a practical necessity of



Declassified in Part - Sanitized Copy Approved for Release 2012/03/12 : CIA-RDP82-00039R000100190014-6

Declassified in Part - Sanitized Copy Approved for Release 2012/03/12 : CIA-RDP82-00039R000100190014-6

further averaging of the field and selection of larger step-intervals of the independent variable.

The fundamental work of A. A. Friedmann and T. Hesselberg /26/ was the first study aiming at the provision of factual characteristics of distribution of first and divided differences of basic meteorological elements necessary for investigations of dynamic meteorology. Indeed, although general principles of the simplification of hydromechanic equations are determined by similarity theory, quantitative evaluation of the error arising on discarding "secondary" members of equations can be effected only on the basis of empirical data. From factual distribution curves of values appearing in the equation of the problem, the researcher must determine how often the error induced by rejection of a certain member of the equation exceeds the definite limit error value, and thus must particularize general considerations relative to unimportance of the given member.

Therefore the study of distribution curves of meteorological elements and divided differences constitutes an indispensible stage in the learning of actual recurring regularities of atmospheric dynamics.

A. A. Friedmann and T. Hesselberg have given in their paper an evaluation of the order of differences in temperature, pressure, and horizontal and vertical wind components. Tables of order values of meteorological elements prepared by these authors/ are up to now, a basic aid of theoretic meteorological studies. It must be noted however that modern knowledge of meteorological field structure



Declassified in Part - Sanitized Copy Approved for Release 2012/03/12 : CIA-RDP82-00039R000100190014-6

Declassified in Part - Sanitized Copy Approved for Release 2012/03/12 : CIA-RDP82-00039R000100190014-6

makes it possible to greatly particularize the characteristic values of various meteorological elements in comparison with values given by A. A. Friedmann and T. Hesselberg. These researchers themselves, especially A. A. Friedmann, have expressed considerable interest in the continuation of studies for a more accurate knowledge of characteristic differences. This is evidenced not only by special remarks adduced to "facilitate future more accurate investigations in this direction" (/26/ page 152), but also by work conducted in the early Twenties at the Mathematic Bureau of Central Geophysical Observatory under the direction of A. A. Friedmann (/16/, /17/).

Let us consider briefly those postulates in the researches of A. A. Friedmann and T. Hesselberg which require at the present time substantial development or particularization.

1. Striving to decrease as much as possible the steps of independent variables, in order that the equations in their terminal differences approximately reproduce the differential equations of atmospheric dynamics, the authors have selected the following steps of independent variables: distance along the horizontal, 10 kilometers; distance along the vertical, 100 meters; time interval, 1 hour. When this work was conducted there could hardly have been suggested/ a different, more accurate selection of the steps. It is only recently that it was ascertained that they are not adequate. Since the steps of independent variables must be selected differently on analyses of distinct physical processes, it is necessary to ascertain the dependence of characteristics values of divided differences upon the step of the independent



Declassified in Part - Sanitized Copy Approved for Release 2012/03/12 : CIA-RDP82-00039R000100190014-6

Declassified in Part - Sanitized Copy Approved for Release 2012/03/12 : CIA-RDP82-00039R000100190014-6

variable, and hence upon the scale of the process. In lieu of the one distribution curve of a given divided difference, which was studied by A. A. Friedmann and T. Hesselberg it thus becomes necessary to study a whole series of such curves and determine from them the functional dependence of given distribution characteristics on the step value. This dependence is found to be a most essential element, especially in the determination of second differences. By doing this we also find some factual errors inherent in the work of A. A. Friedmann and T. Hesselberg.

2. The tables of A. A. Friedmann and T. Hesselberg give very approximate extreme values characterizing the distribution curve. In this connection the authors state: "We cannot at present determine the limits of the order of magnitudes; this requires a statistical study for which the available data are insufficient. We will give the order of magnitude only in the following approximate form. When the magnitude is quite constant, we will give only one value, namely the magnitude value in round figures to the nearest exponent of ten. In general, however, we will indicate the order of magnitude by two exponents of ten, namely $10^n$ and $10^{n+1}$. This implies that the given magnitude, in general, is $a \cdot 10^n$, where $0 < a < 10$, and only in exceptional cases does it exceed the value $5 \cdot 10^{n+1}$. We say then that the order of magnitude is from $10^n$ to $10^{n+1}$."

It is obvious that limits of magnitude determination obtained by the above method are too wide; and this substantially



Declassified in Part - Sanitized Copy Approved for Release 2012/03/12 : CIA-RDP82-00039R000100190014-6

Declassified in Part - Sanitized Copy Approved for Release 2012/03/12 : CIA-RDP82-00039R000100190014-6

limits the possibilities of simplifying equations of atmosphere dynamics. It may be said that simplifications based on tables of A. A. Friedmann and T. Hesselberg have become obvious and almost trivial to Soviet theoretical meteorologists. For further advancement there is a need of more detailed values of statistical characteristics of meteorological fields.

In the present paper there will be considered only one most important distribution characteristic — the standard of divided differences (that is, the root of dispersion).

Study of another interesting characteristic of distribution curves of differences of meteorological elements — that of excess -- still appears considerably less important than the study of standards. For those relatively rough calculations which determine the permissibility of discarding members of ~~dynamics~~ of the dynamics of the atmosphere equations ~~in atmospheric~~, it is in general possible to replace actual distribution curves by those of Gauss.

3. Tables of A. A. Friedmann and T. Hesselberg do not comprise the orders of a number of meteorological elements which are of substantial significance in modern theoretical investigations. Among these are, in first line, characteristics of humidity distribution, and values of radiant heat flows and their differences (heat influxes).

It should also be noted that our views relative to the nature of turbulent intermixing have undergone substantial changes



Declassified in Part - Sanitized Copy Approved for Release 2012/03/12 : CIA-RDP82-00039R000100190014-6

Declassified in Part - Sanitized Copy Approved for Release 2012/03/12 : CIA-RDP82-00039R000100190014-6

since the publication date of the paper of A. A. Friedmann and T. Hesselberg. Recently a number of important general rules determining turbulence characteristics have been derived. All this militates in favor of a need of substantial supplementations of tables of meteorological element characteristics. Work in this direction must be done in the future. Here only a few generalizations and elucidations are to be supplied relative to characteristic values of basic meteorological elements, as set out hereinbefore under sections 1 and 2.

To begin with let us point out that by definition, the structural function constitutes merely the mean square of certain terminal differences. Therefore, for instance:

$$\frac{\sqrt{\left[f\left(k_1+\frac{\Delta_1}{2}, k_2, k_3, k_4\right)-f\left(k_1-\frac{\Delta_1}{2}, k_2, k_3, k_4\right)\right]^2}}{\Delta_1} = \frac{\sqrt{b_x(\Delta_1)}}{\Delta_1}$$

or in a more general form,

$$\frac{\sqrt{\left[\Delta f_{(j)}(k_1, k_2, k_3, k_4)\right]^2}}{\Delta_j} = \frac{\sqrt{b_x(\Delta_j)}}{\Delta} \qquad (25)$$

wherein $\Delta f_{(j)}$ denotes the central difference of function f, with respect to the j argument.

Let us determine now the mean squares of the second divided differences. To do so we express the quantity

$$\left\{\left[f(k_1+\Delta_1, \ldots, k_4+\Delta_4)\right]-2\left[f(k_1, \ldots, k_4)+f(k_1-\Delta_1, \ldots, k_4-\Delta_4)\right]\right\}^2$$



Declassified in Part - Sanitized Copy Approved for Release 2012/03/12 : CIA-RDP82-00039R000100190014-6

Declassified in Part - Sanitized Copy Approved for Release 2012/03/12 : CIA-RDP82-00039R000100190014-6

utilizing equation (3) in the structural function.

On simple computations, we have

$$\overline{\left[f(x_1+\Delta_1,\ldots,x_4+\Delta_4)-2f(x_1,\ldots,x_4)+f(x_1-\Delta_1,\ldots,x_4-\Delta_4)\right]^2} = \tag{26}$$

$$= 4b_f(\Delta_1,\ldots,\Delta_4)-b_f(2\Delta_1,\ldots,2\Delta_4).$$

Therefrom, as a specific case, we obtain for the standard of second divided difference, (central), with respect to the j argument:

$$\frac{\sqrt{\overline{\left[\Delta f_{(j,j)}(x_1,x_2,x_3,x_4)\right]^2}}}{\Delta_j^{\,2}} = \frac{\sqrt{4b_f(\Delta_j)-b_f(2\Delta_j)}}{\Delta_j^{\,2}} \tag{27}$$

Fully analogous ~~is~~ the computation of characteristic values of mixed divided differences $\Delta f_{(j,k)}(x_1,\ldots,x_4)$.

The final result, given directly, is:

$$\frac{\sqrt{\overline{\Delta f_{(j,k)}(x_1,\ldots,x_4)^2}}}{\Delta_j\,\Delta_k} =$$

$$= \frac{\sqrt{2b_f(\Delta_j)+2b_f(\Delta_k)-b_f(\Delta_j,\Delta_k)-b_f(-\Delta_j,\Delta_k)}}{\Delta_j\,\Delta_k} \tag{28}$$



Declassified in Part - Sanitized Copy Approved for Release 2012/03/12 : CIA-RDP82-00039R000100190014-6

Declassified in Part - Sanitized Copy Approved for Release 2012/03/12 : CIA-RDP82-00039R000100190014-6

Calculations of this type could be continued to give standards of differences of any order n, by means of the structural function. Furthermore upon the values of increments of the independent variable tending toward zero, standards of derivatives could be readily obtained, at the same time determining the analytic form of structural function at small values of the arguments (more precisely, in the region where the structural function develops into a Taylor's series). Inasmuch as all such calculations are of a sufficiently elementary nature and are performed by identical methods, we will not consider them but will pass to the more essential problem of empirical determination of standard values of divided differences.

In this there appears immediately a difficulty of fundamental nature. In formulas (25),(27), (28) the physical averaging was used throughout, that is, they require a very detailed analysis of conditions of the given specific problem. It is quite obvious, however, that it is impossible to determine beforehand the characteristic values of differences of meteorological elements in the case of possible physical processes which actually occur in the atmosphere. On the other hand, as a matter of principle it would be incorrect to begin each theoretical investigation with a complete empirical, statistical description of the studied process. If the values of quantities to be obtained as a result of the theoretical investigation were always known beforehand, then the very important function of such investigation — the function of foreseeing facts and establishing new laws — would be completely lost. It



Declassified in Part - Sanitized Copy Approved for Release 2012/03/12 : CIA-RDP82-00039R000100190014-6

Declassified in Part - Sanitized Copy Approved for Release 2012/03/12 : CIA-RDP82-00039R000100190014-6

follows that initial data used by the theoretical meteorologist constitute only in part characteristics of the studied process, and in a major part are general, summative, characteristics of a group of similar processes. The problem which confronts the investigator consists in uncovering those specific laws which differentiate the process studied from other somewhat analagous processes. The more general in form are the initial characteristics given, the more difficult becomes the study; but at the same time the more significant, as a rule, will be the results attained. One should not, however, carry too far such generalizations, since then similarity between a group of processes, with respect to which the averaging is being carried out, and those being studied, may be found to be of such relative nature that the initial data altogether loses all significance. On the basis of considerations set forth, a conclusion may be reached concerning limits of applicability of climatic mean values of structural function. ¶ In the previously mentioned, very extensive investigations of the climatologic section, there were studied deviations of different meteorological elements from their average monthly, or average seasonal, values. Thus, averaging was effected with respect to all processes of a certain month or season which were considered as being analogous.



Declassified in Part - Sanitized Copy Approved for Release 2012/03/12 : CIA-RDP82-00039R000100190014-6

Declassified in Part - Sanitized Copy Approved for Release 2012/03/12 : CIA-RDP82-00039R000100190014-6

The most important characteristic of specificity of a given class of motions is thus the dimensions of area encompassed by these specific motions. Further detailed treatment also comprises differentiation of processes of intensity, by seasons or by geographic areas (See first paper of O. A. Drozdov /9/, which determined to a considerable extent the general trend of subsequent investigations).

Such an approach was found to be fully justified on tackling the practical problem of a rational distribution of a meteorological station network. Obviously, the same data can also be most successfully utilized to simplify formulation of a great many important theoretical problems, among which is included, for instance, the development of standard procedures of weather forecasting.

It should be noted that in the study of processes sharply differentiated by their intensity, such as storms or, on the other hand, calms, many simplifications based solely on analyses of the scale of the phenomena retain their validity. Indeed there can be pointed out large groups of members in equations of motion equally dependent on characteristic velocity. But when one is concerned with simplifications based on comparison of different groups of members, it is necessary to evaluate most carefully the applicability limits of such simplifications. A detailed analysis of structural functions values appears most desirable, and first of all their subdivision by characteristic velocity graduations.

On the whole, however, it must be recognized that in com-



Declassified in Part - Sanitized Copy Approved for Release 2012/03/12 : CIA-RDP82-00039R000100190014-6

Declassified in Part - Sanitized Copy Approved for Release 2012/03/12 : CIA-RDP82-00039R000100190014-6

parison with the scale of motion all other factors appear as secondary, as is indicated for instance by the data of M. V. Zavarinoy /15/. Therefore, in the first approximation it is quite permissible to utilize the mean values of structural function given in the papers of O. A. Drozdov /9/, /18/, O. A. Drozdov and A. A. Shepelevskiy /10/, M. V. Zavarinoy /15/, /19/, E. S. Seleznevoy /14/, and others.

It is most interesting to note that in most of these papers there are given not only graphs of extrapolation errors of

$$F(\Delta)=\sqrt{b(\Delta)+2\sigma_x^2}, \tag{29a}$$

but also graphs of errors of linear interpolation of meteorological elements at middle intervals:

$$f_{\frac{1}{2}}(\Delta)=\sqrt{F^2\left(\frac{\Delta}{2}\right)-\frac{1}{4}F^2(\Delta)}=\sqrt{b\left(\frac{\Delta}{2}\right)-\frac{1}{4}b(\Delta)+\frac{3}{2}\sigma_x^2}. \tag{29b}$$

where $\sigma_x$ characterizes in a summative manner errors of meteorological element measurement and the microclimatic peculiarities inherent thereto /10/; $b(\rho)$ represents no longer the mean physical square of difference but the mean square of difference deviations of the given element from the mean monthly (seasonal) values.

On comparing (29b) and (27) we find that average quadratic error of interpolation is very simply expressed by means of standard of second difference and conversely; and that relative errors



Declassified in Part - Sanitized Copy Approved for Release 2012/03/12 : CIA-RDP82-00039R000100190014-6

Declassified in Part - Sanitized Copy Approved for Release 2012/03/12 : CIA-RDP82-00039R000100190014-6

of determination of either quantity are approximately equal in the case of sufficiently large $\rho$ values. Let us consider now direct determination of characteristic values of some divided differences of the basic meteorological elements: wind, temperature, and pressure.

Most readily determined are values of standards of differences of horizontal wind velocity, in the horizontal direction under free atmosphere conditions.

The law formulated in paper /2/ relative to the proportionality of structural wind function $b_v(\Delta_s)$ and first power of horizontal distance $\Delta_s$ tallies well with results of interpretation of empirical data conducted by M. V. Zaverinoy /15/. It is important that this correlation holds also for various medium velocities of circulatory transfer. At the characteristic transfer velocity of 8-10 meters per second, we have, according to M. V. Zaverinoy, on introducing some small particularizations (see /2/, paper 42-44).

$$\sqrt{b_v(\Delta_s)} = 1.2 \cdot 10^{-2} \Delta_s^{1/2} \quad m/sec. \qquad (30)$$

For a definite period and geographic area the value of the coefficient in formula (30) can be determined with fairly great accuracy. However, on taking into consideration that this coefficient changes from year to year, and with the time of year, and is furthermore different for different altitudes and in different geographic areas, it becomes apparent that on practical utilization of formula (30) it is necessary to consider a possible "extrapolation error" of the coefficient value due to other physical conditions.



Declassified in Part - Sanitized Copy Approved for Release 2012/03/12 : CIA-RDP82-00039R000100190014-6

Declassified in Part - Sanitized Copy Approved for Release 2012/03/12 : CIA-RDP82-00039R000100190014-6

Reviewing the tables and graphs given in the paper of M. V. Zavarinoy, one reaches the conclusion that within a relative error not exceeding 20 percent, correlation (30) can be used over a very wide range of physical and geographic conditions. This 20 percent error will be considered as limiting in further presentation. Conditions under which application of the structural function expression utilized in this paper may result in a relative error substantially exceeding 20 percent, will be always specifically pointed out hereinafter. On consideration of wind structure such a reservation must be made first of all with respect to air layer. For altitudes of less than 30-50 meters, deviations of wind difference standards from the same standards under free atmosphere conditions may attain 50 percent and more. At the same time, substantial changes also occur in the basic regularities of structural function changes with distances, the law of first power. Especially complex is the question of influence of microclimatic peculiarity of the region involved. In this connection it appears best to present in a separate paper the structure of wind field in near-ground atmosphere layer.

At present we do not have available factual data on wind field structure at tropical latitudes, nor in the region of subtropical anticyclones. It can be assumed with some degree of certainty, however, that the regularities of this structure differ substantially from those of wind field structure at moderate latitudes, if for no other reason than the fact that premises upon which are based the deviations of the law of first power, are considerably less justifiable in the case of the above-cited regions.



Declassified in Part - Sanitized Copy Approved for Release 2012/03/12 : CIA-RDP82-00039R000100190014-6

Declassified in Part - Sanitized Copy Approved for Release 2012/03/12 : CIA-RDP82-00039R000100190014-6

Finally it should be recalled that in the case of great distances, when the value of $\sqrt{b_U(\Delta_s)}$, calculated by means of formula (30), exceeds $\sqrt{2}V$, this formula no longer holds and it is necessary to resort to the indicated limit value (/2/ pages 43-44).

Now we can compute the values of standards of first and second divided difference of wind component in a given horizontal direction. To do so we assume:

$$b_U(\Delta_s) = 2b_{U_j}(\Delta_s), \tag{31}$$

where j and s designate any horizontal directions and in particular may assume the values 1, 2.

Equation (31) is not wholly accurate since on the basis of general theoretical considerations it is known that characteristic values of a difference of a wind component depend on the angle between the direction of this component and the direction of the half-line connecting two given points.

However, calculations made by M. V. Zavarinoy, using empirical data (/15/ pages 47-48), show that the indicated dependence is very slight and in practice it is not expedient to take it into account.

On substituting (30) and (31) in equations (25), (27) we have:

$$U_j(s) = 8.5 \times 10^{-3} \Delta_s^{-\frac{1}{2}} \frac{1}{sec.} \tag{32}$$



Declassified in Part - Sanitized Copy Approved for Release 2012/03/12 : CIA-RDP82-00039R000100190014-6

Declassified in Part - Sanitized Copy Approved for Release 2012/03/12 : CIA-RDP82-00039R000100190014-6

and

$$U_j^{(s,s)} = 1.2 \times 10^{-2} \Delta_s^{-\frac{3}{2}} \frac{1}{m/sec.} \quad (j,s = 1,2). \tag{33a}$$

There $U_j^{(s)}$ and $U_j^{(s,s)}$ designate standards of first and second difference of the j velocity component in the s direction. All the dimensional quantities under consideration here and thereafter are expressed by means of the MTS System.

Let us also compute the standard of mixed difference of wind component in the direction $xj$ - $U_j^{(1,2)}$ $(j = 1,2)$.

From (31) it follows that

$$b_{U_j}(\Delta_1, \Delta_2) = b_{U_j}(\Delta_1, -\Delta_2) = 6 \times 10^{-3} (\Delta_1^2 + \Delta_2^2)^{\frac{1}{2}}.$$

wherefrom we find immediately by means of (28) the desired function:

$$U_j^{(1,2)} = 9.2 \times 10^{-3} \Delta_s^{-\frac{3}{2}}. \tag{33b}$$

For rough calculations the values of standards of second divided difference, in a definite direction as well as a composite, are taken as equal to $1.1 \times 10^{-2} \Delta_s^{-\frac{3}{2}} \frac{1}{m/sec.}$. It is desirable however to distinguish these quantities since the difference in the coefficients of formulas (33a) and (33b) exceeds the above-indicated 20 percent limit of relative deviation.

Let us now compare the obtained values of characteristic differences of horizontal wind components with the orders of magnitude indicated by A. A. Friedmann and T. Heerelberg; $10^{-5}$ - $10^{-4}$ for the first and $10^{-10}$ - $10^{-9}$ for the second divided difference.



Declassified in Part - Sanitized Copy Approved for Release 2012/03/12 : CIA-RDP82-00039R000100190014-6

Declassified in Part - Sanitized Copy Approved for Release 2012/03/12 : CIA-RDP82-00039R000100190014-6

If we follow the rules of order determination proposed by these authors, and assume that distribution of differences approximately satisfies the normal law, we find that for distances from 10 kilometers (the step selected by A. A. Friedmann and T. Hesselberg) to 50 kilometers one may utilize the order of first divided difference indicated by them. For distances exceeding 50 kilometers this order is decreased by one unit and is equal to $10^{-6}$ - $10^{-5}$. (Obviously, it is much more advantageous to use directly formula (32a) in conjunction with the law of normal distribution).

Matters stand somewhat differently insofar as order of $U_j^{(s,\sigma)}$ $(j; s, \sigma = 1, 2)$ is concerned. Here the limits indicated in the paper of A. A. Friedmann and T. Hesselberg are found to be not only excessively wide but also clearly erroneous. Indeed when $\Delta_s$ = 10 kilometers, $U_j^{(s,\sigma)}$ is found to be equal to $1.1 \cdot 10^{-8}$, that is, the order of this divided difference is $10^{-9}$ - $10^{-8}$. Determining the value of the step for which the order would be $10^{-10}$ - $10^{-9}$, we can readily ascertain that this is fulfilled when $\Delta_s$ varies within the interval of from approximately 20 to 100 kilometers. (See Table I at the end of the present article and compare with tables of normal distribution law). Thus, A. A. Friedmann and T. Hesselberg have indicated incorrectly the unit of distance in the horizontal direction for which they have determined the terminal difference of wind. In this connection it should be specifically pointed out that determination of differences was effected by means of synoptic charts (/26/ page 153). The authors do not state what procedures they have followed on using the chart, but from the results shown above which are also corro-



Declassified in Part - Sanitized Copy Approved for Release 2012/03/12 : CIA-RDP82-00039R000100190014-6

Declassified in Part - Sanitized Copy Approved for Release 2012/03/12 : CIA-RDP82-00039R000100190014-6

borated by temperature and pressure data, it can be assumed with confidence that these procedures included some additional leveling of meteorological fields. It is also necessary to take into account that in the deviation in the present paper of values of second divided differences, there was excluded the observation error; this apparently was not done in the paper of A. A. Friedmann and T. Hesselberg (the publication does not contain any information on this subject). Therefore the values of differences obtained by these authors should have been too high rather than too low; in fact, however, the latter was the case.

Let us pass now to the determination of standards of time difference of horizontal wind velocity at one definite point. On this subject the basic work was performed by Ye. S. Seleznevoy /14/. We have shown that the hypothesis of transfer of wind fluctuations by the mean current results in very good agreement with the data of Ye. S. Seleznevoy and M. V. Kavarinoy. Therefore the value

$$\sqrt{b_v(\Delta_1)} = 3.5 \times 10^{-2} \Delta_1^{1/2} \frac{m}{sec}, \qquad (34)$$

obtained by means of either data (/2/ page 44, /15/ page 160) may be considered as being sufficiently characteristic.

From this follows:

$$U_j^{(1)} = 2.5 \times 10^{-2} \Delta_1^{-1/2} \frac{m}{sec.^2} \qquad (35)$$

and in accordance with (27):

$$U_f^{(1,1)} = 3.5 \times 10^{-2} \Delta_1^{-3/2} \frac{m}{sec} \qquad (36)$$



Declassified in Part - Sanitized Copy Approved for Release 2012/03/12 : CIA-RDP82-00039R000100190014-6

Declassified in Part - Sanitized Copy Approved for Release 2012/03/12 : CIA-RDP82-00039R000100190014-6

For $\Delta_4 = 3600$ seconds, adopted by A. A. Friedmann and T. Hesselberg as being the elementary time interval, we have:

$$U_j^{(4)} = 4.2 \times 10^{-4} \text{ and } U_j^{(4,4)} = 1.6 \times 10^{-7}$$

Both these values are in accordance with the previously indicated orders of $10^{-4} - 10^{-3}$; and $10^{-8} - 10^{-7}$.

The fact of order agreement between the results obtained and the data of A.A. Friedmann and T. Hesselberg is important since these authors utilized anemogram data. Thus the orders of wind changes in time obtained by them in lower layers of air may be expanded to free atmosphere. On the other hand, as already indicated herein before, it would be erroneous to extend our more accurate characteristics of wind changes in time and along the horizontal to the lower air layer.

## 4. ON STRUCTURE FUNCTIONS OF TEMPERATURE AND PRESSURE

Considering regularities of field of temperature, it is necessary to call attention in the first place to the well known fact of similarity of vertical contours of average wind and average temperature. This fact is demonstrated and extensively utilized in the investigation of turbulent boundary layers (see for example /20/, /21/) and yields no less significant results in the study of atmospheric turbulence. As an outstanding example we may cite the correlation graph of vertical wind gradients and temperature plotted by M. I. Budyko /22/ on the basis of field similarities, and which defines well the experimentally determined regularities. It can be anticipated fully that under certain conditions there exists a



Declassified in Part - Sanitized Copy Approved for Release 2012/03/12 : CIA-RDP82-00039R000100190014-6

Declassified in Part - Sanitized Copy Approved for Release 2012/03/12 : CIA-RDP82-00039R000100190014-6

similarity of not only the vertical but also of the horizontal gradients of temperature and wind, that is, the following condition:

$$\frac{b_T(\Delta_1, \Delta_2, \Delta_3)}{b_U(\Delta_1, \Delta_2, \Delta_3)} = \alpha^2 \frac{\text{degrees}^2 \text{sec.}^2}{M^2} \qquad (37)$$

Such a law was in fact derived by A. M. Obukhov /23/ on the basis of dimensional considerations for the microstructure of temperature field. In other words A. M. Obukhov has shown that within the domain of applicability of the "Two Thirds Law", in the case of wind field, the same law holds for the temperature field.

Within the area in which we are interested, wherein dispersion of horizontal wind component differences is determined by linear law, proof of correlation (37) is based on somewhat different theoretical considerations. We propose to devote a special paper to this subject which will also include a derivation of the linear law of wind field structure based on more general assumptions than those given in paper /2/. Here we will consider this question from an empirical viewpoint. The most important research on horizontal differences of terrestial temperature field in the previously cited paper of O. A. Drozdov /9/. In this paper there was determined the probable average deviation of mean daily temperature differences at two points according to the formula.

$$F = 0.85 \left| \overline{\delta_T}^{(t)} - {}^{(t)}\delta_T \right| \qquad (38)$$

where $\delta_T$ is the difference of temperatures /index (t) to the left of the line denotes that averaging is effected in time/. Then



Declassified in Part - Sanitized Copy Approved for Release 2012/03/12 : CIA-RDP82-00039R000100190014-6

Declassified in Part - Sanitized Copy Approved for Release 2012/03/12 : CIA-RDP82-00039R000100190014-6

there were plotted graphs of probable average deviations of temperature as a function of distance F ( $\Delta_s$ ), and the function was interpolated by straight line $a' + k'\Delta_s$. It must be pointed out that F (0) = $a''$ constitutes an error characterizing the measuring errors and the microclimatic differences of all pairs of points. Since these errors must be eliminated we have, according to O. A. Drozdov, the following correlation for $b_T(\Delta_s)$:

$$b_T(\Delta_s) = 2a\Delta_s + \kappa^2\Delta_s^2. \tag{38a}$$

It is assumed that factors a and k are obtained from $a'$ and $k'$ by multiplication with a constant multiplier of the normal distribution law equal to 1.48.

From the above-indicated standpoint, results not less and possibly more satisfactory should be obtained by means of the simple linear relation:

$$b_T(\Delta_s) = C\Delta_s. \tag{38b}$$

Therefore let us determine how accurately formulas (38a) and (38b) satisfy the empirically determined regularities.

For this determination we will utilize the July data of stations of the Kursk, Voronezh and Orel oblasts (former TsChO), selected by O.A. Drozdov and A. A. Shepelevskiy (/10/, pages 27-28), as an illustration of the correctness of the proposed interpolation theory.

The 83 values of probable mean difference deviations given in the paper of O. A. Drozdov (/9/, pages 75-78) are squared and plotted as a graph (figure 1).



Declassified in Part - Sanitized Copy Approved for Release 2012/03/12 : CIA-RDP82-00039R000100190014-6

Declassified in Part - Sanitized Copy Approved for Release 2012/03/12 : CIA-RDP82-00039R000100190014-6

Figure 1. Structural Function of Temperature

This graph shows that the straight line

$$F^2(\Delta_s) = 0.09 + 4.5 \times 10^{-6} \Delta_s \qquad (39a)$$

represents the function much better than the dotted-line curve obtained by O. A. Drozdov:

$$F^2(\Delta_s) = 0.09 + 2.46 \times 10^{-6} \Delta_s + 1.68 \times 10^{-11} \Delta_s^2. \qquad (39b)$$

Even more convincing is the graph (Figure 2) on which are plotted the squares of probable values of actual interpolation errors. From the table given by O. A. Drozdov (/9/, pages 93-94) there are selected the data for 1931-1933 for three points satisfying the condition:

$$n = \frac{\Delta'}{\Delta} \geqslant 0.4,$$

wherein $\Delta$ is the distance between most remote stations, while $\Delta'$ is the distance between the most closely located stations. In these cases the basic formula of O. A. Drozdov and A. A. Shepelevskiy, which expresses the probable interpolation errors by means of similar extrapolation errors is:

$$f_n^2(\Delta) = n F^2(\Delta - n\Delta) + (1-n) F^2(n\Delta) - n(1-n) F^2(\Delta), \qquad (40)$$

it can be assumed with a considerable degree of accuracy that $n = 0.5$, that is, formula (40) can be replaced by formula (29b).

Figure 2. Interpolation errors of Temperature.



Declassified in Part - Sanitized Copy Approved for Release 2012/03/12 : CIA-RDP82-00039R000100190014-6

Declassified in Part - Sanitized Copy Approved for Release 2012/03/12 : CIA-RDP82-00039R000100190014-6

On the graph (of Figure 2) the solid straight line represents function $f^2_{1/2}(\Delta_s)$ obtained by substituting in (29b) the values of $F^2(\Delta_s)$ determined from (39a):

$$f^2_{1/2}(\Delta_s) = 0.068 + 1.12 \times 10^{-6}\Delta_s . \qquad (41a)$$

while the dotted straight line is the result of substituting in (40) $F^2(\Delta_s)$ values from (39b)

$$f^2_{1/2}(\Delta_s) = 0.068 + 6.15 \times 10^{-7}\Delta_s . \qquad (41b)$$

The advantages of the law of first order (39a) are self-evident. It must also be noted that with the existent distributions of points, determination of form of function $f^2_{1/2}(\Delta_s)$ directly from factual data is most difficult; this has already been pointed out by O. A. Drozdov and A. A. Shepelevskiy.

To obtain the desired value of the standard of periodic temperature differences, it is necessary to perform a double transition:

a. For passing from probable differences of mean daily temperatures to similar differences of standard temperatures we multiply $F(\Delta_s)$ by 1.6, a factor recommended by O.A. Drozdov on the basis of his empirical investigations /9/, /18/;

b. To pass from probable values of difference to the mean quadratic we multiply the value obtained by the coefficient 1.48, corresponding to laws of normal distribution.

Recalling that the free member in the right hand side of formula (39a) is subject to elimination, we finally have:



Declassified in Part - Sanitized Copy Approved for Release 2012/03/12 : CIA-RDP82-00039R000100190014-6

Declassified in Part - Sanitized Copy Approved for Release 2012/03/12 : CIA-RDP82-00039R000100190014-6

$$\sqrt{b_T(\Delta_s)} = 5.0 \times 10^{-3} \Delta_s^{1/2} \text{ degrees} \qquad (42)$$

Even though the transition coefficients are not by their nature definite constants and that figures indicated under a and b, above, must be regarded as approximate mean values of these slightly varying multipliers, the accuracy of correlation (42) is in general sufficient for a characterization of temperature field structure in lower air layers. We do not propose to consider the geographic changes of this structure within the limits of the plain regions of the European part of the Union, nor to take into account the annual range of the coefficient in formula (42) /or correspondingly in (38b)/. It may be noted in this connection that the latter changes somewhat more evenly than the coefficients of O.A. Drozdov's formula (38a).

Greater difficulties are encountered in the problem of applying equation (42) to conditions of a free atmosphere.

Comparison of standard values of temperature differences calculated by means of this equation, with the results of interpolation of factual data conducted by M. V. Zavarinoy /19/, discloses a fully satisfactory agreement of formula (42) with empirical data for the distances interval 300-700 kilometers.

It is precisely [redacted] this interval [redacted] to which the overwhelming majority of M. V. Zavarinoy's data relate and the agreement thus revealed is especially interesting in view of the fact



Declassified in Part - Sanitized Copy Approved for Release 2012/03/12 : CIA-RDP82-00039R000100190014-6

Declassified in Part - Sanitized Copy Approved for Release 2012/03/12 : CIA-RDP82-00039R000100190014-6

that the maximum distance between points of the graph (Figure 1) is 200 kilometers. For relatively short distances between the points the resulting picture is considerably less definite.

While according to data of German atmosphere soundings, Berlin to Lindenberg (distance of 70 kilometers) and especially Norderneitо Hamburg (distance of 190 kilometers), standards of differences obtained are appreciably lower than those calculated on the basis of formula (42), the data of special observations of GGO and TsAP expeditions lead to the opposite conclusion.

It is apparent that in order to obtain the desired accuracy of structural function values, at distances of only several times ten kilometers, it is necessary to have available a considerably greater amount of experimental data. In the present publication equation (42) can be used with adequate justification, for a characteristic of temperature field structure within the lower half of the troposphere. In such a case standards of divided differences are determined by means of formulas (25):

$$T^{(s)} = 5 \times 10^{-3} \Delta_s^{-1/2} \frac{\text{degrees}}{\text{m.}} \quad (s = 1.2); \qquad (43)$$

(27)

$$T^{(s,s)} = 7 \times 10^{-3} \Delta_s^{-3/2} \frac{\text{degrees}}{\text{m.}^2} \qquad (44a)$$

and (28)

$$T^{(1,2)} = 5.4 \times 10^{-3} \Delta_s^{-3/2} \frac{\text{degrees}}{\text{m.}^2} \qquad (44b)$$

Let us consider now the question of temperature changes with



Declassified in Part - Sanitized Copy Approved for Release 2012/03/12 : CIA-RDP82-00039R000100190014-6

Declassified in Part - Sanitized Copy Approved for Release 2012/03/12 : CIA-RDP82-00039R000100190014-6

time. The basic problem thus arising can be formulated as follows: does the temperature field possess, the same as the field of wind, the property of fluctuation transfer by median flow?

If an affirmative answer can be established, this means a substantially increased analogy between fields of horizontal wind and temperature. But such an affirmative answer becomes obvious if the problem stated is formulated in the more usual manner: are temperature changes in time determined in the basic horizontal advection of heat? Then from the correlation

$$\frac{\partial T}{\partial t} \cong -\overline{U}_s \frac{\partial T}{\partial x_s}$$

(axis $X_s$ is selected in the direction of the mean horizontal velocity vector $\overline{U}_s$), it follows:

$$T^{(4)} = 5 \times 10^{-3} \overline{u}_s^{-1/2} \Delta_4^{-1/2} \tag{45}$$

Since the path covered over the time $\Delta_4$ is equal to:

$$\Delta_s = \overline{u}_s \Delta_4 \tag{46}$$

At average transfer velocity $U_s = 30 \frac{km}{hr} = 8.5 m/sec$, we have

$$T^{(4)} = 1.45 \times 10^{-2} \Delta_4^{-1/2} \frac{degrees}{sec.} \tag{47}$$

the standard of second divided difference in time

$$T^{(4,4)} = 2.05 \times 10^{-2} \Delta_4^{-1/2} \frac{degrees}{sec.} \tag{48}$$

Let us now compare formula (47) with the empirical data. It is most convenient to use the final table compiled by Ye. S.



Declassified in Part - Sanitized Copy Approved for Release 2012/03/12 : CIA-RDP82-00039R000100190014-6

Declassified in Part - Sanitized Copy Approved for Release 2012/03/12 : CIA-RDP82-00039R000100190014-6

Seleznevoy (/14/ page 163) containing standards of temperature changes over time intervals from 2 to 24 hours obtained from leveled curves. We are reproducing this table.

TABLE II

Standards in temperature changes in time

| | Time intervals in hours. | | | | | |
|---|---|---|---|---|---|---|
| | 2 | 3 | 4 | 6 | 12 | 24 |
| Altitudes 1-2 kilometers | 0.8 | 1.1 | 1.4 | 2.0 | 2.9 | 3.5 |
| Altitudes 4 kilometers | 1.1 | 1.5 | 1.8 | 2.4 | 3.2 | 3.8 |
| Temperature change from formula (47) | 1.2 | 1.5 | 1.7 | 2.1 | 3.0 | 4.3 |

In the last line of Table II are shown values of temperature change $T(4)\Delta_4$ computed by means of formula (47). Agreement of these values with the actual standards of temperature changes with time at an altitude of 4 kilometers must be recognized as fully satisfactory. Even determination errors of temperature change standards within the 1-2 kilometer layer, where according to data of Ye. S. Seleznevoy fluctuation of temperature with time is at a minimum, are in most instances within the previously adopted 20 percent limit of permissible relative errors.

This formula (47) derived indirectly satisfies with a sufficient degree of accuracy the direct experimental data. This also justifies the use of formula (48) obtained directly from (47).

The next important characteristic of meteorological fields is the structural function of pressure, the values of which have



Declassified in Part - Sanitized Copy Approved for Release 2012/03/12 : CIA-RDP82-00039R000100190014-6

Declassified in Part - Sanitized Copy Approved for Release 2012/03/12 : CIA-RDP82-00039R000100190014-6

been partially investigated empirically. Characteristic differences of pressure in horizontal direction were considered in the papers of M. A. Omshanskiy /24/ and also of O. A. Drozdov and A. A. Shepelevskiy /10/. These investigators have proposed solutions which differ in principle from the very important problem relative to the form of function defining the dependence of the structural function on distance. Whereas O. A. Drozdov and A. A. Shepelevskiy assume that the values of the structural function of pressure, like those of temperature and wind, can be defined by formula (38a), M. A. Omshanskiy assumed that development of structural function as a series by increasing orders of distance $\Delta_s$ must begin with $\Delta_s^2$. Consequently he proposed the following form of dependence between $b_p$ and $\Delta_s$.

$$b_p(\Delta_s) = m^2\Delta_s^2(1 - n\Delta_s) \qquad (49)$$

We know now that in general structural functions expressed as series may contain members of the form $a\Delta_s$, and even $a\Delta_s^n$ where $n<1$ (excluding from considerations very small-scale motions, where direct transformation of kinetic energy into energy of thermal molecular motion is essential). Nevertheless, for a field of air pressure differentiated by especial smoothness due to general properties of atmospheric currents (smallness of vertical accelerations!), the form of structural function (49) proposed by M. A. Omshanskiy appears more natural than the form of O. A. Drozdov and A. A. Shepelevskiy (38a).

For a comparison of both formulas with empirical data it is most convenient to compare values of second differences (interpolation



Declassified in Part - Sanitized Copy Approved for Release 2012/03/12 : CIA-RDP82-00039R000100190014-6

Declassified in Part - Sanitized Copy Approved for Release 2012/03/12 : CIA-RDP82-00039R000100190014-6

errors), since in this computation the difference in analytical form of structural function is expressed most prominently.

Let us determine the mean square of second difference, using equation (26) and utilizing the values of A. M. Omshanskiy's structural function:

$$b_p(\Delta_s) = 9.7 \times 10^{-11} \Delta_s^2 (1 - 8.3 \times 10^{-7} \Delta_s) \, (mm\ Hg)^2$$

and that of O. A. Drozdov and A. A. Shepelevskiy:

$$b_p(\Delta_s) = (6.4 \times 10^{-7} \Delta_s + 4.1 \times 10^{-11} \Delta_s^2) (mm\ Hg)^2$$

the free member, reflecting errors of pressure determination, being omitted. Thus we have, respectively,

$$4 b_p(\Delta_s) - b_p(2\Delta_s) = 3.2 \times 10^{-16} \Delta_s^3 \, (mm\ Hg)^2$$

and

$$4 b_p(\Delta_s) - b_p(2\Delta_s) = 1.28 \times 10^{-6} \Delta_s \, (mm\ Hg)^2$$

while coinciding when $\Delta_s \cong 6 \cdot 10^4$m, these values of second differences diverge very greatly at higher values of $\Delta_s$. Thus when $\Delta_s = 5 \cdot 10^5$m = 500 kilometers according to M. A. Omshanskiy's formula, we have for the mean square value of second pressure difference 6.3 mm Hg = 8.4 mb, while according to O. A. Drozdov and A. A. Shepelevskiy, it is only 0.8 mm Hg = 1.1 mb.



Declassified in Part - Sanitized Copy Approved for Release 2012/03/12 : CIA-RDP82-00039R000100190014-6

Declassified in Part - Sanitized Copy Approved for Release 2012/03/12 : CIA-RDP82-00039R000100190014-6

The result of M. A. Omshanskiy is found to be much closer to the factual characteristic values of second differences, the computation of which is frequently effected in synoptic practice.

Processing of several such series gave values of second difference pressure standards from 4 to 6 millibars. It is obvious that such values cannot be obtained by variation of the initial ordinate in the graph of O. A. Drozdov and A. A. Shepelevskiy (See Figure 6, paper /10/). Therefore we will utilize the analytical form of structural function (49) but with inclusion of certain corrections of coefficients, in M. A. Omshanskiy's equation. The inaccuracy in determination of these coefficients is characterized first of all by utilization of insufficient data (data of only 4 stations located in the area of Kara Sea), and in addition by approximations in determining distances between stations. Having determined these distances more accurately (by orthodromy) we find immediately a substantially lower value for this coefficient $n:n = 6.5 \cdot 10^{-7} \frac{1}{n}$, which will be used hereafter. Coefficient $m^2$ remains practically unchanged. This indicates high values of baric gradients in the Kara Sea area, appreciably exceeding characteristic values of gradients in almost the entire territory of USSR. It should be noted in this connection that pressure differences constitute one of the least uniform characteristics of meteorological fields. Standards of pressure differences depend substantially on the direction of the line joining the stations, change quite noticeably from season to season and from one year to another, and so forth.

Therefore, in order to determine with a sufficient degree of accuracy the regularities of pressure fields, it is imperative



Declassified in Part - Sanitized Copy Approved for Release 2012/03/12 : CIA-RDP82-00039R000100190014-6

Declassified in Part - Sanitized Copy Approved for Release 2012/03/12 : CIA-RDP82-00039R000100190014-6

to process the very considerable amount of empirical data. As a first approximation one may accept the mean value of coefficient $m^2$ as being equal to $m^2 = 10^{-10} \frac{mb.^2}{m.^2}$. This value is obtained as the average on the basis of M. A. Omshanskiy's data, data of O. A. Drozdov and A. A. Shepelevskiy, and additional personal computations.

Transferring now into MTS units (10 millibars) and determining standards of first and second divided differences, we have:

$$P^{(s)} = 1.3 \times 10^{-6} (1 - 8.3 \times 10^{-7} \Delta_s)^{1/2} \quad (s = 1.2) \qquad (50)$$

and

$$P^{(s,s)} = 2.4 \times 10^{-9} \Delta_s^{-1/2}. \qquad (51a)$$



Declassified in Part - Sanitized Copy Approved for Release 2012/03/12 : CIA-RDP82-00039R000100190014-6

Declassified in Part - Sanitized Copy Approved for Release 2012/03/12 : CIA-RDP82-00039R000100190014-6

TABLE III

Standards of Differences of Basic Meteorological Elements in the Horizontal Direction.

| Element | | Step, in kilometers | | | | |
|---|---|---|---|---|---|---|
| | | 20 | 50 | 100 | 200 | 500 |
| Wind component in horizontal direction | $10^5\ U_j^{(s)}$ | 6.0 | 3.8 | 2.7 | 1.9 | 1.2 |
| | $10^{10}\ U_j^{(s,s)}$ | 42 | 11 | 3.8 | 1.3 | 0.34 |
| | $10^{10}\ U_j^{(1,2)}$ | 32 | 8.2 | 2.9 | 1.0 | 0.26 |
| Temperature | $10^5\ T^{(s)}$ | 3.5 | 2.2 | 1.6 | 1.1 | 0.71 |
| | $10^{10}\ T^{(s,s)}$ | 25 | 6.3 | 2.2 | 0.38 | 0.20 |
| | $10^{10}\ T^{(1,2)}$ | 19 | 4.8 | 1.7 | 0.60 | 0.15 |
| Pressure | $10^6\ p^{(s)}$ | 1.0 | 1.0 | 1.0 | 0.9 | 0.8 |
| | $10^{12}\ p^{(s,s)}$ | 1.1 | 7.1 | 5.1 | 3.6 | 2.3 |
| | $10^{12}\ p^{(1,2)}$ | 7.1 | 7.5 | 3.2 | 2.2 | 1.4 |

Substituting values of structural function in equation (28) with $\Delta_1=\Delta_2=\Delta_s$, and assuming the horizontal pressure field to be isotropic, we have for the standard of composite divided difference:

$$-p^{(1,2)} = 1.5\times 10^{-9}\Delta_s^{-1/2} \tag{51b}$$

As previously stated the coefficients of equations (50) and (51) require further particularization. It is of interest that dependence of $p^{(s)}$ and $p^{(s,s)}$ on magnitude of step $\Delta_s$ is found to be so slight that the orders of differences indicated by A. A. Friedmann



Declassified in Part - Sanitized Copy Approved for Release 2012/03/12 : CIA-RDP82-00039R000100190014-6

Declassified in Part - Sanitized Copy Approved for Release 2012/03/12 : CIA-RDP82-00039R000100190014-6

and T. Herselberg, $10^{-7}$ _ $10^{-6}$, and $10^{-12}$ _ $10^{-11}$, are found to be correct for all step values contained in Table III from 20 to 500 kilometers.

In this table are given standards of divided differences in the horizontal direction, horizontal component of wind velocity, temperature and pressure, computed on the basis of equations (32), (33), (43), (44), (50), and (51).

Table IV contains standards of divided differences of horizontal component of wind velocity, and temperature in time, calculated on the basis of equations (35), (36), (47) and (48).

TABLE IV

Standards of Differences of Temperature and Horizontal Component of wind in time.

| Element | | Step, in hours | | | | |
|---|---|---|---|---|---|---|
| | | 1/2 | 1 | 3 | 6 | 12 |
| Wind Component | $10^4\ v_j^{(4)}$ | 5.9 | 4.2 | 2.4 | 1.7 | 1.2 |
| | $10^8\ v_j^{(4,4)}$ | 46 | 16 | 3.1 | 1.1 | 0.38 |
| Temperature | $10^4\ T^{(4)}$ | 3.5 | 2.4 | 1.4 | 1.0 | 0.7 |
| | $10^8\ T^{(4,4)}$ | 27 | 9.5 | 1.8 | 0.65 | 0.23 |

Thus of the 45 differences the order of which is given in the basic table Ia of A. A. Friedmann and T. Herselberg in the present paper there are particularized 10.

Consequently in order to attain essentially new results it is necessary to utilize in conjunction with the empirical computations a number of theoretical considerations.



Declassified in Part - Sanitized Copy Approved for Release 2012/03/12 : CIA-RDP82-00039R000100190014-6